Response and Reliability Problems of Dynamic Systems

Nielsen, Søren R. K.

Publication date:
1997

Document Version
Publisher's PDF, also known as Version of record

RESPONSE AND RELIABILITY PROBLEMS OF DYNAMIC SYSTEMS

Søren R. K. Nielsen

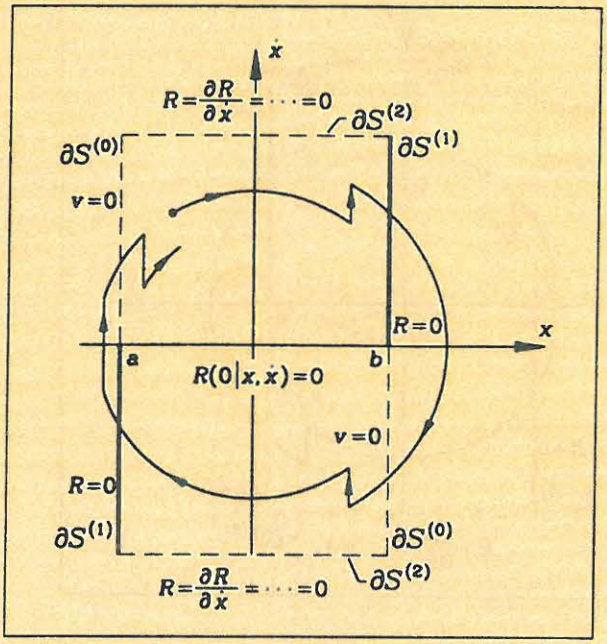

Thesis for the dr.techn. degree

Aalborg Tekniske Universitetsforlag
September, 1997

RESPONSE AND RELIABILITY PROBLEMS OF DYNAMIC SYSTEMS

Søren R. K. Nielsen

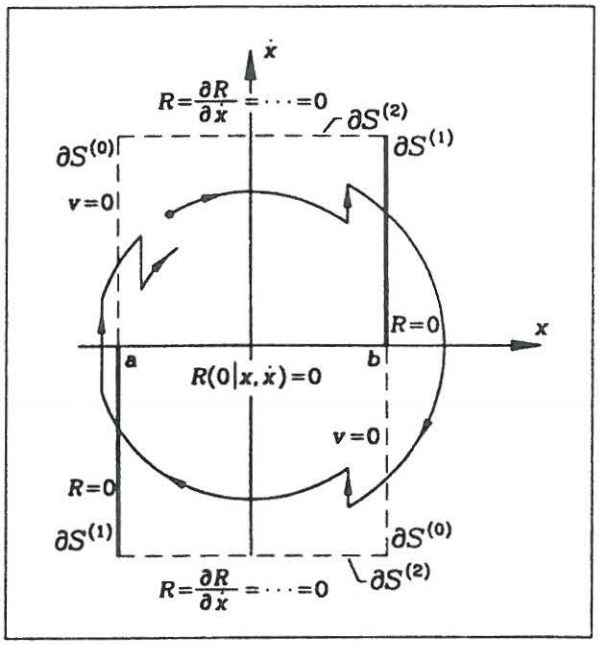

Thesis for the dr.techn. degree

Aalborg Tekniske Universitetsforlag
September, 1997

Denne afhandling er af Det Teknisk-Naturvidenskabelige Fakultet ved Aalborg Universitet antaget til forsvar for doktorgraden i teknik. Forsvaret finder sted på Aalborg Universitet i Auditorium F.108, Sohngaardsholmsvej 57 den 16. januar 1998 kl. 13.00 præcis.

Aalborg den 12. november 1997

Finn Kjærsdam
Dekan

This thesis has been accepted by the Faculty of Engineering and Science at Aalborg University for public defence in fulfilment of the requirements for the doctoral degree in technology . The defence will take place at Aalborg University in Lecture Room F.108, Sohngaardsholmsvej 57 on Jan. 16, 1998 at 1 p.m. punctually.

Aalborg, November 12, 1997

Finn Kjærsdam
Dean

Preface

The present thesis consists of selected parts of the work performed by the author on stochastic dynamics and reliability theory of dynamically excited structures primarily during the period 1986-1996. Since this work in parts has been done in cooperation with colleagues at the Aalborg University and abroad it is mandatory for me to use this opportunity to render my thanks to all of them for their kind encouragements, inspiration and hospitality during visits. Especially, I want to express my gratitude to Professor, Dr.-ing. habil. Radosław Iwankiewicz, Technical University of Wrocław, with whom I have been working with the development of the theory of dynamics of structures exposed to random pulses since 1988. The cooperation has been a great fun from the first day and has influenced the work significantly. Of equally great importance was a visit I paid to Professor Ahmet Ş. Çakmak, Princeton University in the autumn semester of 1990, which initiated a cooperation on stochastic dynamics, earthquake engineering and damage assessment, including mutual visits by Ph.D. students from Aalborg University and Princeton University. One of these students was H.U. Köylüoğlu, who was visiting me for one year in 1992-93. Since his graduation I have continued to work together with Ugur, on various subjects within stochastic dynamics with emphasis on response and reliability of uncertain structures. At Aalborg University I want to thank my colleagues Professor Palle Thoft-Christensen and Associate Professor John Dalsgård Sørensen, who together with myself form the research group on stochastic mechanics and reliability at Aalborg University. Palle employed me in my present position in 1986, and introduced me to several of my international contacts including Professor Iwankiewicz and Professor Çakmak.

The thesis has been written as a coherent text, based on a number of papers. This has necessitated rewriting of larger parts of the underlaying papers. The layout and editing of my messy notes and enclosures was managed with masterful skill of secretary Solveig Hesselvang. The modest English was corrected and improved by senior secretary Kirsten Aakjær and the drawings were prepared by technician Norma Hornung. My gratitude is rendered to all of them.

Aalborg, September 20, 1997

Søren R.K. Nielsen

TABLE OF CONTENTS

1. INTRODUCTION

Let $\{\mathbf{X}(t),\, t \in [t_0, \infty[\}$, $\mathbf{X}(t) : \Omega \rightarrow R^m$ be an m-dimensional stochastic vector process made up by some response quantities of a structural system subjected to external (i.e. non-parametric) dynamic loads applied during the interval $[t_0, \infty[$. Typically, $\{\mathbf{X}(t),\, t \in [t, \infty[\}$ is made up by a combination of stresses and displacement components at a number m of critical material points throughout the structure, in which the structural reliability is controlled.

In principle all material points in a continuous medium must be checked. Hence, the dimension m of the response process $\{\mathbf{X}(t),\, t \in [t_0, \infty[\}$ is infinite for any continuous medium. However, at any numerical application a discretization to a finite number n of degrees-of-freedom becomes mandatory. All m response quantities controlling the reliability can then be expressed as the n selected degrees-of-freedom, and the reliability problem can be mapped into the n-dimensional sample space of the system degrees-of-freedom. Hence, the reliability problem can always be formulated so that m is equal to n. However, if from an engineering judgement it can be decided that the structural reliability can be checked with sufficient accuracy in a few hot-spots m, where $m < n$, it can be advantageous to formulate the reliability problem directly in the sample space of these responses. Both formulations will be applied in the thesis.

The dynamic loads, initial values as well as the mathematical models applied for deriving the responses are generally assumed to be uncertain and will be modelled stochastically. However, modelling uncertainty will only be attributed to imperfect knowledge of the structural parameters such as mass, damping and stiffness parameters. Hence, it is assumed that if these parameters are property calibrated, the selected mathematical dynamic model provides a perfect causal relationship between the loads and the response of the structure to these loads. The uncertainty due to imperfectly known distributed or discrete system parameters is modelled by means of random fields and stochastic variables.

The thesis deals partly with the stochastic response problem, i.e. the determination of the stochastic properties of the process $\{\mathbf{X}(t),\, t \in [t_0, \infty[\}$ measuring the response of the structure, and partly with the solution of the related reliability problem, i.e. the determination of the probability that the structure is able to sustain the dynamic loads in a prescribed time interval $[t_0, t]$, with due consideration to possible uncertain structural parameters and initial values. The contents are primarily a compilation of some 39 papers specified in the list of references on response and reliability analysis of dynamically excited systems, which have been published by the author alone or together with my good friends during the years 1980-82 and 1986-1994. As is the case with a deterministic vibration analysis, any stochastic vibration analysis has no engineering interest in itself. In any case, the result of the stochastic analysis must be incorporated in a reliability measure from which decisions can be made on the acceptance or decline of a certain structural draft proposal or of a partly damaged existing building, which has been exposed to excessive dynamic loads.

Generally, throughout the outline, calligraphic letters signify sets in a sigma-algebra generated on the space Ω. The range of these sets in the sample space of $\mathbf{X}(t)$, deter-

mined by the mapping $\mathbf{X}(t) : \Omega \rightarrow R^m$, are designated by capital letters. It is then assumed that the sample space of $\mathbf{X}(t)$ at any time t can be separated in two disjoint sets, specifying safe and failure conditions of the structure at the time t. The surface ∂S_t of the safe set S_t is considered to be a part of the failure set, S_t^c. The event of safe operation at the time t is given by $\mathcal{S}_t = \{\omega \in \Omega \mid \mathbf{X}(t,\omega) \in S_t\}$.

2. INTEGRAL EQUATION METHODS

2.1 Introduction to integral equation methods

$\mathcal{C}_{]t,t+\Delta t]}$ signifies the events of one in- or out-crossing from the safe domain in the interval $]t, t+\Delta t]$. Correspondingly, $\mathcal{C}^+_{]t,t+\Delta t]}$ and $\mathcal{C}^-_{]t,t+\Delta t]}$ signify the event of one out-crossing from the safe domain and one in-crossing into the safe domain during the interval $]t, t+\Delta t]$. The event of measure 0 that a crossing takes place at the time t, is designated $\mathcal{C}_t$. Correspondingly, the events of an out-crossing from the safe domain or an in-crossing into the safe domain at the time t are designated $\mathcal{C}^+_t$ or $\mathcal{C}^-_t$, respectively. It is assumed that the process and the failure surface are sufficiently regular so that the following relation holds for the probability of $\mathcal{C}_{]t,t+\Delta t]}$

$$P\big(\mathcal{C}_{]t,t+\Delta t]}\big) = f_1(t)\Delta t + \mathrm{O}\big(\Delta t^2\big) \qquad (2-1)$$

The applied order notation means that $\mathrm{O}\big(g(t)\big) \leq A \mid g(t) \mid$, A being a positive constant. The density function $f_1 : [t_0, \infty[\rightarrow R_+$ is termed the first order crossing rate. Due to the regularity properties of the process and the failure surface, $f_1(t)$ may alternatively be interpreted as the expected number of out-crossings per unit of time. Next, consider the non-overlap intervals $]t_1, t_1+\Delta t_1], \ldots,]t_n, t_n+\Delta t_n]$. It is then assumed that the probability of the event $\mathcal{C}_{]t_1,t_1+\Delta t_1]} \cap \cdots \cap \mathcal{C}_{]t_n,t_n+\Delta t_n]}$ can be written

$$P\big(\mathcal{C}_{]t_1,t_1+\Delta t_1]} \cap \cdots \cap \mathcal{C}_{]t_n,t_n+\Delta t_n]}\big) =$$

$$f_n(t_1, \ldots, t_n)\Delta t_1 \cdots \Delta t_n + \mathrm{O}\big((\Delta t_{\max})^{n+1}\big) \qquad (2-2)$$

where $\Delta t_{\max} = \max(\Delta t_1, \ldots, \Delta t_n)$. $f_n(t_1, \ldots, t_n)$ is termed the nth order crossing rate. From (2-2) it follows that $f_n(t_1, \ldots, t_n)$ fulfils the symmetry property

$$f_n(t_1, \ldots, t_n) = f_n(t_{\alpha_1}, \ldots, t_{\alpha_n}) \qquad (2-3)$$

where $\alpha_1, \ldots, \alpha_n$ is an arbitrary permutation of $1, \ldots, n$. If the crossing events $\mathcal{C}_{]t_1,t_1+\Delta t_1]}, \cdots, \mathcal{C}_{]t_n,t_n+\Delta t_n]}$ are mutually independent, it then follows from (2-1) and (2-2) that

$$f_n(t_1, \ldots, t_n) = \prod_{j=1}^{n} f_1(t_j) \qquad (2-4)$$

Occasionally, crossings of sample curves on condition of some event $\mathcal{E}$ will be considered. As an example one may have $\mathcal{E} = \mathcal{S}_{t_0}$, corresponding to the event of being in the safe domain at the time t_0. The probability of the event $\mathcal{C}_{]t_1,t_1+\Delta t_1]} \cap \cdots \cap \mathcal{C}_{]t_n,t_n+\Delta t_n]}$ on condition of $\mathcal{E}$ can then be written

$$P\big(\mathcal{C}_{]t_1,t_1+\Delta t_1]} \cap \cdots \cap \mathcal{C}_{]t_n,t_n+\Delta t_n]} \mid \mathcal{E}\big) =$$

$$f_n(t_1,\dots,t_n \mid \mathcal{E})\Delta t_1 \cdots \Delta t_n + \mathrm{O}\big((\Delta t_{\max})^{n+1}\big) \qquad (2-5)$$

$f_n(t_1,\dots,t_n \mid \mathcal{E})$ is termed the nth order crossing rate on condition of $\mathcal{E}$. Next, sequences of out- and in-crossings will be considered. Depending on the sequence of crossings, the corresponding nth order crossing rates are defined as follows

$$P\big(\mathcal{C}^+_{]t_1,t_1+\Delta t_1]} \cap \mathcal{C}^-_{]t_2,t_2+\Delta t_2]} \cap \cdots \cap \mathcal{C}^+_{]t_n,t_n+\Delta t_n]} \mid \mathcal{E}\big) =$$

$$f_n^{+-\cdots+}(t_1,t_2,\dots,t_n \mid \mathcal{E})\Delta t_1 \cdots \Delta t_n + \mathrm{O}\big((\Delta t_{\max})^{n+1}\big) \qquad (2-6)$$

$f_n^{+-\cdots+}(t_1,t_2,\dots,t_n \mid \mathcal{E})$ is the nth order crossing rate with an out-crossing at the time t_1, an in-crossing at the time $t_2,\dots$, and an out-crossing at the time t_n. In the applied notation, the sequence of out- and in-crossings is indicated by superscripts "$+$" and "$-$", taking place at the corresponding sequential instants of times, as specified explicitly in the argument list. Because of (2-3) it will be assumed in the following that $t_1 < t_2 < \cdots < t_n$. Especially, crossings on condition of $\mathcal{C}_t^+$ and $\mathcal{C}_t^-$ will be considered. The conditioning on these events is everywhere interpreted in the horizontal window sense of Kac and Slepian (1959). As an example one has the relations

$$f_n^{-\cdots-}(t_1,t_2,\dots,t_n \mid \mathcal{C}_t^+) = \frac{f_{n+1}^{-\cdots-+}(t_1,t_2,\dots,t_n,t)}{f_1^+(t)} \qquad (2-7)$$

$$f_n^{+\cdots+}(t_1,t_2,\dots,t_n \mid \mathcal{E} \cap \mathcal{C}_t^+) = \frac{f_{n+1}^{+\cdots++}(t_1,t_2,\dots,t_n,t \mid \mathcal{E})}{f_1^+(t \mid \mathcal{E})} \qquad (2-8)$$

Correspondingly, the probability of the joint event $\mathcal{C}^+_{]t_1,t_1+\Delta t_1]} \cap \mathcal{C}^-_{]t_2,t_2+\Delta t_2]} \cap \cdots \cap \mathcal{C}^+_{]t_n,t_n+\Delta t_n]} \cap \mathcal{E}$ defines an nth order crossing rate denoted $f_n^{+-\cdots+}(t_1,t_2,\dots,t_n\ ;\ \mathcal{E})$, where

$$f_n^{+-\cdots+}(t_1,t_2,\dots,t_n\ ;\ \mathcal{E}) = f_n^{+-\cdots+}(t_1,t_2,\dots,t_n \mid \mathcal{E})\,P(\mathcal{E}) \qquad (2-9)$$

Let $\mathcal{E}_{t_0} \subseteq \mathcal{S}_{t_0}$ be the event that a subset of initial values $\mathbf{X}(t_0)$ of the process belongs to the safe domain S_{t_0}. Further, let $\mathcal{E}_{]t_0,t]} = \bigcap_{\tau\in]t_0,t]} \mathcal{S}_\tau$. We are interested in the probability rate of the first-passage out-crossings of samples originating in $\mathcal{E}_{t_0}$. Two kinds of first-passage problems will be addressed. In the so-called stochastic start problem initial values beyond S_{t_0} may exist. In this case we define $\mathcal{E}_{t_0} = \mathcal{S}_{t_0}$. The other case considered is the so-called deterministic start problem, where almost all sample curves of the process are assumed to initiate from a single point in the safe domain at the time t_0, i.e. $P(\mathcal{E}_{t_0}) = 1$. The event that a first-passage out-crossing from the safe domain takes place in the time interval $]t, t+\Delta t]$ is designated $\mathcal{F}^{(1)}_{]t,t+\Delta t]}$. The event of measure 0

that a first-passage out-crossing takes place at the time t is correspondingly designated $\mathcal{F}_t^{(1)}$. The following relation is assumed to hold for the probability of $\mathcal{F}_{]t,t+\Delta t]}^{(1)}$

$$P(\mathcal{F}_{]t,t+\Delta t]}^{(1)}) = f_{T_1}(t \mid \mathcal{E}_{t_0})\Delta t + \mathrm{O}(\Delta t^2) \qquad (2-10)$$

$f_{T_1}(t \mid \mathcal{E}_{t_0})$ indicates the probability density function of the elapsed random first-passage time interval T_1, until a first out-crossing takes place at the time $t_0 + T_1$. This quantity, which is designated the first-passage time probability density function, can then be defined by the following conditional out-crossing rate at the time t

$$f_{T_1}(t \mid \mathcal{E}_{t_0}) = f_1^+(t\ ;\ \mathcal{E}_{]t_0,t]} \mid \mathcal{E}_{t_0}) \qquad (2-11)$$

The first-passage time probability distribution function is defined from

$$F_{T_1}(t \mid \mathcal{E}_{t_0}) = \int_{t_0}^{t} f_{T_1}(\tau \mid \mathcal{E}_{t_0})\, d\tau \qquad (2-12)$$

$F_{T_1}(t \mid \mathcal{E}_{t_0})$ signifies the probability of failure (at least one out-crossing) in the interval $]t_0, t]$ on condition of the event of being in the safe domain at the time $t_0, \mathcal{E}_{t_0}$. The unconditional probability of failure in the interval $[t_0, t]$ can then be written

$$P_f([t_0, t]) = 1 - P(\mathcal{E}_{t_0}) + P(\mathcal{E}_{t_0})\ F_{T_1}(t \mid \mathcal{E}_{t_0}) \qquad (2-13)$$

In the stochastic start problem $1 - P(\mathcal{E}_{t_0})$ represents the probability of instantaneous failure at the time t_0, i.e. the probability that the system initiates from the unsafe domain. The event that one out-crossing from the safe domain takes place in the time interval $]t, t + \Delta t]$ on condition of the event $\mathcal{E}_{[t_0,t]} = \bigcap_{\tau \in [t_0,t]} \mathcal{S}_\tau$, corresponding to survival of the system up to and including the time t, is designated $\mathcal{H}_{]t,t+\Delta t]}^{(1)}$. The following relation is assumed to hold for the probability of $\mathcal{H}_{]t,t+\Delta t]}^{(1)}$

$$P(\mathcal{H}_{]t,t+\Delta t]}^{(1)}) = h_{T_1}(t \mid \mathcal{E}_{t_0})\Delta t + \mathrm{O}(\Delta t^2) \qquad (2-14)$$

$h_{T_1}(t \mid \mathcal{E}_{t_0})$ is termed the hazard rate for the first out-crossing. This is related to the first-passage probability density function as follows

$$h_{T_1}(t \mid \mathcal{E}_{t_0}) = f_1^+(t \mid \mathcal{E}_{[t_0,t]}) = \frac{f_1^+(t\ ;\ \mathcal{E}_{]t_0,t]} \mid \mathcal{E}_{t_0})}{P(\mathcal{E}_{]t_0,t]} \mid \mathcal{E}_{t_0})} = \frac{f_{T_1}(t \mid \mathcal{E}_{t_0})}{1 - F_{T_1}(t \mid \mathcal{E}_{t_0})} \qquad (2-15)$$

Then,

$$F_{T_1}(t \mid \mathcal{E}_{t_0}) = 1 - \exp\left(-\int_{t_0}^{t} h_{T_1}(\tau \mid \mathcal{E}_{t_0})\, d\tau\right) \qquad (2-16)$$

Hence, (2-13) can be written

$$P_f([t_0,t]) = 1 - P(\mathcal{E}_{t_0})\ \exp\left(-\int_{t_0}^{t} h_{T_1}(\tau \mid \mathcal{E}_{t_0})\,d\tau\right) \qquad (2-17)$$

L_t^- signifies the interval length spent in the safe domain after an in-crossing to the safe domain at the time t. Correspondingly, L_t^+ signifies the interval length spent in the safe domain before an out-crossing at the time t. The probability density functions of L_t^- and L_t^+ fulfil

$$f_{L_t^-}(l) = \frac{f_2^{-+}(t,t+l\ ;\ \mathcal{E}_{]t,t+l[})}{f_1^-(t)} \qquad (2-18)$$

$$f_{L_t^+}(l) = \frac{f_2^{-+}(t-l,t\ ;\ \mathcal{E}_{]t-l,t[})}{f_1^+(t)} \qquad (2-19)$$

Hence, we have the relation

$$f_{L_t^-}(l) = f_{L_{t+l}^+}(l)\ \frac{f_1^+(t+l)}{f_1^-(t)} \qquad (2-20)$$

U_t^- signifies the elapsed time interval until the next out-crossing after an out-crossing from the safe domain at the time t. Correspondingly, U_t^+ signifies the time interval between an out-crossing at the time t and the previous out-crossing. The probability density functions of U_t^- and U_t^+ on condition of $\mathcal{E}_{t_0}$ fulfil

$$f_{U_t^-}(l \mid \mathcal{E}_{t_0}) = \frac{f_2^{++}(t,t+l\ ;\ \{\text{exactly one in-crossing in }]t,t+l[\} \mid \mathcal{E}_{t_0})}{f_1^+(t \mid \mathcal{E}_{t_0})} \qquad (2-21)$$

$$f_{U_t^+}(l \mid \mathcal{E}_{t_0}) = \frac{f_2^{++}(t-l,t\ ;\ \{\text{exactly one in-crossing in }]t-l,t[\} \mid \mathcal{E}_{t_0})}{f_1^+(t \mid \mathcal{E}_{t_0})} \qquad (2-22)$$

leading to the relation

$$f_{U_t^-}(l \mid \mathcal{E}_{t_0}) = f_{U_{t+l}^+}(l \mid \mathcal{E}_{t_0})\ \frac{f_1^+(t+l \mid \mathcal{E}_{t_0})}{f_1^+(t \mid \mathcal{E}_{t_0})} \qquad (2-23)$$

Among the first-passage out-crossings in the interval $]t, t+\Delta t[$, we shall next draw attention to the subset of sample curves, which have additional out-crossings at the instants of times $t_1 < \cdots < t_n$ later than the time t. The corresponding first-passage probability density function at the time t on condition of later joint out-crossings at the times $t_1 < \cdots < t_n$ is designated $f_{T_1}(t \mid \mathcal{E}_{t_0} \cap C_{t_1}^+ \cap \cdots \cap C_{t_n}^+)$, $t_0 < t < t_1 < \cdots < t_n$.

Similarly, we introduce the probability density function of L_t^+ on condition of prior joint in-crossings to the safe domain at the times $t_1 < t_2 < \cdots < t_n$ before the last in-crossing at the time $t-l$, which is designated $f_{L_t^+}(l \mid \mathcal{C}_{t_1}^- \cap \cdots \cap \mathcal{C}_{t_n}^-)$, $t_0 < t_1 < \cdots < t_n < t-l < t$, and the probability density function of U_t^+ on condition of $\mathcal{E}_{t_0}$ and on condition of prior out-crossings from the safe domain at the times $t_1 < t_2 < \cdots < t_n$ before the last out-crossing at the time $t-l$, which is designated $f_{U_t^+}(l \mid \mathcal{E}_{t_0} \cap \mathcal{C}_{t_1}^+ \cap \cdots \cap \mathcal{C}_{t_n}^+)$, $t_0 < t_1 < \cdots < t_n < t-l < t$.

The event that the process makes its nth out-crossing in the time interval $]t, t+\Delta t]$ on condition of $\mathcal{E}_{t_0}$ is designated $\mathcal{F}_{]t,t+\Delta t]}^{(n)}$. The following relation is assumed for the probability of $\mathcal{F}_{]t,t+\Delta t]}^{(n)}$

$$P\big(\mathcal{F}_{]t,t+\Delta t]}^{(n)}\big) = f_{T_n}(t \mid \mathcal{E}_{t_0})\Delta t + O(\Delta t^2) \qquad (2-24)$$

$f_{T_n}(t \mid \mathcal{E}_{t_0})$ indicates the probability density function of the elapsed random nth-passage time interval T_n.

Let $\mathcal{E}_{]t_0,t]}^{(n)}$ signify the event that at least n out-crossings from the safe domain take place during the interval $]t_0, t]$ on condition of sample curves originating from S_{t_0}. Obviously, $P\big(\mathcal{E}_{]t_0,t]}^{(n)}\big) = P(T_n > t) = 1 - F_{T_n}(t \mid \mathcal{E}_{t_0})$. The event that one out-crossing from the safe domain takes place in the interval $]t, t+\Delta t]$ on condition of $\mathcal{E}_{]t_0,t]}^{(n)}$ is designated $\mathcal{H}_{]t,t+\Delta t]}^{(n)}$, for which the following probability is assumed

$$P\big(\mathcal{H}_{]t,t+\Delta t]}^{(n)}\big) = h_{T_n}(t \mid \mathcal{E}_{t_0})\Delta t + O(\Delta t^2) \qquad (2-25)$$

$h_{T_n}(t \mid \mathcal{E}_{t_0})$ signifies the hazard rate for the nth out-crossing event. Obviously,

$$P\big(\mathcal{E}_{]t_0,t+\Delta t]}^{(n)}\big) = \Big(1 - P\big(\mathcal{H}_{]t,t+\Delta t]}^{(n)}\big)\Big)P\big(\mathcal{E}_{]t_0,t]}^{(n)}\big) + P\big(\mathcal{H}_{]t,t+\Delta t]}^{(n-1)}\big)P\big(\mathcal{E}_{]t_0,t]}^{(n-1)}\big) \Rightarrow$$

$$1 - F_{T_n}(t+\Delta t \mid \mathcal{E}_{t_0}) = \Big(1 - h_{T_n}(t \mid \mathcal{E}_{t_0})\Delta t\Big)\Big(1 - F_{T_n}(t \mid \mathcal{E}_{t_0})\Big) +$$

$$h_{T_{n-1}}(t \mid \mathcal{E}_{t_0})\Delta t\Big(1 - F_{T_{n-1}}(t \mid \mathcal{E}_{t_0})\Big) \Rightarrow$$

$$\frac{d}{dt}F_{T_n}(t \mid \mathcal{E}_{t_0}) = f_{T_n}(t \mid \mathcal{E}_{t_0}) =$$

$$h_{T_n}(t \mid \mathcal{E}_{t_0})\Big(1 - F_{T_n}(t \mid \mathcal{E}_{t_0})\Big) - h_{T_{n-1}}(t \mid \mathcal{E}_{t_0})\Big(1 - F_{T_{n-1}}(t \mid \mathcal{E}_{t_0})\Big),\ n = 2, 3, \ldots \quad (2-26)$$

where $F_{T_n}(t \mid \mathcal{E}_{t_0})$ indicates the nth-passage time distribution function. The solution of (2-26) can be written recursively as follows

$$F_{T_n}(t \mid \mathcal{E}_{t_0}) = 1 - \exp\left(-\int_{t_0}^{t} h_{T_n}(\tau \mid \mathcal{E}_{t_0})\, d\tau\right).$$

$$\left(1+\int_{t_0}^{t}\exp\Big(\int_{t_0}^{\tau}h_{T_n}(u\,|\,\mathcal{E}_{t_0})du\Big)h_{T_{n-1}}(\tau\,|\,\mathcal{E}_{t_0})\Big(1-F_{T_{n-1}}(\tau\,|\,\mathcal{E}_{t_0})\Big)d\tau\right)\ ,\ n=2,3,\ldots \quad (2\text{–}27)$$

(2-27) reduces to (2-16) for $n=1$, defining $F_{T_0}(t\mid\mathcal{E}_{t_0})\equiv 1$.

Let $\{N(t), t\in]t_0,\infty[\}$, $\{N^+(t), t\in]t_0,\infty[\}$ and $\{N^-(t), t\in]t_0,\infty[\}$ be regular counting processes, where $N(t)$, $N^+(t)$ and $N^-(t)$ indicate, respectively, the random number of crossings, out-crossings and in-crossings in the interval $]t_0,t]$ on condition of some event $\mathcal{E}$. These counting processes then have the conditional product densities $f_n(t_1,t_2,\ldots,t_n\mid\mathcal{E})$, $f_n^{+\cdots+}(t_1,t_2,\ldots,t_n\mid\mathcal{E})$ and $f_n^{-\cdots-}(t_1,t_2,\ldots,t_n\mid\mathcal{E})$. From the regularity assumptions it follows that

$$E[\Delta N^+(t_1)\Delta N^-(t_2)\cdots\Delta N^+(t_n)\mid\mathcal{E}]=$$

$$f_n^{+-\cdots+}(t_1,\ldots,t_n\mid\mathcal{E})\Delta t_1\cdots\Delta t_n+\mathrm{O}((\Delta t_{\max})^{n+1}) \quad (2-28)$$

where $\Delta N(t)=N(t+\Delta t)-N(t)$ signifies the increment of the counting process during the interval $]t,t+\Delta t]$. At the indicated formulas for the first- and nth passage probabilities then follows the theory of point processes, Srinivasan (1974), Nielsen and Iwankiewicz (1996).

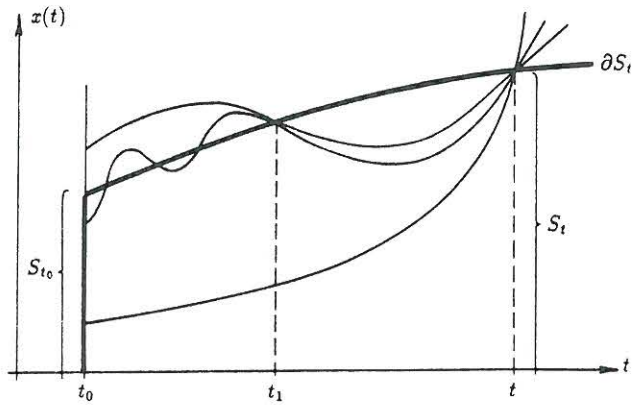

Fig. 2-1: First-passage at the time t and sample curves with last in-crossing to the safe domain at the time t_1 and out-crossing at the time t.

The following identity can be stated, see fig. 2-1.

$$f_{T_1}(t\mid\mathcal{E}_{t_0})P(\mathcal{E}_{t_0})=f_1^+(t)-\int_{t_0}^{t}f_{L_{t_1}^-}(t-t_1)f_1^-(t_1)\,dt_1 \quad (2-29)$$

The last term on the right-hand side of (2-29) withdraws from $f_1^+(t)$ the out-crossing rate of sample curves with their last in-crossing to the safe domain at the time $t_1\in]t_0,t[$,

leaving the out-crossing rate $f_1^+(t\ ;\ \mathcal{E}_{[t_0,t[})$, which is equal to the left-hand side of (2-29). This kind of reasoning will be widely used in the following. From (2-20) it then follows that

$$f_{T_1}(t \mid \mathcal{E}_{t_0}) = \frac{f_1^+(t)}{P(\mathcal{E}_{t_0})} \left(1 - \int_{t_0}^{t} f_{L_t^+}(t - t_1)\, dt_1\right) \qquad (2-30)$$

Assume that $\{\mathbf{X}(t),\ t \in [t_0, \infty)\}$ is a stationary vector process, and that the safe domain is time-invariant. Further, consider the stochastic start problem, i.e. $\mathcal{E}_{t_0} = \mathcal{S}_{t_0}$. L_t^- and L_t^+ are then independent of t, and will be identically distributed as the random variable L with the probability distribution function $F_L(l)$. Further, $f_1^+(t) = f_1^+$ and $P(\mathcal{S}_t)$ become time-constant. (2-30) then reduces to

$$f_{T_1}(t \mid \mathcal{E}_{t_0}) = \frac{f_1^+}{P(\mathcal{S}_{t_0})}(1 - F_L(t - t_0)) = \frac{1}{E[L]}(1 - F_L(t - t_0)) \qquad (2-31)$$

where

$$E[L] = \frac{P(\mathcal{S}_{t_0})}{f_1^+} \qquad (2-32)$$

(2-32) follows from an integration of (2-31) over the interval $]t_0, \infty[$, and using $\lim_{t\to\infty} F_{T_1}(t \mid \mathcal{S}_{t_0}) = 1$.

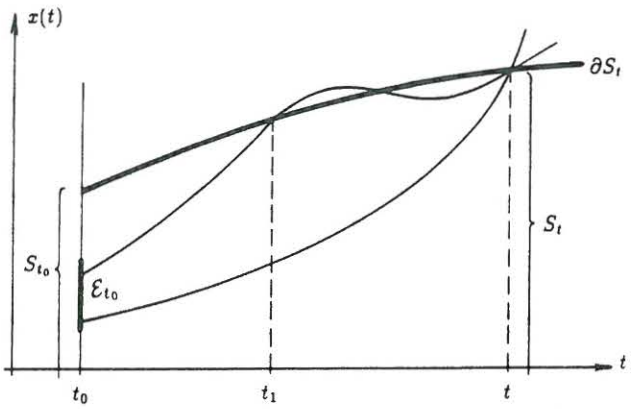

Fig. 2-2: First-passage at the time t and sample curve with last out-crossing from the safe domain at the times t_1 and t on condition of $\mathcal{E}_{t_0}$.

Next, the following identity can be stated, see fig. 2-2.

$$f_{T_1}(t \mid \mathcal{E}_{t_0}) = f_1^+(t \mid \mathcal{E}_{t_0}) - \int_{t_0}^{t} f_{U_{t_1}^-}(t - t_1 \mid \mathcal{E}_{t_0}) f_1^+(t_1 \mid \mathcal{E}_{t_0})\, dt_1 \qquad (2-33)$$

The last term on the right-hand side of (2-33) withdraws from $f_1^+(t \mid \mathcal{E}_{t_0})$ all previous out-crossings conditioned on $\mathcal{E}_{t_0}$ in the interval $]t_0, t[$. Using (2-23) the following relation can then be derived, similar to (2-30), Nielsen and Sørensen (1988)

$$f_{T_1}(t \mid \mathcal{E}_{t_0}) = f_1^+(t \mid \mathcal{E}_{t_0}) \left(1 - \int_{t_0}^{t} f_{U_t^+}(t - t_1 \mid \mathcal{E}_{t_0})\, dt_1 \right) \qquad (2-34)$$

(2-30) and (2-34) expresses $f_{T_1}(t \mid \mathcal{E}_{t_0})$ in terms of the probability density functions of L_t^+ and U_t^+. As will be shown in succeeding sections 2.3 and 2.4, (2-29) and (2-33) turn out to be connected with inclusion-exclusion expansions of $f_{T_1}(t \mid \mathcal{E}_{t_0})$ in unconditioned and conditioned crossing rates, respectively.

A relation similar to (2-31) was first derived by Slepian (1962), considering the probability that a zero mean stationary process remains non-negative in a certain interval. With applications to mechanical reliability problems, (2-31) was rediscovered independently by Cook (1964) and Rice (1964,1966). Concerning Cook's work, see also Crandall et al. (1966). The non-stationary equivalent (2-30) was originally derived by Nielsen and Sørensen (1988) for stochastic start problems of non-stationary processes or time-varying safe domains, based on a proof different from the one applied here. The present formulation provides a further generalization to non-stochastic start problems. (2-31) may be used for estimation of $f_{T_1}(t \mid \mathcal{S}_{t_0})$ by simulation. Assuming sufficient ergodicity, $F_L(l)$ is estimated from a single sample. Robust estimates of $f_{T_1}(t \mid \mathcal{S}_{t_0})$ can then be determined, when $f_{T_1}(0 \mid \mathcal{S}_{t_0}) = 1/E[L] = f_1^+/P(\mathcal{S}_{t_0})$ is either estimated from the simulated sample of interval lengths, Cook (1964), Crandall et al. (1966), or is calculated analytically, Thoft-Christensen and Nielsen (1982), Nielsen and Sørensen (1988), Nielsen (1990a). The latter approach provides exact values of $f_{T_1}(t \mid \mathcal{S}_{t_0})$ at initial first-passage times at the expense that the area below the estimated probability density curve may differ from 1.

2.2 Integral equations for the first-passage time probability density function

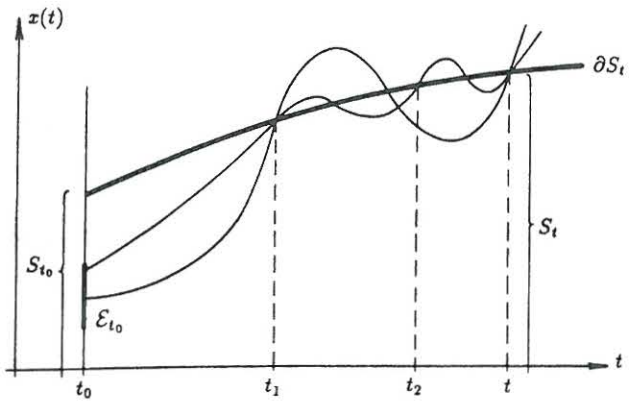

Fig. 2-3: Out-crossing of sample curves at the times t_1, t_2 and t on condition of $\mathcal{E}_{t_0}$.

The following Volterra integral equation may be formulated for the first-passage time probability density function, Nielsen (1980)

$$f_{T_1}(t \mid \mathcal{E}_{t_0}) = f_1^+(t \mid \mathcal{E}_{t_0}) - \int_{t_0}^{t} f_1^+\left(t \mid \mathcal{E}_{t_0} \cap \mathcal{F}_{t_1}^{(1)}\right) f_{T_1}(t_1 \mid \mathcal{E}_{t_0})\, dt_1 \qquad (2-35)$$

$f_1^+\left(t \mid \mathcal{E}_{t_0} \cap \mathcal{F}_{t_1}^{(1)}\right)$ indicates the out-crossing rate at the time t on condition of $\mathcal{E}_{t_0}$ and on condition of a prior first-passage at the time $t_1 \in]t_0, t[$, see fig. 2-3. $f_1^+\left(t \mid \mathcal{E}_{t_0} \cap \mathcal{F}_{t_1}^{(1)}\right) f_{T_1}(t_1 \mid \mathcal{E}_{t_0})$ represents the joint probability density of a first-passage at the time t_1 and an out-crossing from S_t on condition of $\mathcal{E}_{t_0}$, where $t_0 < t_1 < t$. For this quantity the following identity holds

$$f_1^+\left(t \mid \mathcal{E}_{t_0} \cap \mathcal{F}_{t_1}^{(1)}\right) f_{T_1}(t_1 \mid \mathcal{E}_{t_0}) = f_{T_1}\left(t_1 \mid \mathcal{E}_{t_0} \cap \mathcal{C}_t^+\right) f_1^+(t \mid \mathcal{E}_{t_0}) \qquad (2-36)$$

From (2-35) and (2-36) the following relation is then obtained

$$f_{T_1}(t \mid \mathcal{E}_{t_0}) = f_1^+(t \mid \mathcal{E}_{t_0}) \left(1 - \int_{t_0}^{t} f_{T_1}\left(t_1 \mid \mathcal{E}_{t_0} \cap \mathcal{C}_t^+\right) dt_1\right) \qquad (2-37)$$

Upon comparison of (2-34) and (2-37) it should be noticed that $f_{U_t^+}(t - t_1 \mid \mathcal{E}_{t_0}) \neq f_{T_1}(t_1 \mid \mathcal{E}_{t_0} \cap \mathcal{C}_t^+)$. Only the integral of these quantities is equal. $f_1^+\left(t \mid \mathcal{E}_{t_0} \cap \mathcal{F}_{t_1}^{(1)}\right) f_{T_1}(t_1 \mid \mathcal{E}_{t_0})$ fulfils the integral equation

$$f_1^+\left(t \mid \mathcal{E}_{t_0} \cap \mathcal{F}_{t_1}^{(1)}\right) f_{T_1}(t_1 \mid \mathcal{E}_{t_0}) =$$

$$f_2^{++}(t_1,t \mid \mathcal{E}_{t_0}) - \int_{t_0}^{t_1} f_2^{++}(t_1,t \mid \mathcal{E}_{t_0} \cap \mathcal{F}_{t_2}^{(1)}) f_{T_1}(t_2 \mid \mathcal{E}_{t_0})\, dt_2\ ,\ t_0 < t_1 < t \qquad (2-38)$$

$f_2^{++}(t_1,t \mid \mathcal{E}_{t_0} \cap \mathcal{F}_{t_2}^{(1)}) f_{T_1}(t_2 \mid \mathcal{E}_{t_0})$ signifies the joint probability density of a first-passage at the time t_2 and out-crossings from S_{t_1} and S_t on condition of $\mathcal{E}_{t_0}$, where $t_0 < t_2 < t_1 < t$. For this quantity the following identity holds

$$f_2^{++}(t_1,t \mid \mathcal{E}_{t_0} \cap \mathcal{F}_{t_2}^{(1)}) f_{T_1}(t_2 \mid \mathcal{E}_{t_0}) = f_{T_1}(t_2 \mid \mathcal{E}_{t_0} \cap \mathcal{C}_{t_1}^{+} \cap \mathcal{C}_t^{+}) f_2^{++}(t_1,t \mid \mathcal{E}_{t_0}) \qquad (2-39)$$

From (2-35), (2-38) and (2-39) it then follows that

$$f_{T_1}(t \mid \mathcal{E}_{t_0}) = f_1^{+}(t \mid \mathcal{E}_{t_0}) -$$

$$\int_{t_0}^{t} f_2^{++}(t_1,t \mid \mathcal{E}_{t_0}) \left(1 - \int_{t_0}^{t_1} f_{T_1}(t_2 \mid \mathcal{E}_{t_0} \cap \mathcal{C}_{t_1}^{+} \cap \mathcal{C}_t^{+})\, dt_2\right) dt_1 \qquad (2-40)$$

$$f_{T_1}(t \mid \mathcal{E}_{t_0}) = f_1^{+}(t \mid \mathcal{E}_{t_0}) -$$

$$\int_{t_0}^{t} f_2^{++}(t_1,t \mid \mathcal{E}_{t_0})\, dt_1 + \int_{t_0}^{t}\int_{t_0}^{t_1} f_2^{++}(t_1,t \mid \mathcal{E}_{t_0} \cap \mathcal{F}_{t_2}^{(1)}) f_{T_1}(t_2 \mid \mathcal{E}_{t_0})\, dt_2 dt_1 \qquad (2-41)$$

Next, an integral equation similar to (2-38) and a relation similar to (2-36) can be formulated for $f_2^{++}(t_1,t \mid \mathcal{E}_{t_0} \cap \mathcal{F}_{t_2}^{(1)}) f_{T_1}(t_2 \mid \mathcal{E}_{t_0})$, which is substituted into the right-hand sides of (2-38) and (2-41). Continuation of this process until the nth term leads to the following results

$$f_{T_1}(t \mid \mathcal{E}_{t_0}) = f_1^{+}(t \mid \mathcal{E}_{t_0}) - \int_{t_0}^{t} f_2^{++}(t_1,t \mid \mathcal{E}_{t_0})\, dt_1 + \cdots +$$

$$(-1)^{n-1} \int_{t_0}^{t}\int_{t_0}^{t_1} \cdots \int_{t_0}^{t_{n-2}} f_n^{+\cdots+++}(t_{n-1},\ldots,t_2,t_1,t \mid \mathcal{E}_{t_0}) \cdot$$

$$\left(1 - \int_{t_0}^{t_{n-1}} f_{T_1}(t_n \mid \mathcal{E}_{t_0} \cap \mathcal{C}_{t_{n-1}}^{+} \cap \cdots \cap \mathcal{C}_{t_2}^{+} \cap \mathcal{C}_{t_1}^{+} \cap \mathcal{C}_t^{+})\, dt_n\right) dt_{n-1} \cdots dt_2 dt_1 \qquad (2-42)$$

$$f_{T_1}(t \mid \mathcal{E}_{t_0}) = f_1^{+}(t \mid \mathcal{E}_{t_0}) - \int_{t_0}^{t} f_2^{++}(t_1,t \mid \mathcal{E}_{t_0})\, dt_1 + \cdots +$$

$$(-1)^{n-1}\int_{t_0}^{t}\int_{t_0}^{t_1}\cdots\int_{t_0}^{t_{n-2}} f_n^{+\cdots+++}(t_{n-1},\ldots,t_2,t_1,t\mid\mathcal{E}_{t_0})\,dt_{n-1}\cdots dt_2 dt_1 +$$

$$(-1)^{n}\int_{t_0}^{t}\int_{t_0}^{t_1}\cdots\int_{t_0}^{t_{n-1}} f_n^{+\cdots+++}(t_{n-1},\ldots,t_2,t_1,t\mid\mathcal{E}_{t_0}\cap\mathcal{F}_{t_n}^{(1)})f_{T_1}(t_n\mid\mathcal{E}_{t_0})\,dt_n\cdots dt_2 dt_1 \quad (2-43)$$

and

$$f_1^{+}\big(t\mid\mathcal{E}_{t_0}\cap\mathcal{F}_{t_1}^{(1)}\big)f_{T_1}(t_1\mid\mathcal{E}_{t_0}) = f_2^{++}(t_1,t\mid\mathcal{E}_{t_0}) - \int_{t_0}^{t_1} f_3^{+++}(t_2,t_1,t\mid\mathcal{E}_{t_0})\,dt_2 + \cdots +$$

$$(-1)^{n}\int_{t_0}^{t_1}\cdots\int_{t_0}^{t_{n-2}} f_n^{+\cdots+++}(t_{n-1},\ldots,t_2,t_1,t\mid\mathcal{E}_{t_0})\cdot$$

$$\left(1-\int_{t_0}^{t_{n-1}} f_{T_1}\big(t_n\mid\mathcal{E}_{t_0}\cap\mathcal{C}_{t_{n-1}}^{+}\cap\cdots\cap\mathcal{C}_{t_1}^{+}\cap\mathcal{C}_{t}^{+}\big)\,dt_n\right)\,dt_{n-1}\cdots dt_2 \qquad (2-44)$$

The following quantity is introduced

$$F_{n,j}^{+}(t_n,\ldots,t_1\mid\mathcal{E}_{t_0}) =$$

$$\begin{cases} f_n^{+}(t_n,\ldots,t_1\mid\mathcal{E}_{t_0}) & ,\ j=0 \\ \int_{t_0}^{t_n}\cdots\int_{t_0}^{t_{n+j-1}} f_{n+j}^{+\cdots++\cdots+}(t_{n+j},\ldots,t_{n+1},t_n,\ldots,t_1\mid\mathcal{E}_{t_0})\,dt_{n+j}\cdots dt_{n+1} & ,\ j\geq 1 \end{cases} \qquad (2-45)$$

From (2-42) and (2-44) the following formal expansion for the kernel $f_1^{+}\big(t\mid\mathcal{E}_{t_0}\cap\mathcal{F}_{t_1}^{(1)}\big)$ of the integral equation (2-35) is obtained as $n\to\infty$

$$f_1^{+}(t\mid\mathcal{E}_{t_0}\cap\mathcal{F}_{t_1}^{(1)}) = \frac{f_2^{++}(t_1,t\mid\mathcal{E}_{t_0}) - \int_{t_0}^{t_1} f_3^{+++}(t_2,t_1,t\mid\mathcal{E}_{t_0})\,dt_2+\cdots}{f_1^{+}(t_1\mid\mathcal{E}_{t_0}) - \int_{t_0}^{t_1} f_2^{++}(t_2,t_1\mid\mathcal{E}_{t_0})\,dt_2+\cdots} =$$

$$\frac{\sum_{j=0}^{\infty}(-1)^j F_{2,j}^{+}(t_1,t\mid\mathcal{E}_{t_0})}{\sum_{j=0}^{\infty}(-1)^j F_{1,j}^{+}(t_1\mid\mathcal{E}_{t_0})} \qquad (2-46)$$

For the kernel in the integral equation (2-43) the formal expansion becomes

$$f_n^{+\cdots++}(t_{n-1},\ldots,t_1,t \mid \mathcal{E}_{t_0} \cap \mathcal{F}_{t_n}^{(1)}) =$$

$$\frac{f_{n+1}^{++\cdots++}(t_n,t_{n-1},\ldots,t_1,t \mid \mathcal{E}_{t_0}) - \int_{t_0}^{t_n} f_{n+2}^{+++\cdots++}(t_{n+1},t_n,t_{n-1},\ldots,t_1,t \mid \mathcal{E}_{t_0})\,dt_{n+1} + \cdots}{f_1^{+}(t_n \mid \mathcal{E}_{t_0}) - \int_{t_0}^{t_n} f_2^{++}(t_{n+1},t_n \mid \mathcal{E}_{t_0})dt_{n+1} + \cdots} =$$

$$\frac{\sum_{j=0}^{\infty}(-1)^j F_{n+1,j}^{+}(t_n,t_{n-1},\ldots,t_1,t \mid \mathcal{E}_{t_0})}{\sum_{j=0}^{\infty}(-1)^j F_{1,j}^{+}(t_n \mid \mathcal{E}_{t_0})} \qquad (2-47)$$

The conditioned first-passage time probability density function $f_{T_1}\left(t_1 \mid \mathcal{E}_{t_0} \cap \mathcal{C}_t^{+}\right)$, $t_0 < t_1 < t$ on the right-hand side of (2-37) fulfils the integral equation, Nielsen (1990a)

$$f_{T_1}(t_1 \mid \mathcal{E}_{t_0} \cap \mathcal{C}_t^{+}) = f_1^{+}(t_1 \mid \mathcal{E}_{t_0} \cap \mathcal{C}_t^{+}) - \int_{t_0}^{t_1} f_1^{+}(t_1 \mid \mathcal{E}_{t_0} \cap \mathcal{F}_{t_2}^{(1)} \cap \mathcal{C}_t^{+}) f_{T_1}(t_2 \mid \mathcal{E}_{t_0} \cap \mathcal{C}_t^{+})\,dt_2 \qquad (2-48)$$

where

$$f_1^{+}(t_1 \mid \mathcal{E}_{t_0} \cap \mathcal{C}_t^{+}) = \frac{f_2^{++}(t_1,t \mid \mathcal{E}_{t_0})}{f_1^{+}(t \mid \mathcal{E}_{t_0})} \qquad (2-49)$$

$$f_1^{+}(t_1 \mid \mathcal{E}_{t_0} \cap \mathcal{F}_{t_2}^{(1)} \cap \mathcal{C}_t^{+}) =$$

$$\frac{f_2^{++}(t_2,t_1 \mid \mathcal{E}_{t_0} \cap \mathcal{C}_t^{+}) - \int_{t_0}^{t_2} f_3^{+++}(t_3,t_2,t_1 \mid \mathcal{E}_{t_0} \cap \mathcal{C}_t^{+})\,dt_3 + \cdots}{f_1^{+}(t_2 \mid \mathcal{E}_{t_0} \cap \mathcal{C}_t^{+}) - \int_{t_0}^{t_2} f_2^{++}(t_3,t_2 \mid \mathcal{E}_{t_0} \cap \mathcal{C}_t^{+})\,dt_3 + \cdots} =$$

$$\frac{f_3^{+++}(t_2,t_1,t \mid \mathcal{E}_{t_0}) - \int_{t_0}^{t_2} f_4^{+++}(t_3,t_2,t_1,t \mid \mathcal{E}_{t_0})\,dt_3 + \cdots}{f_2^{++}(t_2,t \mid \mathcal{E}_{t_0}) - \int_{t_0}^{t_2} f_3^{++}(t_3,t_2,t \mid \mathcal{E}_{t_0})\,dt_3 + \cdots} =$$

$$\frac{\sum_{j=0}^{\infty}(-1)^j F_{3,j}^{+}(t_2,t_1,t \mid \mathcal{E}_{t_0})}{\sum_{j=0}^{\infty}(-1)^j F_{2,j}^{+}(t_2,t \mid \mathcal{E}_{t_0})} \qquad (2-50)$$

(2-50) is derived by a procedure identical to the one leading to (2-46). Further, (2-8) has been applied in (2-49) and (2-50).

Similarly, $f_{T_1}\left(t_n \mid \mathcal{E}_{t_0} \cap \mathcal{C}^+_{t_{n-1}} \cap \cdots \cap \mathcal{C}^+_{t_1} \cap \mathcal{C}^+_t\right)$, $t_0 < t_n < t_{n-1} < \cdots < t_1 < t$ in (2-42) fulfils the integral equation

$$f_{T_1}\left(t_n \mid \mathcal{E}_{t_0} \cap \mathcal{C}^+_{t_{n-1}} \cap \cdots \cap \mathcal{C}^+_{t_1} \cap \mathcal{C}^+_t\right) = f_1^+\left(t_n \mid \mathcal{E}_{t_0} \cap \mathcal{C}^+_{t_{n-1}} \cap \cdots \cap \mathcal{C}^+_{t_1} \cap \mathcal{C}^+_t\right) -$$

$$\int_{t_0}^{t_n} f_1^+(t_n \mid \mathcal{E}_{t_0} \cap \mathcal{F}^{(1)}_{t_{n+1}} \cap \mathcal{C}^+_{t_{n-1}} \cap \cdots \cap \mathcal{C}^+_{t_1} \cap \mathcal{C}^+_t) f_{T_1}(t_{n+1} \mid \mathcal{E}_{t_0} \cap \mathcal{C}^+_{t_{n-1}} \cap \cdots \cap \mathcal{C}^+_{t_1} \cap \mathcal{C}^+_t)\, dt_{n+1} \quad (2-51)$$

where

$$f_1^+\left(t_n \mid \mathcal{E}_{t_0} \cap \mathcal{C}^+_{t_{n-1}} \cap \cdots \cap \mathcal{C}^+_{t_1} \cap \mathcal{C}^+_t\right) = \frac{f^{++\cdots++}_{n+1}(t_n, t_{n-1}, \ldots, t_1, t \mid \mathcal{E}_{t_0})}{f^{+\cdots++}_n(t_{n-1}, \ldots, t_1, t \mid \mathcal{E}_{t_0})} \quad (2-52)$$

The following formal expansions are obtained for the conditioned first-passage time probability density function and the kernel of the integral equation (2-51)

$$f_{T_1}\left(t_n \mid \mathcal{E}_{t_0} \cap \mathcal{C}^+_{t_{n-1}} \cap \cdots \cap \mathcal{C}^+_{t_1} \cap \mathcal{C}^+_t\right) = \frac{\sum_{j=0}^{\infty} (-1)^j F^+_{n+1,j}(t_{n+1}, t_{n-1}, \ldots, t_1, t \mid \mathcal{E}_{t_0})}{f^{+\cdots++}_n(t_{n-1}, \ldots, t_1, t \mid \mathcal{E}_{t_0})} \quad (2-53)$$

$$f_1^+\left(t_n \mid \mathcal{E}_{t_0} \cap \mathcal{F}^{(1)}_{t_{n+1}} \cap \mathcal{C}^+_{t_{n-1}} \cap \cdots \cap \mathcal{C}^+_{t_1} \cap \mathcal{C}^+_t\right) =$$

$$\frac{f^{+++\cdots++}_{n+2}(t_{n+1}, t_n, t_{n-1}, \ldots, t_1, t \mid \mathcal{E}_{t_0}) - \int_{t_0}^{t_{n+1}} f^{++++\cdots++}_{n+3}(t_{n+2}, t_{n+1}, t_n, t_{n-1}, \ldots, t_1, t \mid \mathcal{E}_{t_0})\, dt_2 + \cdots}{f^{++\cdots++}_{n+1}(t_{n+1}, t_{n-1}, \ldots, t_1, t \mid \mathcal{E}_{t_0}) - \int_{t_0}^{t_{n+1}} f^{+++\cdots++}_{n+2}(t_{n+2}, t_{n+1}, t_{n-1}, \ldots, t_1, t \mid \mathcal{E}_{t_0})\, dt_{n+2} + \cdots}$$

$$\frac{\sum_{j=0}^{\infty} (-1)^j F^+_{n+2,j}(t_{n+1}, t_n, t_{n-1}, \ldots, t_1, t \mid \mathcal{E}_{t_0})}{\sum_{j=0}^{\infty} (-1)^j F^+_{n+1,j}(t_{n+1}, t_{n-1}, \ldots, t_1, t \mid \mathcal{E}_{t_0})} \quad (2-54)$$

If an approximate solution can be obtained for (2-51), the remainder of the series expansion (2-42) of the first-passage time probability density function can be evaluated approximately.

Next, the following identity can be stated for the nth-passage time probability density function, $n \geq 2$, Nielsen (1980)

$$f_{T_n}(t \mid \mathcal{E}_{t_0}) = f_1^+(t \mid \mathcal{E}_{t_0}) - \sum_{j=1}^{n-1} f_{T_j}(t \mid \mathcal{E}_{t_0}) - \int_{t_0}^{t} f_1^+\left(t \mid \mathcal{E}_{t_0} \cap \mathcal{F}^{(n)}_{t_1}\right) f_{T_n}(t_1 \mid \mathcal{E}_{t_0})\, dt_1 \quad (2-55)$$

The second term on the right-hand side of (2-55) withdraws from $f_1^+(t \mid \mathcal{E}_{t_0})$ the rate of out-crossings at the time t of sample curves which are less than an nth-passage. The last term withdraws the rate of out-crossings of sample curves which have had their nth-passage prior to the time t.

By a sequential procedure for $n = 2, 3, \ldots$ similar to the one applied to (2-35) the following expansions can be derived for $f_{T_n}(t \mid \mathcal{E}_{t_0})$, and for the inhomogenity and kernel of the integral equation (2-55), Nielsen (1980)

$$f_{T_n}(t \mid \mathcal{E}_{t_0}) = \sum_{j=n-1}^{\infty} (-1)^{j-n+1} \binom{j}{n-1} F_{1,j}^+(t \mid \mathcal{E}_{t_0}) \qquad (2-56)$$

$$f_1^+(t \mid \mathcal{E}_{t_0}) - \sum_{j=1}^{n-1} f_{T_j}(t \mid \mathcal{E}_{t_0}) = \sum_{j=n}^{\infty} f_{T_j}(t \mid \mathcal{E}_{t_0}) =$$

$$\sum_{j=n-1}^{\infty} (-1)^{j-n+1} \binom{j-1}{n-2} F_{1,j}^+(t \mid \mathcal{E}_{t_0}) \qquad (2-57)$$

$$f_1^+\left(t \mid \mathcal{E}_{t_0} \cap \mathcal{F}_{t_1}^{(n)}\right) = \frac{\sum_{j=n-1}^{\infty} (-1)^{j-n+1} \binom{j}{n-1} F_{2,j}^+(t_1, t \mid \mathcal{E}_{t_0})}{\sum_{j=n-1}^{\infty} (-1)^{j-n+1} \binom{j}{n-1} F_{1,j}^+(t_1 \mid \mathcal{E}_{t_0})} \qquad (2-58)$$

Consider a discrete index set $T = \{\tau_1, \ldots, \tau_m\}$, $t_0 < \tau_1 < \cdots < \tau_m < t$ and let $\mathcal{E}_{\tau_1,\ldots,\tau_m} = \bigcap_{\tau \in T} \mathcal{S}_\tau$. $f_{T_1}(t \mid \mathcal{E}_{t_0})$ then fulfils the integral equation, Thoft-Christensen and Nielsen (1982)

$$f_{T_1}(t \mid \mathcal{E}_{t_0}) = f_1^+\left(t; \mathcal{E}_{\tau_1,\ldots,\tau_m} \mid \mathcal{E}_{t_0}\right) - \int_{t_0}^{t} f_1^+\left(t; \mathcal{E}_{\tau_1,\ldots,\tau_m} \mid \mathcal{E}_{t_0} \cap \mathcal{F}_{t_1}^{(1)}\right) f_{T_1}(t_1 \mid \mathcal{E}_{t_0})\, dt_1 \qquad (2-59)$$

$f_1^+\left(t; \mathcal{E}_{\tau_1,\ldots,\tau_m} \mid \mathcal{E}_{t_0}\right)$ and $f_1^+\left(t; \mathcal{E}_{\tau_1,\ldots,\tau_m} \mid \mathcal{E}_{t_0} \cap \mathcal{F}_{t_1}^{(1)}\right)$ signify the out-crossing rates at the time t of sample curves in the safe set at the times $\tau_1, \ldots, \tau_m$, respectively, on condition of $\mathcal{E}_{t_0}$ and on condition of a first-passage at the time $t_1 \in]t_0, t[$.

(2-59) is quite similar to (2-35). All previous integral equations can in the same way be formulated in out-crossing rates of sample curves which are in the safe set at times $\tau_1, \ldots, \tau_m$. In doing this all the indicated inclusion-exclusion series remain valid, if the quantity $F_{n,j}^+(t_n, \ldots, t_1 \mid \mathcal{E}_{t_0})$ in (2-42) is calculated based on the conditioned nth order the out-crossing rate $f_{n+j}^{+\cdots+}(t_{n+j}, \ldots, t_{n+1}, t_n, \ldots, t_1 \,;\, \mathcal{E}_{\tau_1,\ldots,\tau_m} \mid \mathcal{E}_{t_0})$. By a suitable choice of the intermediate instants of time $\tau_1, \ldots, \tau_m$, this approach results in more accurate approximate solutions to the various integral equations, and in a more

rapid convergence of the various inclusion-exclusion series. Especially, the following expansions are valid for the solution and for the kernel of the integral equation (2-59)

$$f_{T_1}(t \mid \mathcal{E}_{t_0}) = f_1^+\left(t; \mathcal{E}_{\tau_1,\ldots,\tau_m} \mid \mathcal{E}_{t_0}\right) - \int_{t_0}^{t} f_2^{++}\left(t_1, t; \mathcal{E}_{\tau_1,\ldots,\tau_m} \mid \mathcal{E}_{t_0}\right) dt_1 + \cdots$$

$$(-1)^{n-1} \int_{t_0}^{t}\int_{t_0}^{t_1}\cdots\int_{t_0}^{t_{n-2}} f_n^{+\cdots+++}\left(t_{n-1},\ldots,t_2,t_1,t; \mathcal{E}_{\tau_1,\ldots,\tau_m} \mid \mathcal{E}_{t_0}\right)\cdot$$

$$\left(1 - \int_{t_0}^{t_{n-1}} f_{T_1}\left(t_n \mid \mathcal{E}_{t_0} \cap \mathcal{C}^+_{t_{n-1}} \cap \cdots \cap \mathcal{C}^+_{t_2} \cap \mathcal{C}^+_{t_1} \cap \mathcal{C}^+_t\right) dt_n\right) dt_{n-1}\cdots dt_2 dt_1 \quad (2-60)$$

$$f_1^+\left(t; \mathcal{E}_{\tau_1,\ldots,\tau_m} \mid \mathcal{E}_{t_0} \cap \mathcal{F}^{(1)}_{t_1}\right) =$$

$$\frac{f_2^{++}\left(t_1, t; \mathcal{E}_{\tau_1,\ldots,\tau_m} \mid \mathcal{E}_{t_0}\right) - \int_{t_0}^{t_1} f_3^{+++}\left(t_2, t_1, t; \mathcal{E}_{\tau_1,\ldots,\tau_m} \mid \mathcal{E}_{t_0}\right) dt_2 + \cdots}{f_1^+\left(t_1; \mathcal{E}_{\tau_1,\ldots,\tau_m} \mid \mathcal{E}_{t_0}\right) - \int_{t_0}^{t_1} f_2^{++}\left(t_2, t_1; \mathcal{E}_{\tau_1,\ldots,\tau_m} \mid \mathcal{E}_{t_0}\right) dt_2 + \cdots} \quad (2-61)$$

From (2-15) and (2-45) the following formal expansion is obtained for the failure rate

$$h_{T_1}(t \mid \mathcal{E}_{t_0}) = \frac{\sum_{j=0}^{\infty}(-1)^j F^+_{1,j}(t \mid \mathcal{E}_{t_0})}{1 - \int_{t_0}^{t}\sum_{j=0}^{\infty}(-1)^j F^+_{1,j}(t_1 \mid \mathcal{E}_{t_0})\, dt_1} \quad (2-62)$$

Expanding the nominator in (2-15) and applying the symmetry condition (2-3), the following formal series may be obtained, Stratonovich (1963)

$$h_{T_1}(t \mid \mathcal{E}_{t_0}) = f_{T_1}(t \mid \mathcal{E}_{t_0})\cdot$$

$$\left(1 + \int_{t_0}^{t} f_{T_1}(t_1 \mid \mathcal{E}_{t_0})\, dt_1 + \int_{t_0}^{t}\int_{t_0}^{t} f_{T_1}(t_1 \mid \mathcal{E}_{t_0}) f_{T_1}(t_2 \mid \mathcal{E}_{t_0})\, dt_1 dt_2 + \cdots\right) =$$

$$g_1^+(t \mid \mathcal{E}_{t_0}) - \int_{t_0}^{t} g_2^{++}(t_1, t \mid \mathcal{E}_{t_0})\, dt_1 + \cdots +$$

$$(-1)^{n-1} \int_{t_0}^{t}\int_{t_0}^{t_1}\cdots\int_{t_0}^{t_{n-2}} g_n^{+\cdots+++}(t_{n-1},\ldots,t_2,t_1,t \mid \mathcal{E}_{t_0})\, dt_{n-1}\cdots dt_2 dt_1 \cdots \quad (2-63)$$

where

$$\left.\begin{aligned}
&g_1^+(t \mid \mathcal{E}_{t_0}) = f_1^+(t \mid \mathcal{E}_{t_0}) \\
&g_2^{++}(t_1,t \mid \mathcal{E}_{t_0}) = f_2^{++}(t_1,t \mid \mathcal{E}_{t_0}) - f_1^+(t_1 \mid \mathcal{E}_{t_0}) f_1^+(t \mid \mathcal{E}_{t_0}) \\
&g_3^{+++}(t_2,t_1,t \mid \mathcal{E}_{t_0}) = f_3^{+++}(t_2,t_1,t \mid \mathcal{E}_{t_0}) - 3\{f_2^{++}(t_2,t_1 \mid \mathcal{E}_{t_0}) f_1^+(t \mid \mathcal{E}_{t_0})\}_s + \\
&2 f_1^+(t_2 \mid \mathcal{E}_{t_0}) f_1^+(t_1 \mid \mathcal{E}_{t_0}) f_1^+(t \mid \mathcal{E}_{t_0}) \\
&g_4^{++++}(t_3,t_2,t_1,t \mid \mathcal{E}_{t_0}) = f_4^{++++}(t_3,t_2,t_1,t \mid \mathcal{E}_{t_0}) - \\
&4\{f_3^{+++}(t_3,t_2,t_1 \mid \mathcal{E}_{t_0}) f_1^+(t \mid \mathcal{E}_{t_0})\}_s - 3\{f_2^{++}(t_3,t_2 \mid \mathcal{E}_{t_0}) f_2^{++}(t_1,t \mid \mathcal{E}_{t_0})\}_s + \\
&12\{f_2^{++}(t_3,t_2 \mid \mathcal{E}_{t_0}) f_1^+(t_1 \mid \mathcal{E}_{t_0}) f_1^+(t \mid \mathcal{E}_{t_0})\}_s - \\
&6 f_1^+(t_3 \mid \mathcal{E}_{t_0}) f_1^+(t_2 \mid \mathcal{E}_{t_0}) f_1^+(t_1 \mid \mathcal{E}_{t_0}) f_1^+(t \mid \mathcal{E}_{t_0}) \\
&\vdots
\end{aligned}\right\} \quad (2\text{–}64)$$

The symbol $\{\cdot\}_s$ denotes a symmetry operator producing the arithmetric mean of all the terms similar to the one indicated, obtained by permuting all indicated instants of time. As an example, the following expression in (2-64) is evaluated as follows

$$\{f_2^{++}(t_2,t_1 \mid \mathcal{E}_{t_0}) f_1^+(t \mid \mathcal{E}_{t_0})\}_s = \frac{1}{3}\left(f_2^{++}(t_2,t_1 \mid \mathcal{E}_{t_0}) f_1^+(t \mid \mathcal{E}_{t_0}) + f_2^{++}(t_2,t \mid \mathcal{E}_{t_0}) f_1^+(t_1 \mid \mathcal{E}_{t_0}) + f_2^{++}(t_1,t \mid \mathcal{E}_{t_0}) f_1^+(t_2 \mid \mathcal{E}_{t_0})\right) \quad (2-65)$$

Finally, combining (2-15), (2-16) and (2-35) the following non-linear integral equation is derived for the hazard rate

$$h_{T_1}(t \mid \mathcal{E}_{t_0}) = \frac{f_1^+(t \mid \mathcal{E}_{t_0})}{\exp\left(-\int_{t_0}^{t} h_{T_1}(\tau \mid \mathcal{E}_{t_0})\, d\tau\right)} - \int_{t_0}^{t} f_1^+\left(t \mid \mathcal{E}_{t_0} \cap \mathcal{F}_{t_1}^{(1)}\right) \exp\left(\int_{t_1}^{t} h_{T_1}(\tau \mid \mathcal{E}_{t_0})\, d\tau\right) h_{T_1}(t_1 \mid \mathcal{E}_{t_0})\, dt_1 \quad (2-66)$$

Example 2-1: Approximate evaluations of inclusion-exclusion series

A basic problem of the expansion (2-63) is that the series is divergent at truncation of any order as the length $t - t_0$ of the excitation interval grows to infinity. Moreover, the functions $g_n^{+\cdots+}(t_{n-1},\ldots,t \mid \mathcal{E}_{t_0})$ can hardly be calculated for the order $n > 2$ even for Gaussian processes. For this reason several approaches have been suggested to estimate the higher order functions in terms of $g_1^+(t \mid \mathcal{E}_{t_0})$ and $g_2^{++}(t_1,t_2 \mid \mathcal{E}_{t_0})$, and further to evaluate the sum (2-63) based only on this information. In the so-called method of non-approaching random points by Stratonovich (1963) (for a review of the method, see also Lin (1969, 1970)), the following assumption is applied for the higher order out-crossing rates

$$g_n^{+\cdots++}(t_{n-1},\ldots,t_1,t) = (n-1)!\, f_1^+(t_{n-1} \mid \mathcal{E}_{t_0}) \cdots f_1^+(t_1 \mid \mathcal{E}_{t_0}) f_1^+(t \mid \mathcal{E}_{t_0}) \cdot$$

$$\{R(t_{n-1},t)\ldots R(t_1,t)\}_s \ , \ n = 3,4,\ldots \qquad (2-67)$$

where $R(t_1,t)$ is defined by the expression

$$f_2^{++}(t_1,t_2 \mid \mathcal{E}_{t_0}) = f_1^+(t_1 \mid \mathcal{E}_{t_0}) f_1^+(t_2 \mid \mathcal{E}_{t_0})(1 - R(t_1,t_2)) \qquad (2-68)$$

Because $f_1^+(t \mid \mathcal{E}_{t_0})$ as well as $f_2^{++}(t_1,t_2 \mid \mathcal{E}_{t_0})$ are positive, $R(t_1,t_2)$ is bounded above by unity. Moreover, as $\mid t_2 - t_1 \mid \rightarrow \infty$ the crossing at the times t_1 and t_2 becomes independent, so $R(t_1,t_2) \rightarrow 0$ according to (2-4). Stratonovich designated $R(t_1,t_2)$ as the correlation coefficient of the point process made up by the crossing events. The symmetry operator in (2-66) contains n addends and has a quite similar interpretation to the one in (2-65). As an example the interpretation for $n = 4$ reads

$$\{R(t_3,t)R(t_2,t)R(t_1,t)\}_s = \frac{1}{4}\Big(R(t_3,t)R(t_2,t)R(t_1,t)$$

$$R(t_3,t_1)R(t_2,t_1)R(t,t_1) + R(t_3,t_2)R(t_1,t_2)R(t,t_2) + R(t_2,t_3)R(t_1,t_3)R(t,t_3)\Big) \qquad (2-69)$$

Based on the assumption (2-67) the series (2-63) can then be approximately evaluated as follows

$$h_{T_1}(t \mid \mathcal{E}_{t_0}) = \frac{\ln(1+S(t))}{S(t)} f_1^+(t \mid \mathcal{E}_{t_0}) \qquad (2-70)$$

where

$$S(t) = \int_{t_0}^{t} R(\tau,t) f_1^+(\tau \mid \mathcal{E}_{t_0})\, d\tau \qquad (2-71)$$

In case of independent out-crossings, $R(\tau,t) \equiv 0 \ \Rightarrow \ S(t) \equiv 0$. In this case (2-70) reduces to the well-known Poisson solution

$$h_{T_1}(t \mid \mathcal{E}_{t_0}) = f_1^+(t \mid \mathcal{E}_{t_0}) \qquad (2-72)$$

Unfortunately, it is difficult to relate any physical interpretation to the assumptions inherent in (2-67), which seems to have been selected primarily in order to be able to evaluate the infinite series (2-63) on closed form. As an example, (2-67) for $n = 3$ implies the following rather strange result for the 3rd order out-crossing rate as follows from (2-64) and (2-68)

$$f_3^{+++}(t_2,t_1,t \mid \mathcal{E}_{t_0}) = 2\left\{\frac{f_2^{++}(t_2,t \mid \mathcal{E}_{t_0}) f_2^{++}(t_1,t \mid \mathcal{E}_{t_0})}{f_1^+(t \mid \mathcal{E}_{t_0})}\right\}_s -$$

$$\{f_2^{++}(t_2,t_1 \mid \mathcal{E}_{t_0}) f_1^+(t \mid \mathcal{E}_{t_0})\}_s \qquad (2-73)$$

where the symmetry operators are interpreted as indicated by (2-69).

A somewhat similar approach was suggested by Roberts (1968) and Kimura et al. (1987) for evaluating the infinite sum in (2-43). Their assumption can be stated as follows

$$\lambda_1(t) = \frac{\int_{t_0}^{t} f_2^{++}(t_1, t \mid \mathcal{E}_{t_0})\, dt_1}{\int_{t_0}^{t} f_1^{+}(t_1 \mid \mathcal{E}_{t_0})\, dt_1} \simeq \frac{\int_{t_0}^{t}\int_{t_0}^{t_1} f_3^{+++}(t_2, t_1, t \mid \mathcal{E}_{t_0})\, dt_2 dt_1}{\int_{t_0}^{t}\int_{t_0}^{t_1} f_2^{++}(t_2, t_1 \mid \mathcal{E}_{t_0})\, dt_2 dt_1} \simeq \cdots \simeq$$

$$\frac{\int_{t_0}^{t}\int_{t_0}^{t_1}\cdots\int_{t_0}^{t_{n-2}} f_n^{+\cdots+++}(t_{n-1}, \ldots, t_2, t_1, t \mid \mathcal{E}_{t_0})\, d_{n-1} \ldots dt_2\, dt_1}{\int_{t_0}^{t}\int_{t_0}^{t_1}\cdots\int_{t_0}^{t_{n-2}} f_{n-1}^{+\cdots++}(t_{n-1}, \ldots, t_2, t_1 \mid \mathcal{E}_{t_0})\, dt_{n-1} \ldots dt_2\, dt_1} \simeq \ldots \qquad (2-74)$$

As seen from (2-4), (2-74) is fulfilled in case of independent crossings from the safe domain, where $\lambda_1(t) = f_1^{+}(t \mid \mathcal{E}_{t_0})$. Inserting (2-74) into (2-43) provides

$$f_{T_1}(t \mid \mathcal{E}_{t_0}) \simeq f_1^{+}(t \mid \mathcal{E}_{t_0}) - \lambda_1(t)\left(\int_{t_0}^{t} f_1^{+}(t_1 \mid \mathcal{E}_{t_0})\, dt_1 - \int_{t_0}^{t}\int_{t_0}^{t_1} f_2^{++}(t_2, t_1 \mid \mathcal{E}_{t_0}\, dt_2 dt_1 + \cdots\right) =$$

$$f_1^{+}(t \mid \mathcal{E}_{t_0}) - \lambda_1(t) F_{T_1}(t \mid \mathcal{E}_{t_0}) \;\Rightarrow$$

$$F_{T_1}(t \mid \mathcal{E}_{t_0}) = \int_{t_0}^{t} \exp\left(-\int_{t_1}^{t} \lambda_1(\tau)\, d\tau\right) f_1^{+}(t_1 \mid \mathcal{E}_{t_0})\, dt_1 \qquad (2-75)$$

where $\lambda_1(t)$ is evaluated from $f_1^{+}(t \mid \mathcal{E}_{t_0})$ and $f_2^{++}(t_1, t_2 \mid \mathcal{E}_{t_0})$ as follows from the first statement of (2-74). The method of Roberts and Kimura et al. can be generalized if out-crossing frequencies up to and including the order (n_0+1) is available. Then, the following quantity approximation is considered

$$\lambda_{n_0}(t) = \frac{\int_{t_0}^{t}\int_{t_0}^{t_{n_0-1}} f_{n_0+1}^{+\cdots++}(t_{n_0}, \ldots, t_1, t \mid \mathcal{E}_{t_0}) dt_{n_0} \cdots dt_1}{\int_{t_0}^{t}\cdots\int_{t_0}^{t_{n_0-1}} f_{n_0}^{+\cdots+}(t_{n_0}, \ldots, t_1 \mid \mathcal{E}_{t_0})\, dt_{n_0} \cdots dt_1} \simeq$$

$$\frac{\int_{t_0}^{t}\cdots\int_{t_0}^{t_{n_0-1}}\int_{t_0}^{t_{n_0}} f_{n_0+2}^{++\cdots++}(t_{n_0+1}, t_{n_0}, \ldots, t_1, t \mid \mathcal{E}_{t_0})\, dt_{n_0+1} dt_{n_0} \cdots dt_1}{\int_{t_0}^{t}\cdots\int_{t_0}^{t_{n_0-1}}\int_{t_0}^{t_{n_0}} f_{n_0+1}^{++\cdots+}(t_{n_0+1}, t_{n_0}, \ldots, t_1 \mid \mathcal{E}_{t_0})\, dt_{n_0+1} dt_{n_0} \cdots dt_1} \simeq \ldots,\ n_0 = 2, 3, \ldots \qquad (2-76)$$

(2-43) can then be approximated as follows

$$f_{T_1}(t) \mid \mathcal{E}_{t_0}) \simeq \sum_{j=0}^{n_0} (-1)^j F_{1,j}^{+}(t \mid \mathcal{E}_{t_0}) + \lambda_{n_0}(t) \sum_{j=0}^{n_0-1} (-1)^j \int_{t_0}^{t} F_{1,j}^{+}(t_1 \mid \mathcal{E}_{t_0})\, dt_1$$

$$-\lambda_{n_0}(t) F_{T_1}(t \mid \mathcal{E}_{t_0}) \quad , \quad n_0 = 2, 3, \ldots \quad \Rightarrow$$

$$F_{T_1}(t \mid \mathcal{E}_{t_0}) = \int_{t_0}^{t} \exp\left(- \int_{t_1}^{t} \lambda_{n_0}(u)\, du \right) \cdot$$

$$\left(\sum_{j=0}^{n_0} (-1)^j F_{1,j}^{+}(\tau \mid \mathcal{E}_{t_0}) - \lambda_{n_0}(\tau) \sum_{j=0}^{n_0-1} (-1)^j \int_{t_0}^{\tau} F_{1,j}^{+}(u) \mid \mathcal{E}_{t_0})\, du \right) d\tau \qquad (2-77)$$

The generalization of (2-77) was neither considered by Roberts nor Kimura et al.

Closure methods of the inclusion-exclusion series (2-63) for the hazard function and (2-42), (2-43) for the first-passage time probability density function becomes necessary because of the divergent terms at large excitation time intervals, and because only a rather limited number of terms can be evaluated. However, both of the indicated closure methods are based on weak assumptions and seem to be motivated primarily in order to be able to evaluate the series on closed form. Integral equation methods, based on a truncation of the infinite series of the numerator and denominator of the formal representation of the kernel function offer a more accurate and better motivated alternative.

Next, it is assumed that $\{\mathbf{X}(t),\, t \in [t_0, \infty[\}$ and its time derivative $\{\dot{\mathbf{X}}(t),\, t \in [t_0, \infty[\}$ form a Markov vector process

$$\mathbf{Z}(t) = \begin{bmatrix} \mathbf{X}(t) \\ \dot{\mathbf{X}}(t) \end{bmatrix} \qquad (2-78)$$

As an example a non-linear and non-hysteretic single-degree-of-freedom system under external excitation is considered, determined by the stochastic differential equation

$$d\mathbf{Z}(t) = \mathbf{c}\big(\mathbf{Z}(t)\big)\, dt + \mathbf{d}(t) dW(t) + \mathbf{e}(t)\, dV(t)\,,\ t \in]t_0, \infty[\ ,\ \mathbf{Z}(t_0) = \mathbf{Z}_0 \qquad (2-79)$$

$$\mathbf{Z}(t) = \begin{bmatrix} X(t) \\ \dot{X}(t) \end{bmatrix}\ ,\ \mathbf{c}\big(\mathbf{Z}(t)\big) = \begin{bmatrix} \dot{X}(t) \\ -u\big(X(t), \dot{X}(t)\big) \end{bmatrix}\ ,\ \mathbf{d}(t) = \begin{bmatrix} 0 \\ d(t) \end{bmatrix}\ ,\ \mathbf{e}(t) = \begin{bmatrix} 0 \\ e(t) \end{bmatrix} \qquad (2-80)$$

$\mathbf{c}\big(\mathbf{Z}(t)\big)$ is the drift vector and $\mathbf{d}\big(\mathbf{Z}(t)\big)$ and $\mathbf{e}(t)$ represent the diffusion vectors of the system. The component $u\big(X(t), \dot{X}(t)\big)$ in the drift vector indicates the restoring force per unit mass of the oscillator. The generating sources $\{W(t),\, t \in [t_0, \infty[\}$ and $\{V(t),\, t \in [t_0, \infty[\}$ have independent increments, which are also independent of their initial values $W(t_0)$ and $V(t_0)$. $\{W(t),\, t \in [t_0, \infty[\}$ is assumed to have sample curves, which are continuous with the probability 1. These restrictions confine $\{W(t),\, t \in [t_0, \infty[\}$ to be a Wienerprocess, Nielsen and Iwankiewicz (1996). Because of the introduction of the diffusion function $d(t)$ it can without restrictions be assumed that $\{W(t),\, t \in [t_0, \infty[\}$ is a unit intensity Wienerprocess. $\{V(t),\, t \in [t_0, \infty[\}$ have sample curves which are not continuous with probability 1. This confines $\{V(t),\, t \in [t_0, \infty[\}$ to the classes of compound Poisson processes or α stable Lévy motions, Nielsen and Iwankiewicz (1996). $c(t)$ and $d(t)$ signify deterministic modulation function of the generating stationary source processes $\{W(t),\, t \in [t_0, \infty[\}$ and $\{V(t), t \in [t_0, \infty[\}$. A more

general formulation allows the diffusion vectors $\mathbf{d}(t)$ and $\mathbf{e}(t)$ to depend on the state vector $\mathbf{Z}(t)$. Such problems appear in case of parametric excitation processes with independent increments. However, this is never the case for external excitations, which are the only excitations to be considered in this thesis.

Further, if the initial conditions $\mathbf{Z}_0$ are deterministic or stochastically independent of $\{V(t), t \in [t_0, \infty[\}$, and $\{W(t), t \in [t_0, \infty[\}$ the response process $\{\mathbf{Z}(t), t \in [t_0, \infty[\}$ then becomes a 2-dimensional Markov process. The joint transition probability density function of the Markov state vector from the state $\mathbf{z}_0^T = [x_0, \dot{x}_0]$ at the time t_0 to the state $\mathbf{z}^T = [x, \dot{x}]$ at time $t > t_0$ is denoted $q_{\{\mathbf{Z}\}}(x, \dot{x}, t \mid x_0, \dot{x}_0, t_0)$.

In relation to the indicated 2-dimensional response process, first-passsage time failure is considered in relation to the safe domain $S_t = \{(x, \dot{x}) \mid a(t) < x < b(t) \wedge -\infty < \dot{x} < \infty\}$. If both barriers are restrictive the first-passage problem is referred to as a double barrier problem, whereas the case $a(t) \equiv -\infty \vee b(t) \equiv \infty$ is denoted a single barrier problem.

Below, a single barrier problem with constant upper barrier b is first considered. In this case $f_{\dot{X}T_1}(b, \dot{x}, t \mid \mathcal{E}_{t_0})\, dt d\dot{x}$ indicates the joint probability of the first-passages in the time interval $]t, t + dt]$ at the barrier b with out-crossing velocities in the interval $]\dot{x}, \dot{x} + d\dot{x}]$ on condition of $\mathcal{E}_{t_0}$. Using the Markov property the following integral equation can then be formulated for $f_{T_1\dot{X}}(b, \dot{x}, t \mid \mathcal{E}_{t_0})$ with an argumentation identical to the one leading to (2-35), Nielsen (1990b)

$$f_{\dot{X}T_1}(b, \dot{x}, t \mid \mathcal{E}_{t_0}) = \dot{x}\, q_{\{\mathbf{Z}\}}(b, \dot{x}, t \mid \mathcal{E}_{t_0}) - \int_{t_0}^{t} \int_{0}^{\infty} \dot{x} q_{\{\mathbf{Z}\}}(b, \dot{x}, t \mid b, \dot{x}_1, t_1) \cdot$$

$$f_{\dot{X}T_1}(b, \dot{x}_1, t_1 \mid \mathcal{E}_{t_0})\, d\dot{x}_1 dt_1 \qquad (2-81)$$

where

$$q_{\{\mathbf{Z}\}}(b, \dot{x}, t \mid \mathcal{E}_{t_0}) = \frac{\int_{S_{t_0}} q_{\{\mathbf{Z}\}}(b, \dot{x}, t \mid x_0, \dot{x}_0, t_0) f_{\{X\}\{\dot{X}\}}(x_0, \dot{x}_0, t_0)\, dx_0 d\dot{x}_0}{\int_{S_{t_0}} f_{\{X\}\{\dot{X}\}}(x_0, \dot{x}_0, t_0)\, dx_0 \dot{x}_0} \qquad (2-82)$$

$f_{\{X\}\{\dot{X}\}}(x, \dot{x}, t)$ signifies the joint first order probability density function of the processes $\{X(t)\}, \{\dot{X}(t)\}$ at the time t, i.e. the joint probability density function of the stochastic variables $X(t)$ and $\dot{X}(t)$.

In case of non-Markov processes the relevant kernel in (2-81) is given by $\dot{x} q_{\{\mathbf{Z}\}}\big(b, \dot{x}, t \mid \mathcal{E}_{t_0} \bigcap \mathcal{E}_{]t_0,t_1[} \bigcap \{X(t_1) = b \wedge \dot{X}(t_1) = \dot{x}_1\}\big)$, where $\mathcal{E}_{]t_0,t_1[} = \bigcap_{\tau \in]t_0,t_1[} S_\tau$, indicating the rate of out-crossings at the time t on condition of a first-passage at the time t_1 with the out-crossing velocity $\dot{x}_1$. Due to the Markov property of the state vector process $\{\mathbf{Z}(t), t \in [t_0, \infty[\}$ the kernel reduces to the transition probability density function as shown in (2-81). The inner integral in (2-81) provides transition from all possible out-crossing velocities at the time t_1 to out-crossings with velocity $\dot{x}$ at the time t.

From the solution to (2-81) the first-passage time probability density function is given by

$$f_{T_1}(t \mid \mathcal{E}_{t_0}) = \int_0^\infty f_{\dot{X}T_1}(b, \dot{x}, t \mid \mathcal{E}_{t_0})\, d\dot{x} \qquad (2-83)$$

Inserting the right-hand side of (2-81) into the right-hand side of (2-83) and application of Rice's formula provide

$$f_{T_1}(t \mid \mathcal{E}_{t_0}) = f_1^+(t \mid \mathcal{E}_{t_0}) - \int_{t_0}^t \int_0^\infty f_1^+(t \mid b, \dot{x}_1 t_1) f_{\dot{X}T_1}(b, \dot{x}_1 t_1 \mid \mathcal{E}_{t_0})\, d\dot{x}_1 dt_1 \qquad (2-84)$$

$f_1^+(t \mid b, \dot{x}_1, t_1) = \int_0^\infty \dot{x} q_{\{\mathbf{Z}\}}(b, \dot{x}, t \mid b, \dot{x}_1, t_1) d\dot{x}$ is the first order out-crossing rate at the time t on condition of deterministic start in $[X(t_1), \dot{X}(t_1)] = [b, \dot{x}_1]$, $t_1 < t$. The formulation (2-84) should be preferred compared to (2-83) because the boundary condition $f_{T_1}(t_0 \mid \mathcal{E}_{t_0}) = f_1^+(t_0 \mid \mathcal{E}_{t_0})$ is exactly fulfilled.

Using the Markov property the solution to (2-81) can be expressed in a Neumann-series of iterated kernels

$$f_{\dot{X}T_1}(b, \dot{x}, t \mid \mathcal{E}_{t_0}) = \dot{x} q_{\{\mathbf{Z}\}}(b, \dot{x}, t \mid \mathcal{E}_{t_0}) -$$

$$\int_{t_0}^t \int_0^\infty \dot{x} q_{\{\mathbf{Z}\}}(b, \dot{x}, t \mid b, \dot{x}_1, t_1)\, \dot{x}_1 q_{\{\mathbf{Z}\}}(b, \dot{x}_1, t_1 \mid \mathcal{E}_{t_0})\, d\dot{x}_1 dt_1 + \cdots =$$

$$\dot{x} f_{\{X\}\{\dot{X}\}}(b, \dot{x}, t \mid \mathcal{E}_{t_0}) - \int_{t_0}^t \int_0^\infty \dot{x}\dot{x}_1 f_{\{X\}\{\dot{X}\}}(b, \dot{x}, t; b, \dot{x}_1, t_1 \mid \mathcal{E}_{t_0})\, d\dot{x}_1 dt_1 + \cdots \qquad (2-85)$$

If (2-85) is inserted into (2-83) the formal inclusion-exclusion series (2-43) is obtained, using the generalization of the Rice formulas for joint conditioned crossing rates, Rice (1944).

The main difference between the integral equations (2-35) and (2-81) is that the former applies also to non-Markov processes. However, in (2-35) the kernel is introduced as a new unknown function, which must be approximated in applications. This is not the case in the formulation (2-81), which provides an exact calculation procedure for the first-passage time probability density function for Markov vector processes.

For the double barrier problem with time-varying lower and upper barriers $a(t)$ and $b(t)$, (2-81) is replaced with the coupled integral equations

$$f_{\dot{X}T_1}(b(t), \dot{x}, t \mid \mathcal{E}_{t_0}) = (\dot{x} - \dot{b}(t)) q_{\{\mathbf{Z}\}}(b(t), \dot{x}, t \mid \mathcal{E}_{t_0}) -$$

$$\int_{t_0}^{t}\int_{\dot{b}(t_1)}^{\infty}(\dot{x}-\dot{b}(t))q_{\{\mathbf{Z}\}}(b(t),\dot{x},t\mid b(t_1),\dot{x}_1,t_1)f_{\dot{X}T_1}(b(t_1),\dot{x}_1,t_1\mid\mathcal{E}_{t_0})\,d\dot{x}_1dt_1-$$

$$\int_{t_0}^{t}\int_{-\infty}^{\dot{a}(t_1)}(\dot{x}-\dot{b}(t))q_{\{\mathbf{Z}\}}(b(t),\dot{x},t\mid a(t_1),\dot{x}_1,t_1)f_{\dot{X}T_1}(a(t_1),\dot{x}_1,t_1\mid\mathcal{E}_{t_0})\,d\dot{x}_1dt_1 \quad (2-86)$$

$$f_{\dot{X}T_1}(a(t),\dot{x},t\mid\mathcal{E}_{t_0})=(\dot{a}(t)-\dot{x})q_{\{\mathbf{Z}\}}(a(t),\dot{x},t\mid\mathcal{E}_{t_0})-$$

$$\int_{t_0}^{t}\int_{-\infty}^{\dot{a}(t_1)}(\dot{a}(t)-\dot{x})q_{\{\mathbf{Z}\}}(a(t),\dot{x},t\mid a(t_1),\dot{x}_1,t_1)f_{\dot{X}T_1}(a(t_1),\dot{x}_1,t_1\mid\mathcal{E}_{t_0})\,d\dot{x}_1dt_1-$$

$$\int_{t_0}^{t}\int_{\dot{b}(t_1)}^{\infty}(\dot{a}(t)-\dot{x})q_{\{\mathbf{Z}\}}(a(t),\dot{x},t\mid b(t_1),\dot{x}_1,t_1)f_{\dot{X}T_1}(b(t_1),\dot{x}_1,t_1\mid\mathcal{E}_{t_0})\,d\dot{x}_1dt_1 \quad (2-87)$$

From the solution of (2-86) and (2-87) $f_{T_1}(t\mid\mathcal{E}_{t_0})$ is then obtained from

$$f_{T_1}(t\mid\mathcal{E}_{t_0})=\int_{\dot{b}(t)}^{\infty}f_{\dot{X}T_1}(b(t),\dot{x},t\mid\mathcal{E}_{t_0})d\dot{x}+\int_{-\infty}^{\dot{a}(t)}f_{\dot{X}T_1}(a(t),\dot{x},t\mid\mathcal{E}_{t_0})\,d\dot{x} \qquad (2-88)$$

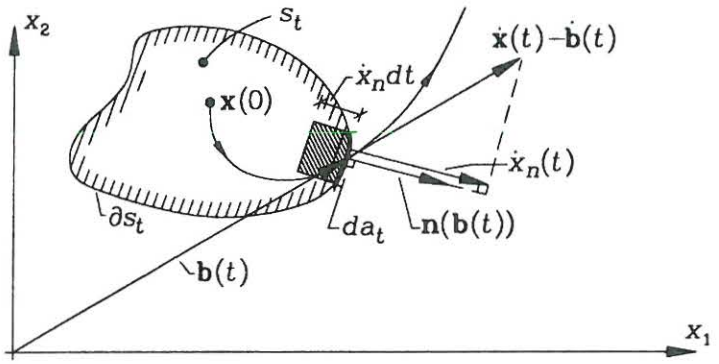

Fig. 2-4: Out-crossings in the interval $]t,t+dt]$ through an area element da_t of the failure surface ∂s_t.

Next, consider a non-linear and a non-hysteretic dynamic system of n degrees-of-freedom. The state vector $\mathbf{Z}^T(t) = [\mathbf{X}(t), \dot{\mathbf{X}}(t)]$ made up by the displacement and velocity response is assumed to be a $2n$-dimensional Markov vector with the transition probability density function $q_{\{\mathbf{Z}\}}(\mathbf{x}, \dot{\mathbf{x}}, t \mid \mathbf{x}_0, \dot{\mathbf{x}}_0, t_0)$.

The safe domain at the time t is given by $S_t = \{(\mathbf{x}, \dot{\mathbf{x}}) \mid \mathbf{x} \in s_t \wedge \dot{\mathbf{x}} \in R^n\}$. The surface of the set s_t is denoted ∂s_t. ∂S_t then becomes a cylinder in R^{2n} with ∂s_t as the perimeter set.

Consider an area element da_t of ∂s_t specified by the position vector $\mathbf{b}(t)$, and moving at the velocity $\dot{\mathbf{b}}(t)$ relative to a fixed frame of reference. The velocity of a sample curve relative to the surface in direction of the outward directed unit normal vector $\mathbf{n}(\mathbf{b}(t))$ is given by

$$\dot{X}_n(\mathbf{b}(t)) = \mathbf{n}^T(\mathbf{b}(t))(\dot{\mathbf{X}}(t) - \dot{\mathbf{b}}(t)) \qquad (2-89)$$

$f_{\dot{\mathbf{X}}T_1}(\mathbf{b}(t), \dot{\mathbf{x}}, t \mid \mathcal{E}_{t_0})\, da_t\, d\dot{\mathbf{x}} dt$ indicates the joint probability of first-passages in the time interval $]t, t+dt]$ at the surface area element da_t at position $\mathbf{b}(t)$ with the out-crossing velocity vector in the volume $d\dot{\mathbf{x}}$ centred at $\dot{\mathbf{x}}$ on condition of $\mathcal{E}_{t_0}$. Out-crossings in the time interval $]t, t+dt]$ take place if $\mathbf{X}(t)$ is placed in the volume element $da_t \dot{X}_n dt$, see fig. 2-4. $f_{\dot{\mathbf{X}}T_1}(\mathbf{b}(t), \dot{\mathbf{x}}, t \mid \mathcal{E}_{t_0})$ then fulfils the following integral equation

$$f_{\dot{\mathbf{X}}T_1}(\mathbf{b}(t), \dot{\mathbf{x}}, t \mid \mathcal{E}_{t_0}) = \mathbf{n}^T(\mathbf{b}(t))(\dot{\mathbf{x}} - \dot{\mathbf{b}}(t)) q_{\{\mathbf{Z}\}}(\mathbf{b}(t), \dot{\mathbf{x}}, t \mid \mathcal{E}_{t_0}) -$$

$$\int_{t_0}^{t} \mathbf{n}^T(\mathbf{b}(t))(\dot{\mathbf{x}} - \dot{\mathbf{b}}(t)) \int_{\partial s_{t_1}} \int_{\Lambda_{t_1}} q_{\{\mathbf{Z}\}}(\mathbf{b}(t), \dot{\mathbf{x}}, t \mid \mathbf{b}(t_1), \dot{\mathbf{x}}_1, t_1) \cdot$$

$$f_{\dot{\mathbf{X}}T_1}(\mathbf{b}(t_1), \dot{\mathbf{x}}_1, t_1 \mid \mathcal{E}_{t_0})\, d\dot{\mathbf{x}}_1\, da_{t_1}\, dt_1 \qquad (2-90)$$

where

$$\Lambda_t = \{\dot{\mathbf{x}} \in R^n \mid \mathbf{n}^T(\mathbf{b}(t))(\dot{\mathbf{x}} - \dot{\mathbf{b}}(t)) > 0\} \qquad (2-91)$$

(2-90) generalizes (2-81) in the same way as the Belyaev formula for the out-crossing rate of a vector stochastic process, Belyaev (1968), generalizes the Rice formula for the out-crossing rate of a scalar process. (2-90) defines the integral equations for all points $\mathbf{b}(t)$ of the surface ∂s_t. In case of numerical solutions the failure surface ∂s_t has to be divided into finite subdomains within each of which $f_{\dot{\mathbf{X}}T_1}(\mathbf{b}(t), \dot{\mathbf{x}}, t \mid \mathcal{E}_{t_0})$ is considered constant as a function of $\mathbf{b}(t)$. A closed system of integral equations for these quantities may then be obtained from (2-90). Hence, in contrast to (2-81) and (2-86), (2-87) no exact formulation of the problem is obtained in this case. The level of approximation depends on the roughness of the discretization of the failure surface.

Obviously, a finer discretization should be applied where out-crossings are likely to occur. The first-passage time probability density function is next obtained from

$$f_{T_1}(t \mid \mathcal{E}_{t_0}) = \int_{\partial s_t} \int_{\Lambda_t} f_{\dot{\mathbf{X}}T_1}(\mathbf{b}(t), \dot{\mathbf{x}}, t \mid \mathcal{E}_{t_0})\, d\dot{\mathbf{x}} da_t \qquad (2-92)$$

Finally, it is assumed that the restoring force of the oscillator (2-79) is related with hysteresis. The equations of motion can then be written

$$d\mathbf{Z}(t) = \mathbf{c}\big(\mathbf{Z}(t)\big)dt + \mathbf{d}(t)dW(t) + \mathbf{e}(t)\,dV(t)\ ,\ t \in [t_0, \infty[\ ,\ \mathbf{Z}(t_0) = \mathbf{Z}_0 \qquad (2-93)$$

$$\mathbf{Z}(t) = \begin{bmatrix} X(t) \\ \dot{X}(t) \\ Q(t) \end{bmatrix},\ \mathbf{c}\big(\mathbf{Z}(t)\big) = \begin{bmatrix} \dot{X}(t) \\ -\alpha u\big(X(t), \dot{X}(t)\big) - (1-\alpha)Q(t) \\ \kappa\big(\dot{X}(t), Q(t)\big)\dot{X}(t) \end{bmatrix} \qquad (2-94a)$$

$$\mathbf{d}(t) = \begin{bmatrix} 0 \\ d(t) \\ 0 \end{bmatrix},\ \mathbf{e}(t) = \begin{bmatrix} 0 \\ e(t) \\ 0 \end{bmatrix} \qquad (2-94b)$$

$Q(t)$ is the hysteretic component of the restoring force, which is confined to the interval $[-q_y, q_y]$ with probability 1, and α is the non-hysteretic fraction of the total restoring force. The 3rd equation in (2-93) represents the constitutive equation of this component. $\kappa\big(\dot{X}(t), Q(t)\big)$ can be interpreted as a state dependent spring stiffness of the restoring force. This is a non-linear and a non-analytical function of the state variables. Expressions for this quantity have been given for various simple models of hysteresis such as the bilinear oscillator, Kaul and Penzien (1974), and the Bouc-Wen hysteresis, Wen (1976), see (3-49), (3-50), (3-51).

(2-81), (2-82) and (2-83) are then replaced with

$$f_{\dot{X}QT_1}(b, \dot{x}, q, t \mid \mathcal{E}_{t_0}) = \dot{x} q_{\{\mathbf{Z}\}}(b, \dot{x}, q, t \mid \mathcal{E}_{t_0}) - \int_{t_0}^{t} \int_{0}^{\infty} \int_{-q_y}^{q_y} \dot{x} q_{\{\mathbf{Z}\}}(b, \dot{x}, q, t \mid b, \dot{x}_1, q_1, t_1) \cdot$$

$$f_{\dot{X}QT_1}(b, \dot{x}_1, q_1, t_1 \mid \mathcal{E}_{t_0})\, d\dot{x}_1 dq_1 dt_1 \qquad (2-95)$$

$$q_{\{\mathbf{Z}\}}(b, \dot{x}, q, t \mid \mathcal{E}_{t_0}) = \frac{\int_{S_{t_0}} q_{\{\mathbf{Z}\}}(b, \dot{x}, q, t \mid x_0, \dot{x}_0, q_0, t_0) f_{\{\mathbf{Z}\}}(x_0, \dot{x}_0, q_0, t_0)\, dx_0 d\dot{x}_0 dq_0}{\int_{S_{t_0}} f_{\{\mathbf{Z}\}}(x_0, \dot{x}_0, q_0, t_0)\, dx_0 \dot{x}_0 dq_0} \qquad (2-96)$$

$$f_{T_1}(t \mid \mathcal{E}_{t_0}) = \int_{0}^{\infty} \int_{-q_y}^{q_y} f_{\dot{X}QT_1}(b, \dot{x}, q, t \mid \mathcal{E}_{t_0})\, d\dot{x} dq \qquad (2-97)$$

q_y is the yield value of the hysteretic restoring force component. In case of a bilinear oscillator this value is attained with finite probability. Consequently, the transition probability density will have delta-spikes at $Q(t) = -q_y$ and $Q(t) = q_y$. As seen (2-95) is a special case of (2-90), where $\partial s_t = b \times [-q_y, q_y]$. The integral equations for more involved hysteretic systems are equally given by (2-90), when ∂s_t indicates the set product of the safe domain of $\mathbf{X}(t)$ and the sample space of all hysteretic components.

The integral equation (2-35) was first obtained by Bernard and Shipley (1972) and Shipley and Bernard (1972) dealing with single-degree-of-freedom systems under white noise excitation. The applied derivation relied on the Markov property of the state vector of this system. In the present notation they obtained the following expression for the kernel in the single barrier problem as follows from (2-84) and comparison with (2-35)

$$f_1^+(t \mid \mathcal{E}_{t_0} \cap \mathcal{F}_{t_1}^{(1)}) = \int_0^\infty f_1^+(t \mid b, \dot{x}_1, t_1) \frac{f_{\dot{X}T_1}(\dot{x}_1, t_1 \mid \mathcal{E}_{t_0})}{f_{T_1}(t_1 \mid \mathcal{E}_{t_0})} \, d\dot{x}_1 \qquad (2-98)$$

It should be noted that Bernard and Shipley did not obtain any of the integral equations (2-81), (2-86), (2-87), (2-90), (2-95) or similar equations valid for Markov systems, but concentrated on specifying various approximations to $f_1^+(t \mid \mathcal{E}_{t_0} \cap \mathcal{F}_{t_1}^{(1)})$.

Bernard and Shipley (1972) claimed that the separation of the integrand in (2-35) into a kernel function and a first-passage probability density function is unique for Markov systems. Nielsen (1980) demonstrated the nature of (2-35) as a fundamental identity, not restricted to Markov processes, and derived from the integral equation the formal inclusion-exclusion series (2-43) and (2-46) for the first-passage probability density function and for the kernel in terms of joint conditioned out-crossing rates. In the same paper the integral equation (2-55) for the nth-passage probability density function was specified, along with the formal expansions (2-56) and (2-58) for this quantity and the associated kernel. The integral equations (2-48), (2-51) for the conditioned first-passage probability density function and the expansions for the associated kernels (2-50), (2-54) were derived by Nielsen (1990a).

The formulation (2-59) and the associated formal expansions (2-60), (2-61) in conditioned crossing rates of samples in the safe domain at specified instants of time, $f_n^{+\cdots+}(t_n, \ldots, t_1; \mathcal{E}_{\tau_1,\ldots,\tau_m} \mid \mathcal{E}_{t_0})$, were suggested by Thoft-Christensen and Nielsen (1982).

For a one-dimensional Markov process $\{Z(t), t \in [t_0, \infty[\}$ in combination with a single barrier problem with time varying upper barrier $b(t)$, the first-passage time probability density function fulfils the integral equation

$$f_{T_1}(t \mid \mathcal{E}_{t_0}) = c_{\{Z\}}(b(t), t \mid \mathcal{E}_{t_0}) - \int_{t_0^+}^{t^-} c_{\{Z\}}(b(t), t \mid b(t_1), t_1) f_{T_1}(t_1 \mid \mathcal{E}_{t_0}) \, dt_1 \qquad (2-99)$$

$$c_{\{Z\}}(b(t), t \mid \mathcal{E}_{t_0}) = \frac{\int_{S_{t_0}} c_{\{Z\}}(b(t), t \mid z_0, t_0) f_{\{X\}}(z_0, t_0) dz_0}{\int_{S_{t_0}} f_{\{X\}}(z_0, t_0) dz_0} \qquad (2-100)$$

$c_{\{Z\}}(b(t), t \mid z_0, t_0)$ is the probability current through the boundary $b(t)$ at the time t on condition of a deterministic start at z_0 at the time t_0. Let $D_N(z,t)$ be the derivative moment of Nth order of the process. Then, see e.g. Stratonovich (1963)

$$c_{\{Z\}}(b(t), t \mid z_0, t_0) = \sum_{N=1}^{\infty} \frac{(-1)^{N-1}}{N!} \frac{\partial^{N-1}}{\partial z^{N-1}} (D_N(b(t), t) q_{\{Z\}}(b(t), t \mid z_0, t_0)) \qquad (2-101)$$

$q_{\{Z\}}(z,t \mid z_0,t_0)$ signifies the transition probability density function of the Markov process. For diffusion processes the derivative moments above the second order vanish. This is not the case if the input noise to the system is a compound Poisson process.

(2-99) has here been stated using the same argumentation as in (2-35). Alternatively, (2-99) was formally derived by Ricciardi et al. (1984) for the case of deterministic start based on an identity by Siegert (1951, eq. (2.12)). In their final result a factor 2 appears in front of both terms on the right-hand side of (2-99), originating from an interpretation of the integration limits different from the one indicated above. The system of integral equations (2-81), (2-86), (2-87), (2-90), (2-95) for Markov systems was derived by Nielsen (1990b).

Example 2-2: Approximations for the kernel and the inhomogeneity of integral equations (2-35) and (2-41) and related bounding technique

Consider a linear single-degree-of-freedom oscillator subjected a Gaussian white noise $\{\dot{W}(t),\ t \in]0,\infty[\}$

$$\left.\begin{aligned} &m(\ddot{X} + 2\zeta\omega_0\dot{X} + \omega_0^2 X) = \dot{W}(t) \quad , \quad t > 0 \\ &X(0) = X_0 \quad , \quad \dot{X}(0) = \dot{X}_0 \end{aligned}\right\} \qquad (2-102)$$

The time will be normalized with respect to the eigenperiod $T_0 = \frac{2\pi}{\omega_0}$. The boundary conditions will be normalized with respect to the stationary variance of the oscillator given by, e.g. Nielsen (1993)

$$\sigma_{X,0}^2 = \frac{\pi S_0}{2\zeta\omega_0^3 m^2} \qquad (2-103)$$

where S_0 is the auto-spectral density function of the Gaussian white noise.

The following 4 first-passage time problems will be analysed

1. Symmetric double barrier deterministic start problem.
   $X_0 = \dot{X}_0 = 0$, $\zeta = 0.08$, $b(t) = -a(t) = 2.5\sigma_{X,0}$

2. Single barrier stochastic start problem.
   $\zeta = 0.01$, $b(t) \equiv 2.0\sigma_{X,0}$

3. Single barrier deterministic start problem.
   $X_0 = \dot{X}_0 = 0$, $\zeta = 0.08$, $b(t) = 2.5\sigma_{X,0}\left(1 - \frac{1}{5}\frac{t}{T_0}\right)$.

4. Symmetric double barrier deterministic start problem.
   $X_0 = \dot{X}_0 = 0$, $\zeta = 0.08$, $b(t) = -a(t) = 2.5\sigma_{X,0}\left(1 - \frac{1}{7}\frac{t}{T_0}\right)$, $t \in [0, 7T_0]$.

The safe domains in the last 2 problems are shown in fig. 2-5.

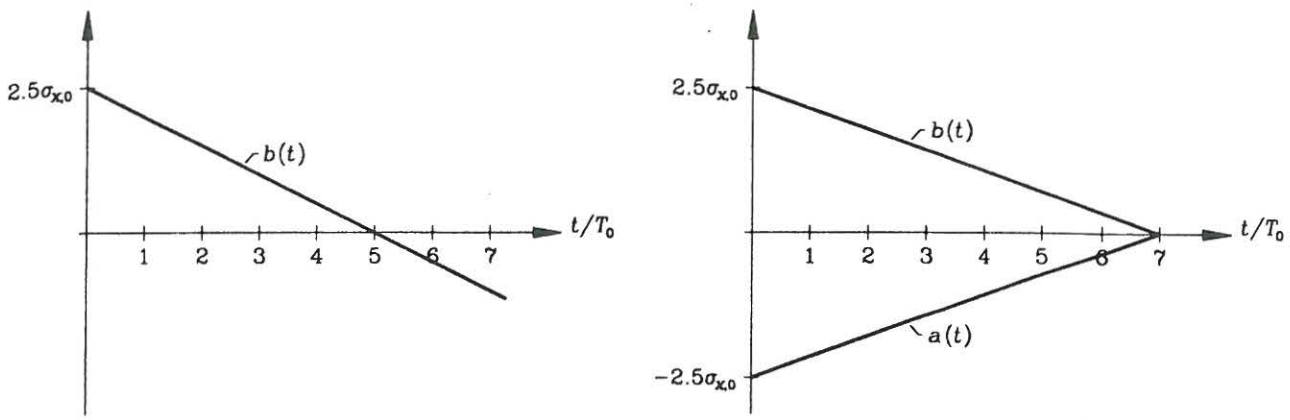

Fig. 2-5: Time varying safe domains.

The following approximation is used for the kernel of the integral equation (2-35), obtained by truncating the numerator and denominator series of (2-46) to the first term

$$f_1^+\left(t \mid \mathcal{E}_0 \cap \mathcal{F}_{t_1}^{(1)}\right) \simeq \frac{f_2^{++}(t_1, t \mid \mathcal{E}_0)}{f_1^+(t_1 \mid \mathcal{E}_0)} \qquad (2-104)$$

The approximation for the first-passage time probability density function obtained by numerical integration of (2-35) with the kernel (2-104) is designated $f_{T_1}^{(a)}(t \mid \mathcal{E}_0)$ in the following.

For the deterministic start problems the approximation (2-104) is always applied based on conditioned crossing rates evaluated from the joint pdf of $[X(t), \dot{X}(t)]$ conditioned on $[X(0), \dot{X}(0)] = [0, 0]$. For the stochastic start problem the following approximations for the kernel and the inhomogeneity will also be considered

$$f_1^+\left(t \mid \mathcal{E}_0 \cap \mathcal{F}_{t_1}^{(1)}\right) \simeq \frac{f_2^{++}(t_1, t)}{f_1^+(t_1)} \qquad (2-105)$$

$$f_1^+(t \mid \mathcal{E}_0) \simeq \frac{f_1^+(t)}{\Phi\left(\frac{b}{\sigma_{X,0}}\right)} \qquad (2-106)$$

The approximation (2-104) is reasonable because both the numerator and the denominator are upper bounds as shown below, and thus counterbalance each other to some extent. At high barrier levels with independent crossing rates $f_1^+(t \mid \mathcal{E}_{t_0} \cap \mathcal{F}_{t_1}^{(1)}) \simeq f_1^+(t)$. As follows from (2-4) this limit is also attained asymptotically by the right-hand sides of (2-104) and (2-105). Hence, both of those approximations are asymptotically correct at high barrier levels.

(2-105) was first suggested by Bernard and Shipley (1972) and Shipley and Bernard (1972). The denominator in (2-106) was a modification due to Nielsen (1980) to insure the fulfilment of the boundary condition $f_{T_1}(0 \mid \mathcal{E}_0) = \frac{f_1^+(0)}{P(S_0)}$ as seen from (2-30). In comparison Bernard and Shipley applied the approximation $f_1^+(t \mid \mathcal{E}_0) \simeq f_1^+(t)$. The approximation for the first-passage probability density function obtained by numerical solution of (2-35) with (2-105), (2-106) is designated $f_{T_1}^{(b)}(t \mid \mathcal{E}_0)$.

The next approximation to the kernel is obtained by truncating the numerator and denominator series after 2 terms. Replacing conditional out-crossing rates by corresponding unconditional out-crossing as in (2-105) the following kernel approximation is obtained, Nielsen (1980)

$$f_1^+\left(t \mid \mathcal{E}_0 \cap \mathcal{F}_{t_1}^{(1)}\right) \simeq \frac{f_2^{++}(t_1, t) - \int_0^{t_1} f_3^{+++}(t_2, t_1)dt_2}{f_1^+(t_1) - \int_0^{t_1} f_2^{++}(t_2, t_1)dt_2} \qquad (2-107)$$

The approximation for the first-passage time probability density function obtained by numerical solution of (2-35) with (2-106), (2-107) is designated $f_{T_1}^{(c)}(t \mid \mathcal{E}_0)$.

Finally, the integral equation (2-41) is considered. For the inhomogeneity and for the kernel the following approximations are applied, Nielsen (1980)

$$f_1^+(t \mid \mathcal{E}_0) - \int_0^t f_2^{++}(t_1, t \mid \mathcal{E}_0) dt_1 \simeq \frac{1}{\Phi\left(\frac{b}{\sigma_{X,0}}\right)} \left(f_1^+(t) - \int_0^t f_2^{++}(t_1, t) dt_1 \right) \qquad (2-108)$$

$$f_2^{++}\left(t_1, t \mid \mathcal{E}_0 \cap \mathcal{F}_{t_2}^{(1)}\right) \simeq \frac{f_3^{+++}(t_2, t_1, t)}{f_1^+(t_2)} \qquad (2-109)$$

The approximation obtained by numerical solution of (2-41) with (2-108), (2-109) is designated $f_{T_1}^{(d)}(t \mid \mathcal{E}_0)$.

Since the integral on the right-hand side of (2-35) is non-negative, one has the following bounding for the first-passage time probability density function

$$f_{T_1}(t \mid \mathcal{E}_0) \leq S_{T_1}^{(1)}(t) = f_1^+(t \mid \mathcal{E}_0) \qquad (2-110)$$

The right-hand side of (2-110) will be referred to as the 1st upper bound.

The general technique for construction bounds follows from (2-42). Ignoring the non-negative integral within the brackets on the right-hand side succeeding upper and lower bounds are constructed depending on the sign of $(-1)^{n-1}$. The 1st lower bound and the 2nd upper bound become

$$f_{T_1}(t \mid \mathcal{E}_0) \geq R_{T_1}^{(1)}(t) = f_1^+(t \mid \mathcal{E}_0) - \int_0^t f_2^{++}(t_1, t \mid \mathcal{E}_0) dt_1 \qquad (2-111)$$

$$f_{T_1}(t \mid \mathcal{E}_0) \leq S_{T_1}^{(2)}(t) = f_1^+(t \mid \mathcal{E}_0) - \int_0^t f_2^{++}(t_1, t \mid \mathcal{E}_0) dt_1 + \int_0^t \int_0^{t_1} f_3^{+++}(t_2, t_1, t \mid \mathcal{E}_0) dt_2 dt_1 \qquad (2-112)$$

Ignoring the non-negative integral within the brackets on the right-hand side of (2-30) the following upper bound is obtained

$$f_{T_1}(t \mid \mathcal{E}_0) \leq \frac{f_1^+(t)}{P(\mathcal{E}_0)} \qquad (2-113)$$

(2-113) is an alternative to (2-110) but is expressed in the unconditioned out-crossing rate.

The various approximate results for the first-passage time probability density function along with the indicated bounds have been shown in fig. 2-6 for problem 1 defined above. The results have been compared to the simulation results of Crandall et al. (1966). Obviously, $f_{T_1}^{(a)}(t \mid \mathcal{E}_0)$ is doing better in this case than the more involved approximations $f_{T_1}^{(c)}(t \mid \mathcal{E}_0)$ and $f_{T_1}^{(d)}(t \mid \mathcal{E}_0)$. Hence, the conclusion is that these approximations should be abandoned. The approximations $f_{T_1}^{(a)}(t \mid \mathcal{E}_0)$ and $f_{T_1}^{(b)}(t \mid \mathcal{E}_0)$ will both be further investigated in the following examples.

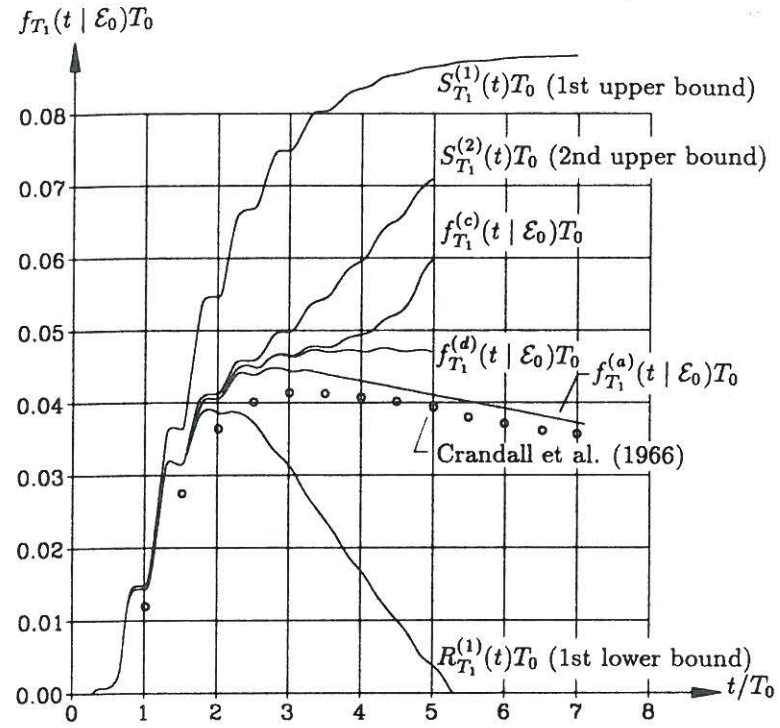

Fig. 2-6: First-passage time probability density function. Deterministic start problem with symmetric constant double barriers. $\zeta = 0.08$, $b(t) = -a(t) = 2.5\sigma_{X,0}$. Nielsen (1980).

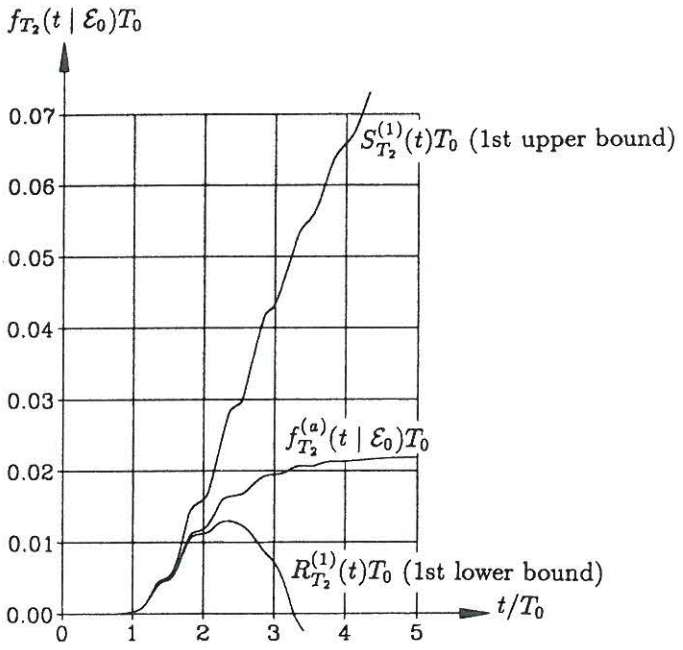

Fig. 2-7: 2nd-passage time probability density function. Deterministic start problem with symmetric constant double barriers. $\zeta = 0.08$, $b(t) = -a(t) = 2.5\sigma_{X,0}$. Nielsen (1980).

Upon inserting any approximation to $f_{T_1}(t \mid \mathcal{E}_0)$ into the right-hand side of (2-55) the 2nd-passage time probability density function can next be evaluated numerically. The kernel given by (2-58) is approximated as follows

$$f_1^+\left(t \mid \mathcal{E}_0 \cap \mathcal{F}_{t_1}^{(2)}\right) \simeq \frac{\int_0^t f_3^{+++}(t_2, t_1, t \mid \mathcal{E}_0)dt_2}{\int_0^t f_2^{++}(t_2, t_1 \mid \mathcal{E}_0)dt_2} \simeq \frac{\int_0^t f_3^{+++}(t_2, t_1, t)dt_2}{\int_0^t f_2^{++}(t_2, t_1)dt_2} \qquad (2-114)$$

The approximation to the 2nd-passage time probability density function obtained by numerical solution of (2-55) with the inhomogeneity $f_1^+(t \mid \mathcal{E}_0) - f_{T_1}^{(a)}(t \mid \mathcal{E}_0)$ and with the kernel approximation (2-114) is designated $f_{T_2}^{(a)}(t \mid \mathcal{E}_0)$.

From (2-55), (2-56) the following bounds can similarly be derived for the 2nd-passage time probability density function, Nielsen (1980)

$$f_{T_2}(t \mid \mathcal{E}_0) \leq S_{T_2}^{(1)}(t) = \int_0^t f_2^{++}(t_1, t \mid \mathcal{E}_0)dt_1 \qquad (2-115)$$

$$f_{T_2}(t \mid \mathcal{E}_0) \geq R_{T_2}^{(1)}(t) = \int_0^t f_2^{++}(t_1, t \mid \mathcal{E}_0)dt_1 - 2\int_0^t \int_0^{t_1} f_3^{+++}(t_2, t_1, t \mid \mathcal{E}_0)dt_2 dt_1 \qquad (2-116)$$

The obtained result along with the indicated bounds has been shown in fig. 2-7. $f_{T_2}^{(a)}(t \mid \mathcal{E}_{t_0})$ will maybe start decreasing at later times than shown in the figure.

Fig. 2-8 shows the results for the approximation $f_T^{(b)}(t \mid \mathcal{E}_0)$ for problem 2 along with associated bounds. The simulation results are obtained from ergodic sampling based on the identity (2-31). Fig. 2-9 shows the first-passage time distribution function $F_{T_1}^{(b)}(t \mid \mathcal{E}_0)$ obtained from the approximation $f_{T_1}^{(b)}(t \mid \mathcal{E}_0)$ of fig. 2-8.

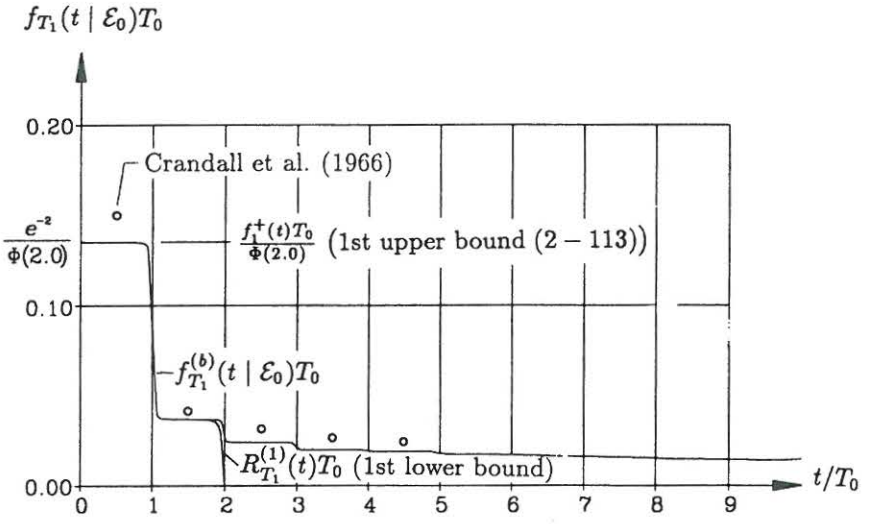

Fig. 2-8: First-passage time probability density function for a single barrier stochastic start problem. $\zeta = 0.01$, $b(t) \equiv 2.0\,\sigma_{X,0}$. Nielsen (1980)

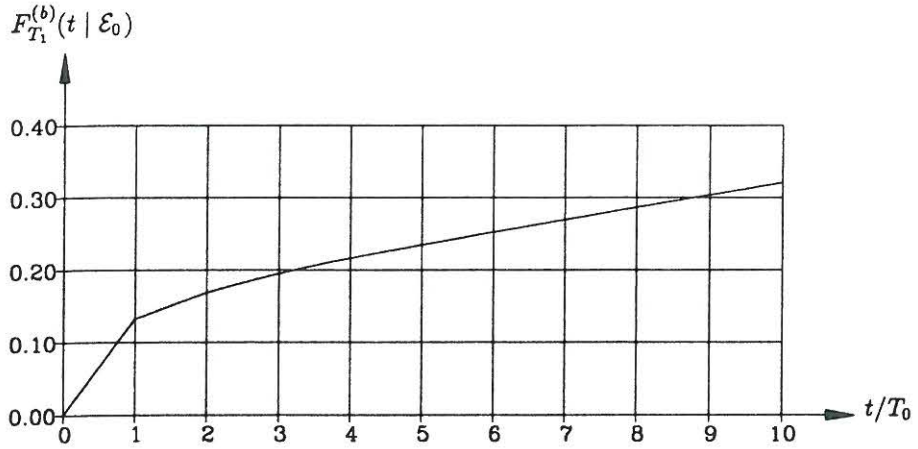

Fig. 2-9: First-passage time probability distribution function for a single barrier stochastic start problem. $\zeta = 0.01$, $b(t) \equiv 2.0\,\sigma_{X,0}$. Nielsen (1980).

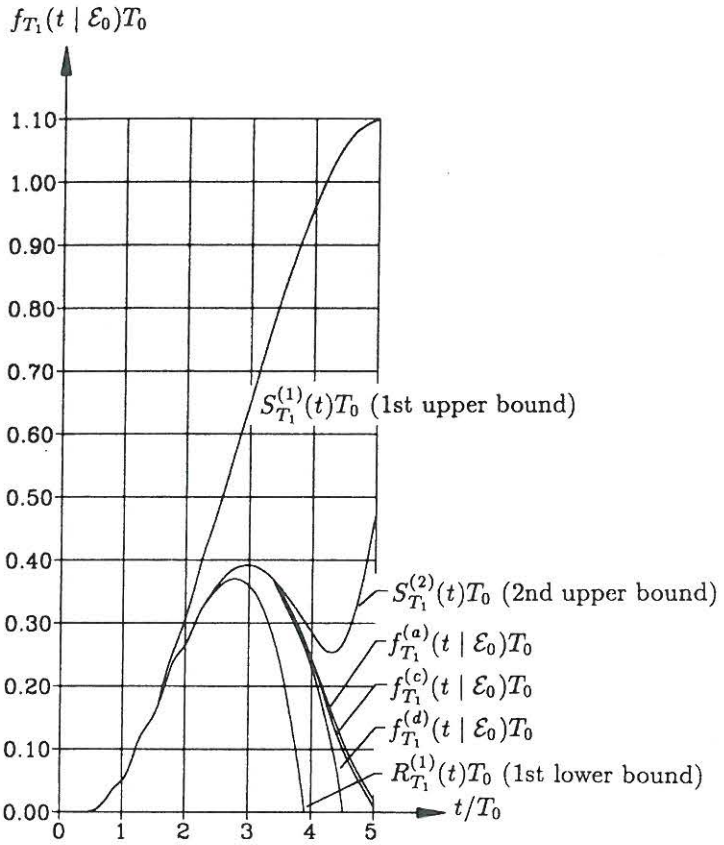

Fig. 2-10: First-passage time probability density function. Deterministic start problem with a single time-varying barrier. $\zeta = 0.08$, $b(t) = 2.5\,\sigma_{X,0}\left(1 - \frac{1}{5}\frac{t}{T_0}\right)$. Nielsen (1980).

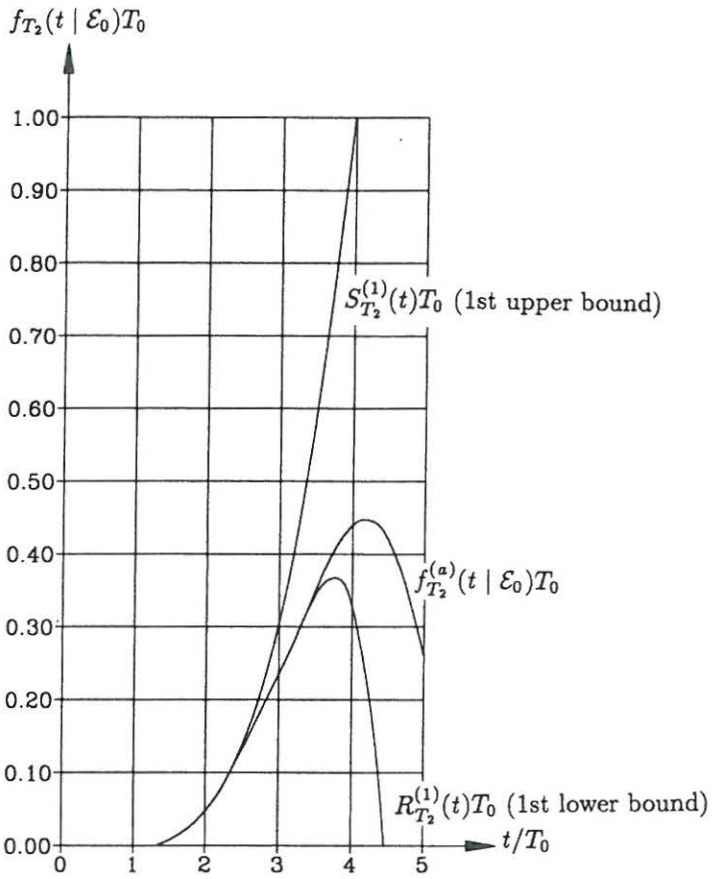

Fig. 2-11: 2nd-passage time probability density function. Deterministic start problem with a single time-varying barrier. $\zeta = 0.08$, $b(t) = 2.5\sigma_{X,0}\left(1 - \frac{1}{5}\frac{t}{T_0}\right)$. Nielsen (1980).

In fig. 2-10 the various approximations for the first-passage time probability density function are shown for problem 3 along with various bounds. It is noted that $f^{(c)}_{T_1}(t \mid \mathcal{E}_0)$ and $f^{(d)}_{T_1}(t \mid \mathcal{E}_0)$ are almost identical as long as the first lower bound remains positive.

Fig. 2-11 indicates the approximation $f^{(a)}_{T_2}(t \mid \mathcal{E}_0)$ to the 2nd-passage time probability density function. The probability of at least 2 failures in the interval $[0, 5T_0]$ can be calculated as $F^{(a)}_{T_2}(5T_0 \mid \mathcal{E}_0) = \int_0^{5T_0} f^{(a)}_{T_2}(t \mid \mathcal{E}_0)dt = 0.8788$.

In fig. 2-12 the approximation $f^{(a)}_{T_1}(t \mid \mathcal{E}_0)$ is shown for problem 4 along with the 1st upper and the 1st lower bounds. Theoretically, the probability of failure in the interval $[0, 7T_0]$ is 1 in this case. The considered approximation provides $F^{(a)}_{T_1}(7T_0 \mid \mathcal{E}_0) = 1.0015$. This accuracy can generally not be expected in case of longer excitation intervals under stationary conditions (stationary excitation with constant barrier).

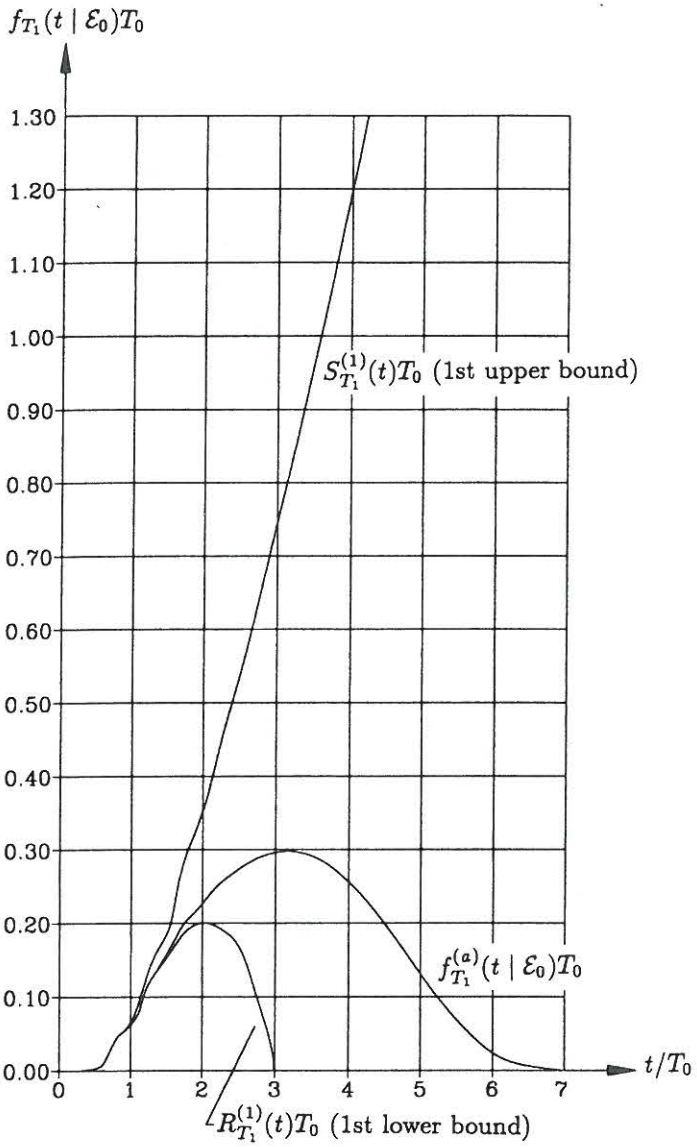

Fig. 2-12: First-passage time probability density function. Deterministic start problem with symmetric time varying double barriers. $\zeta = 0.08, b(t) = -a(t) = 2.5\sigma_{X,0}\left(1 - \frac{1}{7}\frac{t}{T_0}\right)$, $t \in [0, 7T_0]$. Nielsen (1980).

For an oscillatory system with time-invariant safe domain subjected to stationary white noise excitation, the first passage time probability density function for both deterministic and stochastic start problems can be written as follows, Mark (1966)

$$f_{T_1}(t \mid \mathcal{E}_{t_0}) = \sum_{n=1}^{\infty} c_n e^{-\lambda_n (t - t_0)} \qquad (2-117)$$

λ_n signifies the nth eigenvalue of the Kolmogorov forward and backward operators with absorption on the entrance and the exit part of the failure surface ∂S in the phase space, respectively. (2-117) is proved in section 3.2.2, cf. (3-146), to be generally valid for all Markov systems described by (2-80), if

80), if only the structural system and the safe domain are time-invariant, and the increments of the generating sources $dW(t)$ and $dV(t)$ are stationary. The structural system is time invariant if the drift vector and the diffusion vectors are not explicitly dependent on time, i.e. $\mathbf{c}(\mathbf{z}(t),t) = \mathbf{c}(\mathbf{z}(t))$ and $\mathbf{d}(\mathbf{Z}(t),t) = \mathbf{d}(\mathbf{Z}(t))$. The smallest eigenvalue, λ_1, is known as the limiting decay rate, corresponding to the asymptotic behaviour as follows from (2-117), $f_{T_1}(t \mid \mathcal{E}_{t_0}) \propto c_1 e^{-\lambda_1(t-t_0)}$. In case of independent out-crossings, $\lambda_1 = f_1^+$, cf. (2-72). As seen from fig. 2-6 and fig. 2-8 the simulation results are asymptotically parallel as $t - t_0 \to \infty$ to the approximations $f_{T_1}^{(a)}(t \mid \mathcal{E}_0)$ and $f_{T_1}^{(b)}(t \mid \mathcal{E}_0)$. This means that the limiting decay rate can be calculated relatively accurately from this approximation. This property has been observed in other applications to the integral equation method, where similar kernel approximations are applied as seen in the succeeding numerical example 2-4.

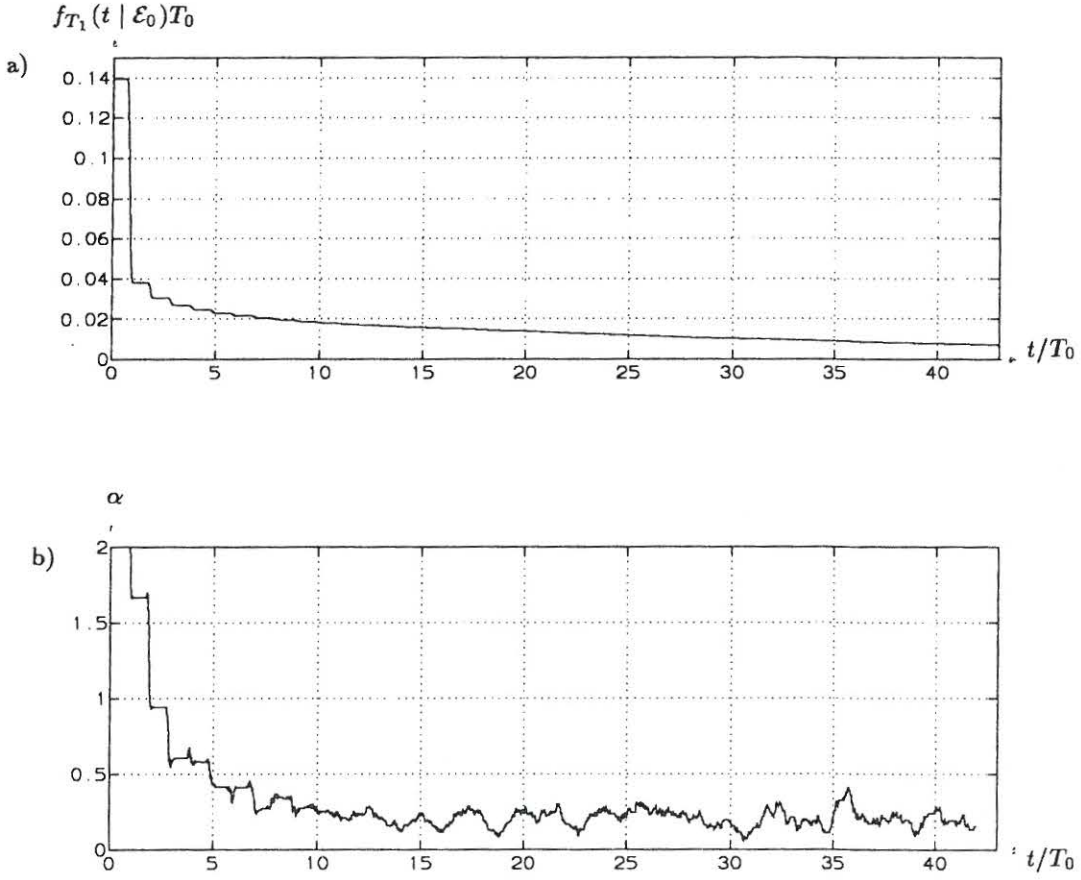

Fig. 2-13: a) First-passage time probability density function. b) Decay rate coefficients. Simulation results based on 100000 out-crossings. Linear SDOF oscillator. Single barrier stochastic start problem. $\zeta = 0.01$, $b = 2.0\sigma_{X,0}$.

The existence of a limiting decay rate has been demonstrated in fig. 2-13, where the first-passage time probability density function has been estimated from Monte-Carlo simulation based on (2-31) for a single barrier stochastic start problem with $\zeta = 0.01$ og $b = 2.0\sigma_{X,0}$. The length of the applied time series has been adjusted so totally 100000 intervals spent in the safe domain is used in the estimation of $F_L(\tau)$. Define the so-called decay rate coefficient $\alpha = \lambda_1/f_1^+$. A running estimate, $\alpha(t)$, is next defined from the estimated values of $f_{T_1}(t \mid \mathcal{E}_0)$ and the value 1 period ahead, $f_{T_1}(t + T_0 \mid \mathcal{E}_0)$ assuming $f_{T_1}(t \mid \mathcal{E}_0) = c_1 e^{-\lambda_1 t}$. As seen from fig. 2-13b a stationary estimate $\alpha \sim 0.2$ is obtained for $t > 10T_0$. At the estimation of $f_{T_1}(t \mid \mathcal{E}_0)$ no attempts were done to adjust the simulation results to

the boundary value $f_{T_1}(0 \mid \mathcal{E}_0) = \frac{1}{E[L]} = \frac{f_1^+}{P(S_0)} = 0.13849$. The corresponding simulated values are $f_{T_1}(0 \mid \mathcal{E}_0) = 0.13966$.

Example 2-3: Bounding techniques related to the integral equation (2-59)

Bounds similar to (2-110), (2-111) and (2-112) can with an identical argumentation be derived from (2-59) and (2-60). The 1st upper bound and the 1st lower bound to the first-passage probability density function based on these results become

$$f_{T_1}(t \mid \mathcal{E}_{t_0}) \leq S_{T_1}^{(1)}(t; \mathcal{E}_{\tau_1,\cdots,\tau_m}) = f_1^+(t; \mathcal{E}_{\tau_1,\cdots,\tau_m} \mid \mathcal{E}_{t_0}) \qquad (2-118)$$

$$f_{T_1}(t \mid \mathcal{E}_{t_0}) \geq R_{T_1}^{(1)}(t; \mathcal{E}_{\tau_1,\cdots,\tau_m}) = f_1^+(t; \mathcal{E}_{\tau_1,\cdots,\tau_m} \mid \mathcal{E}_{t_0}) - \int_{t_0}^{t} f_2^{++}(t_1, t; \mathcal{E}_{\tau_1,\cdots,\tau_m} \mid \mathcal{E}_{t_0})\, dt_1 \qquad (2-119)$$

(2-118) was originally stated by Shinozuka and Yang (1969). Assuming the considered response processes to be sufficiently smooth the right-hand side of (2-118) forms a non-increasing sequence, and the right-hand side of (2-119) forms a non-decreasing sequence as the number m of the control points is increased. Hence, these sequences converge to specific limits as $m \to \infty$. Let $\delta_m = \max(\tau_{i+1} - \tau_i)$. If $\delta_m \to 0$ as $m \to \infty$, it can further be shown that the sequences converge monotonously to the first-passage time probability density function, Thoft-Christensen and Nielsen (1982)

$$S_{T_1}^{(1)}(t; \mathcal{E}_{\tau_1,\cdots,\tau_m}) \downarrow f_{T_1}(t \mid \mathcal{E}_{t_0}) \quad \text{as} \quad \delta_m \to 0 \qquad (2-120)$$

$$R_{T_1}^{(1)}(t; \mathcal{E}_{\tau_1,\cdots,\tau_m}) \uparrow f_{T_1}(t \mid \mathcal{E}_{t_0}) \quad \text{as} \quad \delta_m \to 0 \qquad (2-121)$$

For a fixed m the optimal upper and lower bounds can be found by the instants of time $\tau_1, \cdots, \tau_m$ which minimize the upper bound and maximize the lower bound. These improved bounds become, Thoft-Christensen and Nielsen (1982)

$$S_{T_1}^{(1)*}(t, m) = \min_{t_0 < \tau_1 < \cdots < \tau_m < t} S_{T_1}^{(1)}(t; \mathcal{E}_{\tau_1,\cdots,\tau_m}) \qquad (2-122)$$

$$R_{T_1}^{(1)*}(t, m) = \max_{t_0 < \tau_1 < \cdots < \tau_m < t} R_{T_1}^{(1)}(t; \mathcal{E}_{\tau_1,\cdots,\tau_m}) \qquad (2-123)$$

If the first-passage time probability density function is a non-increasing function with time as is the case for the stochastic start problem with stationary response processes and a time-invariant safe domain, these bounds may be sharpened in the following way, Thoft-Christensen and Nielsen (1982)

$$f_{T_1}(t \mid \mathcal{E}_{t_0}) \leq S_{T_1}^{(1)**}(t, m) = \max_{t_1 \in [t, \infty[} S_{T_1}^{(1)*}(t_1, m) \qquad (2-124)$$

$$f_{T_1}(t \mid \mathcal{E}_{t_0}) \geq R_{T_1}^{(1)**}(t, m) = \min_{t_1 \in]t_0, t]} R_{T_1}^{(1)*}(t_1, m) \qquad (2-125)$$

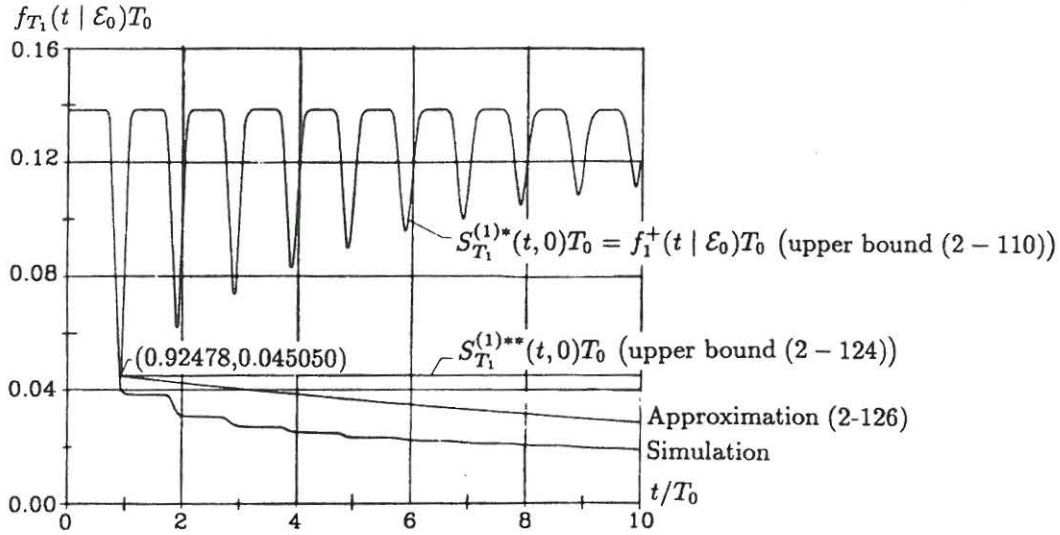

Fig. 2-14: Upper bounds to the first-passage time probability density function. Single barrier stochastic start problem. $m = 0, \quad \zeta = 0.01, \quad b = 2.0\,\sigma_{X,0}$. Thoft-Christensen and Nielsen (1982).

The linear single-degree-of-freedom system oscillator (2-102) is considered again. A single barrier first-passage problem with stochastic start is considered. The damping ratio is $\zeta = 0.01$ and the barrier level is $b = 2.0\sigma_{X,0}$.

Fig. 2-14 shows the variation with the time of the first upper bounds $S_{T_1}^{(1)*}(t,0)$ and $S_{T_1}^{(1)**}(t,0)$ as given by (2-122) and (2-124) for the case of no internal control points, i.e. $m = 0$. The first local minimum $f_1^+(t_1 \mid \mathcal{E}_0)T_0 = 0.045050$ at the time $t = t_1 = 0.92478\,T_0$ is also the global minimum, so $S_{T_1}^{(1)**}(t,0)$ follows $f_1^+(t \mid \mathcal{E}_0)$ up to $t = t_1$ and is given by $S_{T_1}^{(1)**}(t,0) = f_1^+(t_1 \mid \mathcal{E}_0)$ for $t > t_1$. The indicated simulation result was obtained from ergodic sampling based on (2-31) with analytical calculation of $\frac{1}{E[L]} = \frac{f_1^+}{P(S_0)}$ to insure the correct boundary value of $f_{T_1}(0 \mid S_0)$.

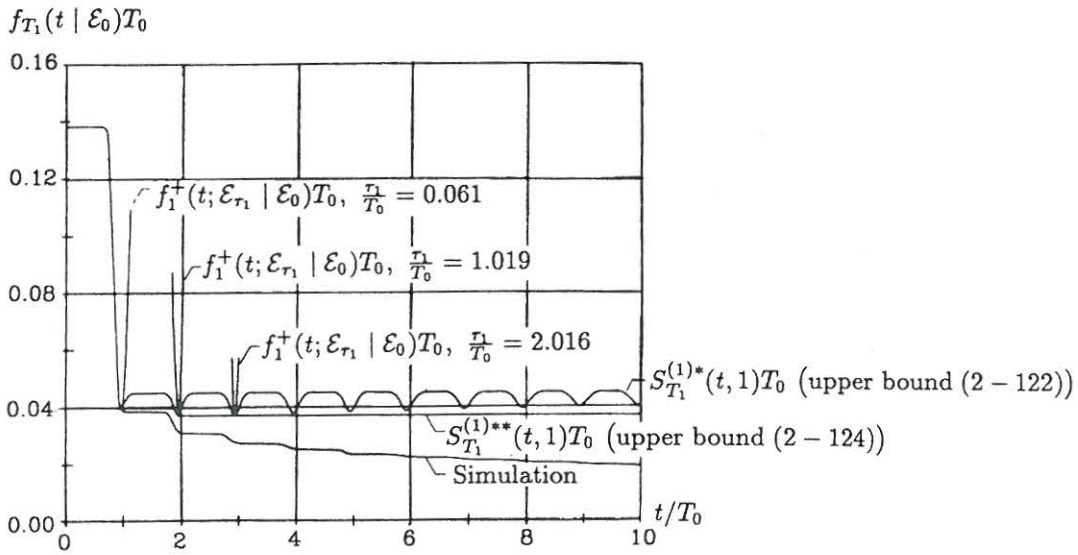

Fig. 2-15: Upper bounds to the first-passage time probability density function. Single barrier stochastic start problem. $m = 1, \quad \zeta = 0.01, \quad b = 2.0\,\sigma_{X,0}$. Thoft-Christensen and Nielsen (1982).

$\frac{\tau_1}{T_0}$	$\frac{t_1}{T_0}$	$f_1^+(t_1, \mathcal{E}_{\tau_1} \mid \mathcal{E}_0)T_0$
0.061	0.961	0.04050
1.019	1.941	0.03723
2.016	2.939	0.03712

Table 2-1: Local minima of the 1st upper bound, $m = 1$.

In fig. 2-15 the time-variation of the corresponding upper bounds $S_{T_1}^{(1)*}(t,1)$ and $S_{T_1}^{(1)**}(t,1)$ with 1 control point is shown. Generally, the optimal position of this control time, τ_1, is placed $0.90T_0 - 0.92T_0$ prior to the variable time t. This is approximately the time needed to perform an eigenvibration in the safe domain from $[x, \dot{x}] = [b, 0]$ until some position on the exit boundary $[b, \dot{x}]$, $\dot{x} > 0$ is reached. For a corresponding symmetric double boundary problem τ_1 will be approximately $0.40T_0 - 0.42T_0$. In any case the search for an optimal position of τ_1 can be restricted to a very narrow interval, and it can be performed correspondingly fast. The local minima of $f_1^+(t; \mathcal{E}_{\tau_1} \mid \mathcal{E}_0)$, attained at the instants of time $t = t_1$, and the corresponding optimal positions of the control time τ_1 are shown in table 2-1. The local minima of $S_{T_1}^{(1)*}(t,1)$ are decreasing up to and including the 3rd local minimum, so $S_{T_1}^{(1)**}(t,1)$ is passing through these minima, and is constant to the right of the 3rd local minimum.

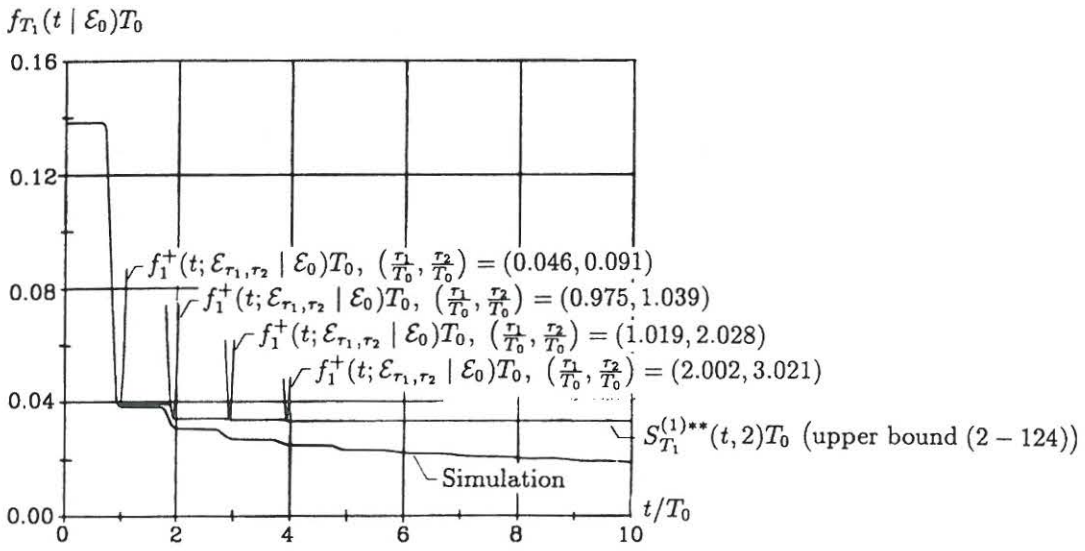

Fig. 2-16: Upper bounds to the first-passage time probability density function. Single barrier stochastic start problem. $m = 2$, $\zeta = 0.01$, $b = 2.0\,\sigma_{X,0}$. Thoft-Christensen and Nielsen (1982).

$\frac{\tau_1}{T_0}$	$\frac{\tau_2}{T_0}$	$\frac{t_1}{T_0}$	$f_1^+(t_1; \mathcal{E}_{\tau_1,\tau_2} \mid \mathcal{E}_0)T_0$
0.046	0.091	0.978	0.03943
0.975	1.039	1.937	0.03415
1.019	2.028	2.950	0.03375
2.002	3.021	3.942	0.03320

Table 2-2: Local 2-2: Local minima of the first upper bound, $m = 2$.

80), if only the structural system and the safe domain are time-invariant, and the increments of the generating sources $dW(t)$ and $dV(t)$ are stationary. The structural system is time invariant if the drift vector and the diffusion vectors are not explicitly dependent on time, i.e. $\mathbf{c}(\mathbf{z}(t),t) = \mathbf{c}(\mathbf{z}(t))$ and $\mathbf{d}(\mathbf{Z}(t),t) = \mathbf{d}(\mathbf{Z}(t))$. The smallest eigenvalue, λ_1, is known as the limiting decay rate, corresponding to the asymptotic behaviour as follows from (2-117), $f_{T_1}(t \mid \mathcal{E}_{t_0}) \propto c_1 e^{-\lambda_1(t-t_0)}$. In case of independent out-crossings, $\lambda_1 = f_1^+$, cf. (2-72). As seen from fig. 2-6 and fig. 2-8 the simulation results are asymptotically parallel as $t - t_0 \to \infty$ to the approximations $f_{T_1}^{(a)}(t \mid \mathcal{E}_0)$ and $f_{T_1}^{(b)}(t \mid \mathcal{E}_0)$. This means that the limiting decay rate can be calculated relatively accurately from this approximation. This property has been observed in other applications to the integral equation method, where similar kernel approximations are applied as seen in the succeeding numerical example 2-4.

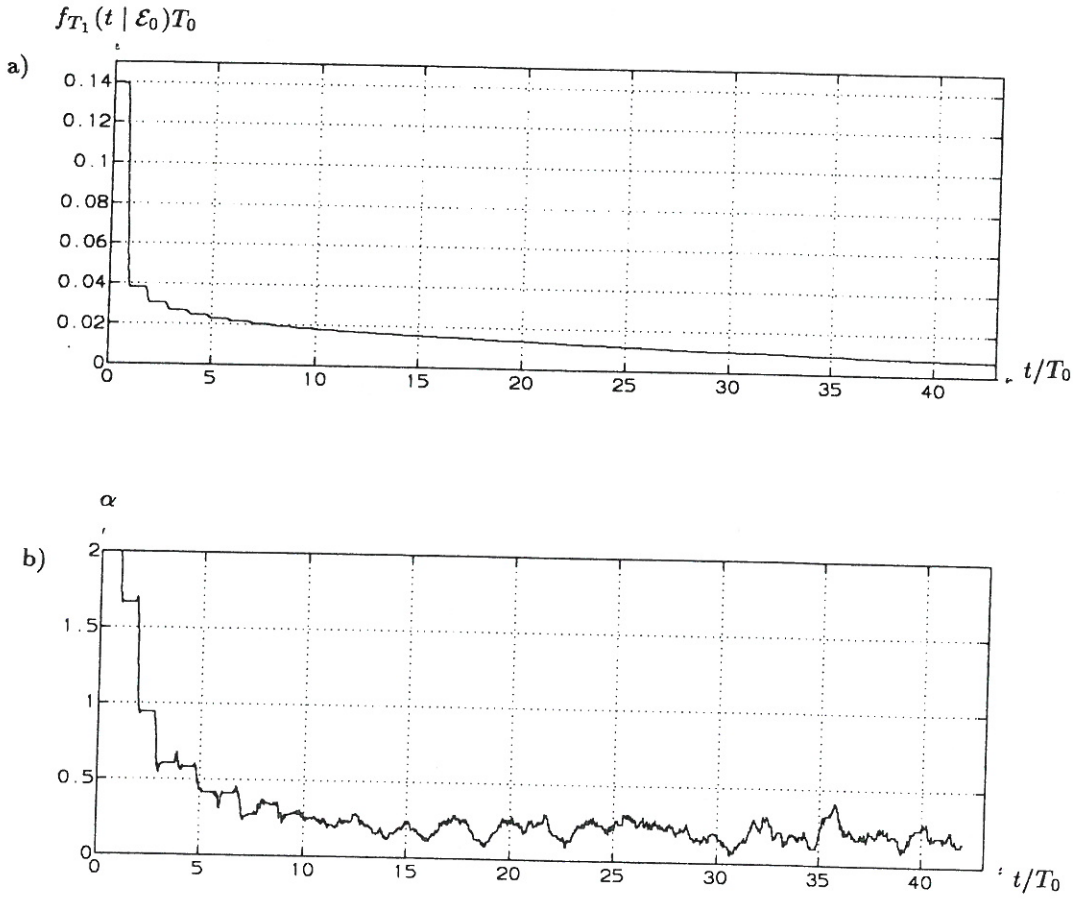

Fig. 2-13: a) First-passage time probability density function. b) Decay rate coefficients. Simulation results based on 100000 out-crossings. Linear SDOF oscillator. Single barrier stochastic start problem. $\zeta = 0.01$, $b = 2.0\sigma_{X,0}$.

The existence of a limiting decay rate has been demonstrated in fig. 2-13, where the first-passage time probability density function has been estimated from Monte-Carlo simulation based on (2-31) for a single barrier stochastic start problem with $\zeta = 0.01$ og $b = 2.0\sigma_{X,0}$. The length of the applied time series has been adjusted so totally 100000 intervals spent in the safe domain is used in the estimation of $F_L(\tau)$. Define the so-called decay rate coefficient $\alpha = \lambda_1/f_1^+$. A running estimate, $\alpha(t)$, is next defined from the estimated values of $f_{T_1}(t \mid \mathcal{E}_0)$ and the value 1 period ahead, $f_{T_1}(t + T_0 \mid \mathcal{E}_0)$ assuming $f_{T_1}(t \mid \mathcal{E}_0) = c_1 e^{-\lambda_1 t}$. As seen from fig. 2-13b a stationary estimate $\alpha \sim 0.2$ is obtained for $t > 10T_0$. At the estimation of $f_{T_1}(t \mid \mathcal{E}_0)$ no attempts were done to adjust the simulation results to

the boundary value $f_{T_1}(0 \mid \mathcal{E}_0) = \frac{1}{E[L]} = \frac{f_1^+}{P(S_0)} = 0.13849$. The corresponding simulated values are $f_{T_1}(0 \mid \mathcal{E}_0) = 0.13966$.

Example 2-3: Bounding techniques related to the integral equation (2-59)

Bounds similar to (2-110), (2-111) and (2-112) can with an identical argumentation be derived from (2-59) and (2-60). The 1st upper bound and the 1st lower bound to the first-passage probability density function based on these results become

$$f_{T_1}(t \mid \mathcal{E}_{t_0}) \leq S_{T_1}^{(1)}(t; \mathcal{E}_{\tau_1,\cdots,\tau_m}) = f_1^+(t; \mathcal{E}_{\tau_1,\cdots,\tau_m} \mid \mathcal{E}_{t_0}) \tag{2-118}$$

$$f_{T_1}(t \mid \mathcal{E}_{t_0}) \geq R_{T_1}^{(1)}(t; \mathcal{E}_{\tau_1,\cdots,\tau_m}) = f_1^+(t; \mathcal{E}_{\tau_1,\cdots,\tau_m} \mid \mathcal{E}_{t_0}) - \int_{t_0}^{t} f_2^{++}(t_1, t; \mathcal{E}_{\tau_1,\cdots,\tau_m} \mid \mathcal{E}_{t_0})\, dt_1 \tag{2-119}$$

(2-118) was originally stated by Shinozuka and Yang (1969). Assuming the considered response processes to be sufficiently smooth the right-hand side of (2-118) forms a non-increasing sequence, and the right-hand side of (2-119) forms a non-decreasing sequence as the number m of the control points is increased. Hence, these sequences converge to specific limits as $m \to \infty$. Let $\delta_m = \max(\tau_{i+1} - \tau_i)$. If $\delta_m \to 0$ as $m \to \infty$, it can further be shown that the sequences converge monotonously to the first-passage time probability density function, Thoft-Christensen and Nielsen (1982)

$$S_{T_1}^{(1)}(t; \mathcal{E}_{\tau_1,\cdots,\tau_m}) \downarrow f_{T_1}(t \mid \mathcal{E}_{t_0}) \quad \text{as} \quad \delta_m \to 0 \tag{2-120}$$

$$R_{T_1}^{(1)}(t; \mathcal{E}_{\tau_1,\cdots,\tau_m}) \uparrow f_{T_1}(t \mid \mathcal{E}_{t_0}) \quad \text{as} \quad \delta_m \to 0 \tag{2-121}$$

For a fixed m the optimal upper and lower bounds can be found by the instants of time $\tau_1, \cdots, \tau_m$ which minimize the upper bound and maximize the lower bound. These improved bounds become, Thoft-Christensen and Nielsen (1982)

$$S_{T_1}^{(1)*}(t, m) = \min_{t_0 < \tau_1 < \cdots < \tau_m < t} S_{T_1}^{(1)}(t; \mathcal{E}_{\tau_1,\cdots,\tau_m}) \tag{2-122}$$

$$R_{T_1}^{(1)*}(t, m) = \max_{t_0 < \tau_1 < \cdots < \tau_m < t} R_{T_1}^{(1)}(t; \mathcal{E}_{\tau_1,\cdots,\tau_m}) \tag{2-123}$$

If the first-passage time probability density function is a non-increasing function with time as is the case for the stochastic start problem with stationary response processes and a time-invariant safe domain, these bounds may be sharpened in the following way, Thoft-Christensen and Nielsen (1982)

$$f_{T_1}(t \mid \mathcal{E}_{t_0}) \leq S_{T_1}^{(1)**}(t, m) = \max_{t_1 \in [t, \infty[} S_{T_1}^{(1)*}(t_1, m) \tag{2-124}$$

$$f_{T_1}(t \mid \mathcal{E}_{t_0}) \geq R_{T_1}^{(1)**}(t, m) = \min_{t_1 \in]t_0, t]} R_{T_1}^{(1)*}(t_1, m) \tag{2-125}$$

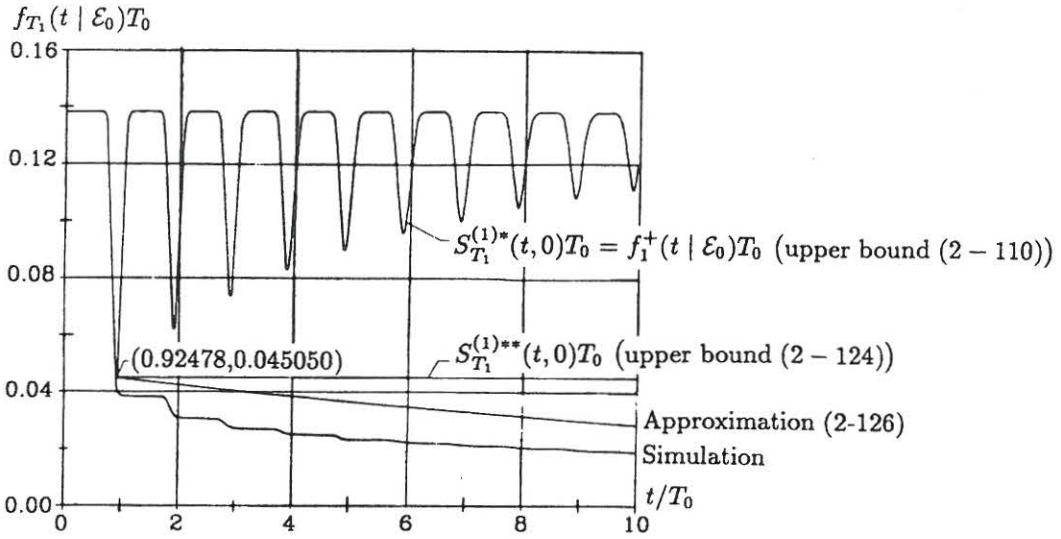

Fig. 2-14: Upper bounds to the first-passage time probability density function. Single barrier stochastic start problem. $m = 0, \quad \zeta = 0.01, \quad b = 2.0\,\sigma_{X,0}$. Thoft-Christensen and Nielsen (1982).

The linear single-degree-of-freedom system oscillator (2-102) is considered again. A single barrier first-passage problem with stochastic start is considered. The damping ratio is $\zeta = 0.01$ and the barrier level is $b = 2.0\sigma_{X,0}$.

Fig. 2-14 shows the variation with the time of the first upper bounds $S_{T_1}^{(1)*}(t,0)$ and $S_{T_1}^{(1)**}(t,0)$ as given by (2-122) and (2-124) for the case of no internal control points, i.e. $m = 0$. The first local minimum $f_1^+(t_1 \mid \mathcal{E}_0)T_0 = 0.045050$ at the time $t = t_1 = 0.92478\,T_0$ is also the global minimum, so $S_{T_1}^{(1)**}(t,0)$ follows $f_1^+(t \mid \mathcal{E}_0)$ up to $t = t_1$ and is given by $S_{T_1}^{(1)**}(t,0) = f_1^+(t_1 \mid \mathcal{E}_0)$ for $t > t_1$. The indicated simulation result was obtained from ergodic sampling based on (2-31) with analytical calculation of $\frac{1}{E[L]} = \frac{f_1^+}{P(S_0)}$ to insure the correct boundary value of $f_{T_1}(0 \mid S_0)$.

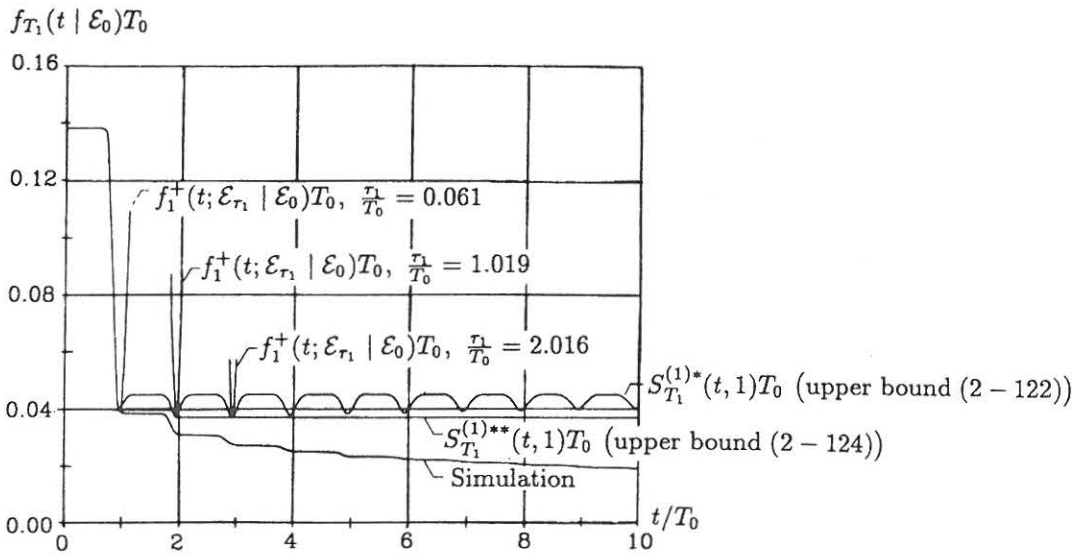

Fig. 2-15: Upper bounds to the first-passage time probability density function. Single barrier stochastic start problem. $m = 1, \quad \zeta = 0.01, \quad b = 2.0\,\sigma_{X,0}$. Thoft-Christensen and Nielsen (1982).

$\frac{\tau_1}{T_0}$	$\frac{t_1}{T_0}$	$f_1^+(t_1, \mathcal{E}_{\tau_1} \mid \mathcal{E}_0)T_0$
0.061	0.961	0.04050
1.019	1.941	0.03723
2.016	2.939	0.03712

Table 2-1: Local minima of the 1st upper bound, $m = 1$.

In fig. 2-15 the time-variation of the corresponding upper bounds $S_{T_1}^{(1)*}(t,1)$ and $S_{T_1}^{(1)**}(t,1)$ with 1 control point is shown. Generally, the optimal position of this control time, τ_1, is placed $0.90T_0 - 0.92T_0$ prior to the variable time t. This is approximately the time needed to perform an eigenvibration in the safe domain from $[x, \dot{x}] = [b, 0]$ until some position on the exit boundary $[b, \dot{x}]$, $\dot{x} > 0$ is reached. For a corresponding symmetric double boundary problem τ_1 will be approximately $0.40T_0 - 0.42T_0$. In any case the search for an optimal position of τ_1 can be restricted to a very narrow interval, and it can be performed correspondingly fast. The local minima of $f_1^+(t; \mathcal{E}_{\tau_1} \mid \mathcal{E}_0)$, attained at the instants of time $t = t_1$, and the corresponding optimal positions of the control time τ_1 are shown in table 2-1. The local minima of $S_{T_1}^{(1)*}(t,1)$ are decreasing up to and including the 3rd local minimum, so $S_{T_1}^{(1)**}(t,1)$ is passing through these minima, and is constant to the right of the 3rd local minimum.

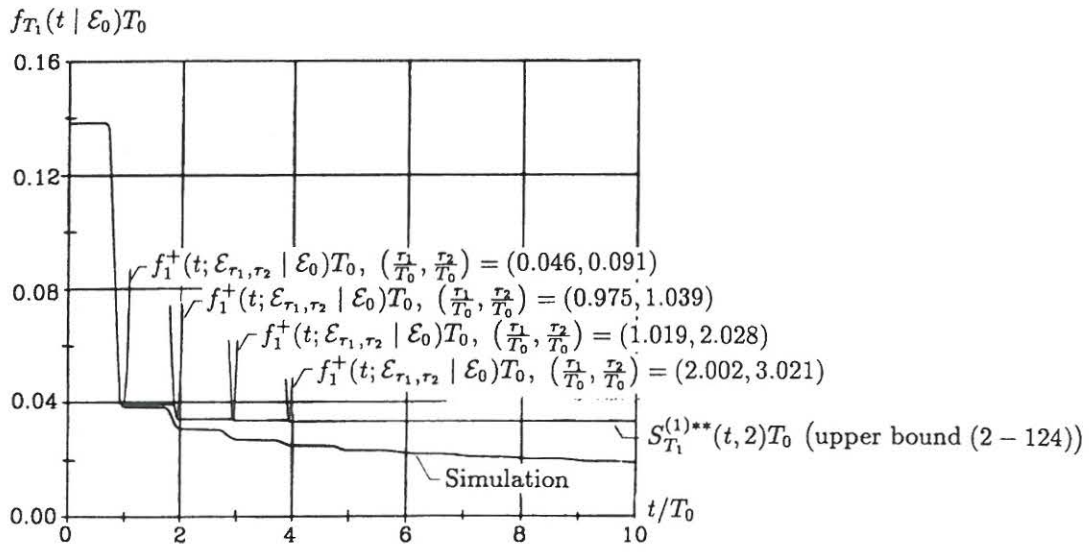

Fig. 2-16: Upper bounds to the first-passage time probability density function. Single barrier stochastic start problem. $m = 2$, $\zeta = 0.01$, $b = 2.0\,\sigma_{X,0}$. Thoft-Christensen and Nielsen (1982).

$\frac{\tau_1}{T_0}$	$\frac{\tau_2}{T_0}$	$\frac{t_1}{T_0}$	$f_1^+(t_1; \mathcal{E}_{\tau_1,\tau_2} \mid \mathcal{E}_0)T_0$
0.046	0.091	0.978	0.03943
0.975	1.039	1.937	0.03415
1.019	2.028	2.950	0.03375
2.002	3.021	3.942	0.03320

Table 2-2: Local 2-2: Local minima of the first upper bound, $m = 2$.

Fig. 2-16 shows the corresponding results with 2 control times τ_1 and τ_2. Again the optimal position of the control times τ_1 and τ_2 is placed at relatively narrow intervals explained by the dynamics of the oscillator, making the minimization of $f_1^+(t; \mathcal{E}_{\tau_1,\tau_2} \mid \mathcal{E}_0)$ relatively simple. The local minima of $S_{T_1}^{(1)*}(t,2)$, attained at the instants of time $t = t_2$, and the corresponding optimal positions of the control times τ_1 and τ_2 are shown in table 2-2. The local minima of $S_{T_1}^{(1)*}(t,2)$ are decreasing up to and including the 4th local minimum, so $S_{T_1}^{(1)**}(t,2)$ is passing through these minima, and is constant to the right of the 4th local minimum.

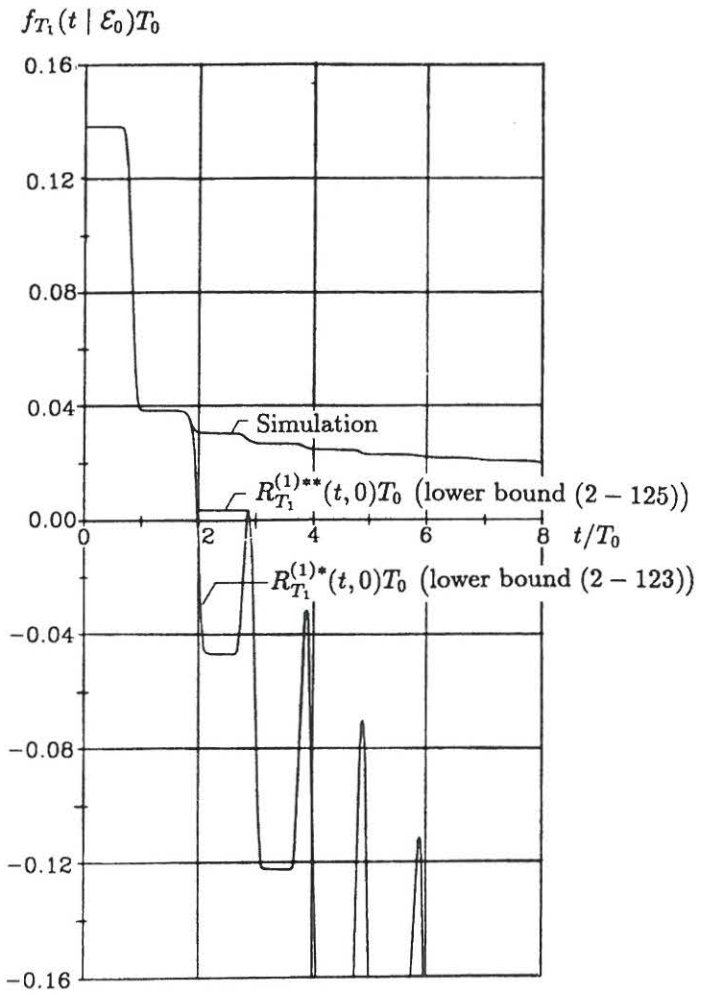

Fig. 2-17: Lower bounds to the first-passage time probability density function. Single barrier stochastic start problem. $m = 0, \quad \zeta = 0.01, \quad b = 2.0\,\sigma_{X,0}$. Thoft-Christensen and Nielsen (1982).

$\frac{t_1}{T_0}$	$R_{T_1}^{(1)*}(t_1,0)T_0$
1.500	0.03872
2.888	0.00374
3.892	−0.03132
4.893	−0.07014
5.893	−0.1110

Table 2-3: Local maxima of the 1st lower bound, $m = 0$.

In fig. 2-17 the variation with the time of the first lower bounds $R_{T_1}^{(1)*}(t,0)$ and $R_{T_1}^{(1)**}(t,0)$ as given by (2-123) and (2-125) for the case of no internal control points is shown. The local maxima of $R_{T_1}^{(1)*}(t,0)$, attained at the instants of time $t = t_1$ are shown in table 2-3. $R_{T_1}^{(1)**}(t,0)$ is passing through these maxima, and is constant to the left until its intersection with $R_{T_1}^{(1)*}(t,0)$, after which $R_{T_1}^{(1)**}(t,0)$ follows $R_{T_1}^{(1)*}(t,0)$ up to the previous local maximum. $R_{T_1}^{(1)**}(t,0)$ is only of interest as long as it remains positive.

Fig. 2-18 shows the corresponding lower bounds $R_{T_1}^{(1)*}(t,1)$ and $R_{T_1}^{(1)**}(t,1)$ with 1 control point. The local maxima of $R_{T_1}^{(1)*}(t,1)$, attained at the instants of time $t = t_1$, and corresponding optimal position of the control time τ_1 are shown in table 2-4.

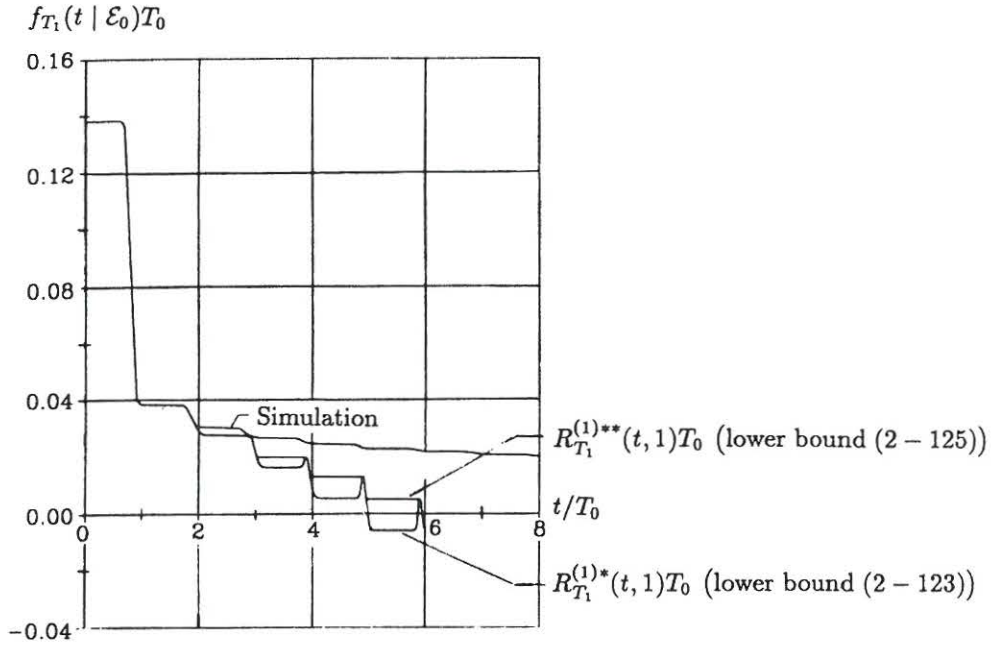

Fig. 2-18: Lower bounds to the first-passage time probability density function. Single barrier stochastic start problem. $m = 1$, $\zeta = 0.01$, $b = 2.0\,\sigma_{X,0}$. Thoft-Christensen and Nielsen (1982).

$\frac{\tau_1}{T_0}$	$\frac{t_1}{T_0}$	$R_{T_1}^{(1)*}(t_1,1)T_0$
1.50	1.50	0.0387
2.50	1.58	0.0278
3.89	2.95	0.0202
4.89	3.96	0.0132
5.89	4.95	0.00530

Table 2-4: Local maxima of the 1st lower bound, $m = 1$.

The conclusion to be drawn from the numerical example is that the bounds (2-122), (2-121) with optimally selected control points are significantly sharper than the corresponding bounds without control

points. Further, the optimal position of the control points is confined to relatively narrow intervals determined by the dynamics of the system, and can hence be determined rather easily.

In stationary start problems with constant safe domain $S_{T_1}^{(1)}(t,0)$ attains a global minimum at the first local minimum, t_1, as shown in fig. 2-13. This observation has motivated the following approximation to the first-passage time probability density function, Thoft-Christensen and Nielsen (1982)

$$f_{T_1}^{(\alpha)}(t \mid \mathcal{E}_0) = \begin{cases} f_1^+(t \mid \mathcal{E}_0) & , \quad t \in [0, t_1] \\ f_1^+(t_1 \mid \mathcal{E}_0) e^{-\alpha f_1^+(0|\mathcal{E}_0)(t-t_1)} & , \quad t \in]t_1, \infty[\end{cases} \qquad (2-126)$$

where

$$\alpha = \frac{f_1^+(t_1 \mid \mathcal{E}_0)}{f_1^+(0 \mid \mathcal{E}_0)} \left(1 - \int_0^{t_1} f_1^+(u \mid \mathcal{E}_0) du \right)^{-1} \qquad (2-127)$$

The decay rate coefficient α as given by (2-127) implies a normalization of (2-126) to unit probability mass. Since $f_1^+(t \mid \mathcal{E}_0)$ is an upper bound for $t \in [0, t_1]$, (2-126) will effectively provide an upper bound to the failure probability. $\alpha f_1^+(0 \mid \mathcal{E}_0) = \alpha \frac{f_1^+(0)}{P(S_0)}$ indicates an approximation to the limiting decay rate, λ_1. For narrow-banded response processes, $\alpha < 1$, unless the barrier level is extremely low. In this case the out-crossing events occur in clumps. $\frac{1}{\alpha}$ is a measure of the average number of out-crossings in a clump, which Lyon (1960, 1961) estimated as the ratio between the out-crossing rate of a narrow-banded process and the out-crossing rate of its envelope.

In fig. 2-19 the variation of α with the barrier level b for four values of the damping ratio is shown. From this figure it is seen that the approximation (2-126) is most favourable, when the damping is low and the barrier level is moderate. For $b = 2.0\sigma_{X,0}$ and $\zeta = 0.01$ is found $\alpha \sim 0,38$, which is well above the simulation result $\alpha \simeq 0.2$ indicated in fig. 2-136. This is another indication that (2-126) provides upper bounds for the failure probability.

Consider a single barrier problem with the upper barrier $b = x$. The probability of failure in the interval $[0, t]$ is denoted $P_f([0, t]; x)$. From (2-13) it follows that

$$P_f([0, t]; x) = 1 - P(X(0) \leq x) + P(X(0) \geq x) F_{T_1}(t; x \mid \mathcal{E}_0) \qquad (2-128)$$

where $F_{T_1}(t; x \mid \mathcal{E}_0)$ is the probability of failure with the upper barrier $b = x$ conditioned upon the event $\mathcal{E}_0$. The probability distribution function of the maximum value $X_{\max} = \max_{\tau \in [0,t]} X(\tau)$ then becomes

$$F_{X_{\max}}(x; [0, t]) = 1 - P_f([0, t]; x) \qquad (2-129)$$

$F_{T_1}(t; x \mid \mathcal{E}_0)$ is calculated based on the approximation (2-126). The so-called peak factor, i.e. the expected value of $X_{\max}$ in units of the stationary standard deviation, $\sigma_{X,0}$, is shown in fig. 2-20 for four values of the damping ratio as a function of the excitation time in units of the linear eigenperiod T_0. As a standard of reference the following well-known approximation for the peak factor of Gaussian response processes is also shown, Davenport (1964)

$$E[X_{\max}] = \sqrt{2 \ln(\tau)} + \frac{0.577216}{\sqrt{2 \ln(\tau)}} \quad , \quad \tau = \frac{t}{T_0} \qquad (2-130)$$

(2-130) provides an upper bound for the peak factor as seen from fig. 2-20.

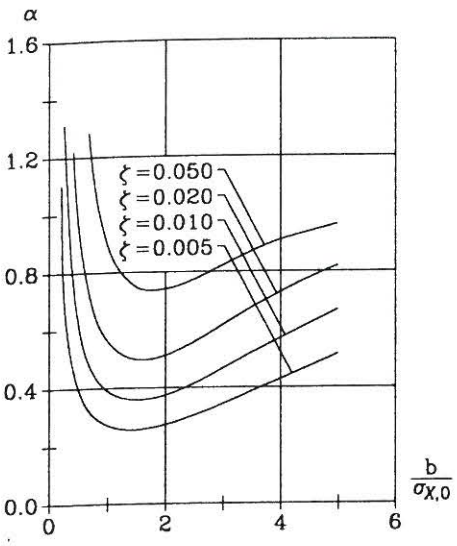

Fig. 2-19: Variation of the decay rate coefficient α as a function of the threshold level and the damping ratio. Thoft-Christensen and Nielsen (1982).

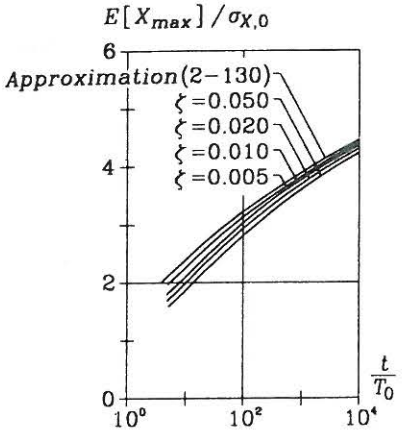

Fig. 2-20: Variation of the peak factor as a function of the excitation time and the damping ratio. Thoft-Christensen and Nielsen (1982).

Example 2-4: Approximations for the kernel of the integral equations (2-48) and (2-51)

If the conditioned first-passage time probability density function $f_{T_1}(t_1 \mid \mathcal{E}_{t_0} \cap C_i^+)$ is determined as solution to the integral equation (2-48), the unconditional first-passage time probability density function next follows from (2-37). In the present example approximate solutions to the integral equation (2-48) are obtained by truncating the series expansions of the numerator and the denominator of the kernel (2-50) to the first term, Nielsen (1990a)

$$f_1^+\left(t_1 \mid \mathcal{E}_{t_0} \cap \mathcal{F}_{t_2}^{(1)} \cap C_i^+\right) \simeq \frac{f_3^{+++}(t_2, t_1, t \mid \mathcal{E}_{t_0})}{f_2^{++}(t_2, t \mid \mathcal{E}_0)} \qquad (2-131)$$

The integral equation is solved with the exact inhomogeneity (2-49). The resulting approximate first-

passage time probability density function obtained from numerical solution of (2-48) and succeeding insertion into (2-37) is designated $f_{T_1}^{(e)}(t \mid \mathcal{E}_{t_0})$. As comparison the approximations $f_{T_1}^{(a)}(t \mid \mathcal{E}_{t_0})$ and $f_{T_1}^{(b)}(t \mid \mathcal{E}_{t_0})$ will also be indicated, obtained from numerical solution of (2-35) with the kernel approximation (2-104), (2-105) and (2-106).

Generally, if the conditioned first-passage time probability density function $f_T(t_n \mid \mathcal{E}_{t_0} \cap C_{t_{n-1}}^+ \cap \cdots \cap C_{t_1}^+ \cap C_t^+)$ is determined from (2-51), the first-passage time probability density can be determined from (2-42). The following approximation can be used for the kernel of (2-51), cf. (2-54)

$$f_1^+\left(t_n \mid \mathcal{E}_{t_0} \cap \mathcal{F}_{t_{n+1}}^{(1)} \cap C_{t_{n-1}}^+ \cap \cdots \cap C_{t_1}^+ \cap C_t^+\right) \simeq \frac{f_{n+2}^{+++\cdots++}(t_{n+1}, t_n, t_{n-1}, \cdots, t_1, t \mid \mathcal{E}_{t_0})}{f_{n+1}^{++\cdots++}(t_{n+1}, t_{n-1}, \cdots, t_1, t \mid \mathcal{E}_{t_0})} \quad (2-132)$$

The inhomogeneity can be evaluated as follows

$$f_1^+(t_n \mid \mathcal{E}_{t_0} \cap C_{t_{n-1}}^+ \cap \cdots \cap C_{t_1}^+ \cap C_t^+) = \frac{f_1^{++\cdots++}(t_n, t_{n-1}, \cdots, t_1, t \mid \mathcal{E}_{t_0})}{f_1^{+\cdots++}(t_{n-1}, \cdots, t_1, t \mid \mathcal{E}_{t_0})} \quad (2-133)$$

Similar to (2-105), (2-106) the following approximations in unconditioned out-crossing rates to the inhomogeneity (2-49) and the kernel (2-50) are considered

$$f_1^+(t_1 \mid \mathcal{E}_{t_0} \cap C_t^+) \simeq \frac{f_2^{++}(t_1, t)}{f_1^+(t)} \quad (2-134)$$

$$f_1^+\left(t_1 \mid \mathcal{E}_{t_0} \cap \mathcal{F}_{t_2}^{(1)} \cap C_t^+\right) \simeq \frac{f_3^{+++}(t_2, t_1, t)}{f_2^{++}(t_2, t)} \quad (2-135)$$

Consistently, the conditioned out-crossing rate $f_1^+(t \mid \mathcal{E}_0)$ entering the right-hand side of (2-37) is approximated by (2-106). The approximation to the first-passage time probability density function thus obtained is denoted $f_{T_1}^{(f)}(t \mid \mathcal{E}_0)$.

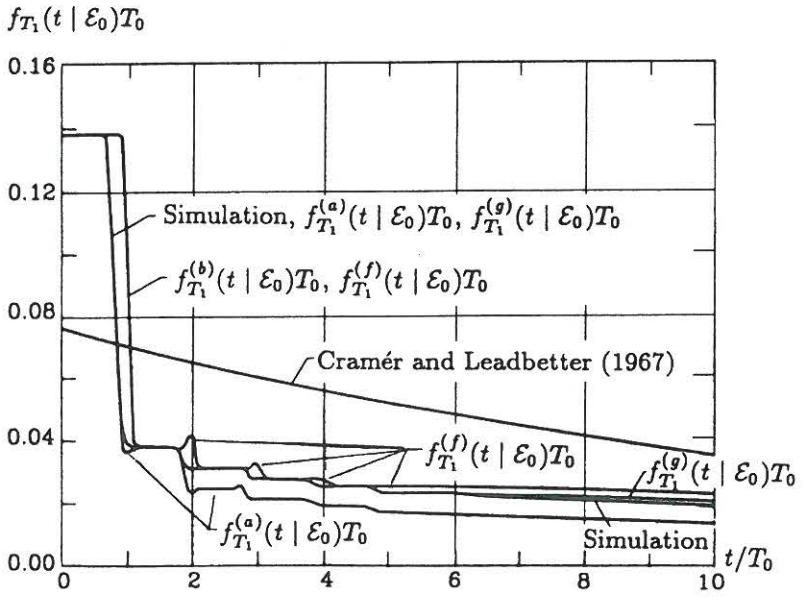

Fig. 2-21: First-passage time probability density function for single barrier stochastic start problem of an SDOF oscillator. $\zeta = 0.01$, $b(t) = 2.0\,\sigma_{X,0}$. $f_{T_1}^{(a)}(t \mid \mathcal{E}_0)$: Eq. (2-104). $f_{T_1}^{(b)}(t \mid \mathcal{E}_0)$: Eqs. (2-105), (2-106). $f_{T_1}^{(f)}(t \mid \mathcal{E}_0)$: Eqs. (2-134), (2-135). $f_{T_1}^{(g)}(t \mid \mathcal{E}_0)$: Eq. (2-197). Nielsen (1990a).

Interval $\frac{t}{T_0}$	Simulation (exact)	$f_{T_1}^{(a)}(t \mid \mathcal{E}_0)T_0$	$f_{T_1}^{(g)}(t \mid \mathcal{E}_0)T_0$	$f_{T_1}^{(f)}(t \mid \mathcal{E}_0)T_0$
0–1	0.13849	0·13849	0·13849	0·13849
1–2	0.03821	0·03822	0·03821	0·03821
2–3	0.03041	0·02507	0·03040	0·03041
3–4	0.02678	0·02124	0·02715	0·02817
4–5	0.02453	0·01938	0·02527	0·02700

Table 2-5: Stair levels of approximations to the first-passage time probability density function of SDOF oscillator.

The linear single degree-of-freedom oscillator (2-102) for a single barrier stochastic start problem is considered again. The stationary auto-correlation coefficient function of the displacement process becomes, see e.g. Nielsen (1993)

$$\rho_{XX}(\tau) = \exp\Big(-\zeta\omega_0 \mid \tau \mid\Big)\left(\cos\Big(\omega_0\sqrt{1-\zeta^2}\,\tau\Big) + \frac{\zeta}{\sqrt{1-\zeta^2}}\sin\Big(\omega_0\sqrt{1-\zeta^2} \mid \tau \mid\Big)\right) \quad (2-136)$$

The damping ratio is $\zeta = 0.01$ and the barrier level is $b(t) \equiv 2.0\,\sigma_{X,0}$. $f_{T_1}^{(a)}(t \mid \mathcal{E}_0)$ as given by (2-104), $f_{T_1}^{(b)}(t \mid \mathcal{E}_0)$ as given by (2-105), (2-106) and $f_{T_1}^{(f)}(t \mid \mathcal{E}_0)$ have been shown in fig. 2-21 in comparison to the simulation results obtained from ergodic sampling based on (2-31), and another approximation, $f_{T_1}^{(g)}(t \mid \mathcal{E}_0)$, related to the identity (2-30), which will be explained further in a succeeding example 2-6. Also shown in the figure 2.21 is the result obtained from an assumption of independent out-crossing events of the Hilbert transform based envelope definition of Cramér and Leadbetter (1966). As seen $f_{T_1}^{(a)}(t \mid \mathcal{E}_0)$, based on conditioned out-crossing rates, follows closely the simulation results up to the 2nd period, whereas the approximations $f_{T_1}^{(b)}(t \mid \mathcal{E}_0)$ and $f_{T_1}^{(f)}(t \mid \mathcal{E}_0)$, based on unconditioned out-crossing rates, deviate considerably from the simulation result at the first downfall of the first-passage time curve. This is so, because the unconditioned out-crossing rates carry no memory of the initial conditions. Compared to $f_{T_1}^{(b)}(t \mid \mathcal{E}_0)$, based on 2nd order unconditioned out-crossing rates, the approximation $f_{T_1}^{(f)}(t \mid \mathcal{E}_0)$ based on 3rd order unconditioned out-crossing rates shows a rapid convergence to the simulation results. From figure 2.21 it is concluded that $f_{T_1}^{(g)}(t \mid \mathcal{E}_0)$ is the best of the approximations shown. The numerical values of the stair levels (the horizontal parts) of the indicated first-passage time curves are shown in table 2-5. As proved in the succeeding example 2-5 the simulation results are exact to the indicated figures.

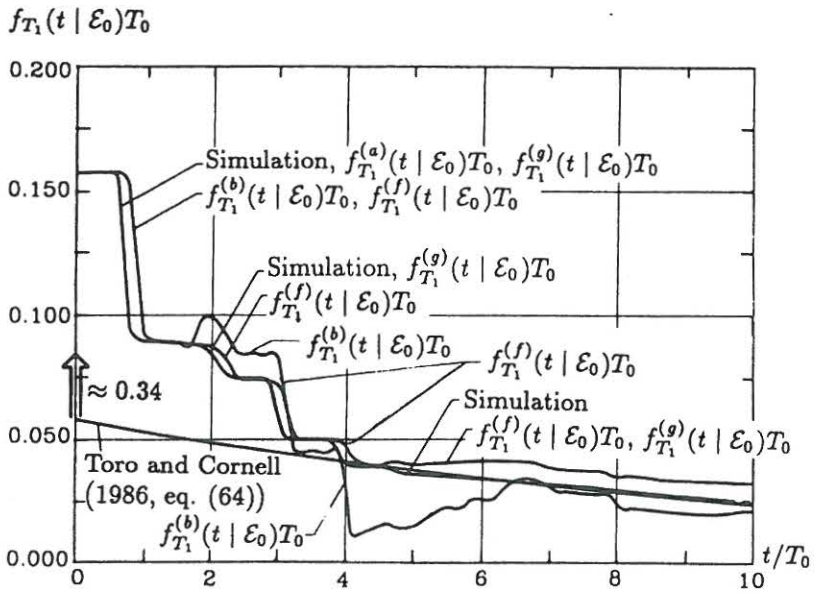

Fig. 2-22: First-passage time probability density function for a single barrier stochastic start problem of a 2 degree-of-freedom system. $\sigma_{X_1}^2 = \sigma_{X_2}^2 = 0.5$, $\zeta_1 = \zeta_2 = 0.01$, $\omega_1 = 2.0\pi$, $\omega_2 = 2.5\pi$, $b(t) = 2.0\,\sigma_{X,0}$. $f_{T_1}^{(a)}(t \mid \mathcal{E}_0)$: Eq. (2-104). $f_{T_1}^{(b)}(t \mid \mathcal{E}_0)$: Eqs. (2-104), (2-105). $f_{T_1}^{(f)}(t \mid \mathcal{E}_0)$: Eqs. (2-134), (2-135). $f_{T_1}^{(g)}(t \mid \mathcal{E}_0)$: Eq. (2-197). Nielsen (1990a).

Next, a slightly damped two-degree-of-freedom system subjected to stationary excitation of Gaussian white noise is considered. The auto-correlation coefficient function $\rho_{XX}(\tau)$ of the displacement response process is assumed to be given by

$$\rho_{XX}(\tau) = \sigma_{X_1}^2 \rho_{X_1X_1}(\tau) + \sigma_{X_2}^2 \rho_{X_2X_2}(\tau) \quad , \quad \sigma_{X_1}^2 + \sigma_{X_2}^2 = 1 \qquad (2-137)$$

$$\rho_{X_iX_i}(\tau) = \exp\left(-\zeta_i\omega_i \mid \tau \mid\right)\left(\cos\left(\omega_i\sqrt{1-\zeta_i^2}\,\tau\right) + \frac{\zeta_i}{\sqrt{1-\zeta_i^2}}\sin\left(\omega_i\sqrt{1-\zeta_i^2} \mid \tau \mid\right)\right) \quad , \; i = 1,2 \qquad (2-138)$$

The result (2-137) is achieved, if $\{X(t),\, t \in R\}$ is obtained from a modal analysis of a structure subjected to broad-banded Gaussian excitation, and only 2 modal coordinates are retained in the modal expansion. If the structure is slightly damped, so $\zeta_i \ll 1$, and the circular frequencies are well separated, the modal processes $\{X_i(t),\, t \in R\}$, $i = 1,2$ can be assumed to be mutually independent. Moreover, the modal loading processes can be replaced by equivalent white noise processes with auto-spectral densities equal to the auto-spectral density function of the modal loading processes evaluated at the circular eigenfrequencies, resulting in the modal auto-correlation coefficient functions (2-138). The circular eigenfrequencies can be considered well separated, if $\omega_1(1 + r\zeta_1) < \omega_2(1 - r\zeta_2)$, where $r \sim 2 - 3$. For a proof of these statements, see Nielsen (1993).

In the example, $\sigma_{X_1}^2 = \sigma_{X_2}^2 = 0.5$, $\zeta_1 = \zeta_2 = 0.01$, $\omega_1 = 2.0\pi$, $\omega_2 = 2.5\pi$. Both modes contribute with equal shares to the displacement variance. The indicated damping ratios and circular eigenfrequencies, represent a limit point for considering the modal processes to be stochastically independent according to the indicated discussion. Again, a single barrier stochastic start first-passage time problem is considered with the barrier level $b(t) = 2.0\sigma_{X,0}$.

In figure 2-22 the approximations $f_{T_1}^{(a)}(t \mid \mathcal{E}_0)$, $f_{T_1}^{(b)}(t \mid \mathcal{E}_0)$, $f_{T_1}^{(f)}(t \mid \mathcal{E}_0)$ and $f_{T_1}^{(g)}(t \mid \mathcal{E}_0)$ are shown in comparison to the simulation results. $f_{T_1}^{(b)}(t \mid \mathcal{E}_0)$ and $f_{T_1}^{(f)}(t \mid \mathcal{E}_0)$ are almost identical during the first

two periods of excitation. Being based on unconditioned out-crossing frequencies, these approximations deviate considerably from the simulation results and from $f_{T_1}^{(a)}(t \mid \mathcal{E}_0)$ and $f_{T_1}^{(g)}(t \mid \mathcal{E}_0)$ at the first downfall of the first-passage time curve as previously stated. The approximation $f_{T_1}^{(b)}(t \mid \mathcal{E}_0)$ fluctuates somewhat about the simulation results, but reasonable results for the first-passage time probability distribution function can be expected. $f_{T_1}^{(f)}(t \mid \mathcal{E}_0)$ and $f_{T_1}^{(g)}(t \mid \mathcal{E}_0)$, based on 3rd order joint crossing rates, give very good results compared with numerical simulation. Also shown in fig. 2-22 is an approximate result of the Poisson type due to Toro and Cornell (1986), which has a Dirac delta spike of the intensity $\simeq 0.34$ at $t = 0$. The staircase character of the first-passage time probability density function is a consequence of the correlated crossing events at moderate to low safety levels. The delta spike is approximating the probability mass below the first few stair levels, and is hence a correction to the Poissonian assumption of independent out-crossings. The approximation is doing well in this case in predicting the limiting decay rate.

Example 2-5: Single barrier stationary start first-passage time problem for single-degree-of-freedom oscillator subjected to Gaussian white noise or to Poisson driven trains of impulses

A linear time-invariant SDOF system is considered subjected to stationary Gaussian white noise excitation, or to a stationary compound Poisson process.

In this case the restoring force $u(X(t), \dot{X}(t))$ and the diffusion function $d(t)$ in (2-80) can be written, cf. (2-102)

$$u(X(t), \dot{X}(t)) = 2\zeta\omega_0 \dot{X}(t) + \omega_0^2 X(t) \tag{2-139}$$

$$d(t) = \frac{1}{m} \tag{2-140}$$

The displacement and the velocity of the system on condition of the initial values $\mathbf{z}_0^T = [X(t_0), \dot{X}(t_0)] = [x_0, \dot{x}_0]$ at the time t_0 can then be written

$$X(t) = c(t \mid \mathbf{z}_0, t_0) + \int_{t_0^+}^{t^-} h(t - t_1)\, dV(t_1) \tag{2-141}$$

$$\dot{X}(t) = \dot{c}(t \mid \mathbf{z}, t_0) + \int_{t_0^+}^{t^-} \dot{h}(t - t_1)\, dV(t_1) \tag{2-142}$$

$$c(t \mid \mathbf{z}_0, t_0) = (\dot{h}(t - t_0) + 2\zeta\omega_0 h(t - t_0))x_0 + h(t - t_0)\dot{x}_0 \tag{2-143}$$

$$\dot{c}(t \mid \mathbf{z}_0, t_0) = -\omega_0^2 h(t - t_0)x_0 + \dot{h}(t - t_0)\dot{x}_0 \tag{2-144}$$

$$h(t) = \begin{cases} 0 & , \quad t < 0 \\ \frac{1}{m\omega_0\sqrt{1-\zeta^2}} e^{-\zeta\omega_0 t} \sin\left(\omega_0\sqrt{1-\zeta^2}t\right) & , \quad t \geq 0 \end{cases} \tag{2-145}$$

$h(t)$ and $\dot{h}(t)$ signify the impulse response functions of the displacement and the velocity. The functions $c(t \mid \mathbf{z}_0, t_0)$ and $\dot{c}(t \mid \mathbf{z}_0, t_0)$ indicate the deterministic drift (the eigenvibrations) of the displacement

and the velocity from the initial value $\mathbf{z}_0$ at the time t_0. The stochastic integrals in (2-141) and (2-142) signify the responses from the excitation process $\{V(\tau),\ \tau \in [t_0, t[\}$.

The joint characteristic function of $X(t)$ and $\dot{X}(t)$ on condition of $\mathbf{Z}(t_0) = \mathbf{z}_0$ is denoted $M_{\{\mathbf{Z}\}}(\theta_1, \theta_2, t \mid x_0, \dot{x}_0, t_0)$. $\kappa_{mn}[\mathbf{Z}(t) \mid \mathbf{z}_0, t_0] = \frac{\partial^{m+n}}{\partial(i\theta_1)^m \partial(i\theta_2)^n} \ln M_{\{\mathbf{Z}\}}(\theta_1, \theta_2, t \mid x_0, \dot{x}_0, t_0) \mid_{\theta_1=\theta_2=0}$ signifies the joint cumulant of the order $m+n$ of $X(t)$ and $\dot{X}(t)$.

For the white noise case the increment of the excitation process is given by

$$dV(t) = \sqrt{2\pi S_0}\, dW(t) \qquad (2-146)$$

$\{W(t), t \in]t_0, \infty[\}$ is a unit intensity Wiener process, and S_0 is the auto-spectral density function of the Gaussian white noise. Since the Wiener process is Gaussian, the response processes also becomes Gaussian. The joint transition probability density function of the Markov state vector can then immediately be indicated as follows

$$q_{\{\mathbf{Z}\}}(x, \dot{x}, t \mid x_0, \dot{x}_0, t_0) = \frac{\varphi_2(\xi_1, \xi_2; \rho[\mathbf{Z}(t) \mid \mathbf{z}_0, t_0])}{\sigma[X(t) \mid \mathbf{z}_0, t_0]\sigma[\dot{X}(t) \mid \mathbf{z}_0, t_0]} \qquad (2-147)$$

$$\xi_1 = \frac{x - c(t \mid \mathbf{z}_0, t_0)}{\sigma[X(t) \mid \mathbf{z}_0, t_0]} \quad , \quad \xi_2 = \frac{\dot{x} - \dot{c}(t \mid \mathbf{z}_0, t_0)}{\sigma[\dot{X}(t) \mid \mathbf{z}_0, t_0]} \qquad (2-148)$$

$$\kappa_{mn}(\mathbf{Z}(t) \mid \mathbf{z}_0, t_0) = \int_{t_0}^{t} h^m(t-\tau)\dot{h}^n(t-\tau) 2\pi S_0 d\tau \quad , \quad m+n=2 \qquad (2-149)$$

In this case, $c(t \mid \mathbf{z}_0, t_0)$ and $\dot{c}(t \mid \mathbf{z}_0, t_0)$ can be identified as the conditional mean value functions of the displacement and the velocity processes. $\sigma[X(t) \mid \mathbf{z}_0, t_0]$, $\sigma[\dot{X}(t) \mid \mathbf{z}_0, t_0]$ and $\rho[\mathbf{Z}(t) \mid \mathbf{z}_0, t_0]$ signify the conditioned standard deviations and conditioned correlation coefficient function of $X(t)$ and $\dot{X}(t)$ as calculated from (2-149). $\varphi_2(\xi_1, \xi_2; \rho)$ is the joint probality density function of a bivariate normal stochastic variable with zero mean values, unit standard deviations and the correlation coefficient ρ. (2-147) was first obtained by Wang and Uhlenbeck (1945) based on direct integration of the associated Fokker-Planck equation.

A stochastic start problem with a constant upper barrier b is considered. In this case the stationary displacement $X(0)$ and the stationary velocity $\dot{X}(0)$ are stochastically independent. The conditional joint probality density function $q_{\{\mathbf{Z}\}}(b, \dot{x}, t \mid \mathcal{E}_0)$ as given by (2-82) then becomes

$$q_{\{\mathbf{Z}\}}(b, \dot{x}, t \mid \mathcal{E}_0) = \frac{1}{\Phi\left(\frac{b}{\sigma_{X,0}}\right)} \cdot \int_{-\infty}^{b} \frac{\varphi_2(\xi_1, \xi_2; \rho)}{\sigma[X(t) \mid \mathbf{z}_0, 0]\, \sigma[\dot{X}(t) \mid \mathbf{z}_0, 0]} \frac{\varphi\left(\frac{x}{\sigma_{X,0}}\right)}{\sigma_{X,0}} dx \qquad (2-150)$$

where $\sigma_{X,0} = \lim_{t\to\infty} \sigma[X(t) \mid \mathbf{z}_0, 0]$, and $\varphi(x)$ and $\Phi(x)$ are the probability density function and the distribution function of a standardized normal variable. The integral in (2-150) can be evaluated analytically in terms of $\varphi(x)$ and $\Phi(x)$.

The integral equation (2-81) was solved numerically, using a trapezoidal scheme with the time step length $\Delta t_1 = 0.025 T_0$ and a Gaussian quadrature scheme with the velocity step length $\Delta \dot{x}_1 = 0.15\sigma_{\dot{X},0}$, where $\sigma_{\dot{X},0} = \lim_{t\to\infty} \sigma[\dot{X}(t) \mid \mathbf{z}_0, 0]$ is the stationary velocity standard deviation. The latter scheme was also used for the quadrature in (2-84). The result has been shown as the full-line curve $\nu T_0 = \infty$ in fig. 2-23. The horizontal stair levels of the first-passage time probability density function are indicated in table 2-6. As seen from table 2-5 the indicated figures coincide with those obtained from ergodic simulation based on (2-31).

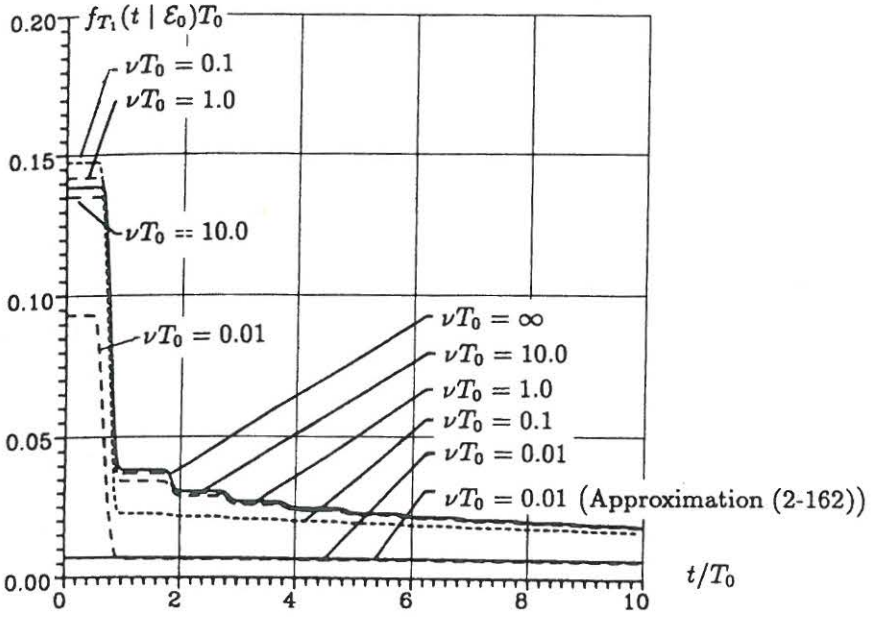

Fig. 2-23: First-passage time probability density functions for white noise and Poisson driven pulses of an SDOF oscillator. Single barrier stochastic start problem $\zeta = 0.01$, $b = 2.0\,\sigma_{X,0}$. Nielsen (1990b).

Interval $\frac{t}{T_0}$	Exact solution $f_{T_1}(t \mid \mathcal{E}_0)T_0$
0–1	0.13849
1–2	0.03821
2–3	0.03041
3–4	0.02678
4–5	0.02453

Table 2-6: Stair levels of first-passage probability density function. SDOF oscillator exposed to Gaussian white noise.

In case of compound Poisson excitation the increment of the excitation process in the interval $]t, t+dt]$ is given by

$$dV(t) = \int_{-\infty}^{\infty} pM(dt, t, dp, p) = dt \sum_{j=1}^{N(t)} P_j \delta(t - t_j) \qquad (2-151)$$

$M(dt, t, dp, p)$ is a random measure specifying the number of impulses into the interval $]p, p+dp]$ during the interval $]t, t+dt]$, see (3-14), (3-17). The Stieltje integration is performed over the sample space of the pulse intensities P_j. $\{N(t),\ t \in]0, \infty[\}$ is a stationary Poisson counting process with the arrival rate ν. Assuming that the moments $E[P^n]$ of sufficiently high order n exist the conditioned mean values and the joint conditioned cumulants of the response process become, Lin (1967), Nielsen and

Iwankiewicz (1996)

$$\mu[X(t) \mid \mathbf{z}_0, t_0] = c(t \mid \mathbf{z}_0, t_0) + \int_{t_0}^{t} h(t-\tau)\nu(\tau)E[P]d\tau \qquad (2-152)$$

$$\mu[\dot{X}(t) \mid \mathbf{z}_0, t_0] = \dot{c}(t \mid \mathbf{z}_0, t_0) + \int_{t_0}^{t} \dot{h}(t-\tau)\nu(\tau)E[P]d\tau \qquad (2-153)$$

$$\kappa_{mn}[\mathbf{Z}(t) \mid \mathbf{z}_0, t_0] = \int_{t_0}^{t} h^m(t-\tau)\dot{h}^n(t-\tau)\nu(\tau)E[P^{m+n}]d\tau \quad , \quad m+n \geq 2 \qquad (2-154)$$

The integrals in (2-152), (2-153), (2-154) can all be evaluated analytically in case of stationary impulse rates ν. From (2-152), (2-153), (2-154) it is seen that the log-characteristic function of the transition probability density function is given by

$$\ln M_{\{\mathbf{Z}\}}(\theta_1, \theta_2, t \mid x_0, \dot{x}_0, t_0) = c(t \mid \mathbf{z}_0, t_0)i\theta_1 + \dot{c}(t \mid \mathbf{z}_0, t_0)i\theta_2 + S(i\theta_1, i\theta_2) \qquad (2-155)$$

$$S(i\theta_1, i\theta_2) = \int_{t_0}^{t} \nu(\tau)\Big(E[\exp(Ph(t-\tau)i\theta_1 + P\dot{h}(t-\tau)i\theta_2)] - 1\Big)d\tau \qquad (2-156)$$

The joint transition probability density function can then be obtained by a double inverse Fourier transformation

$$q_{\{\mathbf{Z}\}}(x, \dot{x}, t \mid x_0, \dot{x}_0, t_0) =$$

$$\frac{1}{(2\pi)^2}\int_{-\infty}^{\infty}\int_{-\infty}^{\infty} M_{\{\mathbf{Z}\}}(\theta_1, \theta_2, t \mid x_0, \dot{x}_0, t_0)\exp(-xi\theta_1 - \dot{x}i\theta_2)d\theta_1 d\theta_2 =$$

$$\frac{1}{(2\pi)^2}\int_{-\infty}^{\infty}\int_{-\infty}^{\infty} \exp\Big(S(i\theta_1, i\theta_2) - (x-c)i\theta_1 - (\dot{x}-\dot{c})i\theta_2\Big)d\theta_1 d\theta_2 \qquad (2-157)$$

(2-157) shows that the joint transition probability density depends on $x, \dot{x}, x_0, \dot{x}_0$ through the differences $x - c(t \mid \mathbf{z}_0, t_0)$ and $\dot{x} - \dot{c}(t \mid \mathbf{z}_0, t_0)$. Unfortunately, (2-157) cannot be solved in closed form for any system of engineering interest. Alternatively, the solution may be represented by the following infinite Gram-Charlier type A series on Edgeworth form, Longuet-Higgins (1964)

$$q_{\{\mathbf{Z}\}}(x, \dot{x}, t \mid x_0, \dot{x}_0, t_0) = \frac{\varphi_2(\xi_1, \xi_2; \rho[\mathbf{Z}(t) \mid \mathbf{z}_0, t_0])}{\sigma[X(t) \mid \mathbf{z}_0, t_0]\,\sigma[\dot{X}(t) \mid \mathbf{z}_0, t_0]}\left(1 + \sum_{k+l=3}^{\infty}\frac{\lambda_{kl}}{k!\,l!}H_{kl}(\xi_1, \xi_2; \rho[\mathbf{Z}(t) \mid \mathbf{z}_0, t_0]) + \right.$$

$$\left.\frac{1}{2}\sum_{k+l=3}^{\infty}\sum_{m+n=3}^{\infty}\frac{\lambda_{kl}\lambda_{mn}}{k!\,l!\,m!\,n!}H_{k+m\,l+n}(\xi_1, \xi_2; \rho[\mathbf{Z}(t) \mid \mathbf{z}_0, t_0]) + \cdots\right) \qquad (2-158)$$

$$\lambda_{mn} = \frac{\kappa_{mn}[\mathbf{Z}(t) \mid \mathbf{z}_0, t_0]}{\sigma[X(t) \mid \mathbf{z}_0, t_0]^m \, \sigma[\dot{X}(t) \mid \mathbf{z}_0, t_0]^n} \qquad (2-159)$$

$$H_{mn}(\xi_1, \xi_2; \rho) = \frac{(-1)^{m+n}}{\varphi_2(\xi_1, \xi_2; \rho)} \frac{\partial^{m+n}}{\partial \xi_1^m \partial \xi_2^n} \varphi_2(\xi_1, \xi_2; \rho) \qquad (2-160)$$

$H_{mn}(\xi_1, \xi_2; \rho)$ signifies the bivariate Hermite polynomial. Eqs. (2-158), (2-159), (2-160) are also valid for the general non-linear system (2-79) under Gaussian white noise or compound Poisson excitation, provided the joint cumulants of sufficiently high order can be calculated. In case of Gaussian responses one has $\lambda_{mn} = 0$, $m + n \geq 3$, and (2-158) reduce to (2-147).

It can be shown that $\lambda_{mn} \to \infty, m + n \geq 2$ as $\nu(t - t_0) \to 0$, implying a prohibitively slow convergence of the series expansion at the transition time intervals for which $\nu(t - t_0) \ll 1$. The indicated singularity can be circumvented by applying the expansion (3-xx) to the first order for the transitional joint pdf in combination with a Gram-Charlier series for the conditioned transitional joint pdf $q^{(1)}_{\{\mathbf{Z}\}}(x, \dot{x}, t \mid x_0, \dot{x}_0, t_0)$. Although this approach is numerically robust it has not been pursued in the following numerical example, which is based on (2-158) with all series expansions truncated up to and including the joint 6th order cumulants. It should be noted that truncation of the series expansion (2-158) at any finite order, corresponding to a finite order polynomial expansion of the log-characteristic function, cannot be mathematically justified. Actually, the theorem of Marcienkiewicz (1939) states that either the log-characteristic function is a polynomial of the 2nd order corresponding to the Gaussian case, or joint cumulants of inifinite order exist. Hence, the justification totally relies on the quality of the obtained results. Similar obstacles arise in the application of cumulant neglect closure schemes in moment methods of Markov systems, see (3-193).

In order to compare the results for the compound Poisson excitation to those of the Gaussian white noise excitation the intensities of the impulses are assumed to be zero-mean normally distributed, $P \sim N(0, \sigma_P^2)$, with the variance σ_P^2 selected as follows

$$\nu \sigma_P^2 = 2\pi S_0 \qquad (2-161)$$

The basis for this is the well-known convergence of the compound Poisson process to a Gaussian white noise as $\nu \to \infty$ under the restriction of (2-161).

The obtained numerical results have been shown as the dotted curves in fig. 2-23 for $\nu T_0 = 0.01$, 0.1, 1.0, 10.0. The convergence to Gaussian white noise may be considered to be attained for $\nu T_0 = 10.0$, so the noticed deviation from the full-line curve ($\nu T_0 = \infty$) can be attributed to the applied truncation of the Gram-Charlier series expansion.

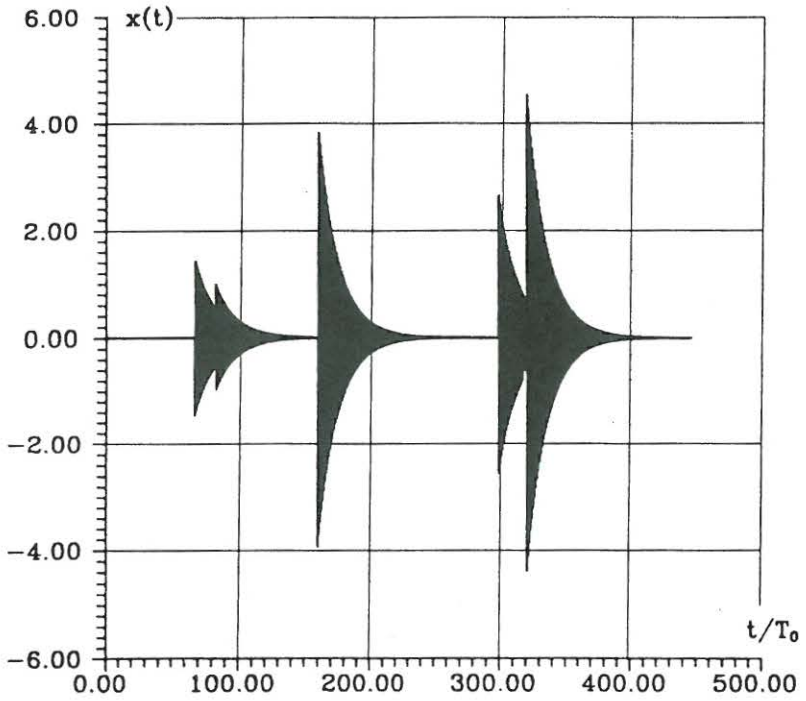

Fig. 2-24: Realization of displacement process for an SDOF system subjected to compound Poisson excitation with low mean arrival rate. $\zeta = 0.01$, $\nu T_0 = 0.01$, $P \sim N(0, \sigma_p^2)$.

It is remarkable that the height of the first stair level is almost constant for $\nu T_0 \gtrsim 0.1$, whereas the height is significantly smaller for $\nu T_0 = 0.01$. This suggests that the out-crossing events tend to become increasingly uncorrelated as $\nu T_0 \to 0$ under the restriction of (2-161). The explanation of this effect can be given with reference to the realizations of the response process in case of excitations with low mean arrival rate of impulses as shown in fig. 2-24. As seen the eigenvibrations have diminished substantially at the arrival of the next impulse.

Due to the stochastic independence of the pulse intensities, the eigenvibrations from adjacent impulses tend to become stochastically independent. Then, assume these eigenvibrations to be completely independent. The eigenvibrations $x(t) = h(t - t_1)P$, initiated by the last previous impulse P with arrival time t_1, will then cross out from the safe domain, if $h_{\max} \mid P \mid > b$. $h_{\max}$ is the maximum value of the impulse response function in (2-145). This provides the following asymptotic solution for the first-passage time probability density function

$$f_{T_1}(t \mid \mathcal{E}_0) \simeq \frac{1}{\lambda_1} \exp(-\lambda_1 t) \tag{2-162}$$

$$\lambda_1 = P(h_{\max} \mid P \mid > b)\nu = \left(1 + F_P\left(-\frac{b}{h_{\max}}\right) - F_P\left(\frac{b}{h_{\max}}\right)\right)\nu \tag{2-163}$$

$$h_{\max} = \max_{t \in [0, \infty[} h(t) = h(t_{\max}) \tag{2-164}$$

$$t_{\max} = \frac{1}{\omega_0 \sqrt{1 - \zeta^2}} \arctan\left(\frac{\sqrt{1 - \zeta^2}}{b}\right) \tag{2-165}$$

where $F_P(p)$ signifies the probability distribution function of P. Since the system and the safe domain are time-invariant, and the state vector $\mathbf{Z}(t)$ is a Markov vector, the first-passage probability density function can be represented by the expansion (2-117). λ_1 as given by (2-163) is an approximation to the 1st eigenvalue of the forward and the backward Kolmogorov operators (the Kolmogorov-Feller operators) of the first-passage time problem. The approximation (2-162) has been plotted in fig. 2-23 as the lowest full-line curve. Since the indicated first-passage time curves for $\nu T_0 = 0.01$ are parallel, (2-163) turns out to be a good approximation to the limiting decay rate of the problem. In case of higher damping the approximation will be even better, because a faster decay of eigenvibrations then takes place, and the assumption of mutually stochastic independence of such eigenvibrations then is better fulfilled.

In case the diffusion function $d(t)$ in (2-80) is a constant the approximation (2-162) can be extended to the general non-linear system (2-79) exposed to compound Poisson excitation. In this case the quantity $h_{\max}$, entering the expression (2-163) for the limiting decay rate, is alternatively defined by

$$h_{\max} = \max_{t \in [0,\infty[} c(t \mid 0,1,0) \qquad (2-166)$$

where $c(t \mid 0,1,0)$ is the displacement eigenvibration $c(t \mid x_0, \dot{x}_0, t_0)$ with the initial value $\mathbf{z}_0^T = [x_0, \dot{x}_0] = [0,1]$ at the time $t_0 = 0$.

In conclusion it has been demonstrated in example 2-5 that the integral equation (2-81) in combination with (2-84) may be used to obtain very accurate solutions for the first-passage time probability density function for simple linear systems exposed to Gaussian white noise. Approximate solutions can be obtained for similar non-linear systems exposed to white noise or to linear or non-linear systems exposed to compound Poisson excitation.

2.3 Integral equations for the probability density function of the time interval spent in the safe domain

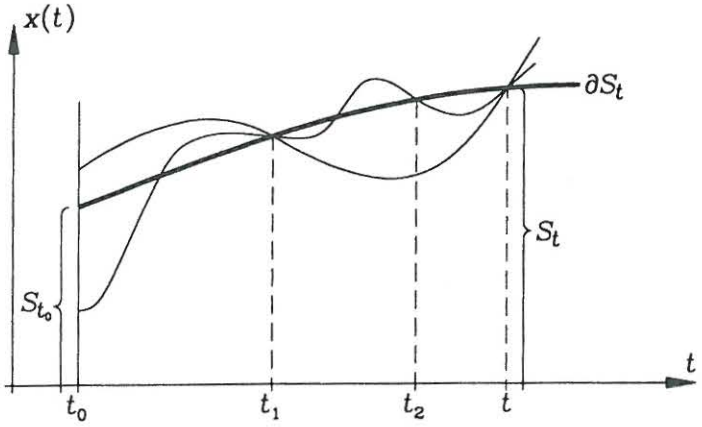

Fig. 2-25: Sample curves with in-crossings to the safe domain at the times t_1 and t_2 and out-crossings at the time t.

$f_{L_t^+}(t-t_1) = f_1^-\left(t_1;\ \mathcal{E}_{]t_1,t[} \mid \mathcal{C}_t^+\right)$, $\mathcal{E}_{]t_1,t[} = \cap_{\tau\in]t_1,t[}\mathcal{S}_\tau$ is the rate of in-crossings to the safe domain at the time t_1 of the sample curves which do not leave the safe domain in the interval $]t_1,t[$ on condition of an out-crossing at the time t, cf. (2-19). This characterizes $f_{L_t^+}(t-t_1)$ as a kind of first-passage time probability density function backwards in time. The following integral equation may be formulated, Nielsen and Sørensen (1988)

$$f_{L_t^+}(t-t_1) = f_1^-\left(t_1 \mid \mathcal{C}_t^+\right) - \int_{t_1}^{t} f_1^-\left(t_1 \mid \mathcal{C}_{t_2}^- \cap \mathcal{E}_{]t_2,t[} \cap \mathcal{C}_t^+\right) f_{L_t^+}(t-t_2)\,dt_2 \quad (2-167)$$

where

$$f_1^-\left(t_1 \mid \mathcal{C}_t^+\right) = \frac{f_2^{-+}(t_1,t)}{f_1^+(t)} \quad , \quad t_0 < t_1 < t \quad (2-168)$$

The last term on the right-hand side of (2-167) withdraws from $f_1^-\left(t_1 \mid \mathcal{C}_t^+\right)$ the rate of in-crossings at the time t_1 of the sample curves which have at least one further in-crossing to the safe domain in the interval $]t_1,t[$ on condition of an out-crossing at the time t.

Define $\mathcal{L}_{t_2,t} = \mathcal{C}_{t_2}^- \cap_\tau \mathcal{E}_{]t_2,t[}\mathcal{S}_\tau \cap \mathcal{C}_t^+$. $\mathcal{L}_{t_2,t}$ signifies the joint event of an in-crossing at the time t_2 and an out-crossing at the time t of the sample curves which are in the safe domain in the interval $]t_2,t[$. Further, $f_1^-(t_1 \mid \mathcal{L}_{t_2,t}) f_{L_t^+}(t-t_2) = f_2^{--}\left(t_1,t_2;\mathcal{E}_{]t_2,t[} \mid \mathcal{C}_t^+\right)$ represents the second order rate of the in-crossings at the times t_1 and t_2 of the sample curves which do not leave the safe domain in the interval $]t_2,t[$ on condition of an out-crossing at the time t. For this quantity the following identity holds

$$f_1^-(t_1 \mid \mathcal{L}_{t_2,t}) f_{L_t^+}(t-t_2) = f_{L_t^+}(t-t_2 \mid \mathcal{C}_{t_1}^-) f_1^-(t_1 \mid \mathcal{C}_t^+) \qquad (2-169)$$

From (2-167) and (2-169) the following relation is then obtained

$$f_{L_t^+}(t-t_1) = f_1^-(t_1 \mid \mathcal{C}_t^+) \left(1 - \int_{t_1}^{t} f_{L_t^+}(t-t_2 \mid \mathcal{C}_{t_1}^-)\, dt_2\right) \qquad (2-170)$$

$f_1^-(t_1 \mid \mathcal{L}_{t_2,t}) f_{L_t^+}(t-t_2)$ fulfils the integral equation

$$f_1^-(t_1 \mid \mathcal{L}_{t_2,t}) f_{L_t^+}(t-t_2) = f_2^{--}(t_1,t_2 \mid \mathcal{C}_t^+) - \int_{t_2}^{t} f_2^{--}(t_1,t_2 \mid \mathcal{L}_{t_3,t}) f_{L_t^+}(t-t_3)\, dt_3 \qquad (2-171)$$

$f_2^{--}(t_1,t_2 \mid \mathcal{L}_{t_3,t}) f_{L_t^+}(t-t_3)$ signifies the 3rd order rate of the in-crossings to S_{t_1}, S_{t_2}, S_{t_3}, $t_0 < t_1 < t_2 < t_3 < t$ of the sample curves which do not leave the safe domain in the interval $]t_3, t[$ on condition of an out-crossing at the time t. For this quantity the following identity holds

$$f_2^{--}(t_1,t_2 \mid \mathcal{L}_{t_3,t}) f_{L_t^+}(t-t_3) = f_{L_t^+}(t-t_3 \mid \mathcal{C}_{t_1}^- \cap \mathcal{C}_{t_2}^-) f_2^{--}(t_1,t_2 \mid \mathcal{C}_t^+) \qquad (2-172)$$

From (2-167), (2-171) and (2-172) the following identities are obtained

$$f_{L_t^+}(t-t_1) = f_1^-(t_1 \mid \mathcal{C}_t^+) -$$

$$\int_{t_1}^{t} f_2^{--}(t_1,t_2 \mid \mathcal{C}_t^+) \left(1 - \int_{t_2}^{t} f_{L_t^+}(t-t_3 \mid \mathcal{C}_{t_1}^- \cap \mathcal{C}_{t_2}^-)\, dt_3\right) dt_2 \qquad (2-173)$$

$$f_{L_t^+}(t-t_1) = f_1^-(t_1 \mid \mathcal{C}_t^+) -$$

$$\int_{t_1}^{t} f_2^{--}(t_1,t_2 \mid \mathcal{C}_t^+)\, dt_2 + \int_{t_1}^{t}\int_{t_2}^{t} f_2^{--}(t_1,t_2 \mid \mathcal{L}_{t_3,t}) f_{L_t^+}(t-t_3)\, dt_3\, dt_2 \qquad (2-174)$$

Continuation of this process until the nth term leads to the result

$$f_{L_t^+}(t-t_1) = f_1^-(t_1 \mid \mathcal{C}_t^+) - \int_{t_1}^{t} f_2^{--}(t_1,t_2 \mid \mathcal{C}_t^+)\, dt_2 + \cdots +$$

$$(-1)^{n-1} \int_{t_1}^{t}\int_{t_2}^{t} \cdots \int_{t_{n-1}}^{t} f_n^{---\cdots-}(t_1,t_2,t_3,\ldots,t_n \mid \mathcal{C}_t^+) \cdot$$

$$\left(1-\int_{t_n}^{t} f_{L_t^+}\left(t-t_{n+1} \mid \mathcal{C}_{t_1}^- \cap \mathcal{C}_{t_2}^- \cap \mathcal{C}_{t_3}^- \cap \cdots \cap \mathcal{C}_{t_n}^-\right) dt_{n+1}\right) dt_n \cdots dt_3 dt_2 \qquad (2-175)$$

and

$$f_1^-(t_1 \mid \mathcal{L}_{t_2,t}) f_{L_t^+}(t-t_2) = f_2^{--}(t_1,t_2 \mid \mathcal{C}_t^+) - \int_{t_2}^{t} f_3^{---}(t_1,t_2,t_3 \mid \mathcal{C}_t^+)\, dt_3 + \cdots +$$

$$(-1)^{n-2} \int_{t_2}^{t} \cdots \int_{t_{n-1}}^{t} f_n^{-----\cdots-}(t_1,t_2,t_3,\ldots,t_n \mid \mathcal{C}_t^+) \cdot$$

$$\left(1-\int_{t_n}^{t} f_{L_t^+}\left(t-t_{n+1} \mid \mathcal{C}_{t_1}^- \cap \mathcal{C}_{t_2}^- \cap \cdots \cap \mathcal{C}_{t_n}^-\right) dt_{n+1}\right) dt_n \cdots dt_3 \qquad (2-176)$$

From (2-7), (2-30) and (2-175), the following series is then obtained for the first-passage time probability density function, Nielsen and Sørensen (1988)

$$f_{T_1}(t \mid \mathcal{E}_{t_0}) P(\mathcal{E}_{t_0}) = f_1^+(t) - \int_{t_0}^{t} f_2^{-+}(t_1,t)\, dt_1 + \cdots +$$

$$(-1)^n \int_{t_0}^{t} \int_{t_1}^{t} \cdots \int_{t_{n-1}}^{t} f_{n+1}^{----\cdots-+}(t_1,t_2,\ldots,t_n,t) \cdot$$

$$\left(1-\int_{t_n}^{t} f_{L_t^+}\left(t-t_{n+1} \mid \mathcal{C}_{t_1}^- \cap \mathcal{C}_{t_2}^- \cap \cdots \cap \mathcal{C}_{t_n}^-\right) dt_{n+1}\right) dt_n \cdots dt_2 dt_1 \qquad (2-177)$$

(2-42) and (2-177) are two exact inclusion-exclusion representations of the first-passage time probability density function. The main difference of these expansions is that (2-42) is in terms of conditioned crossing rates, whereas (2-177) is in terms of simpler unconditioned crossing rates.

The following quantity is introduced, cf. (2-45)

$$F_{n,j}^-(t_1,\ldots,t_n,t) =$$

$$\begin{cases} f_{n+1}^{----\cdots-+}(t_1,\ldots,t_n,t) & , \; j=0 \\ \int_{t_n}^{t} \cdots \int_{t_{n+j-1}}^{t} f_{n+j+1}^{----\cdots-----\cdots-+}(t_1,\ldots,t_n,t_{n+1},\ldots,t_{n+j},t)\, dt_{n+j} \cdots dt_{n+1} & , \; j \geq 1 \end{cases} \qquad (2-178)$$

From (2-175) and (2-176) the following formal expansion for the kernel $f_1^-(t_1 \mid \mathcal{L}_{t_2,t})$ of the integral equation (2-167) is obtained as $n \to \infty$, Nielsen and Sørensen (1988)

$$f_1^-(t_1 \mid \mathcal{L}_{t_2,t}) = \frac{f_2^{--}(t_1,t_2 \mid \mathcal{C}_t^+) - \int_{t_2}^{t} f_3^{---}(t_1,t_2,t_3 \mid \mathcal{C}_t^+)\,dt_3 + \cdots}{f_1^-(t_2 \mid \mathcal{C}_t^+) - \int_{t_2}^{t} f_2^{--}(t_2,t_3 \mid \mathcal{C}_t^+)\,dt_3 + \cdots} =$$

$$\frac{f_3^{--+}(t_1,t_2,t) - \int_{t_2}^{t} f_4^{---+}(t_1,t_2,t_3,t)\,dt_3 + \cdots}{f_2^{-+}(t_2,t) - \int_{t_2}^{t} f_3^{--+}(t_2,t_3,t)\,dt_3 + \cdots} =$$

$$\frac{\sum_{j=0}^{\infty}(-1)^j F_{2,j}^-(t_1,t_2,t)}{\sum_{j=0}^{\infty}(-1)^j F_{1,j}^-(t_2,t)} \qquad (2-179)$$

Upon truncating the series in the numerator and denominator of (2-179), approximate solution for the integral equation (2-167) can be obtained numerically. From (2-30) an approximate solution for the first-passage time probability density function is finally obtained.

Analogous to (2-48) $f_{L_t^+}(t-t_2 \mid \mathcal{C}_{t_1}^-)$ fulfils the integral equation, Nielsen (1990a)

$$f_{L_t^+}(t-t_2 \mid \mathcal{C}_{t_1}^-) = f_1^-(t_2 \mid \mathcal{C}_{t_1}^- \cap \mathcal{C}_t^+) - \int_{t_2}^{t} f_1^-(t_2 \mid \mathcal{C}_{t_1}^- \cap \mathcal{L}_{t_3,t}) f_{L_t^+}(t-t_3 \mid \mathcal{C}_{t_1}^-)\,dt_3,$$

$$t_0 < t_1 < t_2 < t \qquad (2-180)$$

where

$$f_1^-(t_2 \mid \mathcal{C}_{t_1}^- \cap \mathcal{C}_t^+) = \frac{f_3^{--+}(t_1,t_2,t)}{f_2^{-+}(t_1,t)} \qquad (2-181)$$

$$f_1^-(t_2 \mid \mathcal{C}_{t_1}^- \cap \mathcal{L}_{t_3,t}) = \frac{f_2^{--}(t_2,t_3 \mid \mathcal{C}_{t_1}^- \cap \mathcal{C}_t^+) - \int_{t_3}^{t} f_3^{---}(t_2,t_3,t_4 \mid \mathcal{C}_{t_1}^- \cap \mathcal{C}_t^+)\,dt_4 + \cdots}{f_1^-(t_3 \mid \mathcal{C}_{t_1}^- \cap \mathcal{C}_t^+) - \int_{t_3}^{t} f_2^{--}(t_3,t_4 \mid \mathcal{C}_{t_1}^- \cap \mathcal{C}_t^+)\,dt_4 + \cdots} =$$

$$\frac{f_4^{---+}(t_1,t_2,t_3,t) - \int_{t_3}^{t} f_5^{----+}(t_1,t_2,t_3,t_4,t)\,dt_4 + \cdots}{f_3^{--+}(t_1,t_3,t) - \int_{t_3}^{t} f_4^{---+}(t_1,t_3,t_4,t)\,dt_4 + \cdots} =$$

$$\frac{\sum_{j=0}^{\infty}(-1)^j F^-_{3,j}(t_1,t_2,t_3,t)}{\sum_{j=0}^{\infty}(-1)^j F^-_{2,j}(t_1,t_3,t)} \qquad (2-182)$$

Similarly, $f_{L_t^+}(t-t_{n+1} \mid \mathcal{C}^-_{t_1} \cap \cdots \cap \mathcal{C}^-_{t_n})$ in (2-175) fulfils the integral equation, Nielsen (1990a)

$$f_{L_t^+}(t-t_{n+1} \mid \mathcal{C}^-_{t_1} \cap \cdots \cap \mathcal{C}^-_{t_n}) = f_1^-(t_{n+1} \mid \mathcal{C}^-_{t_1} \cap \cdots \cap \mathcal{C}^-_{t_n} \cap \mathcal{C}^+_t) -$$

$$\int_{t_{n+1}}^{t} f_1^-(t_{n+1} \mid \mathcal{C}^-_{t_1} \cap \cdots \cap \mathcal{C}^-_{t_n} \cap \mathcal{L}_{t_{n+2},t}) f_{L_t^+}(t-t_{n+2} \mid \mathcal{C}^-_{t_1} \cap \cdots \cap \mathcal{C}^-_{t_n})\, dt_{n+2},$$

$$t_0 < t_1 < \cdots < t_n < t_{n+1} < t_{n+2} < t \qquad (2-183)$$

where

$$f_1^-(t_{n+1} \mid \mathcal{C}^-_{t_1} \cap \cdots \cap \mathcal{C}^-_{t_n} \cap \mathcal{C}^+_t) = \frac{f^{-\cdots-+}_{n+2}(t_1,\ldots,t_n,t_{n+1},t)}{f^{-\cdots-+}_{n+1}(t_1,\ldots,t_n,t)} \qquad (2-184)$$

$$f_1^-(t_{n+1} \mid \mathcal{C}^-_{t_1} \cap \cdots \cap \mathcal{C}^-_{t_n} \cap \mathcal{L}_{t_{n+2},t}) = \frac{\sum_{j=0}^{\infty}(-1)^j F^-_{n+2,j}(t_1,\ldots,t_n,t_{n+1},t_{n+2},t)}{\sum_{j=0}^{\infty}(-1)^j F^-_{n+1,j}(t_1,\ldots,t_n,t_{n+2},t)} \qquad (2-185)$$

(2-183) is motivated in the same way as the integral equation (2-51). If an approximate solution to (2-183) can be obtained, the remainder of the series (2-177) can be evaluated approximately.

$f_{L^-_{t_1}}(t-t_1) = f_1^+(t;\mathcal{E}_{]t_1,t[} \mid \mathcal{C}^-_{t_1})$ is the rate of out-crossings from the safe domain at the time t of the sample curves which do not leave the safe domain in the interval $]t_1,t[$ on the condition of an in-crossing at the time t_1, cf. (2-18). From (2-11) it follows that $f_{L^-_{t_1}}(t-t_1)$ and $f_{T_1}(t \mid \mathcal{E}_{t_1})$ are identically defined, except from the different conditionings. Analogous to (2-35), $f_{L^-_{t_1}}(t-t_1)$ then fulfils the integral equation

$$f_{L^-_{t_1}}(t-t_1) = f_1^+(t \mid \mathcal{C}^-_{t_1}) - \int_{t_1}^{t} f_1^+(t \mid \mathcal{C}^-_{t_1} \cap \mathcal{F}^{(1)}_{t_2}) f_{L^-_{t_1}}(t_2-t_1)\, dt_2 \qquad (2-186)$$

where

$$f_1^+(t \mid \mathcal{C}_{t_1}^-) = \frac{f_2^{-+}(t_1,t)}{f_1^-(t_1)} \ , \ t_0 < t_1 < t \qquad (2-187)$$

The following expansions for $f_{L_{t_1}^-}(t-t_1)$ and for the kernel $f_1^+(t \mid \mathcal{C}_{t_1}^- \cap \mathcal{F}_{t_2}^{(1)})$ follow immediately from (2-42), (2-43), (2-46)

$$f_{L_{t_1}^-}(t-t_1) = f_1^+(t \mid \mathcal{C}_{t_1}^-) - \int_{t_1}^{t} f_2^{++}(t_2,t \mid \mathcal{C}_{t_1}^-)\, dt_2 + \cdots +$$

$$(-1)^{n-1} \int_{t_1}^{t}\int_{t_1}^{t_2} \cdots \int_{t_1}^{t_{n-1}} f_n^{+\cdots+++}(t_n,\ldots,t_3,t_2,t \mid \mathcal{C}_{t_1}^-) \cdot$$

$$\left(1 - \int_{t_1}^{t_n} f_{L_{t_1}^-}(t_{n+1}-t_1 \mid \mathcal{C}_{t_n}^+ \cap \cdots \cap \mathcal{C}_{t_3}^+ \cap \mathcal{C}_{t_2}^+ \cap \mathcal{C}_t^+)\, dt_{n+1}\right) dt_n \cdots dt_3\, dt_2$$

$$t_1 < t_{n+1} < t_n < t_{n-1} < \cdots < t_3 < t_2 < t \qquad (2-188)$$

$$f_{L_{t_1}^-}(t-t_1) = f_1^+(t \mid \mathcal{C}_{t_1}^-) - \int_{t_1}^{t} f_2^{++}(t_2,t \mid \mathcal{C}_{t_1}^-)\, dt_2 + \cdots +$$

$$(-1)^{n-1} \int_{t_1}^{t}\int_{t_1}^{t_2} \cdots \int_{t_1}^{t_{n-1}} f_n^{+\cdots+++}(t_n,\ldots,t_3,t_2,t \mid \mathcal{C}_{t_1}^-)\, dt_n \cdots dt_3\, dt_2 +$$

$$(-1)^{n} \int_{t_1}^{t}\int_{t_1}^{t_2} \cdots \int_{t_1}^{t_n} f_n^{+\cdots+++}(t_n,\ldots,t_3,t_2,t \mid \mathcal{C}_{t_1}^- \cap \mathcal{F}_{t_{n+1}}^{(1)}) f_{L_{t_1}^-}(t_{n+1}-t_1)\, dt_{n+1} \cdots dt_3\, dt_2 \qquad (2-189)$$

$$f_1^+(t \mid \mathcal{C}_{t_1}^- \cap \mathcal{F}_{t_2}^{(1)}) = \frac{\sum_{j=0}^{\infty}(-1)^j F_{2,j}^+(t_2,t \mid \mathcal{C}_{t_1}^-)}{\sum_{j=0}^{\infty}(-1)^j F_{1,j}^+(t_2 \mid \mathcal{C}_{t_1}^-)} \qquad (2-190)$$

$F_{n,j}^+(t_{n+1},\ldots,t_2 \mid \mathcal{C}_{t_1}^-)$ is given by (2-45) with $\mathcal{E}_{t_0}$ replaced by $\mathcal{C}_{t_1}^-$.

From (2-3) follows that the integrand of the last term in (2-188) is symmetric in the indices $t_{n-1},\ldots,t_3,t_2$. Applying (2-7) and a renaming of the integration parameters, (2-188) can then be written

$$f_{L_{t_1}^-}(t-t_1) = \frac{1}{f_1^-(t_1)} \left(f_2^{-+}(t_1,t) - \int_{t_1}^{t} f_3^{-++}(t_1,t_2,t)\, dt_2 + \cdots +\right.$$

$$(-1)^{n-1}\int_{t_1}^{t}\cdots\int_{t_{n-2}}^{t}\int_{t_{n-1}}^{t} f_{n+1}^{-+\cdots+++}(t_1,t_2,\ldots,t_{n-1},t_n,t)\cdot$$

$$\left(1-\int_{t_1}^{t_2} f_{L_{t_1}^-}(\tau-t_1\mid \mathcal{C}_{t_2}^+\cap\cdots\cap\mathcal{C}_{t_n}^+\cap\mathcal{C}_t^+)d\tau\right)dt_n dt_{n-1}\cdots dt_2\Bigg),$$

$$t_1<t_2<t_3<\cdots<t_n<t \qquad (2-191)$$

From (2-30) and (2-191), the following series is then obtained for the first-passage time probability density function

$$f_{T_1}(t\mid\mathcal{E}_{t_0})P(\mathcal{E}_{t_0})=f_1^+(t)-\int_{t_0}^{t} f_2^{-+}(t_1,t)\,dt_1+\cdots+$$

$$(-1)^n\int_{t_0}^{t}\int_{t_1}^{t}\cdots\int_{t_{n-2}}^{t}\int_{t_{n-1}}^{t} f_{n+1}^{-+\cdots+++}(t_1,t_2,\ldots,t_{n-1},t_n,t)\cdot$$

$$\left(1-\int_{t_1}^{t_2} f_{L_{t_1}^-}\left(\tau-t_1\mid\mathcal{C}_{t_2}^+\cap\cdots\cap\mathcal{C}_{t_n}^+\cap\mathcal{C}_t^+\right)d\tau\right)dt_n dt_{n-1}\cdots dt_2 dt_1 \qquad (2-192)$$

As $n\to\infty$, (2-192) provides an inclusion-exclusion series for the first-passage time probability density function in unconditioned crossing rates of the type $f_{n+1}^{-+\cdots++}(t_1,t_2,\ldots,t_n,t)$, alternatively to the previous expansion (2-177) in unconditioned crossing rates of the type $f_{n+1}^{--\cdots-+}(t_1,t_2,\cdots,t_n,t)$.

Consider the Markov system (2-79) with a safe domain defined by a single constant upper barrier b for the displacement response. Let $f_{\dot{X}L_{t_1}^-}(b,\dot{x},t-t_1)dtd\dot{x}$ be the joint probability of out-crossings in the time interval $]t,t+dt]$ at the barrier b with out-crossing velocities in the interval $]\dot{x},\dot{x}+d\dot{x}]$ of the sample curves, which are not leaving the safe domain in the interval $]t_1,t[$, on condition of an in-crossing at the time t_1. Based on previously mentioned similarity between $f_{L_{t_1}^-}(t-t_1)=f_1^+\left(t;\mathcal{E}_{]t_1,t[}\mid\mathcal{C}_{t_1}^-\right)$ and $f_{T_1}(t\mid\mathcal{E}_{t_1})=f_1^+\left(t;\mathcal{E}_{]t_1,t[}\mid\mathcal{E}_{t_1}\right)$, and with an argumentation identical to the one leading to (2-81), the following integral equation for $f_{\dot{X}L_{t_1}^-}\left(b,\dot{x}_1,t-t_1\right)$ can then be formulated,

$$f_{\dot{X}L_{t_1}^-}(b,\dot{x},t-t_1)=\dot{x}q_{\{\mathbf{Z}\}}(b,\dot{x},t\mid\mathcal{C}_{t_1}^-)-\int_{t_1}^{t}\int_{0}^{\infty}\dot{x}q_{\{\mathbf{Z}\}}(b,\dot{x},t\mid b,\dot{x}_2,t_2)\cdot$$

$$f_{\dot{X}L_{t_1}^-}(b,\dot{x}_2,t_2-t_1)\,d\dot{x}_2dt_2 \qquad (2-193)$$

where

$$q_{\{\mathbf{Z}\}}(b,\dot{x},t \mid \mathcal{C}_{t_1}^-) = \frac{-\int_{-\infty}^{0} \dot{x}_1 \, q_{\{\mathbf{Z}\}}(b,\dot{x},t \mid b,\dot{x}_1,t_1) f_{\{X\}\{\dot{X}\}}(b,\dot{x}_1,t_1)\, d\dot{x}_1}{f_1^-(t_1)} \qquad (2-194)$$

Using (2-20), $f_{L_t^+}(t-t_1)$ is then obtained from the solution of (2-193) as follows

$$f_{L_t^+}(t-t_1) = \frac{f_1^-(t_1)}{f_1^+(t)} \int_0^{\infty} f_{\dot{X}L_{t_1}^-}(b,\dot{x},t-t_1)\, d\dot{x} \qquad (2-195)$$

In complete analogy with (2-86), (2-87), (2-90), (2-95) integral equations similar to (2-193) can be formulated for more involved Markov systems.

Upon inserting (2-195) into (2-30) the following solution is finally obtained for the first-passage time probability density function

$$f_{T_1}(t \mid \mathcal{E}_{t_0})P(\mathcal{E}_{t_0}) = f_1^+(t) - \int_{t_0}^{t} f_1^-(t_1) \int_0^{\infty} f_{\dot{X}L_{t_1}^-}(b,\dot{x},t-t_1)\, d\dot{x}\, dt_1 \qquad (2-196)$$

The integral equation (2-167) and the associated expansion (2-177) and (2-179) for the solution and for the kernel of the integral equation in unconditioned crossing rates of the type $f_{n+1}^{--\cdots-+}(t_1,t_2,\ldots,t_n,t)$ were derived by Nielsen and Sørensen (1988). The solutions of the integral equation (2-180) and (2-183) enter the remainder of the expansion (2-177). These integral equations and the expansions (2-182) and (2-185) of the associated kernels were formulated by Nielsen (1990a). The results (2-186), (2-188), (2-189) based on the resemblance between $f_{L_t^-}(t-t_1) = f_1^+(t;\mathcal{E}_{]t_1,t[} \mid \mathcal{C}_{t_1}^-)$ and $f_{T_1}(t \mid \mathcal{E}_{t_1}) = f_1^+(t;\mathcal{E}_{]t_1,t[} \mid \mathcal{E}_{t_1})$, as well as the resulting alternative expansion (2-192) in unconditioned crossing rates of the type $f_{n+1}^{-+\cdots++}(t_1,t_2,\ldots,t_n,t)$ for the first-passage time probability density function have not previously been published, neither have the results (2-193), (2-194), (2-195), (2-196) for an SDOF Markov system.

Example 2-6: Approximations for the kernel of the integral equation (2-167) and related bounding technique

At the application of the integral equation (2-167) the following approximation may be used for the kernel, obtained by truncating the numerator and the denominator series of (2-179) to the first term and use of (2-7)

$$f_1^-(t_1 \mid \mathcal{L}_{t_2,t}) \simeq \frac{f_2^{--}(t_1,t_2 \mid C_t^+)}{f_1^-(t_2 \mid C_t^+)} = \frac{f_3^{--+}(t_1,t_2,t)}{f_2^{-+}(t_2,t)} \qquad (2-197)$$

Ignoring the conditioning on the C_t^+ the following approximation is obtained

$$f_1^-(t_1 \mid \mathcal{L}_{t_2,t}) \simeq \frac{f_2^{--}(t_1,t_2)}{f_1^-(t_2)} \qquad (2-198)$$

The approximations to the first-passage time probability density function obtained by the numerical solution of (2-167) with the kernel approximations (2-197) and (2-198) and succeeding insertion into (2-30) are designated $f_{T_1}^{(g)}(t \mid \mathcal{E}_0)$ and $f_{T_1}^{(h)}(t \mid \mathcal{E}_0)$, respectively.

The approximation (2-197) is reasonable, because both numerator and denominator are upper bounds, and thus they counterbalance each other to some extent. At high barrier levels with independent crossing events $f_1^-(t_1 \mid \mathcal{L}_{t_2,t}) \simeq f_1^-(t_1)$. As follows from (2-4) this limit is also attained asymptotically by the right-hand sides of (2-197) and (2-198). Hence, both of these approximations are asymptotically correct at high barrier levels.

Finally, it can be noted that (2-198) is related to (2-197) in the same way as (2-105) is related to (2-104). In both cases the conditioning on the considered set of sample curves is ignored in the joint crossing rates.

With the same argument as applied to (2-110), (2-111), the following bounds may be derived for $f_{L_t} + (t - t_1)$ from the integral equation (2-167)

$$f_{L_t} + (t - t_1) \leq f_1^-(t_1 \mid C_t^+) \tag{2-199}$$

$$f_{L_t} + (t - t_1) \geq f_1^-(t_1 \mid C_t^+) - \int_{t_1}^{t} f_2^{--}(t_1, t_2 \mid C_t^+) dt_2 \tag{2-200}$$

Upon inserting these bounds into the right-hand side of (2-30) and using (2-7) the following exact bounds for the first-passage time probability density function are then obtained

$$f_{T_1}(t \mid \mathcal{E}_0) \geq R_{T_1}^{(1)}(t) = \frac{1}{P(\mathcal{E}_0)} \left(f_1^+(t) - \int_0^t f_2^{-+}(t_1, t) dt_1 \right) \tag{2-201}$$

$$f_{T_1}(t \mid \mathcal{E}_0) \leq S_{T_1}^{(2)}(t) = \frac{1}{P(\mathcal{E}_0)} \left(f_1^+(t) - \int_0^t f_2^{-+}(t_1, t) dt_1 + \int_0^t \int_{t_1}^t f_3^{--+}(t_2, t_1, t) dt_2 dt_1 \right) \tag{2-202}$$

(2-201) and (2-202) indicate alternative results in unconditioned crossing rates to (2-111) and (2-112) for the 1st lower bound and the 2nd upper bound. The 1st upper bound in this hierarchy of bounds is given by (2-113).

Initially, the single degree-of-freedom oscillator (2-102) is considered with a single barrier stochastic start first-passage time problem. The damping ratio is $\zeta = 0.01$ and the barrier level is $b(t) \equiv 2.0\sigma_{X,0}$. $f_{T_1}^{(g)}(t \mid \mathcal{E}_0)$ as given by (2-197) and $f_{T_1}^{(h)}(t \mid \mathcal{E}_0)$ as given by (2-198) are shown in fig. 2-26 in comparison with simulation results obtained by ergodic sampling based on (2-31). Further, the results have been compared to the approximation $f_{T_1}^{(b)}(t \mid \mathcal{E}_0)$, obtained from numerical solution of the integral equation (2-35) with the kernel approximation (2-105) and the approximative inhomogeneity (2-106). $f_T^{(h)}(t \mid \mathcal{E}_0)$ involves the unconditioned 2nd order in-coming rate $f_2^{--}(t_1, t_2)$, whereas $f_T^{(b)}(t \mid \mathcal{E}_0)$ involves the unconditioned 2nd order out-crossing rate $f_2^{++}(t_1, t)$. Since these approximations demand the same computational effort they should especially be compared.

The results are shown in fig. 2-26. Both $f_{T_1}^{(g)}(t \mid \mathcal{E}_0)$ and $f_{T_1}^{(h)}(t \mid \mathcal{E}_0)$ follow closely the simulation results up to the 2nd period, whereas the approximation $f_{T_1}^{(b)}(t \mid \mathcal{E}_0)$ deviates significantly from the simulation result at the downfalls of the first-passage time curve. However, the horizontal stair levels of $f_{T_1}^{(b)}(t \mid \mathcal{E}_0)$ and $f_{T_1}^{(h)}(t \mid \mathcal{E}_0)$ are almost identical, as seen from the numeric values indicated in table 2-7. Being able to represent the correlation of the initial values better, it is concluded that $f_{T_1}^{(h)}(t \mid \mathcal{E}_0)$ is superior to $f_{T_1}^{(b)}(t \mid \mathcal{E}_0)$.

$f_{T_1}^{(g)}(t \mid \mathcal{E}_0)$, involving unconditioned 3rd order crossing rates $f_3^{--+}(t_1, t_2, t)$, has previously in fig. 2-21 for the same problem been shown to do better than the approximation $f_{T_1}^{(f)}(t \mid \mathcal{E}_0)$, obtained by solving the integral equation (2-48) with the approximate inhomogeneity (2-134) and the kernel approximation (2-135), and succeeding insertion into (2-37). This approximation involves the unconditioned 3rd order out-crossing rate $f_3^{+++}(t_2, t_1, t)$. Hence, the computational effort is comparable to that of $f_{T_1}^{(g)}(t \mid \mathcal{E}_0)$.

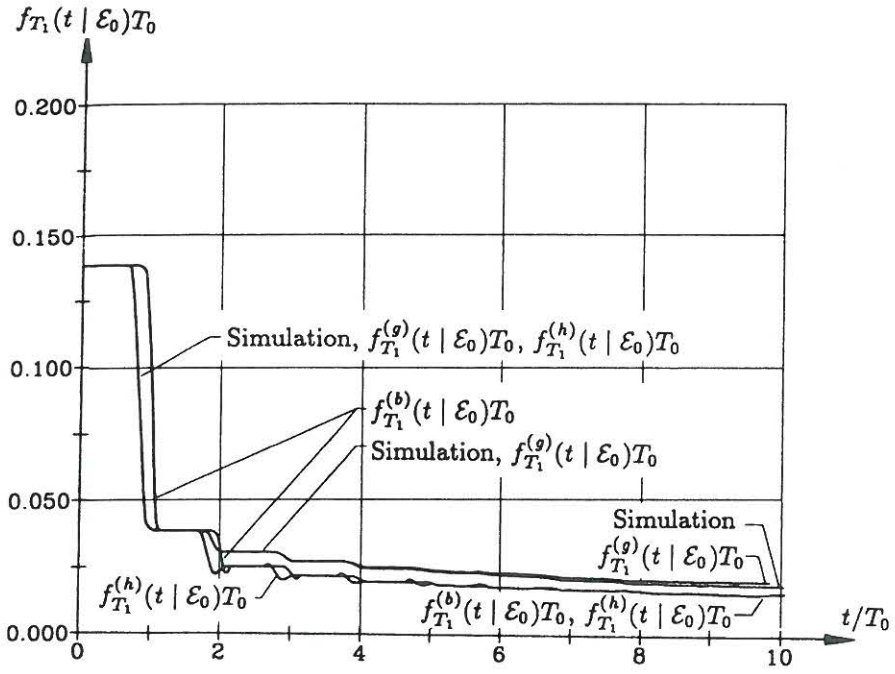

Fig. 2-26: First-passage time probability density function for a single barrier stochastic start problem of an SDOF oscillator. $\zeta = 0.01$, $b(t) = 2\sigma_{X,0}$. $f_{T_1}^{(b)}(t \mid \mathcal{E}_0)$: Eqs. (2-105), (2-106). $f_{T_1}^{(g)}(t \mid \mathcal{E}_0)$: Eq. (2-197). $f_{T_1}^{(h)}(t \mid \mathcal{E}_0)$: Eq. (2-198). Nielsen and Sørensen (1988).

Interval $\frac{t}{T_0}$	Simulation (exact)	$f_{T_1}^{(g)}(t \mid \mathcal{E}_0)T_0$	$f_{T_1}^{(h)}(t \mid \mathcal{E}_0)T_0$	$f_{T_1}^{(b)}(t \mid \mathcal{E}_0)T_0$
0–1	0.13849	0.13849	0.13849	0.13849
1–2	0.03821	0.03821	0.03822	0.03822
2–3	0.03041	0.03040	0.02507	0.02507
3–4	0.02678	0.02715	0.02124	0.02124
4–5	0.02453	0.02527	0.01938	0.01938

Table 2-7: Stair levels of approximations to the first-passage time probability density function of an SDOF oscillator.

In fig. 2-27 the results for the single barrier stochastic start problem for the 2 degree-of-freedom system defined in relation to fig. 2-22 are shown. Again, it is seen that $f_{T_1}^{(h)}(t \mid \mathcal{E}_0)$ is doing better than $f_{T_1}^{(b)}(t \mid \mathcal{E}_0)$ at the downfall of the first-passage time probability density curve, whereas these approximations are comparable elsewhere. The approximate result of Toro and Cornell (1986) has been indicated for comparison as in fig. 2-22.

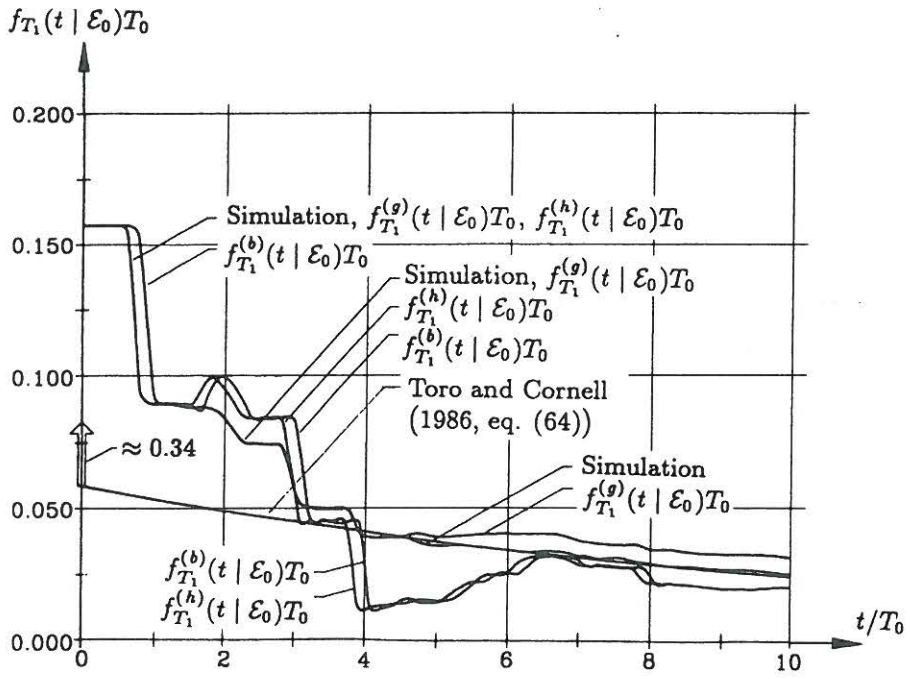

Fig. 2-27: First-passage time probability density function for a single barrier stochastic start problem of a 2 degree-of-freedom system $\sigma_1^2 = \sigma_2^2 = 0.5$, $\zeta_1 = \zeta_2 = 0.01$, $\omega_1 = 2.0\pi$, $\omega_2 = 2.5\pi$, $b(t) = 2.0\sigma_{X,0}^2$. $f_{T_1}^{(b)}(t \mid \mathcal{E}_0)$: Eqs. (2-105), (2-106). $f_{T_1}^{(g)}(t \mid \mathcal{E}_0)$: Eq. (2-197). $f_{T_1}^{(h)}(t \mid \mathcal{E}_0)$: Eq. (2-198). Nielsen and Sørensen (1988).

The general conclusion from this example is that approximations to the first-passage time probability density function, obtained by numerical solution of the integral equation (2-167) with an approximate kernel function and succeeding insertion into (2-30), are superior to approximations based on the integral equations (2-35) and (2-48), involving crossing rates of the same order.

Example 2-7: Approximation for the kernel of the integral equations (2-180) and (2-183)

At the application of the integral equation (2-180) the following approximation may be used for the kernel, obtained by truncating the numerator and the denominator series of (2-182) to the first term, Nielsen (1990a)

$$f_1^-(t_2 \mid C_{t_1}^- \cap \mathcal{L}_{t_3,t}) \simeq \frac{f_4^{---+}(t_1, t_2, t_3, t)}{f_3^{--+}(t_1, t_3, t)} \qquad (2-203)$$

From the numerical solution of (2-180) for $f_{L_t^+}(t - t_2 \mid C_{t_1}^-)$, using the inhomogeneity (2-181) and the kernel (2-203), $f_{L_t^+}(t - t_1)$ is next obtained from (2-170). Finally, $f_{T_1}(t \mid \mathcal{E}_{t_0})$ is obtained from (2-30). Again, the approximation (2-203) is reasonable, because both counter and denominator are upper bounds, and hence tend to counterbalance each other.

Similarly, on application of the integral equation (2-183) the following approximation may be used for the kernel, obtained by truncating the numerator and the denominator series of (2-185) to the first term, Nielsen (1990a)

$$f_1^-(t_{n+1} \mid C_{t_1}^- \cap \cdots \cap C_{t_n}^- \cap \mathcal{L}_{t_{n+2},t}) \simeq \frac{f_{n+3}^{-\cdots---+}(t_1, \ldots, t_n, t_{n+1}, t_{n+2}, t)}{f_{n+2}^{-\cdots--+}(t_1, \ldots, t_n, t_{n+2}, t)} \qquad (2-204)$$

Even though no numerical results are presented, the kernel approximations (2-203) and (2-204) can be

expected to provide the best available approximations to the first-passage time function based on joint unconditioned crossing rates of the order $n + 3$.

Example 2-8: Approximations for the kernel and the inhomogeneity of integral equation (2-186) and related bounding technique

At the application of the integral equation (2-186) the following approximation may be used for the kernel as given by (2-190), obtained by truncating the numerator and the denominator series to the first term

$$f_1^+(t \mid C_{t_1}^- \cap \mathcal{F}_{t_2}^{(1)}) \simeq \frac{f_2^{++}(t_2, t \mid C_{t_1}^-)}{f_1^+(t_2 \mid C_{t_1}^-)} = \frac{f_2^{-++}(t_1, t_2, t)}{f_1^{-+}(t_1, t_2)} \qquad (2-205)$$

In the last statement of (2-205) use of (2-7) has been made. Again the approximation (2-205) is a good one, because both counter and denominator are upper bounds. At high barrier levels with independent crossing events $f_1^+(t \mid C_{t_1}^- \cap \mathcal{F}_{t_2}^{(1)}) \simeq f_1^+(t)$. This limit is also asymptotically attained by the right-hand side of (2-205), which obviously will be asymptotically correct at high barrier levels. The results for the first-passage time probability density function obtained from the kernel approximation (2-205) can be expected to be of the same quality as $f_{T_1}^{(g)}(t \mid \mathcal{E}_0)$, based on the quite similar kernel approximation (2-197). No numerical example is shown.

With the same argument as applied to (2-110) and (2-111), the following bounds may be derived for $f_{L_{t_1}^-}(t - t_1)$ from the integral equation (2-186)

$$f_{L_{t_1}^-}(t - t_1) \leq f_1^+(t \mid C_{t_1}^-) \qquad (2-206)$$

$$f_{L_{t_1}^-}(t - t_1) \geq f_1^+(t \mid C_{t_1}^-) - \int_{t_1}^{t} f_2^{++}(t_2, t \mid C_{t_1}^-) dt_2 \qquad (2-207)$$

From (2-20) and application of (2-7) the following bounds are then obtained for $f_{L_t^+}(t - t_1)$

$$f_{L_t^+}(t - t_1) \leq \frac{1}{f_1^+(t)} f_2^{-+}(t_1, t) \qquad (2-208)$$

$$f_{L_t^+}(t - t_1) \geq \frac{1}{f_1^+(t)} \left(f_2^{-+}(t_1, t) - \int_{t_1}^{t} f_2^{-++}(t_1, t_2, t) dt_2 \right) \qquad (2-209)$$

Upon inserting these bounds into the right-hand side of (2-30) the following exact bounds for the first-passage time probability density function are then obtained

$$f_{T_1}(t \mid \mathcal{E}_0) \geq R_{T_1}^{(1)}(t) = \frac{1}{P(\mathcal{E}_0)} \left(f_1^+(t) - \int_0^t f_2^{-+}(t_1, t) dt_1 \right) \qquad (2-210)$$

$$f_{T_1}(t \mid \mathcal{E}_0) \leq S_{T_1}^{(2)}(t) = \frac{1}{P(\mathcal{E}_0)} \left(f_1^+(t) - \int_0^t f_2^{-+}(t_1, t) dt_1 + \int_0^t \int_{t_1}^t f_3^{-++}(t_1, t_2, t) dt_2 dt_1 \right) \qquad (2-211)$$

(2-210) is identical to (2-201). The difference between (2-202) and (2-211) is due to the different 3rd order crossing rates.

2.4 Integral equations for the probability density function of the time interval between two succeeding out-crossings from the safe domain

$f_{U_t^+}(t-t_1 \mid \mathcal{E}_{t_0}) = f_1^+(t_1;\ \{\text{exactly one in-crossing in }]t_1,t[\} \mid \mathcal{E}_{t_0} \cap \mathcal{C}_t^+)$ is the rate of out-crossings from the safe domain at the time t_1 of the sample curves which make exactly one in-crossing to the safe domain in the interval $]t_1,t[$ on condition of $\mathcal{E}_{t_0}$ and on condition of an out-crossing at the time t, cf. (2-22). The following integral equation may then be formulated

$$f_{U_t^+}(t-t_1 \mid \mathcal{E}_{t_0}) = f_1^+(t_1 \mid \mathcal{E}_{t_0} \cap \mathcal{C}_t^+) -$$

$$\int_{t_1}^{t} f_1^+(t_1 \mid \mathcal{E}_{t_0} \cap \mathcal{C}_{t_2}^+ \cap \{\text{exactly one in-crossing in }]t_2,t[\} \cap \mathcal{C}_t^+) f_{U_t^+}(t-t_2 \mid \mathcal{E}_{t_0})\, dt_2 \tag{2-212}$$

where

$$f_1^+(t_1 \mid \mathcal{E}_{t_0} \cap \mathcal{C}_t^+) = \frac{f_2^{++}(t_1,t \mid \mathcal{E}_{t_0})}{f_1^+(t \mid \mathcal{E}_{t_0})},\ t_0 < t_1 < t \tag{2-213}$$

The last term on the right-hand side of (2-212) withdraws from $f_1^+(t_1 \mid \mathcal{E}_{t_0} \cap \mathcal{C}_t^+)$ the rate of out-crossings at the time t_1 of the sample curves which have at least one further in-crossing to the safe domain in the interval $]t_1,t[$ on condition of an out-crossing at the time t.

Define $\mathcal{U}_{t_2,t} = \mathcal{C}_{t_2}^+ \cap \{\text{exactly one in-crossing in }]t_2,t[\} \cap \mathcal{C}_t^+$. Then, $f_1^+(t_1 \mid \mathcal{E}_{t_0} \cap \mathcal{U}_{t_2,t})$ $f_{U_t^+}(t-t_2 \mid \mathcal{E}_{t_0}) = f_2^{++}(t_1,t_2\ ;\ \mathcal{U}_{t_2,t} \mid \mathcal{E}_{t_0} \cap \mathcal{C}_t^+)$ represents the 2nd order rate of out-crossings at the times t_1 and t_2 of the sample curves which make exactly one in-crossing to the safe domain in the interval $]t_2,t[$ on condition of $\mathcal{E}_{t_0}$ and on condition of an out-crossing at the time t. For this quantity the following identity holds

$$f_1^+(t_1 \mid \mathcal{E}_{t_0} \cap \mathcal{U}_{t_2,t}) f_{U_t^+}(t-t_2 \mid \mathcal{E}_{t_0}) = f_{U_t^+}(t-t_2 \mid \mathcal{E}_{t_0} \cap \mathcal{C}_{t_1}^+) f_1^+(t_1 \mid \mathcal{E}_{t_0} \cap \mathcal{C}_t^+) \tag{2-214}$$

From (2-212) and (2-214) the following relation is obtained, similarly to (2-37) and (2-170)

$$f_{U_t^+}(t-t_1 \mid \mathcal{E}_{t_0}) = f_1^+(t_1 \mid \mathcal{E}_{t_0} \cap \mathcal{C}_t^+) \left(1 - \int_{t_1}^{t} f_{U_t^+}(t-t_2 \mid \mathcal{E}_{t_0} \cap \mathcal{C}_{t_1}^+)\, dt_2\right) \tag{2-215}$$

$f_1^+(t_1 \mid \mathcal{E}_{t_0} \cap \mathcal{U}_{t_2,t}) f_{U_t^+}(t-t_2 \mid \mathcal{E}_{t_0})$ fulfils the integral equation

$$f_1^+(t_1 \mid \mathcal{E}_{t_0} \cap \mathcal{U}_{t_2,t}) f_{U_t^+}(t-t_2 \mid \mathcal{E}_{t_0}) = f_2^{++}(t_1,t_2 \mid \mathcal{E}_{t_0} \cap \mathcal{C}_t^+) -$$

$$\int_{t_2}^{t} f_2^{++}(t_1, t_2 \mid \mathcal{E}_{t_0} \cap \mathcal{U}_{t_3,t}) f_{U_t^+}(t - t_3 \mid \mathcal{E}_{t_0})\, dt_3 \qquad (2-216)$$

$f_2^{++}(t_1, t_2 \mid \mathcal{E}_{t_0} \cap \mathcal{U}_{t_3,t}) f_{U_t^+}(t - t_3 \mid \mathcal{E}_{t_0})$ signifies the 3rd order rate of out-crossings from S_{t_1}, S_{t_2}, S_{t_3}, $t_0 < t_1 < t_2 < t_3 < t$ of the sample curves which make exactly one in-crossing to the safe domain in the interval $]t_3, t[$ on condition of $\mathcal{E}_{t_0}$ and on condition of an out-crossing at the time t. For this quantity the following identity holds

$$f_2^{++}(t_1, t_2 \mid \mathcal{E}_{t_0} \cap \mathcal{U}_{t_3,t}) f_{U_t^+}(t - t_3 \mid \mathcal{E}_{t_0}) =$$

$$f_{U_t^+}(t - t_3 \mid \mathcal{E}_{t_0} \cap \mathcal{C}_{t_1}^+ \cap \mathcal{C}_{t_2}^+) f_2^{++}(t_1, t_2 \mid \mathcal{E}_{t_0} \cap \mathcal{C}_t^+) \qquad (2-217)$$

From (2-212), (2-216) and (2-217) follow

$$f_{U_t^+}(t - t_1 \mid \mathcal{E}_{t_0}) = f_1^+(t_1 \mid \mathcal{E}_{t_0} \cap \mathcal{C}_t^+) -$$

$$\int_{t_1}^{t} f_2^{++}(t_1, t_2 \mid \mathcal{E}_{t_0} \cap \mathcal{C}_t^+) \left(1 - \int_{t_2}^{t} f_{U_t^+}(t - t_3 \mid \mathcal{E}_{t_0} \cap \mathcal{C}_{t_1}^+ \cap \mathcal{C}_{t_2}^+)\, dt_3\right) dt_2 \qquad (2-218)$$

$$f_{U_t^+}(t - t_1 \mid \mathcal{E}_{t_0}) = f_1^+(t_1 \mid \mathcal{E}_{t_0} \cap \mathcal{C}_t^+) -$$

$$\int_{t_1}^{t} f_2^{++}(t_1, t_2 \mid \mathcal{E}_{t_0} \cap \mathcal{C}_t^+)\, dt_2 + \int_{t_1}^{t}\int_{t_2}^{t} f_2^{++}(t_1, t_2 \mid \mathcal{E}_{t_0} \cap \mathcal{U}_{t_3,t}) f_{U_t^+}(t - t_3 \mid \mathcal{E}_{t_0})\, dt_3 dt_2 \qquad (2-219)$$

Continuation of this process until the nth term leads to the result

$$f_{U_t^+}(t - t_1 \mid \mathcal{E}_{t_0}) = f_1^+(t_1 \mid \mathcal{E}_{t_0} \cap \mathcal{C}_t^+) - \int_{t_1}^{t} f_2^{++}(t_1, t_2 \mid \mathcal{E}_{t_0} \cap \mathcal{C}_t^+)\, dt_2 + \cdots +$$

$$(-1)^{n-1} \int_{t_1}^{t}\int_{t_2}^{t} \cdots \int_{t_{n-1}}^{t} f_n^{+++\cdots+}(t_1, t_2, t_3, \ldots, t_n \mid \mathcal{E}_{t_0} \cap \mathcal{C}_t^+) \cdot$$

$$\left(1 - \int_{t_n}^{t} f_{U_t^+}(t - t_{n+1} \mid \mathcal{E}_{t_0} \cap \mathcal{C}_{t_1}^+ \cap \mathcal{C}_{t_2}^+ \cap \mathcal{C}_{t_3}^+ \cap \cdots \cap \mathcal{C}_{t_n}^+)\, dt_{n+1}\right) dt_n \cdots dt_3 dt_2 \qquad (2-220)$$

and

$$f_1^+(t_1 \mid \mathcal{E}_{t_0} \cap \mathcal{U}_{t_2,t}) f_{U_t^+}(t - t_2 \mid \mathcal{E}_{t_0}) = f_2^{++}(t_1, t_2 \mid \mathcal{E}_{t_0} \cap \mathcal{C}_t^+) -$$

$$\int_{t_2}^{t} f_3^{+++}(t_1, t_2, t_3 \mid \mathcal{E}_{t_0} \cap \mathcal{C}_t^+)\, dt_3 + \cdots +$$

$$(-1)^{n-2} \int_{t_2}^{t} \cdots \int_{t_{n-1}}^{t} f_n^{+++\cdots+}(t_1, t_2, t_3, \ldots, t_n \mid \mathcal{E}_{t_0} \cap \mathcal{C}_t^+) \cdot$$

$$\left(1 - \int_{t_n}^{t} f_{U_t^+}(t - t_{n+1} \mid \mathcal{E}_{t_0} \cap \mathcal{C}_{t_1}^+ \cap \mathcal{C}_{t_2}^+ \cap \cdots \cap \mathcal{C}_{t_n}^+)\, dt_{n+1}\right) dt_n \cdots dt_3 \qquad (2-221)$$

From (2-8), (2-34) and (2-220), the following series is then obtained for the first-passage probability density function

$$f_{T_1}(t \mid \mathcal{E}_{t_0}) = f_1^+(t \mid \mathcal{E}_{t_0}) - \int_{t_0}^{t} f_2^{++}(t_1, t \mid \mathcal{E}_{t_0})\, dt_1 + \cdots +$$

$$(-1)^n \int_{t_0}^{t} \int_{t_1}^{t} \cdots \int_{t_{n-2}}^{t} \int_{t_{n-1}}^{t} f_{n+1}^{++\cdots+++}(t_1, t_2, \ldots, t_{n-1}, t_n, t \mid \mathcal{E}_{t_0}) \cdot$$

$$\left(1 - \int_{t_n}^{t} f_{U_t^+}(t - t_{n+1} \mid \mathcal{E}_{t_0} \cap \mathcal{C}_{t_1}^+ \cap \mathcal{C}_{t_2}^+ \cap \cdots \cap \mathcal{C}_{t_{n-1}}^+ \cap \mathcal{C}_{t_n}^+) dt_{n+1}\right) dt_n dt_{n-1} \cdots dt_2 dt_1 \qquad (2-222)$$

From (2-3) it follows that the integrand of the last term of (2-222) is symmetric in the indexes $t_1, \ldots, t_{n-1}$. After renaming of the integration parameters (2-222) can then be written

$$f_{T_1}(t \mid \mathcal{E}_{t_0}) = f_1^+(t \mid \mathcal{E}_{t_0}) - \int_{t_0}^{t} f_2^{++}(t_1, t \mid \mathcal{E}_{t_0})\, dt_1 + \cdots +$$

$$(-1)^n \int_{t_0}^{t} \int_{t_0}^{t_1} \cdots \int_{t_0}^{t_{n-1}} f_{n+1}^{+\cdots+++}(t_n, \ldots, t_2, t_1, t \mid \mathcal{E}_{t_0}) \cdot$$

$$\left(1 - \int_{t_1}^{t} f_{U_t^+}(t - \tau \mid \mathcal{E}_{t_0} \cap \mathcal{C}_{t_n}^+ \cap \cdots \cap \mathcal{C}_{t_2}^+ \cap \mathcal{C}_{t_1}^+)\, d\tau\right) dt_n \cdots dt_2 dt_1 \qquad (2-223)$$

From (2-220) and (2-221) the following formal expansion for $f_1^+(t_1 \mid \mathcal{E}_{t_0} \cap \mathcal{U}_{t_2,t})$ is obtained as $n \to \infty$

$$f_1^+(t_1 \mid \mathcal{E}_{t_0} \cap \mathcal{U}_{t_2,t}) = \frac{f_2^{++}(t_1,t_2 \mid \mathcal{E}_{t_0} \cap \mathcal{C}_t^+) - \int_{t_2}^{t} f_3^{+++}(t_1,t_2,t_3 \mid \mathcal{E}_{t_0} \cap \mathcal{C}_t^+)dt_3 + \cdots}{f_1^+(t_2 \mid \mathcal{E}_{t_0} \cap \mathcal{C}_t^+) - \int_{t_2}^{t} f_2^{++}(t_2,t_3 \mid \mathcal{E}_{t_0} \cap \mathcal{C}_t^+)dt_3 + \cdots} =$$

$$\frac{f_3^{+++}(t_1,t_2,t \mid \mathcal{E}_{t_0}) - \int_{t_2}^{t} f_4^{++++}(t_1,t_2,t_3,t \mid \mathcal{E}_{t_0})\, dt_3 + \cdots}{f_2^{++}(t_2,t \mid \mathcal{E}_{t_0}) - \int_{t_2}^{t} f_3^{+++}(t_2,t_3,t \mid \mathcal{E}_{t_0})\, dt_3 + \cdots} =$$

$$\frac{\sum_{j=0}^{\infty}(-1)^j F_{3,j}^+(t_1,t_2,t \mid \mathcal{E}_{t_0})}{\sum_{j=0}^{\infty}(-1)^j F_{2,j}^+(t_2,t \mid \mathcal{E}_{t_0})} \qquad (2-224)$$

Analogous to (2-48) and (2-180) $f_{U_t^+}(t-t_2 \mid \mathcal{E}_{t_0} \cap \mathcal{C}_{t_1}^+)$ fulfils the integral equation

$$f_{U_t^+}(t-t_2 \mid \mathcal{E}_{t_0} \cap \mathcal{C}_{t_1}^+) = f_1^+(t_2 \mid \mathcal{E}_{t_0} \cap \mathcal{C}_{t_1}^+ \cap \mathcal{C}_t^+) -$$

$$\int_{t_2}^{t} f_1^+(t_2 \mid \mathcal{E}_{t_0} \cap \mathcal{C}_{t_1}^+ \cap \mathcal{U}_{t_3,t}) f_{U_t^+}(t-t_3 \mid \mathcal{E}_{t_0} \cap \mathcal{C}_{t_1}^+)\, dt_3\,, \quad t_0 < t_1 < t_2 < t \quad (2-225)$$

where

$$f_1^+(t_2 \mid \mathcal{E}_{t_0} \cap \mathcal{C}_{t_1}^+ \cap \mathcal{C}_t^+) = \frac{f_3^{+++}(t_1,t_2,t \mid \mathcal{E}_{t_0})}{f_2^{++}(t_1,t \mid \mathcal{E}_{t_0})} \qquad (2-226)$$

$$f_1^+(t_2 \mid \mathcal{E}_{t_0} \cap \mathcal{C}_{t_1}^+ \cap \mathcal{U}_{t_3,t}) =$$

$$\frac{f_2^{++}(t_2,t_3 \mid \mathcal{E}_{t_0} \cap \mathcal{C}_{t_1}^+ \cap \mathcal{C}_t^+) - \int_{t_3}^{t} f_3^{+++}(t_2,t_3,t_4 \mid \mathcal{E}_{t_0} \cap \mathcal{C}_{t_1}^+ \cap \mathcal{C}_t^+)\, dt_4 + \cdots}{f_1^+(t_3 \mid \mathcal{E}_{t_0} \cap \mathcal{C}_{t_1}^+ \cap \mathcal{C}_t^+) - \int_{t_3}^{t} f_2^{++}(t_3,t_4 \mid \mathcal{E}_{t_0} \cap \mathcal{C}_{t_1}^+ \cap \mathcal{C}_t^+)\, dt_4 + \cdots} =$$

$$\frac{f_4^{++++}(t_1,t_2,t_3,t \mid \mathcal{E}_{t_0}) - \int_{t_3}^{t} f_5^{+++++}(t_1,t_2,t_3,t_4,t \mid \mathcal{E}_{t_0})\, dt_4 + \cdots}{f_3^{+++}(t_1,t_3,t \mid \mathcal{E}_{t_0}) - \int_{t_3}^{t} f_4^{++++}(t_1,t_3,t_4,t \mid \mathcal{E}_{t_0})\, dt_4 + \cdots} =$$

$$\frac{\sum_{j=0}^{\infty}(-1)^j F^+_{4,j}(t_1,t_2,t_3,t \mid \mathcal{E}_{t_0})}{\sum_{j=0}^{\infty}(-1)^j F^+_{3,j}(t_1,t_3,t \mid \mathcal{E}_{t_0})} \qquad (2-227)$$

Similarly, $f_{U_t^+}(t-t_{n+1} \mid \mathcal{E}_{t_0} \cap \mathcal{C}^+_{t_1} \cap \cdots \cap \mathcal{C}^+_{t_n})$ fulfils the integral equation

$$f_{U_t^+}(t-t_{n+1} \mid \mathcal{E}_{t_0} \cap \mathcal{C}^+_{t_1} \cap \cdots \cap \mathcal{C}^+_{t_n}) = f_1^+(t_{n+1} \mid \mathcal{E}_{t_0} \cap \mathcal{C}^+_{t_1} \cap \cdots \cap \mathcal{C}^+_{t_n} \cap \mathcal{C}^+_t) -$$

$$\int_{t_{n+1}}^{t} f_1^+(t_{n+1} \mid \mathcal{E}_{t_0} \cap \mathcal{C}^+_{t_1} \cap \cdots \cap \mathcal{C}^+_{t_n} \cap \mathcal{U}_{t_{n+2},t}) f_{U_t^+}(t-t_{n+2} \mid \mathcal{E}_{t_0} \cap \mathcal{C}^+_{t_1} \cap \cdots \cap \mathcal{C}^+_{t_n})\, dt_{n+2}\,,$$

$$t_0 < t_1 < \cdots < t_n < t_{n+1} < t \qquad (2-228)$$

where

$$f_1^+(t_{n+1} \mid \mathcal{E}_{t_0} \cap \mathcal{C}^+_{t_1} \cap \cdots \cap \mathcal{C}^+_{t_n} \cap \mathcal{C}^+_t) = \frac{f^{+\cdots+++}_{n+2}(t_1,\ldots,t_n,t_{n+1},t \mid \mathcal{E}_{t_0})}{f^{+\cdots++}_{n+1}(t_1,\ldots,t_n,t \mid \mathcal{E}_{t_0})} \qquad (2-229)$$

$$f_1^+(t_{n+1} \mid \mathcal{E}_{t_0} \cap \mathcal{C}^+_{t_1} \cap \cdots \cap \mathcal{C}^+_{t_n} \cap \mathcal{U}_{t_{n+2},t}) = \frac{\sum_{j=0}^{\infty}(-1)^j F^+_{n+3,j}(t_1,\ldots,t_{n+1},t_{n+2},t \mid \mathcal{E}_{t_0})}{\sum_{j=0}^{\infty}(-1)^j F^+_{n+2,j}(t_1,\ldots,t_n,t_{n+2},t \mid \mathcal{E}_{t_0})} \qquad (2-230)$$

$f_{U^-_{t_1}}(t-t_1 \mid \mathcal{E}_{t_0}) = f_1^+(t;\ \{\text{exactly one in-crossing in }]t_1,t[\} \mid \mathcal{E}_{t_0} \cap \mathcal{C}^+_{t_1})$ is the rate of out-crossings from the safe domain at the time t of the sample curves which make exactly one in-crossing in the interval $]t_1,t[$ on condition of $\mathcal{E}_{t_0}$ and on condition of an out-crossing at the time t_1, cf. (2-21). $f_{U^-_{t_1}}(t-t_1 \mid \mathcal{E}_{t_0})$ fulfils the integral equation

$$f_{U^-_{t_1}}(t-t_1 \mid \mathcal{E}_{t_0}) = f_1^+(t \mid \mathcal{E}_{t_0} \cap \mathcal{C}^+_{t_1}) - \int_{t_1}^{t} f_1^+(t \mid \mathcal{E}_{t_0} \cap \mathcal{U}_{t_1,t_2}) f_{U^-_{t_1}}(t_2-t_1 \mid \mathcal{E}_{t_0})\, dt_2 \qquad (2-231)$$

where

$$f_1^+(t \mid \mathcal{E}_{t_0} \cap \mathcal{C}^+_{t_1}) = \frac{f_2^{++}(t_1,t \mid \mathcal{E}_{t_0})}{f_1^+(t_1 \mid \mathcal{E}_{t_0})}\,, \quad t_0 < t_1 < t \qquad (2-232)$$

The following expansions for $f_{U_{t_1}^-}(t-t_1 \mid \mathcal{E}_{t_0})$ and for the kernel $f_1^+(t \mid \mathcal{E}_{t_0} \cap \mathcal{U}_{t_1,t_2})$, analogous to (2-188) and (2-190), can be derived from (2-231)

$$f_{U_{t_1}^-}(t-t_1 \mid \mathcal{E}_{t_0}) = f_1^+(t \mid \mathcal{E}_{t_0} \cap \mathcal{C}_{t_1}^+) - \int_{t_1}^{t} f_2^{++}(t_2,t \mid \mathcal{E}_{t_0} \cap \mathcal{C}_{t_1}^+)dt_2 + \cdots +$$

$$(-1)^{n-1} \int_{t_1}^{t}\int_{t_1}^{t_2}\cdots\int_{t_1}^{t_{n-1}} f_n^{+\cdots+++}(t_n,\ldots,t_3,t_2,t \mid \mathcal{E}_{t_0} \cap \mathcal{C}_{t_1}^+) \cdot$$

$$\left(1-\int_{t_1}^{t_n} f_{U_{t_1}^-}(t_{n+1}-t_1 \mid \mathcal{E}_{t_0} \cap \mathcal{C}_{t_n}^+ \cap \cdots \cap \mathcal{C}_{t_3}^+ \cap \mathcal{C}_{t_2}^+ \cap \mathcal{C}_t^+)\, dt_{n+1}\right) dt_n \cdots dt_3 dt_2 \ ,$$

$$t_1 < t_{n+1} < t_n < t_{n-1} < \cdots < t_3 < t_2 < t \qquad (2-233)$$

$$f_1^+(t \mid \mathcal{U}_{t_1,t_2}) = \frac{\sum_{j=0}^{\infty}(-1)^j F_{2,j}^+(t_2,t \mid \mathcal{E}_{t_0} \cap \mathcal{C}_{t_1}^+)}{\sum_{j=0}^{\infty}(-1)^j F_{1,j}^+(t_2 \mid \mathcal{E}_{t_0} \cap \mathcal{C}_{t_1}^+)} =$$

$$\frac{\sum_{j=0}^{\infty}(-1)^j F_{3,j}^+(t_1,t_2,t \mid \mathcal{E}_{t_0})}{\sum_{j=0}^{\infty}(-1)^j F_{2,j}^+(t_1,t_2 \mid \mathcal{E}_{t_0})} \qquad (2-234)$$

From (2-3) follows that the integrand of the last term in (2-233) is symmetric in the indices $t_{n-1},\ldots,t_3,t_2$. After renaming of the integration parameters and application of (2-8), (2-233) can then be written

$$f_{U_{t_1}^-}(t-t_1 \mid \mathcal{E}_{t_0}) = \frac{1}{f_1^+(t_1 \mid \mathcal{E}_{t_0})}\left(f_2^{++}(t_1,t \mid \mathcal{E}_{t_0}) - \int_{t_1}^{t} f_3^{+++}(t_1,t_2,t \mid \mathcal{E}_{t_0})\, dt_2 + \cdots +\right.$$

$$(-1)^{n-1}\int_{t_1}^{t}\cdots\int_{t_{n-1}}^{t} f_{n+1}^{++\cdots++}(t_1,t_2,\ldots,t_n,t \mid \mathcal{E}_{t_0}) \cdot$$

$$\left.\left(1-\int_{t_1}^{t_2} f_{U_{t_1}^-}(\tau-t_1 \mid \mathcal{E}_{t_0} \cap \mathcal{C}_{t_2}^+ \cap \cdots \cap \mathcal{C}_{t_n}^+ \cap \mathcal{C}_t^+)\, d\tau\right) dt_n \cdots dt_2\right) \ ,$$

$$t_1 < t_2 < t_3 < \cdots < t_{n+1} < t \qquad (2-235)$$

From (2-33) and (2-235), the following series is then obtained for the first-passage time probability density function

$$f_{T_1}(t \mid \mathcal{E}_{t_0}) = f_1^+(t \mid \mathcal{E}_{t_0}) - \int_{t_0}^{t} f_2^{++}(t_1, t \mid \mathcal{E}_{t_0})\, dt_1 + \cdots +$$

$$(-1)^n \int_{t_0}^{t} \int_{t_1}^{t} \cdots \int_{t_{n-1}}^{t} f_{n+1}^{++\cdots++}(t_1, t_2, \ldots, t_n, t \mid \mathcal{E}_{t_0}) \cdot$$

$$\left(1 - \int_{t_1}^{t_2} f_{U_{t_1}^-}(\tau - t_1 \mid \mathcal{E}_{t_0} \cap \mathcal{C}_{t_2}^+ \cap \cdots \cap \mathcal{C}_{t_n}^+ \cap \mathcal{C}_t^+)\, d\tau\right) dt_n \cdots dt_2 dt_1 \qquad (2-236)$$

(2-223) and (2-236) are seen to converge to the same inclusion-exclusion series in the conditioned crossing rates as (2-42). These series only differ because of different formulation of the remainders, and are both generated by the identity (2-33).

The Markov system (2-79) with a safe domain defined by a single constant upper barrier b for the displacement response is considered again. Let $f_{\dot{X}U_{t_1}^-}(b, \dot{x}, t - t_1 \mid \mathcal{E}_{t_0})\, dt d\dot{x}$ be the joint probability of out-crossings in the time interval $]t, t + dt]$ at the barrier b with the out-crossing velocities in the interval $]\dot{x}, \dot{x} + d\dot{x}]$ of the sample curves, which make exactly one in-crossing to the safe domain in the interval $]t_1, t[$, on condition of $\mathcal{E}_{t_0}$ and on condition of an out-crossing at the time t_1. With an argumentation similar to the one leading to (2-193) the following integral equation for $f_{\dot{X}U_{t_1}^-}(b, \dot{x}_1, t - t_1 \mid \mathcal{E}_{t_0})$ can then be formulated

$$f_{\dot{X}U_{t_1}^-}(b, \dot{x}, t - t_1 \mid \mathcal{E}_{t_0}) = \dot{x} q_{\{\mathbf{Z}\}}(b, \dot{x}, t \mid \mathcal{E}_{t_0} \cap \mathcal{C}_{t_1}^+) - \int_{t_1}^{t} \int_{0}^{\infty} \dot{x} q_{\{\mathbf{Z}\}}(b, \dot{x}, t \mid b, \dot{x}_2, t_2) \cdot$$

$$f_{\dot{X}U_{t_1}^-}(b, \dot{x}_2, t_2 - t_1 \mid \mathcal{E}_{t_0})\, d\dot{x}_2 dt_2 \qquad (2-237)$$

where

$$q_{\{\mathbf{Z}\}}(b, \dot{x}, t \mid \mathcal{E}_{t_0} \cap \mathcal{C}_{t_1}^+) = \frac{\int_{-\infty}^{b} \int_{0}^{\infty} \dot{x}_1\, q_{\{\mathbf{Z}\}}(b, \dot{x}, t \mid b, \dot{x}_1, t_1) f_{\{X\}\{\dot{X}\}}(x_0, t_0; b, \dot{x}_1, t_1)\, dx_0 d\dot{x}_1}{\int_{-\infty}^{b} \int_{0}^{\infty} \dot{x}_1 f_{\{X\}\{\dot{X}\}}(x_0, t_0; b, \dot{x}_1, t_1)\, dx_0 d\dot{x}_1} \qquad (2-238)$$

Using (2-23), $f_{U_t^+}(t - t_1 \mid \mathcal{E}_{t_0})$ is then obtained from the solution of (2-237) as follows

$$f_{U_t^+}(t - t_1 \mid \mathcal{E}_{t_0}) = \frac{f_1^+(t_1 \mid \mathcal{E}_{t_0})}{f_1^+(t \mid \mathcal{E}_{t_0})} \int_{0}^{\infty} f_{\dot{X}U_{t_1}^-}(b, \dot{x}, t - t_1 \mid \mathcal{E}_{t_0})\, d\dot{x} \qquad (2-239)$$

In complete analogy with (2-86), (2-87), (2-90), (2-95) integral equations similar to (2-237) can be formulated for more involved Markov systems.

Upon inserting (2-239) into (2-34) the following solution is finally obtained for the first-passage time probability density function

$$f_{T_1}(t \mid \mathcal{E}_{t_0}) = f_1^+(t \mid \mathcal{E}_{t_0}) - \int_{t_0}^{t} f_1^+(t_1 \mid \mathcal{E}_{t_0}) \int_0^{\infty} f_{\dot{X}U_{t_1}^-}(b, \dot{x}, t - t_1 \mid \mathcal{E}_{t_0})\, d\dot{x} dt_1 \quad (2-240)$$

(2-193), (2-196) or (2-237), (2-240) involve computational efforts comparable to (2-81), (2-84).

An integral equation with some resemblance to (2-237) was indicated by Siegert (1951, eq. (5.6)), considering the interval length until a zero first-passage crossing at the time t in either upward or downward direction on condition of a zero crossing at the time $t_1 < t$ for a stationary 2-dimensional Markov vector process. All results in this section 2.4 have not previously been published by the author.

2.5 Summary and conclusions

Initially, in section 2.1 relationships are derived between the first-passage time probability density function on condition of the event $\mathcal{E}_{t_0}$, $f_{T_1}(t \mid \mathcal{E}_{t_0})$, and the probability density functions $f_{L_t^+}(t-t_1)$ and $f_{U_t^+}(t-t_1 \mid \mathcal{E}_{t_0})$ of, respectively, the length of the time interval spent in the safe domain from the previous in-crossing at the time t_1 until an out-crossing at the time t, and the elapsed time interval from the previous out-crossing at the time t_1 until an out-crossing at the time t on condition of $\mathcal{E}_{t_0}$. $\mathcal{E}_{t_0}$ denotes the event that a subset of initial values belongs to the safe domain at the time t_0. The relationship of these functions to the probability of failure $P_f([t_0,t])$ in the interval $[t_0,t]$ is also indicated.

In section 2.2 a Volterra integral equation is stated for $f_{T_1}(t \mid \mathcal{E}_{t_0})$. In this formulation the kernel function is introduced as a new unknown function. Based on the said integral equation inclusion-exclusion series in the joint conditioned out-crossing rates $f_n^{+\cdots+}(t_1,\ldots,t_n \mid \mathcal{E}_{t_0})$ are derived for $f_{T_1}(t \mid \mathcal{E}_{t_0})$, and for the nominator and denominator of the kernel function of the integral equation. Next, an integral equation is formulated for the first-passage time probability density function at the time t on condition of later out-crossings at the times $t_1,\ldots,t_n$, which is denoted $f_{T_1}(t \mid \mathcal{E}_{t_0} \cap \mathcal{C}_{t_1}^+ \cap \cdots \cap \mathcal{C}_{t_n}^+)$, $t_0 < t < t_1 < \cdots < t_n$. This quantity occurs in the remainder of the inclusion-exclusion series for $f_{T_1}(t \mid \mathcal{E}_{t_0})$. The idea is to obtain an approximate solution to this quantity from the integral equation. By resubstitution into the truncated series for $f_{T_1}(t \mid \mathcal{E}_{t_0})$, rapid convergence can then be expected. Further, an integral equation is formulated for the nth-passage probability density function, $f_{T_n}(t \mid \mathcal{E}_{t_0})$, and the associated inclusion-exclusion series for this quantity and for the nominator and denominator of the kernel function are derived. Next, it is shown that all the integral equations and inclusion-exclusion series referred to alternatively may be formulated in the joint crossing rates $f_n^{+\cdots+}(t_1,\ldots,t_n\ ;\ \mathcal{S}_{\tau_1} \cap \cdots \cap \mathcal{S}_{\tau_m} \mid \mathcal{E}_{t_0})$ of the sample curves in the safe domain at the discrete instants of the time $\tau_1,\ldots,\tau_m$ on condition of $\mathcal{E}_{t_0}$. In case of suitable choice of the intermediate instants of time $\tau_1,\ldots,\tau_m$, this approach results in more accurate approximate solutions to the various integral equations, and in a more rapid convergence of the various inclusion-exclusion series. Next, an inclusion-exclusion series is formulated for the hazard rate, which is of more direct applicability in reliability problems, and a non-linear integral equation of the Volterra type is formulated for this quantity. A basic problem of all the mentioned inclusion-exclusion expansions is that the series are divergent at truncation of any order as the time length of the excitation grows to infinity. Moreover, a rather limited number of terms can generally be evaluated. Various ways of truncating these series are reviewed in example 2-1. The conclusion drawn is that all available closure methods are based on weak assumptions and seem to be motivated primarily by their ability to evaluate the series on closed form. Instead, integral equation methods with appropriate approximations to the kernel functions and involving the same computational effort are advocated for. Finally, dynamic systems driven by processes with independent increment, such as the Wiener process or a compound Poisson process are considered. The state vector made up by displacement components, velocity components and possible hysteretic components then forms a Markov state vector. Integral equations of the Volterra type

are formulated for the joint probability density function of the first-passage time and the associated velocity and hysteretic components at a first passage. The first-passage time probability density function is next obtained by marginalization. The kernel of these integral equations is formed by the transition probability density function of the Markov vector, which is assumed to be known with sufficient accuracy. Hence, no new unknown functions are introduced, and exact solutions can in principle be obtained. Integral equations are formulated for the single and double barrier problem of a single degree-of-freedom non-linear and non-hysteretic oscillator, for a non-linear and non-hysteretic multi-degree-of-freedom system, and for a single-degree-of-freedom hysteretic oscillator. In example 2-2 various kernel approximations and bounding techniques related to the integral equation for $f_{T_1}(t \mid \mathcal{E}_{t_0})$ are investigated. The considered problem is a linear single-degree-of-freedom oscillator subjected to Gaussian white noise. The conclusion of the investigation is that the best kernel approximation is obtained if the series expansions of the numerator and the denominator of the kernel expansion are truncated to the first term. This is so, because both the numerator and the denominator of the truncated series are then upper bounds, and hence counterbalance each other to some extent. Two of such kernel approximations are selected for further examination. The first is expressed in terms of 2nd order joint conditioned out-crossing rates of the type $f_2^{++}(t_1, t_2 \mid \mathcal{E}_{t_0})$ and the other is in terms of 2nd order joint unconditioned out-crossing rates of the type $f_2^{++}(t_1, t_2)$. The corresponding solutions for the first-passage time probability density function are designated $f_{T_1}^{(a)}(t \mid \mathcal{E}_{t_0})$ and $f_{T_1}^{(b)}(t \mid \mathcal{E}_{t_0})$. In example 2-3 bounds are formulated for $f_{T_1}(t \mid \mathcal{E}_{t_0})$ in terms of the joint crossing rates $f_n^{+\cdots+}(t_1, \ldots, t_n; S_{\tau_1} \cap \cdots \cap S_{\tau_m} \mid \mathcal{E}_{t_0})$, and the optimal position of the control points $\tau_1, \ldots, \tau_m$ to narrow these bounds is investigated. The considered physical system is a single barrier stochastic start problem of the linear single degree-of-freedom system of example 2-2. The conclusion drawn from the numerical example is that the bounds with optimally positioned control points become significantly sharper than corresponding bounds without control points. Further, the optimal position of the control points is confined to relatively narrow intervals determined by the dynamics of the system, and hence they can be determined rather easily. An approximation for the first-passage time probability density function is formulated based on the 1st upper bound with no control points. The approximation takes into consideration the clumping of out-crossings of narrow-banded response processes at low to medium barrier levels. In example 2-4 approximations for the kernel of the integral equations for $f_{T_1}(t \mid \mathcal{E}_{t_0} \cap C_{t_1}^+)$ are considered. Specifically, a kernel approximation involving joint 3rd order unconditioned out-crossing rates of the type $f_3^{+++}(t_2, t_1, t)$ is investigated. The corresponding solution for the first-passage time probability density function is designated $f_{T_1}^{(f)}(t \mid \mathcal{E}_{t_0})$. For the single barrier stochastic start problem for a single degree-of-freedom oscillator as well for a 2 degree-of-freedom system, both subjected to Gaussian white noise, a rapid convergence to the results obtained by Monte-Carlo simulation is noticed, compared to the similar approximations based on unconditioned 2nd order out-crossing rates. In all the mentioned examples the approximate first-passage time probability density curves tend to be parallel to the simulated curve. Hence, the so-called limiting decay rate of the first-passage time probability density function can be estimated in case of time-invariant Markov systems subjected to stationary excitation and with a time-

invariant safe domain. The limiting decay rate is nothing but the lowest eigenvalues of the Kolmogorov forward and the Kolmogorov backward operators with absorption on the entrance and exit part of the accessible part of the failure surface, respectively. In example 2-5 solutions are obtained for the single barrier stationary start problem of a linear time-invariant single degree-of-freedom oscillator subjected to stationary white noise or stationary compound Poisson process excitation by numerical integration of the integral equation for the joint probability density function of the velocity at out-crossings from the barrier b and the first-passage time, $f_{\dot{X}T_1}(b, \dot{x}, t \mid \mathcal{E}_{t_0})$. In the case of white noise excitation exact solutions are obtained to the extent of the accuracy of the applied numerical integration scheme. In case of compound Poisson process driven systems, only approximate results are obtained, because the transition probability density function is approximated by a Gram-Charlier expansion truncated after the 6th order. Finally, an approximation for the first-passage time probability density function is indicated valid for systems driven by compound Poisson processes with very sparse pulse arrivals, based on assumed stochastic independence of the eigenvibrations from adjacent impulses. The approximation becomes increasingly accurate, as the mean pulse arrival rate goes to zero or the structural damping is increased.

In section 2.3 a Volterra integral equation is formulated for $f_{L_t^+}(t - t_1)$. Based on this integral equation inclusion-exclusion series in the unconditioned crossing rates $f_{n+1}^{-\cdots-+}(t_1, \ldots, t_n, t)$ are derived for $f_{L_t^+}(t - t_1)$ and for the nominator and denominator of the kernel of the said integral equation. Based upon the relationship between $f_{T_1}(t \mid \mathcal{E}_{t_0})$ and $f_{L_t^+}(t - t_1)$ an alternative inclusion-exclusion series for $f_{T_1}(t \mid \mathcal{E}_{t_0})$ in the indicated joint unconditioned crossing rates is then obtained. Next, an integral equation is stated for the probability density function of L_t^+ on condition of in-crossings to the safe domain at the times $t_1, \ldots, t_n$, previous to the in-crossing at the time t_{n+1} at the start of the interval L_t^+. This quantity, which is denoted $f_{L_t^+}(t - t_{n+1} \mid C_{t_1}^- \cap \cdots \cap C_{t_n}^-)$, $t_1 < \cdots < t_n < t_{n+1} < t$, occurs in the remainder of the inclusion-exclusion series for $f_{L_t^+}(t - t_1)$. If an approximate solution to the integral equation for this quantity can be obtained, fast convergence of the inclusion-exclusion series for $f_{L_t^+}(t - t_1)$ and hence for $f_{T_1}(t \mid \mathcal{E}_{t_0})$ can be expected by resubstitution. The following identities can be proved to be valid, $f_{T_1}(t_2 \mid \mathcal{E}_{t_1}) = f_1^+(t; \cap_{\tau \in]t_1, t[} S_\tau \mid \mathcal{E}_{t_1})$ and $f_{L_{t_1}^-}(t - t_1) = f_1^+(t; \cap_{\tau \in]t_1, t[} S_\tau \mid C_t^-)$. As seen, the functions on the right-hand sides only differ with respect to the conditioning. Based on this observation an integral equation for $f_{L_{t_1}^-}(t - t_1)$ is formulated, identical to the one, previously mentioned for $f_{T_1}(t \mid \mathcal{E}_{t_1})$, replacing the conditioning on the event $\mathcal{E}_{t_1}$ with the event C_t^- in the conditioned crossing rates. From this integral equation inclusion-exclusion series in the joint unconditioned crossing rates $f_{n+1}^{-+\cdots+}(t_1, \ldots, t_n, t)$ are derived for $f_{L_t^-}(t - t_1)$ and for the nominator and denominator of the kernel of the said integral equation. Based on the mentioned relation between $f_{L_t^-}(t - t_1)$ and $f_{L_t^+}(t - t_1)$ an alternative inclusion-exclusion series in these unconditioned crossing rates can then be derived for $f_{T_1}(t \mid \mathcal{E}_{t_0})$. Next, the single barrier first-passage time problem of a linear single degree-of-freedom oscillator exposed to Gaussian white noise is considered again for which case the displacement and the velocity form a Markov vector. From the mentioned resemblance between the integral equations for $f_{T_1}(t \mid \mathcal{E}_{t_1})$ and $f_{L_t^-}(t - t_1)$ an integral equation for the joint probability density function

$f_{\dot{X}L_{t_1}^-}(b,\dot{x},t-t_1)$ of the out-crossing velocities $\dot{X}$ at the time t and L_t^- can immediately be formulated from the corresponding integral equation for $f_{\dot{X}T_1}(b,\dot{x},t \mid \mathcal{E}_{t_1})$. From the numerical solution of this equation $f_{L_t^-}(t-t_1)$ is obtained by marginalization. $f_{L_T^+}(t-t_1)$ and finally $f_{T_1}(t \mid \mathcal{E}_{t_0})$ can then be calculated from the relations linking these quantities to $f_{L_t^-}(t-t_1)$. In example 2-6 approximations to the kernel of the integral equation for $L_t^+(t-t_1)$ are investigated. Two approximations are considered, one in terms of joint 3rd order joint crossing rates of the type $f_3^{--+}(t_1,t_2,t)$ and one in terms of joint 2nd order crossing rates of the type $f_2^{--}(t_1,t_2)$. The corresponding solutions for the first-passage time probability density function are designated $f_{T_1}^{(g)}(t \mid \mathcal{E}_{t_0})$ and $f_{T_1}^{(h)}(t \mid \mathcal{E}_{t_0})$, respectively. For the considered single barrier stationary start problem of the linear single degree-of-freedom and the 2 degrees-of-freedom oscillators subjected to Gaussian white noise, $f_{T_1}^{(h)}(t \mid \mathcal{E}_{t_0})$ turns out to give almost identical results to the approximation $f_{T_1}^{(b)}(t \mid \mathcal{E}_{t_0})$, also based on unconditioned joint 2nd order crossing rates. However, $f_{T_1}^{(h)}(t \mid \mathcal{E}_{t_0})$ is doing better during the first few periods of first-passage times. In the same way, $f_{T_1}^{(g)}(t \mid \mathcal{E}_{t_0})$ is doing better than the approximation $f_{T_1}^{(f)}(t \mid \mathcal{E}_{t_0})$, also based on unconditioned joint 3rd crossing rates. The general conclusion drawn from the example is that $f_{T_1}^{(g)}(t \mid \mathcal{E}_{t_0})$ and $f_{T_1}^{(h)}(t \mid \mathcal{E}_{t_0})$ are the best considered approximations based on joint 3rd and 2nd order unconditioned crossing rates. Example 2-7 shows the appropriate kernel approximations to be used in the integral equation for $f_{L_t^+}(t-t_2 \mid C_{t_1}^-)$ and for $f_{L_t^+}(t-t_{n+1} \mid C_{t_1}^- \cap \cdots \cap C_{t_n}^-)$, which appear in the remainder of the inclusion-exclusion series for $f_{L_t^+}(t-t_1)$. No numerical results are presented, but with reference to the conclusion in example 2-6 these approximations can be expected to provide the best approximations available based on joint unconditioned crossing rates of the order $n+3$. Finally, in example 2-8 an appropriate approximation to the kernel of the integral equation for $f_{L_{t_1}^-}(t-t_1)$ are formulated. The said kernel approximation is expected to give results of equally quality as $f_{T_1}^{(g)}(t \mid \mathcal{E}_{t_0})$, based on the integral equation for $f_{L_{t_1}^-}(t-t_1)$, although no numerical example is shown.

In section 2.4 a Volterra integral equation is formulated for $f_{U_t^+}(t-t_1 \mid \mathcal{E}_{t_0})$. Based on this integral equation inclusion-exclusion series are formulated for $f_{U_t^+}(t-t_1 \mid \mathcal{E}_{t_0})$ and for the nominator and denominator of the kernel of the said integral equation in the same joint conditioned out-crossing rates $f_n^{+\cdots+}(t_1,\ldots,t_n \mid \mathcal{E}_{t_0})$ as used for $f_{T_1}(t \mid \mathcal{E}_{t_0})$. Based upon the relationship between $f_{T_1}(t \mid \mathcal{E}_{t_0})$ and $f_{U_t^+}(t-t_1 \mid \mathcal{E}_{t_0})$ an alternative inclusion-exclusion series for $f_{T_1}(t \mid \mathcal{E}_{t_0})$ in these conditioned crossing rates is then obtained. Next, an integral equation is stated for the probability density function of U_t^+ on condition of $\mathcal{E}_{t_0}$ and on condition of out-crossings from the safe domain at the times $t_1,\ldots,t_n$, prior to the out-crossing at the end of the interval U_t^+. This quantity, which is denoted $f_{U_t^+}(t-t_{n+1} \mid \mathcal{E}_{t_0} \cap C_{t_1}^+ \cap \cdots \cap C_{t_n}^+)$, $t_1 < \cdots < t_n < t-l < t$, occurs in the remainder of the inclusion-exclusion series for $f_{U_t^+}(t-t_1 \mid \mathcal{E}_{t_0})$. If an approximate solution to this integral equation can be obtained, fast convergence of the inclusion-exclusion series for $f_{U_t^+}(t-t_1 \mid \mathcal{E}_{t_0})$ and hence for $f_{T_1}(t \mid \mathcal{E}_{t_0})$ is obtained by resubstitution. Next, an integral equation is formulated for the probability density function $f_{U_t^-}(t-t_1 \mid \mathcal{E}_{t_0})$ of the interval U_t^- until the next out-crossing after an out-crossing from the safe domain

has taken place at the time t. From this integral equation an inclusion-exclusion series for this quantity and for the numerator and denominator of the kernel function is derived for still the same joint conditioned out-crossing rates $f_n^{+\cdots+}(t_1,\ldots,t_n \mid \mathcal{E}_{t_0})$. Based on a relation between $f_{U_t^-}(t-t_1 \mid \mathcal{E}_{t_0})$ and $f_{U_t^+}(t-t_1 \mid \mathcal{E}_{t_0})$ a 3rd inclusion-exclusion series in these conditioned out-crossing rates can then be derived for $f_{T_1}(t \mid \mathcal{E}_{t_0})$. Hence, the three alternative series turn out to be merely different formulations of the remainder of the inclusion-exclusion series. Next, the single barrier first-passage time problem with stationary start of a single degree-of-freedom oscillator excited by Gaussian white noise is considered again, for which an integral equation is formulated for the joint probability density function $f_{\dot{X}U_{t_1}^-}(b,\dot{x},t-t_1 \mid \mathcal{E}_{t_0})$ of the out-crossing velocities $\dot{X}$ at the time t and the interval U_t^- on condition of $\mathcal{E}_{t_0}$. From the numerical solution of this equation, $f_{U_t^-}(t-t_1 \mid \mathcal{E}_{t_0})$ is obtained by marginalization. $f_{U_t^+}(t-t_1 \mid \mathcal{E}_{t_0})$ and finally $f_{T_1}(t \mid \mathcal{E}_{t_0})$ can then be calculated from the relation linking these quantities to $f_{U_t^-}(t-t_1 \mid \mathcal{E}_{t_0})$. No numerical example of the theory of section 2-4 has been presented.

Finally, it should be mentioned that the main obstacle of all the presented methods is that the areas of application are limited to the problems for which the necessary crossing rates can be calculated. At present this means that only linear problems and a very restricted class of non-linear systems can be analysed. Further, the dimension of the considered response vector must be low. Even for the Gaussian vector processes of medium high dimensionality the calculation of joint crossing rates will soon be practically impossible.

3. MARKOV VECTOR METHODS

3.1 Introduction to Markov vector methods

In this section various models for the generating source of a vibratory system are presented. By a generating source is meant the final stochastic excitation on a vibratory system, and not merely the loads. The actual dynamic loads may also be obtained by a filtration of the generating sources.

The main distinction will be made between generating source processes, which have sample curves that are continuous with probability 1, and those, which may be discontinuous (perform jumps). The scalar and n_3-dimensional vector continuous source processes are designated $\{W(t), t \in [0, \infty[\}$ and $\{\mathbf{W}(t), t \in [0, \infty[\}$, respectively. Similarly, the scalar and n_4-dimensional vector discontinuous source processes are designated $\{V(t), t \in [0, \infty[\}$ and $\{\mathbf{V}(t), t \in [0, \infty[\}$. A basic approach in the following outline is that all generating source processes have independent increments, i.e. for any $0 \leq t_0 < t_1 < \cdots < t_n$ the stochastic variables $\Delta W(t_0) = W(t_1) - W(t_0), \Delta W(t_1) = W(t_2) - W(t_1), \cdots \Delta W(t_{n-1}) = W(t_n) - W(t_{n-1})$ are mutually stochastically independent and independent of the initial value $W(t_0)$. This assumption restricts $\{W(t), t \in [0, \infty[\}$ to a Wiener process, $\{\mathbf{W}(t), t \in [0, \infty[\}$ to a vector (multivariate) Wiener process, $\{V(t), t \in [0, \infty[\}$ to a compound Poisson process or an α-stable Lévy motion process and $\{\mathbf{V}(t), t \in [0, \infty[\}$ to a vector (multivariate) compound Poisson process or α-stable Lévy motion.

The dynamic loading processes on an SDOF or n_1-degrees-of-freedom system are designated $\{F(t), t \in [0, \infty[\}$ or $\{\mathbf{F}(t), t \in [0, \infty[\}$, respectively. The corresponding scalar and n_1-dimensional displacement processes are designated $\{X(t), t \in [0, \infty[\}$ and $\{\mathbf{X}(t), t \in [0, \infty[\}$, respectively. The n-dimensional state vector process, describing the integrated dynamic system made up of displacements and velocities, possible hysteretic components and filter state variables for the load, is designated $\{\mathbf{Z}(t), t \in [0, \infty[\}$. The basic assumption in the present outline is that the state vector process can be modelled as a Markov vector process, with the transitional probability density function $q_{\{\mathbf{Z}\}}(\mathbf{z}, t \mid \mathbf{z}_0, t_0)$.

In section 3.1.1 the properties of Wiener, compound Poisson and α-stable Lévy motion processes are described. In section 3.1.2 the dynamic modelling of loads obtained by filtering of the generating sources is described and finally, in section 3.1.3, the modelling of dynamic systems and the final formulation of systems with Markov properties are given.

3.1.1 Generating sources with independent increments

3.1.1.1 Wiener process

A stochastic process $\{W(t), t \in [0, \infty[\}$ is a Wiener process (or Brownian motion), if

1: $P(W(0) = 0) = 1$.

2: The process has zero mean, i.e. the mean value function $\mu_W(t) = E[W(t)] \equiv 0$.

3: For arbitrary $0 < t_0 < t_1 < \cdots < t_n$ the increments $\Delta W(t_0) = W(t_1) - W(t_0)$, $\Delta W(t_1) = W(t_2) - W(t_1), \cdots, \Delta W(t_{n-1}) = W(t_n) - W(t_{n-1})$ are stochastically independent.

4: For arbitrary t and Δt the increment $\Delta W(t) = W(t + \Delta t) - W(t)$ has a Gaussian distribution with the zero mean and with the variance

$$E[(\Delta W(t))^2] = D\Delta t \qquad (3-1)$$

The diffusion coefficient D is assumed to be 1 for simplicity, a so-called unit intensity Wiener process.

From the definitions a Wiener process can equivalently be described as a zero mean Gaussian process with the auto-covariance function

$$\kappa_{WW}(t_1, t_2) = \min(t_1, t_2) \qquad (3-2)$$

Since, the auto-covariance function $\kappa_{WW}(t_1, t_2)$ is continuous at the diagonal $t_1 = t_2 = t$, the Wiener process is continuous in the mean square, see e.g. Arnold (1974). Further, since the 2nd order mixed derivative $\frac{\partial^2}{\partial t_1 \partial t_2}\kappa_{WW}(t_1, t_2)$ does not exist at the diagonal $t_1 = t_2 = t$, the Wiener process is not differentiable in the mean square. The mentioned properties of continuity and differentiability can even be proved to hold with probability 1.

An n_3-dimensional Wiener vector process $\{\mathbf{W}(t), t \in [0, \infty[\}$ is defined as a vector process, where all component processes $\{W_\alpha(t), t \in [0, \infty[\}$, $\alpha = 1, \ldots, n_3$ are assumed to be mutually independent, and unit intensity Wiener processes. One then has the cross-covariance function of the process,

$$\kappa_{W_\alpha W_\beta}(t_1, t_2) = E[W_\alpha(t_1) W_\beta(t_2)] = \delta_{\alpha\beta} \min(t_1, t_2) \qquad (3-3)$$

where $\delta_{\alpha\beta}$ signifies the Kronecker delta.

3.1.1.2 Compound Poisson process

The Poisson process is characterized as a regular (orderly) stochastic point process with independent increments. Let the increment of the counting process (the random number of points) in $[t, t + dt[$ be denoted by $dN(t) = N(t + dt) - N(t)$. A compound Poisson process $\{V(t), t \in [0, \infty[\}$ is represented as

$$V(t) = \sum_{i=1}^{N(t)} P_i = \sum_{i=1}^{N(t)} P_i(1 - H(t_i - t)) = \int_0^t dV(\tau) = \int_0^t P(\tau) dN(\tau) \qquad (3-4)$$

where $H(x)$ is the Heaviside unit step function given by

$$H(x) = \begin{cases} 1 & , \quad x \geq 0 \\ 0 & , \quad x < 0 \end{cases} \qquad (3-5)$$

The specific definition of the unit step function becomes important, because impulses up to but not including the time t_j are being counted.

The generalized derivative of the compound Poisson process can then formally be represented as the following random train of Dirac delta impulses,

$$\frac{d}{dt}V(t) = \sum_{i=1}^{N(t)} P_i \delta(t - t_i) \qquad (3-6)$$

where $\delta(x)$ is the Dirac delta function (or, rather pseudofunction), which is the generalized derivative of a unit step function. $\{N(t), t \in [0, \infty[\}$ is a Poisson counting process giving the random number of time points t_i in the time interval $[0, t[$ (with the additional assumption, $P(N(0) = 0) = 1$), and P_i are independent random variables, identically distributed as a random variable P. Each of the variables P_i is assigned to a random point t_i. The variables P_i are also assumed to be statistically independent of the random times t_i, or of the counting process $N(t)$. Since, the counting process counts the number of jumps up to, but excluding the one at the time t, the sample paths are continuous to the left.

In the Stieltje integral representation (3-4) $P(t)$ denotes the random variable assigned to the time point occurring in the time interval $[t,\ t+dt[$. Since $P(t_1)$ and $P(t_2)$ for disjoint differential intervals are stochastically independent and independent of the Poisson counting process, and the increments $dN(t_1)$ and $dN(t_2)$ of the Poisson counting process are independent as well, it also follows that the increments $dV(t_1) = P(t_1)dN(t_1)$, and $dV(t_2) = P(t_2)dN(t_2)$ are stochastically independent, i.e. the compound Poisson process has independent increments.

From the regularity properties it follows that

$$E\big[dN(t)\big] = E\Big[\big(dN(t)\big)^n\Big] = \nu(t)dt + \mathrm{O}(dt^2) \qquad (3-7)$$

for any n, where $\nu(t)$ is interpreted as a mean arrival (or occurrence) rate of events (points). The probability function of the first order of the Poisson counting proccess is given by, e.g. Snyder (1975)

$$P_{\{N\}}(n,t,0) = P\Big(N(t) = n\Big) = \frac{\left(\int_0^t \nu(\tau)d\tau\right)^n}{n!} \exp\left(-\int_0^t \nu(\tau)d\tau\right) \qquad (3-8)$$

Making use of (3-4) and of the stochastic independence of $P(\tau)$ and $dN(\tau)$ the following results are obtained for the mean value function $\mu_V(t)$ and the auto-covariance function $\kappa_{VV}(t_1, t_2)$

$$\mu_V(t) = E[P] \int_0^t \nu(\tau) d\tau \tag{3-9}$$

$$\kappa_{VV}(t_1, t_2) = E[P^2] \int_0^{\min(t_1, t_2)} \nu(\tau) d\tau \tag{3-10}$$

The joint characteristic function of $\mathbf{V}^T(t) = [V(t_1), V(t_2), \dots, V(t_n)]$ is given as, Roberts (1972)

$$M_{\mathbf{V}}(\boldsymbol{\theta}; t_1, t_2, \dots t_n) = E\left[\exp\left(i \sum_{j=1}^{n} \theta_j V(t_j)\right)\right] =$$

$$\int_0^t \left[M_P\left(\sum_{j=1}^{n} \theta_j (1 - H(\tau - t_j))\right) - 1\right] \nu(\tau) d\tau \tag{3-11}$$

where $M_P(\theta)$ is the characteristic function of the impulse strength. The corresponding log-characteristic function can be expanded in MacLaurin series in terms of $\boldsymbol{\theta}$ as follows

$$\ln M_{\mathbf{V}}(\boldsymbol{\theta}; t_1, \dots, t_n) =$$

$$\sum_{j=1}^{n} \kappa_1[V(t_j)](i\theta_j) + \frac{1}{2!} \sum_{j,k=1}^{n} \kappa_2[V(t_j), V(t_j)](i\theta_j)(i\theta_k) + \cdots \tag{3-12}$$

where

$$\kappa_n[V(t_1), \dots, V(t_n)] =$$

$$E[P^n] \int_0^t \prod_{j=1}^{n} (1 - H(\tau - t_j)) \nu(\tau) d\tau = E[P^n] \int_0^{\min(t_1, \dots, t_n)} \nu(\tau) d\tau \tag{3-13}$$

is the joint nth order cumulant of the vector $\mathbf{V}^T(t) = [V(t_1), V(t_2), \dots, V(t_n)]$. Since, the auto-covariance function (3-10) is continuous at the diagonal $t_1 = t_2 = t$ it follows that the compound Poisson process is continuous in mean square. Of course, this is not the case with probability 1.

Alternatively, the compound Poisson process may be described by the random measure $M(dt,t,dp,p)$, which gives the random number of jumps during the time interval $[t,t+dt[$ into the differential interval $[p,p+dp[$ of the mark variable P. Since, the underlying counting process is regular (i.e. the probability of occurrence of more than one jump in the infinitesimal time interval is negligible) this measure has the following properties

$$
\begin{aligned}
&1: \int_{\mathcal{P}} M(dt,t,dp,p) = dN(t) \\
&2: P\big(M(dt,t,dp,p) = M^n(dt,t,dp,p)\big) = 1 \ , \ n = 2,3,\ldots \\
&3: P\big(M(dt,t,dp,p) = 1\big) = \nu(t) f_P(p) dt dp \\
&4: P\big(M(dt,t,dp,p) = 0\big) = 1 - \nu(t) f_P(p) dt dp \\
&5: P\big(M(dt,t,dp_1,p_1) \cdot M(dt,t,dp_2,p_2) = 0\big) = 1 \ , \ p_1 \neq p_2 \\
&6: P\big(M(dt_1,t_1,dp_1,p_1) = M(dt_2,t_2,dp_2,p_2) = 1\big) = \\
&\quad \nu(t_1) f_P(p_1) dt_1 dp_1 \nu(t_2) f_P(p_2) dt_2 dp_2 \ , \ t_1 \neq t_2
\end{aligned}
\qquad (3-14)
$$

where $\mathcal{P} \subseteq R$ is the sample space of the random variable P, and $f_P(p)$ is its probability density function. Notice, that the remainders of the order $O(dt^2)$ and $O(dp^2)$ have not been indicated in (3-14). The first relation of (3-14) states that the total number $dN(t)$ of jumps in the interval $[t,\ t+dt[$ is obtained by summing up the jumps to all possible intervals $[p,\ p+dp[$. This is so, since the possibility of multiple jumps during $[t,\ t+dt[$ has been excluded by the regularity condition. The remaining properties all follow from the regularity property of the Poisson counting process and the stochastically independent increments of the compound Poisson process.

From the above properties it follows that

$$
E\big[M(dt,t,dp,p)\big] = E\big[M^n(dt,t,dp,p)\big] = \nu(t) f_P(p) dt dp, \ n = 2,3,\ldots \qquad (3-15)
$$

$$
\begin{aligned}
&E\big[M(dt_1,t_1,dp_1,p_1) M(dt_2,t_2,dp_2,p_2)\big] = \\
&E\big[M(dt_1,t_1,dp_1,p_1)\big] E\big[M(dt_2,t_2,dp_2,p_2)\big], \ t_1 \neq t_2
\end{aligned}
\qquad (3-16)
$$

If the jump during $[t,t+dt[$ takes place into interval $[p,p+dp[$, i.e. the jump has the magnitude $P(t) = p$ and $M(dt,t,dp,p) = 1$, the increment of the compound Poisson process is $dV(t) = p = pM(dt,t,dp,p)$. Summing up the possible jumps into all the contiguous intervals, i.e. summing over the whole sample space $\mathcal{P}$ of the random variable P, yields the following integral representation for the unconditional increment of the compound Poisson process

$$
dV(t) = \int_{\mathcal{P}} pM(dt,t,dp,p) \qquad (3-17)
$$

Alternatively, the compound Poisson process may then be written as the following stochastic integral

$$V(t) = \int_0^t \int_{\mathcal{P}} pM(d\tau, \tau, dp, p) \qquad (3-18)$$

More generally, it follows that with probability 1

$$(dV(t))^n = \left(\int_{\mathcal{P}} pM(dt, t, dp, p) \right)^n = \int_{\mathcal{P}} p^n M(dt, t, dp, p) \qquad (3-19)$$

In the context of (3-17) the left-hand side of (3-19) represents an n-fold Stieltjes integral over $\mathcal{P}^n$. However, because of the 5th shown property of (3-14) all off-diagonal terms cancel, and only the diagonal terms on the right-hand side of (3-19) give the contribution to the integral.

Next, a multivariate compound Poisson process $\{\mathbf{V}(t),\ t \in [0, \infty[\}$ is defined as an n_4-dimensional vector process, where all component processes $\{V_\alpha(t),\ t \in [0, \infty[\}, \alpha = 1, \ldots, n_4$ are mutually statistically independent compound processes. Each component process is defined by a random measure $M_\alpha(dt, t, dp, p)$ corresponding to a certain mean arrival rate $\nu_\alpha(t)$ and a mark variable P_α.

3.1.1.3 α–stable Lévy motion

Quite a wide class of random excitation processes with jumps can be described in terms of α–stable Lévy motions, which turn out to have independent increments and discontinuous sample paths. Initially, some fundamental notations and definitions are introduced.

A random variable is said to have a stable distribution if it can be represented as the sum of independent, identically distributed random variables whose probability distributions follow the same law as the distribution of this variable.

A generalized Central Limit Theorem (see e.g. Samorodnitsky and Taqqu (1994)) states that the limit distribution for the sum of independent, identically distributed random variables is a stable distribution. It is a Gaussian distribution (according to the usual Central Limit Theorem) if these variables have finite variance.

There is a large family of distributions known as α–stable distributions satisfying the stability condition. The α–stable random variables X, denoted as $X \sim S_\alpha(\sigma, \beta, \mu)$, are defined by the characteristic function expressed in the general form of

$$M_X(\theta) = \begin{cases} \exp\{i\mu\theta - \sigma^\alpha |\theta|^\alpha (1 - i\beta \mathrm{sgn}(\theta) \tan \frac{\alpha\pi}{2})\} & , \alpha \in]0,1[\text{ or }]1,2], \\ \exp\{i\mu\theta - \sigma|\theta|\} & , \alpha = 1, \beta = 0 \end{cases} \qquad (3-20)$$

where $\alpha \in]0,2]$ is the index of stability or the characteristic exponent, $\beta \in [-1,1]$ is the skewness or asymmetry parameter, $\sigma \in]0,\infty[$ is the scale or dispersion parameter and $\mu \in]-\infty,+\infty[$ is the shift or location parameter.

Unfortunately, the analytical inversion of the characteristic function (3-20) is only feasible in a few special cases, e.g. for $S_2(\sigma,0,\mu)$ which is the Gaussian distribution $N(\mu,\sigma^2)$, or in the case $S_1(\sigma,0,\mu)$ which is the Cauchy distribution with the density function

$$f_X(x) = \frac{1}{\pi}\,\frac{\sigma}{\sigma^2+(x-\mu)^2} \qquad (3-21)$$

The characteristic property of α–stable random variables is that, except for the case $\alpha = 2$, they have infinite variance and higher order moments, since for $\alpha \in]0,2[$

$$\begin{aligned} &E\big[|X|^p\big] = \infty,\ p \in [\alpha,\infty[\\ &E\big[|X|^p\big] < \infty,\ p \in]0,\alpha[\end{aligned} \qquad (3-22)$$

For example, if $\alpha = 1$, the distribution has infinite mean value (Cauchy distribution). Of course, in the case $\alpha = 2$ (Gaussian distribution) all the moments are finite.

For different sets of parameters, a wide variety of probability density curves can be modelled with the help of α–stable distributions, both with positive and negative skewness. Positive values of the skewness parameter β correspond to 'positive skewness', where the right-hand side tail of the density curve is heavier, or thicker, than the left hand-side tail. A characteristic property of these curves is that they have inverse power (or algebraic) tails, which means that the tails decay more slowly than the tails of the Gaussian distribution. Hence, the α–stable distributions are suitable in modelling the distributions with 'heavy' tails. This may be relevant to the phenomena in which the jumps, or impulses, occur, since in those cases the high values of the observed quantity are more likely to occur than in the case of a Gaussian process.

Next, an α–stable Lévy (standard) motion is defined as a stochastic process $\{V(t),\ t \in [0,\infty[\}$ for which

1: $P\big(V(0)=0\big) = 1.$

2: $\big\{V(t), t \in [0,\infty[\big\}$ has independent increments.

3: For arbitrary t and Δt the increment $\Delta V(t) = V(t+\Delta t) - V(t)$ has an α–stable distribution, $S_\alpha\big((a\Delta t)^{1/\alpha},\beta,0\big)$, where a is a positive constant.

An α–stable Lévy motion is a Wiener process, when $\alpha = 2$ and it is symmetric for $\beta = 0$.

The characteristic function of the increment $\Delta V(t)$ during the interval $[t, t+\Delta t[$ becomes

$$M_{\Delta V(t)}(\theta) = \begin{cases} \exp\Big(-(a\Delta t)|\theta|^\alpha\big(1 - i\beta\,\mathrm{sign}\,(\theta)\tan\frac{\alpha\pi}{2}\big)\Big) & ,\ \alpha \in]0,1[\text{or }]1,2] \\ \exp\Big(-a\Delta t|\theta|\Big) & ,\ \alpha = 1, \beta = 0 \end{cases} \qquad (3\text{–}23)$$

A random measure $M(dt, t, dp, p)$ may be introduced for the α–stable Lévy motion, defined in the same way as for the compound Poisson process. Moreover, the integral representation (3-18) is valid for α–stable Lévy motions as well.

The probability of making a jump into the interval $[p, p + dp[$ during the time interval $[t, t + \Delta t[$ is given by $f_{\Delta V(t)}(p)dp$. If Δt is sufficiently small this probability can also be expressed as $P\big(M(\Delta t, t, dp, p) = 1\big)$. Hence, one may write

$$\lim_{\Delta t \to 0} P\big(M(\Delta t, t, dp, p) = 1\big) = \lim_{\Delta t \to 0} f_{\Delta V(t)}(p)dp \qquad (3-24)$$

Similarly, a multivariate α–stable Lévy motion $\{\mathbf{V}(t),\ t \in [0, \infty[\}$ can be defined as an n_4-dimensional vector process, where all component processes $\{V_\alpha(t),\ t \in [0, \infty[\}, \alpha = 1, \ldots, n_4$ are mutually independent and defined by the individual random measures $M_\alpha(dt, t, dp, p)$.

In what follows it will be assumed in general that the n_4-dimensional generating source process $\{\mathbf{V}(t),\ t \in [0, \infty[\}$ is made up of mutually independent component processes $\{V_\alpha(t),\ t \in [0, \infty[\}$, which may be either compound Poisson processes or α–stable Lévy motions. Due to the independent increments each component process is then completely defined by its so-called jump probability intensity function $J_{\{V_\alpha\}}(p_\alpha, t)$ defined as

$$J_{\{V_\alpha\}}(p_\alpha, t) = \lim_{\Delta t \to 0, \Delta p \to 0} \frac{1}{\Delta t \Delta p_\alpha} P\Big(M_\alpha\big(\Delta t, t, \Delta p_\alpha, p_\alpha\big) = 1\Big) \qquad (3-25)$$

Seeing that there may be no jump or one jump in $[t, t + dt[$, (3-25) implies that the expectation $E\big[M_\alpha(dt, t, dp_\alpha, p_\alpha)\big]$, if it exists, is evaluated as

$$E\big[M_\alpha(dt, t, dp_\alpha, p_\alpha)\big] = J_{\{V_\alpha\}}(p_\alpha, t)dp_\alpha dt \qquad (3-26)$$

From the 3rd mentioned property in (3-14) it follows that the jump probability intensity function of a compound Poisson process is

$$J_{\{V\}}(p, t) = \nu(t) f_P(p) \qquad (3-27)$$

For the α–stable Lévy motion from (3-24) it follows that

$$J_{\{V\}}(p, t) = \lim_{\Delta t \to 0} \frac{1}{\Delta t} f_{\Delta V(t)}(p) = \lim_{\Delta t \to 0} \frac{1}{\Delta t} \frac{1}{2\pi} \int_{-\infty}^{\infty} \exp(-i\theta p) M_{\Delta V(t)}(\theta) d\theta \qquad (3-28)$$

Upon inserting (3-23) into (3-28) and substituting $x = |p|\theta$ and $u = \frac{a\Delta t}{|p|^\alpha}$ the following result can be obtained

$$J_{\{V\}}(p, t) = \frac{1}{\pi} \frac{a}{|p|^{\alpha+1}} f\big(\alpha, \beta, \mathrm{sign}(p)\big) \qquad (3-29)$$

where

$$f(\alpha,\beta,\mathrm{sign}(p)) = \lim_{u\to 0}\frac{1}{u}\int_0^\infty \cos\left(x\,\mathrm{sign}(p) - ux^\alpha\beta\tan\frac{\alpha\pi}{2}\right)\exp(-ux^\alpha)dx \;=$$

$$\lim_{u\to 0}\int_0^\infty \left(\beta\tan\frac{\alpha\pi}{2}\mathrm{sign}(p)\cos\left(x - \mathrm{sign}(p)ux^\alpha\beta\tan\frac{\alpha\pi}{2}\right) +\right.$$

$$\left.\sin\left(x - \mathrm{sign}(p)ux^\alpha\beta\tan\frac{\alpha\pi}{2}\right)\right)\alpha x^{\alpha-1}\exp(-ux^\alpha)dx \qquad (3-30)$$

The last statement follows from the integration by parts of the first part. The last-mentioned formulation is preferable at numerical applications, since the numerical differentiation is avoided. It should be noted that the integral does not converge uniformly as u approaches zero. Hence, the integration and the limiting operation cannot be interchanged. As seen the function $f(\alpha,\beta,\mathrm{sign}(p))$ only depends on p through its sign and then it merely acts as different constants for positive and negative values of p. It is then seen that the jump probability intensity function of an α–stable Lévy motion has a singularity of the order $|p|^{\alpha+1}$ as $p\to 0$, i.e. the probability intensity of performing small jumps is much higher than the one of performing larger jumps. For $\beta = 0$ (3-30) provides

$$f(\alpha,0,\mathrm{sign}(p)) = \lim_{u\to 0}\int_0^\infty \alpha x^{\alpha-1}\sin(x)\exp(-ux^\alpha)dx \qquad (3-31)$$

As it is seen, $f(\alpha,0,\mathrm{sign}(p))$ is completely independent of p in this case. For $\alpha = 1$ and $\alpha = 2$ (3-31) provides, respectively,

$$f(1,0,\mathrm{sign}(p)) = 1,\;\; f(2,0,\mathrm{sign}(p)) = 0 \qquad (3-32)$$

Further, it can be shown that $f(\alpha,0,\mathrm{sign}(p))$ tends to infinity as $\alpha\to 0$. Relationships (3-29) and (3-32) imply that the jump probability intensity function of the Cauchy process and the Wiener process are, respectively,

$$J_{\{V\}}(p,t) = \frac{1}{\pi}\frac{a}{p^2} \qquad (3-33)$$

$$J_{\{V\}}(p,t) = 0 \qquad (3-34)$$

3.1.2 Dynamic loads obtained by filtration of processes with independent increments

Consider the linear SDOF oscillator

$$m\left(\ddot{X} + 2\zeta\omega_0\dot{X} + \omega_0^2 X\right) = F(t) \qquad (3-35)$$

In general, the stochastic excitation process $\{F(t), t \in [0,\infty[\}$ has no independent increments. Hence, the vector process $[X, \dot{X}]^T$ is not Markovian.

One way to remain within the framework of the Markov approach is to regard such excitation processes as an r-th order differential form of an auxiliary process, which in turn is the result of filtering the generating source with independent increments through an sth order filter $(s > r)$.

Hence, the loading process can be expressed as

$$F(t) = p_0 Y^{(r)} + p_1 Y^{(r-1)} + \cdots + p_r Y \qquad (3-36)$$

where $Y^{(r)}(t) = \frac{d^r}{dt^r} Y(t)$ and $Y(t)$ are the response of an sth order linear time invariant filter, governed by the differential equation

$$Y^{(s)} + q_1 Y^{(s-1)} + \cdots + q_s Y = \dot{V}(t) \qquad (3-37)$$

$p_0, p_1, \ldots, p_r, q_1, \ldots, q_s$ in (3-36), (3-37) are real constants. The process $\dot{V}(t)$ stands for the generalized derivative of any generating source process with independent increments, i.e. of a Wiener process, of a compound Poisson process, or of an α–stable Lévy motion. Then, the augmented state vector $\left[X, \dot{X}, Y, \dot{Y}, \ldots, Y^{(s-1)}\right]^T$ is a Markov vector process.

The differential rules (3-36) and (3-37) can alternatively be given in the following integral form

$$F(t) = \int_0^t h(t-\tau) dV(\tau) \qquad (3-38)$$

where

$$h(t) = \frac{1}{2\pi} \int_{-\infty}^{\infty} e^{i\omega t} H(i\omega) d\omega = \frac{1}{2\pi} \int_{-\infty}^{\infty} e^{i\omega t} \frac{P(i\omega)}{Q(i\omega)} d\omega \qquad (3-39)$$

and $P(z)$ and $Q(z)$ are polynomials of order r and s, respectively,

$$P(z) = p_0 z^r + p_1 z^{r-1} + \cdots + p_r z$$

$$Q(z) = z^s + q_1 z^{s-1} + \cdots + p_s z \qquad (3-40)$$

In (3-38) and (3-39) $h(t)$ and $H(i\omega) = P(i\omega)/Q(i\omega)$ are the impulse response and the frequency response functions of the shaping filter, respectively. In formulation (3-38) it is assumed that the load prior to $t = 0$ is zero. If $r < s$ and the roots z_j of $Q(z_j) = 0$ have negative real parts, i.e. $\mathrm{Re}(z_j) < 0$, the integral (3-39) can be evaluated as follows, see e.g. Nielsen (1993)

$$h(t) = \begin{cases} 0 & , \quad t \leq 0, \\ \sum_{j=1}^{s} e^{z_j t} \dfrac{P(z_j)}{\prod_{\substack{k=1 \\ k \neq j}}^{s} (z_j - z_k)} & , \quad t > 0 \end{cases} \qquad (3-41)$$

The frequency response function of other time-invariant linear systems can often be approximated by a rational one.

The Poisson-driven train of general pulses may in the simplest case be regarded directly as the result of filtering the train of Dirac delta impulses (3-5) through a rational linear filter such as (3-35) and (3-36). Upon inserting (3-5) into (3-38) one obtains

$$F(t) = \sum_{i=1}^{N(t)} P_i h(t - t_i) \qquad (3-42)$$

More generally, the filter equation may be a non-linear and time-varying sth order differential equation, and the output equation (3-36) can be a non-linear time-varying transformation of the filter state variables up to and including the rth derivative.

3.1.3 Governing stochastic differential equations in state vector form

The general equation of motion of a non-linear, non-hysteretic, SDOF system with the mass m is, cf. (2-80)

$$m\Big(\ddot{X} + u(X, \dot{X})\Big) = F(t) \qquad (3-43)$$

Especially, for the Duffing oscillator, (3-43) attains the form

$$m\Big(\ddot{X} + 2\zeta\omega_0\dot{X} + \omega_0^2(1 + \varepsilon X^2)X\Big) = F(t) \qquad (3-44)$$

where the constant ε may assume any value, $\varepsilon \in R$, and ω_0 and ζ are the circular eigenfrequency and the damping ratio of the corresponding linear oscillator, respectively.

The differential equation (3-43) can be recast into the following set of first order equations, cf. (2-80)

$$\frac{d}{dt}\mathbf{Z}(t) = \mathbf{c}\big(\mathbf{Z}(t)\big) + \mathbf{d}F(t) \qquad (3-45)$$

$$\mathbf{Z}(t) = \begin{bmatrix} X(t) \\ \dot{X}(t) \end{bmatrix}, \ \mathbf{c}\big(\mathbf{Z}(t)\big) = \begin{bmatrix} \dot{X}(t) \\ -u\big(X(t), \dot{X}(t)\big) \end{bmatrix}, \ \mathbf{d} = \begin{bmatrix} 0 \\ \frac{1}{m} \end{bmatrix} \qquad (3-46)$$

Equation (3-45) is known as the state vector formulation, where $\mathbf{Z}(t)$ is the state vector and $\mathbf{c}\big(\mathbf{Z}(t)\big)$ is termed as the drift vector.

In the case of a hysteretic SDOF oscillator the time-history dependence (hereditary property) of the restoring force acting on the mass can be taken into account by introducing an extra endochronic state variable Q. Assume that the restoring force is made up of its hysteretic component $m\omega_0^2(1-\alpha)Q$, its linear elastic part $m\omega_0^2\alpha X$, and its linear viscous part $m2\zeta\omega_0\dot{X}$, in parallel. The parameter α, which is termed the secondary to primary (post- to pre-yielding) stiffness ratio, specifies the fraction of the linear elastic part of the restoring force, remaining during plastic loadings, due to the strain hardening or strain softening effects. The equation of motion then becomes

$$m\Big(\ddot{X} + 2\zeta\omega_0\dot{X} + \omega_0^2\big(\alpha X + (1-\alpha)Q\big)\Big) = F(t) \qquad (3-47)$$

In order to close the system, a constitutive relation must be introduced, which relates the hysteretic state variable Q to the state variables X and $\dot{X}$. This is given in differential form as follows

$$\dot{Q} = \kappa(\dot{X}, Q)\dot{X} \qquad (3-48)$$

where κ may be interpreted as a non-linear state-dependent spring stiffness of the hysteretic component of the restoring force.

The state vector formulation of (3-47), (3-48) is still given by (3-45) with the following new definitions, cf. (2-93)

$$\mathbf{Z}(t) = \begin{bmatrix} X(t) \\ \dot{X}(t) \\ Q(t) \end{bmatrix}, \ \mathbf{c}\big(\mathbf{Z}(t)\big) = \begin{bmatrix} \dot{X} \\ -2\zeta\omega_0\dot{X} - \omega_0^2\big(\alpha X + (1-\alpha)Q\big) \\ \kappa(\dot{X}, Q)\dot{X} \end{bmatrix}, \ \mathbf{d} = \begin{bmatrix} 0 \\ \frac{1}{m} \\ 0 \end{bmatrix} \qquad (3-49)$$

Various hysteretic models are determined from various constitutive equations. For a bilinear oscillator the non-dimensional spring stiffness assumes the following form, Kaul and Penzien (1974)

$$\kappa(\dot{X}, Q) = 1 - H\big(Q - q_y\big)\big(1 - H(-\dot{X})\big) - H\big(-Q - q_y\big)\big(1 - H(\dot{X})\big) \qquad (3-50)$$

where $H(x)$ is the Heaviside unit step function (3-5). The quantity q_y is the yield limit, which is equal to the displacement, at which yielding takes place for the first time. As seen in figure 3.1a, $\kappa = 0$ when the oscillator is in the elastic range or at the point of moving into this range. The corresponding bilinear behaviour of the total restoring force $\alpha Y + (1-\alpha)Q$ is depicted in figure 3.1b.

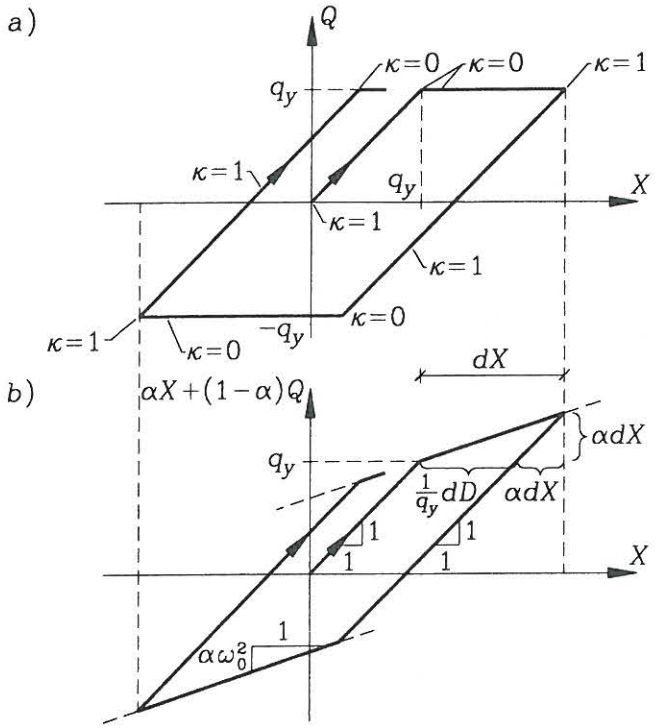

Fig. 3-1: Bilinear oscillator. a) Constitutive relation for the hysteretic state variable. b) Constitutive relation for the total restoring force $\alpha X + (1-\alpha)Q$.

The Bouc-Wen smooth hysteretic model is given by, Bouc (1967), Wen (1976)

$$\kappa(\dot{X}, Q) = 1 - \beta \text{sign}(\dot{X}) \frac{Q}{q_y} \left| \frac{Q}{q_y} \right|^{n-1} - \gamma \left| \frac{Q}{q_y} \right|^n \qquad (3-51)$$

where β, γ, n are the parameters to be calibrated from available tests. If $\beta + \gamma = 1$, q_y can be identified as the yield level.

Furthermore, if the loading process $\{F(t),\ t \in [0, \infty[\}$ is the result of the filtering described above, the state vector as given by (3-49) must be augmented by the state variables of the filter $[Y, \dot{Y}, \ldots, Y^{(s-1)}]$ and the augmented state vector is governed by the following system of first order ordinary differential equations obtained from (3-36), (3-37), (3-47), (3-48)

$$\frac{d}{dt}\mathbf{Z}(t) = \mathbf{c}(\mathbf{Z}(t)) + \mathbf{d}\dot{V}(t),\ t > 0 \qquad (3-52)$$

$$\mathbf{Z}(t) = \begin{bmatrix} X \\ \dot{X} \\ Q \\ Y \\ \dot{Y} \\ . \\ . \\ . \\ Y^{(s-2)} \\ Y^{(s-1)} \end{bmatrix}, \quad \mathbf{d} = \begin{bmatrix} 0 \\ 0 \\ 0 \\ 0 \\ 0 \\ . \\ . \\ . \\ 0 \\ d_0 \end{bmatrix} \qquad (3-53)$$

$$\mathbf{c}(\mathbf{Z}(t)) = \begin{bmatrix} \dot{X} \\ -2\zeta\omega_0\dot{X} - \omega_0^2\big(\alpha X + (1-\alpha)Q\big) + \frac{p_0}{m}Y^{(r)} + \frac{p_1}{m}Y^{(r-1)} + \cdots + \frac{p_r}{m}Y \\ \kappa(\dot{X}, Q)\dot{X} \\ \dot{Y} \\ \ddot{Y} \\ . \\ . \\ . \\ Y^{(s-1)} \\ -q_1 Y^{(s-1)} - \cdots - q_s Y \end{bmatrix} \qquad (3-54)$$

Equation (3-52) may be termed as the state vector formulation in terms of the generating source process, where d_0 is the suitable constant. Equation (3-52) should be solved with suitable initial condition $\mathbf{Z}(0) = \mathbf{Z}_0$, which may be deterministic as well as stochastic.

With the help of standard techniques of structural dynamics (the d'Alembert principle in combination with the principle of virtual work) the equations of motion of a general non-linear and hysteretic MDOF system can be written in the following matrix form, Nielsen, Mørk and Thoft-Christensen (1989)

$$\mathbf{M}\ddot{\mathbf{X}} + \mathbf{C}\dot{\mathbf{X}} + \mathbf{K}_0\mathbf{X} + \mathbf{g}^T\mathbf{Q} = \mathbf{F}(t) \qquad (3-55)$$

$\mathbf{X}(t)$ is an n_1-dimensional vector and $\mathbf{F}(t)$ are the external loads conjugated to $\mathbf{X}(t)$. $\mathbf{M}$, $\mathbf{C}$ and $\mathbf{K}_0$ signify the global mass matrix, the global linear viscous damping matrix and the global stiffness matrix from the linear elastic part of the structure, all of dimension $n_1 \times n_1$. $\mathbf{M}$ is symmetric and positive definite, and $\mathbf{K}_0$ is symmetric and positive semi-definite. $\mathbf{C}$ is generally non-symmetric and positive definite for dissipative systems. $\mathbf{Q}(t)$ is a vector of dimension n_2 of generalized stresses from all plastic elements, conjugated to the generalized strains, $\mathbf{q}(t)$. The relationship between the rates of the generalized strains and the rate of the external degree-of-freedom is defined by the following geometrical condition

$$\dot{\mathbf{q}} = \mathbf{g}\dot{\mathbf{X}} \qquad (3-56)$$

The geometrical matrix $\mathbf{g} = \mathbf{g}(\mathbf{X}(t))$ of the dimension $n_2 \times n_1$ is an analytical function of the external degrees of freedom $\mathbf{X}(t)$ in the general geometrically non-linear case. For geometrically linear structures, $\mathbf{g}$ becomes a constant, and (3-56) can directly be integrated.

In order to close the differential system (3-55) a constitutive equation for the generalized stresses must be formulated. For an ideal elasto-plastic structure this can be given on the form, Nielsen, Mørk and Thoft-Christensen (1989)

$$\dot{\mathbf{Q}} = \boldsymbol{\kappa}(\dot{\mathbf{q}}, \mathbf{Q})\dot{\mathbf{q}} \qquad (3-57)$$

For a physical linear system, the symmetric positive semi-definite stiffness matrix $\boldsymbol{\kappa}(\dot{\mathbf{q}}, \mathbf{Q})$ of dimension $n_2 \times n_2$ is independent of the state variables $\dot{\mathbf{q}}(t)$ and $\mathbf{Q}(t)$, in which case (3-57) can be integrated. For non-linear elastic systems, $\boldsymbol{\kappa} = \boldsymbol{\kappa}(\mathbf{Q})$ is an analytical function of $\mathbf{Q}$ and is independent of $\dot{\mathbf{q}}$. For a physically linear or physically non-linear system $\mathbf{Q}(t)$ can be eliminated in favour of the linear or non-linear function of $\mathbf{X}(t)$ in (3-55). For elasto-plastic systems, $\boldsymbol{\kappa} = \boldsymbol{\kappa}(\dot{\mathbf{q}}, \mathbf{Q})$ is a non-analytical function of $\mathbf{Q}$ and $\dot{\mathbf{q}}$. In this case $\mathbf{Q}$ serves as endocronic state variables. If the system is both physically and geometrically linear, the global stiffness matrix from the corresponding structural elements becomes $\mathbf{K}_1 = \mathbf{g}^T \boldsymbol{\kappa} \mathbf{g}$.

Taking into account the possible equations for the hysteretic behaviour and those for a filter, one can build up the state vector of all the displacements, velocities, hysteretic components and state variables for the filter. The augmented state vector $\mathbf{Z}(t)$ is governed by the equations in the form of (3-57). Taking due account of the fact that the generating source may consist of an n_3-dimensional Wiener vector process $\{\mathbf{W}(t),\ t \in [0, \infty[\}$ and an n_4-dimensional jump vector process $\{\mathbf{V}(t),\ t \in [0, \infty[\}$ the usual differential equations are next converted into the following state vector formulation

$$\left.\begin{aligned} &d\mathbf{Z}(t) = \mathbf{c}\big(\mathbf{Z}(t), t\big)dt + \mathbf{d}d\mathbf{W}(t) + \mathbf{e}d\mathbf{V}(t),\ t > 0 \\ &\mathbf{Z}(0) = \mathbf{Z}_0 \end{aligned}\right\} \qquad (3-58)$$

$$\mathbf{Z}(t) = \begin{bmatrix} \mathbf{X} \\ \dot{\mathbf{X}} \\ \mathbf{Q} \\ \mathbf{Y} \\ \cdot \\ \cdot \\ \mathbf{Y}^{(s-2)} \\ \mathbf{Y}^{(s-1)} \end{bmatrix}, \quad \mathbf{c}\big(\mathbf{Z}(t)\big) = \begin{bmatrix} \dot{\mathbf{X}} \\ \mathbf{M}^{-1}\big(-\mathbf{C}\dot{\mathbf{X}} - \mathbf{K}_0\mathbf{X} - \mathbf{g}^T\mathbf{Q} + \mathbf{p}_0\mathbf{Y}^{(r)} + \cdots + \mathbf{p}_r\mathbf{Y}\big) \\ \boldsymbol{\kappa}(\mathbf{g}\dot{\mathbf{X}}, \mathbf{Q})\mathbf{g}\dot{\mathbf{X}} \\ \dot{\mathbf{Y}} \\ \cdot \\ \cdot \\ \mathbf{Y}^{(s-1)} \\ -\mathbf{q}_1\mathbf{Y}^{(s-1)} - \cdots - \mathbf{q}_s\mathbf{Y} \end{bmatrix} \qquad (3-59)$$

$$\mathbf{d} = \begin{bmatrix} \mathbf{0} \\ \mathbf{0} \\ \mathbf{0} \\ \mathbf{0} \\ \cdot \\ \cdot \\ \mathbf{0} \\ \mathbf{d}_0 \end{bmatrix}, \quad \mathbf{e} = \begin{bmatrix} \mathbf{0} \\ \mathbf{0} \\ \mathbf{0} \\ \mathbf{0} \\ \cdot \\ \cdot \\ \mathbf{0} \\ \mathbf{e}_0 \end{bmatrix} \qquad (3-60)$$

As seen, $\mathbf{q}(t)$ has been eliminated by means of the geometrical relation. In what follows $\mathbf{c}$ will be termed as the drift vector and $\mathbf{d}$ as the diffusion matrix.

Equation (3-60) can be generalized further, assuming the structural system to be time-varying, so the drift vector becomes especially dependent on time, and that the matrices $\mathbf{d}$ and $\mathbf{e}$ may depend on the state of the system and time. Hence, the following formulations are arrived at

$$\left.\begin{aligned} d\mathbf{Z}(t) &= \mathbf{c}\big(\mathbf{Z}(t),t\big)dt + \mathbf{d}\big(\mathbf{Z}(t),t\big)d\mathbf{W}(t) + \mathbf{e}\big(\mathbf{Z}(t),t\big)d\mathbf{V}(t),\ t>0 \\ \mathbf{Z}(0) &= \mathbf{Z}_0 \end{aligned}\right\} \qquad (3-61)$$

The governing stochastic differential equations (3-61) together with the random initial condition can be converted into the integral form of

$$\mathbf{Z}(t) = \mathbf{Z}_0 + \int_0^t \mathbf{c}\big(\mathbf{Z}(\tau),\tau\big)d\tau + \int_0^t \mathbf{d}\big(\mathbf{Z}(\tau),\tau\big)d\mathbf{W}(\tau) + \int_0^t \mathbf{e}\big(\mathbf{Z}(\tau),\tau\big)d\mathbf{V}(\tau) \quad (3-62)$$

If the dynamic behaviour of the system is governed by the set of first order differential equations (3-61) and the generating source processes are the ones with independent increments and are statistically independent of random initial conditions $\mathbf{Z}_0$, then the state vector $\{\mathbf{Z}(t),\ t\in[0,\infty[\}$ is a Markov process.

Example 3-1: Equivalent shear models for reinforced concrete structures exposed to earthquakes

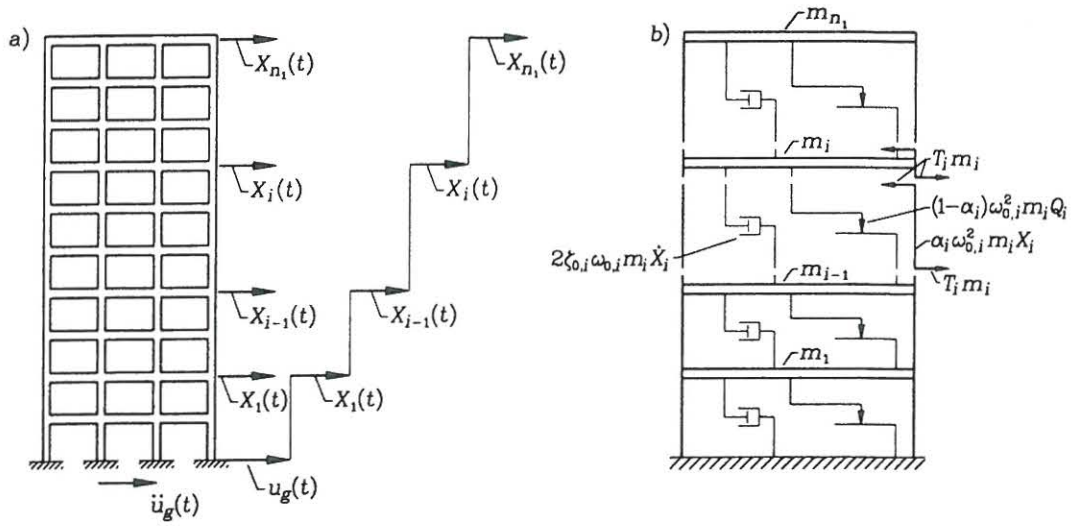

Figur 3-2: A) Instrumented reinforced concrete structure. b) Equivalent shear model.

It is common practice to instrument important structures in seismic active areas to control the damage development. Assume, the horizontal ground surface accelerator $\ddot{u}_g(t)$ and the horizontal displacement are measured at a number, n_1, of points along the building, not necessarily coinciding with the storey beams as shown in fig. 3-2a. $X_i(t)$ signifies the displacement of the ith measurement point relative to the displacement of the $(i-1)$th measurement point. Generally, the n_1th measurement point is assumed to be located at the top storey. Especially, $X_1(t)$ signifies the horizontal displacement of the 1st measurement point relative to the ground surface.

Next, an equivalent shear building with n_1 degrees-of-freedom is introduced, see fig. 3-2b. In this case, $X_i(t)$ is assumed to represent the relative displacement between the $(i-1)$th and the ith storey beam of the equivalent shear structure. Then, $X_i(t)$ is assumed to cause an interstorey shear force of magnitude $m_i T_i$, where m_i is the ith storey mass. The equations of motion in terms of the relative displacements can be written as

$$\left.\begin{aligned}
&\ddot{X}_1 = \mu_2 T_2 - T_1 - \ddot{u}_g && , \quad t>0 && \\
&\ddot{X}_i = \mu_{i+1} T_{i+1} - (\mu_i + 1) Q_i + Q_{i-1} && , \quad t>0 && , \quad i = 2,3,\cdots,n_1-1 \\
&\ddot{X}_{n_1} = -(\mu_{n_1}+1) T_n + T_{n_1-1} && , \quad t>0 && \\
&X_i(0) = \dot{X}_i(0) = 0 && && , \quad i = 1,2,\cdots,n_1
\end{aligned}\right\} \qquad (3-63)$$

$$T_i = 2\zeta_{0,i}\omega_{0,i}\dot{X}_i + \omega_{0,i}^2(\alpha_i X_i + (1-\alpha_i)Q_i) \quad , \quad i = 1,2,\cdots,n_1 \qquad (3-64)$$

$$\dot{Q}_i = \kappa(\dot{X}_i, Q_i, D_i)\dot{X}_i \quad , \quad t>0 \quad , \quad z_i(t_0) = 0 \quad , \quad i = 1,2,\cdots,n_1 \qquad (3-65)$$

$$\dot{D}_i = g(\dot{X}_i, Q_i)\dot{X}_i \quad , \quad t>0 \quad , \quad D_i(0) = D_{i,0} \quad , \quad i = 1,2,\cdots,n_1 \qquad (3-66)$$

$$\alpha_i = \left(\frac{2q_{y,i}}{2q_{y,i}+D_i}\right)^{a_i} \quad , \quad i = 1,2,\cdots,n_1 \qquad (3-67)$$

$$\mu_i = \frac{m_i}{m_{i-1}} \quad , \quad i = 2,3,\cdots,n_1 \qquad (3-68)$$

where $m_i 2\zeta_{0,i}\omega_{0,i}\dot{X}_i$ and $m_i\omega_{0,i}^2\alpha_i X_i$ are, respectively, the linear viscous part and the linear elastic part of the shear force per unit mass, T_i, as given by (3-64). Hence, $\omega_{0,i}$ and $\zeta_{0,i}$, $i = 1,2,\cdots n_1$, are merely parameters to specify the linear parts of the shear forces and should not be confused with the natural frequencies and modal damping ratios of the structure. These parameters along with the mass ratios μ_i, $i = 2,3,\cdots n_1$, must be identified so that the elastic version of (3-63) and (3-64) with $\alpha_i = 1$ provides the same undamped circular eigenfrequencies ω_i, modal damping ratios ζ_i and modal participation factors β_i of the undamaged structure, as calculated or measured by non-destructive testing. Notice, that the indicated discrete linear system has $3n_1 - 1$ free parameters, $\omega_{0,i}$, $\zeta_{0,i}$ and μ_i, to fit the $3n_1$ parameters, ω_i, ζ_i and β_i, obtained from the primary linear system identification of the structure. Assuming that modal parameters of the lowest n_1 modes of the primary linear structure have been identified, the indicated indeterminateness in the secondary system identification means that conditions can only be met at the lowest $n_1 - 1$ modes.

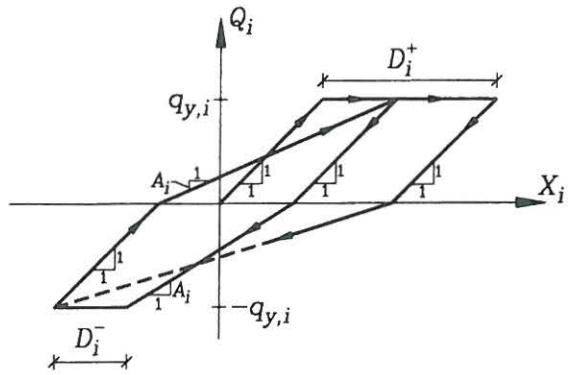

Fig. 3-3: Clough-Johnston hysteretic model.

The hysteretic component of the shear force, $Q_i(t)$, along with the attached state variable $D_i(t)$, is modelled using the Clough-Johnston model as given by (3-65) and (3-66) with the non-dimensional spring stiffness $\kappa(\dot{X}_i,\, Q_i,\, D_i)$ and the function $g(\dot{X}_i, Q_i)$ given as

$$\kappa(\dot{X}_i, Q_i, D_i) = H(Q_i)\Big(A_i(t)H(\dot{X})(1 - H(Q - q_{y,i})) + H(-\dot{X}_i)\Big) +$$

$$H(-Q_i)\Big(A_i(t)H(-\dot{X})(1 - H(-Q_i - q_{y,i})) + H(\dot{X}_i)\Big) \qquad (3-69)$$

$$g(\dot{X}_i, Q_i) = H(\dot{X}_i)H(Q_i - q_{y,i}) - H(-\dot{X}_i)H(-Q_i - q_{y,i}) \qquad (3-70)$$

$$A_i(t) = \frac{q_{y,i}}{q_{y,i} + D_i(t)} \qquad (3-71)$$

The stiffness degrading hysteretic constitutive law of the model can be represented as shown in fig. 3-3. The Clough-Johnston model deals with the stiffness degradation by changing the slope $A_i(t)$ of the elastic branches as the accumulated plastic deformations, $D_i^+(t)$, and $D_i^-(t)$, at positive and negative yielding increase as shown in fig. 3-3. $D_i(t) = D_i^+(t) + D_i^-(t)$ are the total accumulated plastic deformations. For loading branches, the slope $A_i(t)$ is selected such that the elastic branch always aims at the previous unloading point with the other sign. At unloadings, the slope is 1. $D_{i,0}$ is the initial value of the total accumulated damage which is zero before the first earthquake hits and is assumed to be calculated from previous earthquake and displacement response records for the succeeding earthquakes. $H(x)$ is the unit step function as given by (3-5).

The novelty of the present model primarily stems from the modelling of the elastic fraction of the shear force, $\alpha_i(D(t))$, as a non-increasing function of the accumulated plastic deformation as indicated by (3-67). The initial undamped structure is elastic. Hence, $\alpha_i = 1$ in this case. As larger and larger parts of the structure between the $(i-1)$th and ith measure point become plastic and damaged, $\alpha_i(t)$ is comparably decreasing.

The model of the shear force has 2 free parameters, $q_{y,i}$ and a_i. These $2n_1$ parameters are updated after each significant earthquake so the shear model predicts the measured response when the measured ground surface acceleration is applied to the model. Subjecting a stochastic design earthquake $\{\ddot{u}_g(t),\, t \in [0, \infty[\}$ to the calibrated shear model the residual reliability can next be estimated from the stochastic behaviour of the damage indicators.

This necessitates an introduction of a damage indicator for the substructure between the $(i-1)$th and the ith measurement point. In the hysteretic model an equivalent linear spring stiffness for the hysteretic component is defined by the slope, $s_i(t)$, connecting the previous extreme unloading points at positive and negative yielding. As seen from fig. 3-3 this is given as

$$s_i(t) = \frac{2q_{y,i}}{2q_{y,i} + D_i(t)} \qquad (3-72)$$

The so-called softening of the considered section of the structure is then defined as

$$\delta_i(t) = 1 - \frac{\omega_i(t)}{\omega_{i,0}} = 1 - \sqrt{\alpha_i + (1-\alpha_i)s_i} =$$
$$1 - \sqrt{\frac{2q_{y,i}}{2q_{y,i} + D_i(t)}\Big(1 - \alpha_i(D_i(t))\Big) + \alpha_i(D_i(t))} \qquad (3-73)$$

In (3-73) $\omega_i(t)$ signifies the value of $\omega_{i,0}$ at the time t to be used in an equivalent linear shear model in (3-64). For the case $n_1 = 1$, $\omega_1(t)$ can be identified as an estimate of the fundamental circular eigenfrequency of the equivalent linear structure. (3-73) is a non-decreasing function of time and hence displays the maximum softening encountered up to the time t. $\delta_i(t)$ can also be measured from the time series $X_i(t)$ using time-windowed ARMA-models (DiPasquale and Çakmak (1990), Köylüoğlu, Nielsen, Çakmak and Kirkegaard (1996)), time-windowed Fourier transforms (Mullen, Micaletti and Çakmak (1995)) or wavelet transforms (Micaletti, Çakmak, Nielsen and Kirkegaard (1996)). The free parameters, $q_{y,i}$ and a_i, can then be updated from a weighted least square criterion, minimizing the deviations between measured and estimated inter-storey displacements $X_1(t), \cdots, X_{n_1}(t)$ and damage indicators $\delta_i(t), \cdots, \delta_{n_1}(t)$ in the last encountered earthquake.

In this case the state vector of the integrated dynamic system of dimension $n = 4n_1$ becomes

$$\mathbf{Z}(t) = \begin{bmatrix} \mathbf{X}(t) \\ \dot{\mathbf{X}}(t) \\ \mathbf{Q}(t) \\ \mathbf{D}(t) \end{bmatrix}, \ \mathbf{X}(t) = \begin{bmatrix} X_i(t) \\ \vdots \\ X_{n_1}(t) \end{bmatrix}, \ \mathbf{Q}(t) = \begin{bmatrix} Q_i(t) \\ \vdots \\ Q_{n_1}(t) \end{bmatrix}, \ \mathbf{D}(t) = \begin{bmatrix} D_i(t) \\ \vdots \\ D_{n_1}(t) \end{bmatrix} \qquad (3-74)$$

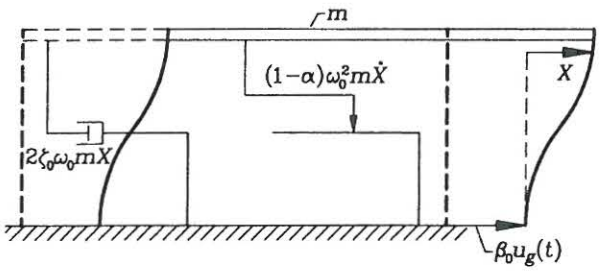

Fig. 3-4: SDOF hysteretic oscillator model.

Especially, for the case $n_1 = 1$ the shear model reduces to the hysteretic single-degree-of-freedom hysteretic oscillator shown in fig. 3-4. The equations of motion and the maximum softening become

$$\left.\begin{aligned} &\ddot{X}(t) + 2\zeta_0\omega_0\dot{X}(t) + \omega_0^2\Big(\alpha(t)X(t) + (1-\alpha(t))Q(t)\Big) = -\beta_0\ddot{u}_g(t) \quad , \quad t > 0 \\ &X(0) = \dot{X}(0) = 0 \end{aligned}\right\} \qquad (3-75)$$

$$\dot{Q}(t) = \Big[H(Q)\Big(A(t)H(\dot{X})(1 - H(Q - q_y)) + H(u - \dot{X})\Big) +$$
$$H(-Q)\Big(A(t)H(-\dot{X})(1 - H(-Q - q_y)) + H(\dot{X})\Big)\Big]\dot{X}(t) \quad , \quad Q(0) = 0 \qquad (3-76)$$

$$\dot{D}(t) = \Big(H(\dot{X})H(Q-q_y) - H(-\dot{X})H(-Q-q_y)\Big)\dot{X}(t) \quad , \quad D(0) = D_0 \tag{3-77}$$

$$\alpha(t) = \left(\frac{2q_y}{2q_y + D}\right)^a \tag{3-78}$$

$$A(t) = \frac{q_y(t)}{q_y(t) + D(t)} \tag{3-79}$$

$$\delta(t) = 1 - \sqrt{\frac{2q_y}{2q_y + D(t)}\Big(1-\alpha(t)\Big) + \alpha(t)} \tag{3-80}$$

The top storey displacement of the structure relative to the ground surface, $X(t)$, can be interpreted as the first modal coordinate in a modal expansion if the mode shape is suitably normalized. The linear circular eigenfrequency, ω_0, the damping ratio, ζ_0, and the mode participation factor, β_0, of the first mode are assumed to be known before the arrival of the first earthquake.

The 10 storey 3 bay structure shown in figure 3-2a was tested experimentally by Cecen (1979) in the model scale 1:10. The circular eigenfrequency, damping ratio and modal participation factor for the first mode of the undamaged structure are $\omega_1 = 6\pi s^{-1}$, $\zeta_1 = 0.035$ and $\beta_1 = 1.32$. The first eigenvector has been selected so the displacement of the top storey is $1.32\ X(t)$. The model was exposed to 3 sequential earthquakes shown in fig. 3-5, which are simulated versions of the 1940 El Centro NS earthquake component. The time has been compressed with a factor 2.5 compared to prototype time according to the applied model law.

The top storey displacement relative to the ground surface in the 3 runs has been shown as the unbroken curves in fig. 3-6. The softening $\delta(t)$ has next been derived from these data using an overlapping time-windowing ARMA model suited for the displacement response. The time window is chosen as 2.4 seconds and the ARMA model is fitted for each such window. The estimates are located at the centre of each window and the estimates are smoothed.

Test	q_y (mm)	a
Run1	2.68	0.83
Run2	3.01	0.77
Run3	3.14	0.73

Table 3-1: Estimated hysteretic parameters.

Applying the SDOF model (3-75)-(3-80) in combination with the weighted least square deviation of measured and estimated relative displacements $x(t)$ and softenings $\delta(t)$ in each of the 3 runs, the parameters shown in table 3-1 are obtained. Even though the excitation level and the structural properties change dramatically throughout the 3 runs, these parameters only change slightly, which is an indication of the feasibility of the whole concept of modelling. A perfect model would provide constant parameters.

In fig. 3-6 the predicted displacements of the calibrated SDOF hysteretic model compared to those obtained by measurements are shown. The agreements are generally good and comparable to what can be achieved by much more involved finite element modelling, see Mørk and Nielsen (1991b), Mørk (1992, 1993). The development of the maximum softening predicted by the calibrated model has been shown in fig. 3-7.

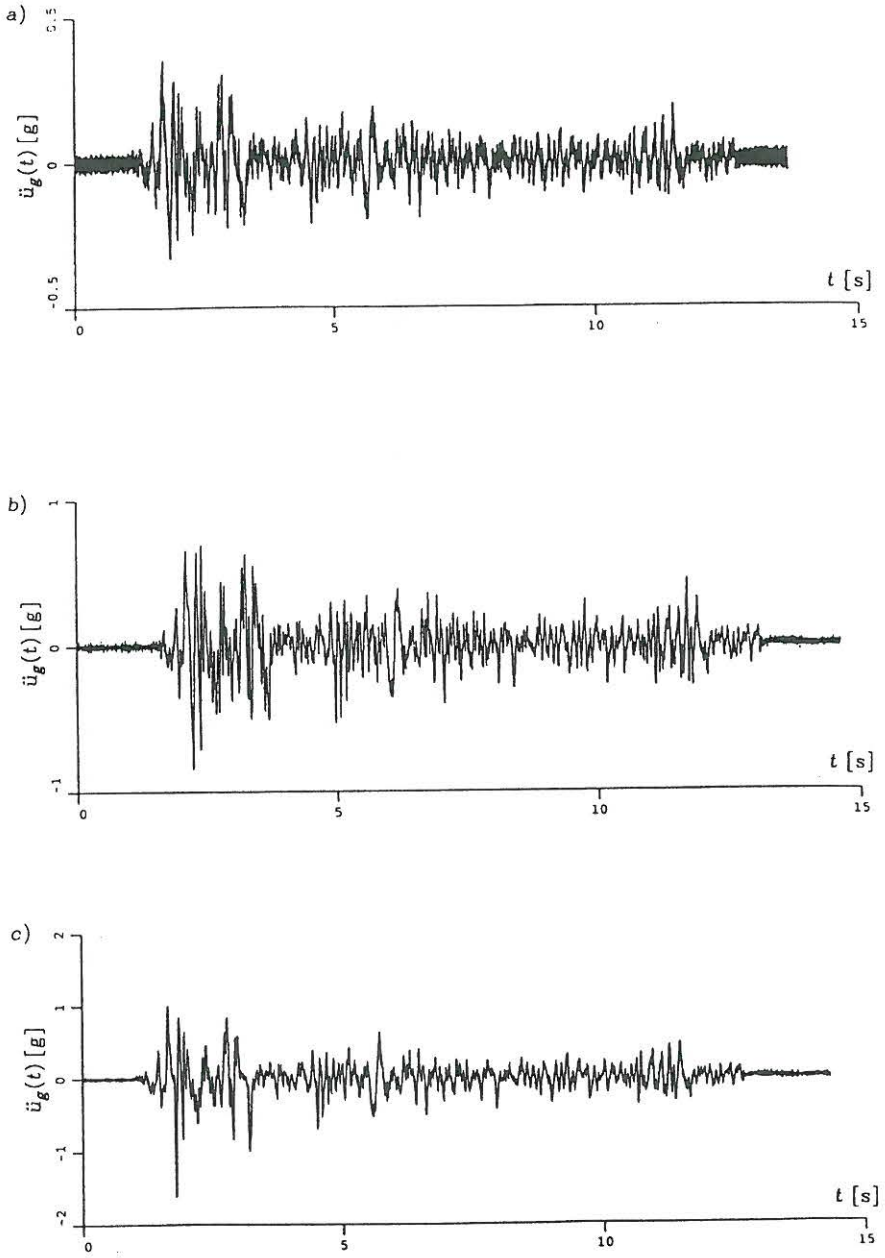

Fig. 3-5: Ground surface accelerations. Structure H1, Cecen (1979). a) Run1, $a_{\text{peak}} = 0.36$ g. b) Run2, $a_{\text{peak}} = 0.84$ g. c) Run3, $a_{\text{peak}} = 1.60$ g.

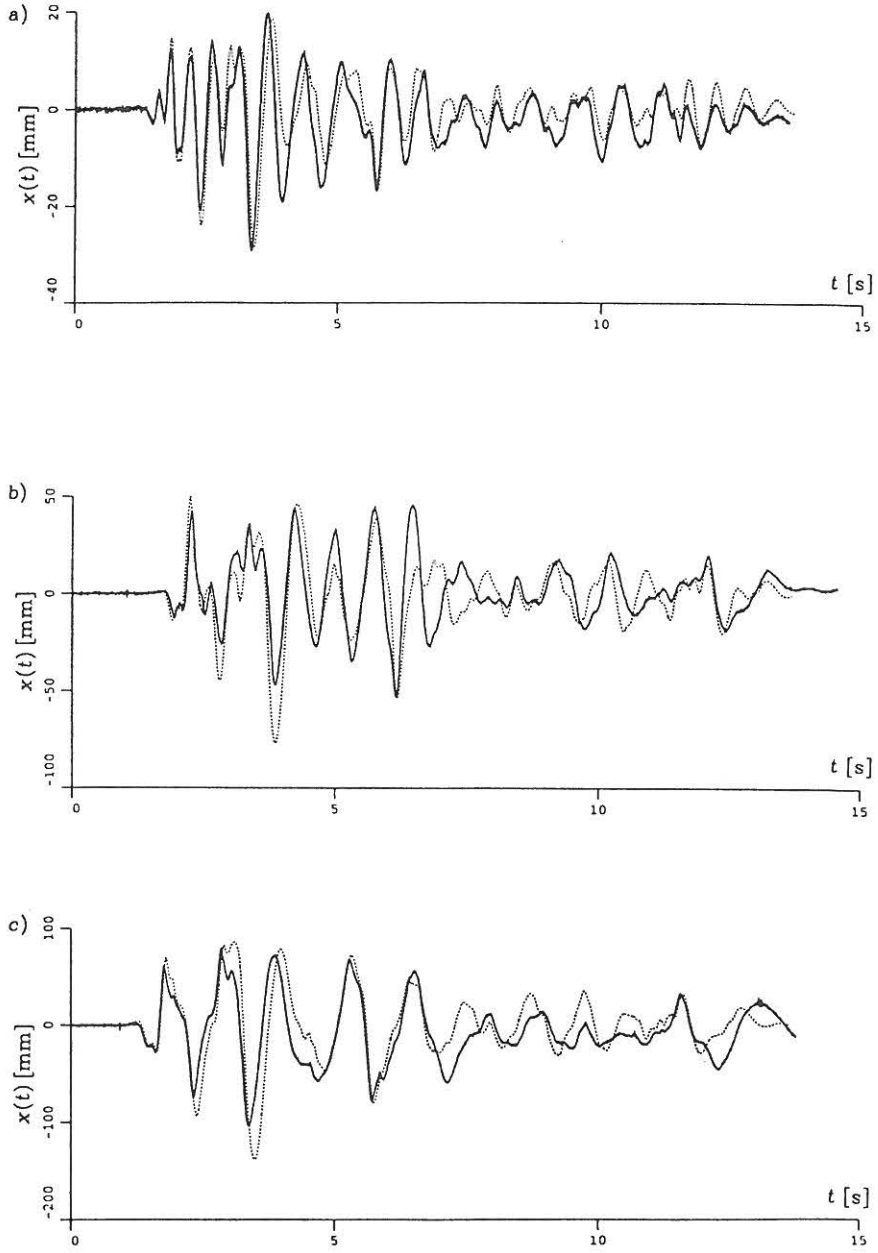

Fig. 3-6: Displacement of top-storey. Structure H1, Cecen (1979). (——): measurement. (- - -): calibrated SDOF hysteretic model. a) Run1, $a_{\text{peak}} = 0.36$ g. b) Run2, $a_{\text{peak}} = 0.84$ g. c) Run3, $a_{\text{peak}} = 1.60$ g. Köylüoğlu, Nielsen, Çakmak and Kirkegaard (1996).

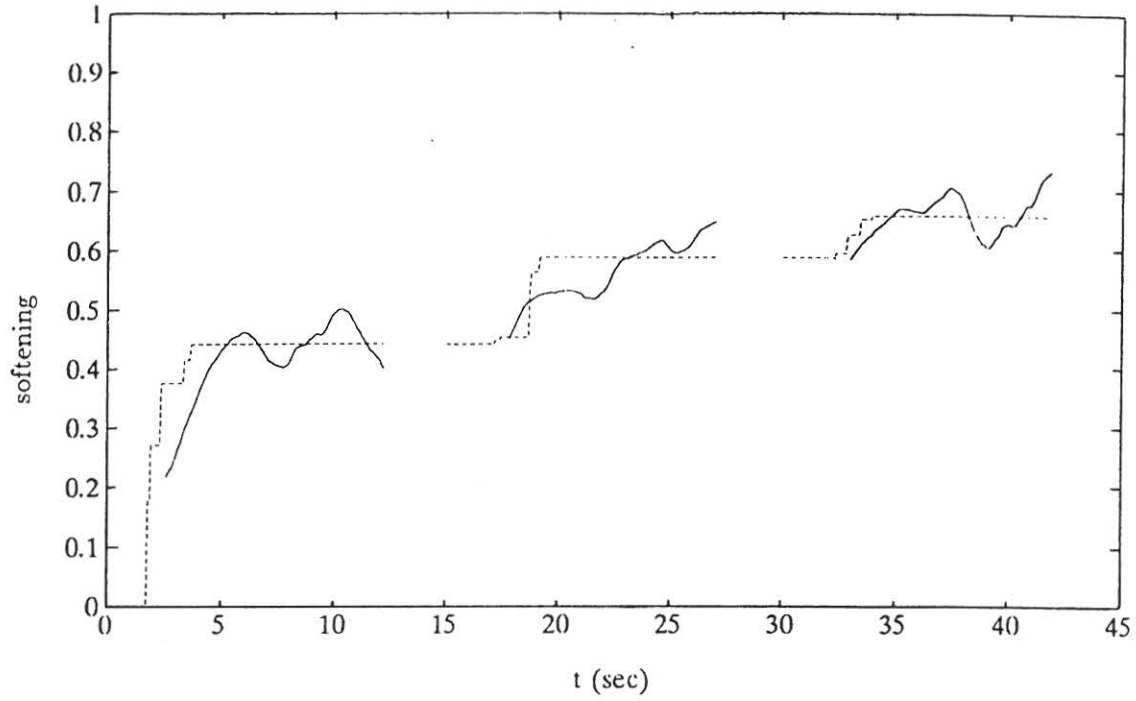

Figur 3-7: Development of maximum softening index in Run1, Run2 and Run3 with SDOF hysteretic model calibrated to each run. Structure H1, Cecen (1979). (——): measurement. (- - -): calibrated hysteretic model. Köylüoğlu, Nielsen, Çakmak and Kirkegaard (1996).

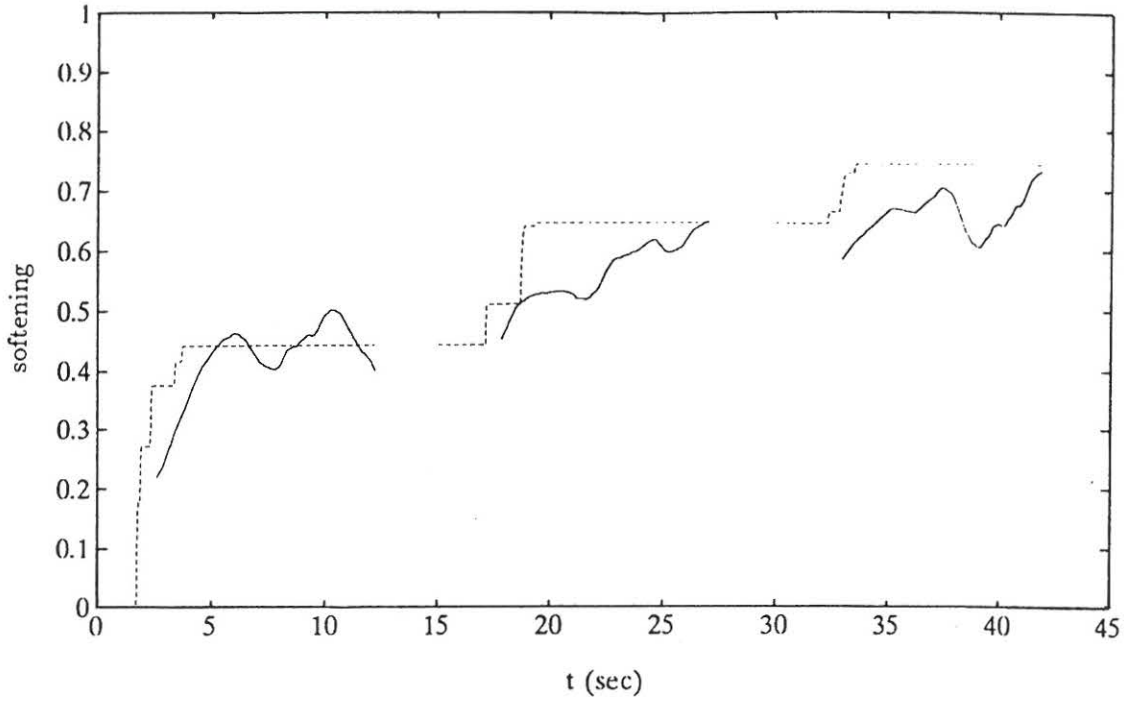

Fig. 3-8: Prediction of maximum softening index in Run2 and Run3 with SDOF hysteretic model calibrated to Run1. Structure H1, Cecen (1979). (——): measurement. (- - -): calibrated hysteretic model. Köylüoğlu, Nielsen, Çakmak and Kirkegaard (1996).

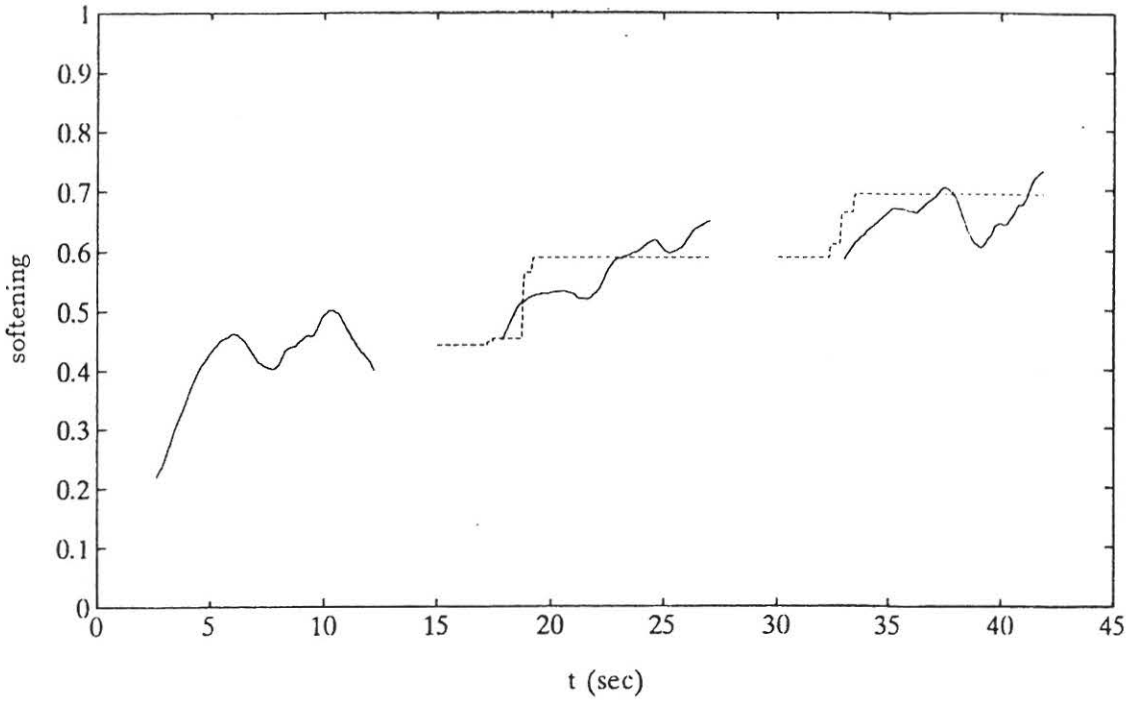

Fig. 3-9: Prediction of maximum softening index in Run3 with SDOF hysteretic model calibrated to Run2. Structure H1, Cecen (1979). (——): measurement. (- - -): calibrated hysteretic model. Köylüoğlu, Nielsen, Çakmak and Kirkegaard (1996).

The capability of the SDOF hysteretic oscillator for predicting the development of the maximum softening in future earthquakes has been demonstrated in figs. 3-8 and 3-9. Fig. 3-8 shows the prediction of the maximum softening index in Run2 and Run3 with the free parameters of the model calibrated to Run1. In this case the extrapolation from the 0.31 g earthquake in Run1 to the 0.84 g earthquake in Run2 is possible, whereas the extrapolation to the 1.60 g earthquake in Run3 is too far, since the shear model seems to overestimate the damage. However, if the free parameters are updated after Run2 the damage development can still be observed very well in Run3 as shown in fig. 3-9.

The maximum softening damage index as a global damage indicator was introduced by DiPasquale and Çakmak (1991). Strong correlation was demonstrated between actual damage levels and damage levels with the maximum softening damage index computed through seismic assessment of actual strong-motion records from medium-size RC-structures subjected to the 1971 San Fernando earthquake. By means of Monte Carlo simulations, Nielsen and Çakmak (1991) demonstrated that maximum softening damage index values encountered in a sequence of earthquakes form a Markov chain. This property is essential for using the index as a predictor of the residual structural reliability on condition that only its last observed value is taken into consideration. Nielsen, Köylüoğlu and Çakmak (1992) devised a method for damage localization based on maximum softening damage indicators defined for various parts of the structure, which were identified from an equal number of smoothed circular eigenfrequencies of the equivalent linear shear structure. The method was only elaborated for the case $n_1 = 2$. The Clough-Johnston hysteretic model was originally devised to model the stiffness degradation in RC shear beams, Clough and Johnston (1966). The differential description of the model is due to Minai and Suzuki (1985) and Mørk (1989). The equivalent shear model presented in this example was formulated by Köylüoğlu, Nielsen, Çakmak and Kirkegaard (1996). The capability of the model in predicting the expectation and the coefficient of variation of the damage in a future earthquake on condition of a certain damage encountered during the previous earthquake was investigated by Nielsen, Skjærbæk, Köylüoğlu and Çakmak (1995) based on Monte Carlo simulations with 1000 independent realizations.

The reference was chosen as the predictions obtained by the much more involved SARCOF finite element program (Mørk and Nielsen (1991a, 1991b), Mørk (1992, 1993)). Only the predictions of the SDOF version of the model was considered. In the paper it was concluded that the model predicts the conditional mean values sufficiently correct, whereas the conditional variance is overestimated. The sensitivity of the residual reliability of partly damaged RC-structure as predicted by the SDOF model on the estimated hysteretic parameters q_y and a was investigated by Iwankiewicz and Nielsen (1995). The failure event was defined as the first-passage of the maximum softening of a critical level of $\delta_c = 0.5$. Again, Monte Carlo simulation with 1000 independent realizations was used and the predictions of the SARCOF program were used as a reference. The results indicate that the residual reliability shows much larger elasticity with respect to q_y than to a for significantly damaged structures ($\delta \in [0.30; 0.50[$). For this reason it is recommended that q_y is modelled as a random variable with expected value equal to the calibrated value. The variational coefficient of the random variable should not be selected larger than 0.1. Finally, Köylüoğlu, Nielsen, Abbott and Çakmak (1996) have examined the damage localization capability of the n_1-dimensional version of the model. It was demonstrated how the damage localization depends on the frequency contents of the excitation. The damage is generally larger and more uniformly distributed, when primarily the 1st eigenmode is excited, which is the basic assumption behind the concept of the global maximum softening damage index, Di Pasquale and Çakmak (1991). Further, a high correlation between the softening $\delta_i(t)$ as given by (3-73) and the energy absorption between measurement points was verified.

3.2 Forward and backward integro-differential Chapman-Kolmogorov equations for stochastic response and reliability problems

3.2.1 Forward and backward integro-differential Chapman-Kolmogorov equations and related initial and boundary values

The sample paths of a Markov process are continuous functions of time with probability one if for any $\varepsilon > 0$ the following condition is satisfied uniformly in $\mathbf{z}$, t and Δt, see e.g. Bharucha-Reid (1960)

$$\lim_{\Delta t \to 0} \frac{1}{\Delta t} \int_{|\mathbf{x}-\mathbf{z}|>\varepsilon} q_{\{\mathbf{Z}\}}(\mathbf{x}, t+\Delta t|\mathbf{z}, t)d\mathbf{x} = 0 \qquad (3-81)$$

This condition expresses the property of continuous sample paths that the probability of increments $|\mathbf{x}-\mathbf{z}|$ larger than some small ε of the process during a small time interval Δt tends to zero faster than Δt.

If the sample paths are discontinuous, the following relationship must hold, for all $\varepsilon > 0$, uniformly in $\mathbf{z}$, and t and for $|\mathbf{x}-\mathbf{z}| > \varepsilon$

$$\int_{|\mathbf{x}-\mathbf{z}|>\varepsilon} J_{\{\mathbf{Z}\}}(\mathbf{x}|\mathbf{z}, t)d\mathbf{x} > 0 \qquad (3-82)$$

where

$$J_{\{\mathbf{Z}\}}(\mathbf{x}|\mathbf{z}, t) = \lim_{\Delta t \to 0} \frac{1}{\Delta t} q_{\{\mathbf{Z}\}}(\mathbf{x}, t+\Delta t|\mathbf{z}, t) \qquad (3-83)$$

is designated the jump probability intensity function on the state vector $\mathbf{Z}(t)$.

The so-called derivate moments are defined as the following limits valid for all $\varepsilon > 0$, and uniformly in $\mathbf{x}$ and t:

$$\lim_{\Delta t \to 0} \frac{1}{\Delta t} \int_{|\mathbf{x}-\mathbf{z}|<\varepsilon} (x_i - z_i) q_{\{\mathbf{Z}\}}(\mathbf{x}, t+\Delta t|\mathbf{z}, t) d\mathbf{x} = C_i(\mathbf{z}, t) + \mathrm{O}(\varepsilon) \qquad (3-84)$$

$$\lim_{\Delta t \to 0} \frac{1}{\Delta t} \int_{|\mathbf{x}-\mathbf{z}|<\varepsilon} (x_i - z_i)(x_j - z_j) q_{\{\mathbf{Z}\}}(\mathbf{x}, t+\Delta t|\mathbf{z}, t) d\mathbf{x} = D_{ij}(\mathbf{z}, t) + \mathrm{O}(\varepsilon) \qquad (3-85)$$

Alternatively, the derivate moments are defined as

$$\lim_{\Delta t \to 0} \frac{1}{\Delta t} E\big[Z_i(t+\Delta t) - Z_i(t) | \mathbf{Z}(t) = \mathbf{z}\big] = C_i(\mathbf{z}, t) + \mathrm{O}(\varepsilon) \qquad (3-86)$$

$$\lim_{\Delta t \to 0} \frac{1}{\Delta t} E\big[\big(Z_i(t+\Delta t) - Z_i(t)\big)\big(Z_j(t+\Delta t) - Z_j(t)\big) | \mathbf{Z}(t) = \mathbf{z}\big] = D_{ij}(\mathbf{z}, t) + \mathrm{O}(\varepsilon) \qquad (3-87)$$

Since, the expectations in (3-84) and (3-85) are performed only for jumps $|\mathbf{x} - \mathbf{z}| < \varepsilon$, these quantities should be interpreted as the rates of moments of the continuous part of the increment in $\mathbf{Z}(t)$ during $[t, t + \Delta t[$, conditional on $\mathbf{Z}(t) = \mathbf{z}$.

Upon insertion of (3-61) into (3-86) and (3-87) and observing that only the continuous part, i.e. $d\mathbf{Z}(t) = \mathbf{c}\big(\mathbf{Z}(t), t\big)dt + \mathbf{d}\big(\mathbf{Z}(t), t\big)d\mathbf{W}(t)$ is to be inserted into these expressions, one has, upon using the incremental properties of the Wiener process,

$$C_i(\mathbf{z}, t) = c_i(\mathbf{z}, t) \qquad (3-88)$$

$$D_{ij}(\mathbf{z}, t) = \sum_{\alpha=1}^{n_3} d_{i\alpha}(\mathbf{z}, t) d_{j\alpha}(\mathbf{z}, t) \qquad (3-89)$$

In order to derive the jump probability intensity function $J_{\{\mathbf{Z}\}}(\mathbf{z}|\mathbf{x}, t)$ of the state vector, assume that a jump of magnitude p_α in the αth component $V_\alpha(t)$ of the generating source process $\{\mathbf{V}(t),\ t \in [0, \infty[\}$ takes place during the interval $[t, t + dt[$. On condition that the system is at the state $\mathbf{Z}(t) = \mathbf{x}$, the increment of the state vector becomes $d\mathbf{Z}(t) = \mathbf{e}_\alpha(\mathbf{x}, t)p_\alpha$, where $\mathbf{e}_\alpha(\mathbf{x}, t)$ is the αth column of the matrix $\mathbf{e}(\mathbf{x}, t)$, cf. (3-61). The transition probability density function can then be represented by the Dirac delta spike

$$q_{\{\mathbf{Z}\}}(\mathbf{z}, t+dt|\mathbf{x}, t) = \delta\Big(\mathbf{z} - \big(\mathbf{x} + \mathbf{e}_\alpha(\mathbf{x}, t)p_\alpha\big)\Big) \qquad (3-90)$$

Since the probability of making a jump into $[p_\alpha, p_\alpha + dp_\alpha[$ during the infinitesimal time interval $[t, t + dt[$ is given by $J_{\{V_\alpha\}}(p_\alpha, t)dtdp_\alpha$, cf. (3-25), the unconditional transition probability is obtained by summing over all contiguous intervals as follows

$$q_{\{\mathbf{Z}\}}(\mathbf{z}, t+dt|\mathbf{x}, t) = dt \int_{\mathcal{P}_\alpha} \delta\Big(\mathbf{z} - \big(\mathbf{x} + \mathbf{e}_\alpha(\mathbf{x}, t)p_\alpha\big)\Big) J_{\{V_\alpha\}}(p_\alpha, t) dp_\alpha \qquad (3-91)$$

Relation (3-91) represents the probability density contribution in case of jumping from $\mathbf{Z}(t) = \mathbf{x}$ to $\mathbf{Z}(t+dt) = \mathbf{z}$ due to a jump in the αth component. Since the components have been assumed to be mutually statistically independent, the probability density contribution from all n_4 component processes can be obtained as the sum of the contributions (3-91)

$$q_{\{\mathbf{Z}\}}(\mathbf{z}, t+dt|\mathbf{x}, t) = dt \sum_{\alpha=1}^{n_4} \int_{\mathcal{P}_\alpha} \delta\Big(\mathbf{z} - \big(\mathbf{x} + \mathbf{e}_\alpha(\mathbf{x}, t)p_\alpha\big)\Big) J_{\{V_\alpha\}}(p_\alpha, t) dp_\alpha \qquad (3-92)$$

From (3-83) and (3-92) the jump probability intensity function of the state vector is finally obtained as

$$J_{\{\mathbf{Z}\}}(\mathbf{z}|\mathbf{x}, t) = \sum_{\alpha=1}^{n_4} \int_{\mathcal{P}_\alpha} \delta\Big(\mathbf{z} - \big(\mathbf{x} + \mathbf{e}_\alpha(\mathbf{x}, t)p_\alpha\big)\Big) J_{\{V_\alpha\}}(p_\alpha, t) dp_\alpha \qquad (3-93)$$

(3-93) was derived by Nielsen and Iwankiewicz (1996).

The development of the transitional probability density function $q_{\{\mathbf{Z}\}}(\mathbf{z}, t \mid \mathbf{x}, t_0)$ is governed by the forward and backward integro-differential Chapman-Kolmogorov equations. For systems with combined deterministic drift, Wiener process driven (diffusions) and jump process driven, these were derived by Gardiner (1985). For all $\mathbf{z} \in S_t$, $\mathbf{x} \in S_{t_0}$, where $t > t_0$, $q_{\{\mathbf{Z}\}}(\mathbf{z}, t \mid \mathbf{x}, t_0)$ is shown to fulfil the following forward integro-differential Chapman-Kolmogorov equation:

$$\frac{\partial}{\partial t} q_{\{\mathbf{Z}\}}(\mathbf{z}, t \mid \mathbf{x}, t_0) = \mathcal{K}_{\mathbf{z},t}\big[q_{\{\mathbf{Z}\}}(\mathbf{z}, t \mid \mathbf{x}, t_0)\big] \ , \ t \in]t_0, t_1] \qquad (3-94)$$

$$\mathcal{K}_{\mathbf{z},t}\big[q_{\{\mathbf{Z}\}}(\mathbf{z}, t \mid \mathbf{x}, t_0)\big] =$$

$$-\sum_{i=1}^{n} \frac{\partial}{\partial z_i}\Big(C_i(\mathbf{z}, t) q_{\{\mathbf{Z}\}}\big(\mathbf{z}, t \mid \mathbf{x}, t_0\big)\Big) + \frac{1}{2}\sum_{i=1}^{n}\sum_{j=1}^{n} \frac{\partial^2}{\partial z_i \partial z_j}\Big(D_{ij}(\mathbf{z}, t) q_{\{\mathbf{Z}\}}\big(\mathbf{z}, t \mid \mathbf{x}, t_0\big)\Big) +$$

$$\int_{S_t}\Big(J_{\{\mathbf{Z}\}}\big(\mathbf{z} \mid \mathbf{y}, t\big) q_{\{\mathbf{Z}\}}\big(\mathbf{y}, t \mid \mathbf{x}, t_0\big) - J_{\{\mathbf{Z}\}}\big(\mathbf{y} \mid \mathbf{z}, t\big) q_{\{\mathbf{Z}\}}\big(\mathbf{z}, t \mid \mathbf{x}, t_0\big)\Big) d\mathbf{y} \ =$$

$$-\sum_{i=1}^{n} \frac{\partial}{\partial z_i}\big[c_i(\mathbf{z}, t) q_{\{\mathbf{Z}\}}(\mathbf{z}, t|\mathbf{x}, t_0)\big] +$$

$$\frac{1}{2}\sum_{i=1}^{n}\sum_{j=1}^{n} \frac{\partial^2}{\partial z_i \partial z_j}\left(\sum_{\alpha=1}^{n_3} d_{i\alpha}\big(\mathbf{z}, t\big) d_{j\alpha}\big(\mathbf{z}, t\big)\, q_{\{\mathbf{Z}\}}(\mathbf{z}, t|\mathbf{x}, t_0)\right) +$$

$$\sum_{\alpha=1}^{n_4} \int_{\mathcal{P}_\alpha}\Big(q_{\{\mathbf{Z}\}}\big(\mathbf{z} - \mathbf{e}_\alpha(t)p_\alpha, t|\mathbf{x}, t_0\big) - q_{\{\mathbf{Z}\}}\big(\mathbf{z}, t|\mathbf{x}, t_0\big)\Big) J_{\{V_\alpha\}}(p_\alpha) dp_\alpha \qquad (3-95)$$

where (3-88), (3-89) and (3-93) have been applied.

Similarly, for any $\mathbf{y} \in S_{t_1}$, $\mathbf{z} \in S_t$ where $t_1 > t, q_{\{\mathbf{Z}\}}(\mathbf{y}, t_1 \mid \mathbf{z}, t)$ fulfils the backward integro-differential Chapman-Kolmogorov equation

$$\frac{\partial}{\partial t} q_{\{\mathbf{Z}\}}(\mathbf{y}, t_1 \mid \mathbf{z}, t) + \mathcal{K}^T_{\mathbf{z},t}\left[q_{\{\mathbf{Z}\}}(\mathbf{y}, t_1 \mid \mathbf{z}, t)\right] = 0 \ , \ t \in [t_0, t_1[\qquad (3-96)$$

$$\mathcal{K}^T_{\mathbf{z},t}\left[q_{\{\mathbf{Z}\}}(\mathbf{y}, t_1 \mid \mathbf{z}, t)\right] =$$

$$\sum_{i=1}^{n} C_i(\mathbf{z}, t) \frac{\partial}{\partial z_i} q_{\{\mathbf{Z}\}}(\mathbf{y}, t_1 \mid \mathbf{z}, t) + \frac{1}{2} \sum_{i=1}^{n} \sum_{j=1}^{n} D_{ij}(\mathbf{z}, t) \frac{\partial^2}{\partial z_i \partial z_j} q_{\{\mathbf{Z}\}}(\mathbf{y}, t_1 \mid \mathbf{z}, t) +$$

$$\int_{S_t} J_{\{\mathbf{Z}\}}(\mathbf{x} \mid \mathbf{z}, t)\Big(q_{\{\mathbf{Z}\}}(\mathbf{y}, t_1 \mid \mathbf{x}, t) - q_{\{\mathbf{Z}\}}(\mathbf{y}, t_1 \mid \mathbf{z}, t)\Big) d\mathbf{x} \ =$$

$$\sum_{i=1}^{n} c_i(\mathbf{z}, t) \frac{\partial}{\partial z_i} q_{\{\mathbf{Z}\}}(\mathbf{y}, t_1 | \mathbf{z}, t) +$$

$$\frac{1}{2} \sum_{i=1}^{n} \sum_{j=1}^{n} \left(\sum_{\alpha=1}^{n_3} d_{i\alpha}(\mathbf{z}, t) d_{j\alpha}(\mathbf{z}, t) \frac{\partial^2}{\partial z_i \partial z_j} q_{\{\mathbf{Z}\}}(\mathbf{y}, t_1 | \mathbf{z}, t) \right) +$$

$$\sum_{\alpha=1}^{n_4} \int_{\mathcal{P}_\alpha} \Big(q_{\{\mathbf{Z}\}}(\mathbf{y}, t_1 | \mathbf{z} + \mathbf{e}_\alpha(\mathbf{z}, t) p_\alpha, t) - q_{\{\mathbf{Z}\}}(\mathbf{y}, t_1 | \mathbf{z}, t)\Big) J_{\{V_\alpha\}}(p_\alpha) dp_\alpha \qquad (3-97)$$

The linear functionals $\mathcal{K}_{\mathbf{z},t}[\cdot]$ and $\mathcal{K}^T_{\mathbf{z},t}[\cdot]$ indicate the forward and backward integro-differential Chapman-Kolmogorov operators, respectively. $\mathbf{z}$ and t in (3-94) signify the forward state and the forward time, whereas $\mathbf{z}$ and t in (3-96) represent the backward state and the backward time.

At the evaluation of the last statement of (3-95) the vector $\mathbf{e}_\alpha(t)$ has been assumed to be state independent (independent of $\mathbf{y}$). Then, the evaluation of the integral of $\delta\Big(\mathbf{z} - (\mathbf{y} + \mathbf{e}_\alpha(\mathbf{y}, t) p_\alpha)\Big)$ with respect to $\mathbf{y}$ is very much simplified. If $\mathbf{e}_\alpha = \mathbf{e}_\alpha(\mathbf{y}, t)$, i.e. it is state dependent, a preliminary change of integration variables must be performed, which is defined by the transformations

$$\left.\begin{aligned} \mathbf{u} &= \mathbf{y} + \mathbf{e}_\alpha(\mathbf{y}, t) p_\alpha \\ \mathbf{y} &= \mathbf{a}_\alpha(\mathbf{u}, p_\alpha, t) \\ d\mathbf{y} &= \frac{d\mathbf{u}}{\left|\det\left(\mathbf{I} + \frac{\partial \mathbf{e}_\alpha}{\partial \mathbf{y}^T} p_\alpha\right)\right|} \end{aligned}\right\} \qquad (3-98)$$

where $\mathbf{a}_\alpha(\mathbf{u}, p_\alpha, t)$ is the inverse transformation, $\frac{\partial \mathbf{e}_\alpha}{\partial \mathbf{y}^T}$ is the gradient matrix of $\mathbf{e}_\alpha(\mathbf{y}, t)$

with respect to $\mathbf{y}$ and $\det\left(\mathbf{I}+\frac{\partial \mathbf{e}_\alpha}{\partial \mathbf{y}^T}p_\alpha\right)$ denotes the Jacobian. Then (3-95) becomes

$$\mathcal{K}_{\mathbf{z},t}\left[q_{\{\mathbf{Z}\}}(\mathbf{z},t|\mathbf{x},t_0)\right] = -\sum_{i=1}^{n}\frac{\partial}{\partial z_i}\left(c_i(\mathbf{z},t)q_{\{\mathbf{Z}\}}(\mathbf{z},t|\mathbf{x},t_0)\right)+$$

$$\frac{1}{2}\sum_{i=1}^{n}\sum_{j=1}^{n}\frac{\partial^2}{\partial z_i \partial z_j}\left(\sum_{\alpha=1}^{n_3} d_{i\alpha}(\mathbf{z},t)d_{j\alpha}(\mathbf{z},t)q_{\{\mathbf{Z}\}}(\mathbf{z},t|\mathbf{x},t_0)\right)+$$

$$\sum_{\alpha=1}^{n_4}\int_{p_\alpha}\left(\frac{q_{\{\mathbf{Z}\}}\left(\mathbf{a}_\alpha(\mathbf{z},p_\alpha,t),t|\mathbf{x},t_0\right)}{\left|\det\left(\mathbf{I}+\frac{\partial \mathbf{e}_\alpha\left(\mathbf{a}_\alpha(\mathbf{z},p_\alpha,t),t\right)}{\partial \mathbf{y}^T}p_\alpha\right)\right|}-q_{\{\mathbf{Z}\}}(\mathbf{z},t|\mathbf{x},t_0)\right)J_{\{V_\alpha\}}(p_\alpha)dp_\alpha \quad (3-99)$$

The derivation of (3-95), (3-97) and (3-99) based on (3-93) was given by Nielsen and Iwankiewicz (1996).

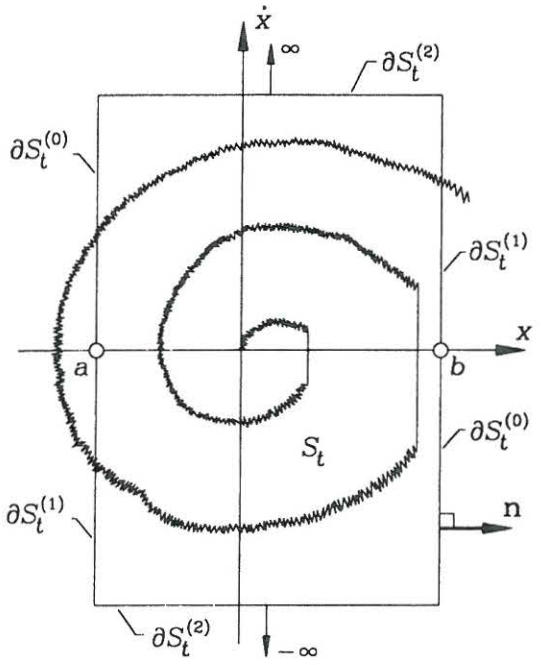

Fig. 3-10. Sample path of the state vector of SDOF non-hysteretic oscillator subjected to combined Wiener process and jump process excitation. Double barrier deterministic start problem.

The forward and backward integro-differential Chapman-Kolmogorov equations must be solved with proper boundary and initial conditions, which will next be derived based on a requirement that $q_{\{\mathbf{Z}\}}(\mathbf{z},t|\mathbf{x},t_0)$ and initial conditions should fulfill both equations.

In fig. 3-10 the sample path and the double barrier deterministic start first-passage time problem for the single-degree-of-freedom non-hysteretic oscillator subjected to a combined Wiener process and jump process excitation are illustrated.

The surface (boundary) ∂S_t of the safe domain S_t may be divided into the accessible part $\partial S_t^{(a)}$, which can be reached in a finite transition time and the non-accessible part $\partial S_t^{(2)}$, which can only be reached after infinitely long time intervals. These parts are defined as follows

$$\partial S_t^{(a)} = \left\{ \mathbf{z} \in \partial S_t \mid \forall \mathbf{x} \in S_{t_0} : \; q_{\{\mathbf{Z}\}}(\mathbf{z}, t \mid \mathbf{x}, t_0) > 0 \right\} \tag{3-100}$$

$$\partial S_t^{(2)} = \left\{ \mathbf{z} \in \partial S_t \mid \forall \mathbf{x} \in S_{t_0} : \; q_{\{\mathbf{Z}\}}(\mathbf{z}, t \mid \mathbf{x}, t_0) = 0 \right\} \tag{3-101}$$

In the example shown in fig. 3-10 the accessible and non-accessible parts of the boundary are given as $\partial S_t^{(a)} = \{(x, \dot{x}) | (x = a \vee x = b) \wedge -\infty < \dot{x} < \infty\}$ and $\partial S_t^{(2)} = \{(x, \dot{x}) | a < x < b \wedge (\dot{x} = -\infty \vee \dot{x} = \infty)\}$.

For the considered system a jump of the generating source process $\{V(t),\, t \in [0, \infty[\}$ causes a discontinuity (jump) in the velocity component of the state vector, cf. (3-45), (3-46). Especially, the jumps close to the accessible surface $\partial S_t^{(a)}$ are tangential, hence no jumps out of the domain are possible. Generally, this is assumed to be true, i.e. the jump probability intensity function fulfils $J_{\{\mathbf{Z}\}}(\mathbf{z} \mid \mathbf{y}, t) = 0$ for all $\mathbf{y} \in S_t$ and $\mathbf{z} \in S_t^c$. Any finite jump at $\mathbf{z}$ close to the accessible part of the surface $\partial S_t^{(a)}$ then takes place in the tangential direction. Since the jumps of the state vector due to the jumps of the αth component of the generating source are in the direction of $\mathbf{e}_\alpha(\mathbf{z}, t)$ these jumps will only be tangential to the surface $\partial S_t^{(a)}$ if

$$\forall t \in]t_0, t_1[\; , \; \mathbf{z} \in \partial S_t^{(a)} \colon \mathbf{n}^T(\mathbf{z}, t) \mathbf{e}_\alpha(\mathbf{z}, t) = 0 \tag{3-102}$$

where $\mathbf{n}(\mathbf{z}, t)$ signifies the unit normal vector in the outward direction of the surface ∂S_t with components $n_i(\mathbf{z}, t)$, see fig. 2-4.

Hence, the flux of probability mass through the accessible surface $\partial S_t^{(a)}$ is caused totally by the convection and diffusion components. The abbreviates $q^{(0)}(\mathbf{z}, t) \equiv q_{\{\mathbf{Z}\}}(\mathbf{z}, t \mid \mathbf{x}, t_0)$ and $q^{(1)}(\mathbf{z}, t) \equiv q_{\{\mathbf{Z}\}}(\mathbf{y}, t_1 \mid \mathbf{z}, t)$ are introduced. Application of the divergence theorem then provides

$$\begin{aligned} &\int_{t_0}^{t_1} \int_{S_t} q^{(1)}(\mathbf{z}, t) \left(\frac{\partial q^{(0)}(\mathbf{z}, t)}{\partial t} - \mathcal{K}_{\mathbf{z},t}\left[q^{(0)}(\mathbf{z}, t) \right] \right) d\mathbf{z} dt = \\ &- \int_{t_0}^{t_1} \int_{S_t} q^{(0)}(\mathbf{z}, t) \left(\frac{\partial q^{(1)}(\mathbf{z}, t)}{\partial t} + \mathcal{K}^T_{\mathbf{z},t}\left[q^{(1)}(\mathbf{z}, t) \right] \right) d\mathbf{z} dt + R\left[q^{(0)}(\mathbf{z}, t), q^{(1)}(\mathbf{z}, t) \right] \end{aligned} \tag{3-103}$$

where $\mathcal{K}_{\mathbf{z},t}[\cdot]$ and $\mathcal{K}^T_{\mathbf{z},t}[\cdot]$ are the forward and backward integro-differential Chapman-Kolmogorov operators as given by (3-95), (3-97) and (3-99), and

$$R\left[q^{(0)}(\mathbf{z}, t), q^{(1)}(\mathbf{z}, t) \right] =$$

$$\int_{S_{t_1}} q_{\{\mathbf{Z}\}}(\mathbf{y},t_1 \mid \mathbf{z},t_1) q_{\{\mathbf{Z}\}}(\mathbf{z},t_1 \mid \mathbf{x},t_0) d\mathbf{z} - \int_{S_{t_0}} q_{\{\mathbf{Z}\}}(\mathbf{y},t_1 \mid \mathbf{z},t_0) q_{\{\mathbf{Z}\}}(\mathbf{z},t_0 \mid \mathbf{x},t_0) d\mathbf{z} +$$

$$\sum_{i=1}^{n} \int_{t_0}^{t_1} \int_{\partial S_t} n_i(\mathbf{z},t) \Big[\Big(C_i(\mathbf{z},t) q^{(0)}(\mathbf{z},t) - \sum_{j=1}^{n} \frac{1}{2} \frac{\partial}{\partial z_j} \big(D_{ij}(\mathbf{z},t) q^{(0)}(\mathbf{z},t) \big) \Big) q^{(1)}(\mathbf{z},t) +$$

$$\sum_{j=1}^{n} q^{(0)}(\mathbf{z},t) \frac{1}{2} D_{ij}(\mathbf{z},t) \frac{\partial}{\partial z_j} q^{(1)}(\mathbf{z},t) \Big] da_t dt \qquad (3-104)$$

$C_i(\mathbf{z},t)$ and $D_{ij}(\mathbf{z},t)$ are given by (3-88), (3-89). If $q^{(0)}(\mathbf{z},t) \equiv q_{\{\mathbf{Z}\}}(\mathbf{z},t \mid \mathbf{x},t_0)$ and $q^{(1)}(\mathbf{z},t) \equiv q_{\{\mathbf{Z}\}}(\mathbf{y},t_1 \mid \mathbf{z},t)$ are assumed to fulfil the forward and backward Chapman-Kolmogorov integro-differential equations (3-94) and (3-96) throughout S_t, the left-hand side and the first term on the right-hand side of (3-103) cancel. Hence, $R\big[q^{(0)}(\mathbf{z},t), q^{(1)}(\mathbf{z},t)\big] \equiv 0$. The initial time t_0 and the terminal time t_1 may be varied. From (3-104) the necessity of the following initial and boundary conditions for $q_{\{\mathbf{Z}\}}(\mathbf{z},t \mid \mathbf{x},t_0)$ and $q_{\{\mathbf{Z}\}}(\mathbf{y},t_1 \mid \mathbf{z},t)$ is then deduced

$$\forall \mathbf{x},\mathbf{z} \in S_{t_0}\colon\ q_{\{\mathbf{Z}\}}(\mathbf{z},t_0 \mid \mathbf{x},t_0) = \delta(\mathbf{z}-\mathbf{x}) \qquad (3-105)$$

$$\forall \mathbf{y},\mathbf{z} \in S_{t_1}\colon\ q_{\{\mathbf{Z}\}}(\mathbf{y},t_1 \mid \mathbf{z},t_1) = \delta(\mathbf{z}-\mathbf{y}) \qquad (3-106)$$

$$\forall t \in]t_0,t_1[\ ,\ \mathbf{x} \in S_{t_0}\ ,\ \mathbf{z} \in \partial S_t^{(2)}\colon\ q^{(0)}(\mathbf{z},t) = q_{\{\mathbf{Z}\}}(\mathbf{z},t \mid \mathbf{x},t_0) = 0 \qquad (3-107)$$

$$\forall t \in]t_0,t_1[\ ,\ \mathbf{y} \in S_{t_1}\ ,\ \mathbf{z} \in \partial S_t^{(2)}\colon\ q^{(1)}(\mathbf{z},t) = q_{\{\mathbf{Z}\}}(\mathbf{y},t_1 \mid \mathbf{z},t) = 0 \qquad (3-108)$$

$\forall t \in]t_0,t_1[\ ,\ \mathbf{x} \in S_{t_0}\ ,\ \mathbf{y} \in S_{t_1}\ ,\ \mathbf{z} \in \partial S_t$:

$$\sum_{i=1}^{n} \int_{\partial S_t^{(a)}} n_i(\mathbf{z},t) \Big[\Big(C_i(\mathbf{z},t) q^{(0)}(\mathbf{z},t) - \frac{1}{2} \sum_{j=1}^{n} \frac{\partial}{\partial z_j} \big(D_{ij}(\mathbf{z},t) q^{(0)}(\mathbf{z},t) \big) \Big) q^{(1)}(\mathbf{z},t) +$$

$$\sum_{j=1}^{n} q^{(0)}(\mathbf{z},t) \frac{1}{2} D_{ij}(\mathbf{z},t) \frac{\partial}{\partial z_j} q^{(1)}(\mathbf{z},t) \Big] da_t = 0 \qquad (3-109)$$

The conditions (3-105) and (3-106) specify the initial and terminal conditions to be used for the forward and backward Chapman-Kolmogorov integro-differential equations, respectively.

The condition (3-107) signifies that the probability density for arriving at a boundary point $\mathbf{z}$ on the non-accessible boundary $\partial S_t^{(2)}$ from an internal point $\mathbf{x}$ in the domain S_{t_0} is zero for the finite transition times $t - t_0$. Similarly the condition (3-108) states that the transitions from a boundary point $\mathbf{z}$ at ∂S_t to an internal point $\mathbf{y}$ in S_{t_1} are zero for the finite transition times $t_1 - t$.

Due to these conditions the surface integral in (3-109) can be confined to the accessible part $\partial S_t^{(a)}$ of the boundary. (3-109) is the necessary condition which must be fulfilled by the forward and backward differential Chapman-Kolmogorov equations in combination, Nielsen and Iwankiewicz (1996). For example, (3-109) may be fulfilled by the forward equation on some part of $\partial S_t^{(a)}$ and by the backward equation on the remaining part.

Consider two sufficiently smooth functions $u(\mathbf{z})$ and $v(\mathbf{z})$ defined on S_t. If these functions in combination fulfil the boundary conditions (3-107), (3-108) and (3-109), it follows from the indicated derivation that

$$\int_{S_t} u(\mathbf{z})\mathcal{K}_{\mathbf{z},t}[v(\mathbf{z})]d\mathbf{z} = \int_{S_t} v(\mathbf{z})\mathcal{K}^T_{\mathbf{z},t}[u(\mathbf{z})]d\mathbf{z} \qquad (3-110)$$

This means that (3-107), (3-108) and (3-109) are the necessary conditions in order for $\mathcal{K}_{\mathbf{z},t}[\cdot]$ and $\mathcal{K}^T_{\mathbf{z},t}[\cdot]$ to be mutually adjoint operators.

$\partial S_t^{(a)}$ may be further divided into the entrance part, $\partial S_t^{(0)}$, and the exit part, $\partial S_t^{(1)}$, which in case of the indicated jump condition are defined in the same way as for diffusion processes, Fichera (1960)

$$\partial S_t^{(0)} = \Big\{\mathbf{z} \in \partial S_t^{(a)} \Big| \sum_{i=1}^{n} n_i(\mathbf{z},t)\Big(C_i(\mathbf{z},t) - \frac{1}{2}\frac{\partial}{\partial z_j}D_{ij}(\mathbf{z},t)\Big) < 0\Big\} \qquad (3-111)$$

$$\partial S_t^{(1)} = \Big\{\mathbf{z} \in \partial S_t^{(a)} \Big| \sum_{i=1}^{n} n_i(\mathbf{z},t)\Big(C_i(\mathbf{z},t) - \frac{1}{2}\frac{\partial}{\partial z_j}D_{ij}(\mathbf{z},t)\Big) > 0\Big\} \qquad (3-112)$$

(3-111) and (3-112) cover all $\partial S_t^{(a)}$ except at certain isolated points, where the probability current is tangential to the surface. Further, the boundary may be divided into the degenerated part, where $\sum_{i,j} D_{ij}(\mathbf{z},t)n_i(\mathbf{z},t)n_j(\mathbf{z},t) = 0$, and the non-degenerated part, where $\sum_{i,j} D_{ij}(\mathbf{z},t)n_i(\mathbf{z},t)n_j(\mathbf{z},t) \neq 0$, Fichera (1960). For the present dynamic system and the indicated jump condition, all accessible parts of the boundary are degenerated, and only the non-accessible parts can be non-degenerated.

For the system shown in fig. 3-2 the entrance part is $\partial S_t^{(0)} = \{(x,\dot{x})|(x = a \wedge \dot{x} > 0) \vee (x = b \wedge \dot{x} < 0)\}$ and the exit part is $\partial S_t^{(1)} = \{(x,\dot{x})|(x = a \wedge \dot{x} < 0) \vee (x = b \wedge \dot{x} > 0)\}$. The surface parts have been indicated in the figure along with the non-accessible part $\partial S_t^{(2)}$.

The unconditional probability density function of the state vector at the time t_0 becomes

$$f_{\{\mathbf{Z}\}}(\mathbf{z},t) = \int_{S_{t_0}} q_{\{\mathbf{Z}\}}(\mathbf{z},t|\mathbf{x},t_0) f_{\{\mathbf{Z}\}}(\mathbf{x},t_0) d\mathbf{x} \qquad (3-113)$$

Upon multiplying (3-94) by $f_{\{\mathbf{Z}\}}(\mathbf{x},t_0)$ and integrating over $\mathbf{x}$, this is seen also to be governed by the forward integro-differential Chapman-Kolmogorov equation

$$\frac{\partial}{\partial t} f_{\{\mathbf{Z}\}}(\mathbf{z},t) = \mathcal{K}_{\mathbf{z},t}\left[f_{\{\mathbf{Z}\}}(\mathbf{z},t)\right] \qquad (3-114)$$

The relevant initial condition is obtained applying (3-105) in (3-113)

$$f_{\mathbf{Z}}(\mathbf{z},t)\big|_{t=t_0} = f_{\mathbf{Z}}(\mathbf{z},t_0) \qquad (3-115)$$

3.2.1.1 Wiener process driven systems

Consider the system driven by an n_3-dimensional Wiener process $\{\mathbf{W}(t), t \in [t_0,\infty[\}$. The governing stochastic equation (3-61) reduces to the classical Itô's differential equation, Arnold (1974)

$$\left.\begin{aligned} &d\mathbf{Z}(t) = \mathbf{c}\big(\mathbf{Z}(t),t\big)dt + \mathbf{d}\big(\mathbf{Z}(t),t\big)d\mathbf{W}(t) \quad , \quad t \in]t_0,\infty[\\ &\mathbf{Z}(t_0) = \mathbf{Z}_0 \end{aligned}\right\} \qquad (3-116)$$

For this case the names Fokker-Planck-Kolmogorov and Kolmogorov backward operators are coined for the forward and backward differential Chapman-Kolmogorov operators. These become, cf. (3-95), (3-97)

$$\mathcal{K}_{\mathbf{z},t}\Big[q_{\{\mathbf{Z}\}}(\mathbf{z},t|\mathbf{x},t_0)\Big] = -\sum_{i=1}^{n} \frac{\partial}{\partial z_i}\Big(c_i(\mathbf{z},t) q_{\{\mathbf{Z}\}}(\mathbf{z},t|\mathbf{x},t_0)\Big) +$$

$$\frac{1}{2}\sum_{i=1}^{n}\sum_{j=1}^{n} \frac{\partial^2}{\partial z_i \partial z_j}\left(\sum_{\alpha=1}^{n_3} d_{i\alpha}(\mathbf{z},t) d_{j\alpha}(\mathbf{z},t) q_{\{\mathbf{Z}\}}(\mathbf{z},t|\mathbf{x},t_0)\right) \qquad (3-117)$$

$$\mathcal{K}^T_{\mathbf{z},t}\Big[q_{\{\mathbf{Z}\}}(\mathbf{y},t_1|\mathbf{z},t)\Big] = \sum_{i=1}^{n} c_i(\mathbf{z},t) \frac{\partial}{\partial z_i} q_{\{\mathbf{Z}\}}(\mathbf{y},t_1|\mathbf{z},t) +$$

$$\frac{1}{2}\sum_{i=1}^{n}\sum_{j=1}^{n}\left(\sum_{\alpha=1}^{n_3} d_{i\alpha}(\mathbf{z},t) d_{j\alpha}(\mathbf{z},t) \frac{\partial^2}{\partial z_i \partial z_j} q_{\{\mathbf{Z}\}}(\mathbf{y},t_1|\mathbf{z},t)\right) \qquad (3-118)$$

3.2.1.2 Compound Poisson process driven systems

Now consider the system driven only by an n_4-dimensional multivariate compound Poisson process, $\{\mathbf{V}(t),\, t \in [t_0, \infty[\}$. The governing stochastic equation (3-61) then reduces to the following stochastic differential equation

$$\left.\begin{aligned} d\mathbf{Z}(t) &= \mathbf{c}\big(\mathbf{Z}(t),t\big)dt + \mathbf{e}\big(\mathbf{Z}(t),t\big)d\mathbf{V}(t) \quad , \quad t \in]t_0, \infty[\\ \mathbf{Z}(t_0) &= \mathbf{Z}_0 \end{aligned}\right\} \qquad (3-119)$$

Using the jump probability intensity function for the component Poisson processes as given by (3-27) the jump probability intensity function of the dynamic system (3-93) becomes

$$J_{\{\mathbf{Z}\}}(\mathbf{z} \mid \mathbf{x}, t) = \sum_{\alpha=1}^{n_4} \nu_\alpha(t) \int_{\mathcal{P}_\alpha} \delta\Big(\mathbf{z} - \big(\mathbf{x} + \mathbf{e}_\alpha(\mathbf{x}, t)p_\alpha\big)\Big) f_{P_\alpha}(p_\alpha) dp_\alpha \qquad (3-120)$$

The forward integro-differential Chapman-Kolmogorov operators (3-95) and (3-99) become

$$\mathcal{K}_{\mathbf{z},t}\Big[q_{\{\mathbf{Z}\}}(\mathbf{z}, t|\mathbf{x}, t_0)\Big] = -\sum_{i=1}^{n} \frac{\partial}{\partial z_i}\Big(c_i(\mathbf{z}, t) q_{\{\mathbf{Z}\}}(\mathbf{z}, t|\mathbf{x}, t_0)\Big) +$$

$$\sum_{\alpha=1}^{n_4} \nu_\alpha(t) \int_{\mathcal{P}_\alpha} \Big(q_{\{\mathbf{Z}\}}(\mathbf{z} - \mathbf{e}_\alpha(t)p_\alpha, t|\mathbf{x}, t_0) - q_{\{\mathbf{Z}\}}(\mathbf{z}, t|\mathbf{x}, t_0)\Big) f_{P_\alpha}(p_\alpha) dp_\alpha \qquad (3-121)$$

$$\mathcal{K}_{\mathbf{z},t}\Big[q_{\{\mathbf{Z}\}}(\mathbf{z}, t|\mathbf{x}, t_0)\Big] = -\sum_{i=1}^{n} \frac{\partial}{\partial z_i}\Big(c_i(\mathbf{z}, t) q_{\{\mathbf{Z}\}}(\mathbf{z}, t|\mathbf{x}, t_0)\Big) +$$

$$\sum_{\alpha=1}^{n_4} \nu_\alpha(t) \int_{\mathcal{P}_\alpha} \left(\frac{q_{\{\mathbf{Z}\}}\big(\mathbf{a}_\alpha(\mathbf{z}, p_\alpha, t), t|\mathbf{x}, t_0\big)}{\left|\det\left(\mathbf{I} + \frac{\partial \mathbf{e}_\alpha\left(\mathbf{a}_\alpha(\mathbf{z}, p_\alpha, t), t\right)}{\partial \mathbf{y}^T} p_\alpha\right)\right|} - q_{\{\mathbf{Z}\}}(\mathbf{z}, t|\mathbf{x}, t_0) \right) f_{P_\alpha}(p_\alpha) dp_\alpha \qquad (3-122)$$

(3-122) was derived by Renger (1979) using a different approach than used here.

The backward integro-differential Chapman-Kolmogorov operator corresponding to (3-97) becomes

$$\mathcal{K}^T_{\mathbf{z},t}\Big[q_{\{\mathbf{Z}\}}(\mathbf{y}, t_1|\mathbf{z}, t)\Big] = \sum_{i=1}^{n} c_i(\mathbf{z}, t) \frac{\partial}{\partial z_i} q_{\{\mathbf{Z}\}}(\mathbf{y}, t_1|\mathbf{z}, t) +$$

$$+ \sum_{\alpha=1}^{n_4} \nu_\alpha(t) \int_{\mathcal{P}_\alpha} \Big(q_{\{\mathbf{Z}\}}(\mathbf{y}, t_1|\mathbf{z} + \mathbf{e}_\alpha(\mathbf{z}, t)p_\alpha, t) - q_{\{\mathbf{Z}\}}(\mathbf{y}, t_1|\mathbf{z}, t)\Big) f_{P_\alpha}(p_\alpha) dp_\alpha \qquad (3-123)$$

Alternatively, using a Taylor expansion of the function $q_{\{\mathbf{Z}\}}(\mathbf{z}-\mathbf{e}_\alpha(t)p_\alpha,t\mid\mathbf{x},t_0)$ and $q_{\{\mathbf{Z}\}}(\mathbf{y},t_1\mid\mathbf{z}+\mathbf{e}_\alpha(\mathbf{z},t)p_\alpha)$ the forward and backward integro-differential Chapman-Kolmogorov operators (3-121) and (3-123) are recast into a purely differential form with infinite sum of the partial derivatives. Thus

$$\mathcal{K}_{\mathbf{z},t}\left[q_{\{\mathbf{Z}\}}(\mathbf{z},t\mid\mathbf{x},t_0)\right]=-\sum_{i=1}^{n}\frac{\partial}{\partial z_i}\Big(c_i(\mathbf{z},t)q_{\{\mathbf{Z}\}}(\mathbf{z},t\mid\mathbf{x},t_0)\Big)+$$

$$\sum_{k=1}^{\infty}\frac{(-1)^k}{k!}\sum_{\alpha=1}^{n_4}\nu_\alpha(t)E\left[P_\alpha^k\right]\sum_{i_1,\ldots,i_k=1}^{n}e_{i_1\alpha}(\mathbf{z},t)\cdots e_{i_k\alpha}(\mathbf{z},t)\frac{\partial^k}{\partial z_{i_1}\cdots\partial z_{i_k}}q_{\{\mathbf{Z}\}}(\mathbf{z},t\mid\mathbf{x},t_0)\quad(3-124)$$

$$K^T_{\mathbf{z},t}\Big[q_{\{\mathbf{Z}\}}(\mathbf{y},t_1\mid\mathbf{z},t)\Big]=\sum_{i=1}^{n}c_i(\mathbf{z},t)\frac{\partial}{\partial z_i}q_{\{\mathbf{Z}\}}(\mathbf{y},t_1\mid\mathbf{z},t)+$$

$$\sum_{k=1}^{\infty}\frac{1}{k!}\sum_{\alpha=1}^{n_4}\nu_\alpha(t)E\left[P_\alpha^k\right]\sum_{i_1,\ldots,i_k=1}^{n}e_{i_1\alpha}(\mathbf{z},t)\cdots e_{i_k\alpha}(\mathbf{z},t)\frac{\partial^k}{\partial z_{i_1}\cdots\partial z_{i_k}}q_{\{\mathbf{Z}\}}(\mathbf{y},t_1\mid\mathbf{z},t)\quad(3-125)$$

(3-124) and (3-125) are valid if the expectations $E\left[P_\alpha^k\right]$ exist for all $\alpha=1,\ldots,n_4$ and $k=1,2,\ldots$. The expansion (3-124) is valid even for state dependence of the vector $\mathbf{e}_\alpha(\mathbf{z},t)$, as indicated. In physics (3-124) is known as the Kramer-Moyal expansion of the forward integro-differential Chapman-Kolmogorov operator, Gardiner (1985), Risken (1984).

3.2.1.3 α-stable Lévy motion driven systems

The stochastic equation governing the behaviour of the system driven by an α-stable Lévy motion is still given by (3-119) where $\{\mathbf{V}(t),t\in[t_0,\infty[\}$ now represents an n_4-dimensional vector of statistically independent components of α-stable Lévy motions $\{V_\alpha(t),t\in[t_0,\infty[\}$.

The jump probability intensity function $J_{\{\mathbf{Z}\}}(\mathbf{z}|\mathbf{x},t)$ of the state vector is then given by (3-93), where the jump probability intensity function $J_{\{V_\alpha\}}(p_\alpha,t)$ of the αth component process is given by (3-29), (3-30).

The forward integro-differential Chapman-Kolmogorov operator corresponding to (3-95) becomes

$$\mathcal{K}_{\mathbf{z},t}\left[q_{\{\mathbf{Z}\}}(\mathbf{z},t|\mathbf{x},t_0)\right]=-\sum_{i=1}^{n}\frac{\partial}{\partial z_i}\Big(c_i(\mathbf{z},t)q_{\{\mathbf{Z}\}}(\mathbf{z},t|\mathbf{x},t_0)\Big)+$$

$$\sum_{\alpha=1}^{n_4}\int_{\mathcal{P}_\alpha}\Big(q_{\{\mathbf{Z}\}}(\mathbf{z}-\mathbf{e}_\alpha(t)p_\alpha,t|\mathbf{x},t_0)-q_{\{\mathbf{Z}\}}(\mathbf{z},t|\mathbf{y},t_0)\Big)J_{\{V_\alpha\}}(p_\alpha,t)dp_\alpha\qquad(3-126)$$

The backward integro-differential Chapman-Kolmogorov operator corresponding to (3-97) becomes

$$\mathcal{K}^T_{\mathbf{z},t}\Big[q_{\{\mathbf{Z}\}}(\mathbf{y},t_1|\mathbf{z},t)\Big] = \sum_{i=1}^{n} c_i(\mathbf{z},t)\frac{\partial}{\partial z_i} q_{\{\mathbf{Z}\}}(\mathbf{y},t_1|\mathbf{z},t) + \sum_{\alpha=1}^{l} \int_{\mathcal{P}_\alpha} \Big(q_{\{\mathbf{Z}\}}(\mathbf{y},t_1|\mathbf{z}+\mathbf{e}_\alpha(\mathbf{z},t)p_\alpha,t) - q_{\{\mathbf{Z}\}}(\mathbf{y},t_1|\mathbf{z},t)\Big) J_{\{V_\alpha\}}(p_\alpha)dp_\alpha \qquad (3-127)$$

3.2.2 First-passage time problems

Consider a Markov system with the deterministic start in $\mathbf{x} \in S_{t_0}$. Transitions from this state to a later state $\mathbf{z}$ at the time t are governed by the forward integro-differential Chapman-Kolmogorov equation (3-94). The system can only leave the safe domain S_t through the exit part of the boundary $\partial S_t^{(1)}$, and re-enter in the safe domain through the entrance part $\partial S_t^{(0)}$. In the reliability problems one is concerned with sample curves which have not left the safe domain in a given interval $]t_0,t]$. Transitions from any point $\mathbf{x} \in S_{t_0}$ in the safe domain at the time t_0 to some point $\mathbf{z} \in \partial S_t^{(0)}$ on the entrance part of the boundary should then be prevented, corresponding to the boundary condition $q_{\{\mathbf{Z}\}}(\mathbf{z},t|\mathbf{x},t_0) = 0$. This implies that any realization at the point of re-entering the safe domain through the entrance part of the boundary is absorbed or extracted from the sample and all remaining sample curves have never left the safe domain up to the time t. $q_{\{\mathbf{Z}\}}(\mathbf{z},t|\mathbf{x},t_0)$ is then seen to fulfil the following boundary and initial value problem, cf. (3-94), (3-105)

$$\left.\begin{aligned} &\frac{\partial}{\partial t} q_{\{\mathbf{Z}\}}(\mathbf{z},t|\mathbf{x},t_0) = \mathcal{K}_{\mathbf{z},t}\big[q_{\{\mathbf{Z}\}}(\mathbf{z},t \mid \mathbf{x},t_0)\big] \ , \ \forall\, t \in]t_0,t_1] \ , \ \forall\, \mathbf{z} \in S_t \\ &q_{\{\mathbf{Z}\}}(\mathbf{z},t_0|\mathbf{x},t_0) = \delta(\mathbf{z}-\mathbf{x}) \ , \ \forall\, \mathbf{z} \in S_{t_0} \\ &q_{\{\mathbf{Z}\}}(\mathbf{z},t|\mathbf{x},t_0) = 0 \ , \ \forall\, t \in]t_0,t_1] \ , \ \mathbf{z} \in \partial S_t^{(0)} \cup \partial S_t^{(2)} \end{aligned}\right\} \qquad (3-128)$$

where $\mathcal{K}_{\mathbf{z},t}[\cdot]$ are the forward integro-differential Chapman-Kolmogorov operators (3-95) or (3-99). No boundary condition need to be formulated on the exit part of the boundary $\partial S_t^{(1)}$.

Knowing the solution of (3-128), the first-passage time distribution function, $F_{T_1}(t|\mathbf{x},t_0)$ on condition of a deterministic start in $\mathbf{x} \in S_{t_0}$ is given as

$$F_{T_1}(t|\mathbf{x},t_0) = 1 - \int_{S_t} q_{\{\mathbf{Z}\}}(\mathbf{z},t|\mathbf{x},t_0)d\mathbf{z} \qquad (3-129)$$

Let $f_{\{\mathbf{Z}\}}(\mathbf{x},t_0)$ be the 1st order probability density function of the state vector process $\{\mathbf{Z}(t), t \in [t_0,t_1]\}$ at the time t_0. The probability density function at the time t on

condition of being in the safe domain at the time t_0 is then given as

$$f_{\{\mathbf{Z}\}}(\mathbf{z},t|\mathcal{E}_{t_0}) = \frac{\int\limits_{S_{t_0}} q_{\{\mathbf{Z}\}}(\mathbf{z},t|\mathbf{x},t_0) f_{\{\mathbf{Z}\}}(\mathbf{x},t_0)d\mathbf{x}}{\int\limits_{S_{t_0}} f_{\{\mathbf{Z}\}}(\mathbf{x},t_0)d\mathbf{x}} \qquad (3-130)$$

Since $\mathcal{K}_{\mathbf{z},t}[\cdot]$ is a linear operator, it follows from (3-128) that $f_{\{\mathbf{Z}\}}(\mathbf{z},t|\mathcal{E}_{t_0})$ fulfils the boundary and initial value problem

$$\left.\begin{aligned} &\frac{\partial}{\partial t} f_{\{\mathbf{Z}\}}(\mathbf{z},t \mid \mathcal{E}_{t_0}) = \mathcal{K}_{\mathbf{z},t}[f_{\{\mathbf{Z}\}}(\mathbf{z},t \mid \mathcal{E}_{t_0})] \ , \ \forall t \in]t_0,t_1] \ , \ \forall \ \mathbf{z} \in S_t \\ &f_{\{\mathbf{Z}\}}(\mathbf{z},t_0 \mid \mathcal{E}_{t_0}) = \frac{f_{\{\mathbf{Z}\}}(\mathbf{z},t_0)}{\int\limits_{S_{t_0}} f_{\{\mathbf{Z}\}}(\mathbf{x},t_0)d\mathbf{x}} \ , \ \forall \ \mathbf{z} \in S_{t_0} \\ &f_{\{\mathbf{Z}\}}(\mathbf{z},t_0 \mid \mathcal{E}_{t_0}) = 0 \ , \ \forall \ t \in]t_0,t_1] \ , \ \mathbf{z} \in \partial S_t^{(0)} \cup \partial S_t^{(2)} \end{aligned}\right\} \qquad (3-131)$$

The first-passage time distribution function on condition of stochastic start at the time t_0 is then given as

$$F_{T_1}(t|\mathcal{E}_{t_0}) = 1 - \int\limits_{S_t} f_{\{\mathbf{Z}\}}(\mathbf{z},t \mid \mathcal{E}_{t_0})d\mathbf{z} \qquad (3-132)$$

Alternatively, the reliability problem can be formulated based on the backward integro-differential Chapman-Kolmogorov equation. In order to specify the boundary conditions for absorbtion of sample curves it is noticed that any state $\mathbf{z} \in \partial S_t^{(1)}$ on the exit part of the boundary inevitably leads to an outcrossing into the unsafe domain. Hence, it is not possible to have a state $\mathbf{z} \in \partial S_t^{(1)}$, and a state $\mathbf{y} \in S_{t_1}$ in the safe domain at the later time t_1, without performing one or more outcrossings into the unsafe domain in the intermediate interval $]t,t_1]$. Since one is interested in the sample curves, which remain in the safe domain throughout the interval $]t,t_1]$, transitions from $\mathbf{z} \in \partial S_t^{(1)}$ to $\mathbf{y} \in S_{t_1}$ should then be prevented. Hence, $q_{\{\mathbf{Z}\}}(\mathbf{y},t_1|\mathbf{z},t)$ should fulfil the following boundary and terminal value problem, cf. (3-96), (3-106)

$$\left.\begin{aligned} &\frac{\partial}{\partial t} q_{\{\mathbf{Z}\}}(\mathbf{y},t_1|\mathbf{z},t) + \mathcal{K}^T_{\mathbf{z},t}[q_{\{\mathbf{Z}\}}(\mathbf{y},t_1 \mid \mathbf{z},t)] = 0 \ , \ \forall t \in [t_0,t_1[\ , \ \forall \mathbf{z} \in S_t \\ &q_{\{\mathbf{Z}\}}(\mathbf{y},t_1|\mathbf{z},t_1) = \delta(\mathbf{z}-\mathbf{y}) \ , \ \forall \mathbf{z} \in S_{t_1} \\ &q_{\{\mathbf{Z}\}}(\mathbf{y},t_1|\mathbf{z},t) = 0 \ , \ \forall t \in]t_0,t_1[\ , \ \mathbf{z} \in \partial S_t^{(1)} \cup \partial S_t^{(2)} \end{aligned}\right\} \qquad (3-133)$$

where $\mathcal{K}^T_{\mathbf{z},t}[\cdot]$ is the backward integro-differential Chapman-Kolmogorov operator (3-97). No boundary condition need to be formulated on the entrance part of the

boundary $\partial S_t^{(0)}$. In combination the absorption boundary conditions in (3-128) and (3-133) fulfil the necessary boundary condition (3-109).

Upon inserting into (3-133), the first-passage time distribution function $F_T(t_1|\mathbf{z},t)$ at the time t_1 on condition of the deterministic start in $\mathbf{z} \in S_t$ as defined by (3-129) is seen to fulfil the following boundary and terminal value problem

$$\left.\begin{aligned} &\frac{\partial}{\partial t} F_{T_1}(t_1|\mathbf{z},t) + \mathcal{K}_{\mathbf{z},t}^T\left[F_{T_1}(t_1 \mid \mathbf{z},t)\right] = 0 \ , \ \forall t \in [t_0,t_1[\ , \ \forall \mathbf{z} \in S_t \\ &F_{T_1}(t_1|\mathbf{z},t_1) = 0 \ , \ \forall \mathbf{z} \in S_{t_1} \\ &F_{T_1}(t_1|\mathbf{z},t) = 1 \ , \ \forall t \in]t_0,t_1[\ , \ \mathbf{z} \in \partial S_t^{(1)} \cup \partial S_t^{(2)} \end{aligned}\right\} \qquad (3-134)$$

Assume that (3-134) is integrated backwards until the time $t = t_0$. From the obtained solution $F_{T_1}(t_1|\mathbf{z},t_0)$, the first-passage time probability distribution function at the time t_1 on condition of stochastic start at the time t_0 is then obtained as follows

$$F_{T_1}(t_1 \mid \mathcal{E}_{t_0}) = \frac{\int\limits_{S_{t_0}} F_{T_1}(t_1 \mid \mathbf{z},t_0) f_{\{\mathbf{Z}\}}(\mathbf{z},t_0) d\mathbf{z}}{\int\limits_{S_{t_0}} f_{\{\mathbf{Z}\}}(\mathbf{z},t_0) d\mathbf{z}} \qquad (3-135)$$

A significant facilitation is obtained, when the following stationarity conditions are fulfilled

$$q_{\{\mathbf{Z}\}}(\mathbf{y},t_1 \mid \mathbf{z},t) = q_{\{\mathbf{Z}\}}(\mathbf{y} \mid \mathbf{z},t_1 - t) \qquad (3-136)$$

$$S_t \equiv S \qquad \text{(time-invariant)} \qquad (3-137)$$

Equation (3-136) will be fulfilled, if the generating source processes $\{\mathbf{W}(t), t \in [t_0,t_1]\}$ and $\{\mathbf{V}(t), t \in [t_0,t_1]\}$ are stationary, and if the structural system is time invariant, i.e. if the drift vector and the diffusion matrices fulfil $\mathbf{c}\big(\mathbf{Z}(t),t\big) \equiv \mathbf{c}\big(\mathbf{Z}(t)\big)$, $\mathbf{d}\big(\mathbf{Z}(t),t\big) \equiv \mathbf{d}\big(\mathbf{Z}(t)\big)$ and $\mathbf{e}\big(\mathbf{Z}(t),t\big) \equiv \mathbf{e}\big(\mathbf{Z}(t)\big)$.

Then, the forward and backward integro-differential Chapman-Kolmogorov operators are not explicitly depending on time, i.e. $\mathcal{K}_{\mathbf{z},t}[\cdot] \equiv \mathcal{K}_{\mathbf{z}}[\cdot]$ and $\mathcal{K}_{\mathbf{z},t}^T[\cdot] \equiv \mathcal{K}_{\mathbf{z}}^T[\cdot]$. From (3-129) it follows that $F_{T_1}(t_1 \mid \mathbf{z},t) \equiv F_{T_1}(\tau \mid \mathbf{z})$, where $\tau = t_1 - t$ signifies the elapsed time interval. Equation (3-134) can then be reformulated in the following way

$$\left.\begin{aligned} &\frac{\partial}{\partial \tau} F_{T_1}(\tau \mid \mathbf{z}) - \mathcal{K}_{\mathbf{z}}^T\left[F_{T_1}(\tau \mid \mathbf{z})\right] = 0 \ , \ \forall \tau \in]0,\infty[\ , \ \forall \mathbf{z} \in S \\ &F_{T_1}(0 \mid \mathbf{z}) = 0 \ , \ \forall \mathbf{z} \in S \\ &F_{T_1}(\tau \mid \mathbf{z}) = 1 \ , \ \forall \tau \in]0,\infty[\ , \ \mathbf{z} \in \partial S^{(1)} \cup \partial S^{(2)} \end{aligned}\right\} \qquad (3-138)$$

(3-134) must be solved for each terminal time t_1 to get (3-135), whereas (3-138) only requires a single solution of the same initial and boundary problem to obtain all terminal

times. Finally, $F_{T_1}(t \mid \mathcal{E}_{t_0})$ can be obtained from the solution of (3-138) as follows, cf. (3-135)

$$F_{T_1}(t \mid \mathcal{E}_{t_0}) = \frac{\int\limits_S F_{T_1}(t - t_0 \mid \mathbf{z}) f_{\{\mathbf{Z}\}}(\mathbf{z}) d\mathbf{z}}{\int\limits_S f_{\{\mathbf{Z}\}}(\mathbf{z}) d\mathbf{z}} \qquad (3-139)$$

$F_{T_1}(\tau \mid \mathbf{z}), \tau = t - t_0$, as determined from (3-138) specifies the first-passage probability distribution function, in case of deterministic start in the state $\mathbf{Z}(t_0) = \mathbf{z} \in S$ at the time t_0. From (3-138) it follows that the Nth order moment of the first-passage time, $m_N(\mathbf{z}) = E\big[T_1^N \mid \mathbf{Z}(t_0) = \mathbf{z} \in S\big], N = 1, 2, \ldots$, can be obtained from the following recursive system of boundary value problems

$$\left.\begin{aligned} &N m_{N-1}(\mathbf{z}) + \mathcal{K}_{\mathbf{z}}^T\big[m_N(\mathbf{z})\big] = 0 \ , \ \forall \mathbf{z} \in S \ , \ N = 1, 2, \ldots \\ &m_N(\mathbf{z}) = 0 \ , \ \forall \mathbf{z} \in \partial S^{(1)} \cup \partial S^{(2)} \end{aligned}\right\} \qquad (3-140)$$

where $m_0(\mathbf{z}) \equiv 1$. The case $N = 1$ represents the classical Andronov-Pontriagin-Vitt equation. The general equation (3-140) is known as the generalized Andronov-Pontriagin-Vitt equation, Andronov, Pontriagin and Vitt (1933), Bolotin (1967).

The solution of (3-138) is given by the uniformly convergent series

$$F_{T_1}(\tau \mid \mathbf{z}) = 1 - \sum_{n=1}^{\infty} d_n e^{-\lambda_n \tau} \Phi^{(n)}(\mathbf{z}) \qquad (3-141)$$

$$d_n = \frac{\int\limits_S \Psi^{(n)}(\mathbf{z}) d\mathbf{z}}{\int\limits_S \Psi^{(n)}(\mathbf{z}) \Phi^{(n)}(\mathbf{z}) d\mathbf{z}} \qquad (3-142)$$

where $\Psi^{(n)}(\mathbf{z})$ and $\Phi^{(n)}(\mathbf{z})$ are the eigenfunctions of the forward and backward operators with the appropriate absorbing boundary conditions, and λ_n are the corresponding eigenvalues, which are all assumed to be simple. The indicated quantities are determined from the eigenvalue problems

$$\left.\begin{aligned} &\lambda_n \Psi^{(n)}(\mathbf{z}) + \mathcal{K}_{\mathbf{z}}\big[\Psi^{(n)}(\mathbf{z})\big] = 0 \ , \ \forall \mathbf{z} \in S \ , \ n = 1, 2, \ldots \\ &\Psi^{(n)}(\mathbf{z}) = 0 \ , \ \forall \mathbf{z} \in \partial S^{(0)} \cup \partial S^{(2)} \end{aligned}\right\} \qquad (3-143)$$

$$\left.\begin{aligned} &\lambda_n \Phi^{(n)}(\mathbf{z}) + \mathcal{K}_{\mathbf{z}}^T\big[\Phi^{(n)}(\mathbf{z})\big] = 0 \ , \ \forall \mathbf{z} \in S \ , \ n = 1, 2, \ldots \\ &\Phi^{(n)}(\mathbf{z}) = 0 \ , \ \forall \mathbf{z} \in \partial S^{(1)} \cup \partial S^{(2)} \end{aligned}\right\} \qquad (3-144)$$

The solutions $(\lambda_n, \Phi^{(n)})$ and $(\lambda_n, \Psi^{(n)})$ may be complex. If so, the said solutions appear as pairwise mutually complex conjugated. Above, the eigenspectrum has been assumed to be discrete. In the case of a continuous spectrum, (3-141) is replaced by

$$F_{T_1}(\tau \mid \mathbf{z}) = 1 - \int_0^\infty d(\lambda) e^{-\lambda\tau} \Phi(\mathbf{z}, \lambda) d\lambda \qquad (3-145)$$

From (3-139), (3-141) and (3-142) the following solution can be obtained for the probability density function and the probability distribution function of the first-passage time on condition of stationary start at t_0

$$f_{T_1}(t \mid \mathcal{E}_{t_0}) = \sum_{n=1}^{\infty} c_n e^{-\lambda_n (t-t_0)} \qquad (3-146)$$

$$F_{T_1}(t \mid \mathcal{E}_{t_0}) = 1 - \sum_{n=1}^{\infty} \frac{c_n}{\lambda_n} e^{-\lambda_n (t-t_0)} \qquad (3-147)$$

$$c_n = \lambda_n \frac{\int_S \Psi^{(n)}(\mathbf{z}) d\mathbf{z}}{\int_S \Psi^{(n)}(\mathbf{z}) \Phi^{(n)}(\mathbf{z}) d\mathbf{z}} \frac{\int_S \Phi^{(n)}(\mathbf{z}) f_{\{\mathbf{Z}\}}(\mathbf{z}) d\mathbf{z}}{\int_S f_{\{\mathbf{Z}\}}(\mathbf{z}) d\mathbf{z}} \qquad (3-148)$$

The numerical solution of the initial and boundary value problems (3-128), (3-131), (3-133), (3-134), (3-138), (3-140), as well as the eigenvalue problems (3-143), (3-144) primarily involves a discretization of the forward and backward integro-differential Chapman-Kolmogorov operators. This problem will be dealt with in sections 3.4 and 3.5.

In case of a discrete eigenspectrum it follows from (3-146) that $f_{T_1}(t|\mathcal{E}_{t_0}) \propto c_1 e^{-\lambda_1 (t-t_0)}$, i.e. the first-passage time probability density function has an asymptotic exponential decay as $t \to \infty$. The limiting decay rate, λ_1, forms the lowest eigenvalue of the forward and backward integro-differential Chapman-Kolmogorov operators with absorbing boundary condition. On the other hand, the existence of a limiting decay rate of $f_{T_1}(t|S_{t_0})$ is an indication of a discrete eigenspectrum as explained subsequent to (2-117).

Example 3-2: Single- and double barrier first-passage time problems for 1-dimensional Markov processes

Consider the non-linear SDOF oscillator (3-43) exposed to a Gaussian white noise with the auto-spectral density S_0, and assume that the inertial forces $m\ddot{X}$ are negligible compared to the other terms entering the equation. Further, it is assumed that $u(X, \dot{X}) = g(X)\dot{X} + k(X)X$. The stochastic equations of motion can then be written as the following Itô differential equation

$$\left.\begin{aligned} &dZ(t) = c(Z(t))dt + d(Z(t))dW(t) \ , \ Z(0) = x_0 \\ &Z(t) = X(t) \ , \ c(Z(t)) = -\frac{k(Z(t))}{g(Z(t))} Z(t) - \frac{\pi S_0}{m^2} \frac{\frac{d}{dz} g(Z(t))}{g^3((t))} \ , \ d(Z(t)) = -\frac{\sqrt{2\pi S_0}}{m g(Z(t))} \end{aligned}\right\} \qquad (3-149)$$

where $\{W(t), t \in [0,\infty[\}$ is a unit intensity Wiener process, and x_0 is the initial value. Above, the Gaussian white noise has been interpreted as the limit of a sequence of broad-banded Gaussian processes, for which the solution process fulfils a Stratonovich stochastic differential equation with drift- and diffusion functions $c(Z(t)) = -k(Z(t)Z(t)/g(Z(t))$ and $d(Z(t)) = -\sqrt{2\pi S_0}/(mg(Z(t)))$, Wong and Zakai (1965), Sobczyk (1991). The drift function for the equivalent Itô equation as indicated by (3-149) includes a correction term due to the state dependent diffusion function, Arnold (1974).

The drift and diffusion functions become, cf. (3-88), (3-89)

$$C(z) = c(z) \quad , \quad D(z) = d^2(z) \tag{3-150}$$

In the case of a double barrier first-passage time problem, (3-138) can be written

$$\left.\begin{aligned} &\frac{\partial}{\partial \tau} F_{T_1}(\tau \mid z) - C(z)\frac{\partial}{\partial z} F_{T_1}(\tau \mid z) - \frac{D(z)}{2}\frac{\partial^2}{\partial z^2} F_{T_1}(\tau \mid z) = 0 \ , \ \forall \tau \in]0,\infty[\ , \ \forall z \in]a,b[\\ &F_{T_1}(0 \mid z) = 0 \ , \ \forall z \in]a,b[\\ &F_{T_1}(\tau \mid z) = 1 \ , \ \forall \tau \in]0,\infty[\ , \ z = a \vee z = b \end{aligned}\right\} \tag{3-151}$$

and (3-143), (3-144) become

$$\left.\begin{aligned} &\lambda_n \Psi^{(n)}(z) - \frac{d}{dz}\left(C(z)\Psi^{(n)}(z)\right) + \frac{1}{2}\frac{d^2}{dz^2}\left(D(z)\Psi^{(n)}(z)\right) = 0 \ , \ z \in]a,b[\ , \ n = 1,2,\ldots \\ &\Psi^{(n)}(a) = \Psi^{(n)}(b) = 0 \end{aligned}\right\} \tag{3-152}$$

$$\left.\begin{aligned} &\lambda_n \Phi^{(n)}(z) + C(z)\frac{d}{dz}\Phi^{(n)}(z) + \frac{D(z)}{2}\frac{d^2}{dz^2}\Phi^{(n)}(z) = 0 \ , \ z \in]a,b[\ , \ n = 1,2,\ldots \\ &\Phi^{(n)}(a) = \Phi^{(n)}(b) = 0 \end{aligned}\right\} \tag{3-153}$$

The eigenvalues λ_n obtained from (3-152) and (3-153) will be well separated, i.e. the eigenspectrum is discrete. From the solution of (3-152), (3-153) the first-passage time probability distribution function on condition of deterministic start in $x_0 \in]a,b[$ becomes, cf. (3-141), (3-142)

$$F_{T_1}(t - t_0 \mid x_0) = 1 - \sum_{n=1}^{\infty} d_n \Phi^{(n)}(x_0) e^{-\lambda_n (t - t_0)} \tag{3-154}$$

$$d_n = \frac{\int_a^b \Psi^{(n)}(z)dz}{\int_a^b \Psi^{(n)}(z)\Phi^{(n)}(z)dz} \tag{3-155}$$

The single barrier problem is obtained as $a \to -\infty$. In this case it is observed that the separation of eigenvalues $\Delta\lambda_n = \lambda_{n+1} - \lambda_n$ approaches zero, i.e. a continuous eigenspectrum is obtained. Correspondingly, the discrete eigenvalue expansion (Fourier series expansion) is replaced by the continuous eigenvalue integral transform (Fourier transform) (3-145).

As an example, consider a linear SDOF oscillator, where also the linear elastic restoring forces are negligible $m2\zeta\omega_0|\dot{X}| >> m|\ddot{X}|$, $m2\zeta\omega_0|\dot{X}| >> m\omega_0^2|X|$. In this case $g(Z) = 2\zeta\omega_0$, $c(Z) = 0$, so (3-149) reduces to

$$dZ(t) = \frac{1}{m2\zeta\omega_0} dW(t) \ , \ Z(0) = x_0 \tag{3-156}$$

This case is the classical Brownian motion equation, studied by Einstein (1905). The drift and diffusion constants become, cf. (3-150)

$$C = 0 \ , \ D = \frac{2\pi S_0}{(m2\zeta\omega_0)^2} \tag{3-157}$$

The eigenvalues, eigenfunctions and expansion coefficients become, cf. (3-152), (3-153), (3-155)

$$\left.\begin{aligned} \lambda_n &= \left(\frac{n\pi}{b-a}\right)^2 \frac{D}{2} \\ \Phi^{(n)}(z) &= \Psi^{(n)}(z) = \sin\left(\sqrt{\frac{2\lambda_n}{D}}(b-z)\right) \\ d_n &= \frac{\int_a^b \Phi^{(n)}(z)dz}{\int_a^b (\Phi^{(n)}(z))^2 dz} = \frac{2}{n\pi}\left(1-(-1)^n\right) \end{aligned}\right\} \tag{3-158}$$

With initial start at $z = x_0$ the solution (3-154) becomes

$$F_{T_1}(t-t_0 \mid x_0) = 1 - \sum_{n=1}^{\infty} \frac{2}{n\pi}\left(1-(-1)^n\right) \sin\left(\sqrt{\frac{2\lambda_n}{D}}\left(b-x_0\right)\right) e^{-\lambda_n(t-t_0)} \tag{3-159}$$

The difference between the eigenvalues becomes

$$\Delta\lambda_n = \lambda_{n+1} - \lambda_n = \frac{2n+1}{(b-a)^2}\frac{\pi^2 D}{2} \tag{3-160}$$

For the single barrier problem, obtained as $a \to -\infty$, $\Delta\lambda_n$ approaches zero and the continuous eigenspectrum is obtained. Hence, the solution becomes, cf. (3-145)

$$F_{T_1}(t-t_0 \mid x_0) = 1 - \int_0^{\infty} d(\lambda) \sin\left(\sqrt{\frac{2\lambda}{D}}(b-x_0)\right) e^{-\lambda(t-t_0)} d\lambda \tag{3-161}$$

Applying the initial value $F_{T_1}(0|x_0) = 0$ one has

$$1 = \int_0^{\infty} d(\lambda) \sin\left(\sqrt{\frac{2\lambda}{D}}(b-x_0)\right) d\lambda \tag{3-162}$$

Multiplying by $\sin\left(\sqrt{\frac{2\mu}{D}}(b-x_0)\right)$ and integrating over $[0,\infty[$, $d(\lambda)$ is finally obtained as the following inverse sine Fourier transform

$$d(\lambda) = \frac{1}{\pi}\frac{1}{\lambda} \tag{3-163}$$

The solutions (3-161), (3-163) can next be shown to have the following closed form representation

$$F_{T_1}(t-t_0 \mid x_0) = 2 - 2\Phi\left(\frac{b-x_0}{\sqrt{D(t-t_0)}}\right) \tag{3-164}$$

The validity of (3-164) can alternatively be proved directly upon insertion into (3-151).

3.3 Moment equation methods

A jump of magnitude p_α in the αth component $V_\alpha(t)$ of the generating source process $\{\mathbf{V}(t), t \in [0,\infty[\}$ at the time t results in a jump of magnitude $d\mathbf{Z}(t) = \mathbf{e}_\alpha\big(\mathbf{Z}(t),t\big)p_\alpha$ of the state vector $\mathbf{Z}(t)$. Consider next an arbitrary sufficiently smooth function $f\big(\mathbf{Z}(t),t\big)$ of the state vector $\mathbf{Z}(t)$ and of the time t. A jump of magnitude $d\mathbf{Z}(t) = \mathbf{e}_\alpha\big(\mathbf{Z}(t),t\big)p_\alpha$ of the state vector implies a jump of magnitude $df\big(\mathbf{Z}(t),t\big) = f\big(\mathbf{Z}(t) + \mathbf{e}_\alpha(\mathbf{Z}(t),t)p_\alpha, t\big) - f\big(\mathbf{Z}(t),t\big)$ of the function f. The jumps to all contiguous intervals from all n_4 components can then be written as the following sum, Nielsen and Iwankiewicz (1996)

$$df\big(\mathbf{Z}(t),t\big) = \sum_{\alpha=1}^{n_4} \int_{\mathcal{P}_\alpha} \Big(f\big(\mathbf{Z}(t)+\mathbf{e}_\alpha(\mathbf{Z}(t),t)p_\alpha,t\big) - f\big(\mathbf{Z}(t),t\big)\Big) M_\alpha(dt,t,dp_\alpha,p_\alpha) \quad (3-165)$$

Making use of the fact that any increment during the infinitesimal time interval is the sum of the increments due to a continuous motion and due to a possible jump, one can then write

$$df\big(\mathbf{Z}(t),t\big) = f\big(\mathbf{Z}(t+dt),t+dt\big) - f\big(\mathbf{Z}(t),t\big) =$$

$$\frac{\partial f\big(\mathbf{Z}(t),t\big)}{\partial t}dt + \sum_{i=1}^{n} \frac{\partial f\big(\mathbf{Z}(t),t\big)}{\partial z_i}\Big(c_i\big(\mathbf{Z}(t),t\big)dt + \sum_{\alpha=1}^{n_3} d_{i\alpha}\big(\mathbf{Z}(t),t\big)dW_\alpha(t)\Big) +$$

$$\frac{1}{2}\sum_{i=1}^{n}\sum_{j=1}^{n}\left(\sum_{\alpha=1}^{n_3} d_{i\alpha}\big(\mathbf{Z}(t),t\big)d_{j\alpha}\big(\mathbf{Z}(t),t\big)\right)\frac{\partial^2 f\big(\mathbf{Z}(t),t\big)}{\partial z_i \partial z_j}dt +$$

$$\sum_{\alpha=1}^{n_4}\int_{\mathcal{P}_\alpha}\Big(f\big(\mathbf{Z}(t)+\mathbf{e}_\alpha(\mathbf{Z}(t),t)p_\alpha,t\big) - f\big(\mathbf{Z}(t),t\big)\Big)M_\alpha(dt,t,dp_\alpha,p_\alpha) \quad (3-166)$$

where (3-87), (3-116) have been used for the Wiener process driven part of the increment $d\mathbf{Z}(t)$. Equation (3-166) is the generalized Itô differential rule for the diffusion and jump excited systems.

Taking the expectation of both sides of (3-166) and using (3-26) the generating equation for moments the following is obtained

$$\frac{d}{dt}E\Big[f\big(\mathbf{Z}(t),t\big)\Big] = E\Big[\frac{\partial}{\partial t}f\big(\mathbf{Z}(t),t\big)\Big] + E\Big[\mathcal{K}^T_{\mathbf{z},t}\Big[f\big(\mathbf{Z}(t),t\big)\Big]\Big] \quad (3-167)$$

where $\mathcal{K}^T_{\mathbf{z},t}[\cdot]$ is the backward integro-differential Chapman-Kolmogorov operator, (3-97). Equation (3-167) can alternatively be derived as follows

$$\frac{d}{dt}E\Big[f(\mathbf{Z}(t),t)\Big] = E\Big[\frac{d}{dt}f(\mathbf{Z}(t),t)\Big] = \int\limits_{S_t} \frac{d}{dt}\Big(f(\mathbf{z},t)q_{\{\mathbf{Z}\}}(\mathbf{z},t \mid \mathbf{y},t_0)\Big)d\mathbf{z} =$$

$$E\Big[\frac{\partial}{\partial t}f(\mathbf{Z}(t),t)\Big] + \int\limits_{S_t} f(\mathbf{z},t)\mathcal{K}_{\mathbf{z},t}\big[q_{\{\mathbf{Z}\}}(\mathbf{z},t \mid \mathbf{y},t_0)\big]d\mathbf{z} =$$

$$E\Big[\frac{\partial}{\partial t}f(\mathbf{Z}(t),t)\Big] + \int\limits_{S_t} \mathcal{K}^T_{\mathbf{z},t}\big[f(\mathbf{z},t)\big]q_{\{\mathbf{Z}\}}(\mathbf{z},t \mid \mathbf{y},t_0)d\mathbf{z} =$$

$$E\Big[\frac{\partial}{\partial t}f(\mathbf{Z}(t),t)\Big] + E\Big[\mathcal{K}^T_{\mathbf{z},t}\big[f(\mathbf{Z}(t),t)\big]\Big] \qquad (3-168)$$

where the commutation of $\mathcal{K}_{\mathbf{z},t}[\cdot]$ and $\mathcal{K}^T_{\mathbf{z},t}[\cdot]$ as specified by (3-110) has been used. Hence, it has been implicitly assumed at the derivation of both (3-167) and (3-168) that either the entire boundary ∂S_t is non-accessible, i.e. $\partial S_t = \partial S_t^{(2)}$, or the jump condition (3-102) and the boundary condition (3-104) are fulfilled at the accessible boundary $\partial S_t^{(a)}$.

The zero time-lag joint statistical moments of the order k are defined as

$$\mu_{i_1\cdots i_k}(t) = E\Big[Z_{i_1}(t)\cdots Z_{i_k}(t)\Big] \qquad (3-169)$$

The corresponding zero time-lag joint central statistical moments of the order N are defined as

$$\lambda_{i_1\cdots i_k}(t) = E\big[Z^0_{i_1}(t)\cdots Z^0_{i_k}(t)\big] \qquad (3-170)$$

where

$$Z^0_i(t) = Z_i(t) - \mu_i(t) \qquad (3-171)$$

Differential equations for these quantities are obtained choosing $f\big(\mathbf{Z}(t),t\big) = Z_{i_1}(t)\cdots Z_{i_k}(t)$ and $f\big(\mathbf{Z}(t),t\big) = \big(Z_{i_1}(t) - \mu_{i_1}(t)\big)\cdots\big(Z_{i_N}(t) - \mu_{i_k}(t)\big)$, respectively in (3-167). Hence

$$\frac{d}{dt}\mu_{i_1\cdots i_k}(t) = E\Big[\mathcal{K}^T_{\mathbf{z},t}\Big[Z_{i_1}(t)\cdots Z_{i_k}(t)\Big]\Big] \quad , \quad k = 1,\ldots,N \qquad (3-172)$$

$$\frac{d}{dt}\lambda_{i_1\cdots i_k}(t) = E\left[\frac{\partial}{\partial t}\Big(\big(Z_{i_1}(t) - \mu_{i_1}(t)\big)\cdots\big(Z_{i_N}(t) - \mu_{i_k}(t)\big)\Big)\right] +$$

$$E\Big[\mathcal{K}^T_{\mathbf{z},t}\Big[\big(Z_{i_1}(t) - \mu_{i_1}(t)\big)\cdots\big(Z_{i_N}(t) - \mu_{i_k}(t)\big)\Big]\Big] \quad , \quad k = 2,\ldots,N \qquad (3-173)$$

These moment equations do not exist for α-stable Lévy motion driven processes. For compound Poisson process driven processes they only exist if the moment $E[P^N]$ of the order N of the mark variable exists.

Upon truncating of the hierarchy of moment equation at the order N, and taking all the symmetries into consideration, (3-172) contains totally $n + \frac{1}{2!}n(n+1) + \cdots + \frac{1}{N!}n$ $(n+1)\cdots(n+N-1) = \sum_{j=1}^{N} \binom{n-1+j}{n-1}$ differential equations. Consequently, these become increasingly difficult to handle as n or N become large. By numerical solution of the moment equations the tensor notation should be maintained through an indirect addressing of the various tensor components into a 1 dimensional array. Manual handling of these equations is only possible for low values of n and N.

3.3.1 Closure schemes for hierarchy of moment equations

A closure scheme simply means a procedure for evaluating the expectations on the right-hand sides of (3-172), (3-173) by means of a tentative joint probability density function $f_{\{\mathbf{Z}\}}(\mathbf{z},t)$ of the state vector $\mathbf{Z}(t) = \left[Z_1(t),\cdots,Z_n(t)\right]^T$, containing a number of free parameters, which are calibrated in a way that the joint pdf displays all the provided moments $\mu_{i_1\cdots i_n}(t)$ or $\lambda_{i_1\cdots i_n}(t)$ as determined by the hierarchy of moment equations (3-172) or (3-173). Consequently, the number of free parameters must be equal to the number of moment equations.

The joint nth variate characteristic and log-characteristic functions of the process $\mathbf{Z}(t)$ admit the following Taylor-expansions

$$M_{\{\mathbf{Z}\}}(\boldsymbol{\theta},t) = 1 + \sum_{k=1}^{\infty} \frac{i^k}{k!} \sum_{i_1,\cdots,i_k=1}^{n} \mu_{i_1 i_2\cdots i_k}(t)\theta_{i_1}\theta_{i_2}\cdots\theta_{i_k} \qquad (3-174)$$

$$\ln M_{\{\mathbf{Z}\}}(\boldsymbol{\theta},t) = \sum_{k=1}^{\infty} \frac{i^k}{k!} \sum_{i_1,\cdots,i_k=1}^{n} \kappa_{i_1 i_2\cdots i_k}(t)\theta_{i_1}\theta_{i_2}\cdots\theta_{i_k} \qquad (3-175)$$

where $\kappa_{i_1 i_2\cdots i_N}(t)$ signifies the joint cumulants of the order N. Comparing (3-174) with (3-175) the following relations between joint moments and joint cumulants are obtained

$$1 + \sum_{k=1}^{\infty} \frac{i^k}{k!} \sum_{i_1,\cdots,i_k}^{n} \mu_{i_1 i_2\cdots i_k}(t)\theta_{i_1}\theta_{i_2}\cdots\theta_{i_k} =$$

$$\exp\left(\sum_{k=1}^{\infty} \frac{i^k}{k!} \sum_{i_1,\cdots,i_k}^{n} \kappa_{i_1 i_2\cdots i_k}(t)\theta_{i_1}\theta_{i_2}\cdots\theta_{i_k}\right) \qquad (3-176)$$

$$\ln\left(1+\sum_{k=1}^{\infty} \frac{i^k}{k!} \sum_{i_1,\cdots,i_k}^{n} \mu_{i_1 i_2\cdots i_k}(t)\theta_{i_1}\theta_{i_2}\cdots\theta_{i_k}\right) = \sum_{k=1}^{\infty} \frac{i^k}{k!} \sum_{i_1,\cdots,i_k}^{n} \kappa_{i_1 i_2\cdots i_k}(t)\theta_{i_1}\theta_{i_2}\cdots\theta_{i_k}$$

$$(3-177)$$

Upon expanding the exponential in (3-176) and comparing terms of the common factor $\theta_{i_1}\theta_{i_2}\cdots\theta_{i_k}$ the joint moments $\mu_{i_1 i_2\cdots i_k}(t)$ may be expressed in terms of the joint cumulants $\kappa_{i_1 i_2\cdots i_k}(t)$. Similarly, upon expanding the logarithm in (3-177) as a Taylor series the inverse relation expressing the joint cumulants in terms of the joint moments is obtained. These take the form

$$\left.\begin{aligned}
&\kappa_i(t) = \mu_i(t)\\
&\kappa_{ij}(t) = \lambda_{ij}(t)\\
&\kappa_{ijk}(t) = \lambda_{ijk}(t)\\
&\kappa_{ijkl}(t) = \lambda_{ijkl}(t) - 3\left\{\lambda_{ij}(t)\lambda_{kl}(t)\right\}_s\\
&\kappa_{ijklm}(t) = \lambda_{ijklm}(t) - 10\left\{\lambda_{ij}(t)\lambda_{klm}(t)\right\}_s\\
&\kappa_{ijklmn}(t) = \lambda_{ijklmn}(t) - 15\left\{\lambda_{ij}(t)\lambda_{klmn}(t)\right\}_s - 10\left\{\lambda_{ijk}(t)\lambda_{lmn}(t)\right\}_s\\
&\quad + 30\left\{\lambda_{ij}(t)\lambda_{kl}(t)\lambda_{mn}(t)\right\}_s\\
&\vdots
\end{aligned}\right\} \quad (3-178)$$

where $\{\cdot\}_s$ indicates the symmetry operator defined by (2-69).

The so-called quasi-moments $\beta_{i_1 i_2\cdots i_N}(t)$ are introduced by the relation, Stratonovich (1963)

$$\exp\left(\sum_{k=3}^{\infty}\frac{i^k}{k!}\sum_{i_1,\ldots,i_k=1}^{n}\kappa_{i_1 i_2\cdots i_k}(t)\theta_{i_1}\theta_{i_2}\cdots\theta_{i_k}\right) = 1+\sum_{k=3}^{\infty}\frac{i^k}{k!}\sum_{i_1,\ldots,i_k}^{n}\beta_{i_1 i_2\cdots i_k}(t)\theta_{i_1}\theta_{i_2}\cdots\theta_{i_k} \quad (3-179)$$

Expanding the exponential of (3-179) as a Taylor series one can express the quasi-moments in terms of cumulants, i.e.

$$\left.\begin{aligned}
&\beta_{ijk}(t) = \kappa_{ijk}(t)\\
&\beta_{ijkl}(t) = \kappa_{ijkl}(t)\\
&\beta_{ijklm}(t) = \kappa_{ijklm}(t)\\
&\beta_{ijklmn}(t) = \kappa_{ijklmn}(t) + 10\left\{\kappa_{ijk}(t)\kappa_{lmn}(t)\right\}_s\\
&\beta_{ijklmnp}(t) = \kappa_{ijklmnp}(t) + 35\left\{\kappa_{ijk}(t)\kappa_{lmnp}(t)\right\}_s\\
&\beta_{ijklmnpq}(t) = \kappa_{ijklmnpq}(t) + 35\left\{\kappa_{ijkl}(t)\kappa_{mnpq}(t)\right\}_s + 56\left\{\kappa_{ijk}(t)\kappa_{lmnpq}(t)\right\}_s\\
&\vdots
\end{aligned}\right\} \quad (3-180)$$

The inverse relationships are obtained by taking the logarithm on both sides of (3-179) and expanding the logarithm on the right-hand side as a Taylor series.

The multivariate probability density function can be evaluated as an inverse Fourier transform of a characteristic function. Using (3-175), (3-179) one has, Stratonovich (1963)

$$f_{\{\mathbf{Z}\}}(\mathbf{z},t) = \int_{-\infty}^{\infty} \cdots \int_{-\infty}^{\infty} \exp\left(-i\sum_{l=1}^{n}\theta_l z_l\right) M_{\{\mathbf{Z}\}}(\boldsymbol{\theta},t)d\theta_1 d\theta_2 \cdots d\theta_n =$$

$$\int_{-\infty}^{\infty} \cdots \int_{-\infty}^{\infty} \exp\left(-i\sum_{l=1}^{n}\theta_l z_l\right) \exp\left(i\sum_{i_1=1}^{n}\kappa_{i_1}(t)\theta_{i_1} + \frac{i^2}{2}\sum_{i_1,i_2=1}^{n}\kappa_{i_1 i_2}(t)\theta_{i_1}\theta_{i_2}\right) \cdot$$

$$\left(1 + \sum_{k=3}^{\infty}\frac{i^k}{k!}\sum_{i_1,\cdots,i_k=1}^{n}\beta_{i_1 i_2 \cdots i_k}(t)\theta_{i_1}\theta_{i_2}\cdots\theta_{i_k}\right)d\theta_1 d\theta_2 \cdots d\theta_n =$$

$$f_{\{\mathbf{Z}\}}(\mathbf{z},t) = \varphi_n(\mathbf{z})\left(1 + \sum_{k=3}^{\infty}\frac{1}{k!}\sum_{i_1,\cdots,i_k=1}^{n}\beta_{i_1 i_2 \cdots i_k}(t)H_{i_1 i_2 \ldots i_k}(\mathbf{z})\right) \qquad (3-181)$$

where $H_{i_1 i_2 \ldots i_k}(\mathbf{z}) = H_{i_1 i_2 \ldots i_k}(\mathbf{z};\boldsymbol{\mu},\boldsymbol{\kappa})$ are the multivariate Hermite polynomials defined from

$$H_{i_1 i_2 \ldots i_k}(\mathbf{z};\boldsymbol{\mu},\boldsymbol{\kappa}) = \frac{(-1)^k}{\varphi_n(\mathbf{z};\boldsymbol{\mu},\boldsymbol{\kappa})}\frac{\partial^k}{\partial z_{i_1}\cdots\partial z_{i_k}}\varphi_n(\mathbf{z};\boldsymbol{\mu},\boldsymbol{\kappa}) \qquad (3-182)$$

and $\varphi_n(\mathbf{z}) = \varphi_n(\mathbf{z};\boldsymbol{\mu},\boldsymbol{\kappa})$ is the multivariate Gaussian joint probability density function with mean values $\mu_i = \kappa_i$ and covariances $\kappa_{ij} = \lambda_{ij}$.

The expansion of (3-181) in terms of multivariate Hermite polynomials will be referred to as a Gram-Charlier type A expansion.

$\beta_{i_1 i_2 \cdots i_k}(t)$ may alternatively be determined from the expectation

$$\beta_{i_1 i_2 \cdots i_k}(t) = k!E\left[G_{i_1 i_2 \cdots i_k}\left(\frac{Z_1^0}{\sigma_{Z_1}},\frac{Z_2^0}{\sigma_{Z_2}},\cdots,\frac{Z_n^0}{\sigma_{Z_n}}\right)\right] \qquad (3-183)$$

where $Z_i^0(t)$ is defined by (3-171) and $\sigma_{Z_i}(t)$ is the standard deviation function of the ith component process. $G_{i_1 i_2 \cdots i_k}(\mathbf{z}) = G_{i_1 i_2 \cdots i_k}(\mathbf{z};\boldsymbol{\mu},\boldsymbol{\kappa}) = H_{i_1 i_2 \cdots i_k}(\mathbf{z};\boldsymbol{\mu},\boldsymbol{\kappa}^{-1})$ is the multivariate adjoint Hermite polynomial, determined from

$$G_{i_1 \cdots i_k}(\mathbf{z};\boldsymbol{\mu},\boldsymbol{\kappa}) = \frac{(-1)^k}{\varphi_n(\mathbf{z};\boldsymbol{\mu},\boldsymbol{\kappa}^{-1})}\frac{\partial^k}{\partial z_{k_1}\cdots\partial z_{i_k}}\varphi_n(\mathbf{z};\boldsymbol{\mu},\boldsymbol{\kappa}^{-1}) \qquad (3-184)$$

where $\varphi_n(\mathbf{z};\boldsymbol{\mu},\boldsymbol{\kappa}^{-1})$ is the multivariate Gaussian joint probability density function evaluated for the inverse covariance matrix $\boldsymbol{\kappa}^{-1}$. It is easily demonstrated that the following orthonormality condition prevails

$$\int_{-\infty}^{\infty} \cdots \int_{-\infty}^{\infty} G_{i_1 \cdots i_r}(\mathbf{z};\boldsymbol{\mu},\boldsymbol{\kappa})H_{j_1 \cdots j_s}(\mathbf{z};\boldsymbol{\mu},\boldsymbol{\kappa})\varphi_n(\mathbf{z};\boldsymbol{\mu},\boldsymbol{\kappa})d\mathbf{z} =$$

$$\begin{cases} 0 & , \quad r \neq s \\ \delta_{i_1 j_1} \cdots \delta_{i_r j_r} & , \quad r = s \end{cases} \qquad (3-185)$$

where δ_{ij} signifies the Kronecker delta. (3-183) follows immediately using (3-185) in (3-181). Upon expanding the adjoint multivariate polynomial (3-183) provides a relation between the quasi-moment and the centralized moments $\lambda_{i_1 i_2 \cdots i_N}(t)$.

Alternatively, the tentative joint pdf can be written in terms of the following expansion in terms of products of univariate Hermite polynomials

$$f_{\mathbf{Z}}(\mathbf{z},t) = \frac{\varphi(\xi_1)\cdots\varphi(\xi_n)}{\sigma_{Z_1}(t)\cdots\sigma_{Z_n}(t)} \sum_{i_1+i_2+\cdots+i_n=0}^{\infty} \gamma_{i_1 i_2 \cdots i_n}(t) H_{i_1}(\xi_1)\cdots H_{i_n}(\xi_n) \qquad (3-186)$$

$$\xi_i = \frac{z_i - \mu_i(t)}{\sigma_{Z_i}(t)} \qquad (3-187)$$

$H_i(x)$ is the univariate Hermite polynomials of the ith order defined by

$$H_i(x) = \frac{(-1)^i}{\varphi(x)} \frac{d^i}{dx^i}\varphi(x) = \sum_{\alpha=0}^{[\frac{i}{2}]} (-1)^\alpha p_{i,\alpha} x^{i-2\alpha} \quad , \quad p_{i,\alpha} = \frac{i!\, 2^{-\alpha}}{\alpha!\,(i-2\alpha)!} \qquad (3-188)$$

$$\gamma_{i_1 i_2 \cdots i_n}(t) = \frac{1}{i_1! i_2! \cdots i_n!} E\left[H_{i_1}\left(\frac{Z^0_{i_1}}{\sigma_{Z_{i_1}}}\right) H_{i_2}\left(\frac{Z^0_{i_2}}{\sigma_{Z_{i_2}}}\right) \cdots H_{i_n}\left(\frac{Z^0_{i_n}}{\sigma_{Z_{i_n}}}\right)\right] =$$

$$\frac{1}{i_1! \cdots i_n!} \sum_{\alpha_1=0}^{[\frac{i_1}{2}]} \cdots \sum_{\alpha_n=0}^{[\frac{i_n}{2}]} (-1)^{\alpha_1+\cdots+\alpha_n} p_{i_1,\alpha_1} \cdots p_{i_n,\alpha_n} \frac{E\left[\left(Z^0_{i_1}(t)\right)^{i_1-2\alpha_1} \cdots \left(Z^0_{i_n}(t)\right)^{i_n-2\alpha_n} \right]}{\sigma^{i_1-2\alpha_1}_{Z_{i_1}}(t) \cdots \sigma^{i_k-2\alpha_n}_{Z_{i_n}}(t)} \qquad (3-189)$$

where $[\cdot]$ signifies the integer part of the argument. The 1st statement of (3-189) follows from the orthogonality property of the Hermite polynomials

$$\int_{-\infty}^{\infty} H_i(x) H_j(x) \varphi(x) dx = \begin{cases} 0 & , \quad i \neq j \\ i! & , \quad i = j \end{cases} \qquad (3-190)$$

$\gamma_{i_1 i_2 \cdots i_N}(t)$ are termed the Hermite moments. Since, $H_0(x) = 1$, $H_1(x) = x$ and $H_2(x) = x^2 - 1$ one sees that $\gamma_{00\cdots0} = 1$, $\gamma_{10\cdots0} = \gamma_{01\cdots0} = \gamma_{00\cdots1} = 0$, $\gamma_{20\cdots0} = \gamma_{02\cdots0} = \gamma_{00\cdots2} = 0$. The last statement of (3-189) provides an explicit relation between the remaining non-linear Hermite moments and the joint centralized moments $\lambda_{i_1 i_2 \cdots i_N}(t)$.

(3-174), (3-175), (3-181) and (3-186) represent various expansions of the joint characteristic function and the joint probability density function. The free parameters of these expansions are the joint moments $\mu_{i_1\cdots i_N}(t)$, the joint cumulants $\kappa_{i_1\cdots i_N}(t)$, the joint quasi-moments including the mean values $\mu_i(t)$ and the covariances $\kappa_{ij}(t)$, and the Hermite moments $\gamma_{i_1\cdots i_N}(t)$, respectively. Closure schemes are obtained upon truncating any of these expansions at the order $k = N$ and calibrate the free parameters by the relations derived above to the provided joint moment $\mu_{i_1\cdots i_k}(t)$ or $\lambda_{i_1\cdots i_k}(t)$, $k = 1, \ldots, N$, obtained from the solution of (3-172) or (3-173).

In case the hierarchy of moment equation (3-172), (3-173) are truncated at the order N, moment neglect closure simply means that all joint moments above the order N are ignored in (3-174). Hence, the following characteristic function of the tentative joint pdf is obtained.

$$M_{\{\mathbf{Z}\}}(\boldsymbol{\theta}, t) = 1 + \sum_{k=1}^{N} \frac{i^k}{k!} \sum_{i_1,\ldots,i_k=1}^{n} \mu_{i_1 i_2 \cdots i_k}(t)\theta_{i_1}\theta_{i_2}\cdots\theta_{i_k} \qquad (3-191)$$

In case of polynomial drift vectors unprovided moments of the order $\mu_{i_1\cdots i_{N+1}}(t)$, $\mu_{i_1\cdots i_{N+2}}(t)\cdots$, occur on the right-hand side of (3-172) in case the hierarchy of moment equations is truncated at the order N. Moment neglect closure involves that these moments are simply ignored. Normally, such an approach leads to poor results and bad numerical stability of the differential system.

Cumulant neglect closure means that all joint cumulants above the order N are ignored in (3-175). Hence, the following log-characteristic function of the tentative joint pdf is obtained

$$\ln M_{\{\mathbf{Z}\}}(\boldsymbol{\theta}, t) = \sum_{k=1}^{N} \frac{i^k}{k!} \sum_{i_1,\ldots,i_k=1}^{n} \kappa_{i_1 i_2 \cdots i_k}(t)\theta_{i_1}\theta_{i_2}\cdots\theta_{i_k} \qquad (3-192)$$

As mentioned subsequent to (2-160), the theorem by Marcienkiewicz (1939) raises serious theoretical objection against the truncation (3-192) for $N > 2$. This means that the moments evaluated by means of the joint pdf originating from (3-192) cannot be exact for any stochastic process.

In case of closure of the hierarchy of moment equations at the order N for systems with polynomial drift vectors, explicit expressions for the unprovided joint central moments $\gamma_{i_1\cdots i_{N+1}}(t)$, $\lambda_{i_1\cdots i_{N+1}}(t), \ldots$ can be derived from the conditions $\kappa_{i_1\cdots i_{N+1}}(t) = 0$, $\kappa_{i_1\cdots i_{N+1}}(t) = 0, \ldots$ From (3-178) the following expressions are obtained for $N = 4$

$$\left.\begin{aligned}
&\lambda_{ijklm}(t) = 10\,\{\lambda_{ij}(t)\lambda_{klm}(t)\}_s \\
&\lambda_{ijklmn}(t) = 15\,\{\lambda_{ij}(t)\lambda_{klmn}(t)\}_s + 10\,\{\lambda_{ijk}(t)\lambda_{lmn}(t)\}_s - 30\,\{\lambda_{ij}(t)\lambda_{kl}(t)\lambda_{mn}(t)\}_s \\
&\vdots
\end{aligned}\right\} \qquad (3-193)$$

The lowest-order cumulant neglect closure, obtained by neglecting the cumulants of orders higher than two, is the so-called Gaussian closure. Then the hierarchy of moment equations is truncated at second-order moments.

Quasi-moment neglect closure means that all joint quasi-moments above the order N are ignored in (3-181). In this case the following tentative joint pdf is obtained

$$f_{\{\mathbf{z}\}}(\mathbf{z},t) = \varphi_n(\mathbf{z})\Big\{1 + \sum_{k=3}^{N} \frac{1}{k!} \sum_{i_1,\dots i_k=1}^{n} \beta_{i_1 i_2 \cdots i_k}(t) H_{i_1 i_2 \dots i_k}(\mathbf{z})\Big\} \qquad (3-194)$$

In case of polynomial drift vectors, explicit expressions for the unprovided joint central moments $\lambda_{i_1 \cdots i_{N+1}}(t)$, $\lambda_{i_1 \cdots i_{N+2}}(t), \cdots$ can be derived from the conditions $\beta_{i_1 \cdots i_{N+1}}(t) = 0$, $\beta_{i_1 \cdots i_{N+2}}(t) = 0, \dots$ for the corresponding quasi-moments. For $N = 4$ it follows from (3-178), (3-180) the joint central moments of the order 5, 6, ... that

$$\left.\begin{aligned} 0 &= \kappa_{ijklm}(t) = \lambda_{ijklm}(t) - 10\{\lambda_{ij}(t)\lambda_{klm}(t)\}_s \\ 0 &= \kappa_{ijklmn}(t) + 10\{\kappa_{ijk}(t)\kappa_{lmn}\}_s = \\ &\lambda_{ijklmn}(t) - 15\{\lambda_{ij}(t)\lambda_{klmn}(t)\}_s + 30\{\lambda_{ij}(t)\lambda_{kl}(t)\lambda_{mn}(t)\}_s \\ &\vdots \end{aligned}\right\} \Rightarrow$$

$$\left.\begin{aligned} \lambda_{ijklm}(t) &= 10\{\lambda_{ij}(t)\lambda_{klm}(t)\}_s \\ \lambda_{ijklmn}(t) &= 15\{\lambda_{ij}(t)\lambda_{klmn}(t)\}_s - 30\{\lambda_{ij}(t)\lambda_{kl}(t)\lambda_{mn}(t)\}_s \\ &\vdots \end{aligned}\right\} \qquad (3-195)$$

As seen the expressions for $\lambda_{ijklmn}(t)$ in (3-193) and (3-195) differ by the term involving 3rd order moments.

Hermite moment neglect closure means that all joint Hermite moments above the order N are ignored in (3-186). Hence, the following tentative joint pdf is obtained

$$f(\mathbf{z},t) = \frac{\varphi(\xi_1)\cdots\varphi(\xi_n)}{\sigma_{Z_1}(t)\cdots\sigma_{Z_n}(t)} \sum_{i_1+i_2+\cdots+i_n=0}^{N} \gamma_{i_1 i_2 \cdots i_n}(t) H_{i_1}(\xi_1)\cdots H_{i_n}(\xi_n) \qquad (3-196)$$

In case of polynomial drift vectors, explicit expressions for the unprovided joint central moments $\lambda_{i_1 \cdots i_{N+1}}(t)$, $\lambda_{i_1 \cdots i_{N+1}}(t), \dots$ can be derived by means of (3-189) from the conditions $\gamma_{i_1 i_2 \cdots i_n}(t) = 0$, $i_1 + i_2 + \cdots + i_n = N+1,\ N+2, \dots$

The indicated closure schemes (save the moment neglect closure) all work well if the joint pdf is almost Gaussian, i.e. of the monomodal and smooth type. Then the joint cumulants above the 2nd order are relatively small, so the expansion (3-175) is supposed to converge rapidly with k. Simularly, the Gram-Charlier type A expansions (3-181)

and (3-186) can be seen as expansions around basic Gaussian distributions. Hence, the joint quasi-moments and joint Hermite moments are relatively small in case of almost Gaussian distributions, and rapid convergence of these series is expected as assumed in the closure schemes. However, joint pdfs of the multimode type or the mixed continuous discrete type do arise in numerous cases in stochastic dynamics. Well-known examples are the so-called two-well potential problem, arising in globally stable postbuckling vibrations of systems with cubic non-linearities, SDOF hysteretic oscillators and Poisson driven systems with low pulse arrival rate. If the indicated closure schemes are applied in such cases with significant deviation from Gaussianity, the resulting moment equations may turn out to give inaccurate results even at relatively high order of closure N (say $N \geq 6$) or may even become unstable, so no solution at all can be obtained. Rather than merely increase the order N in these cases it may be more favourable to modify the tentative joint pdf (i.e. the closure scheme) in a way that it has the degree-of-freedom of modelling such anomalies. Such modified closure schemes will briefly be presented below.

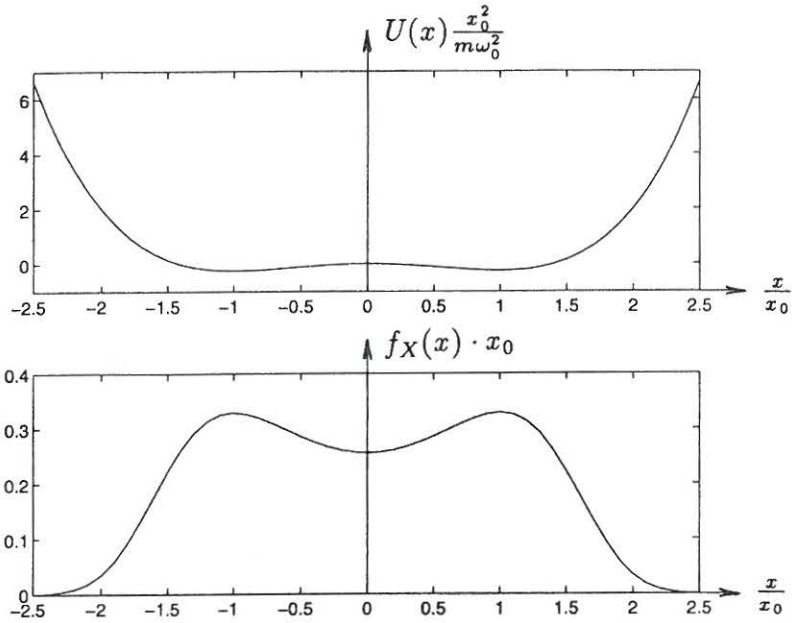

Fig. 3-11: Two-well problem, $x_0 = \sqrt{\frac{1}{\varepsilon}}$. a) Potential function. b) Stationary marginal probability density function of displacement, white noise excitation, $\frac{2\zeta\omega_0^3 m^2}{\pi S_0} \cdot x_0^2 = 1$.

The classical two-well problem deals with the Duffing oscillator in case of post-buckling vibrations with hardening non-linearities. The functions $u\big(X(t), \dot{X}(t)\big)$ in (3-43) can then be written, cf. (3-44),

$$u\big(X(t), \dot{X}(t)\big) = 2\zeta\omega_0\dot{X}(t) - \omega_0^2\big(1 - \varepsilon X^2(t)\big)X(t)\ ,\ \omega_0^2 > 0\ ,\ \varepsilon > 0 \qquad (3-197)$$

The non-dimensional potential energy function $U(x)\frac{x_0^2}{\omega_0^2}$, where $x_0 = \sqrt{\frac{1}{\varepsilon}}$ is the equilibrium distance, has been shown in fig. 3-11 along with the stationary marginal pdf

of $X(t)$ in case of Gaussian white noise excitation. In this case the following tentative joint pdf of $X(t)$ and $\dot{X}(t)$ is appropriate.

$$f_{X\dot{X}}(x,\dot{x},t) = \frac{1}{2}\Big(f_{V\dot{X}}(x+x_0,\dot{x},t) + f_{V\dot{X}}(-x+x_0,-\dot{x},t)\Big) \qquad (3-198)$$

$f_{V\dot{X}}(v,\dot{x},t)$ is a temporarily unknown joint pdf of $\dot{X}(t)$ and the auxiliary variable $V(t)$, which is assumed to be monomodal with the mode value at $(v,\dot{x}) = (0,0)$. Then, the mode values of (3-198) will be close to $x = \pm x_0$, if $f_{V\dot{X}}(\pm 2x_0,\dot{x},t) \simeq 0$. As seen the setting (3-198) ensures that the stationary joint pdf fulfils $f_{X\dot{X}}(x,\dot{x},t) = f_{X\dot{X}}(-x,-\dot{x},t)$, which is caused by the anti-symmetry of the drift vector $\mathbf{c}\big(\mathbf{Z}(t)\big) = -\mathbf{c}\big(-\mathbf{Z}(t)\big)$ in combination with zero initial conditions, cf. (3-46), (3-197). Joint moments of $X(t)$ and $\dot{X}(t)$ are related to joint moments of $V(t)$ and $\dot{X}(t)$ as follows

$$E\big[X^m(t)\dot{X}^n(t)\big] = \frac{1}{2}\big(1+(-1)^{m+n}\big)E\big[\big(V(t)-x_0\big)^m\dot{X}^n(t)\big] =$$

$$\frac{1}{2}\big(1+(-1)^{m+n}\big)\sum_{j=0}^{m}\binom{m}{j}(-x_0)^{m-j}E\big[V^j(t)\dot{X}^n(t)\big] \qquad (3-199)$$

The joint moments $\big[V^j(t)\dot{X}^n(t)\big]$, $j+n \le N$, can all be expressed in terms of the provided joint moments $E\big[X^m(t)\dot{X}^n(t)\big]$, $m+n \le N$, upon solving the linear equations (3-199). For $m+n = N+1, N+2,\ldots$ joint moments $E\big[V^j(t),\dot{X}^n(t)\big]$, $j+n = N+1, N+2,\cdots$ appear on the right-hand side. However, since $f_{V\dot{X}}(v,\dot{x},t)$ is assumed to be almost Gaussian these moments can be expressed in terms of lower order joint moments $E\big[V^j(t)\dot{X}^n(t)\big]$, $j+n \le N$ by means of a cumulant neglect closure scheme and hence by the provided joint moments $E\big[X^m(t)\dot{X}^n(t)\big]$, $m+n \le N$. A modified cumulant neglect closure scheme has then been formulated for the evaluation of the unprovided joint moments $E\big[X^m(t)\dot{X}^n(t)\big]$, $m+n = N+1, N+2,\ldots$

For $N = 2,4$ the following equations can be derived for the stationary variance $\sigma^2_{X,0}$ in case of ordinary cumulant neglect closure, Köylüoğlu and Nielsen (1996)

$$\left.\begin{aligned} &\frac{\pi S_0}{2\zeta\omega_0^3 m^2} + \sigma^2_{X,0} - \frac{3}{x_0^2}\sigma^4_{X,0} = 0 \\ &\frac{\pi S_0}{2\zeta\omega_0^3 m^2} + \sigma^2_{X,0} - \frac{1}{x_0^2}\left(\frac{30\sigma^6_{X,0} + 3\frac{\pi S_0}{2\zeta\omega_0^3 m^2}x_0^2\sigma^2_{X,0}}{15\sigma^2_{X,0} - x_0^2}\right) = 0 \end{aligned}\right\} \qquad (3-200)$$

These equations represent quadratic and cubic equations in $\sigma^2_{X,0}$, respectively. The 1st equation provides the identical solution as obtained by the Gaussian closure. The corresponding results for modified cumulant closure at the order $N = 2$ and 4, obtained by the procedure explained above, read

$$\left.\begin{aligned} &2x_0^2 + \frac{\pi S_0}{2\zeta\omega_0^3 m^2} + \sigma_{X,0}^2 - \frac{3}{x_0^2}\sigma_{X,0}^4 = 0 \\ &\frac{\pi S_0}{2\zeta\omega_0^3 m^2} + \sigma_{X,0}^2 - \frac{1}{x_0^2}\left(\frac{-16x_0^6 + 30\sigma_{X,0}^6 + 3\frac{\pi S_0}{2\zeta\omega_0^3 m^2} x_0^2 \sigma_{X,0}^2}{15\sigma_{X,0}^2 - x_0^2}\right) = 0 \end{aligned}\right\} \qquad (3-201)$$

For $N = 2$ the result (3-201) is tantamount to assuming $V(t) \sim N(0, \sigma_V^2)$, $\sigma_V^2 = \sigma_{X,0}^2 - x_0^2$. As shown in example 3-7 below, even the case $N = 2$ improves the results significantly compared to the exact result.

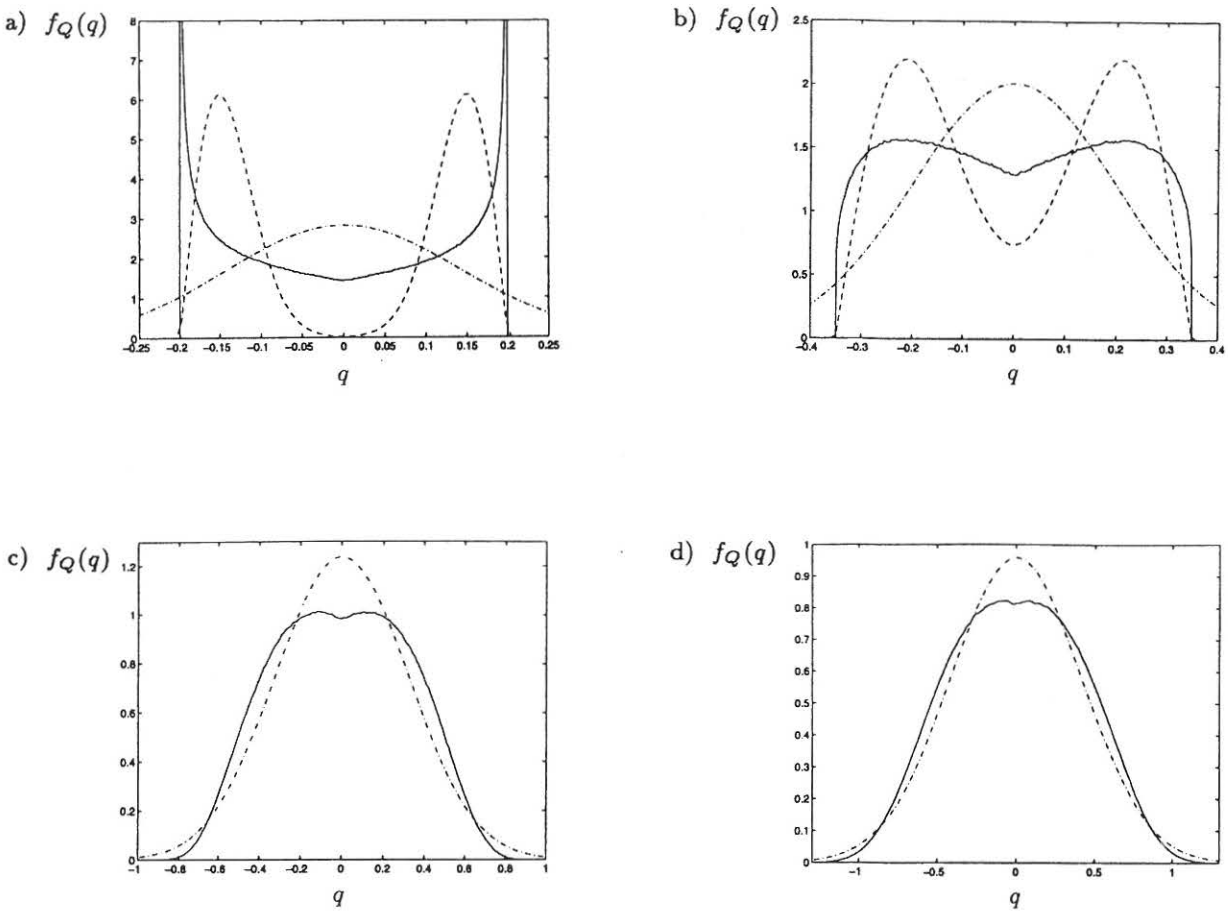

Fig. 3-12: Stationary probability density function of hysteretic component in Bouc-Wen hysteresis and equivalent replacement at closure at the order $N = 4$, $\omega_0 = 1$, $\zeta = 0.01$, $\alpha = 0.05$, $\beta = \gamma = 0.5$, $n = 1.0$, $\sigma_{X,0}^2 = \frac{\pi S_0}{2\zeta\omega_0^3 m^2} = 1$, ergodic sampling after 300000 T_0. a) $q_y = 0.20$. b) $q_y = 0.35$. c) $q_y = 1.00$. d) $q_y = 2.00$.

Fig. 3-12 shows with unbroken line the marginal pdf $f_Q(q)$ of the hysteretic component $Q(t)$ for the Bouc-Wen oscillator (3-49), (3-51) for variable values of the yield level q_y, exposed to stationary Gaussian white noise at an intensity producing the stationary variance $\sigma^2_{X,0} = \frac{\pi S_0}{2\zeta\omega_0^3 m^2} = 1$ of the corresponding linear oscillator. The results have been obtained by ergodic sampling with the sampling interval $300000T_0$, $T_0 = \frac{2\pi}{\omega_0}$. As seen, the marginal pdf has a marked double peak appearance, noticeable even at the relatively high yield level of $q_y = 2\sigma_{X,0}$. Consequently, a modification of the closure scheme along the same line as specified for the two-well potential problem should be applied. However, a substantial difference between the two problems appears, since the modal value q_0 of $f_Q(q)$ is not known in advance, but has to estimated from the available moment equations.

The following tentative joint pdf of the state variables $X(t)$, $\dot{X}(t)$ and $Q(t)$ will be applied

$$f_{X\dot{X}Q}(x,\dot{x},q,t) = \frac{1}{2}\Big(f_{X\dot{X}V}(x,\dot{x},q,t) + f_{X\dot{X}V}(-x,-\dot{x},-q,t)\Big) \qquad (3-202)$$

where the marginal pdf $f_V(v)$ of the auxiliary variable $V(t)$ is assumed to have its modal value in the vicinity of $v = q_0$. Further, $f_V(v)$ is assumed to be effectively equal to zero outside the interval $[-q_y, q_y]$. (3-202) insures the symmetry property $f_{X\dot{X}Q}(x,\dot{x},q,t) = f_{X\dot{X}Q}(-x,-\dot{x},-q,t)$, as caused by the anti-symmetric drift-vector in (3-49) with zero initial conditions. Similar to (3-199) the following expectations of combined stochastic variables, $h\big(X(t),\dot{X}(t),Q(t)\big)$ and $X^l(t)\dot{X}^m(t)Q^n(t)$ can be formulated

$$E\Big[h\big(X(t),\dot{X}(t),Q(t)\big)\Big] = \frac{1}{2}\Big(h\big(X(t),\dot{X}(t),V(t)\big)+h\big(-X(t),-\dot{X}(t),-V(t)\big)\Big) \qquad (3-203)$$

$$E\big[X^l(t)\dot{X}^m(t)Q^n(t)\big] = \frac{1}{2}\Big(1+(-1)^{l+m+n}\Big)E\big[X^l(t)\dot{X}^m(t)V^n(t)\big] \qquad (3-204)$$

The auxiliary joint distribution $f_{X\dot{X}V}(x,\dot{x},v,t)$ is assumed to be monomodal, for which reason the following Gram-Charlier type A expansion may be stated, cf. (3-196)

$$f_{X\dot{X}V}(x,\dot{x},v,t) = \frac{\varphi(\xi_1)\varphi(\xi_2)}{\sigma_X(t)\sigma_{\dot{X}}(t)}\, f_V(v) \sum_{i_1+i_2+i_3=0}^{N} \gamma_{i_1 i_2 i_3}(t) H_{i_1}(\xi_1) H_{i_2}(\xi_2) V_{i_3}(v) \qquad (3-205)$$

$$\xi_{i_1} = \frac{x}{\sigma_X(t)} \quad , \quad \xi_{i_2} = \frac{\dot{x}}{\sigma_{\dot{X}}(t)} \qquad (3-206)$$

$$V_i(v) = \sum_{\alpha=0}^{i} v_{i,\alpha} v^\alpha \qquad (3-207)$$

As seen from (3-187) and (3-206), (3-205) has the prerequisite that $E[X(t)] = E[\dot{X}(t)] \equiv 0$. $H_i(\xi)$ are the Hermite polynomials as given by (3-188) and $V_i(v)$ signifies the orthonormal polynomials of the distribution $f_V(v)$, fulfilling

$$\int_{-\infty}^{\infty} V_{i_1}(v)V_{i_2}(v)f_V(v)dv = \delta_{i_1 i_2} \qquad (3-208)$$

Insertion of(3-207) into (3-208) provides the following equations for the determination of the coefficients of the polynomials (3-207)

$$\sum_{\alpha_1=0}^{i_1}\sum_{\alpha_2=0}^{i_2} v_{i_1,\alpha_1}v_{i_2,\alpha_2}E\left[V^{\alpha_1+\alpha_2}\right] = \delta_{i_1 i_2} \qquad (3-209)$$

(3-209) can be solved sequentially for $v_{i,\alpha}$ in ascending order of i. Using the orthogonality properties (3-190) and (3-208) the expansion coefficients $\gamma_{i_1 i_2 i_3}(t)$ in the series (3-205) can finally be determined from, cf. (3-189)

$$\gamma_{i_1 i_2 i_3}(t) = \frac{1}{i_1!i_2!}E\left[H_{i_1}\left(\frac{X}{\sigma_X}\right)H_{i_2}\left(\frac{\dot{X}}{\sigma_{\dot{X}}}\right)V_{i_3}(V)\right] =$$

$$\frac{1}{i_1!i_2!}\sum_{\alpha_1=0}^{[\frac{i_1}{2}]}\sum_{\alpha_2=0}^{[\frac{i_2}{2}]}\sum_{\alpha_3=0}^{i_3}(-1)^{\alpha_1+\alpha_2}p_{i_1,\alpha_1}p_{i_2,\alpha_2}v_{i_3,\alpha_3}\frac{E\left[\left(X(t)\right)^{i_1-2\alpha_1}\left(\dot{X}(t)\right)^{i_1-2\alpha_2}\left(V(t)\right)^{\alpha_3}\right]}{\sigma_X^{i_1-2\alpha_1}(t)\sigma_{\dot{X}}^{i_1-2\alpha_1}(t)\sigma_V^{\alpha_3}(t)} \qquad (3-210)$$

The first of the expansion coefficients $\gamma_{i_1 i_2 i_3}(t)$ read

$$\left.\begin{array}{lll} \gamma_{000} = 1 & & \\ \gamma_{100} = 0 & , \quad \gamma_{010} = 0 & , \quad \gamma_{001} = 0 \\ \gamma_{200} = 0 & , \quad \gamma_{020} = 0 & , \quad \gamma_{002} = 0 \\ \gamma_{110} = \frac{\mu_{12}}{\sigma_X\sigma_{\dot{X}}} & , \quad \gamma_{101} = \frac{v_{1,1}}{\sigma_X} & , \quad \gamma_{011} = \frac{v_{1,1}}{\sigma_{\dot{X}}} \\ \vdots & & \end{array}\right\} \qquad (3-211)$$

The expectations $E\left[c_j\left(\mathbf{Z}(t)\right)Z_i(t)\right]$ appear in the covariance part of the moment equations (3-237) and (3-239) below. Only the non-linear 3rd component with the drift vector component $c_3\left(\mathbf{Z}(t)\right) = -c_3\left(-\mathbf{Z}(t)\right)$ as given by (3-51) need to be calculated by means of (3-205). Using (3-203) the following results may be derived

$$E\left[c_3\left(\mathbf{Z}(t)\right)Z_i(t)\right] = E\left[c_3\left(\mathbf{Z}(t)\right)V_i(t)\right] =$$

$$\begin{cases} \mu_{12} - \frac{\sigma_X \sigma_{\dot{X}}}{q_y^n} \sum\limits_{i_1+i_2+i_3=0}^{N} \gamma_{i_1 i_2 i_3} f_{i_1}(1,0)\Big(\beta f_{i_2}(0,1) g_{i_3}(1,n-1) + \gamma f_{i_2}(1,0) g_{i_3}(0,n)\Big), & i=1 \\ \mu_{22} - \frac{\sigma_{\dot{X}}^2}{q_y^n} \sum\limits_{i_2+i_3=0}^{N} \gamma_{0 i_2 i_3}\Big(\beta f_{i_2}(1,1) g_{i_3}(1,n-1) + \gamma f_{i_2}(2,0) g_{i_3}(0,n)\Big) & , \quad i=2 \\ \mu_{23} - \frac{\sigma_{\dot{X}}}{q_y^n} \sum\limits_{i_2+i_3=0}^{N} \gamma_{0 i_2 i_3}\Big(\beta f_{i_2}(0,1) g_{i_3}(2,n-1) + \gamma f_{i_2}(1,0) g_{i_3}(1,n)\Big) & , \quad i=3 \end{cases}$$

$$(3-212)$$

where $V_i(t)$ signifies the components of the auxiliary vector $\mathbf{V}^T(t) = [X(t), \dot{X}(t), V(t)]$, and

$$f_i(m,n) = \int_{-\infty}^{\infty} \xi^m |\xi|^n H_i(\xi) \varphi(\xi) d\xi \qquad (3-213)$$

$$g_i(m,n) = \int_{-\infty}^{q_y} v^m |v|^n V_i(v) f_V(v) dv \qquad (3-214)$$

(3-213) and (3-214) are defined for integer values of m and arbitrary real values of n. However, analytical evaluation of the quadratures in terms of $\varphi(\cdot)$ and $\Phi(\cdot)$ is only possible for integer values of n. (3-212) will do at closure at the order $N = 2$. In case of closure at the order $N > 2$, expectations of the type $E\Big[c_3\big(\mathbf{Z}(t)\big) Z_{i_1}(t) \cdots Z_{i_{N-1}}(t)\Big]$ must be evaluated. These can be represented by sums of products of one-dimensional quadratures similar to (3-212).

The number of free parameters of the marginal pdf $f_V(v)$ reflects the order of closure. At closure at the order $N = 2$, $f_V(v)$ may have 1 free parameter, which is calibrated from the following condition following from (3-204)

$$E[V^2(t)] = E[Q^2(t)] = \mu_{33}(t) \qquad (3-215)$$

Similarly, at closure at the order $N = 4$, $f_V(v)$ may have 2 free parameters, which are calibrated from the conditions $E[V^2(t)] = E[Q^2(t)] = \mu_{33}(t)$ and $E[V^4(t)] = E[Q^4(t)] = \mu_{3333}(t)$, etc.

Hence, at closure at the order $N = 2$ the following reversed orientated Rayleigh distribution may be applied

$$f_V(v) = \begin{cases} 0 & , \quad v \in [q_y, \infty[\\ \frac{q_y - v}{(q_y - q_0)^2} \exp\Big(-\frac{1}{2}\big(\frac{q_y - v}{q_y - q_0}\big)^2\Big) & , \quad v \in]-\infty, q_y[\end{cases} \qquad (3-216)$$

(3-216) has its modal value at $v = q_0$. q_0 is the only free parameter of the distribution, which can be determined as follows

$$q_0 = q_y\left(1 - \sqrt{\frac{\pi}{8}} + \sqrt{\frac{\pi}{8} - \frac{1}{2} + \frac{1}{2}\frac{\mu_{33}}{q_y^2}}\right) \qquad (3-217)$$

Obviously, (3-217) requires $\mu_{33}(t) \geq q_y^2\left(1 - \frac{\pi}{4}\right)$. This will be fulfilled for severe non-linear cases, where q_y is significantly smaller then the stationary standard deviation of the corresponding linear oscillator $\sigma_{X,0}$ as given by (2-103), i.e. for the cases for which the present modified closure approximation has been devised. In figs. 3-12a and 3-12b the dashed line signifies the approximation for $f_Q(q) = \frac{1}{2}\left(f_V(q) + f_V(-q)\right)$, calibrated using the simulated value of μ_{33} in (3-217), as well as the normal distribution $f_Q(q) = \frac{1}{\sigma_Q}\varphi\left(\frac{q}{\sigma_Q}\right)$, $\sigma_Q = \sqrt{\mu_{33}}$, assumed by the Gaussian closure scheme. Obviously, the modified closure approximation at the order $N = 2$ is a more realistic approximation to the simulation result than the Gaussian approximation. Figs. 3-12c and 3-12d show various cases, where $\mu_{33}(t) < q_y^2\left(1 - \frac{\pi}{4}\right)$, and the present modification is then no longer useable. However, in these cases the Gaussian approximation resembles the simulation results far better. Gaussian closure, and ordinary cumulant neglect closure approximations in general, may then be used in these cases.

The few lower moments and expansion coefficient $v_{i,\alpha}$ of the distribution (3-216) read

$$\left.\begin{aligned}
E[V] &= (q_y - q_0)\left(\alpha_y - \sqrt{\tfrac{\pi}{2}}\right)\\
E[V^2] &= (q_y - q_0)^2\left(\alpha_y^2 - 2\sqrt{\tfrac{\pi}{2}}\alpha_y + 2\right)\\
E[V^3] &= (q_y - q_0)^3\left(\alpha_y^3 - 3\sqrt{\tfrac{\pi}{2}}\alpha_y^2 + 6\alpha_y - 3\sqrt{\tfrac{\pi}{2}}\right)\\
E[V^4] &= (q_y - q_0)^4\left(\alpha_y^4 - 4\sqrt{\tfrac{\pi}{2}}\alpha_y^3 + 12\alpha_y^2 - 3\sqrt{\tfrac{\pi}{2}}\alpha_y + 8\right)\\
&\vdots
\end{aligned}\right\} \qquad (3-218)$$

$$\left.\begin{aligned}
v_{0,0} &= 1\\
v_{1,0} &= -\left(\alpha_y - \sqrt{\tfrac{\pi}{2}}\right)\sqrt{\tfrac{2}{4-\pi}}\\
v_{1,1} &= \tfrac{1}{q_y - q_0}\sqrt{\tfrac{2}{4-\pi}}\\
v_{2,0} &= \left(\alpha_y^2 - \tfrac{\sqrt{2\pi}}{4-\pi}\alpha_y + \tfrac{3\pi-8}{4-\pi}\right)\sqrt{\tfrac{4-\pi}{16-5\pi}}\\
v_{2,1} &= -\tfrac{1}{q_y - q_0}\left(2\alpha_y - \tfrac{\sqrt{2\pi}}{4-\pi}\right)\sqrt{\tfrac{4-\pi}{16-5\pi}}\\
v_{2,2} &= \tfrac{1}{(q_y - q_0)^2}\sqrt{\tfrac{4-\pi}{16-5\pi}}\\
&\vdots
\end{aligned}\right\} \qquad (3-219)$$

where

$$\alpha_y = \frac{q_y}{q_y - q_0} \qquad (3-220)$$

In case of ideal elastic-ideal plastic systems the plastic branches of the constitutive equations may be attained with finite probability. Hence, the joint pdf of the state vector $f_{\{\mathbf{Z}\}}(\mathbf{z},t)$ will be of the mixed type with a continuous part representing the elastic branches, and discrete probabilities, formally indicated by delta spikes, representing the various plastic branches. Minai and Suzuki (1985) and Suzuki and Minai (1985) suggested the following closure scheme to be used for the bilinear elasto-plastic oscillators as given by (3-49), (3-50)

$$f_{X\dot{X}Q}(x,\dot{x},q) = f_{X\dot{X}V}(x,\dot{x},q) + \delta(q-q_y)\int_{q_y}^{\infty} f_{X\dot{X}V}(x,\dot{x},u)du +$$

$$\delta(-q-q_y)\int_{-\infty}^{-q_y} f_{X\dot{X}V}(x,\dot{x},u)du, \quad (x,\dot{x},q)\in R\times R\times[-q_y,q_y] \qquad (3-221)$$

$$f_{X\dot{X}V}(x,\dot{x},q) = \frac{1}{\sigma_X\sigma_{\dot{X}}\sigma_V}\varphi\left(\frac{x}{\sigma_X}\right)\varphi\left(\frac{\dot{x}}{\sigma_{\dot{X}}}\right)\varphi\left(\frac{q}{\sigma_V}\right)\cdot$$

$$\sum_{i+j+k=0}^{N}\gamma_{ijk}H_i\left(\frac{x}{\sigma_X}\right)H_j\left(\frac{\dot{x}}{\sigma_{\dot{X}}}\right)H_k\left(\frac{q}{\sigma_V}\right) \qquad (3-222)$$

where $\varphi(\cdot)$ is the frequency function of a standardized normal variate and $H_i(\cdot)$ is the Hermite polynomium of the ith degree given by (3-188). γ_{ijk} signifies the Hermite moments as given by (3-189), evaluated with respect to the auxiliary joint pdf $f_{X\dot{X}V}(x,\dot{x},v)$. The relationship between the joint moments of $(X(t),\dot{X}(t),Q(t))$ and $(X(t),\dot{X}(t),V(t))$ reads

$$E\left[X^l(t)\dot{X}^m(t)Q^n(t)\right] = \sigma_X^l(t)\sigma_{\dot{X}}^m(t)\sigma_V^n(t)\sum_{i+j+k=0}^{4}\gamma_{ijk}r_{l,i}r_{m,j}s_{n,k}(\beta) \qquad (3-223)$$

where $\beta = q_y/\sigma_V$ and

$$r_{l,i} = \int_{-\infty}^{\infty} x^l H_i(x)\varphi(x)dx = \begin{cases} 0 & , \quad l=0\vee(l-i) \text{ odd} \\ i!p_{l,(l-i)/2} & , \quad i\le l\wedge(l-i) \text{ even} \end{cases} \qquad (3-224)$$

$$s_{n,k}(\beta) = \int_{-\beta}^{\beta} x^n H_k(x)\varphi(x)dx + \beta^n\int_{\beta}^{\infty} H_k(x)\varphi(x)dx + (-\beta)^n\int_{-\infty}^{-\beta} H_k(x)\varphi(x)dx =$$

$$\begin{cases} 0 & , \quad (n-k) \text{ odd} \\ r_{n,k} + 2\sum_{\alpha=0}^{[\frac{k}{2}]}(-1)^\alpha p_{k,\alpha}\left(\beta^n t_{k-2\alpha}(\beta) - t_{n+k-2\alpha}(\beta)\right) & , \quad (n-k) \text{ even} \end{cases} \qquad (3-225)$$

$$t_k(\beta) = \int_{\beta}^{\infty} x^k \varphi(x) dx \qquad (3-226)$$

where $p_{i,\alpha}$ is given by (3-188). $t_k(\beta)$ can be explicitly expressed in terms of $\varphi(\cdot)$ and $\Phi(\cdot)$.

However, rather than using (3-223) σ_V is calculated from the transcendent equation

$$E[Q^2] = \sigma_V^2 s_{2,0}\Big(\frac{q_y}{\sigma_V}\Big) \qquad (3-227)$$

(3-227) implies the assumption $\gamma_{004} = 0$ in (3-223). This restriction has been imposed in order to prevent significant negative side loops of the approximate joint pdf, and has the consequence that (3-221), (3-222) cannot be calibrated to the moment $E[Q^4(t)]$. In principle this means that the marginal pdf $f_Q(q,t)$ is represented by a closure scheme at the order $N = 2$.

The closure scheme (3-221), (3-222) will be used in the examples (3-3), (3-4) and (3-5) below, which deal with the stochastic analysis of ideal elastic-ideal plastic systems, in combination with an equivalent cubic expansion technique derived by the author especially for such systems.

A dynamic system driven by a compound Poisson process with low pulse arrival rate represents still another example, where modification of any ordinary closure scheme such as cumulant neglect closure, quasi-moment neglect closure, Hermite moment neglect closure, etc. may be necessary in order to achieve accuracy and numerical stability of the moment equation method. Assume, that the said system is defined with initial conditions $\mathbf{Z}(t) = \mathbf{z}_0$ at the time t_0. Then, the system performs a deterministic drift (eigenvibration) from the initial values, $\mathbf{Z}(t) = \mathbf{d}(t|\mathbf{z}_0, t_0)$, until the first impulse arrives. The probability $P_0(t, t_0)$ of no impulse arrivals in the interval $]t_0, t]$ follows from (3-8)

$$P_0(t,t_0) = P\Big(N(t) = 0\Big) = \exp\Big(-\int_{t_0}^{t} \nu(\tau) d\tau\Big) \qquad (3-228)$$

The probability $P_0(t, t_0)$ is large, if either the length $t - t_0$ of the time interval is small or the mean arrival rate $\nu(\tau)$ is small. It follows that with the probability $P_0(t, t_0)$ the system will be placed at the position $\mathbf{d}(t|\mathbf{z}_0, t_0)$. The remaining probability mass $1 - P_0(t, t_0)$ will be continuously distributed in the state space, due to one or more impulses in the interval $]t_0, t]$. The joint probability density function of the state vector can then be written

$$f_{\{\mathbf{Z}\}}(\mathbf{z},t) = P_0(t,t_0) f_{\{\mathbf{Z}\}}(\mathbf{z},t|N(t)=0) + \big(1 - P_0(t,t_0)\big) f_{\{\mathbf{Z}\}}(\mathbf{z},t|N(t)>0) \;=$$

$$P_0(t,t_0)\delta\big(\mathbf{z}-\mathbf{d}(t|\mathbf{z}_0,t_0)\big)+\big(1-P_0(t,t_0)\big)f_{\{\mathbf{V}\}}(\mathbf{z},t) \qquad (3-229)$$

The auxiliary process $\{\mathbf{V}(t), t\in[t_0,\infty[\}$ signifies the state vector on condition of at least one pulse arrival. In contrast to $f_{\{\mathbf{Z}\}}(\mathbf{z},t)$ the joint probability density function of $\mathbf{V}(t)$ will be continuously distributed without any discrete contributions. Hence, any of the above-mentioned closure schemes may apply to this distribution. The joint moments and joint centralized moments of $\mathbf{Z}(t)$ and $\mathbf{V}(t)$ are designated $\mu_{i_1 i_2\cdots i_n}(t)$, $\lambda_{i_1 i_2\cdots i_n}(t)$ and $\mu^0_{i_1 i_2\cdots i_n}(t)$, $\lambda^0_{i_1 i_2\cdots i_n}(t)$, respectively. From (3-229) it follows that

$$\mu_{i_1 i_2\cdots i_n}(t)=P_0(t,t_0)\prod_{j=1}^{n}d_{i_j}(t|\mathbf{z}_0,t_0)+\big(1-P_0(t,t_0)\big)\mu^0_{i_1 i_2\cdots i_n}(t) \qquad (3-230)$$

where $d_i(t|\mathbf{z}_0,t_0)$ signifies a component of the deterministic drift vector. Especially, the mean values of $\mathbf{Z}(t)$ and $\mathbf{V}(t)$ are related as

$$\mu_i(t)=P_0(t,t_0)d_i(t|\mathbf{z}_0,t_0)+\big(1-P_0(t,t_0)\big)\mu^0_i(t) \qquad (3-231)$$

The relationship between the centralized joint moments of $\mathbf{Z}(t)$ and $\mathbf{V}(t)$ then becomes

$$\lambda_{i_1 i_2\cdots i_n}(t)=E\Big[\prod_{j=1}^{n}Z^0_{i_j}(t)\Big]=P_0\prod_{j=1}^{n}\big(d_{i_j}-\mu_{i_j}(t)\big)+\big(1-P_0\big)E\Big[\prod_{j=1}^{n}Z^0_{i_j}(t)\Big]_0=$$

$$P_0\prod_{j=1}^{n}\big(d_{i_j}-\mu_{i_j}(t)\big)+\big(1-P_0\big)E\Big[\prod_{j=1}^{n}\Big(Z_{i_j}(t)-\mu^0_{i_j}(t)+\frac{P_0}{1-P_0}\big(\mu_{i_j}(t)-d_{i_j}\big)\Big)\Big]_0=$$

$$\Big(P_0+\frac{\big(-P_0\big)^n}{\big(1-P_0\big)^{n-1}}\Big)\prod_{j=1}^{n}\big(d_{i_j}-\mu_{i_j}(t)\big)+$$

$$\big(1-P_0\big)\sum_{j=0}^{n-1}\binom{n}{j}\Big\{\lambda^0_{i_1 i_2\cdots i_{n-j}}(t)\prod_{k=n-j+1}^{n}\big(\mu_{i_k}(t)-d_{i_k}\big)\Big\}_s\cdot\Big(\frac{P_0}{1-P_0}\Big)^j \qquad (3-232)$$

where (3-231) has been used. Further, $E[\cdot]_0$ signifies expectations with respect to $f_{\{\mathbf{V}\}}(\mathbf{z},t)$, and the arguments of $P_0(t,t_0)$ and $d_i(t|\mathbf{z}_0,t_0)$ have been omitted for ease of notation. The inverse relation can be derived in a similar few steps

$$\lambda^0_{i_1 i_2\cdots i_n}(t)=E\Big[\prod_{j=1}^{n}\big(Z_{i_j}(t)-\mu^0_{i_j}(t)\big)\Big]_0=$$

$$-\frac{P_0}{1-P_0}\prod_{j=1}^{n}\big(d_{i_j}-\mu^0_{i_j}(t)\big)+\frac{1}{1-P_0}E\Big[\prod_{j=1}^{n}\big(Z_{i_j}(t)-\mu^0_{i_j}(t)\big)\Big]=$$

$$-\frac{P_0}{(1-P_0)^{n+1}}\prod_{j=1}^{n}(d_{i_j}-\mu_{i_j}(t))+\frac{1}{1-P_0}E\Big[\prod_{j=1}^{n}\Big(Z^0_{i_j}(t)+\frac{P_0}{1-P_0}(d_{i_j}-\mu_{i_j}(t))\Big)\Big]=$$

$$\frac{P_0^n-P_0}{(1-P_0)^{n+1}}\prod_{j=1}^{n}(d_{i_j}-\mu_{i_j}(t))+$$

$$\frac{1}{1-P_0}\sum_{j=0}^{n-1}\binom{n}{j}\Big\{\lambda_{i_1 i_2\cdots i_{n-j}}(t)\prod_{k=n-j+1}^{n}(d_{i_k}-\mu_{i_k}(t))\Big\}_s\cdot\Big(\frac{P_0}{1-P_0}\Big)^j \qquad (3-233)$$

For systems with polynomial drift vectors the following modified cumulant neglect closure scheme may be used. In case of closure at the order N all centralized moments $\lambda^0_{i_1 i_2\cdots i_j}(t)$, $j>N$ with respect to the continuous joint pdf $f_{\{\mathbf{v}\}}(\mathbf{z},t)$ are first expressed in terms of corresponding centralized moments of the order $j\le N$ by means of the cumulant neglect closure approximations (3-193). Then, $\lambda_{i_1 i_2\cdots i_n}(t)$, $n>N$ may be expressed in terms of the centralized moments $\lambda^0_{i_1 i_2\cdots i_j}(t)$, $j\le N$ by means of (3-232). Finally, all joint moments $\lambda^0_{i_1 i_2\cdots i_j}(t)$, $j\le N$ within this expression can be expressed by $\lambda_{i_1 i_2\cdots i_j}(t)$, $j\le N$ by means of (3-233), and the requested closure scheme is obtained. In case of closure at the order $N=4$ the following explicit closure approximations for the 5th and 6th order joint centralized moments may be derived for the case $d_i(t\mid \mathbf{z}_0,t_0)\equiv 0$

$$\lambda_{ijklm}(t)=\frac{1}{1-P_0}10\{\lambda_{ij}\lambda_{klm}\}_s-\frac{P_0(1+P_0)}{(1-P_0)^2}10\{\mu_i\mu_j\lambda_{klm}\}_s-$$

$$\frac{2P_0}{(1-P_0)^2}15\{\mu_i\lambda_{jk}\lambda_{lm}\}_s+\frac{P_0}{1-P_0}5\{\mu_i\lambda_{jklm}\}_s+$$

$$\frac{P_0(1+4P_0+P_0^2)}{(1-P_0)^3}10\{\mu_i\mu_j\mu_k\lambda_{lm}\}_s+$$

$$\frac{P_0(1+11P_0+11P_0^2+P_0^3)}{(1-P_0)^4}\mu_i\mu_j\mu_k\mu_l\mu_m \qquad (3-234)$$

$$\lambda_{ijklmn}(t)=\frac{15}{1-P_0}\{\lambda_{ij}\lambda_{klmn}\}_s-\frac{15P_0}{1-P_0}\{\mu_i\mu_j\lambda_{klmn}\}_s+$$

$$\frac{10}{1-P_0}\{\lambda_{ijk}\lambda_{lmn}\}_s+\frac{P_0(1+P_0-2P_0^2)}{1-P_0^3}20\{\mu_i\mu_j\mu_k\lambda_{lmn}\}_s-$$

$$\frac{60P_0}{(1-P_0)^2}\{\mu_i\lambda_{jk}\lambda_{lmn}\}_s-\frac{2\cdot 15}{(1-P_0)^2}\{\lambda_{ij}\lambda_{kl}\lambda_{mn}\}_s+$$

$$\frac{2P_0\cdot 45}{(1-P_0)^3}\{\mu_i\mu_j\lambda_{kl}\lambda_{mn}\}_s-$$

$$\frac{P_0(1+7P_0-5P_0^2-3P_0^3)}{(1-P_0)^4}15\{\mu_i\mu_j\mu_k\mu_l\lambda_{mn}\}_s+$$

$$\frac{P_0\left(1+20P_0-40P_0^3-5P_0^4\right)}{\left(1-P_0\right)^5}\mu_i\mu_j\mu_k\mu_l\mu_m\mu_n \qquad (3-235)$$

In case of stationary excitation, $P_0(t,t_0) \to 0$ as $t - t_0 \to \infty$. Hence, the discrete part of the joint probability density function (3-229) vanishes, and the ordinary cumulant neglect closure approximations (3-193) are obtained from (3-234) and (3-235).

The indicated modified cumulant neglect closure scheme for compound Poisson process driven systems was first suggested by Iwankiewicz and Nielsen (1992a,1992b). The method was applied to the problems described in example 3-9, and turned out to improve the numerical stability significantly in case of small values of $P_0(t,t_0)$. The derivations (3-232), (3-233), (3-234), (3-335) are due to Nielsen and Iwankiewicz (1995).

The method of equivalent linearization was introduced by Booton (1954), Kazakov (1956) and Caughey (1963). Further development to MDOF systems is due to Atalik and Utku (1976), Kaul and Penzien (1974), Iwan and Mason (1980), Wen (1980) and Ahmadi (1980). The technique, intended for slightly non-linear systems, was found to produce reasonable results even for large non-linearities in some cases. A review of applications was given by Spanos (1981) and by Roberts and Spanos (1990). Uniqueness and existence of the equivalent linear system were discussed by Spanos and Iwan (1978). However, as demonstrated by Langley (1988a) and Fan and Ahmadi (1990) for a three-well potential problem, uniqueness is not guaranteed in multi-modal systems. Further, the accuracy of the system is very bad in such cases.

Gaussian closure technique was suggested by Iyengar and Dash (1978), Dash and Iyengar (1982). As mentioned, and first pointed out by Wu and Lin (1984), Ahmadi and Orabi (1987) and Noori and Davoodi (1988), these technique is identical to the equivalent linearization technique with Gaussian evaluation of the equivalent linearization coefficient for the mean value and covariance equations. The evaluation of higher order moments by means of a joint Gaussian pdf, calibrated entirely from the second moment equations, is questionable and inconsistent.

The rate of convergence of cumulant neglect closure schemes in almost Gaussian systems was studied by Wu and Lin (1984). The lack of accuracy and instability in systems which are essentially multi-modal was discovered by Sun and Hsu (1987), Fan and Ahmadi (1990) and Soong and Grigoriu (1993). The lack of convergence of the ordinary cumulant neglect closure scheme for the two-well potential problem was observed by Bergman et al. (1994) using closure schemes up to the order $N = 8$. In contrast, the indicated modified cumulant neglect closure scheme due to Köylüoğlu and Nielsen (1996) converges at the usual rate of convergence of almost Gaussian systems as shown in examples 3-5 and 3-8 below. The general conclusion seems to be that applications of the cumulant neglect closure scheme to any highly non-Gaussian case require modification, guided by physical insight into the system dynamics. Hermite moment neglect closure schemes were first suggested by Crandall (1980, 1985), and have been further developed by Minai and Suzuki (1985) and Suzuki and Minai (1985).

3.3.2 Wiener process driven systems

Using the Kolmogorov backward operator (3-118) in (3-172) and (3-173) the following differential equations for the mean value and the joint central moments are obtained.

$$\frac{d}{dt}\mu_i(t) = E\Big[c_i(\mathbf{Z}(t),t)\Big] \tag{3-236}$$

$$\left.\begin{aligned}
&\frac{d}{dt}\lambda_{ij}(t) = 2\left\{E\Big[c_i^0(\mathbf{Z}(t),t)\,Z_j^0(t)\Big]\right\}_s + \sum_{\alpha=1}^{n_3} E\Big[d_{i\alpha}(\mathbf{Z}(t),t)\,d_{j\alpha}(\mathbf{Z}(t),t)\Big] \\
&\frac{d}{dt}\lambda_{ijk}(t) = 3\left\{E\Big[c_i^0(\mathbf{Z}(t),t)\,Z_j^0(t)Z_k^0(t)\Big]\right\}_s \\
&+ 3\sum_{\alpha=1}^{n_3}\left\{E\Big[d_{i\alpha}(\mathbf{Z}(t),t)\,d_{j\alpha}(\mathbf{Z}(t),t)\,Z_k^0(t)\Big]\right\}_s \\
&\frac{d}{dt}\lambda_{ijkl}(t) = 4\left\{E\Big[c_i^0(\mathbf{Z}(t),t)\,Z_j^0(t)Z_k^0(t)Z_l^0(t)\Big]\right\}_s \\
&+ 6\sum_{\alpha=1}^{n_3}\left\{E\Big[d_{i\alpha}(\mathbf{Z}(t),t)\,d_{j\alpha}(\mathbf{Z}(t),t)\,Z_k^0(t)Z_l^0(t)\Big]\right\}_s \\
&\frac{d}{dt}\lambda_{i_1\ldots i_N}(t) = N\left\{E\Big[c_{i_1}^0(\mathbf{Z}(t),t)\,Z_{i_2}^0(t)\cdots Z_{i_N}^0(t)\Big]\right\}_s + \\
&\frac{N(N-1)}{2}\sum_{\alpha=1}^{n_3}\left\{E\Big[d_{i_1\alpha}(\mathbf{Z}(t),t)\,d_{i_2\alpha}(\mathbf{Z}(t),t)\,Z_{i_3}^0(t)\cdots Z_{i_N}^0(t)\Big]\right\}_s
\end{aligned}\right\} \tag{3-237}$$

where the centralized drift vector has been introduced, defined as

$$\mathbf{c}^0(\mathbf{Z}(t),t) = \mathbf{c}(\mathbf{Z}(t),t) - E\Big[\mathbf{c}(\mathbf{Z}(t),t)\Big] \tag{3-238}$$

In the case of state-independent diffusion terms (3-237) reduces to

$$\left.\begin{aligned}
&\frac{d}{dt}\lambda_{ij}(t) = 2\left\{E\Big[c_i^0(\mathbf{Z}(t),t)\,Z_j^0(t)\Big]\right\}_s + \sum_{\alpha=1}^{n_3} d_{i\alpha}(t)d_{j\alpha}(t) \\
&\frac{d}{dt}\lambda_{ijk}(t) = 3\left\{E\Big[c_i^0(\mathbf{Z}(t),t)\,Z_j^0(t)Z_k^0(t)\Big]\right\}_s \\
&\frac{d}{dt}\lambda_{ijkl}(t) = 4\left\{E\Big[c_i^0(\mathbf{Z}(t),t)\,Z_j^0(t)Z_k^0(t)Z_l^0(t)\Big]\right\}_s + \\
&6\sum_{\alpha=1}^{n_3}\left\{d_{i\alpha}(t)d_{j\alpha}(t)\lambda_{kl}(t)\right\}_s \\
&\frac{d}{dt}\lambda_{i_1\cdots i_N}(t) = N\left\{\Big[c_{i_1}^0(\mathbf{Z}(t),t)\,Z_{i_2}^0(t)\cdots Z_{i_N}^0(t)\Big]\right\}_s + \\
&\frac{N(N-1)}{2}\sum_{\alpha=1}^{n_3}\Big\{d_{i_1\alpha}(t)d_{i_2\alpha}(t)\lambda_{i_3\cdots i_N}(t)\Big\}_s
\end{aligned}\right\} \tag{3-239}$$

Of special interest is the case of a system with polynomial non-linearity, e.g. in terms of a cubic form of the state variables as for the van der Pol and Duffing oscillators. In this case the following cubic expansions of the drift vector and the centralized drift terms of the centralized state variables can be formulated

$$c_i(\mathbf{Z}(t),t) = A_i + B_{im}Z_m^0 + C_{imn}Z_m^0 Z_n^0 + D_{imnp}Z_m^0 Z_n^0 Z_p^0 \qquad (3-240)$$

$$c_i^0(\mathbf{Z}(t),t) = B_{im}Z_m^0 + C_{imn}(Z_m^0 Z_n^0 - \lambda_{mn}) + D_{imnp}(Z_m^0 Z_n^0 Z_p^0 - \lambda_{mnp}) \qquad (3-241)$$

In (3-240), (3-241) and below the summation convention has been used for simplicity, with the dummy indices ranging from 1 to n. The explicit time dependence of the left-hand sides of (3-240) and (3-241) suggests that the tensor component A_i, B_{im}, C_{imn} and D_{imnp} may be time-dependent for time-varying systems.

The expectations of the drift term multiplied by the state variables can now be explicitly performed. (3-239) becomes

$$\left.\begin{aligned}
&\frac{d}{dt}\mu_i = A_i + C_{imn}\lambda_{mn} + D_{imnp}\lambda_{mnp} \\
&\frac{d}{dt}\lambda_{ij}(t) = 2\{B_{im}\lambda_{mj}\}_s + 2\{C_{imn}\lambda_{mnj}\}_s + 2\{D_{imnp}\lambda_{mnpj}\}_s + \sum_{\alpha=1}^{n_3} d_{i\alpha}(t)d_{j\alpha}(t) \\
&\frac{d}{dt}\lambda_{ijk}(t) = 3\{B_{im}\lambda_{mjk}\}_s + 3\{C_{imn}(\lambda_{mnjk} - \lambda_{mn}\lambda_{jk})\}_s + \\
&3\{D_{imnp}(\lambda_{mnpjk} - \lambda_{mnp}\lambda_{jk})\}_s \\
&\frac{d}{dt}\lambda_{ijkl}(t) = 4\{B_{im}\lambda_{mjkl}\}_s + 4\{C_{imn}(\lambda_{mnjkl} - \lambda_{mn}\lambda_{jkl})\}_s + \\
&4\{D_{imnp}(\lambda_{mnpjkl} - \lambda_{mnp}\lambda_{jkl})\}_s + 6\sum_{\alpha=1}^{n_3}\{d_{i\alpha}(t)d_{j\alpha}(t)\lambda_{kl}(t)\}_s
\end{aligned}\right\} \qquad (3-242)$$

The cumulant neglect closure scheme (3-193) or the quasi-moment neglect closure scheme (3-195) can immediately be used in (3-242).

In case of hysteretic systems, the drift vector is non-linear and non-analytical. Hence, it is neither polynomial nor admits an approximate Taylor-expansion. In order to handle such systems an equivalent strucural system may be introduced for which the drift vector $c_{i,eq}(\mathbf{Z}(t),t)$ admits the cubic expansion in the centralized state variables (3-240).

The difference between the drift vector of the original system and the equivalent system is specified by the error vector

$$\varepsilon_i = c_i - c_{eq,i} = c_i - A_i - B_{im}Z_m^0 - C_{imn}Z_m^0 Z_n^0 - D_{imnp}Z_m^0 Z_n^0 Z_p^0 \qquad (3-243)$$

For the class of systems with drift vectors specified by (3-54) or (3-59), the optimal choice for the equivalent system is taken to be the one for which the expectation $E[\varepsilon_k\varepsilon_k]$

becomes minimum. The expansion coefficients are then determined from the conditions

$$\frac{\partial}{\partial A_i}E[\varepsilon_k\epsilon_k] = 0, \quad \frac{\partial}{\partial B_{im}}E[\varepsilon_k\epsilon_k] = 0, \text{ etc.} \tag{3-244}$$

resulting in the following system of linear algebraic equations

$$\left.\begin{aligned}
&E[c_i] = A_i + C_{imn}\lambda_{mn} + D_{imnp}\lambda_{mnp}\\
&E[c_i^0 Z_j^0] = B_{im}\lambda_{mj} + C_{imn}\lambda_{mnj} + D_{imnp}\lambda_{mnpj}\\
&E[c_i^0 Z_j^0 Z_k^0] = B_{im}\lambda_{mjk} + C_{imn}(\lambda_{mnjk} - \lambda_{mn}\lambda_{jk}) +\\
&D_{imnp}(\lambda_{mnpjk} - \lambda_{mnp}\lambda_{jk})\\
&E[c_i^0 Z_j^0 Z_k^0 Z_l^0] = B_{im}\lambda_{mjkl} + C_{imn}(\lambda_{mnjkl} - \lambda_{mn}\lambda_{jkl}) +\\
&D_{imnp}(\lambda_{mnpjkl} - \lambda_{mnp}\lambda_{jkl})
\end{aligned}\right\} \tag{3-245}$$

Especially, equivalent linearization implies that the drift vector of the equivalent system admits the expansion

$$c_{eq,i}(\mathbf{Z}(t), t) = A_i + B_{im}Z_m^0 \tag{3-246}$$

The next step is to investigate to which extent the equivalent system with expansion coefficients determined by (3-245) represents the original system. First, it is noticed that all the expectations entering the right-hand sides of (3-239) also occur in (3-245) for the determination of the expansion coefficients. Further, if (3-245) is inserted into the right-hand sides of (3-239), these become identical to the right-hand sides of (3-242).

Hence, the following theorem has been proved (Nielsen, Mørk and Thoft-Christensen (1990a, 1990b)): *The propagation of the mean values and the joint central moments up to order $N = 4$ will be identical for the original and the equivalent cubic system, provided the same approximate pdf is applied to both systems for evaluation of all the expectations, and provided the coefficients of the polynomial expansion of the equivalent system are determined from a least mean square criterion.*

A generalization to equivalent systems with a polynomial expansion of arbitrary order $N \geq 1$, including $N = 1$ corresponding to equivalent linearization, is straightforward. Actually, this system and the original system predict identical mean values and joint central moments up to the order $N+1$, provided the same approximate pdf is applied to both systems for evaluation of the expectations including unprovided joint central moments of order $N+2, \ldots, 2N$ appearing in the equations for the equivalent coefficients, and provided the coefficients of the polynomial expansion of the equivalent system are determined from a least mean square criterion. Especially, if the exact joint pdf is applied to both systems, exact joint moments up to and including the order $N+1$ are obtained.

For the equivalent linear system (3-246) the following results are derived for the tensor components A_i and B_{im} from (3-245)

$$\left.\begin{aligned} A_i &= E\Big[c_i\big(\mathbf{Z}(t),t\big)\Big] \\ B_{im} &= E\Big[c_i^0\big(\mathbf{Z}(t),t\big)Z_j^0(t)\Big]\kappa_{jm}^{-1} \end{aligned}\right\} \qquad (3-247)$$

where κ_{jm}^{-1} signifies the components of the inverse covariance matrix $\kappa_{jm} = \lambda_{jm}$. The equivalent linear system (3-246) predicts a Gaussian response, when applied to the system (3-116) with state independent drift vector and deterministic or Gaussian distributed initial values. In these cases the consistent choice for the evaluation of the expectations in (3-247) will be a Gaussian closure scheme. Using the following well-known property for the expected value of combined stochastic variables generated by a normal vector

$$E\Big[c_i^0\big(\mathbf{Z}(t),t\big)Z_j^0\Big] = E\left[\frac{\partial c_i^0\big(\mathbf{Z}(t),t\big)}{\partial z_m}\right]\kappa_{mj} = E\left[\frac{\partial c_i\big(\mathbf{Z}(t),t\big)}{\partial z_m}\right]\kappa_{mj} \qquad (3-248)$$

then (3-219) can be written

$$B_{im} = E\left[\frac{\partial c_i\big(\mathbf{Z}(t),t\big)}{\partial z_m}\right] \qquad (3-249)$$

(3-249) is due to Atalik and Utku (1976). Gaussian closure will not give consistent results, when applied to hierarchy of moment equations for non-linear systems truncated above $N > 2$.

Quite often structural systems possess the following symmetry properties

$$\left.\begin{aligned} \mathbf{c}\big(\mathbf{Z}(t),t\big) &= -\mathbf{c}\big(-\mathbf{Z}(t),t\big) \\ \mathbf{d}\big(\mathbf{Z}(t),t\big) &= \mathbf{d}\big(-\mathbf{Z}(t),t\big) \end{aligned}\right\} \qquad (3-250)$$

If further the initial value $\mathbf{Z}_0 = \mathbf{Z}(0) = \mathbf{0}$ in (3-116) it can be stated that $\mu_{i_1\cdots i_N}(t) = \lambda_{i_1\cdots i_N}(t) \equiv 0$, N odd. (3-250) is referred to as the zero mean condition. For the cubic polynomial system (3-240) this implies that $A_i = C_{imn} = 0$. (3-240) and (3-242) then reduce to

$$c_{eq,i}\big(\mathbf{Z}(t),t\big) = B_{im}Z_m + D_{imnp}Z_mZ_nZ_p \qquad (3-251)$$

$$\left.\begin{aligned} \frac{d}{dt}\mu_{ij} &= 2\big\{B_{im}\mu_{mj}\big\}_s + 2\big\{D_{imnp}\mu_{mnp}\big\}_s + \sum_{\alpha=1}^{n_3} d_{i\alpha}(t)d_{j\alpha}(t) \\ \frac{d}{dt}\mu_{ijkl} &= 4\big\{B_{im}\mu_{mjkl}\big\}_s + 4\big\{D_{imnp}\mu_{mnpjkl}\big\}_s + \\ & 6\sum_{\alpha=1}^{n_3}\big\{d_{i\alpha}(t)d_{j\alpha}(t)\lambda_{kl}\big\}_s \end{aligned}\right\} \qquad (3-252)$$

where B_{im} and D_{imnp} are determined from, cf. (3-245)

$$\left.\begin{aligned} E[c_i Z_j] &= B_{im}\mu_{mj} + D_{imnp}\mu_{mnpj} \\ E[c_i Z_j Z_k Z_l] &= B_{im}\mu_{mjkl} + D_{imnp}\mu_{mnpjkl} \end{aligned}\right\} \qquad (3-253)$$

Example 3-3: Stochastic response analysis of hysteretic oscillators driven by Wiener processes

Upon calculating the expansion coefficients in (3-245) or (3-253) an analytical form of the joint pdf $f_{\mathbf{Z}}(\mathbf{z},t)$ with a number of free parameters must be specified in order to evaluate the expectations on the left-hand sides. These free parameters are then sequentially calibrated from an equal number of statistics available. If the same joint pdf is applied in the original system with moment equations (3-239) the same joint moments are predicted according to the indicated theorem. Then, at first sight nothing seems to be gained by the introduction of an equivalent polynomial system. However, in hysteretic systems only the differential equations specifying the hysteretic components will be non-linear and non-analytical. The idea to be presented in this example and the following examples 3-4 and 3-5 is then to replace only these components with an equivalent cubic expansion, whereas the linear components remain unchanged. In contrast, the mean least square solutions obtained from (3-245) and (3-253) provide a polynomial expansion even for the linear components. Since fewer parameters are varied such a method no longer predicts correct joint moments even if the exact joint pdf is used for the evaluation of the equivalent polynomial expansion coefficients.

The SDOF hysteretic oscillator (3-47), (3-48) is considered, where $\{F(T), t \in R\}$ is a stationary Gaussian white noise with the autospectral density S_0. The constitutive equation of the oscillator is modelled as a bilinear oscillator with the non-dimensional spring stiffness given by (3-50). As seen from (3-49) the zero-mean conditions (3-250) are then fulfilled. Since, the system is analyzed with the zero initial conditions, $\mathbf{Z}(0) = \mathbf{0}$, the reduced equivalent cubic expansion (3-251) of the drift vector in (3-49) as well as the reduced moment equations (3-252) is then valid.

The first two drift vector components $c_i(\mathbf{Z}(t))$ in (3-49) can be written in the following way

$$c_i(\mathbf{Z}(t)) = B_{im} Z_m(t) \ , \ i = 1,2 \qquad (3-254)$$

$$\begin{pmatrix} B_{11} = 0 & , & B_{12} = 1 & , & B_{13} = 0 \\ B_{21} = -\alpha\omega_0^2 & , & B_{22} = -2\zeta\omega_0 & , & B_{23} = -\omega_0^2(1-\alpha) \end{pmatrix}$$

As mentioned, the idea of the present method is to keep this linear expansion for these state variables unchanged. Only the component $c_3(\mathbf{Z}(t))$ is replaced by an equivalent cubic expansion in the form

$$c_{3,eq}(\mathbf{Z}(t)) = \kappa(\dot{X},Q)\dot{X} = B_{32}\dot{X} + B_{33}Q + D_{3222}\dot{X}^3 + D_{3223}\dot{X}^2 Q + D_{3233}\dot{X}Q^2 + D_{3333}Q^3 \qquad (3-255)$$

The expansion coefficients in (3-255) are determined from the least mean square criterion, leading to the following system of linear equations, similar to (3-253)

$$\begin{bmatrix} \mu_{22} & \mu_{23} & \mu_{2222} & \mu_{2223} & \mu_{2233} & \mu_{2333} \\ & \mu_{33} & \mu_{2223} & \mu_{2233} & \mu_{2333} & \mu_{3333} \\ & & \mu_{222222} & \mu_{222223} & \mu_{222233} & \mu_{222333} \\ & & & \mu_{222233} & \mu_{222333} & \mu_{223333} \\ & \text{symm.} & & & \mu_{223333} & \mu_{233333} \\ & & & & & \mu_{333333} \end{bmatrix} \begin{bmatrix} B_{32} \\ B_{33} \\ D_{3222} \\ D_{3223} \\ D_{3233} \\ D_{3333} \end{bmatrix} = \begin{bmatrix} E[\dot{X}^2\kappa] \\ E[\dot{X}Q\kappa] \\ E[\dot{X}^4\kappa] \\ E[\dot{X}^3Q\kappa] \\ E[\dot{X}^2Q^2\kappa] \\ E[\dot{X}Q^3\kappa] \end{bmatrix} \qquad (3-256)$$

The expectations on the right-hand side of (3-256) as well as the joint 6th order moments on the left-hand side are calculated by means of the following marginal version of the Minai-Suzuki closure scheme (3-221), (3-222)

$$f_{\dot{X}Q}(\dot{x},q) = f_{\dot{X}V}(\dot{x},q) + \delta(q-q_y)\int_{q_y}^{\infty} f_{\dot{X}V}(\dot{x},u)du +$$

$$\delta(-q-q_y)\int_{-\infty}^{-q_y} f_{\dot{X}V}(\dot{x},u)du \quad , \quad (\dot{x},q) \in R \times [-q_y,q_y] \qquad (3-257)$$

$$f_{\dot{X}V}(\dot{x},v) = \frac{1}{\sigma_{\dot{X}}\sigma_V}\varphi\left(\frac{\dot{x}}{\sigma_{\dot{X}}}\right)\varphi\left(\frac{v}{\sigma_V}\right)\sum_{j+k=0}^{N}\gamma_{0jk}H_j\left(\frac{\dot{x}}{\sigma_{\dot{X}}}\right)H_k\left(\frac{v}{\sigma_V}\right) \qquad (3-258)$$

The joint 6th order joint moments appearing in the global moment equations (3-252) are still approximated by the ordinary cumulant neglect closure approximation given by (3-193).

The following approximate methods have been investigated:

a: equivalent linearization using Gaussian closure with the system of differential equations for the joint central moments closed at covariance level.

b: closure of the original system (3-192) at the order $N = 4$ using the full 3-dimensional expansion (3-221), (3-222).

c: present method. All expectations in (3-256) are calculated from the marginal pdf (3-257), (3-258). The joint 6th order moments of (3-252) are calculated by an ordinary cumulant neglect closure scheme.

d: present method. All expectations in (3-256) are calculated from the marginal pdf (3-257), (3-258). The joint 6th order moments of (3-252) are calculated using the full 3-dimensional expansion (3-221), (3-222) at the order $N = 4$.

Any difference between results for the cases b and c is partly due to the fact that in the latter case only a single drift vector component is replaced by an equivalent cubic polynomial expansion, and partly to the application of the ordinary cumulant neglect closure scheme in the moment equations (3-252), which works bad for any joint 6th order moments involving $Q(t)$. If all 3 components of the drift vector in case d had been replaced by cubic polynomial expansions, this case would have given results identical to case b for all joint moments up to and including the order 4 according to the theorem on page 142. Discrepancies of results between these cases may then be attributed entirely to the replacement of only the non-linear and non-algebraic hysteretic incremental equation of the original system with an equivalent substitution in cubic polynomial form.

To verify the obtained results, a numerical Monte-Carlo simulation has been carried out. Generation of realizations of a broad-banded zero mean Gaussian process was performed by the method of Penzien, Clough and Penzien (1974). The integrated dynamic system (3-49), (3-50) with the system data $\omega_0 = 1$, $\zeta = 0.05$, $q_y = 1.0$ was solved by a 4th order Runge-Kutta scheme, with the initial conditions $\mathbf{Z}(0) = 0$. The excitation level of the Gaussian white noise was chosen so the stationary variance of the corresponding linear oscillator becomes $\sigma^2_{X,0} = \frac{\pi S_o}{2\zeta\omega_0^3 m^2} = 1$. The time step was selected as $\Delta t = \frac{T_0}{50}$, $T_0 = \frac{2\pi}{\omega_0}$ being the period of linear, undamped eigenvibrations. The sample size of ensemble response time-histories was 5000, from which the relevant response statistics were determined.

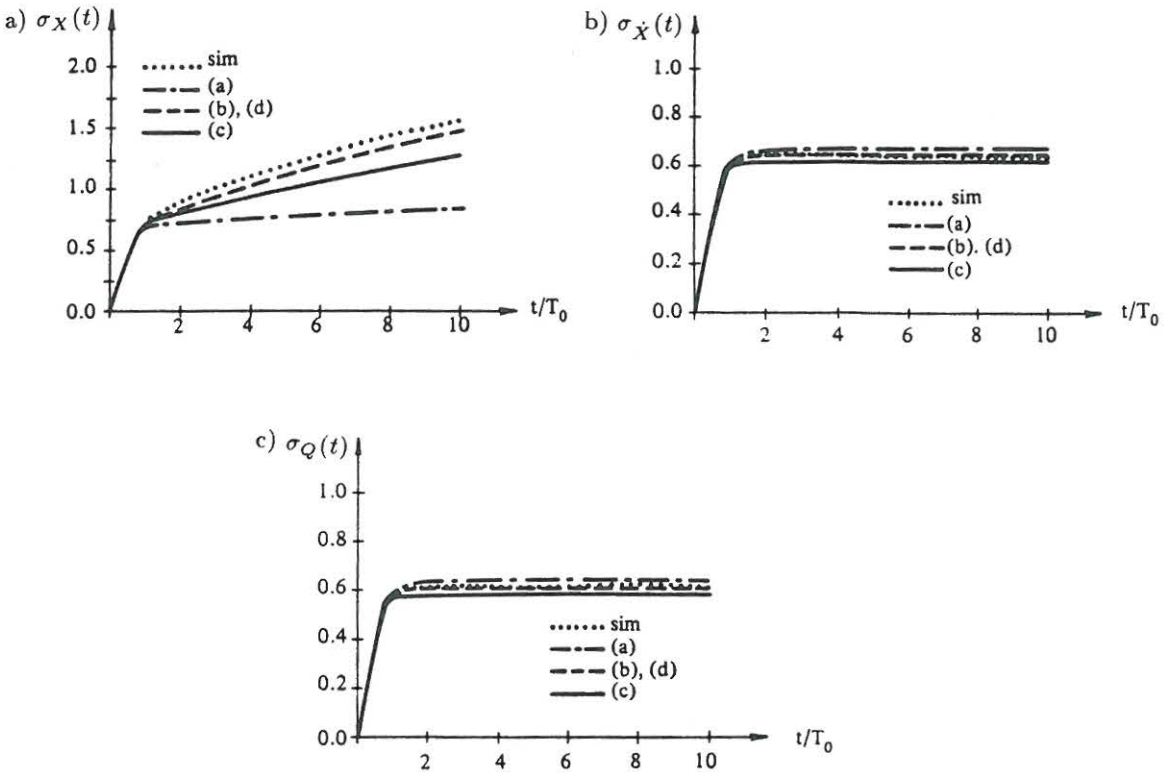

Fig. 3-13: Time-dependence of standard deviations. a) Displacement response. b) Velocity response. c) Hysteretic component. $\omega_0 = 1$, $\zeta = 0.05$, $\alpha = 0.0$, $q_y = 1$, $\sigma^2_{X,0} = \frac{\pi S_0}{2\zeta\omega_0^3 m^2} = 1$. Nielsen, Mørk and Thoft-Christensen (1990a).

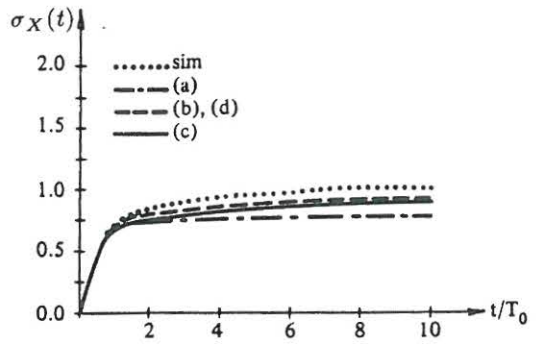

Fig. 3-14: Time-dependent standard deviation of displacement response. $\omega_0 = 1$, $\zeta = 0.05$, $\alpha = 0.1$, $q_y = 1$, $\sigma^2_{X,0} = \frac{\pi S_0}{2\zeta\omega_0^3 m^2} = 1$. Nielsen, Mørk og Thoft-Christensen (1990a).

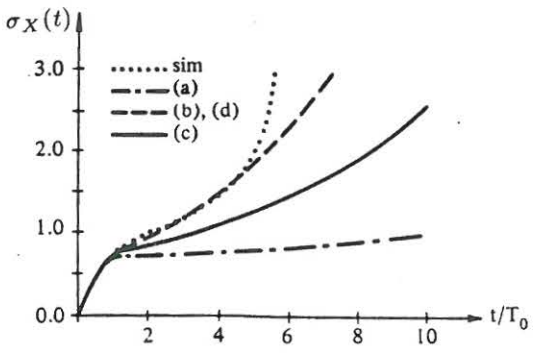

Fig. 3-15: Time-dependent standard deviation of displacement response. $\omega_0 = 1$, $\zeta = 0.05$, $\alpha = -0.1$, $q_y = 1$, $\sigma^2_{X,0} = \frac{\pi S_0}{2\zeta\omega_0^3 m^2} = 1$. Nielsen, Mørk og Thoft-Christensen (1990a).

Fig. 3-13 shows the time-dependent variation of the standard deviation for $X(t)$, $\dot{X}(t)$ and $Q(t)$ with post-yielding stiffness ratio $\alpha = 0.0$, corresponding to an ideal elastic-ideal plastic oscillator. From fig. 3-13a it is evident that equivalent linearization with Gaussian closure significantly underestimates the displacement variance. Moreover, the method predicts a stationary displacement variance in contrast to the characteristic variance drift displayed by the simulation result, resembling the linearly increasing variance in classical Brownian motion exposed to stationary Gaussian white noise. The cases b and d give almost identical results. Actually, the relative difference in the prediction of $\sigma_X(t)$, both in the example shown in fig 3-13a and the following examples in figs. 3-14 and 3-15, is everywhere below 0.4%. Consequently, it may be concluded that it is allowable to replace only the constitutive equation by a polynomial expansion. The difference between cases b and c can then be attributed primarily to the application of the ordinary cumulant neglect closure scheme in (3-252).

As reported by many authors, equivalent linearization is capable of describing the response characteristics for the velocity and the hysteretic restoring components, both of which attain stationarity. This is also the case for the present system. However, as shown in figs. 3-13b and 3.13c the closure approximations applied in cases b, c and d all give slightly improved results compared to those obtained by Gaussian closure.

In order to evaluate the applicability range for the proposed method, an investigation with various degrees of non-linearity represented by the post-yielding stiffness ratio α has been performed. The results for $\alpha = 0.1$ and $\alpha = -0.1$ for the time-varying standard deviation of the displacement are given in figs. 3-14 and 3-15. From these it may be concluded that the proposed approximate method in combination with an ordinary cumulant neglect closure scheme is generelly applicable and offers substantial improvements compared to equivalent linearization. The results for velocities and hysteretic restoring components have not been indicated, but they do not differ qualitatively from those shown in figures 3-13a and 3-13b. Notice that the case of softening post-yielding stiffness ratio $\alpha = -0.1$ implies instability in case of static loading on this branche.

In the present example a method for approximate stochastic analysis of hysteretic systems driven by Wiener processes is presented. The basic idea of the method, which is considered to be a generalization of equivalent linearization, is to replace the non-linear and non-analytical constitutive equations of the system with an equivalent polynomial expansion in the state variables entering these equations, leaving all linear and polynomial non-linear components unchanged. Next, the coefficients of the polynomial expansion are determined from a least mean square criterion. The constitutive equations of a structural system are normally specified within each structural element. The present method makes it possible to break down the problem of calibrating a tentative joint pdf of the state variables from system level to element level. This is because only the joint pdf of the state variables entering the constitutive equation of a certain structural element need to be specified in order to estimate the parameters of the polynomial expansion. Especially for multi degrees of freedom systems this turns out to be a decisive facilitation as demonstrated in example 3-5. The method is combined with an ordinary cumulant neglect closure of the global moment equations. The method has been applied to a bilinear SDOF system subjected to Gaussian white noise excitation, using an equivalent 3rd order polynomial expansion for the constitutive equation. The expansion coefficients are evaluated utilizing a 2-dimensional joint pdf based on a truncated Gram-Charlier series with a Minai-Suzuki modification. Comparison has been made both to equivalent linearization with Gaussian closure, to a closure scheme of the original system based on a truncated 3-dimensional Gram-Charlier series with a Minai-Suzuki modification, and to a scheme which makes it possible to evaluate the errors inherent in only replacing the non-analytical constitutive equations entering the drift vector with equivalent polynomial expansions. Results obtained from these cases have been compared to those obtained by Monte Carlo simulation. From the obtained results it is concluded that the assumption of only expanding the non-analytical constitutive equations gives insignificant errors. Further, the present method offers significant improvements compared to equivalent linearization with Gaussian closure. The main deviation of the method relative to a truncated 3-dimensional Gram-Charlier series with a Minai-Suzuki modification can then be attributed to the application of an ordinary cumulant neglect closure scheme in the global moment equations, where the discrete probabilities at the plastic branches

are ignored. A modified cumulant neglect closure scheme taking this problem into consideration for bilinear oscillators with an equivalent polynomial expansion is presented in the following example 3-4.

The equivalent polynomial expansion technique was proposed by Nielsen, Mørk and Thoft-Christensen (1990a), who also investigated the implications of replacing only the non-algebraic components with equivalent polynomial expansions, and of the application of ordinary cumulant neglect closure schemes in the resulting global moment equations.

Example 3-4: Reliability analysis of hysteretic systems driven by Wiener processes

During hysteretic deformations the micro-structure of the material is partly damaged due to dislocation migration, development of micro-cracks, etc. So-called damage indicators are introduced as a macroscopic measure of the integrated effect of such microscopic deterioration of the structural material over finite domains. Damage indicators are designated as global or local depending on whether they are controlling the damage in the entire structure or only in a part of it. Damage indicators should be included in the state vector in order to get a complete description of the instantanous state of the system. In order to close the integrated dynamic system differential equations must then be formulated, specifying the development of these new state variables. From the physics of the problem it is clear that any damage indicator will be an irreversible non-decreasing function with time. The right-hand sides of the said differential equations then become non-negative and non-linear functions of all introduced structural and damage state variables in their most general formulation. The non-linearity may even be non-analytical for some damage indicators, as demonstrated by (3-66), (3-70) and by the following equation (3-261).

In this example the SDOF bilinear oscillator defined by (3-47), (3-48), (3-50) is considered again. The excitation $F(t)$ on the right-hand side of (3-47) is obtained from filtration of non-stationary Gaussian white noise through a time-invariant rational filter of the order $(r, s) = (1, 2)$. $F(t)$ then becomes, cf. (3-36), (3-37)

$$F(t) = p_0 \dot{Y}(t) + p_1 Y(t) \qquad (3-259)$$

$$\ddot{Y} + q_1 \dot{Y} + q_2 Y = d(t) \dot{W}(t) \qquad (3-260)$$

where p_0, p_1, q_1, q_2 are constants. $\{W(t), t \in [0, \infty[\}$ signifies a unit intensity Wiener process, and $d(t)$ is a non-stationary deterministic modulation function.

The accumulated plastic energy dissipated by the system is used as damage indicator $D(t)$. The differential equation specifying the evolution of $D(t)$ becomes

$$\dot{D}(t) = (1-\alpha) q_y \Big(H(\dot{X}) H(Q - q_y) - H(-\dot{X}) H(-Q - q_y) \Big) \dot{X} = g(\dot{X}, Q) \dot{X}(t) \qquad (3-261)$$

(3-261) is easily derived from the sketch shown in fig. 3-1b. $H(\cdot)$ is the Heaviside unit step function given by (3-5). The equations of motion can then be written by (3-52) with the state vector, the diffusion vector and the drift vector given as follows, cf. (3-54)

$$\mathbf{Z}(t) = \begin{bmatrix} X(t) \\ \dot{X}(t) \\ Q(t) \\ D(t) \\ Y(t) \\ \dot{Y}(t) \end{bmatrix} \quad , \quad \mathbf{d}(t) = \begin{bmatrix} 0 \\ 0 \\ 0 \\ 0 \\ 0 \\ d(t) \end{bmatrix} \qquad (3-262a)$$

$$\mathbf{c}(\mathbf{Z}(t)) = \begin{bmatrix} \dot{X} \\ -2\zeta\omega_0\dot{X} - \omega_0^2(\alpha X + (1-\alpha)Q) + \frac{p_0}{m}\dot{Y} + \frac{p_1}{m}Y \\ \kappa(\dot{X},Q)\dot{X} \\ g(\dot{X},Q)\dot{X} \\ \dot{Y} \\ -q_1\dot{Y} - q_2 Y \end{bmatrix} \qquad (3-262b)$$

$\kappa(\dot{X},Q)$ is given by (3-50). (3-52) is solved with the initial values $\mathbf{Z}(0) = \mathbf{Z}_0 = \mathbf{0}$, i.e. the system is at rest and undamaged at the time $t = 0$. It follows that the functions $\kappa(\dot{X},Q)$ and $g(\dot{X},Q)$ fulfil the symmetry and anti-symmetry conditions

$$\kappa(\dot{X},Q) = \kappa(-\dot{X},-X) \qquad (3-263)$$

$$g(\dot{X},Q) = -g(-\dot{X},-Q) \qquad (3-264)$$

In case of zero initial values, (3-263) implies that $E[X^l(t)\dot{X}^m(t)Q^n(t)] = 0$ for odd values of $l+m+n$.

$d(t)$ specifies the intensity of the white noise. This is assumed in the following form, Saragoni and Hart (1974)

$$d(t) = d_0 \exp\left(-b\left(\frac{t}{T_m} - \ln\frac{t}{T_m} - 1\right)\right) \qquad (3-265)$$

T_m is the time of maximum intensity d_0, and b is a limiting decay rate of the excitation. d_0 is specified so it produces a prescribed value of the stationary standard deviation $\sigma_{X,0}$ of the corresponding linear system under stationary excitation. d_0 is then related to $\sigma_{X,0}$ as follows

$$d_0 = \sqrt{\frac{2e_4(e_3^2 + e_1^2 e_4 - e_1 e_2 e_3)}{e_3 - e_1 e_2}} \cdot \sigma_{X,0} \qquad (3-266)$$

where

$$\left.\begin{array}{lll} e_1 = q_1 + 2\zeta\omega_0 & , & e_2 = q_2 + \omega_0^2 + 2\zeta\omega_0 q_1 \\ e_3 = 2\zeta\omega_0 q_2 + \omega_0^2 q_1 & , & e_4 = \omega_0^2 q_2 \end{array}\right\} \qquad (3-267)$$

The relation (3-266) can be derived from a well-known result for the stationary variance of a linear system with rational frequency response function exposed to Gaussian white noise, see e.g. Nielsen (1990).

The system is assumed to fail, whenever the damage indicator exceeds a critical value d_{cr} for the first time. Since, $D(t)$ is non-decreasing with probability 1 the first-passage time probability distribution function of the problem becomes

$$F_{T_1}(t) = 1 - F_{D(t)}(d_{cr}) \qquad (3-268)$$

Hence, the reliability problem is reduced to the determination of the probability distribution function $F_{D(t)}(d)$ of the damage indicator $D(t)$. More generally, when an n_3-dimensional damage indicator vector $\mathbf{D}(t)$ has been defined as in (3-74), the structure is assumed to operate safely, when $\mathbf{D}(t) \in S_t$, where $S_t \subset R^{n_3}$. In this case $F_{T_1}(t)$ becomes

$$F_{T_1}(t) = 1 - \int_{S_t} f_{\mathbf{D}(t)}(\mathbf{d})\, d\mathbf{d} \qquad (3-269)$$

where $f_{\mathbf{D}(t)}(\mathbf{d})$ signifies the joint probability density function of the damage vector $\mathbf{D}(t)$.

The objective of the present example is primarily to determine the distribution of $D(t)$ in terms of its time-varying moments by means of an equivalent polynomial expansion of the drift vector (3-262b). In example 3-3 it has been demonstrated that application of an ordinary cumulant neglect closure scheme in the global moment equations in connection with the equivalent polynomial expansion technique leads to reduced accuracy of the estimated moments. Actually, when the equivalent polynomial expansion coefficients are evaluated by means of a closing scheme taking the discrete probability mass at the plastic branches into consideration, simultanous application of an ordinary cumulant neglect closure scheme ignoring such probabilities seems to be inconsistent. For this reason a modification of the ordinary cumulant neglect closure scheme based on the same 2-dimensional Gram-Charlier type A expansion with a Minai-Suzuki modification (3-257), (3-258), as used at the evaluation of the equivalent polynomial expansion coefficients has also been suggested in the example.

Only the non-linear and non-analytical components $\kappa(\dot{X},Q)\dot{X}$ and $g(\dot{X},Q)\dot{X}$ of the drift vector (3-262b) are replaced by equivalent polynomial expansion, whereas the remaining linear components are kept unchanged. As shown in example 3-3 this will only introduce insignificant errors compared to a complete polonomial expansion of all components. The equivalent polynomial expansions must meet the symmetry and anti-symmetry properties (3-263) and (3-264). For $\kappa(\dot{X},Q)\dot{X}$ the relevant cubic polynomial expansion is given by (3-254) with the equivalent cubic expansion coefficient determined from (3-256). For $g(\dot{X},Q)\dot{X}$ the corresponding expansion reads, cf. (3-240)

$$g(\dot{X},Q)\dot{X} = A_4 + C_{422}\dot{X}^2 + C_{423}\dot{X}Q + C_{433}Q^2 \qquad (3-270)$$

The expansion coefficients of (3-270) are determined from the least square criterion, leading to the following system of linear equations

$$\begin{bmatrix} 1 & \mu_{22} & \mu_{23} & \mu_{33} \\ & \mu_{2222} & \mu_{2223} & \mu_{2233} \\ \text{symm.} & & \mu_{2233} & \mu_{2333} \\ & & & \mu_{3333} \end{bmatrix} \begin{bmatrix} A_4 \\ C_{422} \\ C_{423} \\ C_{433} \end{bmatrix} = \begin{bmatrix} 0 \\ E[\dot{X}^2 g] \\ E[\dot{X}Qg] \\ E[Q^2 g] \end{bmatrix} \qquad (3-271)$$

The expectations on the left-hand side of (3-271) are all provided by the joint moment equation (3-252) at closure at the order $N = 4$. The expectations on the right-hand side are obtained by the 2-dimensional closure scheme (3-257), (3-258).

Equivalent linearization corresponds to $C_{imn} = D_{imnp} = 0$ in (3-240). (3-271) then gives $A_4 = 0$. This means that all the coefficients in (3-270) are zero. Consequently, damage indicators for which (3-264) is fulfilled cannot be analysed by equivalent linearization techniques.

Consider the auxiliary vector $\mathbf{V}^T(t) = [X, \dot{X}, V, D, Y, \dot{Y}]$ and its sub-vector $\mathbf{V}_0^T(t) = [X, D, Y, \dot{Y}]$ with the joint pdfs $f_{\mathbf{V}}(\mathbf{v},t)$ and $f_{\mathbf{V}_0}(\mathbf{v}_0,t)$. Instead of (3-221) the following scheme is suggested

$$f_{\mathbf{Z}}(\mathbf{z},t) = f_{\mathbf{V}}(\mathbf{z},t) + \delta(q-q_y) f_{\mathbf{V}_0}(\mathbf{z}_0,t) \int_{q_y}^{\infty} f_{\dot{X}V}(\dot{x},u)du +$$

$$\delta(-q-q_y) f_{\mathbf{V}_0}(\mathbf{z}_0,t) \int_{-\infty}^{-q_y} f_{\dot{X}V}(\dot{x},u)du \qquad (3-272)$$

The difference between (3-221) and (3-272) is that $\mathbf{V}_0(t)$ and $[\dot{X},q]$ have been assumed mutually independent in the evaluation of the discrete probabilities. This is merely a formal setting. The right-hand side of (3-272) will still be calibrated to represent all provided moments of the moment equations at closure at a certain order N. The benefit of the formulation (3-272) is that the same

2-dimensional Gram-Charlier type A expansion with a Minai-Suzuki modification (3-257), (3-258) as used in the evaluation of the expectation in (3-256) may be applied without further calculations of Hermite moments. From (3-272) the following expression can be derived for the joint central moments of the order $L = i+j+k+l+m+n$

$$E[X^i \dot{X}^j Q^k D^l Y^m \dot{Y}^n] = E[X^i \dot{X}^j Q^k D^l Y^m \dot{Y}^n]_0 + E[X^i D^l Y^m \dot{Y}^n]_0 \cdot P_{jk} \qquad (3-273)$$

where

$$P_{jk} = \int_{-\infty}^{\infty} \int_{q_y}^{\infty} \dot{x}^j (q_y^k - u^k) f_{\dot{X}V}(\dot{x}, u) d\dot{x} du + \int_{-\infty}^{\infty} \int_{-\infty}^{-q_y} \dot{x}^j ((-q_y)^k - u^k) f_{\dot{X}V}(\dot{x}, u) d\dot{x} du \qquad (3-274)$$

$E[\cdot]_0$ signifies expectations with respect to the joint pdf $f_{\mathbf{V}}(\mathbf{v}, t)$. For $L \leq N$ these can all be expressed in terms of the provided joint moments upon solving the linear equations (3-273). However, since $f_{\mathbf{V}}(\mathbf{v}, t)$ has been assumed to be monomodal and almost Gaussian, joint moments $E[X^i \dot{X}^j Q^k D^l Y^m \dot{Y}^n]_0$, $L > N$, appearing on the right-hand side of (3-273) can all be expressed in terms of similar moments of order $L \leq N$ by means of an ordinary cumulant neglect closure and hence by the provided joint moments. In what follows this approach will be referred to as the modified cumulant neglect closure scheme for bilinear oscillator with an equivalent polynomial expansion.

The following approximate methods have been investigated:

a: Monte Carlo simulation.

b: Cubic polynomial expansion with an ordinary cumulant neglect closure scheme.

c: Cubic polynomial expansion with a modified cumulant neglect closure scheme.

To verify the obtained results, a numerical Monte-Carlo simulation has been carried out. Generation of realizations of a broad-banded zero mean Gaussian process was performed by the method of Penzien, Clough and Penzien (1974). The integrated dynamic system (3-52), (3-262) was solved by a 4th order Runge-Kutta scheme, with the initial conditions $\mathbf{Z}(0) = \mathbf{0}$. The time step was selected as $\Delta t = \frac{T_0}{50}$, $T_0 = \frac{2\pi}{\omega_0}$ being the period of linear, undamped eigenvibrations. The sample size of ensemble response time-histories was 5000, from which the relevant response statistics were determined. The moment estimates stabilized already after 1000 realizations.

The following system data, all in SI-units, are used in the example

$$\left.\begin{array}{llllll} m = 1.0 & , & \omega_0 = 1.0 & , & \zeta = 0.01 & , \quad \alpha = 0.0 \quad , \quad q_y = 1.0 \\ p_0 = 0.0 & , & p_1 = 1.0 & , & q_1 = 2.0 & , \quad q_2 = 4.0 \\ b = 0.20 & , & T_m = 9.0 & , & \sigma_{X,0} = 2.0 & \end{array}\right\} \qquad (3-275)$$

Notice that an ideal elasto-plastic oscillator has been considered ($\alpha = 0.0$). Further, $\frac{\sigma_{X,0}}{q_y} = 2.0$ corresponds to a relatively strong excitation, so the considered system should be classified as highly non-linear.

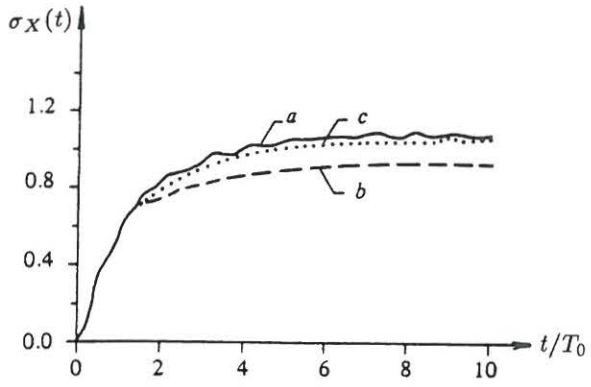

Fig. 3-16: Time-dependent standard deviation of displacement response, $\sigma_X(t)$. Nielsen, Mørk and Thoft-Christensen (1990b).

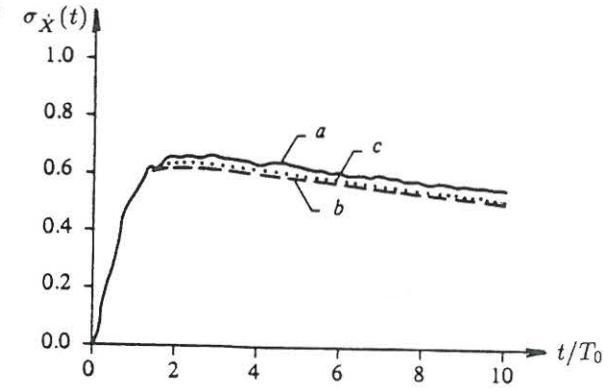

Fig. 3-17: Time-dependent standard deviation of velocity response, $\sigma_{\dot{X}}(t)$. Nielsen, Mørk and Thoft-Christensen (1990b).

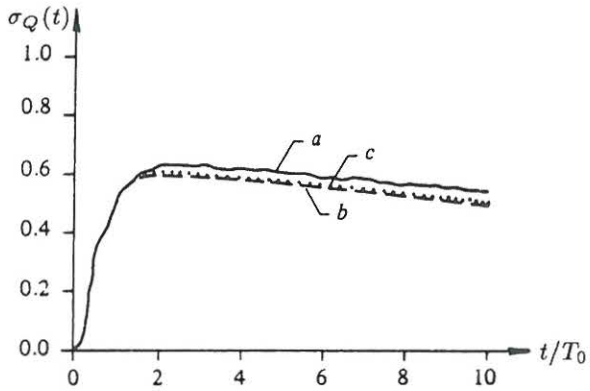

Fig. 3-18: Time-dependent standard deviation of hysteretic component, $\sigma_Q(t)$. Nielsen, Mørk and Thoft-Christensen (1990b).

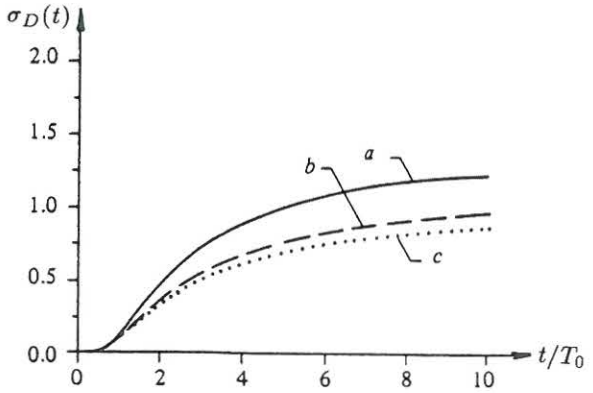

Fig. 3-19: Time-dependent standard deviation of damage component, $\sigma_D(t)$. Nielsen, Mørk and Thoft-Christensen (1990b).

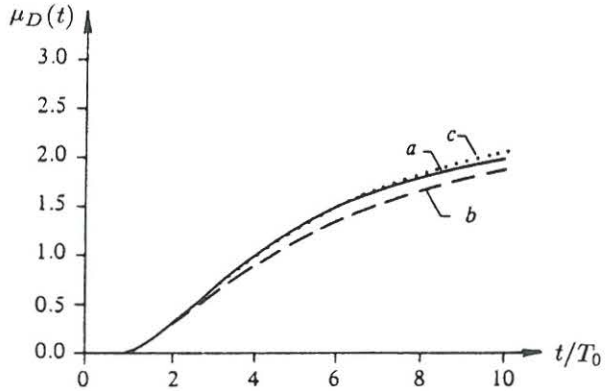

Fig. 3-20: Time-dependent mean value function of damage component, $\mu_D(t)$. Nielsen, Mørk and Thoft-Christensen (1990b).

Fig. 2-16 shows the time-dependent variation of the standard deviation of the displacement $X(t)$. Time has been normalized with respect to $T_0 = \frac{2\pi}{\omega_0}$. As seen the modified cumulant neglect closure scheme produces significantly better results than the ordinary cumulant neglect closure scheme. Figs. 2-17 and 2-18 show the corresponding time-dependent variation of the standard deviations of the velocity $\dot{X}(t)$ and the hysteretic component $Q(t)$. Again, the modified closure scheme produces the best results in comparison to those obtained by Monte Carlo simulation, although both schemes give acceptable results for these components as expected. Figs. 2-19 and 2-20 show the time-dependence of the standard deviation and the mean value function of the damage component $D(t)$, respectively. The ordinary cumulant closure scheme produces slightly better results than the modified closure scheme. However, both closure schemes underestimate the standard deviation significantly. In contrast, the modified cumulant neglect closure scheme produces very accurately estimates for the mean value function, which is underestimated by the ordinary cumulant neglect scheme. The general conclusion that can be drawn from these results is that the modified cumulant neglect closure scheme provides more accurate predictions than the conventional cumulant neglect closure scheme. From the physics of the problem and the inherent properties of the modification (3-272) this is believed to be the case for any system undergoing heavy yielding.

The application of the equivalent polynomial expansion technique to non-linear and non-analytical damage indicator differential equations was suggested in Nielsen, Mørk and Thoft-Christensen (1990b), where also the indicated modified cumulant neglect closure scheme was presented.

Example 3-5: Stochastic response analysis of hysteretic multi-storey frames under earthquake excitation

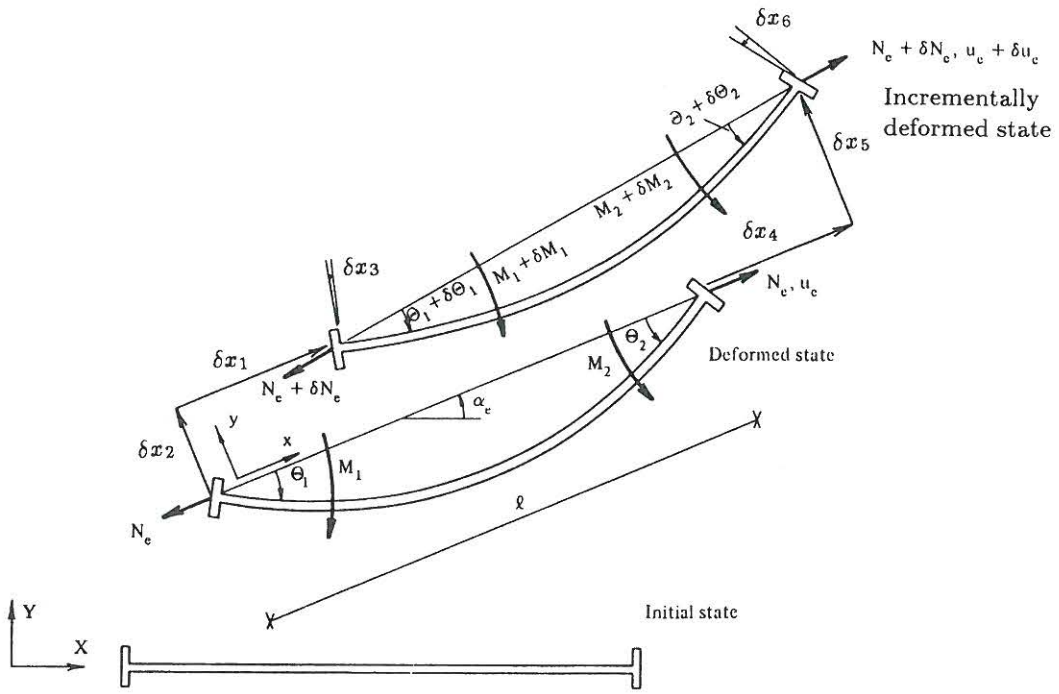

Fig. 3-21: Plane beam element in initial state, deformed state and incrementally deformed state.

Fig. 3-21 shows a plane beam element in the initial unloaded state, in the deformed state and in the incrementally changed deformed state. The generalized strains of the element are selected as

$$\mathbf{q}_e = \begin{bmatrix} \Theta_e \\ u_e \end{bmatrix} \tag{3-276}$$

$\Theta_e^T = (\Theta_1, \Theta_2)$ signifies the member end rotations relative to the chord line and u_e is the elongation along the chord line with signs as defined in fig. 3-21. The generalized stresses conjugated to $\mathbf{q}_e$ are

$$\mathbf{Q}_e = \begin{bmatrix} \mathbf{M}_e \\ N_e \end{bmatrix} \tag{3-277}$$

$\mathbf{M}_e^T = [M_1, M_2]$ are the member end section moments, and N_e is the axial force along the chord line in the deformated state. The rate of the internal degrees of freedom $\dot{\mathbf{q}}_e$ is related to the rates of nodal point degrees of freedom $\mathbf{x}_e^T = [\dot{x}_1, \ldots, \dot{x}_6]$, with components defined relative to the local element fixed (x, y, z)-coordinate system shown in fig. 3-21, through the geometrical conditions

$$\dot{\mathbf{q}}_e = \mathbf{g}_e \dot{\mathbf{x}}_e \tag{3-278}$$

where

$$\mathbf{g}_e = \begin{bmatrix} 0 & -1/l & -1 & 0 & 1/l & 0 \\ 0 & 1/l & 0 & 0 & -1/l & 1 \\ -1 & 0 & 0 & 1 & 0 & 0 \end{bmatrix} \tag{3-279}$$

l is the chord length of the beam element in the deformed state. $\mathbf{g}_e$ is the geometrical matrix at element level, relating external and internal degrees of freedom.

The beam elements are assumed to follow an elasto-plastic behaviour. Hence, the existence of a strain rate independent yield function, $f_e(\mathbf{Q}_e)$, is assumed, which separates elastic states, $f_e(\mathbf{Q}_e) < 0$, and plastic states, $f_e(\mathbf{Q}_e) = 0$. For the sake of simplicity $fe(\mathbf{Q}_e)$ is assumed to be differentiable. Using plastic potential theory with the associated flow rule the incremental constitutive equation can be written, cf. (3-57)

$$\dot{\mathbf{Q}}_e = \boldsymbol{\kappa}_e(\dot{\mathbf{q}}_e, \mathbf{Q}_e)\dot{\mathbf{q}}_e \tag{3-280}$$

$$\boldsymbol{\kappa}_e(\dot{\mathbf{q}}_e, \mathbf{Q}_e) = \boldsymbol{\kappa}_{e,0}(\mathbf{Q}_e) - H(\dot{\lambda})H(f_e(\mathbf{Q}_e))\frac{\boldsymbol{\kappa}_{e,0}\frac{\partial f_e}{\partial \mathbf{Q}_e^T}\left(\frac{\partial f_e}{\partial \mathbf{Q}_e^T}\right)^T\boldsymbol{\kappa}_{e,0}}{\left(\frac{\partial f_e}{\partial \mathbf{Q}_e^T}\right)^T\boldsymbol{\kappa}_{e,0}\frac{\partial f_e}{\partial \mathbf{Q}_e^T}} \tag{3-281}$$

$$\dot{\lambda} = \frac{\left(\frac{\partial f_e}{\partial \mathbf{Q}_e^T}\right)^T\boldsymbol{\kappa}_{e,0}\dot{\mathbf{q}}_e}{\left(\frac{\partial f_e}{\partial \mathbf{Q}_e^T}\right)^T\boldsymbol{\kappa}_{e,0}\frac{\partial f_e}{\partial \mathbf{Q}_e^T}} \tag{3-282}$$

$\boldsymbol{\kappa}_{e,0}$ signifies the local incremental elastic stiffness matrix , which may depend on $\mathbf{Q}_e$ in case of non-linear elasticity, $\dot{\lambda}$ is the plastic potential multiplier and $H(x)$ is the Heaviside unit step function as given by (3-5). Generalization of (3-280) to hardening plasticity and to non-differential yield surfaces is straightforward using the classical plasticity theory. Hardening rules require the introduction of extra state variables to be included in the integrated state vector of the dynamic system, see Mørk (1989).

In the present case (3-280) will be specified with the following additional assumptions

1: The material is assumed to be linear elastic perfectly plastic, and all unloadings are linear elastic with unchanged elasticity modulus.

2: Axial forces have negligible influence on the load-bearing capacity.

3: External loads are applied at system nodes, i.e. all elements are free of external loading.

The elements act as a yield hinge element with plastic deformations confined to the end sections. Further, the axial elongations are assumed to be linear elastic. Hence

$$\dot{N}_e = \frac{AE}{l}\dot{u}_e \qquad (3-283)$$

where A is the cross-sectional area and E is the modulus of elasticity. For the remaining internal degrees of freedom, the stiffness matrix equation (3-280), can be written

$$\boldsymbol{\kappa}_e(\dot{\Theta}_e, \mathbf{M}_e) = (1-\alpha_1)(1-\alpha_2)\boldsymbol{\kappa}_0 + \alpha_1(1-\alpha_2)\boldsymbol{\kappa}_1 + \alpha_2(1-\alpha_1)\boldsymbol{\kappa}_2 \qquad (3-284)$$

$$\boldsymbol{\kappa}_0 = \frac{2EI_0}{l}\begin{bmatrix} 2 & -1 \\ -1 & 2 \end{bmatrix},\ \boldsymbol{\kappa}_1 = \frac{3EI_0}{l}\begin{bmatrix} 0 & 0 \\ 0 & 1 \end{bmatrix},\ \boldsymbol{\kappa}_2 = \frac{3EI_0}{l}\begin{bmatrix} 1 & 0 \\ 0 & 0 \end{bmatrix} \qquad (3-285)$$

where I_0 denotes the bending moment of inertia. The indicator function, α_i, can be written

$$\alpha_i(\dot{\Theta}_i, M_i) = H(-M_y + M_i)(1 - H(-\dot{\Theta}_i)) + H(-M_y - M_i)(1 - H(\dot{\Theta}_i)),\ i = 1,2 \qquad (3-286)$$

where M_y is the yield moment. It follows from equation (3-286) that

$\alpha_i = 1$ when yield hinge i is open and loaded,

$\alpha_i = 0$ when yield hinge i is closed or is at the point of being unloaded into the elastic range.

The above-mentioned assumption 2 may not be valid if the axial forces are sufficiently large, and the storey drift is substantial. However, such $P-\delta$ effects can be taken approximately into consideration by a slight modification of the indicated expression for the incremental stiffness matrix.

Below, the loading process $\mathbf{F}(t)$ in (3-55) is obtained by filtering amplitude modulated Gaussian white noise through a Kanai-Tajimi-filter, Tajimi (1973), with filter parameters ζ_g, ω_g, corresponding to the case $(r,s) = (1,2)$ in (3-36), (3-37). Neglecting linear viscous damping (3-55), (3-57) then attains the form

$$\mathbf{M}\ddot{\mathbf{X}} + \mathbf{K}_0\mathbf{X} + \mathbf{g}^T\mathbf{Q} = \mathbf{M}\mathbf{U}(2\zeta_g\omega_g\dot{Y} + \omega_g^2 Y) \qquad (3-287)$$

$$\ddot{Y} + 2\zeta_g\omega_g\dot{Y} + \omega_g^2 Y = -\ddot{u}_g(t) = -d(t)\dot{W}(t) \qquad (3-288)$$

$$\dot{\mathbf{Q}} = \boldsymbol{\kappa}(\dot{\mathbf{q}}, \mathbf{Q})\dot{\mathbf{q}} \qquad (3-289)$$

$\mathbf{X}(t)$ of the dimension n_1 contains the global translational and rotational degrees of freedom measured relative to the ground surface. $\mathbf{Q}(t)$ of the dimension n_2 is an assemblage of the generalized stresses $\mathbf{Q}_e(t)$ from all plastic elements. The global geometrical matrix $\mathbf{g}$ of the dimension $n_2 \times n_1$ contains the local geometrical matrices $\mathbf{g}_e$ given by (3-279) transformed to global coordinates. $\mathbf{U}$ of the dimension $n_1 \times 1$ is a vector specifying the stiff-body motion of all global degrees-of-freedom due to a unit horizontal translation of the ground surface. Finally, (3-289) represents an assemblage of local constitutive relations (3-280). The local stiffness matrices $\boldsymbol{\kappa}_e(\dot{\mathbf{q}}_e, \mathbf{Q}_e)$ appear as block-matrices in $\boldsymbol{\kappa}(\dot{\mathbf{q}}, \mathbf{Q})$. $\{W(t), t \in [0, \infty[\}$ is a unit intensity Wiener process and $d(t)$ is a deterministic modulation function.

The Kanai-Tajimi filter may be interpreted physically as a shear response model of a sub-soil overlaying a bedrock. ω_g and ζ_g are then the undamped circular frequency and damping ratio of the sub-soil in shear, $Y(t)$ is the ground surface displacement relative to the bedrock, and $\ddot{u}_g(t)$ signifies the horizontal acceleration time-series at the top of the bedrock. This interpretation is valid as long as the mass of the structural system is negligible compared to the mass of the sub-soil within a characteristic area surrounding the structure, i.e. that no significant feed-back from the structure occurs in the coupled soil-structure dynamic problem.

The state vector formulation of the system is then given by, cf. (3-58), (3-59)

$$\left.\begin{aligned} &d\mathbf{Z}(t) = \mathbf{c}(\mathbf{Z}(t))dt + \mathbf{d}(t)dW(t),\ t > 0 \\ &\mathbf{Z}(0) = \mathbf{0} \end{aligned}\right\} \qquad (3-290)$$

$$\mathbf{Z}(t) = \begin{bmatrix} \mathbf{X} \\ \dot{\mathbf{X}} \\ \mathbf{Q} \\ Y \\ \dot{Y} \end{bmatrix},\ \mathbf{c}(\mathbf{Z}(t)) = \begin{bmatrix} \dot{\mathbf{X}} \\ -\mathbf{M}^{-1}(\mathbf{K}_0\mathbf{X} + \mathbf{g}^T\mathbf{Q}) + \mathbf{U}(2\zeta_g\omega_g\dot{Y} + \omega_g^2 Y) \\ \boldsymbol{\kappa}(\mathbf{g}\dot{\mathbf{X}}, \mathbf{Q})\mathbf{g}\dot{\mathbf{X}} \\ \dot{Y} \\ -2\zeta_g\omega_g\dot{Y} - \omega_g^2 Y \end{bmatrix},\ \mathbf{d}(t) = \begin{bmatrix} \mathbf{0} \\ \mathbf{0} \\ \mathbf{0} \\ 0 \\ -d(t) \end{bmatrix} \qquad (3-291)$$

It is assumed that the following symmetry conditions are fulfilled

$$\boldsymbol{\kappa}(\mathbf{Z}(t)) = \boldsymbol{\kappa}(-\mathbf{Z}(t)) \ \wedge\ \mathbf{g}(\mathbf{Z}(t)) = \mathbf{g}(-\mathbf{Z}(t)) \qquad (3-292)$$

Then, the symmetry properties (3-250) are also valid. Together with the initial values $\mathbf{Z}(0) = \mathbf{0}$ the equivalent cubic expansion (3-251) and the moment equations (3-252) are then valid.

The idea of the present method is to replace the constitutive equations (3-280) by equivalent cubic polynomial expansions in the local state variables $\mathbf{Q}_e$ and $\dot{\mathbf{q}}_e$, where the equivalent cubic expansion coefficients are determined at element level by a least square criterion. The global cubic expansion coefficients B_{ij} and D_{ijkl} can next be synthesized from the local expansions by a transformation and assemblage procedure. Compared to the global least square procedure for the determination of B_{ij} and D_{ijkl} as follows from (3-253) some accuracy is lost at the expense of obtaining a much simpler identification procedure. Hence, the local constitutive equation (3-280) is replaced with the following equivalent cubic expansion

$$\left(\boldsymbol{\kappa}_e(\dot{\mathbf{q}}_e, \mathbf{Q}_e)\dot{\mathbf{q}}_e\right)_\alpha \simeq b_{\alpha A}R_{e,I} + d_{\alpha IJK}R_{e,I}R_{e,J}R_{e,K}\ ,\ \alpha = 1, \cdots, n_{2,e} \qquad (3-293)$$

where $R_{e,I}$ is a component of the $2n_{2,e}$ dimensional sub-state vector $\mathbf{R}_e$, defined by

$$\mathbf{R}_e = \begin{bmatrix} \dot{\mathbf{q}}_e \\ \mathbf{Q}_e \end{bmatrix} \qquad (3-294)$$

and $n_{2,e}$ is the dimension of $\mathbf{Q}_e$ or $\mathbf{q}_e$. In (3-294) summation convention has been assumed over dummy indexes I, J, K over the range 1 to $2n_{2,e}$.

The theory has been applied to the simply supported two-storey single bay frame shown in fig. 3-22. μ_i, A_i, I_i and $M_{y,i}$ specify the mass per unit length, cross-sectional area, bending second moment of inertia and yield moment of element i, respectively. All elements have the same moduli of elasticity. For all members the yield hinge model with the incremental stiffness matrices (3-284), (3-285) and a consistent mass matrix are applied. The frame is loaded by horizontal acceleration forces f_1, f_2 applied symmetrically to the system nodes. Deformations of the frame will then be asymmetric and the symmetry can be utilized to reduce the problem as shown in fig. 3-22b. Further, high frequency modes corresponding to the axial degrees-of-freedom X_1, X_4 have been condensed from the system by a Guyan-like reduction scheme. Hence, the global displacement vector of dimension $n_1 = 4$ becomes

$\mathbf{X}^T(t) = [X_2(t), X_3(t), X_5(t), X_6(t)]$. The intensity function $d(t)$ of the excitation process $\{\ddot{u}_g(t)\}$ is assumed to be constant for $t > 0$, and all earthquake excitations are horizontal in the plane of the frame. The system data are shown in table 3-2.

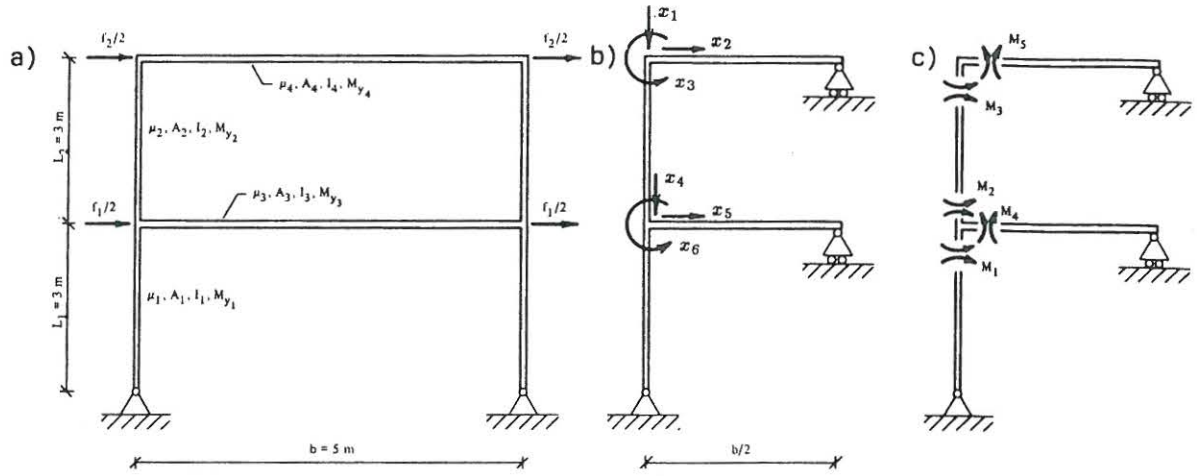

Fig. 3-22: a) Two-storey frame. Geometrical and physical designations. b) Global degrees of freedom. c) Designation of potential yield hinges.

Beam	μ_i (kg/m)	A_i (10^{-3}m^2)	I_i (10^{-5}m^4)	$M_{y,i}$ (10^3 Nm)
1	46·0	5·86	2·63	80
2	46·0	5·86	2·63	80
3	2000	∞	3·89	90
4	1000	∞	1·945	40

Table 3-2: System data for the two-storey frame. $E = 2.1 \cdot 10^{11}$ N/m^2, $\omega_g = 15.6s^{-1}$, $\zeta_g = 0.6$, $d^2 = 0.15$ m$^2/s^3$.

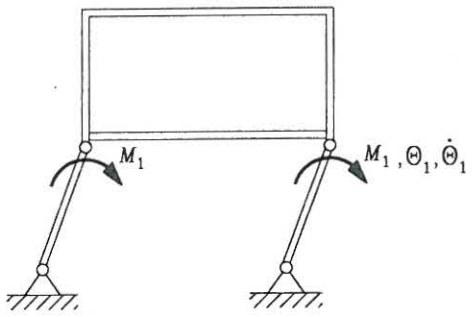

Fig. 3-23: Assumed plastic deformation.

For the present frame it will be assumed that primarily the lower columns behave plastically, see fig. 3-23. For this reason an equivalent cubic expansion for the constitutive relation for this beam element will be introduced, whereas equivalent linear expansions are introduced for the remaining

beam elements 2, 3 and 4. In principle all beam elements are then assumed to be plastic, so $\mathbf{K}_0 = \mathbf{0}$ in (3-287). For the simply supported beams elements 1, 3 and 4 in fig. 3-22b only a single generalized stress variable, selected as the end-section moments M_1, M_4 and M_5 from fig. 3-22c, need to be introduced. The state vector of the integrated system of dimention $n = 15$ then becomes $\mathbf{Z}^T(t) = [\mathbf{X}^T(t), \dot{\mathbf{X}}^T(t),\ M_1, \ldots, M_5, Y(t), \dot{Y}(t)]$. Using $\alpha_1 = 1$ in (3-284), the constitutive equation relating M_1 to the conjugated end-section rotation Θ_1, reads

$$\kappa(M_1, \dot{\Theta}_1)\dot{\Theta}_1 = 3\frac{EI_1}{l_1}(1 - \alpha_2(M_1, \dot{\Theta}_1))\dot{\Theta}_1 \qquad (3-295)$$

(3-295) is replaced by the following equivalent system with a cubic polynomial expansion in M_1, and $\dot{\Theta}_1$

$$(\kappa(M_1, \dot{\Theta}_1)\dot{\Theta}_1)_{eq} = b_1 M_1 + b_2\dot{\Theta}_1 + d_1 M_1^3 + d_2 M_1^2\dot{\Theta}_1 + d_3 M_1\dot{\Theta}_1^2 + d_4\dot{\Theta}_1^3 \qquad (3-296)$$

The expansion coefficients in equation (3-296) are determined from the least mean square criterion, which leads to the following system of linear equations, similar to equation (3-253)

$$\begin{bmatrix} E[M_1^2] & E[M_1\dot{\Theta}_1] & E[M_1^4] & E[M_1^3\dot{\Theta}_1] & E[M_1^2\dot{\Theta}_1^2] & E[M_1\dot{\Theta}_1^3] \\ & E[\dot{\Theta}_1^2] & E[M_1^3\dot{\Theta}_1] & E[M_1^2\dot{\Theta}_1^2] & E[M_1\dot{\Theta}_1^3] & E[\dot{\Theta}_1^4] \\ & & E[M_1^6] & E[M_1^5\dot{\Theta}_1] & E[M_1^4\dot{\Theta}_1^2] & E[M_1^3\dot{\Theta}_1^3] \\ & \text{Symm.} & & E[M_1^4\dot{\Theta}_1^2] & E[M_1^3\dot{\Theta}_1^3] & E[M_1^2\dot{\Theta}_1^4] \\ & & & & E[M_1^2\dot{\Theta}_1^4] & E[M_1\dot{\Theta}_1^5] \\ & & & & & E[\dot{\Theta}_1^6] \end{bmatrix} \begin{bmatrix} b_1 \\ b_2 \\ d_1 \\ d_2 \\ d_3 \\ d_4 \end{bmatrix} = \begin{bmatrix} E[M_1\dot{\Theta}_1\kappa] \\ E[\dot{\Theta}_1^2\kappa] \\ E[M_1^3\dot{\Theta}_1\kappa] \\ E[M_1^2\dot{\Theta}_1^2\kappa] \\ E[M_1\dot{\Theta}_1^3\kappa] \\ E[\dot{\Theta}_1^4\kappa] \end{bmatrix} \qquad (3-297)$$

The expectations on the left- and right-hand sides of equation (3-297) are evaluated by means of an approximate joint pdf $f_{M_1\dot{\Theta}_1}(m, \dot{\theta})$ of M_1 and $\dot{\Theta}_1$. The marginal pdf of M_1 is of mixed type with a continuous part for $m \in]-M_{y,1}, M_{y,1}[$, and discrete probabilities for $m = -M_{y,1}$ and $m = M_{y,1}$, formally represented by delta functions. This fact is displayed by the following tentative joint pdf based on a Hermite moment closure at the order $N = 4$ with a Minai-Suzuki (1985) type of modification

$$f_{M_1\dot{\Theta}_1}(m, \dot{\theta}) = f_{V\dot{\Theta}_1}(m, \dot{\theta}) + \delta(m - M_{y,1})\int_{M_{y,1}}^{+\infty} f_{V\dot{\Theta}_1}(u, \dot{\theta})du + \delta(-m - M_{y,1})\int_{-\infty}^{-M_{y,1}} f_{V\dot{\Theta}_1}(u, \dot{\theta})du,$$

$$(m, \dot{\theta}) \in [-M_{y,1}, M_{y,1}]\times]-\infty, \infty[\qquad (3-298)$$

$$f_{V\dot{\Theta}_1}(m, \dot{\theta}) = \frac{1}{\sigma_V\sigma_{\dot{\Theta}_1}}\varphi\left(\frac{m}{\sigma_V}\right)\varphi\left(\frac{\dot{\theta}}{\sigma_{\dot{\Theta}_1}}\right)\sum_{i+j=0}^{N}\gamma_{ij}H_i\left(\frac{m}{\sigma_V}\right)H_j\left(\frac{\dot{\theta}}{\sigma_{\dot{\Theta}_1}}\right),\ N = 4 \qquad (3-299)$$

where the standard deviations σ_V and $\sigma_{\dot{\Theta}_1}$ as well as the Hermite moments $\gamma_{ij}(t)$ are evaluated with respect to the auxiliary continuous joint pdf $f_{V\dot{\Theta}_1}(m, \dot{\theta})$.

Due to the symmetry condition (3-292) it follows that $\gamma_{ij} = 0$, $i + j$ odd. Moreover, $\gamma_{00} = 1$ and $\gamma_{20} = \gamma_{02} = 0$. The remaining 8 non-trivial free parameters, including σ_V and $\sigma_{\dot{\Theta}}$, are determined from the following joint moment relations similar to (3-223)

$$E[M_1^k\dot{\Theta}_1^l] = \sigma_V^k\sigma_{\dot{\Theta}_1}^l\sum_{i+j=0}^{4}\gamma_{ij}r_{l,j}s_{k,i}\left(\frac{M_{y,1}}{\sigma_{M_1}}\right) \qquad (3-300)$$

where $r_{l,j}$ and $s_{k,i}(\beta)$ are given by (3-224) and (3-225). The calculation of $E[M_1^k \dot{\Theta}^l]$ is explained below. Rather than using (3-300) σ_V is determined from the transcendent equation

$$E[M_1^2] = \sigma_V^2 s_{2,0}\left(\frac{M_{y,1}}{\sigma_V}\right) \qquad (3-301)$$

Equation (3-301) implies that $\gamma_{40} = 0$. This restriction has been imposed in order to prevent negative side loops of the approximate joint pdf, and has the consequence that this quantity cannot be calibrated to $E[M_1^4]$.

For the general beam element with yield hinges at both ends the equivalent constitutive relation (3-293) is used. With $n_{2,e} = 2$ this contains 4 linear terms and 20 cubic terms. Consequently, a total of 48 different expansion coefficients enters the polynomial expansion. These are determined from a system of linear symmetric equations similar to equation (3-297).

The equivalent to equation (3-298) for this case can also be given, Nielsen, Mørk and Thoft-Christensen (1989). The tentative pdf must display the discrete probabilities that one hinge is yielding and the other hinge is elastic, or both hinges are yielding. The latter formally occurs as a product of two delta functions in the tentative joint pdf.

$\dot{\Theta}_1(t)$ is related to the global degrees of freedom $\mathbf{X}(t)$ through the compatibility condition

$$\dot{\Theta}_1 = -\frac{\dot{X}_5(t)}{l_1} + \dot{X}_6(t) \qquad (3-302)$$

The expectations $E[M_1^k \dot{\Theta}_1^l], k+l \leq 4$, on the left-hand side of (3-300) can then be related to the provided moments $\mu_{i_1 i_2 \cdots i_n}(t)$, $n \leq 4$ upon insertion of (3-302) and expanding the expectation. Further, if (3-302) is inserted into the equivalent cubic expansion (3-296), and the result is introduced into the drift vector (3-291) the global tensor components B_{im} and D_{imnp} of the equivalent cubic expansion (3-251) can be evaluated.

It should be emphasized that even if the exact least mean square solution to the coefficients in equation (3-296) could be obtained, this would not necessarily provide exact estimates of the joint central moments, when inserted into equation (3-252) as stated by the theorem on p. 143. This is because only the constitutive equations are represented by an equivalent polynomial expansion, whereas the expansion coefficients of equation (3-251) in principle should originate from an equivalent cubic representation of all components of the drift vector, whether these are linear or not. However, as learned from example 3-3 these additional errors are quite ignorable.

Finally, the resulting moment equations (3-252) are closed by the cumulant neglect closure scheme (3-193).

To verify the results obtained by the present approximate method, a numerical simulation study based on the Monte Carlo technique has been carried out. Generation of realizations of a broad-banded, zero mean and stationary Gaussian process was performed by the method of Penzien, Clough and Penzien (1974).

The differential equations were solved by a 4th order Runge-Kutta scheme, with the initial conditions $\mathbf{X}(0) = \mathbf{0}$. The time step was selected as $\Delta t = T_0/300$. The sample size of response time-histories was 2000. For each of these the system equations have been integrated from 0 to 6 T_0, where the fundamental period of linear eigenvibrations is $T_0 = 0.98$ s.

The following approximate methods have been investigated:

a: equivalent linearization using Gaussian closure

b: equivalent linearization using (3-298), (3-299) with $N = 2$

c: cubic series expansion in yield hinge 1 using (3-298), (3-299) with $N = 4$

d: cubic series expansion in yield hinge 1 using (3-298), (3-299) with $N = 4$

In cases a and b the constitutive relations in all 5 yield hinges have been linearized. However, in case b the expansion coefficients of the equivalent linear system have been calculated from a more realistic joint pdf of the state variables. In cases c and d the cubic expansion equation (3-296) has been applied to yield hinge 1, where excessive yielding is likely to take place. For the remaining yield hinges equivalent linearization with Gaussian closure is applied in case c, whereas equivalent linearization using (3-298), (3-299) with $N = 2$ is applied in case d.

From figs. 3-24 and 3-25 it is evident that equivalent linearization with Gaussian closure significantly underestimates the displacement response of the upper and lower storey. Utilizing the more realistic pdf as in case b to determine the linearization constants improve the results only slightly. Further, it is seen that equivalent linearization in both cases predicts a stationary variance response in contradiction to the characteristic drift in the storey displacement displayed by the simulation result and by cases c and d. Further, the standard deviations of the 2 storeys approach each other as time goes by. This behaviour can be explained with respect to the deformation mode shown in fig. 3-23. Ignoring the elastic deformations of the upper storey, the frame deforms as an SDOF ideal elastic-plastic oscillator. The non-stationary variance response under stationary Gaussian excitation is similar to the time-linear variance response in classical Brownian motion. The indicated analysis shows that this effect is hidden in the joint central moments of the 4th order, whereas closure at 2nd order (covariance level) will always predict a stationary response.

As reported by many authors, equivalent linearization is capable of describing the response characteristics for velocities and end-section moments. This is indeed the case for the present system. In figs. 3-26 and 3-27 the velocity response for the upper and lower storey is shown. The cubic expansion of (3-296) is seen to improve the result compared to the simulation result. The time-dependent standard deviations of the end-section moments M_1 and M_5 are shown in figs. 3-28 and 3-29.

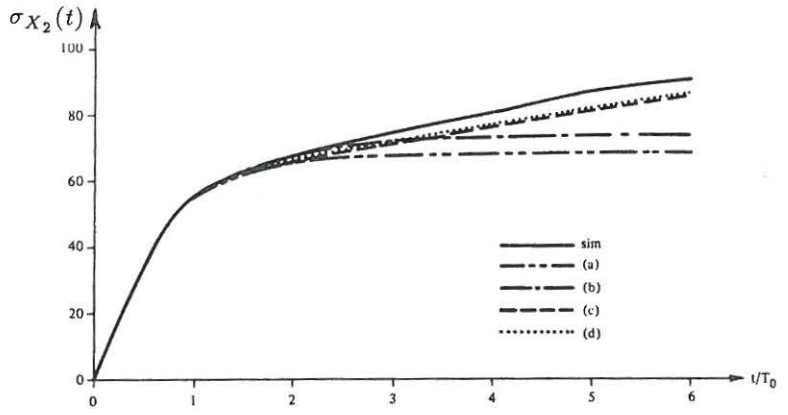

Fig. 3-24: Time-dependent standard deviation of upper storey displacement.
Nielsen, Mørk and Thoft-Christensen (1989).

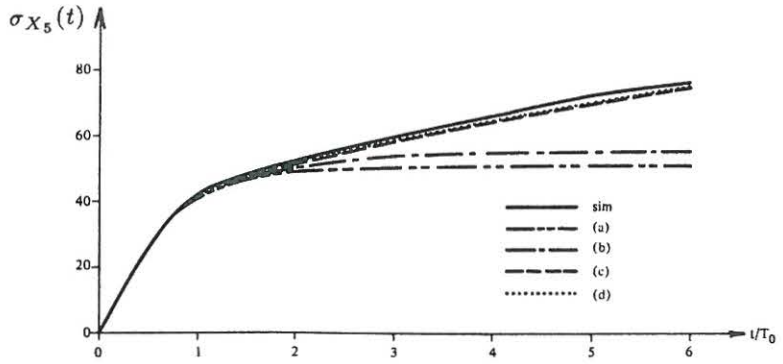

Fig. 3-25: Time-dependent standard deviation of lower storey displacement. Nielsen, Mørk and Thoft-Christensen (1989).

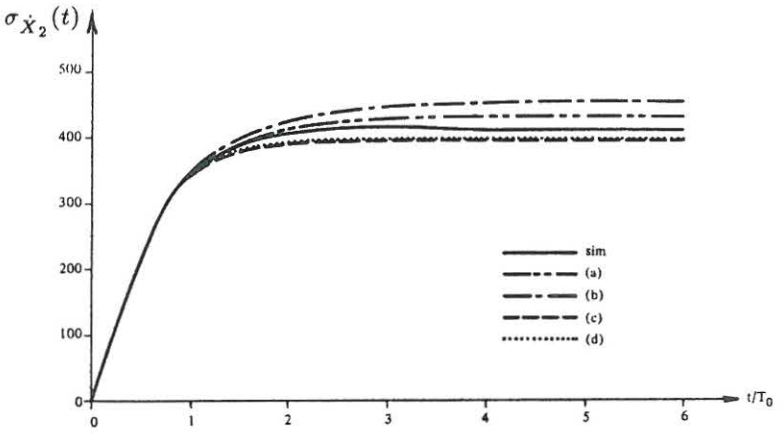

Fig. 3-26: Time-dependent standard deviation of upper storey velocity. Nielsen, Mørk and Thoft-Christensen (1989).

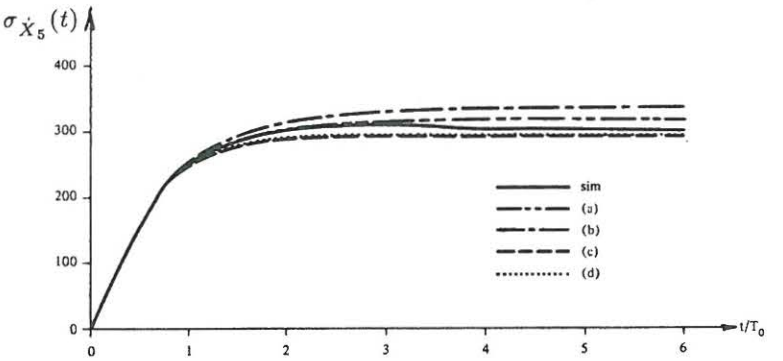

Fig. 3-27: Time-dependent standard deviation of lower storey displacement. Nielsen, Mørk and Thoft-Christensen (1989).

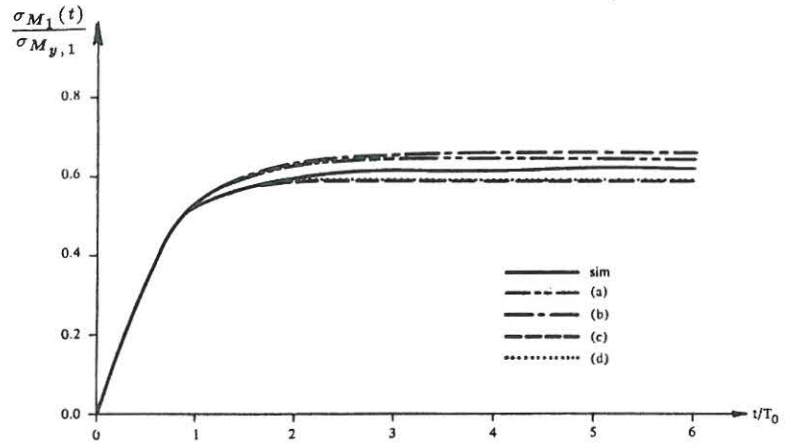

Fig. 3-28: Time-dependent standard deviation of end-section moment of lower columns. Nielsen, Mørk and Thoft-Christensen (1989).

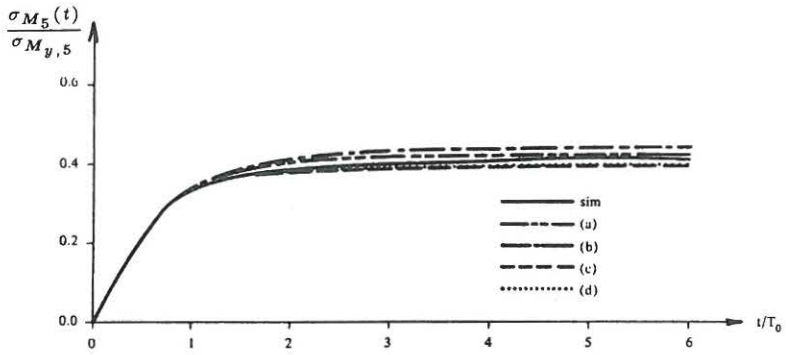

Fig. 3-29: Time-dependent standard deviation of end-section moment of upper storey beam element. Nielsen, Mørk and Thoft-Christensen (1989).

In the present example a method is presented for approximate stochastic analysis of hysteretic, framed structures. The basic idea of the method is to replace the non-analytical and non-linear constitutive equations of beam elements, which are likely to be exposed to severe damage, with an equivalent cubic expansion in the state variables entering these equations. For the remaining beam elements an equivalent linear expansion or a linear elastic analysis is performed. The expansion coefficients of the equivalent polynomial expansions are evaluated by means of a mean least square criterion, where unprovided expectations are evaluated using a truncated Gram-Charlier series in terms of univariate Hermite polynomials with a Minai-Suzuki modification. The global hierarchy of joint central moments is next closed at the order $N = 4$ by means of a cumulant neglect closure scheme. The method has been applied to a two-storey linear elastic-ideal plastic framed structure subjected to Gaussian white noise of relatively high intensity, filtered through a Kanai-Tajimi filter. For comparison a Monte Carlo simulation analysis has been performed. From this it is concluded that equivalent linearization procedures give qualitatively and quantitatively erroneous results. Only if equivalent cubic expansions are introduced for the most exposed elements a Brownian motion type of non-stationary variance drift

can be reproduced. Being a moment equation procedure the method suffers from the well-known drawback that the calculation time increases dramatically with the dimension n of the state vector and the order N of the closure scheme. A system reduction of the external degrees of freedom, e.g. by means of Guyan reduction as in the example, should be performed and the number of plastic elements critically selected.

The indicated method was presented by Nielsen, Mørk and Thoft-Christensen (1989). Previous to that time Baber and Wen (1982) and Baber (1986) have presented methods for hysteretic frames, where the yield hinges are replaced by hysteretic springs with a Bouc-Wen type of constitutive relations between moments and spring rotations. Since equivalent linearization was applied, these results are confined to relatively small plastic deformations. Casciati and Farivelli (1984) used an identical analytical technique. The calculated Gaussian response inherent in the equivalent linearization technique was used to calculate the structural reliability based on certain damage measures. Such an approach is only possible in case of very small plastic deformations.

Example 3-6: Reliability analysis of saturated sand deposits under earthquake excitation

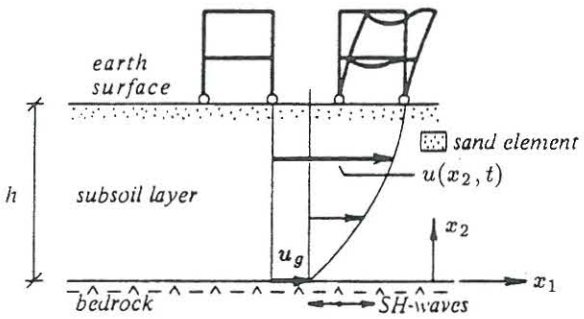

Fig. 3-30. Subsoil layer under earthquake excitation.

Fig. 3-30 shows a saturated sand layer of thickness h covering a rock surface. During an earthquake SH-waves propagate from bedrock upwards through the sand layer. The horizontal displacements at the surface of the bedrock $u_g(t)$ and of the sandlayer $u(x_2,t)$ are assumed to occur under plane strain condition, where x_2 is a vertical coordinate measured from the bedrock surface towards the free surface, and x_1 is the horizontal coordinate axis parallel with the direction of the bedrock displacements. During an earthquake, shear stresses $\sigma_{12}(x_2,t)$ act on the planes perpendicular to the coordinate axes with irregularly varying sign and magnitude.

In the present example the relevance of damage equations of the type (3-261) for saturated sand deposits under earthquake excitation will be investigated and verified in cases where liquefaction is considered the principal failure mode of the soil. Liquefaction is loss of strength due to pore pressure built up during cyclic loads of soil. In complete analogy with the failure event defined in example 3-4 liquefaction in soil is assumed to take place, when the accumulated energy dissipated in a certain unit volume reaches a critical limit. The rate of dissipated energy per unit volume is given by

$$\dot{E} = 2\sigma_{12}\dot{\epsilon}_{12} \qquad (3-303)$$

where $\dot{\epsilon}_{12}$ signifies the shear strain rate.

Test specimens	Vestbjerg Sand	Lund No. 0
Mean diameter d (mm)	0.11	0.40
Uniformity U	3.6	1.7
Void ratio e	0.62	0.63
Density index I	0.77	0.70

Table 3-3: Properties of test sands.

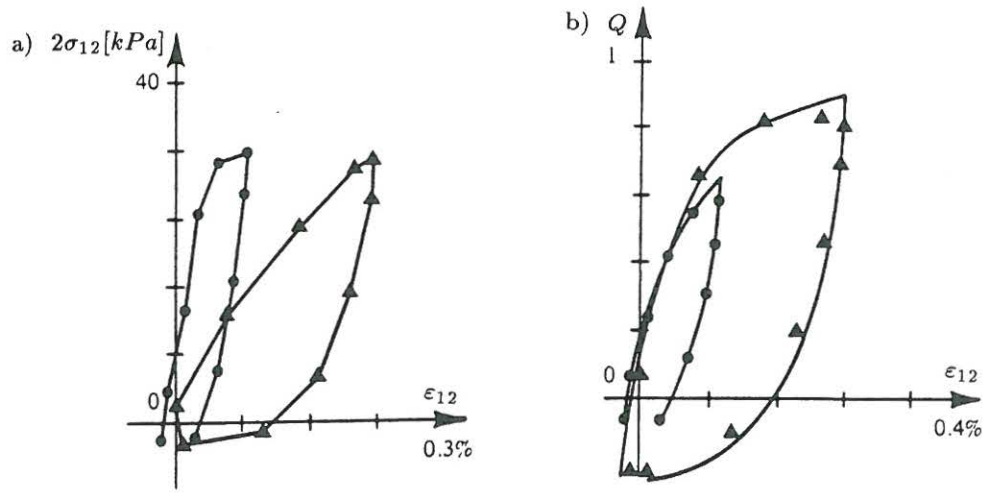

Fig. 3-31. Hysteretic curves. a) Stress versus strain. b) Mobilization factor versus strain. Test results with calibrated Bouc-Wen representation.

Fig. 3-31a shows the stress-strain relationship obtained by triaxial testing for the samples described in table 3-3. The behaviour of the sand is seen to be strongly hysteretic. Fig. 3-31b shows the same results using the socalled mobilization factor $Q(t) = \frac{\sigma_{12}}{\sigma_{12,y}}$ as dependent variable. $\sigma_{12,y} = \sigma_{12,y}(t)$ signifies the shear strength at the time t. Notice, that the mobilization factor is usually defined as the fraction of the deviatoric stress to its maximum value, and consequently refers to 3-dimensional stress states. The present interpretation only applies to the considered case of pure shear. From the tests it was concluded, that the shear strength $\sigma_{12,y}(t)$ and the elastic shear modulus $\mu(t)$, defined as the averaged slope of the hysteretic loops, both decrease from initial values $\sigma_{12,y}(0)$ and $\mu(0)$ as the pore pressure builds up. An interesting finding was that the deterioration of these quantities was almost proportional, i.e.

$$\frac{\mu(x_2,t)}{\sigma_{12,y}(x_2,t)} \simeq \frac{\mu(x_2,0)}{\sigma_{12,y}(x_2,0)} \simeq 1800 \qquad (3-304)$$

The figure 1800 applies to all considered tests and even for different sorts of sand. Apparently, the hysteretic loops in fig. 3-31b is much smoother than those in fig. 3-31a. As shown by the unbroken curve in fig. 3-31b the hysteresis related to the mobilization factor may then be represented by the Bouc-Wen hysteretic model (3-48), (3-51). For applications of the Bouc-Wen model the following normalized shear strain turns out to be useful

$$X(t) = 2\frac{\mu(t)}{\sigma_{12,y}(t)}\varepsilon_{12}(t) = 2\frac{\mu(0)}{\sigma_{12,y}(0)}\varepsilon_{12}(t) \qquad (3-305)$$

Per definition $Q(t)$ is restricted to the interval $]-1,1[$, so $q_y = 1.0$ must be used in (3-51). The best fit was obtained with $\beta = 1.0$, $\gamma = 0.0$, $n = 0.5$ for the other Bouc-Wen parameters. Again, these values applied to all tests and all investigated sorts of sand.

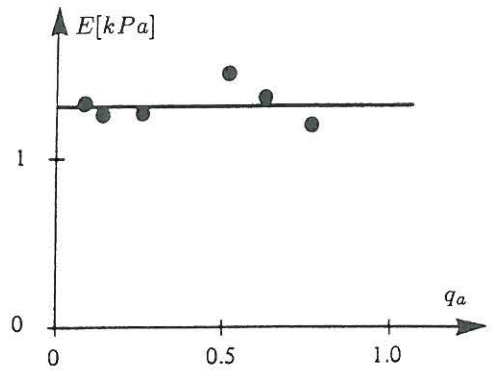

Fig. 3-32: Measured value of damage indicator in cyclical testing with variable amplitude q_a.

As a damage measure the accumulated energy per unit volume is introduced, normalized with respect to the quantity $\frac{\sigma^2_{12,y}(x_2,0)}{\mu(x_2,0)}$. The normalization factor may be interpreted as twice the strain energy per unit volume, if linear elastic deformations were present up to the maximum shear stress $\sigma_{12,y}(x_2,0)$. Introducing the mobilization factor and the generalized strain defined by (3-305) in (3-301), the differential equation specifying the development of the damage indicator can be written

$$\dot{D}(t) = f(D)\ Q\dot{X}(t) \qquad (3-306)$$

where the following non-dimensional function has been introduced

$$f(D) = \frac{\sigma_{12,y}(t)}{\sigma_{12,y}(0)} = \frac{\mu(t)}{\mu(0)} \qquad (3-307)$$

As seen, the consecutive deterioration of the strength and the stiffness have been related to the damage parameter through the non-dimensional function $f(D)$. The validity of (3-306) has been verified in fig. 3-32, where the value of $E(t)$ at liquefaction has been measured for 6 cyclic tests performed at different stress amplitudes q_a. Under complete liquefaction corresponding to $D(t) = d_{cr}$ the shear strength vanishes, so $f(D) \to 0$ as $D \to d_{cr}$. An appropriate assumption for the unknown function $f(D)$ then is

$$f(D) = \begin{cases} 1 - \left(\frac{D}{d_{cr}}\right)^l & , \quad D < d_{cr} \\ 0 & , \quad D \geq d_{cr} \end{cases} \qquad (3-308)$$

Equation (3-208) does not describe the test results in full detail, and the value of l has to be estimated by experience. l seems to vary in the interval $]0.5, 2.0]$. To omit the problem of specifying this parameter the following linear expansion will be applied

$$f(D) \simeq C_{423} + D_{4234} D \quad , \quad C_{423} = 1 \quad , \quad D_{4234} = -\frac{1}{d_{cr}} \qquad (3-309)$$

In the numerical example simulation results based on (3-308) with $l = 0.5$ will be compared with the analytical results obtained using (3-309) Insertion of the expansion (3-309) into (3-306) provides a polynomial expansion similar to (3-270). The major difference is that (3-206), (3-309) is a polynomial expansion of the original system, whereas (3-270) is a polynomial expansion of an equivalent system, which will produce the same moments as the original system up to some order under certain specified conditions.

The indicated damage indicator may be used in a reliability analysis in the considered context of ordinary stochastic differential equations, if the sublayer continuum is appropriately discretized. In this connection the following shape functions for the shear stress and for the shear strain may be used

$$\sigma_{12}(x_2,t) = \sigma_{12}(0,t)\left(1-\left(1-\frac{\mu(h,D)}{\mu(0,D)}\right)\xi\right)\Phi'(\xi) \quad , \quad \xi = \frac{x_2}{h} \tag{3-310}$$

$$\varepsilon_{12}(x_2,t) = \varepsilon_{12}(0,t)\Phi'(\xi) \tag{3-311}$$

$\Phi(\xi)$ is a non-dimensional shape function, fulfilling the boundary conditions $\Phi(0) = \Phi'(1) = 0$, and normalized so $\Phi'(0) = 1$. $\Phi'(\xi)$ signifies the derivative with respect to ξ. In (3-310) the shear modulus $\mu(x_2, D)$ has been assumed to vary linearly between a minimum value $\mu(h, D)$ at the free surface to the maximum value $\mu(0, D)$ at the surface of the bedrock, i.e.

$$\mu(x_2,D) = \mu(0,D)\left(1-\left(1-\frac{\mu(h,D)}{\mu(0,D)}\right)\frac{x_2}{h}\right) \tag{3-312}$$

The equation of motion for the shear layer reads

$$\frac{\partial\sigma_{12}(x_2,t)}{\partial x_2} = \rho\frac{\partial^2 u(x_2,t)}{\partial t^2} \simeq \rho\left(2h\Phi\left(\frac{x_2}{h}\right)\ddot{\varepsilon}_{12}(0,t) + \ddot{u}_g(t)\right) \tag{3-313}$$

where ρ is the mass density of the soil, and the indicated approximation for the displacement field follows from integration of (3-311). Next, (2-313) is multiplied with the variational field followed by an integration over $[0, h]$, resulting in the SDOF equation of motion

$$2\ddot{\varepsilon}_{12}(0,t) + \omega_0^2\frac{\sigma_{12}(0,t)}{\mu(0,0)} = -\frac{a_0}{h}\ddot{u}_g(t) \tag{3-314}$$

where a_0 is the mode participation factor and ω_0 is the circular eigenfrequency of the sublayer defined as

$$a_0 = \frac{\int_0^1 \Phi(\xi)d\xi}{\int_0^1 \Phi^2(\xi)d\xi} = (1.180) \tag{3-315}$$

$$\omega_0^2 = \frac{\int_0^1 \left(1-\left(1-\frac{\mu(h,0)}{\mu(0,0)}\right)\xi\right)(\Phi'(\xi))^2 d\xi}{\int_0^1 \Phi^2(\xi)\,d\xi}\cdot\frac{\mu(0,0)}{\rho h^2} = \left(1.620\,\frac{\mu(0,0)}{\rho h^2}\right) \tag{3-316}$$

In (3-216), the fraction $\frac{\mu(h,D)}{\mu(0,D)}$ has been assumed constant and equal to its initial undamaged value $\frac{\mu(h,0)}{\mu(0,0)}$ as a further assumption. As shape function the first undamped eigenvibration mode is used, fulfilling the eigenvalue problem

$$\left.\begin{array}{l} \frac{d}{d\xi}\left(\left(1-(1-\frac{\mu(h,0)}{\mu(0,0)})\xi\right)\frac{d}{d\xi}\Phi(\xi)\right) + \frac{\rho h^2}{\mu(0,0)}\omega_0^2\,\Phi(\xi) = 0 \\ \Phi(0) = \Phi'(1) = 0\ ,\ \Phi'(0) = 1 \end{array}\right\} \tag{3-317}$$

The results for a_0 and ω_0^2 in the outermost right-hand brackets of (3-315) and (3-316) relate to solution of (3-317) for $\frac{\mu(h,0)}{\mu(0,0)} = \frac{1}{10}$. Notice that the product $\frac{\rho h^2}{\mu(0,0)}\omega_0^2$ in (3-317), and hence $\Phi(\xi)$, is independent of $\frac{\rho h^2}{\mu(0,0)}$ as follows from (3-216). Finally, upon eliminating $\varepsilon_{12}(0,t)$ and $\sigma_{12}(0,t)$ in favour of the generalized strain $X(t)$ and the mobilization factor $Q(t)$ at the surface of the bedrock, (3-314) can be written in the form (3-47) as follows

$$\ddot{X}(t) + \omega_0^2 f(D) Q(t) = F(t) \qquad (3-318)$$

$$F(t) = -\frac{a_0}{h}\frac{\mu(0,0)}{\sigma_{12,y}(0,0)} \cdot \ddot{u}_g(t) \qquad (3-319)$$

It is interesting to compare (3-318) to the SDOF model (3-75) for RC-structures. In both cases the hysteretic fraction $(1-\alpha)$ of the restoring force is dependent on the damage parameter. However as specified by $f(D)$, the hysteretic fraction has the opposite variation from 1 to 0 in the present case as the liquefaction develops.

Nielsen, Thoft-Christensen and Moust Jakobsen (1989) applied the described dynamic model (3-48), (3-51), (3-306), (3-318) to a reliability analysis of the problem defined in fig. 3-30. The loading process $F(t)$ was modelled by the non-stationary white noise filtration (3-259), (3-260), (3-265) with the following parameters of the output equation (3-259) and amplitude of the intensity function (3-265)

$$p_0 = 0 \quad , \quad p_1 = -\frac{a_0}{h}\frac{\mu(0,0)}{\sigma_{12,y}(0,0)} \quad , \quad d_0 = \sqrt{2 q_1 q_2}\ \sigma^0_{\ddot{u}_g} \qquad (3-220)$$

The specified expressions for p_0 and p_1 mean that the auxiliary variable $Y(t)$ in (3-259), (3-260) can be identified directly as the bedrock acceleration $\ddot{u}_g(t)$. The indicated expression for d_0 implies, that the stationary surface bedrock accelerations at stationary white noise excitation become equal to $\sigma^0_{\ddot{u}_g}$. The constitutive equation for the hysteretic component $Q(t)$ was approximated with the following equivalent linear expansion, cf. (3-246)

$$\left(\kappa(\dot{X}, Q)\dot{X}\right)_{eq} = B_{32}\dot{X} + B_{33}Q \qquad (3-321)$$

Equivalent linearization of the Bouc-Wen model was first suggested by Wen (1980), who applied a Gaussian closure scheme for the evaluation of the equivalent expansion coefficients, leading to (3-249). In the present case the 2-dimensional version of the Hermite moment neglect closure scheme (3-196) at the order $N = 2$ has been applied instead. (3-309) was truncated at the indicated 1st order level, resulting in a cubic expansion of (3-306). The resulting moment equations (4-352) were closed at the order $N = 4$ by means of an ordinary cumulant neglect closure scheme.

To verify the obtained results, a numerical Monte-Carlo simulation has been carried out. Generation of realizations of a broad-banded zero mean Gaussian process was performed by the method of Penzien, Clough and Penzien (1974). The integrated dynamic system (3-51), (3-52), (3-262), (3-306), (3-308), (3-318) was solved by a 4th order Runge-Kutta scheme, with the initial conditions $\mathbf{Z}(0) = \mathbf{0}$. The time step was selected as $\Delta t = \frac{T_0}{50}$, $T_0 = \frac{2\pi}{\omega_0}$ being the period of linear, undamped eigenvibrations. The sample size of ensemble response time-histories was 1000.

The following data in agreement with test results have been used in the numerical study

$$\left.\begin{array}{lll}
\omega_0 = 11.06\ \mathrm{s}^{-1} & , \ a_0 = 1.180 & , \ h = 30.5\ \mathrm{m} \\
\rho = 1850\ \mathrm{kg/m}^3 & , \ l = 0.5 & , \ d_{cr} = 119 \\
\mu(0,0) = 2.18 \cdot 10^8\ \mathrm{Pa} & , \ \mu(h,0) = 2.18 \cdot 10^7\ \mathrm{Pa} & , \ \sigma_{12,y}(0,0) = 1.21 \cdot 10^5\ \mathrm{Pa} \\
\beta = 1.0 & , \ \gamma = 0.0 & , \ n = 0.5 \\
b = 0.2 & , \ T_m = 1\ \mathrm{s} & , \ \sigma^0_{\ddot{u}_g} = 4.5\ \mathrm{m/s}^2 \\
q_1 = 14.25\ \mathrm{s}^{-1} & , \ q_2 = 242.1\ \mathrm{s}^{-2} &
\end{array}\right\} \qquad (3-322)$$

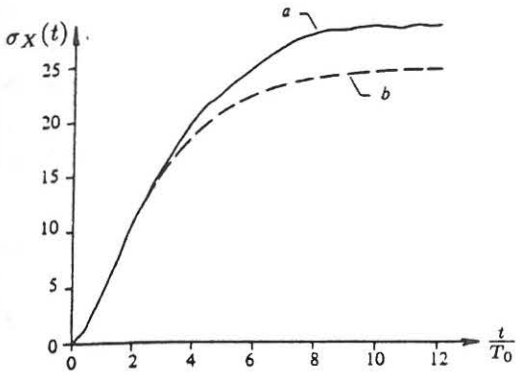

Fig. 3-33: Time-dependent standard deviation of normalized strain, $\sigma_X(t)$. Nielsen, Thoft-Christensen and Moust Jakobsen (1989).

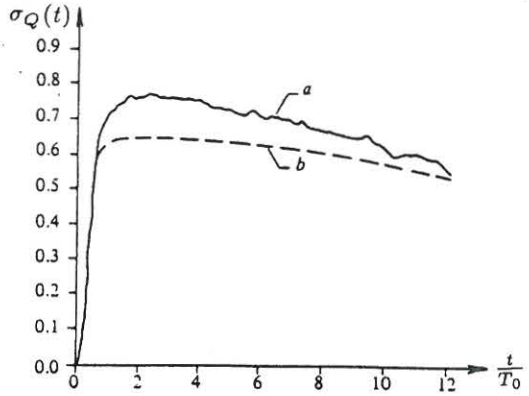

Fig. 3-34: Time-dependent standard deviation of mobilization factor, $\sigma_Q(t)$. Nielsen, Thoft-Christensen and Moust Jakobsen (1989).

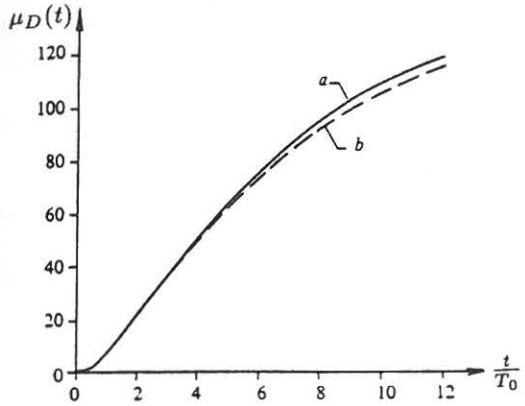

Fig. 3-35: Time-dependent mean value function of damage component, $\mu_D(t)$. Nielsen, Thoft-Christensen and Moust Jakobsen (1989).

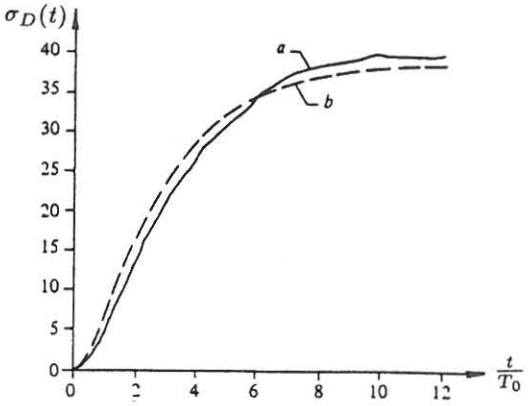

Fig. 3-36: Time-dependent standard deviation of damage component, $\sigma_D(t)$. Nielsen, Thoft-Christensen and Moust Jakobsen (1989).

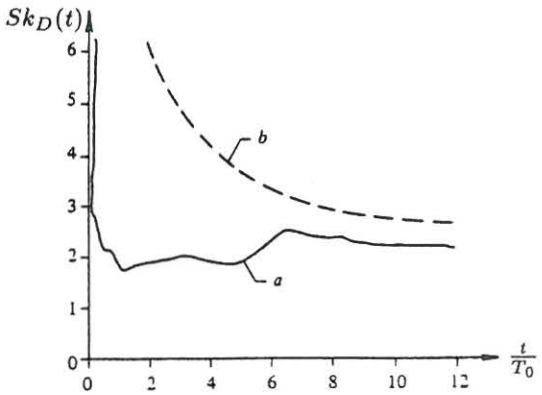

Fig. 3-37: Time-dependent skewness of damage parameter, $Sk_D(t)$. Nielsen, Thoft-Christensen and Moust Jakobsen (1989).

In the figs. 3-33 - 3-37 time dependent response statistics for $X(t)$, $Q(t)$ and $D(t)$ have been shown. Curve a indicates results obtained by Monte Carlo simulation and curve b results from equivalent polynomial expansion. Time has been normalized with respect to the period of linear eigenvibrations $T_0 = \frac{2\pi}{\omega_0}$. Fig. 3-33 shows the time dependence of the standard deviation of $X(t)$. Apparently, equivalent linearization underestimates the variance response of the normalized strain $X(t)$, confirming the similar observations in examples 3-3 and 3-5. In fig. 3-34 the standard deviation of the mobilization factor $Q(t)$ is shown. Again, in agreement with previous observations equivalent linearization produces results in acceptable agreement with simulation for this quantity. $Q(t)$ indicates the shear stress normalized to the present shear strength. Hence, the slight decrease of $\sigma_Q(t)$ with time is not due to the deterioration of the shear strength, but should be attributed to the the decreasing intensity of the excitation process, cf. (3-265). Figs. 3-35 - 3-37 show the time dependence of the mean value function, the standard deviation and the skewness coefficient of the damage indicator $D(t)$. The latter quantity is defined as $Sk_D(t) = E[(D(t) - \mu_D(t))^3]/\sigma_D^3(t)$. A good agreement between semi-analytical and simulated results is obtained for the mean value function and for the standard deviation, whereas the semi-analytical values for the skewness coefficient are only acceptable for $\frac{t}{T_0} > 8$. This verifies that a precise modelling of the $f(D)$ is not nescessary, as long as only the lower-order momemts of $D(t)$ are requested. The considered severe earthquake with $\sigma_{\ddot{u}_g^0} = 4.5\frac{m}{s^2}$ causes mean damage values larger than $d_{cr} = 119$ at the end of the considered interval, indicating a high risk for liquefaction.

In the present example it was demonstrated that liquefaction in saturated sand deposits under earthquake excitation is highly correlated to the accumulated dissipated energy in the soil. Secondly, it was demonstrated that the hysteretic behaviour of the so-called mobilization factor may be modelled by a Bouc-Wen model with parameters that apply to all tests and to all considered sorts of sand. Finally, a SDOF model for the sublayer was formulated, with cubic polynomial expansion of the damage equation based on a linear expansion of the function $f(D)$, and an equivalent linear expansion of the Bouc-Wen constitutive equation. The accelerations of the bedrock surface was modelled by a non-stationary rational filtration of Gaussian white noise.

The indicated SDOF model is primarily aimed at a relatively crude modelling of single layered deposits. A MDOF generalization, aimed at more accurate modelling of single layer or multilayered subsoils, was devised by Mørk and Nielsen (1990).

Example 3-7: Modified cumulant neglect closure of two-well potential oscillator and modified closure scheme for the Bouc-Wen oscillator

In this example the modified cumulant neglect closure scheme for the two-well potential problem will be compared to the results obtained by ordinary cumulant neglect closure scheme at the orders $N = 2,\ 4$ for the parameter values $\frac{\pi S_0}{2\zeta\omega_0^3 m^2} = 1$, $\omega_0 = 1$, $\zeta = 0.01$.

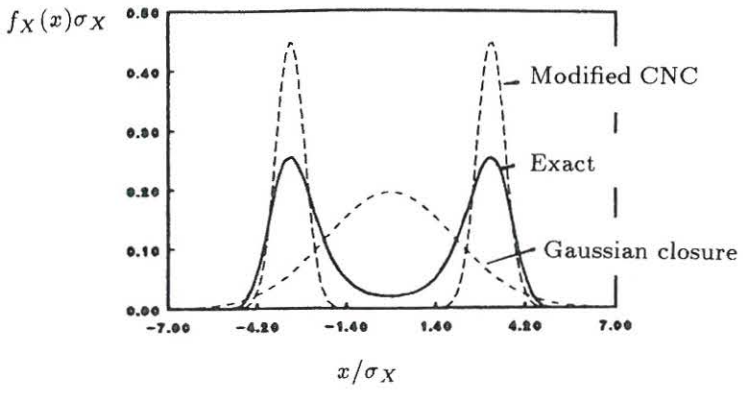

Fig. 3-38: Stationary probability density function of displacement component of two-well potential SDOF oscillator and equivalent replacements at closure at the order $N = 2$. $\frac{\pi S_0}{2\zeta\omega_0^3 m^2} = 1$, $\omega_0 = 1$, $\zeta = 0.01$. Köylüoğlu and Nielsen (1996).

Fig. 3-38 shows with unbroken line the exact stationary marginal pdf $f_X(x)$ of the displacement component $X(t)$ for the modal value $x_0 = \sqrt{10}$. Besides, the modified cumulant neglect approximation $f_X(x) = \frac{1}{2\sigma_V}(\varphi(\frac{x+x_0}{\sigma_V}) + \varphi(\frac{-x+x_0}{\sigma_V}))$, $\sigma_V^2 = \sigma_{X,0}^2 - x_0^2$, as well as the Gaussian closure approximation $f_X(x) = \frac{1}{\sigma_{X,0}}\varphi(\frac{x}{\sigma_{X,0}})$ is shown. $\sigma_{X,0}^2$ of the replacements have been determined from the modified and ordinary closure approximations (3-201) and (3-200). For the present case these become $\sigma_{X,0}^2 = 10.0333$ and $\sigma_{X,0}^2 = 4.1387$, respectively. For comparison the exact stationary variance is $\sigma_{X,0}^2 = 8.7136$. Hence, at the order of closure $N = 2$, (3-201) represents a significant improvement compared to (3-200).

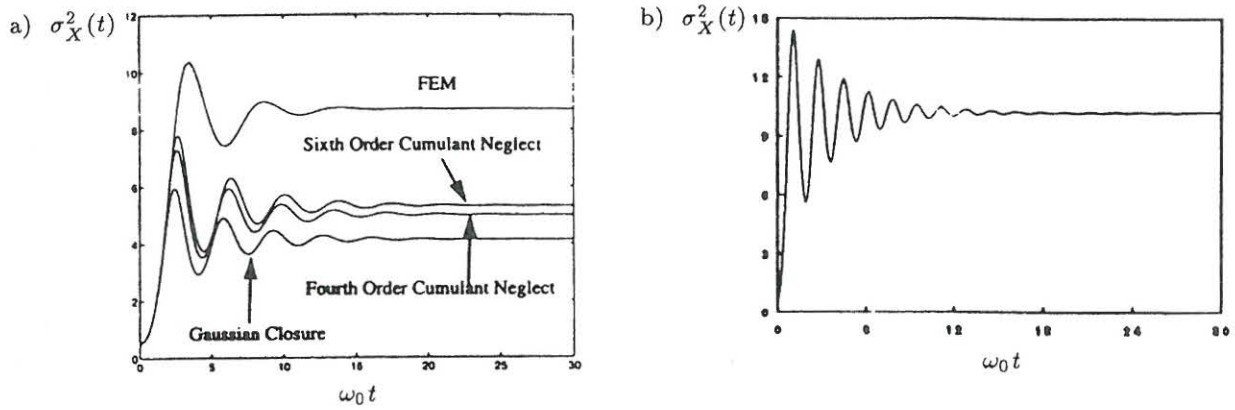

Fig. 3-39: Non-stationary development of displacement variance. a) $\sigma_X^2(t)$ versus time for ordinary cumulant neglect closure at the orders $N = 2, 4, 6$ compared to exact solution, Bergman et al. (1994). b) $\sigma_X^2(t)$ versus time for modified cumulant neglect closure at the order $N = 2$. $\frac{\pi S_0}{2\zeta\omega_0^3 m^2} = 1$, $\omega_0 = 1$, $\zeta = 0.01$. Köylüoğlu and Nielsen (1996).

In fig. 3-39a the development of the non-stationary displacement variance predicted by ordinary cumulant neglect closure is shown in comparison with the exact solution obtained by a Petrov-Galerkin variation of the Fokker-Planck equation. As seen, no convergence to the exact result is achieved. Fig. 3-39b shows the corresponding result obtained by the modified cumulant neglect closure scheme.

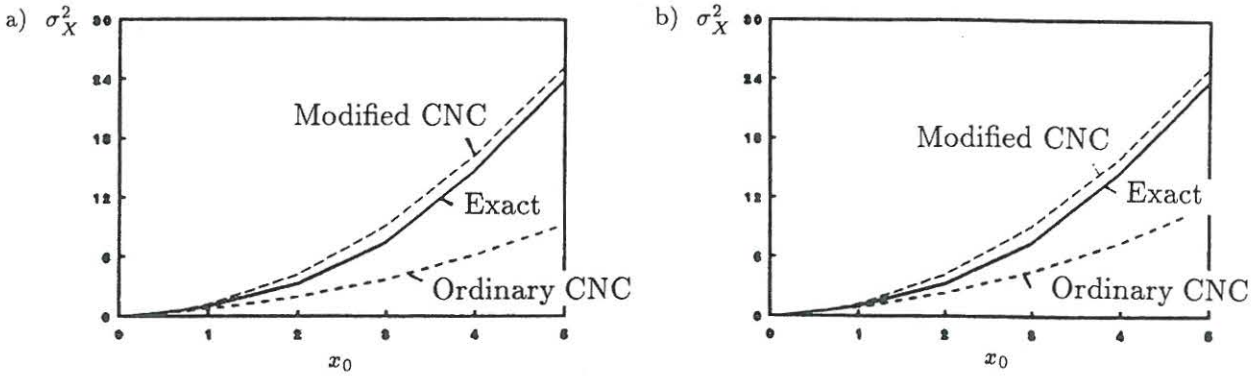

Fig. 3-40: Stationary displacement variance $\sigma_{X,0}^2$ as a function of the modal value x_0. a) Closure at the order $N = 2$. b) Closure at the order $N = 4$. $\frac{\pi S_0}{2\zeta\omega_0^3 m^2} = 1$, $\omega_0 = 1$, $\zeta = 0.01$. Köylüoğlu and Nielsen (1996).

Fig. 3-40 shows the results for the modified and ordinary cumulant neglect closure in comparison with the exact solution as a function of the modal value x_0. The modified cumulant neglect closure

solutions as obtained from (3-201) are much closer to the exact solution than the ordinary cumulant neglect closure solutions for all values of x_0. However, convergence of the modified cumulant neglect closure to the exact solution is slow. Apparently, the significant improvement of the modified cumulant neglect closure is already present at closure at the order $N = 2$, and is caused by the more realistic representation of the tentative joint pdf applied in this scheme.

Monte Carlo simulation	Modified closure, order $N = 2$	Gaussian closure, Wen (1980)
0.662	0.5568	0.6932

Table 3.4: Bouc-Wen oscillator. Stationary standard deviation $\sigma_{X,0}$ of displacement.

Next, the Bouc-Wen oscillator (3-47), (3-48), (3-51) exposed to stationary Gaussian white noise is considered. The parameters of the oscillator are $\zeta_0 = 0.01$, $\alpha = 0.05$, $\beta = \gamma = 0.5$ $n = 1$, $q_y = 0.35$ and $\frac{\pi S_0}{2\zeta\omega_0^3 m^2} = 1.0$, and the system is assumed at rest at the time $t = 0$ with the initial conditions $\mathbf{Z}_0 = \mathbf{0}$. In table 3.4 the results obtained by Monte Carlo simulation, by the Gaussian closure scheme and by the modified closure scheme (3-205) closed at the order $N = 2$ are shown. The stationary result for the Gaussian closure scheme was obtained as the transient values after elapsed time $30T_0$. For the modified scheme the results were calculated by means of a Newton iteration scheme from the stationary moment equations with the left-hand sides of (3-329) set equal to zero. The indicated result is similar to that of the two-well potential problem. Substantially improved results are obtained if the applied closure scheme reflects the physics of the considered problem.

Ordinary closure schemes such as the cumulant neglect closure, the Hermite moment neglect closure scheme, the quasi moment neglect closure scheme will definitely converge to the correct result, if the underlying assumed joint pdf as specified by the expansions (3-192), (3-194), (3-196) converge to the actual joint pdf. Basically, these expansions are specified as deviations from a Gaussian or almost Gaussian distribution. For multi-peaked problems or even joint pdfs of the mixed type with discrete probability components the convergence of these essential mono-modal series expansions is slow or non-existing, which explains the poor performance of these methods in such problems. Instead, the closure scheme should reflect the physics of the considered problem as demonstrated in the considered example. The main drawback of modified closure schemes is the more involved mathematical formulations required.

The modified closure scheme for the two-well potential problem was formulated by Köylüoğlu and Nielsen (1996). The modified Hermite moment neglect closure scheme applied in the Bouc-Wen problem is due to Nielsen and Köylüoğlu (1997).

3.3.3 Compound Poisson process driven systems

Using the Kolmogorov backward operator (3-125) in (3-172) and (3-173) the following differential equations for the mean value and for the joint central moments are obtained for dynamic systems exposed to an n_4 dimensional compound Poisson process $\{\mathbf{V}(t), t \in [0, \infty[\}$ as defined in section 3.1.1.2.

$$\frac{d}{dt}\mu_i(t) = E\Big[c_i(\mathbf{Z}(t),t)\Big] + \sum_{\alpha=1}^{n_4} \nu_\alpha(t) E[P_\alpha] E\Big[e_i(\mathbf{Z}(t),t)\Big] \tag{3-323}$$

$$\left.\begin{aligned}
&\tfrac{d}{dt}\lambda_{ij}(t) = 2\left\{E\Big[c_i^0(\mathbf{Z}(t),t)\, Z_j^0(t)\Big]\right\}_s + \\
&\sum_{\alpha=1}^{n_4} \nu_\alpha(t) E[P_\alpha] 2\left\{E\Big[e_{i\alpha}^0(\mathbf{Z}(t),t)\, Z_j^0(t)\Big]\right\}_s + \\
&\sum_{\alpha=1}^{n_4} \nu_\alpha(t) E[P_\alpha^2] E\Big[e_{i\alpha}(\mathbf{Z}(t),t)\, e_{j\alpha}(\mathbf{Z}(t),t)\Big] \\
&\tfrac{d}{dt}\lambda_{ijk}(t) = 3\left\{E\Big[c_i^0(\mathbf{Z}(t),t)\, Z_j^0(t) Z_k^0(t)\Big]\right\}_s + \\
&\sum_{\alpha=1}^{n_4} \nu_\alpha(t) E[P_\alpha] 3\left\{E\Big[e_{i\alpha}^0(\mathbf{Z}(t),t)\, Z_j^0(t) Z_k^0(t)\Big]\right\}_s + \\
&\sum_{\alpha=1}^{n_4} \nu_\alpha(t) E[P_\alpha^2] 3\left\{E\Big[e_{i\alpha}(\mathbf{Z}(t),t)\, e_{j\alpha}(\mathbf{Z}(t),t)\, Z_k^0(t)\Big]\right\}_s + \\
&\sum_{\alpha=1}^{n_4} \nu_\alpha(t) E[P_\alpha^3] \Big[e_{i\alpha}(\mathbf{Z}(t),t)\, e_{j\alpha}(\mathbf{Z}(t),t)\, e_{k\alpha}(\mathbf{Z}(t),t)\Big] \\
&\tfrac{d}{dt}\lambda_{ijkl}(t) = 4\left\{E\Big[c_i^0(\mathbf{Z}(t),t)\, Z_j^0(t) Z_k^0(t) Z_l^0(t)\Big]\right\}_s + \\
&\sum_{\alpha=1}^{n_4} \nu_\alpha(t) E[P_\alpha] 4\left\{E\Big[e_{i\alpha}^0(\mathbf{Z}(t),t)\, Z_j^0(t) Z_k^0(t) Z_l^0(t)\Big]\right\}_s + \\
&\sum_{\alpha=1}^{n_4} \nu_\alpha(t) E[P_\alpha^2] 6\left\{E\Big[e_{i\alpha}(\mathbf{Z}(t),t)\, e_{j\alpha}(\mathbf{Z}(t),t)\, Z_k^0(t) Z_l^0(t)\Big]\right\}_s + \\
&\sum_{\alpha=1}^{n_4} \nu_\alpha(t) E[P_\alpha^3] 4\left\{E\Big[e_{i\alpha}(\mathbf{Z}(t),t)\, e_{j\alpha}(\mathbf{Z}(t),t)\, e_{k\alpha}(\mathbf{Z}(t),t)\, Z_l^0(t)\Big]\right\}_s + \\
&\sum_{\alpha=1}^{n_4} \nu_\alpha(t) E[P_\alpha^4] \Big[e_{i\alpha}(\mathbf{Z}(t),t)\, e_{j\alpha}(\mathbf{Z}(t),t)\, e_{k\alpha}(\mathbf{Z}(t),t)\, e_{l\alpha}(\mathbf{Z}(t),t)\Big] \\
&\tfrac{d}{dt}\lambda_{i_1\ldots i_N}(t) = N\left\{E\Big[c_{i_1}^0(\mathbf{Z}(t),t)\, Z_{i_2}^0(t)\cdots Z_{i_N}^0(t)\Big]\right\}_s - \\
&\sum_{\alpha=1}^{n_4} \nu_\alpha(t) E[P_\alpha] N\left\{E\Big[e_{i_1\alpha}(\mathbf{Z}(t),t)\Big]\lambda_{i_2\ldots i_N}(t)\right\}_s + \\
&\sum_{k=1}^{N}\sum_{\alpha=1}^{n_4} \nu_\alpha(t) E[P_\alpha^k] \binom{N}{k} \left\{E\Big[e_{i_1\alpha}(\mathbf{Z}(t),t)\cdots e_{i_k\alpha}(\mathbf{Z}(t),t)\, Z_{i_{k+1}}^0(t)\cdots Z_{i_N}^0(t)\Big]\right\}_s
\end{aligned}\right\} \tag{3-324}$$

(3-324) are valid for all impulses for which the moments $E[P_\alpha^N]$ for $\alpha = 1, \ldots, n_4$ exist. Further, in (3-324) the centralized drift vector (3-238) has been introduced, as well as the centralized diffusion vector defined as

$$\mathbf{e}^0(\mathbf{Z}(t),t) = \mathbf{e}(\mathbf{Z}(t),t) - E\Big[\mathbf{e}(\mathbf{Z}(t),t)\Big] \qquad (3-325)$$

In case of scalar compound Poissonian excitation, and the diffusion terms is state independent (3-323) and (3-324) reduce to

$$\left.\begin{aligned}
&\frac{d}{dt}\mu_i(t) = E\Big[c_i(\mathbf{Z}(t),t)\Big] + \nu(t)E[P]e_i(t)\\
&\frac{d}{dt}\lambda_{ij}(t) = 2\left\{E\Big[c_i^0(\mathbf{Z}(t),t)Z_j^0(t))\Big]\right\}_s + \nu(t)E[P^2]e_i(t)e_j(t)\\
&\frac{d}{dt}\lambda_{ijk}(t) = 3\left\{E\Big[c_i^0(\mathbf{Z}(t),t)Z_j^0(t)Z_k^0(t)\Big]\right\}_s + \nu(t)E[P^3]e_i(t)e_j(t)e_k(t)\\
&\frac{d}{dt}\lambda_{ijkl}(t) = 4\left\{E\Big[c_i^0(\mathbf{Z}(t),t)Z_j^0(t)Z_k^0(t)Z_k^0(t)\Big]\right\}_s +\\
&\nu(t)E[P^2]6\left\{e_i(t)e_j(t)\lambda_{kl}(t)\right\}_s + \nu(t)E[P^4]e_i(t)e_j(t)e_k(t)e_l(t)\\
&\frac{d}{dt}\lambda_{i_1\ldots i_N}(t) = N\left\{E\Big[c_{i_1}^0(\mathbf{Z}(t),t)Z_{i_2}^0(t)\cdots Z_{i_N}^0(t)\Big]\right\}_s +\\
&\sum_{k=2}^{N}\nu(t)E[P^k]\binom{N}{k}\left\{e_{i_1}(t)\cdots e_{i_k}(t)\lambda_{i_{k+1}\ldots i_N}(t)\right\}_s
\end{aligned}\right\} \quad (3-326)$$

In case of cubic polynomial expansions of the drift vector and the centralized drift terms in the centralized state variables, as given by (3-240) and (3-241), (3-326) become

$$\left.\begin{aligned}
&\tfrac{d}{dt}\mu_i(t) = A_i + C_{imn}\lambda_{mn} + D_{imnp}\lambda_{mnp} + \nu(t)E[P]e_i(t)\\
&\tfrac{d}{dt}\lambda_{ij}(t) = 2\{B_{im}\lambda_{mj}\}_s + \{C_{imn}\lambda_{mnj}\}_s + 2\{D_{imnp}\lambda_{mnpj}\}_s +\\
&\nu(t)E[P^2]e_i(t)e_j(t)\\
&\tfrac{d}{dt}\lambda_{ijk}(t) = 3\{B_{im}\lambda_{mjk}\}_s + 3\{C_{imn}(\lambda_{mnjk} - \lambda_{mn}\lambda_{jk})\}_s +\\
&3\{D_{imnp}(\lambda_{mnpjk} - \lambda_{mnp}\lambda_{jk})\}_s + \nu(t)E[P^3]e_i(t)e_j(t)e_k(t)\\
&\tfrac{d}{dt}\lambda_{ijkl}(t) = 4\{B_{im}\lambda_{mjkl}\}_s + 4\{C_{imn}(\lambda_{mnjkl} - \lambda_{mn}\lambda_{jkl})\}_s +\\
&4\{D_{imnp}(\lambda_{mnpjkl} - \lambda_{mnp}\lambda_{jkl})\}_s + \nu(t)E[P^2]6\{e_i(t)e_j(t)\lambda_{kl}(t)\}_s +\\
&\nu(t)E[P^4]e_i(t)e_j(t)e_k(t)e_l(t)\\
&\tfrac{d}{dt}\lambda_{i_1\ldots i_N}(t) = N\{B_{i_1m}\lambda_{mi_2\ldots i_N}\}_s + N\{C_{i_1mn}(\lambda_{mni_2\ldots i_N} - \lambda_{mn}\lambda_{i_2\ldots i_N})\}_s +\\
&N\{D_{i_1mnp}(\lambda_{mnpi_2\ldots i_N} - \lambda_{mnp}\lambda_{i_2\ldots i_N})\}_s +\\
&\sum_{k=2}^{N}\nu(t)E[P^k]\tbinom{N}{k}\{e_{i_1}(t)\cdots e_{i_k}(t)\lambda_{i_{k+1}\ldots i_N}(t)\}_s
\end{aligned}\right\} \quad (3-327)$$

Again, in (3-327) the summation convention has been used for simplicity, with the dummy indices ranging from 1 to n. For a linear system ($C_{imn} = D_{imnp} = 0$), (3-327) is automatically closed at any order of truncation. Hence, the response moments of a linear system driven by a compound Poisson process can be calculated with arbitrary accuracy. For any non-linear system identical closing problems appear as encountered for Wiener process driven systems.

For hysteretic systems exposed to compound Poisson process driven systems the equivalent polynomial expansion technique for the non-analytical and non-linear drift vector may be used in the same way as explained in section 3.3.2 for Wiener process driven systems.

Example 3-8: Duffing oscillator subjected to a train of filtered Poisson driven pulses

Consider the dynamic response of the Duffing oscillator (3-44) with the loading process $\{F(t), t \in [0, \infty[\}$ obtained as the output process from a filtration through a rational filter of the order $(r, s) = (0, 2)$ of a homogeneous compound Poisson process $\{V(t), t \in [0, \infty[\}$ with mean arrival rate ν. Then the drift vector becomes cubic polynomial and the moment equations (3-327) apply. The idea of the present example is to demonstrate the applicability of the modified cumulant neglect closure scheme (3-234), (3-235) at closure of the moment equations (3-327) at the order $N = 4$.

The equations of motion are given by (3-52) with the following definitions of the state vector, diffusion vector and drift vector

$$\mathbf{Z}(t) = \begin{bmatrix} X(t) \\ \dot{X}(t) \\ Y(t) \\ \dot{Y}(t) \end{bmatrix} \quad , \quad \mathbf{d}(t) = \mathbf{e}(t) = \begin{bmatrix} 0 \\ 0 \\ 0 \\ 1 \end{bmatrix} \qquad (3-328a)$$

$$\mathbf{c}(\mathbf{Z}(t)) = \begin{bmatrix} \dot{X} \\ -2\zeta\omega_0\dot{X} - \omega_0^2(X + \varepsilon X^3) + \frac{p_0}{m}Y \\ \dot{Y} \\ -q_1\dot{Y} - q_2 Y \end{bmatrix} \qquad (3-328b)$$

Introducing centralized state variables in (3-328b) a cubic polynomial expansion of type (3-240) is obtained. The non-zero tensor components become

$$\left.\begin{aligned} A_1 &= \mu_2 \\ A_2 &= -2\zeta\omega_0\mu_2 - \omega_0^2(\mu_1 + \varepsilon\mu_1^3) + \tfrac{p_0}{m}\mu_3 \\ A_3 &= \mu_4 \\ A_4 &= -q_1\mu_4 - q_2\mu_3 \\ \\ B_{12} &= 1 \\ B_{21} &= -\omega_0^2(1 + 3\varepsilon\mu_1^2) \quad , \quad B_{22} = -2\zeta\omega_0 \quad , \quad B_{23} = \tfrac{p_0}{m} \\ B_{34} &= 1 \\ B_{43} &= -q_2 \quad , \quad B_{44} = -q_1 \\ \\ C_{211} &= -3\varepsilon\omega_0^2\mu_1 \\ \\ D_{2111} &= -\varepsilon\omega_0^2 \end{aligned}\right\} \qquad (3-329)$$

The following methods have been investigated:

a: Monte Carlo simulation.

b: ordinary cumulant neglect closure scheme at the order $N = 3$.

c: ordinary cumulant neglect closure scheme at the order $N = 4$.

d: ordinary cumulant neglect closure scheme at the order $N = 5$.

e: modified cumulant neglect closure scheme at the order $N = 4$.

The generation of time histories for the Monte-Carlo simulation approach has been performed in the following way. Assume that an impulse arrives at the time t_i, where a sample p_i of the mark variable P is generated. The impulse strength $P = p_i$ causes a jump of the state vector of magnitude $\Delta \mathbf{Z}(t_i) = \mathbf{Z}(t_i^+) - \mathbf{Z}(t_i^-) = \mathbf{e}(t)p_i$. Next, a sample of the following impulse arrival time t_{i+1} is generated, using that the interarrival times of a homogeneous Poisson counting process is exponentially distributed with mean value $\frac{1}{\nu}$. The system then performs eigenvibrations in the interval $]t_i, t_{i+1}[$, with the initial values $\mathbf{Z}(t_i^+)$. The eigenvibrations of the dynamic system (3-52), (3-328) are solved by a 4th order Runge-Kutta scheme, with the time step $\Delta t = \frac{T_0}{40}$, $T_0 = \frac{2\pi}{\omega_0}$ being the period of linear, undamped eigenvibrations. The sample size of ensemble response time-histories was 50000, from which the relevant response statistics were determined.

The following system data are used in the example

$$\left.\begin{array}{llll} m = 1.0 & , \ \omega_0 = 1.0 & , \ \zeta = 0.05 & , \ \epsilon = 0.5 \\ p_0 = 1.0 & , \ q_1 = 4.56 & , \ q_2 = 5.76 & \end{array}\right\} \qquad (3-330)$$

The indicated values for q_1 and q_2 correspond to a circular eigenfrequency of $\omega_f = 2.4\omega_0$ and a damping ratio of $\zeta_f = 0.95$ of the shaping filter. Hence, the filter is almost critically damped, and the filtered compound Poisson process $\{F(t), t \in [0, \infty[\}$ given by (3-42) appears as a sequence of non-oscillating general pulses. The strength of the impulses is assumed to be Rayleigh distributed, $P \sim R(\sigma^2)$, where the parameter σ^2 is determined, so $\frac{\nu E[P^2]}{4\zeta\omega_0^3 m^2} = \frac{\nu\sigma^2}{2\zeta\omega_0^3 m^2} = 1$. This level of excitation implies the stationary variance $\sigma_{X,0}^2 = 1$ of the corresponding linear oscillator exposed to an equivalent Gaussian white noise with the auto-spectral density $2\pi\nu E[P^2]$. Then, for $\epsilon = 0.5$ the linear part $X(t)$ and non-linear part $\epsilon X^3(t)$ contribute equally to the restoring force of the oscillator, and the system should be classified as substantially non-linear. Two values of ν are considered, namely $\nu = 0.05\omega_0$ and $\nu = 0.1\omega_0$, corresponding to an average number of impulse arrivals of 0.1π and 0.2π per eigenperiod T_0. $\nu = 0.1\omega_0$ signifies in some sense a limiting case. If ν is below this value the response of the system appears as highly non-Gaussian, Janssen and Lambert (1967).

Fig. 3-41 shows the results for the time-dependent variance of the displacement $X(t)$ at the relatively high mean rate of impulses $\nu = 0.1\omega_0$, obtained for the ordinary cumulant neglect closure at the order $N = 3$, $N = 4$ and $N = 5$. Closure at the order $N = 4$ and $N = 5$ gives practically identical results for $\frac{t}{T_0} > 2$, where only the latter has been shown. As expected, the best result is obtained for closure at the order $N = 5$, but all approximations give acceptable results. Fig. 3-42 shows the time-dependence of the mean-value function for $\nu = 0.1\omega_0$. The results obtained by ordinary cumulant neglect closure at the order $N = 4$ have been compared to those obtained by the modified cumulant neglect closure at the order $N = 4$. The latter scheme improves the results substantially compared to simulation in the initial part of the excitation, where the modification of the joint pdf as given by (3-229) is most important. Fig. 3-43 shows the corresponding time-dependence of the variance function. Results obtained by ordinary cumulant neglect closure at the order $N = 4$ have been compared to those obtained by the modified cumulant neglect closure scheme at the order $N = 4$. Again, substantial improvements are noticed in the initial phase. Fig. 3-44 shows the time-dependence of the mean value function at the lower mean arrival rate $\nu = 0.05\omega_0$. Ordinary and modified cumulant neglect closure schemes at the order $N = 4$ have been compared. The ordinary cumulant neglect closure scheme becomes numerically unstable at $\frac{t}{T_0} \simeq 0.5$, whereas the modified closure remains stable. Finally, fig. 3-45 shows the corresponding results for the variance.

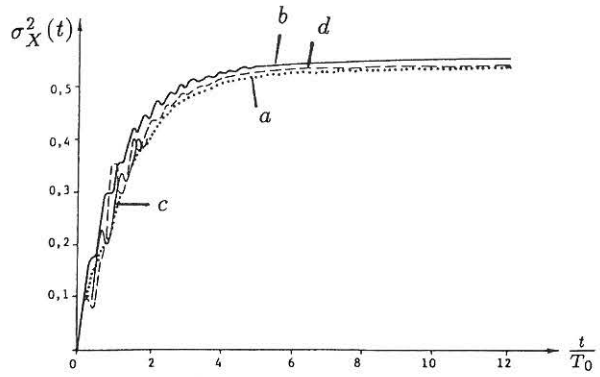

Fig. 3-41: Time-dependent variance of displacement response, $\sigma_X^2(t)$. $\nu = 0.1\omega_0$. Iwankiewicz, Nielsen and Thoft-Christensen (1990).

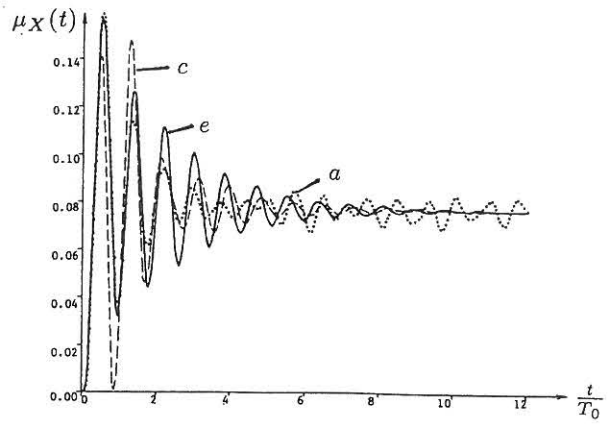

Fig. 3-42: Time-dependent mean value function of displacement response, $\mu_X(t)$. $\nu = 0.1\omega_0$ Iwankiewicz, Nielsen and Thoft-Christensen (1990).

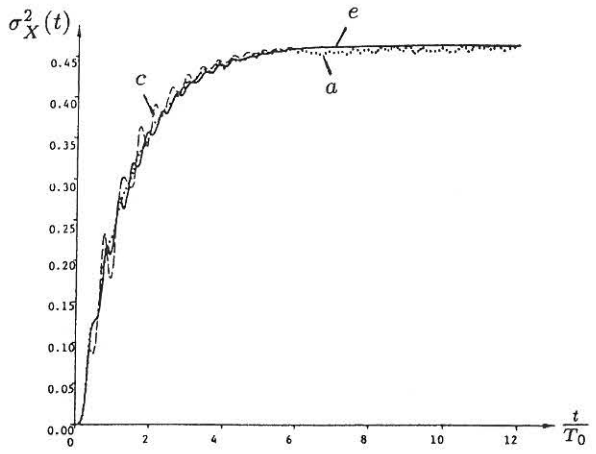

Fig. 3-43: Time-dependent variance of displacement response, $\sigma_X^2(t)$. $\nu = 0.1\omega_0$. Iwankiewicz, Nielsen and Thoft-Christensen (1990).

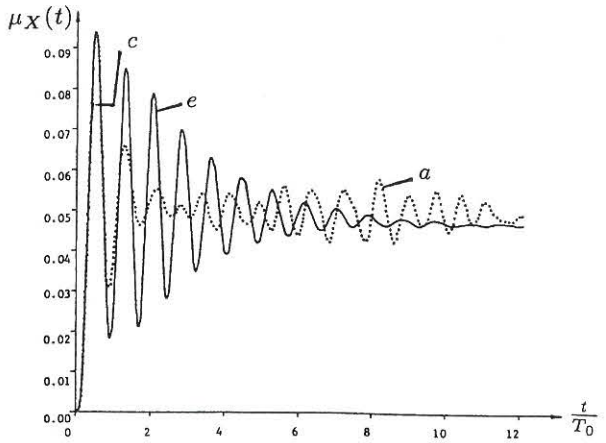

Fig. 3-44: Time-dependent mean value function of displacement response, $\mu_X(t)$. $\nu = 0.05\omega_0$. Iwankiewicz, Nielsen and Thoft-Christensen (1990).

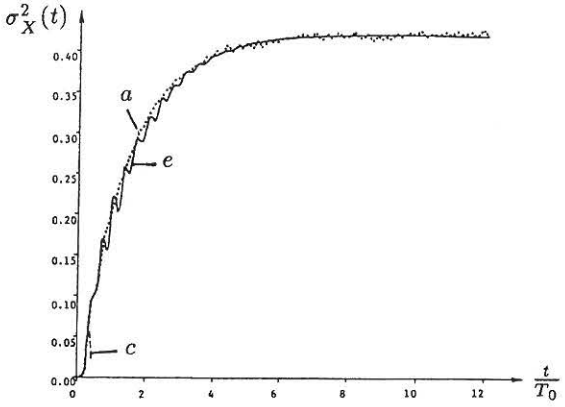

Fig. 3-45: Time-dependent variance of displacement response, $\sigma_X^2(t)$. $\nu = 0.05\omega_0$. Iwankiewicz, Nielsen and Thoft-Christensen (1990).

The general conclusion that can be drawn from these results is that the modified cumulant neglect closure scheme derived from the setting (3-229) provides more accurate predictions in the early phases of excitation and increases the stability of the numerical scheme. This improvement is especially pronounced if the mean arrival rate of impulses is very low, and the response is correspondingly non-Gaussian. However, even the modified cumulant neglect closure scheme runs into numerical instability at sufficiently low mean arrival rates. In the present example this was noticed around $\nu \simeq 0.01\omega_0$. Hence, moment equation methods for compound Poisson process driven systems are best applied at medium to high mean arrival rates of impulses.

The present modified cumulant neglect closure scheme was devised by Iwankiewicz, Nielsen and Thoft-Christensen (1990). The first attempt to apply moment methods to geometrically non-linear dynamic systems driven by compound Poisson processes was made by Iwankiewicz and Nielsen (1992a), using an ordinary cumulant neglect closure scheme.

3-9: Reliability analysis of hysteretic systems driven by compound Poisson processes

The aim of the present example is to demonstrate the applicability of the equivalent polynomial expansion technique for hysteretic systems exposed to compound Poisson processes. The Bouc-Wen oscillator (3-47), (3-48), (3-51) is considered with various specifications for the excitation $\{F(t), t \in [0, \infty[\}$. Further, a reliability analysis will be performed, using the accumulated dissipated energy on the hysteretic component as the damage indicator, leading to the damage indicator differential equation

$$\dot{D}(t) = Q\dot{X}(t) \qquad (3-331)$$

(3-331) corresponds to the general damage indicator format (3-261) with $g(\dot{X}, Q) = Q$.

In one case the loading process is given by an unfiltered homogeneous compound Poisson process with the mean arrival rate ν. Then, the equations of motion of the integrated dynamic system is given by (3-52) with the following definitions of the state vector, the diffusion vector and the drift vector

$$\mathbf{Z}(t) = \begin{bmatrix} X(t) \\ \dot{X}(t) \\ Q(t) \\ D(t) \end{bmatrix} \quad , \quad \mathbf{d}(t) = \mathbf{e}(t) = \begin{bmatrix} 0 \\ \frac{1}{m} \\ 0 \\ 0 \end{bmatrix} \qquad (3-332a)$$

$$\mathbf{c}(\mathbf{Z}(t)) = \begin{bmatrix} \dot{X} \\ -2\zeta\omega_0\dot{X} - \omega_0^2(\alpha X + (1-\alpha)Q) \\ \kappa(\dot{X}, Q)\dot{X} \\ Q\dot{X} \end{bmatrix} \qquad (3-332b)$$

$\kappa(\dot{X}, Q)$ is given by (3-51). In the other case the loading process is obtained from a filtration of the stationary compound Poisson process through a time-invariant rational filter of the order $(r, s) = (0, 2)$. In this case the state vector, the diffusion vector and the drift vector can be written

$$\mathbf{Z}(t) = \begin{bmatrix} X(t) \\ \dot{X}(t) \\ Q(t) \\ D(t) \\ Y(t) \\ \dot{Y}(t) \end{bmatrix} \quad , \quad \mathbf{d}(t) = \mathbf{e}(t) = \begin{bmatrix} 0 \\ 0 \\ 0 \\ 0 \\ 0 \\ 1 \end{bmatrix} \qquad (3-333a)$$

$$\mathbf{c}(\mathbf{Z}(t)) = \begin{bmatrix} \dot{X} \\ -2\zeta\omega_0\dot{X} - \omega_0^2(\alpha X + (1-\alpha)Q) + \frac{p_0}{m}Y \\ \kappa(\dot{X},Q)\dot{X} \\ Q\dot{X} \\ \dot{Y} \\ -q_1\dot{Y} - q_2 Y \end{bmatrix} \qquad (3-333b)$$

The systems (3-332) and (3-333) will be analyzed by means of an equivalent cubic polynomial expansion. In the present case the right-hand sides of the damage differential equations are analytic and quadratic. Then, only $\kappa(\dot{X},Q)\dot{X}$ in the drift vectors is replaced by a cubic polynomial expansion, whereas the remaining linear or quadratic components are kept unchanged. Since, the system is non-zero mean the following expansion in the centralized state variables $\dot{X}^0 = \dot{X} - E[\dot{X}]$ and $Q^0 = Q - E[Q]$ is appropriate, cf. (3-240)

$$c_{3,eq}(\mathbf{Z}(t)) = \kappa(\dot{X},Q)\dot{X} = A_3 + B_{32}\dot{X}^0 + B_{33}Q^0 + C_{322}(\dot{X}^0)^2 + C_{323}\dot{X}^0Q^0 + C_{333}(Q^0)^2 + D_{3222}(\dot{X}^0)^3 + D_{3223}(\dot{X}^0)^2Q^0 + D_{3233}\dot{X}^0(Q^0)^2 + D_{3333}(Q^0)^3 \qquad (3-334)$$

The expansion coefficients in (3-334) are determined by a least mean square criterion, leading to the following system of linear equations

$$\begin{bmatrix} 1 & 0 & 0 & \lambda_{22} & \lambda_{23} & \lambda_{33} & \lambda_{222} & \lambda_{223} & \lambda_{233} & \lambda_{333} \\ & \lambda_{22} & \lambda_{23} & \lambda_{222} & \lambda_{223} & \lambda_{233} & \lambda_{2222} & \lambda_{2223} & \lambda_{2233} & \lambda_{2333} \\ & & \lambda_{33} & \lambda_{223} & \lambda_{233} & \lambda_{333} & \lambda_{2223} & \lambda_{2233} & \lambda_{2333} & \lambda_{3333} \\ & & & \lambda_{2222} & \lambda_{2223} & \lambda_{2233} & \lambda_{22222} & \lambda_{22223} & \lambda_{22233} & \lambda_{22333} \\ & \text{symm.} & & & \lambda_{2233} & \lambda_{2333} & \lambda_{22223} & \lambda_{22233} & \lambda_{22333} & \lambda_{23333} \\ & & & & & \lambda_{3333} & \lambda_{22233} & \lambda_{22333} & \lambda_{23333} & \lambda_{33333} \\ & & & & & & \lambda_{222222} & \lambda_{222223} & \lambda_{222233} & \lambda_{222333} \\ & & & & & & & \lambda_{222233} & \lambda_{222333} & \lambda_{223333} \\ & & & & & & & & \lambda_{223333} & \lambda_{233333} \\ & & & & & & & & & \lambda_{333333} \end{bmatrix} \begin{bmatrix} A_3 \\ B_{32} \\ B_{33} \\ C_{322} \\ C_{323} \\ C_{333} \\ D_{3222} \\ D_{3223} \\ D_{3233} \\ D_{3333} \end{bmatrix} =$$

$$\begin{bmatrix} \kappa(\dot{X},Q)\dot{X} \\ \kappa(\dot{X},Q)\dot{X}\dot{X}^0 \\ \kappa(\dot{X},Q)\dot{X}Q^0 \\ \kappa(\dot{X},Q)\dot{X}(\dot{X}^0)^2 \\ \kappa(\dot{X},Q)\dot{X}\dot{X}^0Q^0 \\ \kappa(\dot{X},Q)\dot{X}(Q^0)^2 \\ \kappa(\dot{X},Q)\dot{X}(\dot{X}^0)^3 \\ \kappa(\dot{X},Q)\dot{X}(\dot{X}^0)^2Q^0 \\ \kappa(\dot{X},Q)\dot{X}\dot{X}^0(Q^0)^2 \\ \kappa(\dot{X},Q)\dot{X}(Q^0)^3 \end{bmatrix} \qquad (3-335)$$

The expectations on the right-hand side of (3-335) as well as the unprovided joint central moments of the 5th and 6th order on the left-hand side are calculated by means of the following quasi-moment neglect closure scheme at the order N, cf. (3-194)

$$f_{\dot{X}Q}(\dot{x},q,t) = \varphi_2(\dot{x},q;\boldsymbol{\mu}(t),\boldsymbol{\kappa}(t))\left\{1+\sum_{k=3}^{N}\frac{1}{k!}\sum_{i_1,\ldots,i_k=1}^{n}\beta_{i_1i_2\ldots i_k}(t)H_{i_1i_2\ldots i_k}(\dot{x},q;\boldsymbol{\mu}(t),\boldsymbol{\kappa}(t))\right\} \qquad (3-336)$$

where $n = 4$ or $n = 6$ signify the dimension of the state vectors (3-332a) og (3-333a). $\varphi_2(\dot{x}, q; \boldsymbol{\mu}(t), \boldsymbol{\kappa}(t))$ indicates the bivariate Gaussian joint probability density function of $[\dot{X}(t), Q(t)]$, and $H_{i_1 i_2 \ldots i_k}(\dot{x}, q; \boldsymbol{\mu}(t), \boldsymbol{\kappa}(t))$ are the related multivariate Hermite polynomials defined from (3-182). Notice, since $N = 4$ that all joint quasi-moments $\beta_{i_1 i_2 \ldots i_k}(t)$ entering (3-336) are identical to the corresponding joint cumulants, cf. (3-180). The joint central moments of the 5th and 6th order may be evaluated analytically in terms of the parameters entering (3-336). Analytical evaluation of the expectations on the right-hand side of (3-335) in terms of $\varphi(\cdot)$ and $\Phi(\cdot)$ can only be performed for integer values of n in the Bouc-Wen model (3-51). Closed form solutions for the case $n = 1$ have been derived by Iwankiewicz and Nielsen (1992b).

Results will also be derived for the equivalent linear expansion version, where only the linear terms are retained in (3-334). The equivalent linear expansion coefficients will still be calculated by (3-336) truncated both at the orders $N = 2$ and $N = 4$, where the former corresponds to Gaussian closure.

The global moment equations of the equivalent cubic system is given by (3-327). The system is closed by an ordinary cumulant neglect closure scheme at the order $N = 4$ for both the equivalent linear expansion and the equivalent cubic expansion procedures with equivalent coefficients calculated by means of (3-336) truncated at the order $N = 4$. The ordinary cumulant neglect procedure is appropriate in the present case, since relatively high mean arrival rates are considered. However, in case of equivalent linearization with Gaussian evaluation of the expansion coefficients closure of the global moment equations at the order $N = 2$ is performed. Even though the cumulant neglect closure and the quasi-moment neglect closure schemes differ for the joint 6th order moments as seen from (3-180), the local closure scheme (3-336) and the applied global closure scheme are consistent in the sense that modifications as specified by (3-229) for the discrete component of the underlying joint probability density functions, representing the probability of no impulse arrivals during the interval $[t_0, t[$, have not been performed in any of these cases. As learned from example 3-4, the modification for discrete probability components should be performed at the determination of the local equivalent polynomial expansion as well as at the closure of the global moment equations, if increased accuracy and stability are to be achieved.

The results of the moment equation method will be compared to those obtained by Monte Carlo simulation. The generation of time-histories is performed in the same way as explained in Example 3-8. The eigenvibrations of the dynamic systems (3-52), (3-332), (3-333) are solved by a 4th order Runge-Kutta scheme with the time step $\Delta t = \frac{T_0}{40}$, $T_0 = \frac{2\pi}{\omega_0}$ being the period of linear, undamped eigenvibrations. The size of ensemble response time-histories is 50000, from which the relevant response statistics are determined.

The following system data are used in the example

$$\left.\begin{array}{llll} m = 1.0 & , \ \omega_0 = 1.0 & , \ \zeta = 0.01 & , \ \alpha = 0.05 \\ \beta = 0.5 & , \ \gamma = 0.5 & , \ n = 1 & \\ p_0 = 1.0 & , \ q_1 = 4.56 & , \ q_2 = 5.76 & \end{array}\right\} \qquad (3-337)$$

The filter constants q_1 and q_2 are identical to those used in example 3-8 with the consequence that the filtered compound Poisson process $\{F(t), t \in [0, \infty[\}$ applied to the system defined by (3-52), (3-333) appears as a sequence of non-oscillating general pulses.

For the system defined by (3-52), (3-332) two different distributions for the impulse strength P are considered. In the 1st case P is assumed to be Rayleigh distributed, $P \sim R(\sigma^2)$, where the parameter σ^2 is determined from $E[P^2] = 2\sigma^2$. In the 2nd case $P = R - E[R]$, $R \sim R(\sigma^2)$, which implies $E[P^2] = \frac{4-\pi}{2}\sigma^2$. σ^2 of the various distributions and the mean arrival rate of impulses, ν, are next specified, so $\frac{\nu E[P^2]}{4\zeta\omega_0^3 m^2} = 5\pi$. For the present example, as defined in (3-337), this corresponds to $\nu\sigma^2 = 0.1\pi$ or $\nu\sigma^2 = \frac{0.4\pi}{4-\pi}$, respectively. Notice that the indicated level of excitation causes a stationary variance $\sigma^2_{X,0} = 5\pi$ of the linear oscillator exposed to an equivalent Gaussian white noise with the auto-spectral

density $2\pi\nu E[P^2]$. The modification of the setting $\sigma^2_{X,0} = 1$ used in previous examples has been performed in order to make direct comparison with the zero mean and non-zero mean equivalent linearization results of Wen (1976) and Baber (1986) for the white noise excitated problem, identical to equivalent linearization of the present system with Gaussian evaluation of the equivalent linear expansion coefficients and with zero mean and non-zero mean impulse strengths, respectively. Hence, a mean excitation of $\nu E[P] = \nu\sigma\sqrt{\frac{\pi}{2}} = 0.8$ is used in the non-zero mean case equal to the one used by Baber (1986), leading to a mean arrival rate of impulses as high as $\nu = 1.297\omega_0$, or 8.149 impulses per linear eigenperiod T_0 on average. It is known that the Poisson distributed train of impulses tends to a Gaussian white noise as $\nu \to \infty$ in such a way that $\nu E[P^2]$ is kept constant. Another of the ideas of the example is to demonstrate the effect of substituting a compound Poisson driven systems by an equivalent white noise excitation. It is shown that for strongly non-linear hysteretic systems as the present significant deviations in the displacement response may occur even with the indicated relatively high impulse arrival rate.

The obtained results have been shown below in figs. 3-46 - 3-57 versus the non-dimensional time $\frac{t}{T_0}$. The solid line represents simulation, the dash-dotted curves denote the results obtained by equivalent statistical linearization with the closure scheme (3-334). The dashed curve represents equivalent cubic expansion, and the dotted curve indicates the results obtained by Gaussian white noise, i.e. global closure at the order $N = 2$ and equivalent linearization with Gaussian evaluation of expansion coefficients.

Figs. 3-46, 3-47 and 3-48 show the time-dependent mean value functions of the displacement, the hysteretic component and the damage indicator for the case of non-zero mean impulse strengths. All considered methods give acceptable results for these quantities, although the white noise approximation is overestimating the mean value of the hysteretic component somewhat at larger excitation intervals. Since, $E[\ddot{X}(t)] = E[\dot{X}(t)] = 0$ in the stationary state as $t \to \infty$ it follows that $\omega_0^2(\alpha E[X(t)] + (1 - \alpha)E[Q(t)]) \to \frac{\nu E[P]}{m}$. As seen from (3-347), $\lim E[Q(t)] \simeq 0$ and so $\lim E[X(t)] \simeq \frac{\nu E[P]}{\alpha\omega_0^2 m} = 16$ as $t \to \infty$.

Figs. 3-49, 3-50 and 3-51 show the corresponding results for the time-dependent variances of the displacement, the hysteretic component and the damage indicator. The equivalent linearization schemes clearly underestimate the variances of the displacement and the hysteretic component, but are still qualitatively in agreement with the simulation result. However, the variance predictions for the damage indicator obtained by the linearized schemes are completely wrong. Instead of predicting an increasing variance similar to the one observed for stationary white noise excitation of hysteretic systems, cf. figs. 3-19 and fig. 3-36, a decreasing behaviour is predicted. Equivalent linearization technique will predict the exact variance, if all the expectation entering the mean least square criterion are evaluated from the exact joint distribution, as stated by the theorem on p. 143. The expansion (3-336) truncated at the order $N = 4$ was thought of as a better approximation to the exact distribution than the normal distribution, and hence some improvements of the variance predictions were expected. However, since no such improvement is observed, it can be concluded that (3-336) truncated at the order $N = 4$ is still not sufficiently accurate to accomplish any significant improvement. In contrast, the equivalent cubic expansion procedure with an ordinary cumulant neglect closure scheme gives accurate variance prediction of all three state variables. The relatively good agreement for the variance of the damage indicator is mainly due to the fact that the damage rate is quadratic in the state variable, and hence it is exactly represented by a cubic polynomial expansion. As already learned from examples 3-3, 3-4 and 3-5 the characteristic behaviour of strongly non-linear hysteretic systems is hidden in the 4th order correlations, for which the equivalent cubic expansion is the consistent level of expansion.

Figs. 3-52, 3-53 and 3-54 show the results obtained for the time-dependent mean value functions of the displacement, the hysteretic component and the damage indicator for the case of zero mean impulse strengths, $E[P] = 0$. In this case one has the asymptotic behaviour of the mean values $\lim E[X(t)] = -\frac{1-\alpha}{\alpha}\lim E[Q(t)]$. With $\lim E[Q(t)] \simeq -0.025$, as seen in fig. (3-54), it follows that $\lim E[X(t)] \simeq 0.475$. The Gaussian white noise case predicts $E[X(t) \equiv 0$, coincident with the abscissa axis in fig. 3-52. The observed non-zero mean values of the displacement response for the compound Poisson driven system are a consequence of non-zero higher order odd moments of the impulse strength in combination

with strong non-linearity of the oscillator (small value of α), and represent a significant difference to the equivalent Gaussian white noise replacement. As seen in fig. 3-52, equivalent linearization based on the series (3-352) truncated at the order $N = 4$ gives qualitatively correct non-zero mean predictions of the displacement mean value, although the quantitative agreement is not good. An acceptable agreement with the simulation results is only obtained for the equivalent cubic expansion approach.

Figs. 3-55, 3-56 and 3-57 show the results for the corresponding time-varying variances. The equivalent linearization methods significantly underestimate the variances of the displacement and the hysteretic component compared to the simulation results, whereas the equivalent cubic expansion approach overestimates these quantities somehow. Again, the various equivalent linearization schemes were incapable predicting even qualitatively correct results for the variance of the damage indicator, and have been omitted in fig. 3-57. In contrast the results of the equivalent cubic expansion approach are in good agreement with the simulation results. The irregular behaviour of the simulation results for the hysteretic components displays the absolute error of the Monte Carlo method with 50000 generated realizations.

For the system (3-52), (3-333) driven by a filtered compound Poisson process the impulses are assumed to be non-zero mean Rayleigh distributed, $P \sim R(\sigma^2)$. The mean arrival rate and the parameter σ are chosen as $\nu = 1.0\,\omega_0$ and $\sigma = 3.708$. This specific choice is based on evaluations similar to those given by (3-266), (3-267), and implies approximately the same mean value and variance for the displacement as obtained for the system (3-52), (3-332).

The results obtained are shown below in figs. 3-58 - 3-63. The solid line curves represent simulation, the dash-dotted curves denote the results obtained by equivalent statistical linearization with the closure scheme (3-334), and the dashed curve represents equivalent cubic expansion. No results are presented for the equivalent Gaussian white noise representation.

Figs. 3-58, 3-59 and 3-60 show the time-dependent mean value functions of the displacement, the hysteretic component and the damage indicator. All methods considered give acceptable results for these quantities as expected from the similar results for the unfiltered case. Figs. 3-61, 3-62 and 3-63 show the corresponding results for the time-dependent variances of the displacement, the hysteretic component and the damage indicator. Again, the equivalent linearization schemes clearly underestimate the variances of the displacement and the hysteretic component, and give completely misleading results for the damage indicator. The variance predictions of the equivalent cubic expansion are in much better agreement with the simulation results and are of the same quality as those of the unfiltered case. The calculation time for the various methods in comparison to those used for the Monte Carlo simulation was 0.88% for the equivalent linearization and 6% for the equivalent cubic expansion technique.

The following conclusions may be drawn from the the study in this example. Both of the considered equivalent linearization schemes are able to predict the mean value function of the state variables with acceptable accuracy. However, the variances of the displacement and the hysteretic component are significantly underestimated, and the variance prediction of the damage indicator is completely misleading. Since, the results of the two equivalent linearization methods are of the same quality, the idea of using a Gram-Charlier type A expansion for the joint pdf in the one method in order to approximate the true distribution better, and hence achieve better results as suggested by the theorem on p. 143, does not work when the series is truncated at the order $N = 4$. In contrast the equivalent cubic expansion technique in combination with an ordinary cumulant neglect closure approximation provides accurate estimates of the mean value function and variance of all state variables, and seems to provide one of the best semi-analytical schemes available for the analysis of hysteretic system driven by compound Poisson processes.

Further, it has been demonstrated that significant non-zero mean displacement responses may occur in hysteretic systems with small elastic restoring forces exposed to a compound process with zero mean impulses and non-zero odd moments of higher order, even at the relatively high mean arrival rate of impulses of $\nu = \frac{8.149}{T_0}$. Hence, the replacement of compound Poisson process excitations with an equivalent Gaussian white noise on these conditions, as is often claimed to be legal, should be performed with caution.

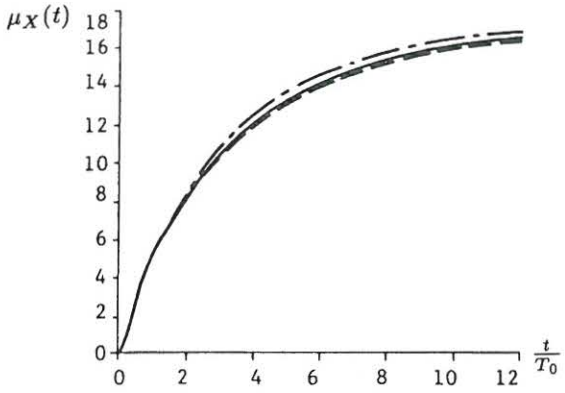

Fig. 3-46: Mean value function of displacement response, $\mu_X(t)$. Non-zero mean case. Iwankiewicz and Nielsen (1992b).

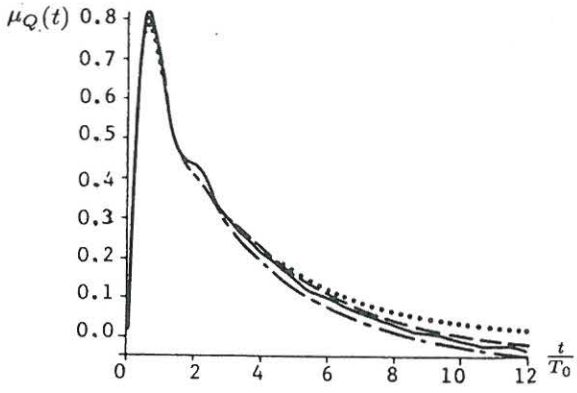

Fig. 3-47: Mean value function of hysteretic component, $\mu_Q(t)$. Non-zero mean case. Iwankiewicz and Nielsen (1992b).

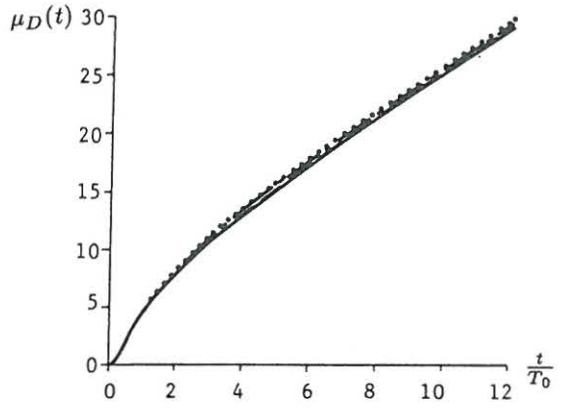

Fig. 3-48: Mean-value function of damage indicator, $\mu_D(t)$. Non-zero mean case. Iwankiewicz and Nielsen (1992b).

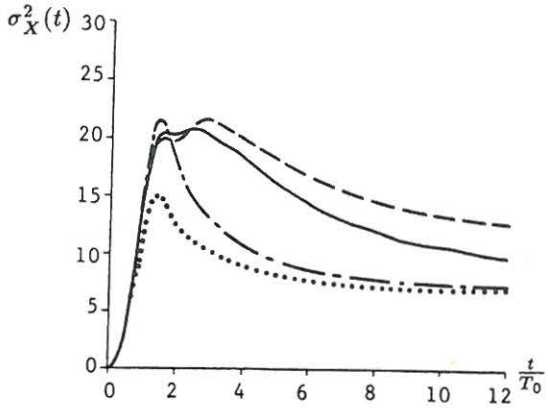

Fig. 3-49: Time-dependent variance of displacement response, $\sigma_X^2(t)$. Non-zero mean case. Iwankiewicz and Nielsen (1992b).

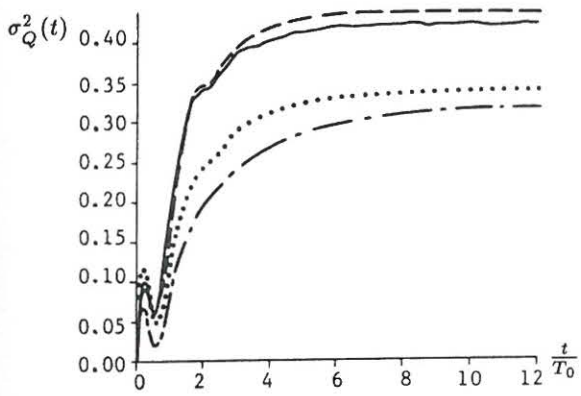

Fig. 3-50: Time-dependent variance of hysteretic component, $\sigma_Q^2(t)$. Non-zero mean case. Iwankiewicz and Nielsen (1992b).

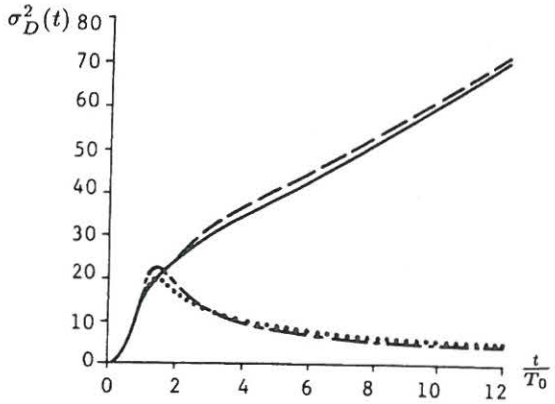

Fig. 3-51: Time-dependent variance of damage indicator, $\sigma_D^2(t)$. Non-zero mean case. Iwankiewicz and Nielsen (1992b).

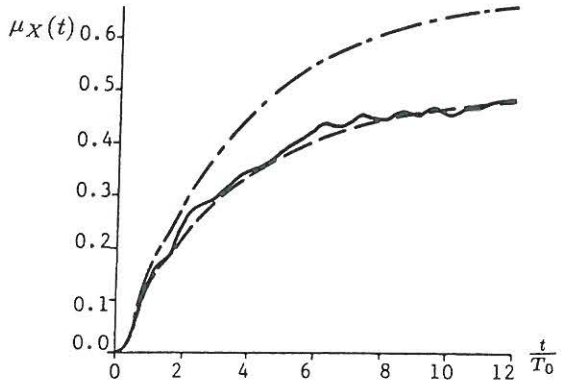

Fig. 3-52: Mean value function of displacement response, $\mu_X(t)$. Zero mean case. Iwankiewicz and Nielsen (1992b).

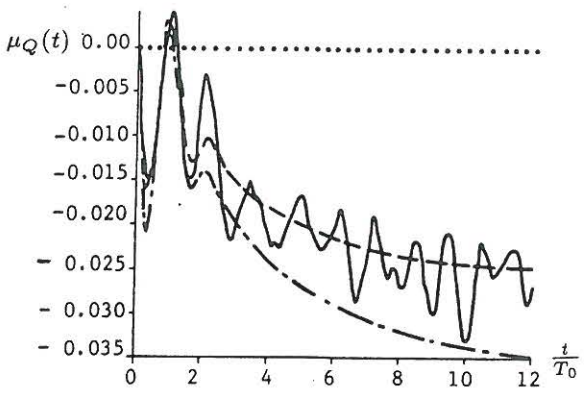

Fig. 3-53: Mean value function of hysteretic component, $\mu_Q(t)$. Zero mean case. Iwankiewicz and Nielsen (1992b).

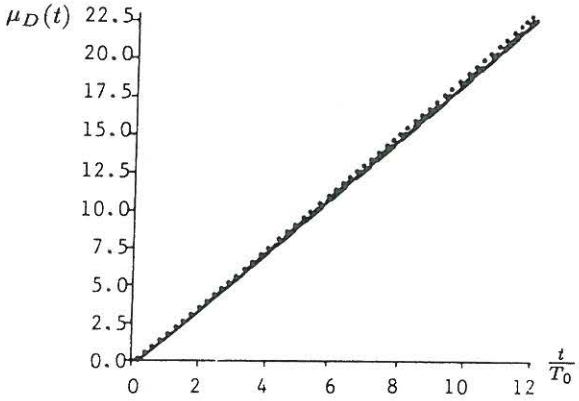

Fig. 3-54: Mean-value function of damage indicator, $\mu_D(t)$. Zero mean case. Iwankiewicz and Nielsen (1992b).

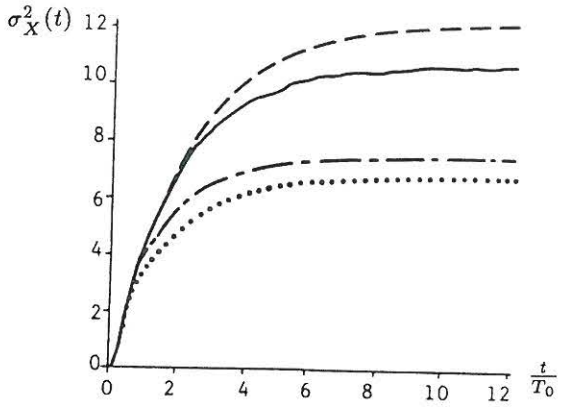

Fig. 3-55: Time-dependent variance of displacement response, $\sigma_X^2(t)$. Zero mean case. Iwankiewicz and Nielsen (1992b).

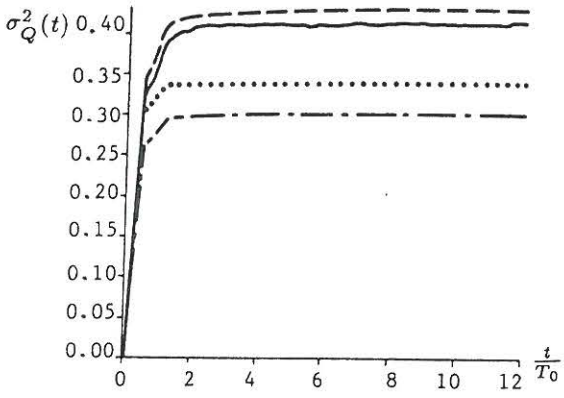

Fig. 3-56: Time-dependent variance of hysteretic component, $\sigma_Q^2(t)$. Zero mean case. Iwankiewicz and Nielsen (1992b).

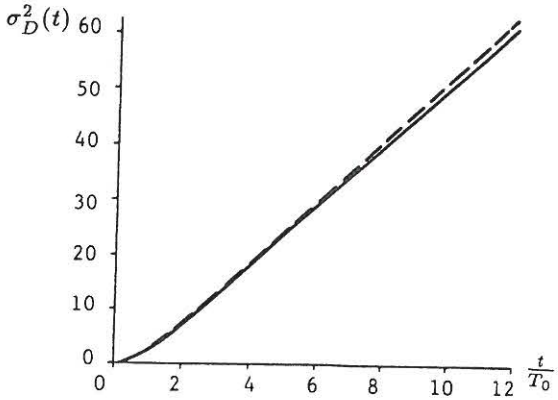

Fig. 3-57: Time-dependent variance of damage indicator, $\sigma_D^2(t)$. Zero mean case. Iwankiewicz and Nielsen (1992b).

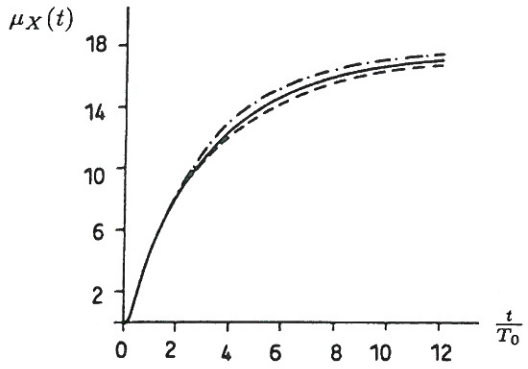

Fig. 3-58: Mean value function of displacement response, $\mu_X(t)$. General pulses. Iwankiewicz and Nielsen (1992b).

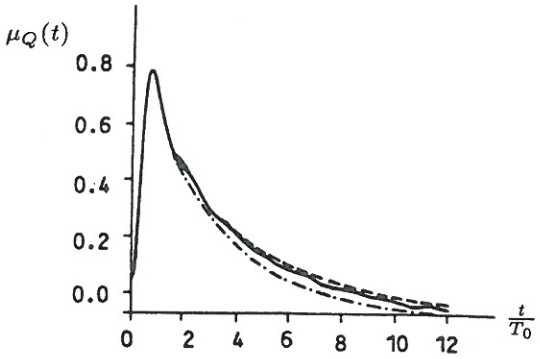

Fig. 3-59: Mean value function of hysteretic component, $\mu_Q(t)$. General pulses. Iwankiewicz and Nielsen (1992b).

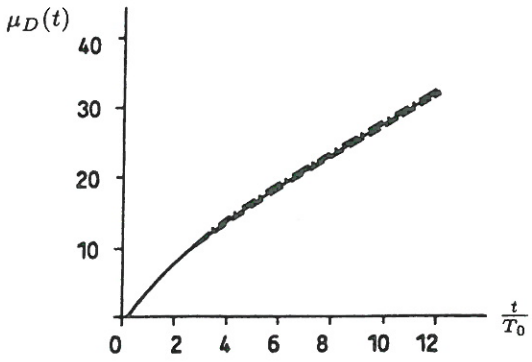

Fig. 3-60: Mean-value function of damage indicator, $\mu_D(t)$. General pulses. Iwankiewicz and Nielsen (1992b).

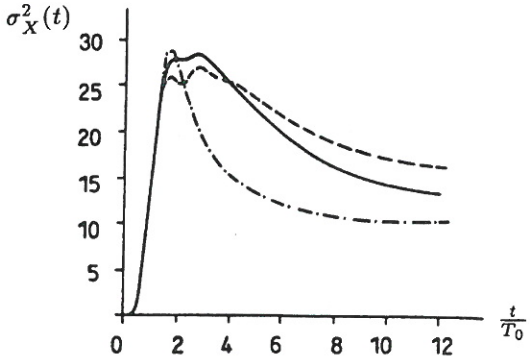

Fig. 3-61: Time-dependent variance of displacement response, $\sigma_X^2(t)$. General pulses. Iwankiewicz and Nielsen (1992b).

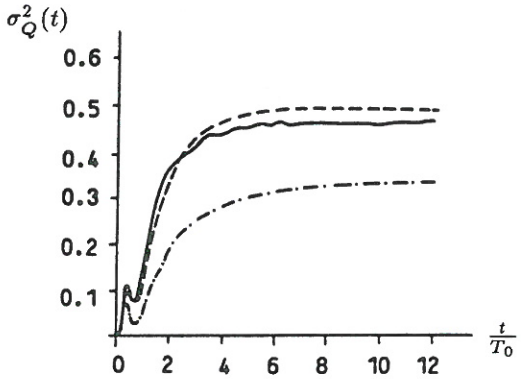

Fig. 3-62: Time-dependent variance of hysteretic component, $\sigma_Q^2(t)$. General pulses. Iwankiewicz and Nielsen (1992b).

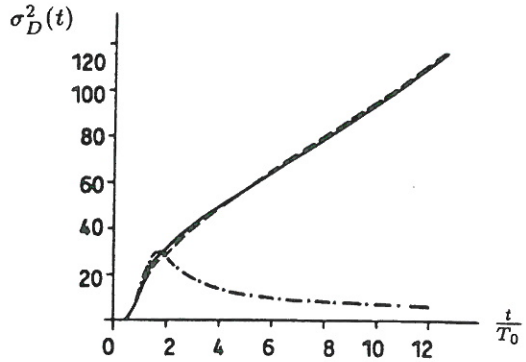

Fig. 3-63: Time-dependent variance of damage indicator, $\sigma_D^2(t)$. General pulses. Iwankiewicz and Nielsen (1992b).

3.3.4 Compound renewal process driven systems

A renewal counting process $\{N_r(t), t \in]t_0, \infty[\}$ can be defined as a sequence of random time points $t_1, t_2, \dots, t_n$ on the positive real line, such that the interarrival times $I_i = t_i - t_{i-1}$, $i = 2, 3, \dots$ are positive, mutually independent and identically distributed random variables. The point process is called an ordinary renewal counting process if the time $I_1 = t_1$ measured from the origin to the first event has the same distribution as other time intervals $I_2, I_3, \dots$, Cox (1962), Cox and Isham (1980). This means that the counting starts at the time t_0 after the arrival of the 0th impulse, which is not counted. If I_1 has a distribution different from other time intervals I_i, the point process is denoted a general or delayed renewal counting process. In that case the time origin is placed arbitrarily. An ordinary renewal process can be defined equivalently as the sequence of positive, mutually independent and identically distributed random variables $\{I_i,\ i = 1, 2, \dots\}$.

Let $\mathcal{C}_{]t,t+\Delta t]}$ signify the event of an impulse arrival during the interval $]t, t+\Delta t]$. For the ordinary and the general renewal processes the probability that a random point occurs in each of the disjoint intervals $]t_1, t_1 + \Delta t_1], \dots,]t_n, t_n + \Delta t_n]$ can be written

$$P\left(\mathcal{C}_{]t_1,t_1+\Delta t_1]} \cap \cdots \cap \mathcal{C}_{]t_n,t_n+\Delta t_n]}\right) = \begin{cases} f_{n,o}(t_1, \dots, t_n)\Delta t_1 \cdots \Delta t_n + O\left((\Delta t_{\max})^{n+1}\right) \\ f_{n,g}(t_1, \dots, t_n)\Delta t_1 \cdots \Delta t_n + O\left((\Delta t_{\max})^{n+1}\right) \end{cases} \tag{3-338}$$

where $\Delta t_{\max} = \max(\Delta t_1, \dots \Delta t_n)$. $f_{n,o}(t_1, \dots, t_n)$ and $f_{n,g}(t_1, \dots, t_n)$ signify the product densities of the order n for the various definitions of the reneval process. These have identical meaning to the nth order crossing rates defined in section 2.1, which are actually product densities for underlying processes counting the number of specific crossing events. $f_{n,o}(t_1, \dots, t_n)$ and $f_{n,g}(t_1, \dots, t_n)$ may easily be expressed in terms of the product densities of the 1st order $f_{1,o}(t)$ and $f_{1,g}(t)$. With $t_1 < \cdots < t_n$ it follows from the assumption of mutually independent interarrival times that

$$P\left(\mathcal{C}_{]t_1,t_1+\Delta t_1]} \cap \cdots \cap \mathcal{C}_{]t_n,t_n+\Delta t_n]}\right) = P\left(\mathcal{C}_{]t_1,t_1+\Delta t_1]}\right) \prod_{i=2}^{n} P\left(\mathcal{C}_{]t_i,t_i+\Delta t_i]} \mid \mathcal{C}_{]t_{i-1},t_{i-1}+\Delta t_{i-1}]}\right) \Rightarrow$$

$$f_{n,o}(t_1, \dots, t_n) = f_{1,o}(t_1) \prod_{i=2}^{n} f_{1,o}(t_i - t_{i-1}) \tag{3-339}$$

$$f_{n,g}(t_1, \dots, t_n) = f_{1,g}(t_1) \prod_{i=2}^{n} f_{1,o}(t_i - t_{i-1}) \tag{3-340}$$

If the probability density functions of I_1 and $\{I_i,\ i = 2, 3, \dots\}$ are denoted $f_{I_1}(\cdot)$ and $f_I(\cdot)$, the 1st order product densities are obtained from the following integral equations, known as the renewal equations, Srinivasan (1974)

$$f_{1,o}(t) = f_{I_1}(t) + \int_0^t f_{1,o}(t-u) f_{I_1}(u) du \tag{3-341}$$

$$f_{1,g}(t) = f_I(t) + \int_0^t f_{1,g}(t-u) f_{I_1}(u) du \qquad (3-342)$$

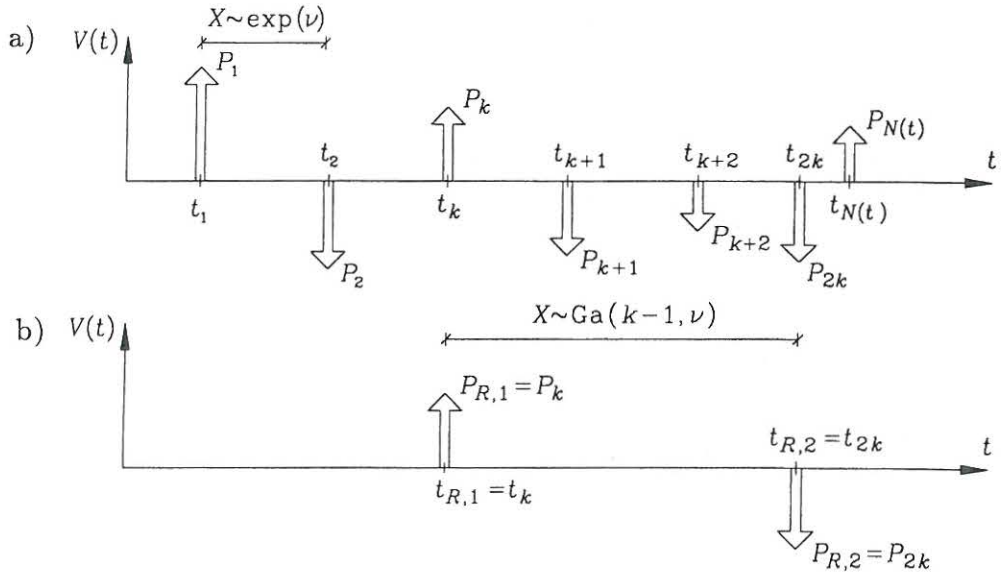

Figur 3-64: Realizations of compound point processes. a) Compound Poisson process. b) Compound Erlang renewal process.

Let the considerations be confined to the class of Erlang renewal processes, i.e. the ones for which the interarrival times I_i are independent, gamma distributed random variables, $I_i \sim \mathrm{G}(k-1,\nu)$, with the probability density function given by

$$f_I(t) = \frac{\nu^k t^{k-1}}{(k-1)!} \exp(-\nu t) \quad , \quad t > 0 \quad , \quad k = 1, 2, \ldots \qquad (3-343)$$

The case $k = 1$ corresponds to a negative exponential density function, hence it is the case of a Poisson process. Since, the gamma distributed random variable with parameters $(k-1,\nu)$ has the same distribution as the sum of k independent, negative exponentially distributed random variables with parameter ν, the events driven by an Erlang renewal process $\{N_r(t), t \in]t_0, \infty[\}$ with parameter k can be regarded as every kth Poisson event, taken out of a stationary Poisson process $\{N(t), t \in]t_0, \infty[\}$ with the mean arrival rate ν, cf. e.g. Osaki (1992). Since, the increment of a Poisson counting process is independent, I_1 is exponentially distributed with mean value $\frac{1}{\nu}$, no matter if the 0th impulse has arrived at the time t_0 or previous. Hence, the distinction between ordinary and general renewal counting processes becomes immaterial in this case.

The idea is to recast the renewal-driven impulse process, or the excitation term of the dynamic system in such a way as to obtain a non-zero impulse magnitude for every $k, 2k, 3k, \ldots$ Poisson event and zero magnitudes for all other Poisson events. The

governing stochastic equations (3-119) can then be written in terms of the following stochastic integro-differential equations as follows

$$d\mathbf{X}(t) = \mathbf{a}\big(\mathbf{X}(t),t\big)dt + \mathbf{b}\big(\mathbf{X}(t),t\big)\rho\big(N(t)\big)\int_{\mathcal{P}} pM(dt,t,dp,p) \qquad (3-344)$$

As seen, the structural state vector, the drift vector and the diffusion vector have temporarily been denoted $\mathbf{X}(t)$, $\mathbf{a}\big(\mathbf{X}(t),t\big)$ and $\mathbf{b}\big(\mathbf{X}(t),t\big)$, respectively. $M(dt,t,dp,p)$ is a Poisson random measure, cf. (3-14), and $\rho\big(N(t)\big)$ is the required zero-memory transformation of the Poisson counting process $\{N(t), t \in]t_0,\infty[\}$ with the property

$$\rho\big(N(t)\big) = \begin{cases} 1 & , \quad N(t) = k-1,\ 2k-1,\ 3k-1,\ldots \\ 0 & , \quad \text{else} \end{cases} \qquad (3-345)$$

The transformation satisfying the required property is found to be

$$\rho\big(N(t)\big) = \frac{1}{k}\sum_{j=0}^{k-1}\exp\left(i2\pi\frac{j\big(N(t)+1\big)}{k}\right) = \frac{1}{k}\sum_{j=0}^{k-1}U_j(t) \qquad (3-346)$$

The equivalence of (3-345) and (3-346) follows from direct evaluation of the power series (3-346) in the quantity $\exp\big(i2\pi(N(t)+1)/k\big)$. Noticing, that $U_j(t) = U^*_{k-j}(t)$, where * denotes the complex conjugate, the right-hand side of (3-346) can be evaluated as

$$\rho\big(N(t)\big) = \begin{cases} \frac{1}{k}\left(1+2\sum\limits_{j=1}^{k_0-1}C_j(t)\right) & , \quad k \text{ odd} \\ \frac{1}{k}\left(1+2\sum\limits_{j=1}^{k_0-1}C_j(t)+C_{k_0}(t)\right) & , \quad k \text{ even} \end{cases} \qquad (3-347)$$

where

$$C_j(t) = \mathrm{Re}\big(U_j(t)\big) = \cos\left(2\pi\frac{j\big(N(t)+1\big)}{k}\right) \quad , \quad j = 1,2,\ldots,k_0-1 \qquad (3-348)$$

$$C_{k_0}(t) = \exp\Big(i\pi\big(N(t)+1\big)\Big) = (-1)^{N(t)+1} \quad , \quad k \text{ even} \qquad (3-349)$$

$$S_j(t) = \mathrm{Im}\big(U_j(t)\big) = \sin\left(2\pi\frac{j\big(N(t)+1\big)}{k}\right) \quad , \quad j = 1,2,\ldots,k_0-1 \qquad (3-350)$$

$$k_0 = \left[\frac{k+1}{2}\right] \qquad (3-351)$$

$[\cdot]$ denotes the integer part. Next, $C_j(t)$, $S_j(t)$, $j = 1,\ldots,k_0-1$, and $C_{k_0}(t)$ in case of k even, will be considered as additional auxiliary new state variables, somewhat similar

to the auxiliary state variables introduced for the shaping filter (3-36), (3-37). This means that stochastic differential equations specifying the development of these new state variables must be formulated, which is done in the following few steps

$$dU_j(t) = U_j(t+dt) - U_j(t) =$$

$$\exp\left(i2\pi\frac{j\big(N(t)+dN(t)+1\big)}{k}\right) - \exp\left(i2\pi\frac{j\big(N(t)+1\big)}{k}\right) =$$

$$U_j(t)\Big(\exp\left(i2\pi\frac{j}{k}dN(t)\right)-1\Big) = U_j(t)\Big(\exp\left(i2\pi\frac{j}{k}\right)-1\Big)dN(t)\ ,\ j=1,2,\dots,k_0 \quad (3-352)$$

The equivalence of the last two statements of (3-352) follows from the fact that the right-hand sides give the same result for both $dN(t)=0$ and $dN(t)=1$.

Specifically, the equations for the real and imaginary parts become

$$dC_j(t) = \left[C_j(t)\Big(\cos\left(2\pi\frac{j}{k}\right)-1\Big) - S_j(t)\sin\left(2\pi\frac{j}{k}\right)\right]dN(t)\ ,\ j=1,\dots,k_0-1 \quad (3-353)$$

$$dC_{k_0}(t) = -2C_{k_0}(t)dN(t) \quad , \quad k \text{ even} \quad (3-354)$$

$$dS_j(t) = \left[C_j(t)\sin\left(2\pi\frac{j}{k}\right) + S_j(t)\Big(\cos\left(2\pi\frac{j}{k}\right)-1\Big)\right]dN(t)\ ,\ j=1,\dots,k_0-1 \quad (3-355)$$

The state vector augmented by these new variables is governed by the stochastic integro-differential equations

$$d\mathbf{Z}(t) = \mathbf{c}\big(\mathbf{Z}(t),t\big)dt + \int_{\mathcal{P}} \mathbf{e}\big(\mathbf{Z}(t),t,p\big)M(dt,t,dp,p) \quad (3-356)$$

where for k even

$$\mathbf{Z}(t) = \begin{bmatrix} \mathbf{X}(t) \\ C_1(t) \\ S_1(t) \\ C_2(t) \\ S_2(t) \\ \vdots \\ C_{k_0-1}(t) \\ S_{k_0-1}(t) \\ C_{k_0}(t) \end{bmatrix} \quad , \quad \mathbf{c}\big(\mathbf{Z}(t),t\big) = \begin{bmatrix} \mathbf{a}\big(\mathbf{X}(t),t\big) \\ 0 \\ 0 \\ 0 \\ 0 \\ \vdots \\ 0 \\ 0 \\ 0 \end{bmatrix} \quad (3-357)$$

$$\mathbf{e}\big(\mathbf{Z}(t),t,p\big)=\begin{bmatrix}\frac{1}{k}\Big(1+2\sum\limits_{j=1}^{k_0-1}C_j(t)+C_{k_0}(t)\Big)\mathbf{b}\big(\mathbf{X}(t),t\big)p\\ C_1(t)\Big(\cos\big(2\pi\frac{1}{k}\big)-1\Big)-S_1(t)\sin\big(2\pi\frac{1}{k}\big)\\ C_1(t)\sin\big(2\pi\frac{1}{k}\big)+S_1(t)\Big(\cos\big(2\pi\frac{1}{k}\big)-1\Big)\\ C_2(t)\Big(\cos\big(2\pi\frac{2}{k}\big)-1\Big)-S_2(t)\sin\big(2\pi\frac{2}{k}\big)\\ C_2(t)\sin\big(2\pi\frac{2}{k}\big)+S_2(t)\Big(\cos\big(2\pi\frac{2}{k}\big)-1\Big)\\ \vdots\\ C_{k_0-1}(t)\Big(\cos\big(2\pi\frac{k_0-1}{k}\big)-1\Big)-S_{k_0-1}(t)\sin\big(2\pi\frac{k_0-1}{k}\big)\\ C_{k_0-1}(t)\sin\big(2\pi\frac{k_0-1}{k}\big)+S_{k_0-1}(t)\Big(\cos\big(2\pi\frac{k_0-1}{k}\big)-1\Big)\\ -2C_{k_0}(t)\end{bmatrix}\qquad(3-358)$$

and for k odd

$$\mathbf{Z}(t)=\begin{bmatrix}\mathbf{X}(t)\\ C_1(t)\\ S_1(t)\\ C_2(t)\\ S_2(t)\\ \vdots\\ C_{k_0-1}(t)\\ S_{k_0-1}(t)\end{bmatrix}\quad,\quad \mathbf{c}\big(\mathbf{Z}(t),t\big)=\begin{bmatrix}\mathbf{a}\big(\mathbf{X}(t),t\big)\\ 0\\ 0\\ 0\\ 0\\ \vdots\\ 0\\ 0\end{bmatrix}\qquad(3-359)$$

$$\mathbf{e}\big(\mathbf{Z}(t),t,p\big)=\begin{bmatrix}\frac{1}{k}\Big(1+2\sum\limits_{j=1}^{k_0-1}C_j(t)\Big)\mathbf{b}\big(\mathbf{X}(t),t\big)p\\ C_1(t)\Big(\cos\big(2\pi\frac{1}{k}\big)-1\Big)-S_1(t)\sin\big(2\pi\frac{1}{k}\big)\\ C_1(t)\sin\big(2\pi\frac{1}{k}\big)+S_1(t)\Big(\cos\big(2\pi\frac{1}{k}\big)-1\Big)\\ C_2(t)\Big(\cos\big(2\pi\frac{2}{k}\big)-1\Big)-S_2(t)\sin\big(2\pi\frac{2}{k}\big)\\ C_2(t)\sin\big(2\pi\frac{2}{k}\big)+S_2(t)\Big(\cos\big(2\pi\frac{2}{k}\big)-1\Big)\\ \vdots\\ C_{k_0-1}(t)\Big(\cos\big(2\pi\frac{k_0-1}{k}\big)-1\Big)-S_{k_0-1}(t)\sin\big(2\pi\frac{k_0-1}{k}\big)\\ C_{k_0-1}(t)\sin\big(2\pi\frac{k_0-1}{k}\big)+S_{k_0-1}(t)\Big(\cos\big(2\pi\frac{k_0-1}{k}\big)-1\Big)\end{bmatrix}\qquad(3-360)$$

The state vector $\mathbf{Z}(t)$, augmented by additional auxiliary state variables as governed by equation (3-356), is driven by a Poisson process, and hence forms a Markov vector process. The differential rule and the equations for joint central moments then follow

from (3-166) and (3-324) with the minor correction that only the components of the diffusion vector $\mathbf{e}(\mathbf{Z}(t),t,P)$ belonging to the structural state variables are proportional to the impulse strength P. The resulting equations read

$$df(\mathbf{Z}(t),t) = \frac{\partial f(\mathbf{Z}(t),t)}{\partial t}dt + \mathcal{K}^T_{\mathbf{z},t}\Big[f(\mathbf{Z}(t),t)\Big]dt = \frac{\partial f(\mathbf{Z}(t),t)}{\partial t}dt +$$

$$\sum_{i=1}^{n} c_i(\mathbf{Z}(t),t)\frac{\partial f(\mathbf{Z}(t),t)}{\partial z_i}dt + \int_{\mathcal{P}}\Big(f\Big(\mathbf{Z}(t)+\mathbf{e}(\mathbf{Z}(t),t,p),t\Big)-f(\mathbf{Z}(t),t)\Big)M(dt,t,dp,p) \quad (3-361)$$

$$\left.\begin{aligned}
&\tfrac{d}{dt}\mu_i(t) = E\Big[c_i(\mathbf{Z}(t),t)\Big] + \nu E\Big[e_i(\mathbf{Z}(t),t,E[P])\Big]\\
&\tfrac{d}{dt}\lambda_{ij}(t) = 2\Big\{E\Big[c^0_i(\mathbf{Z}(t),t)Z^0_j(t)\Big]\Big\}_s +\\
&\nu\cdot 2\Big\{E\Big[e^0_i(\mathbf{Z}(t),t,P)Z^0_j(t)\Big]\Big\}_s +\\
&\nu E\Big[e_i(\mathbf{Z}(t),t,P)e_j(\mathbf{Z}(t),t,P)\Big]\\
&\tfrac{d}{dt}\lambda_{ijk}(t) = 3\Big\{E\Big[c^0_i(\mathbf{Z}(t),t)Z^0_j(t)Z^0_k(t)\Big]\Big\}_s +\\
&\nu\cdot 3\Big\{E\Big[e^0_i(\mathbf{Z}(t),t,P)Z^0_j(t)Z^0_k(t)\Big]\Big\}_s +\\
&\nu\cdot 3\Big\{E\Big[e_i(\mathbf{Z}(t),t,P)e_j(\mathbf{Z}(t),t,P)Z^0_k(t)\Big]\Big\}_s +\\
&\nu E\Big[e_i(\mathbf{Z}(t),t,P)e_j(\mathbf{Z}(t),t,P)e_k(\mathbf{Z}(t),t,P)\Big]\\
&\tfrac{d}{dt}\lambda_{ijkl}(t) = 4\Big\{E\Big[c^0_i(\mathbf{Z}(t),t)Z^0_j(t)Z^0_k(t)Z^0_l(t)\Big]\Big\}_s +\\
&\nu\cdot 4\Big\{E\Big[e^0_i(\mathbf{Z}(t),t,P)Z^0_j(t)Z^0_k(t)Z^0_l(t)\Big]\Big\}_s +\\
&\nu\cdot 6\Big\{E\Big[e_i(\mathbf{Z}(t),t,P)e_j(\mathbf{Z}(t),t,P)Z^0_k(t)Z^0_l(t)\Big]\Big\}_s +\\
&\nu\cdot 4E\Big[e_i(\mathbf{Z}(t),t,P)e_j(\mathbf{Z}(t),t,P)e_k(\mathbf{Z}(t),t,P)Z^0_l(t)\Big] +\\
&\nu E\Big[e_i(\mathbf{Z}(t),t,P)e_j(\mathbf{Z}(t),t,P)e_k(\mathbf{Z}(t),t,P)e_l(\mathbf{Z}(t),t,P)\Big]\\
&\tfrac{d}{dt}\lambda_{i_1\ldots i_N}(t) = N\Big\{E\Big[c^0_{i_1}(\mathbf{Z}(t),t)Z^0_{i_2}(t)\cdots Z^0_{i_N}(t)\Big]\Big\}_s -\\
&\nu\cdot N\Big\{E\Big[e_{i_1}(\mathbf{Z}(t),t,P)\Big]\lambda_{i_2\ldots i_N}(t)\Big\}_s +\\
&\sum_{k=1}^{N}\nu\cdot\binom{N}{k}\Big\{E\Big[e_{i_1}(\mathbf{Z}(t),t,P)\cdots e_{i_k}(\mathbf{Z}(t),t,P)Z^0_{i_{k+1}}(t)\cdots Z^0_{i_N}(t)\Big]\Big\}_s
\end{aligned}\right\} \quad (3-362)$$

In case of low mean arrival rates of impulses it may be necessary to modify the applied closure scheme in order to take into consideration the probability that no compound Erlang impulses have yet excited the structure during the interval $]t_0,t[$. The probability of no Erlang events, $P(t,t_0)$, is equal to the probability of less than k Poisson event. Hence, cf. (3-8)

$$P(t,t_0) = \sum_{n=0}^{k-1} \frac{\big(\nu(t-t_0)\big)^n}{n!} \exp\Big(-\nu(t-t_0)\Big) \qquad (3-363)$$

Only the structural state vector components $\mathbf{X}(t)$ should be subjected to the modification, whereas the remaining auxiliary state variables, assembled in the subvector $\mathbf{Y}(t)$, are unchanged. Hence, the closure scheme (3-229) should be reformulated in the following way

$$f_{\{\mathbf{X}\}\{\mathbf{Y}\}}(\mathbf{x},\mathbf{y},t) = P(t,t_0)\delta\big(\mathbf{x}-\mathbf{d}(t|\mathbf{x}_0,t_0)\big)f_{\{\mathbf{Y}\}}(\mathbf{y},t) + \big(1-P(t,t_0)\big)f_{\{\mathbf{V}\}\{\mathbf{Y}\}}(\mathbf{x},\mathbf{y},t) \quad (3-364)$$

where $P(t,t_0))$ is given by (3-363) and $\mathbf{d}(t|\mathbf{x}_0,t_0))$ signifies the eigenvibrations of the structural system (3-344). For polynomial non-linearities modified cumulant neglect closure schemes similar to (3-232), (3-233), (3-234) and (3-235) may be derived next.

The moment equations for the special case $k = 2$ were originally devised by Iwankiewicz and Nielsen (1994). The theory presented, covering systems driven by an arbitrary compound Erlang process and using a completely different approach, is due to Nielsen, Iwankiewicz and Skjærbæk (1996).

Example 3-10: Excitation processes reducible to compound Poisson processes

Consider the point process $\{V(t), t \in]t_0,\infty[\}$ with the increments

$$dV(t) = \rho(N(t))dN(t) \qquad (3-365)$$

where $\rho(N(t))$ is a zero memory transformation of the homogeneous Poisson process $\{N(t), t \in]t_0,\infty[\}$ with the mean arrival rate ν. If $\rho(N(t))$ is given by (3-346) the Erlang process is obtained, for which it has just been demonstrated that introduction of the auxiliary state variables (3-348), (3-349) and (3-350) reduces the augmented dynamic system to a Markov system with the state vector given by (3-357) or (3-359). In this example the conditions for such a reduction will be closer investigated. The product densities of (3-365) become

$$f_1(t) = \nu E\Big[\rho(N(t))\Big] \qquad (3-366)$$

$$f_n(t_1,\ldots,t_n) = \nu^n E\Big[\rho(N(t_1))\cdots\rho(N(t_n))\Big] \qquad (3-367)$$

Introduce $Y_j(t) = \rho(N(t)+j-1)$, $j = 1,2,\ldots,$ as new auxiliary state variables. The differential equation specifying the development of these state variables can then be written

$$\left.\begin{aligned} &dY_1(t) = \rho(N(t)+dN(t)) - \rho(N(t)) = \Big(\rho(N(t)+1) - \rho(N(t))\Big)dN(t) \Rightarrow \\ &dY_1(t) = (Y_2(t) - Y_1(t))dN(t) \\ &dY_2(t) = (Y_3(t) - Y_2(t))dN(t) \\ &\vdots \\ &dY_k(t) = (Y_{k+1}(t) - Y_k(t))dN(t) \end{aligned}\right\} \qquad (3-368)$$

(3-368) is proved in the same way as (3-352), using that either $dN(t) = 0$ or $dN(t) = 1$. The hierarchy of differential equations (3-368) cannot be closed unless $Y_{k+1}(t)$ can be expressed in terms of the previous auxiliary state variables. As an example assume the following linear dependence

$$Y_{k+1}(t) = -\frac{1}{a_{k+1}}\Big(a_1 Y_1(t) + a_2 Y_2(t) + \cdots + a_k Y_k(t)\Big) \quad , \quad a_j \in R \tag{3-369}$$

(3-368) then attains the form

$$\left.\begin{aligned} dY_1(t) &= \big(Y_2(t) - Y_1(t)\big)dN(t) \\ dY_2(t) &= \big(Y_3(t) - Y_2(t)\big)dN(t) \\ &\vdots \\ dY_k(t) &= -\Big(\tfrac{a_1}{a_{k+1}} Y_1(t) + \cdots + \tfrac{a_{k-1}}{a_{k+1}} Y_{k-1}(t) + \big(1 + \tfrac{a_k}{a_{k+1}}\big) Y_k(t)\Big)dN(t) \end{aligned}\right\} \tag{3-370}$$

(3-369) implies that $\rho\big(N(t)\big)$ must fulfil the AR difference equation

$$a_1 \rho\big(N(t)\big) + a_2 \rho\big(N(t)+1\big) + \cdots + a_{k+1} \rho\big(N(t)+k\big) = 0 \tag{3-371}$$

The solution of (3-371) reads

$$\rho\big(N(t)\big) = \sum_{j=1}^{k} b_j \lambda_j^{N(t)} \tag{3-372}$$

where $b_j \in C$, and λ_j denote the solutions of the characteristic equation

$$a_1 + a_2 \lambda + \cdots + a_{k+1} \lambda^k = 0 \tag{3-373}$$

If $|\lambda_j| \neq 1$ the corresponding term in (3-372) either extincts or explodes. Hence, in case the point process (3-365) is assumed to be homogeneous, it is necessary that the eigenvalues all have the magnitude 1, so

$$\lambda_j = \exp\big(i\gamma_j\big) \quad , \quad \gamma_j \in R \quad , \quad j = 1, 2, \ldots, k \tag{3-374}$$

The solutions of (3-373) are either real or complex conjugates in pairs. For a homogeneous point process all solutions of the former kind, save $\lambda_j \pm 1$, are excluded by the stationarity requirement, from which it follows that the most general expression fulfilling (3-371) has the appearance

$$\rho\big(N(t)\big) = b_0 + 2\sum_{j=1}^{k_0} \Big(\mathrm{Re}(b_j)\cos\big(\gamma_j N(t)\big) - \mathrm{Im}(b_j)\sin\big(\gamma_j N(t)\big)\Big) + b_{k_0+1}\big(-1\big)^{N(t)} \tag{3-375}$$

b_0 and b_{k_0+1} signify the coefficients in (3-371) related to the eigenvalues $\lambda_j = 1$ and $\lambda_j = -1$, and $2k_0$ denotes the number of complex eigenvalues with $\gamma_j \neq 0$. Imposing the extra conditions on the invariants $a_1, \ldots, a_{k+1}$ of (3-373) that only solutions of magnitude 1 are permitted, γ_j is related to $a_1, \ldots, a_{k+1}$ via a one-to-one correspondence. As seen from (3-346) the Erlang process follows from (3-372) upon specialization of the parameters b_j and γ_j.

Upon insertion of (3-373) into (3-367) the following expression is obtained for the product densities

$$f_n(t_1,\dots,t_n) = \nu^n \sum_{j_1=1}^{k} \cdots \sum_{j_n=1}^{k} b_{j_1}\cdots b_{j_n} E\left[\lambda_{j_1}^{N(t_1)}\cdots\lambda_{j_n}^{N(t_n)}\right] =$$
$$\nu^n \sum_{j_1=1}^{k} \cdots \sum_{j_n=1}^{k} b_{j_1}\cdots b_{j_n}\lambda_{j_n}^{n-1}\lambda_{j_{n-1}}^{n-2}\cdots\lambda_{j_2}^{2}\lambda_{j_2}\exp\Big(\nu(t_n-t_{n-1})(\lambda_{j_n}-1)\Big)$$
$$\exp\Big(\nu(t_{n-1}-t_{n-2})(\lambda_{j_n}\lambda_{j_{n-1}}-1)\Big)\cdots\exp\Big(\nu(t_1-t_0)(\lambda_{j_n}\lambda_{j_{n-1}}\cdots\lambda_{j_1}-1)\Big) \qquad (3-376)$$

where it has been assumed that $t_1 < t_2 < \cdots < t_n$. Consider an arbitrarily regular counting process with product densities $f_n(t_1,\dots,t_n)$. The eigenvalues with argument γ_j and the coefficients b_j as well as the order of expansion k may then be determined, so the right-hand side of (3-376) approximates the left-hand side up to a certain order. Next, from the obtained parameters γ_j, the expansion coefficients a_k in (3-369) are determined, and a closed system of auxiliary differential equations (3-370) is obtained. By then, an approximate representation of the actual counting process with an equivalent Poissonian process has been achieved.

Example 3-11: Duffing oscillator exposed to compound Erlang process with k = 2, k = 3 and k = 4

Consider the Duffing oscillator (3-44) with the following parameter values

$$m = 1.0 \quad , \quad \omega_0 = 1.0 \quad , \quad \zeta = 0.05 \quad , \quad \varepsilon = 0.5 \qquad (3-377)$$

The excitation process $\{F(t), t \in]0,\infty[\}$ is modelled as a compound Erlang process with the cases $k = 2$, $k = 3$, $k = 4$. In order to make meaningful comparison between these cases, the mean arrival rate ν of the impulses will be adjusted so that $\frac{\nu}{k} = 10\omega_0$. The impulse strengths are assumed to be Rayleigh distributed, $P \sim R(\sigma^2)$, with $\sigma = 0.1$. The stationary mean value and variance of the corresponding linear oscillator exposed to Poissonian impulses with the mean arrival rate $\frac{\nu}{k}$ then become

$$\left.\begin{aligned} \mu_{X,0} &= \frac{\nu}{k}\frac{E[P]}{\omega_0^2 m} = \frac{\nu}{k}\frac{\sqrt{\frac{\pi}{2}}\sigma}{\omega_0^2 m} \\ \sigma_{X,0}^2 &= \frac{\nu}{k}\frac{E[P^2]}{4\zeta\omega_0^3 m^2} = \frac{\nu}{k}\frac{\sigma^2}{2\zeta\omega_0^3 m^2} \end{aligned}\right\} \qquad (3-378)$$

Hence, $\mu_{X,0} = \sqrt{\frac{\pi}{2}}$ and $\sigma_{X,0} = 1.0$. Deviation of results obtained from these figures can be attributed partly to the non-linearity and partly to distributions of interarrival times different from the exponential distribution. To estimate the effect of non-linearities on the result the moments for a linear oscillator with $\varepsilon = 0$ exposed to a compound Poisson process excitation with mean arrival rate $\nu = 10\omega_0$ will also be calculated.

The hierarchy of joint statistical moments (3-362) is truncated at the order $N = 4$. Since the drift terms $c_i^0(\mathbf{Z}(t))$ are cubic polynomial in the state variables, joint central moments of the 5th order appear in the equations for the 3rd order moments, and 5th and 6th order moments appear in the equations for 4th order moments. The mean arrival rate of Erlang impulses is as high as $\frac{\nu}{k} = 10\omega_0 = \frac{20\pi}{T_0}$. In this case it is not necessary to modify the closure scheme according to (3-366), and the unprovided moments of the closure scheme are all obtained by means of the ordinary cumulant neglect closure scheme (3-193).

The results of the moment equation method are compared to those obtained by Monte Carlo simulation. The simulated results have been based on averaging over an ensemble of 32000 independent response realizations, each obtained by numerical integration of the governing equations of motion (3-52), (3-332), (3-333). The interarrival times of the Erlang process between sequential impulses are generated as a sum of k mutually independent exponentially distributed random variables. The discontinuous change of the state vector due to the generated impulse strength, and succeeding eigenvibrations of the system until the arrival of the next Erlang impulse are performed in the same way as explained for compound Poisson driven systems in example 3-8. The eigenvibrations of the system between impulse arrivals were calculated by a 4th order Runge-Kutta scheme with the time step $\Delta t = \frac{T_0}{40}$, $T_0 = \frac{2\pi}{\omega_0}$ being the period of linear, undamped eigenvibrations.

The obtained results for the mean value function and the variance function of the displacement are shown in figs. 3-65, 3-66 and 3-70 for the cases $k = 2$, $k = 3$ and $k = 4$, respectively. The unbroken curves signify the approximate analytical results from the moment equation method, the dotted curves indicate the results from Monte Carlo simulation, and the dashed-dotted curve indicates the results for the linear oscillator, when exposed to an equivalent Poisson process. The first thing to notice is that the agreement between the approximate analytical results and the simulation results is very good. Secondly, the mean value functions are practically the same in all cases, meaning that this quantity is insensible to the distribution of the interarrival times. The variances, however, have a marked tendency to decrease with increasing values of k. The stationary value of these become $\sigma_X^2(\infty) \simeq 0.30$, $\sigma_X^2(\infty) \simeq 0.24$ and $\sigma_X^2(\infty) \simeq 0.21$ for the 3 cases. Hence, it may be concluded that the displacement variance depends significantly on the specific distribution of the interarrival time between Erlang impulses.

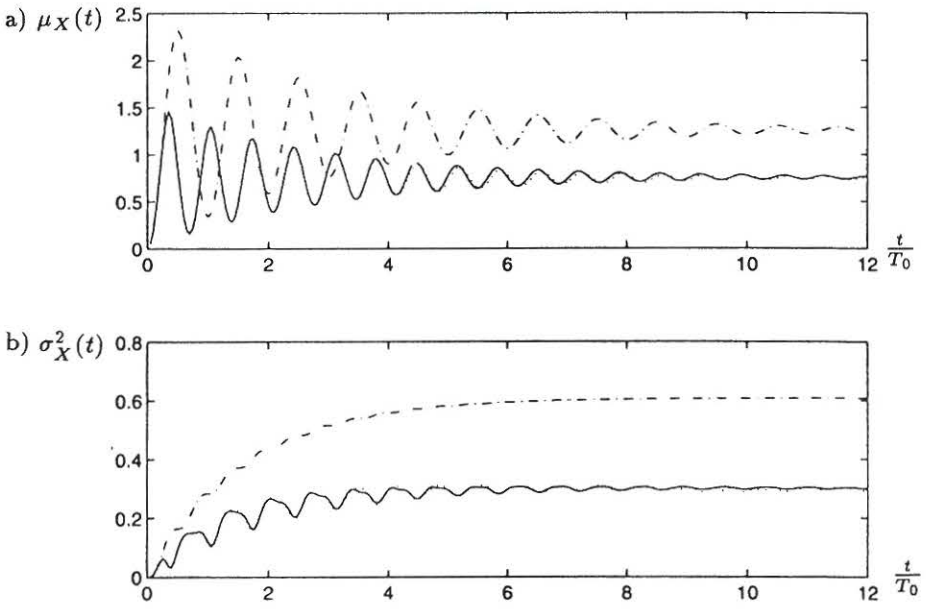

Fig. 3-65: Compound Erlang process, case $k = 2$. a) Time-dependent mean value function, $\mu_X(t)$. b) Time dependent variance function, $\sigma_X^2(t)$. Nielsen, Iwankiewicz and Skjærbæk (1996).

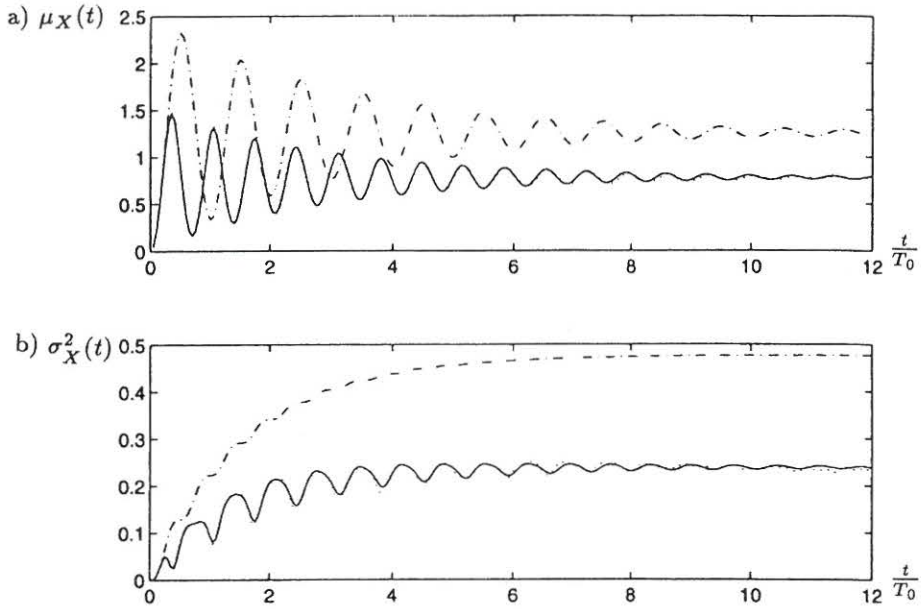

Fig. 3-66: Compound Erlang process, case $k = 3$. a) Time-dependent mean value function, $\mu_X(t)$. b) Time dependent variance function, $\sigma_X^2(t)$. Nielsen, Iwankiewicz and Skjærbæk (1996).

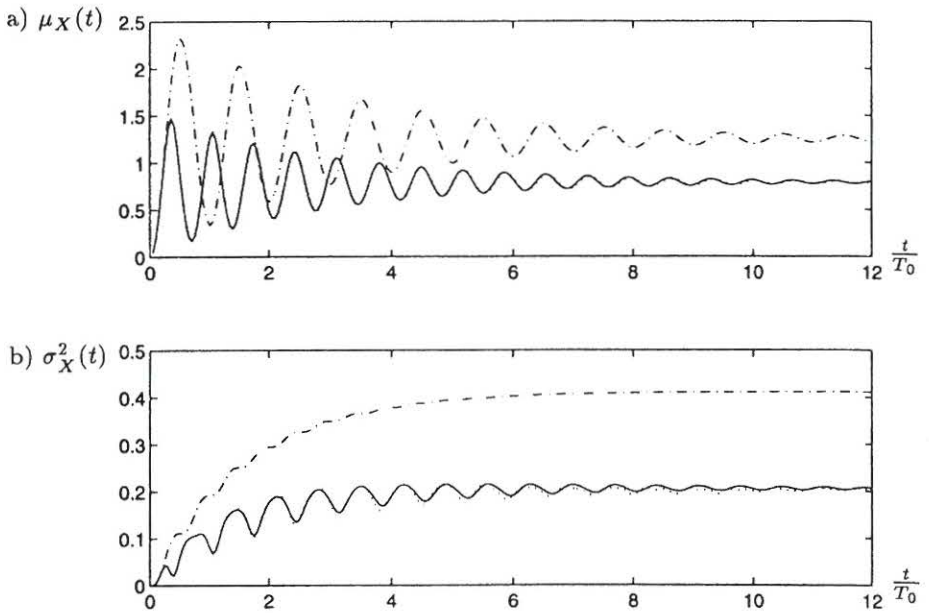

Fig. 3-67: Compound Erlang process, case $k = 4$. a) Time-dependent mean value function, $\mu_X(t)$. b) Time dependent variance function, $\sigma_X^2(t)$. Nielsen, Iwankiewicz and Skjærbæk (1996).

The considered example demonstrates the applicability of the moment equation method for the problem of a Duffing oscillator driven by a compound Erlang process after reducing the problem to an equivalent compound Poisson driven system. The obtained results of the example clearly show that the mean value function of the displacement process is insensible to the distribution of the interarrival times, whereas the variance function strongly depends on this distribution.

3.4 Path integration techniques

For a long time in physics e.g. Wehner and Wolfert (1987), Kleinert (1992), path integration methods have been applied to the numerical solution of the Fokker-Planck equation for the case of white noise excited non-linear systems. The application of the method to structural mechanics problems is due to Naess and Johnsen (1991) and Johnsen (1992). The basis of path integration approach is reducing the time continuous state continuous Markov vector process to a Markov chain by considering the process at discrete instants of time and by discretizing the sample space of the process. Sun and Hsu (1988), (1990), used a similar approach, named cell-to-cell mapping, following the earlier work of Crandall, Chandiramani and Cook (1966) on the method. However, as shown below, cell-to-cell mapping turns out to be merely a different way of evaluating the convolution integrals at transitions, and hence the discretization of the state space. Hence, path integration and cell-to-cell mapping are merely different names for one and the same thing. In what follows the former name will be coined.

Let $q_{\{\mathbf{Z}\}}(\mathbf{z}, t \mid \mathbf{x}, t_0)$ signify the joint transition probability density function of the Markov vector process $\{\mathbf{Z}(t), t \in [t_0, t_1]\}$. Further, let $f_{\{\mathbf{Z}\}}(\mathbf{z}, t_i)$ be the 1st order probability density function at the time $t_i = t_0 + i\Delta t$, $i = 0, 1, 2, \ldots$. Next, the 1st order probability density function at the following instant of time t_{i+1} is given by the convolution integral

$$f_{\{\mathbf{Z}\}}(\mathbf{z}, t_{i+1}) = \int_{S_{t_i}} q_{\{\mathbf{Z}\}}(\mathbf{z}, t_{i+1} \mid \mathbf{x}, t_i) f_{\{\mathbf{Z}\}}(\mathbf{x}, t_i) d\mathbf{x} \qquad (3-379)$$

From (3-379) the time continuous vector process has been discretized to the instants of time $t_i = t_0 + i\Delta t$. In order to discretize the state space, the sample space S_{t_i} is divided into a finite number N of small volumes $\Delta \mathbf{z}_k$ with an interior centre at $\mathbf{z}_k$. If $\Delta \mathbf{z}_k$ is sufficiently small for $q_{\{\mathbf{Z}\}}(\mathbf{z}_j, t_i + \Delta t \mid \mathbf{z}_k, t_i)$ and $f_{\{\mathbf{Z}\}}(\mathbf{z}_k, t_i)$ is approximately constant throughout the cell, the probability $\pi_j^{(i+1)}$ of being in the jth cell $\Delta \mathbf{z}_j$ at the time t_{i+1} is then given by the Riemann sum

$$\pi_j^{(i+1)} = \sum_{k=1}^{N} Q_{jk}^{(i)} \pi_k^{(i)} \quad , \quad j = 1, \ldots, N \qquad (3-380)$$

$$\pi_k^{(i)} \simeq \Delta \mathbf{z}_k f_{\{\mathbf{Z}\}}(\mathbf{z}_k, t_i) \qquad (3-381)$$

$$Q_{jk}^{(i)} \simeq \Delta \mathbf{z}_j q_{\{\mathbf{Z}\}}(\mathbf{z}_j, t_i + \Delta t \mid \mathbf{z}_k, t_i) \qquad (3-382)$$

More accurate calculations of the nodal probabilities (3-381) and the components (3-382) of the transition probability matrix $\mathbf{Q}^{(i)}$ of the Markov chain were performed by Naess and Johnsen (1991) and Johnsen (1992) upon interpolating among adjacent nodal point values by means of B - splines.

If the Markov process $\{\mathbf{Z}(t), t \in [t_0, t_1]\}$ is stationary and the intervals Δt between observations of the process are equidistant, the transition probability matrix becomes independent of the time of transition t_i, i.e. $\mathbf{Q}^{(i)} = \mathbf{Q}$, and the Markov chain becomes stationary, as well. The transition of states (3-380) can then be represented by the matrix equation

$$\boldsymbol{\pi}^{(i+1)} = \mathbf{Q}\boldsymbol{\pi}^{(i)} = \mathbf{Q}^i\boldsymbol{\pi}^{(0)} \qquad (3-383)$$

where $\boldsymbol{\pi}^{(i)}$ is an N-dimensional vector of the state probabilities $\pi_k^{(i)}$ after i transitions, and $\boldsymbol{\pi}^{(0)}$ signifies the initial distribution at the time t_0.

In reliability problems absorbing states on the exit part of the boundary $\partial S_{t_i}^{(1)}$ are characterized by the transition probability $Q_{kk} = 1 \Rightarrow Q_{jk} = 0,\ j \neq k$. Each absorbing state then forms a recurrent class, whereas all non-absorbing states make up a single class of transient states. The transient states are all the cells within the safe domain S_{t_i}. The non-absorbed probability mass, which remains in the transient states after i transitions represents the reliability of the system at the time t_{i+1}.

In stochastic response problems no absorbing states within the sample space should be specified. However, in practical calculations one needs to delimit the sample space, so artificial absorbing states are specified at sufficiently distant positions for the probability of accessing these states to be small enough. The application of cell-to-cell mapping methods to reliability problems and to stochastic response problems is then completely identical.

For the stochastic response problem in case of stationary Markov chains one may be interested in the question, whether a stationary distribution $\boldsymbol{\pi}^{(\infty)}$ to (3-383) exists, obtained after infinitely many transitions as $i \to \infty$, irrespective of the initial distribution $\boldsymbol{\pi}^{(0)}$ applied. Since the Markov chain in this case is irreducible, positive recurrent and aperiodic, the answer to this question is positive, see e.g. Osaki (1992). The limiting distribution must be invariant to further transitions, and can then be determined from the equation

$$\boldsymbol{\pi}^{(\infty)} = \mathbf{Q}\boldsymbol{\pi}^{(\infty)} \qquad (3-384)$$

(3-384) determines $\boldsymbol{\pi}^{(\infty)}$ as the normalized eigenvector to a linear eigenvalue problem with the known eigenvalue $\lambda = 1$. This eigenvalue is simple, since the Markov chain is irreducible, and the solution $\boldsymbol{\pi}^{(\infty)}$ to (3-384) then is unique. Hence the coefficient matrix $\mathbf{I} - \mathbf{Q}$ has the rank $N - 1$ and (3-384) can be rearranged into a system of linear equations of the order $N - 1$. Alternatively, $\boldsymbol{\pi}^{(\infty)}$ can be obtained by iterating in the transition equation until convergence for an arbitrary initial value distribution $\boldsymbol{\pi}^{(0)}$ is attained. Since $\lambda = 1$ is the largest eigenvalue of $\mathbf{Q}$, this corresponds to the power method approach in numerical solution of linear eigenvalue problems. Since the eigenvalue $\lambda = 1$ is known, the former approach is normally the most efficient one. Moreover, for symmetric problems, such as double barrier problems, the size of eigenvector problem can be further reduced.

As seen from (3-382) the transition probability matrix relies on the transition probability density function. Since this is not known in general, nothing seems to be gained at first. However, the method benefits from certain asymptotic results for $q_{\{\mathbf{Z}\}}(\mathbf{z}_j, t_i+\Delta t \mid \mathbf{z}_k, t_i)$, valid for small transition time intervals Δt. In sections 3.4.1 and 3.4.2 it is demonstrated how these results are obtained for systems driven by Wiener processes and for systems driven by generating source processes with jumps. In both cases the illustrative example is a non-linear, non-hysteretic SDOF oscillator. This is so, because at present path integration methods have not yet been extended to MDOF systems.

3.4.1 Path integration methods for Wiener process driven systems

The Wiener process driven system (3-116) is considered. At transitions from the state $\mathbf{Z}(t_i) = \mathbf{z}_k$ it is assumed that the transition time interval $t - t_i$ is sufficiently small for the drift vector $\mathbf{c}\big(\mathbf{Z}(t), t\big)$ to be approximated by a linear function of the state vector $\mathbf{Z}(t)$, and the diffusion matrix $\mathbf{d}\big(\mathbf{Z}(t), t\big)$ to be considered a constant as a function of $\mathbf{Z}(t)$, although it may still be a function of time. Hence, for $t \in]t_i, t_i + \Delta t]$ it is assumed, cf. (3-326)

$$\mathbf{c}\big(\mathbf{Z}(t), t\big) \simeq \mathbf{A}(t) + \mathbf{B}(t)\mathbf{Z}(t) \qquad (3-385)$$

$$\mathbf{d}\big(\mathbf{Z}(t), t\big) \simeq \mathbf{d}_0(t) \qquad (3-386)$$

The process cannot perform any jumps, so (3-385) and (3-386) will certainly be acceptable, if only the transition time interval is sufficiently small. Since the approximated system is linear under Gaussian white noise excitation, the response becomes Gaussian too. This is the principle of local Gaussianity, valid for non-linear Markov systems, during small transition time intervals. The transition probability density function $q_{\{\mathbf{Z}\}}(\mathbf{z}, t \mid \mathbf{z}_k, t_i)$ then becomes

$$q_{\{\mathbf{Z}\}}(\mathbf{z}, t \mid \mathbf{z}_k, t_i) \simeq \frac{1}{(2\pi)^{\frac{n}{2}} \Big(\det\big(\boldsymbol{\lambda}(t)\big)\Big)^{\frac{1}{2}}} \exp\Big(-\frac{1}{2}\big(\mathbf{z}-\boldsymbol{\mu}(t)\big)^T \boldsymbol{\lambda}^{-1}(t)\big(\mathbf{z}-\boldsymbol{\mu}(t)\big)\Big) \qquad (3-387)$$

where $\boldsymbol{\mu}(t) = E\big[\mathbf{Z}(t) \mid \mathbf{Z}(t_i) = \mathbf{z}_k\big]$ and $\boldsymbol{\lambda}(t) = E\big[\big(\mathbf{Z}(t) - \boldsymbol{\mu}(t)\big)\big(\mathbf{Z}(t) - \boldsymbol{\mu}(t)\big)^T \mid \mathbf{Z}(t_i) = \mathbf{z}_k\big]$ are the conditional mean value vector and the conditional covariance matrix function, respectively. These are the solutions of the following ordinary differential equations, (3-240), (3-242)

$$\frac{d}{dt}\boldsymbol{\mu}(t) = \mathbf{A}(t) + \mathbf{B}(t)\boldsymbol{\mu}(t) \quad , \quad t > t_i \quad , \quad \boldsymbol{\mu}(t_i) = \mathbf{z}_k \qquad (3-388)$$

$$\frac{d}{dt}\boldsymbol{\lambda}(t) = \mathbf{B}(t)\boldsymbol{\lambda}(t) + \boldsymbol{\lambda}(t)\mathbf{B}^T(t) + \mathbf{d}_0(t)\mathbf{d}_0^T(t) \quad , \quad \boldsymbol{\lambda}(t_i) = 0 \qquad (3-389)$$

Normally, the linearization parameters $\mathbf{A}(t), \mathbf{d}_0(t), \mathbf{B}(t)$ depend on the initial state $\mathbf{z}_k$. In case of applications in path integration methods (3-388) and (3-389) should then be solved for initial values $\mathbf{z}_k$ in all N cells, and for each transition from t_i to t_{i+1}. In case of stationary excitation in time-invariant problems $\mathbf{A}(t), \mathbf{d}_0(t)$ and $\mathbf{B}(t)$ no longer depend explicitly on time.

Moreover, if the time interval Δt between transitions is constant, the Markov chain becomes stationary, and (3-388), (3-389) need only be integrated once for all N considered states.

The various path integration methods are characterized by the way the functions $\mathbf{A}(t), \mathbf{d}_0(t)$ and $\mathbf{B}(t)$ are defined. In ascending order of complexity at least the following four specifications can be used

$$\left.\begin{aligned} \mathbf{A} &\equiv \mathbf{c}(\mathbf{z}_k, t_i) \\ \mathbf{d}_0 &\equiv \mathbf{d}(\mathbf{z}_k, t_i) \\ \mathbf{B} &\equiv \mathbf{0} \end{aligned}\right\} \qquad (3-390)$$

$$\left.\begin{aligned} \mathbf{A}(t) &= \mathbf{c}(\mathbf{z}_k, t) - \mathbf{B}(t)\mathbf{z}_k \\ \mathbf{d}_0(t) &= \mathbf{d}(\mathbf{z}_k, t) \\ \mathbf{B}(t) &= \tfrac{\partial}{\partial \mathbf{z}^T}\mathbf{c}(\mathbf{z}_k, t) \end{aligned}\right\} \qquad (3-391)$$

$$\left.\begin{aligned} \mathbf{A}(t) &= \mathbf{c}\big(\boldsymbol{\mu}(t), t\big) - \mathbf{B}(t)\boldsymbol{\mu}(t) \\ \mathbf{d}_0(t) &= \mathbf{d}\big(\boldsymbol{\mu}(t), t\big) \\ \mathbf{B}(t) &= \tfrac{\partial}{\partial \mathbf{z}^T}\mathbf{c}\big(\boldsymbol{\mu}(t), t\big) \end{aligned}\right\} \qquad (3-392)$$

$$\left.\begin{aligned} \mathbf{A}(t) &= E\Big[\mathbf{c}\big(\mathbf{Z}(t), t\big)\Big] - \mathbf{B}(t)\boldsymbol{\mu}(t) \\ \mathbf{d}_0(t) &= E\Big[\mathbf{d}\big(\mathbf{Z}(t), t\big)\Big] \\ \mathbf{B}(t) &= E\Big[\tfrac{\partial}{\partial \mathbf{z}^T}\mathbf{c}\big(\mathbf{Z}(t), t\big)\Big] \end{aligned}\right\} \qquad (3-393)$$

Insertion of (3-390) into (3-388), (3-389) provides the following solutions for the conditional moments

$$\left.\begin{aligned} \boldsymbol{\mu}(t) &\simeq \mathbf{z}_k + \mathbf{c}(\mathbf{z}_k, t_i)(t - t_i) \\ \boldsymbol{\lambda}(t) &\simeq \mathbf{d}(\mathbf{z}_k, t_i)\mathbf{d}^T(\mathbf{z}_k, t_i)(t - t_i) \end{aligned}\right\} \qquad (3-394)$$

(3-387), (3-394) are identical to the asymptotic solution by Risken (1984), which was used by Naess and Johnsen (1981) and Johnsen (1992). Because of the crude level of approximation inherent in the linearization scheme (3-390) this approximation can only be expected to give accurate results for very small time steps. This may cause numerical inconveniences in the non-stationary case, where transitions from an initial distribution $\boldsymbol{\pi}^{(0)}$ are requested, and in reliability problems, because a large number of transitions (3-383) are requested for evolutions of the system in any finite time interval. However, if only a stationary distribution $\boldsymbol{\pi}^{(\infty)}$ is required, this problem is omitted using the

eigenvalue approach (3-384) in favour of iterating (3-383) until convergence. The use of the method is due to the simple analytical results (3-394) for $\boldsymbol{\mu}(t)$ and $\boldsymbol{\lambda}(t)$.

Relationships (3-391) correspond to a first order Taylor expansion of $\mathbf{c}\big(\mathbf{Z}(t),t\big)$ and zero order Taylor expansion of $\mathbf{d}\big(\mathbf{Z}(t),t\big)$ from $\mathbf{Z}(t_i)=\mathbf{z}_k$. In this case the differential equations (3-388) and (3-389) become mutually uncoupled systems of differential equations, which usually have to be solved numerically. Because of the more accurate linearization somehow larger time steps Δt between transitions can be applied compared to the previous case.

In turn, relationship (3-392) corresponds to a first order Taylor expansion of $\mathbf{c}(\mathbf{Z}(t),t)$ and zero order Taylor expansion of $\mathbf{d}(\mathbf{Z}(t),t)$ from the running mean value $\boldsymbol{\mu}(t)$. Now, the systems of differential equations (3-388) and (3-389) become mutually coupled and non-linear. This does not imply any practical problems since these equations must be solved numerically anyway.

The unknown expectations at the right-hand sides of (3-393) are supposed to be evaluated by the running joint probability density function (3-387). Then the result corresponds to the equivalent linearization scheme in the expected least square sense by Atalik and Utku (1976), cf. (3-249). The resulting expectations will be non-linear functions of $\boldsymbol{\mu}(t)$ and $\boldsymbol{\lambda}(t)$, resulting in mutually coupled systems of ordinary differential equations upon insertion into (3-388), (3-389). This method was first used by Sun and Hsu (1990) (in their previous work Sun and Hsu (1988) the transition probability matrix $\mathbf{Q}$ was obtained by a simulation procedure). The methods resulting from the assertions (3-392) and (3-393) are assumed to give results of the same quality. In both cases much larger transition time intervals Δt, than for the assertions (3-390) and (3-391), can be assumed. In some cases Δt can be chosen as large as $0.5T_0$, T_0 being the fundamental eigenperiod of the linear oscillator.

The linearization schemes (3-391), (3-392) were suggested by Nielsen and Iwankiewicz (1996). The principle of local Gaussianity was also used by Aşkar, Köylüoğlu, Nielsen and Çakmak (1996) and by Köylüoğlu, Nielsen and Çakmak (1996a), (1996b) in devising various Monte Carlo simulation schemes for geometrically non-linear and hysteretic systems, allowing for larger time steps than conventional explicit numerical integration schemes. The schemes were based on the Ermak-Allen algorithms, Ermak and Buckholtz (1980), Allen (1982), devised for Monte Carlo simulation in molecular dynamics. Such algorithms require a piecewise linearization for which the the linearization schemes (3-391), (3-392) and (3-393) were considered again.

Example 3-12: Duffing oscillator subjected to a Gaussian white noise

The Duffing oscillator (3-44), (3-45), (3-46) is considered with the following parameter values

$$m=1.0\quad,\quad \omega_0=1.0\quad,\quad \zeta=0.03\quad,\quad \varepsilon=0.2 \qquad (3-395)$$

Since $\mathbf{d}$ is constant in time and independent of the state vector no approximation is needed for this quantity. For the cases (3-390) - (3-394) the quantities $\mathbf{A}(t)$ and $\mathbf{B}(t)$ defining the equivalent linearization

of the drift vector become

$$\left.\begin{aligned}\mathbf{A} &= \begin{bmatrix} \dot{x}_k \\ -2\omega_0\dot{x}_k - \omega_0^2(x_k + \epsilon x_k^3)\end{bmatrix} \\ \mathbf{B} &= \begin{bmatrix} 0 & 0 \\ 0 & 0 \end{bmatrix}\end{aligned}\right\} \qquad (3-396)$$

$$\left.\begin{aligned}\mathbf{A} &= \begin{bmatrix} 0 \\ 2\epsilon\omega_0^2 x_k^3 \end{bmatrix} \\ \mathbf{B} &= \begin{bmatrix} 0 & 1 \\ -\omega_0^2(1+3\epsilon x_k^2) & -2\zeta\omega_0 \end{bmatrix}\end{aligned}\right\} \qquad (3-397)$$

$$\left.\begin{aligned}\mathbf{A}(t) &= \begin{bmatrix} 0 \\ 2\epsilon\omega_0^2 \mu_1^3(t) \end{bmatrix} \\ \mathbf{B}(t) &= \begin{bmatrix} 0 & 1 \\ -\omega_0^2(1+3\epsilon\mu_1^2(t)) & -2\zeta\omega_0 \end{bmatrix}\end{aligned}\right\} \qquad (3-398)$$

$$\left.\begin{aligned}\mathbf{A}(t) &= \begin{bmatrix} 0 \\ 2\epsilon\omega_0^2 \mu_1^3(t) \end{bmatrix} \\ \mathbf{B}(t) &= \begin{bmatrix} 0 & 1 \\ -\omega_0^2\Big(1+3\epsilon\big(\mu_1^2(t)+\lambda_{11}(t)\big)\Big) & -2\zeta\omega_0 \end{bmatrix}\end{aligned}\right\} \qquad (3-399)$$

Hence, the 1st order Taylor linearization from the running mean, (3-398), and the expected least-square minimization (3-399) only deviate in the component B_{21} of the gradient matrix. (3-398) is significantly easier to a apply in case of hysteretic multi-degrees-of-freedom systems.

(3-398) will be applied for the determination of the stochastic response and reliability of the Duffing oscillator exposed to Gaussian white noise. In the numerical calculations the limits of the mesh are taken as $[-4\sigma_{X,0}, 4\sigma_{X,0}] \times [-4\sigma_{\dot{X},0}, 4\sigma_{\dot{X},0}]$, where $\sigma_{X,0}$ and $\sigma_{\dot{X},0}$ denote the stationary standard deviations of the displacement and velocity of the corresponding linear oscillator. A uniform coarse 20×20 mesh is applied, so $\Delta x = 0.4\sigma_{X,0}, \Delta\dot{x} = 0.4\sigma_{\dot{X},0}$. The transition probability density at one transition time-interval has been obtained from (3-385), (3-386), (3-388), (3-389), (3-398) for all 400 cells using a 4th order Runge-Kutta scheme. The transition time-interval was selected as $\Delta t = \frac{T_0}{4}$, where T_0 is the eigenperiod of the linear oscillator. The auto-spectral density function of the Gaussian white noise has been selected, so $\sigma_{X,0} = \sigma_{\dot{X},0} = 1$.

The results for the stationary marginal pdfs of the displacement and velocity have been shown in figs. 3-68 - 3-71. To emphasize on the tails of the distributions the results have also been shown in semi-logarithmic scale. The solid line curves represent the analytical solutions, whereas the results marked with • and ○ signify the numerical results obtained from iterating (3-383) $n = 60$ times and from the eigenvector solution (3-384), respectively. The iteration solution was started with deterministic start in the origin $\mathbf{Z}(0) = 0$. From these results it is concluded that the path integration method provides very accurate results for Wiener process driven systems at all levels of probability including the tails even with the applied coarse mesh and the applied large time step. In turn, the applicability of large time steps is a consequence of the relative accuracy of the linearization schemes (3-392) and (3-393). The calculation times were 39s for the iteration approach, and 139s for the eigenvector approach. Notice, for the present problem the number n of iteration required to achieve convergence is determined by the criterion $n\zeta\Delta t\omega_0 \simeq 2.8$. Hence the benefit of using the iteration approach is partly due to the relatively large time step of $\Delta t = \frac{T_0}{4}$ and the large damping ratio of $\zeta = 0.03$. Johnsen (1992) used a time step of $\Delta t = \frac{T_0}{2000\pi}$ and a 47×47 for the same problem with a damping ratio of $\zeta = 0.10$. In this case the eigenvector solution will turn out to be beneficial, especially in case of lower damping ratios.

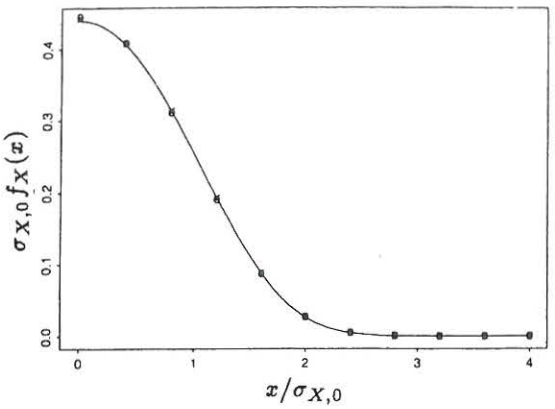

Fig. 3-68: Stationary pdf of displacement, $f_X(x)$. Linear scale. • iteration, ○ eigenvector solution. Köylüoğlu, Nielsen and Çakmak (1995).

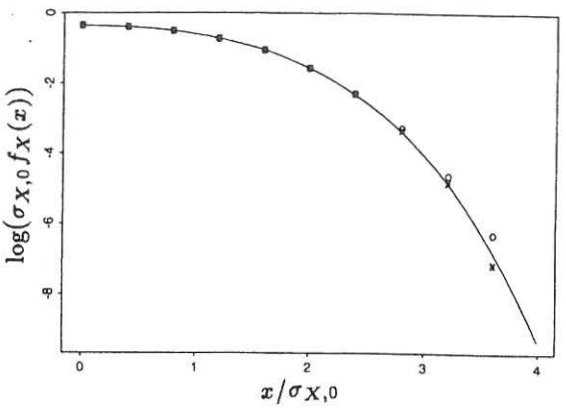

Fig. 3-69: Stationary pdf of displacement, $f_X(x)$. Semi-log scale. • iteration, ○ eigenvector solution. Köylüoğlu, Nielsen and Çakmak (1995).

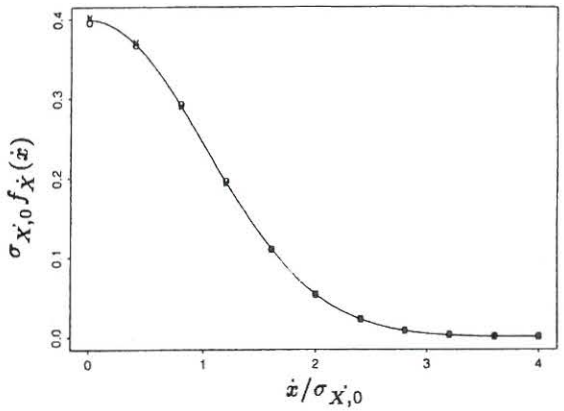

Fig. 3-70: Stationary pdf of velocity, $f_{\dot{X}}(\dot{x})$. Linear scale. • iteration, ○ eigenvector solution. Köylüoğlu, Nielsen and Çakmak (1995).

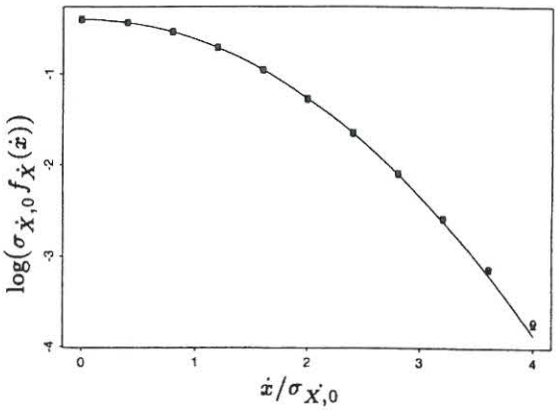

Fig. 3-71: Stationary pdf of velocity, $f_{\dot{X}}(\dot{x})$. Semi-log scale. • iteration, ○ eigenvector solution. Köylüoğlu, Nielsen and Çakmak (1995).

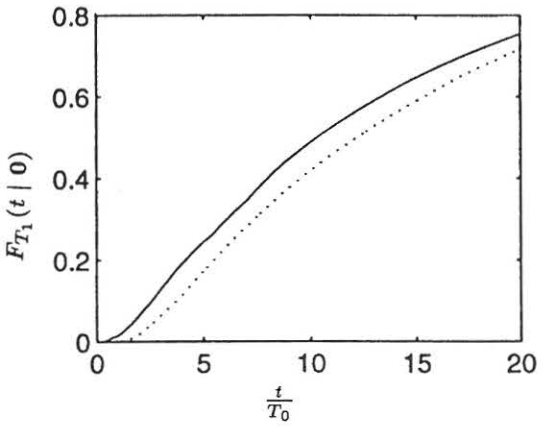

Fig. 3-72: First-passage time probability distribution function, $F_{T_1}(t \mid 0)$. Deterministic start with a single constant barrier, $b = 2.0\sigma_X(\infty)$. (—) Simulation, (· · ·) path integration. Nielsen and Iwankiewicz (1996).

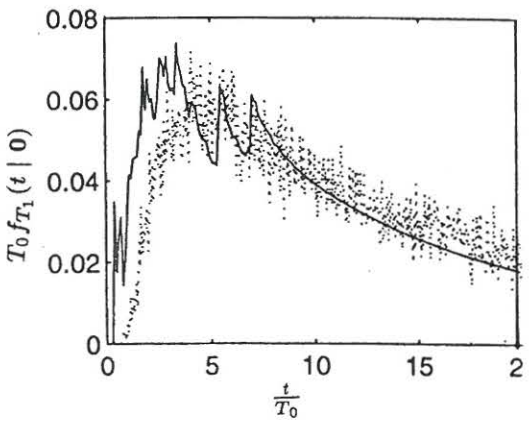

Fig. 3-73: First-passage time probability density function, $f_{T_1}(t \mid 0)$. Deterministic start with a single constant barrier, $b = 2.0\sigma_X(\infty)$. (—) Simulation, (· · ·) path integration. Nielsen and Iwankiewicz (1996).

In figs. 3-72 and 3-73 the time dependence of the first-passage time probability distribution function and the first-passage time probability density functions are shown for the same Duffing oscillator in case of a single constant barrier first-passage time problem with deterministic start at $\mathbf{Z}(0 = 0$, obtained by Monte-Carlo path integration and simulation, respectively. The path integration results are shown with an unbroken curve and the simulation results with a dotted curve. The barrier level is $2.0\sigma_X(\infty)$, where the stationary variance $\sigma_X^2(\infty) = 0.721023$ was obtained from the analytical 4th order cumulant neglect closure solution, Wu and Lin (1984). The simulation results are based on 32000 independent realizations, obtained from numerical integration of the equations of motion (3-44), (3-45), (3-46), by means of the 4th order Runge-Kutta scheme with the time step $\Delta t = \frac{T_0}{40}$. Generation of realizations of a broad-band broken line zero mean Gaussian process was performed by the method of Penzien, Clough and Penzien (1974). As seen from fig. 3-72 the computed results overestimate the probability of failure somehow during the first period of the excitation, which provides a parallel translation of the first-pasage time probability distribution curve obtained by path integration compared to the one obtained by simulation. This effect can be attributed to the problem of convecting and diffusing the probability mass, initially concentrated at $\mathbf{Z}(0) = \mathbf{0}$, to the nodes of the mesh, with the relatively large transition time step of $T_0/4$ in combination with the applied coarse 20×20 mesh. The first-passage time probability density functions on fig. 3-73 were obtained by numerical differentiation, which caused the highly irregular behaviour.

The general conclusion from this example is that path integration methods are useful both for stochastic response problems and for reliablity problems of SDOF non-linear oscillators. For stochastic response problems very coarse meshes may be used, whereas a somewhat finer mesh should be used in reliability problems. The main shortcoming of path integration methods is the rapid growth of the cpu time for problems of higher dimension than 2. According to Naess and Johnsen (1991) the cpu time for the path integration method applied by them easily runs up to many hours on a work station (Dec 3100) for 3-dimensional problems. Hence supercomputing (parallel computing) becomes nescessary at even higher dimensions.

3.4.2 Path integration methods for systems driven by processes with jumps

In this section attention will be restricted to systems driven by a scalar generating source process with jumps $\{V(t), t \in [t_0, \infty[\}$.

Initially, the case of a system driven by a scalar compound Poisson process is considered. Let $q^{(n)}_{\{\mathbf{Z}\}}(\mathbf{z}, t \mid \mathbf{z}_k, t_i)$ be the transition probability density function of the state vector from the state $\mathbf{Z}(t_0) = \mathbf{z}_k$ on condition of exact n impulse arrivals in the time interval $[t_i, t[$, and let $P_{\{N\}}(n, t, t_i)$ denote the probability function of exactly n arrivals in this time interval as given by (3-8). Using the total probability theorem the unconditional transition probability density function can then be written as

$$q_{\{\mathbf{Z}\}}(\mathbf{z}, t \mid \mathbf{z}_k, t_i) = \sum_{n=0}^{\infty} P_{\{N\}}(n, t, t_i) q^{(n)}_{\{\mathbf{Z}\}}(\mathbf{z}, t \mid \mathbf{z}_k, t_i) \qquad (3-400)$$

The 1st term in the sum (3-400) is identical to the 1st term in the modified closure (3-229). $q^{(0)}_{\{\mathbf{Z}\}}(\mathbf{z}, t \mid \mathbf{z}_k, t_i)$ describes the purely deterministic drift (eigenvibration) of the system from the state $\mathbf{Z}(t_i) = \mathbf{z}_k$, since the states are conditioned on no impulse arrival.

Then $q^{(0)}_{\{\mathbf{Z}\}}(\mathbf{z},t \mid \mathbf{z}_k,t_i)$ is given as

$$q^{(0)}_{\{\mathbf{Z}\}}(\mathbf{z},t \mid \mathbf{z}_k,t_i) = \prod_{j=1}^{n} \delta\Big(z_j - d_j(t|\mathbf{z}_k,t_i)\Big) \qquad (3-401)$$

where $\mathbf{d}(t|\mathbf{z}_k,t_i)$ with the components $d_i(t|\mathbf{z}_k,t_i)$ denotes the deterministic drift motion of the system from the initial state $\mathbf{z}_k$ at the time t_i. The vector $\mathbf{d}(t|\mathbf{z}_k,t_i)$ is the solution of the initial value problem originating from (3-119)

$$\frac{\partial}{\partial t}\mathbf{d}(t|\mathbf{z}_k,t_i) = \mathbf{c}\big(\mathbf{d}(t|\mathbf{z}_k,t_i),t\big) \quad , \quad t > t_i \quad , \quad \mathbf{d}(t_i|\mathbf{z}_k,t_i) = \mathbf{z}_k \qquad (3-402)$$

For linear systems (3-402) may be solved analytically, depending on whether a fundamental basis of solutions can be found. This is the case of linear vibratory systems, for which modal decoupling can be used. For other linear systems and for non-linear systems (3-402) must be solved numerically.

The remaining conditional transition probability density functions, $q^{(n)}_{\{\mathbf{Z}\}}(\mathbf{z},t \mid \mathbf{z}_k,t_i)$, $n \geq 1$, are all continuous functions without delta spikes, and of the same order of magnitude, cf. (3-229). Since $P_{\{N\}}(n,t,t_i) = \mathrm{O}\Big(\big(\nu(t_i)(t-t_i)\big)^n\Big)$, it follows that (3-400) can be written as

$$\begin{aligned} &q_{\{\mathbf{Z}\}}(\mathbf{z},t \mid \mathbf{z}_k,t_i) = P_0(t,t_i)q^{(0)}_{\{\mathbf{Z}\}}(\mathbf{z},t \mid \mathbf{z}_k,t_i) + \\ &\big(1-P_0(t,t_0)\big)q^{(1)}_{\{\mathbf{Z}\}}(\mathbf{z},t \mid \mathbf{z}_k,t_i) + \mathrm{O}\Big(\big(\nu(t_i)(t-t_i)\big)^2\Big) \end{aligned} \qquad (3-403)$$

where the probability of no impulse arrivals in the interval $[t_i,t[$, $P_0(t,t_i) = P_{\{N\}}(0,t,t_i)$, is given by (3-228). The asymptotic relationship (3-403) forms the basis for path integration methods for Poisson driven systems. The specific formulation of (3-403) ensures that upon chopping the remainder, the quality of a genuine (actual) probability density function is preserved, i.e. the integral of the function over the sample space is exactly equal to one, for any choice of the transition time interval $t - t_i$. Further, it is important to notice that the remainder depends on the magnitude of the product $\nu(t_i)(t-t_i)$, rather than of the interval length $t - t_i$ itself. Hence, truncation is permitted if

$$\nu(t_i)(t-t_i) \ll 1 \qquad (3-404)$$

For any finite transition interval (3-404) is more easily fulfilled for sparse pulse trains, for which $\nu(t_i)T_0 \ll 1$, T_0 being the fundamental eigenperiod of the corresponding linear structure, than for dense pulse trains. Hence, in contrast to the moment equations method of section 3.3.3 and the Petrov-Galerkin finite element formulation of section 3.5, which both work well for rather dense pulse trains and run into numerical instability for sparse pulses, the indicated path integration method is designed to work the other way around in providing the best results for sparse pulses.

On the other hand the coarseness of the mesh sets lower bounds for the admissibility of the transition time interval, $t - t_i$. This is so, because the distribution of the convected probability masses to the adjacent nodes in the mesh cannot be done sufficiently accurately, if $t - t_i$ is too small. Let $c^{(k)} = |\mathbf{c}(\mathbf{z}_k, t_i)|$ be the magnitude of the convection vector at the centre of the kth cell, and let $\Delta z^{(k)}$ be the diameter of the cell in the direction of $\mathbf{c}(\mathbf{z}_k, t_i)$. It is then required that a convection at least of the length $\Delta z^{(k)}$ should take place during the interval $t - t_i$ in all cells, i.e.

$$c^{(k)}(t - t_i) > \Delta z^{(k)} \quad \Rightarrow \quad C^{(k)} = \frac{c^{(k)}(t - t_i)}{\Delta z^{(k)}} > 1 \qquad (3-405)$$

where $C^{(k)}$ is the local Courant number for the kth cell. Numerical instability and inaccurate results occur if $C^{(k)}$ becomes too large in some part of the mesh. For a SDOF system $c^{(k)} \simeq \Delta\dot{x}$ in the most critical cells close to origo. Then $C^{(k)} \simeq \frac{\Delta\dot{x}(t-t_i)}{\Delta x} \simeq \frac{\sigma_{\dot{X},0}(t-t_i)}{\sigma_{X,0}} \simeq \omega_0(t - t_i)$ follows. Hence, the following lower bound for the transition time interval is obtained from (3-405), $t - t_i \geq \frac{T_0}{2\pi}$. Therefore, a decrease in the transition time interval must be accompanied by a finer mesh to guarantee stability and higher accuracy.

At the determination of $q^{(1)}_{\{\mathbf{Z}\}}(\mathbf{z}, t \mid \mathbf{z}_k, t_i)$ the state is conditioned on exactly one impulse arrival in $[t_i, t[$. The arrival time (first-passage time), T_1, of this impulse has the probability density function, e.g. Osaki (1992)

$$f_{T_1}(\tau) = \frac{\nu(\tau)}{\int_{t_i}^{t} \nu(u)du} \quad , \quad \tau \in [t_i, t[\qquad (3-406)$$

Assume that the impulse arrives at the time $T_1 = \tau$ and has the strength $P = p$. Up to the time τ the system has been performing eigenvibrations from the initial state $\mathbf{z}_k$ at the time t_i. Then the state at the time τ^- is given by $\mathbf{Z}(\tau^-) = \mathbf{d}(\tau|\mathbf{z}_k, t_i)$. At the time τ a discontinuous change of the state of magnitude $\Delta\mathbf{Z}(\tau) = \mathbf{e}\big(\mathbf{d}(\tau|\mathbf{z}_k, t_i), \tau\big)p$ takes place, so the state at the time τ^+ becomes $\mathbf{Z}(\tau^+) = \mathbf{d}(\tau|\mathbf{z}_k, t_i) + \mathbf{e}\big(\mathbf{d}(\tau|\mathbf{z}_k, t_i), \tau\big)p$, cf. (3-165). $\mathbf{e}\big(\mathbf{Z}(\tau), \tau\big)$ signifies the diffusion vector of the system, cf. (3-119). Succeedingly, during the time interval $]\tau, t]$ the system continues performing eigenvibrations with these initial values, so the state at the time t is

$$Z_i(t) = d_i\Big(t\Big|\mathbf{d}(\tau|\mathbf{z}_k, t_i) + \mathbf{e}\big(\mathbf{d}(\tau|\mathbf{z}_k, t_i), \tau\big)p, \tau\Big) \qquad (3-407)$$

Joint statistical moments conditioned on the state $\mathbf{z}_k$ at the time t_i and on exactly one impulse can then be evaluated from

$$E\big[Z_{i_1}(t) \cdots Z_{i_n}(t) \mid \mathbf{z}_k, t_i, N(t) = 1\big] =$$
$$\int_{t_i}^{t} \int_{-\infty}^{\infty} \prod_{j=1}^{n} d_{i_j}\Big(t\Big|\mathbf{d}(\tau|\mathbf{z}_k, t_i) + \mathbf{e}\big(\mathbf{d}(\tau|\mathbf{z}_k, t_i), \tau\big)p, \tau\Big) f_P(p) f_{T_1}(\tau) dp d\tau \qquad (3-408)$$

At the derivation of (3-408), the mutual statistical independence of T_1 and P has been taken into account. In the same manner the joint characteristic function is obtained as, cf. (2-155)

$$M_{\{\mathbf{Z}\}}(\boldsymbol{\theta}, t \mid \mathbf{z}_k, t_i, N(t)=1) = E\left[\exp\left(i\boldsymbol{\theta}^T\mathbf{Z}(t)\right) \mid \mathbf{z}_k, t_i, N(t)=1\right] =$$

$$\int_{t_i}^{t}\int_{-\infty}^{\infty} \exp\left(i\sum_{j=1}^{n}\theta_j d_j\left(t\middle|\mathbf{d}(\tau|\mathbf{z}_k,t_i)+\mathbf{e}\big(\mathbf{d}(\tau|\mathbf{z}_k,t_i),\tau\big)p,\tau\right)\right) f_P(p) f_{T_1}(\tau)\,dp\,d\tau \quad (3\text{-}409)$$

The results (3-408), (3-409) were derived by Nielsen and Iwankiewicz (1996). Next, the function $q^{(1)}_{\{\mathbf{Z}\}}(\mathbf{z}, t \mid \mathbf{z}_k, t_i)$ can be obtained as an inverse Fourier transform of (4-409). Since this can be performed numerically since no severe singularities are present, the problem has, in principle, been solved. However, the indicated method calls for an enormous numerical effort. Alternatively, $q^{(1)}_{\{\mathbf{Z}\}}(\mathbf{z}, t \mid \mathbf{z}_k, t_i)$ can be represented as a Gram-Charlier or Edgeworth expansion, see (2-158). Again, extensive computations are necessary, and only approximate solutions are obtained, due to the mandatory truncation of this expansion. Instead, two numerically stable methods, derived by Köylüoğlu, Nielsen and Iwankiewicz (1995) and Köylüoğlu, Nielsen and Çakmak (1995), respectively, are presented below, which requires much less numerical effort. The methods will be explained by a 2-dimensional state vector with the expanding domain $[-4\sigma_X(t), 4\sigma_X(t)] \times [-4\sigma_{\dot{X}}(t), 4\sigma_{\dot{X}}(t)]$ as shown in fig. 3-74. $\sigma_X(t)$ and $\sigma_{\dot{X}}(t)$ signify the nonstationary standard deviations of the corresponding linear oscillator exposed to a comparable Gaussian white noise, which can be determined analytically. For the sake of simplicity the method will be explained for the case where the diffusion vector $\mathbf{e}$ is assumed to be state- and time-independent. However the method is equally valid if this is not so.

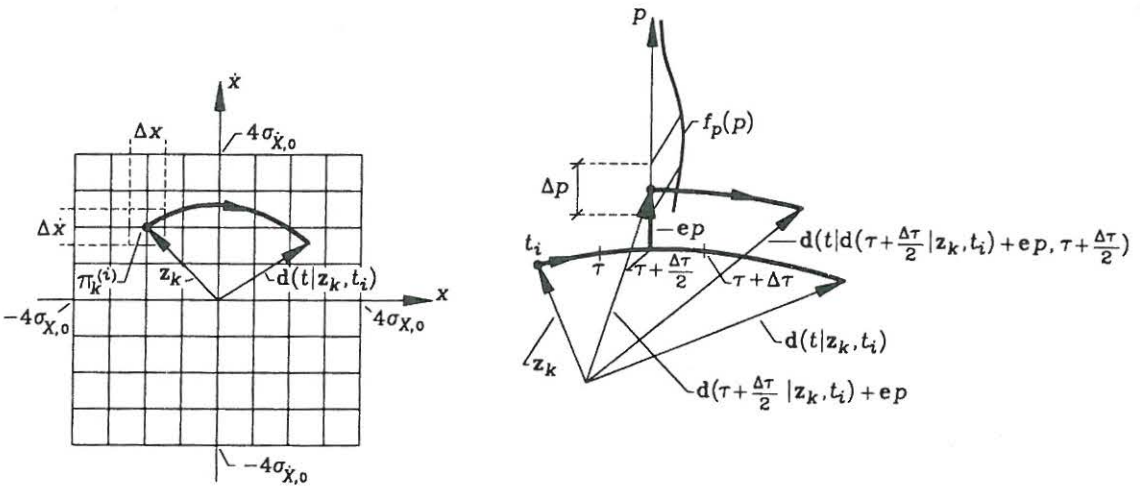

Fig. 3-74: Path integration of compound Poisson process driven system. Method 1: Discretization of phase plane, and convection and diffusion of probability mass.

On condition of being in node $\mathbf{z}_k$ at the time t_i, the transition probability Q_{jk} of being in node j at the time t can now be evaluated as shown in fig. 3-74. The discrete probability mass $\pi_k^{(i)}$ attached to node $\mathbf{z}_k$ at the time t_i is partly convected to $\mathbf{d}(t|\mathbf{z}_k, t_i)$ with the probability $P_0 = P_0(t, t_i)$ on condition that no impulses arrive in $]t_i, t]$. The rest of the probability mass $\pi_k^{(i)}(1 - P_0)$ is continuously distributed according to the transition probability density $q_{\{\mathbf{Z}\}}^{(1)}(\mathbf{z}, t \mid \mathbf{z}_k, t_i)$ of exactly one pulse arrival in $]t_i, t]$. Numerically, this is attained by dividing the time interval $[t_i, t[$ into a number of subintervals of the length $\Delta\tau$. In the subinterval $[\tau, \tau+\Delta\tau]$ a probability mass of magnitude $f_{T_1}(\tau)\Delta\tau\pi_k^{(i)}$ is lumped at the time $\tau + \frac{1}{2}\Delta\tau$, and succeedingly diffused and lumped along the direction $\mathbf{e}$ according to the probability density function $f_P(p)$, see fig. 3-74. At the position $\mathbf{d}(\tau + \frac{1}{2}\Delta\tau|\mathbf{z}_k, t_i) + \mathbf{e}p$ a probability mass of magnitude $f_{T_1}(\tau)\Delta\tau f_P(p)\Delta p(1 - P_0)\pi_k^{(i)}$ is lumped. Next, this probability mass is convected to the position $\mathbf{d}\big(t|\mathbf{d}(\tau + \frac{1}{2}\Delta\tau|\mathbf{z}_k, t_i) + \mathbf{e}p, \tau + \frac{1}{2}\Delta\tau\big)$. Finally, at the time t all the convected probability masses are distributed to the 4 neighbouring nodal points, weighted according to their distances.

The second method is based on the following identity, valid for any $\tau \in]t_i, t[$

$$\mathbf{d}\big(t|\mathbf{d}(\tau|\mathbf{z}_k, t_i), \tau\big) = \mathbf{d}\big(t|\mathbf{z}_k, t_i\big) \qquad (3-410)$$

The left- and right-hand sides of (3-410) just state that the oscillator arrives at the same position at the time t, if it starts on the very same trajectory at the position $\mathbf{d}\big(\tau|\mathbf{z}_k, t_i\big)$ at the time τ or at the position $\mathbf{d}\big(t_i|\mathbf{z}_k, t_i\big) = \mathbf{z}_k$ at the time t_i. From (3-410) the following Taylor expansion prevails for $\mathbf{Z}(t)$ given by (3-407)

$$\mathbf{Z}(t) = \mathbf{d}\big(t|\mathbf{d}(\tau|\mathbf{z}_k, t_i) + \mathbf{e}P, \tau\big) = \mathbf{d}\big(t|\mathbf{d}(\tau|\mathbf{z}_k, t_i), \tau\big) + \frac{\partial \mathbf{d}\big(t|\mathbf{d}(\tau|\mathbf{z}_k, t_i), \tau\big)}{\partial \mathbf{z}_k^T}\mathbf{e}P + \cdots =$$

$$\mathbf{d}\big(t|\mathbf{z}_k, t_i\big) + \mathbf{d}^{(1)}\big(t|\mathbf{z}_k, t_i\big)P + \mathbf{d}^{(2)}\big(t|\mathbf{z}_k, t_i\big)P^2 + \cdots \qquad (3-411)$$

where

$$\left.\begin{aligned} \mathbf{d}^{(1)}\big(t|\mathbf{z}_k, t_i\big) &= \tfrac{\partial \mathbf{d}(t|\mathbf{z}_k, t_i)}{\partial \mathbf{z}_k^T}\mathbf{e} \\ \mathbf{d}^{(2)}\big(t|\mathbf{z}_k, t_i\big) &= \tfrac{1}{2}\mathbf{e}^T \tfrac{\partial^2 \mathbf{d}(t|\mathbf{z}_k, t_i)}{\partial \mathbf{z}_k \partial \mathbf{z}_k^T}\mathbf{e} \\ &\vdots \end{aligned}\right\} \qquad (3-412)$$

Equation (3-411) is basically a Taylor expansion in the impulse magnitude P. Notice that the random time τ entering the left-hand side of (3-411) has totally disappeared at the right-hand side. Instead the unknown Taylor expansion vectors $\mathbf{d}^{(1)}, \mathbf{d}^{(2)}, \ldots$ appear. Differential equations for these quantities can be derived upon multiple partial differentiations of (3-403) with respect to $\mathbf{z}_k$ and contractions with the vector $\mathbf{e}$

$$
\left.
\begin{aligned}
&\frac{\partial}{\partial t}\Big(\frac{\partial \mathbf{d}(t|\mathbf{z}_k,t_i)}{\partial \mathbf{z}_k^T}\Big) = \frac{\partial \mathbf{c}\big(\mathbf{d}(t|\mathbf{z}_k,t_i),t\big)}{\partial \mathbf{z}^T}\frac{\partial \mathbf{d}(t|\mathbf{z}_k,t_i)}{\partial \mathbf{z}_k^T} \quad , \quad \frac{\partial \mathbf{d}(t_i|\mathbf{z}_k,t_i)}{\partial \mathbf{z}_k^T} = \mathbf{I} \;\Rightarrow \\
&\frac{\partial}{\partial t}\mathbf{d}^{(1)}(t|\mathbf{z}_k,t_i) = \frac{\partial \mathbf{c}\big(\mathbf{d}(t|\mathbf{z}_k,t_i),t\big)}{\partial \mathbf{z}^T}\mathbf{d}^{(1)}(t|\mathbf{z}_k,t_i) \quad , \quad \mathbf{d}^{(1)}(t_i|\mathbf{z}_k,t_i) = \mathbf{e} \\
&\frac{\partial}{\partial t}\mathbf{d}^{(2)}(t|\mathbf{z}_k,t_i) = \frac{\partial \mathbf{c}\big(\mathbf{d}(t|\mathbf{z}_k,t_i),t\big)}{\partial \mathbf{z}^T}\mathbf{d}^{(2)}(t|\mathbf{z}_k,t_i) + \\
&\frac{1}{2}\mathbf{d}^{(1)T}(t|\mathbf{z}_k,t_i)\frac{\partial^2 \mathbf{c}\big(\mathbf{d}(t|\mathbf{z}_k,t_i),t\big)}{\partial \mathbf{z}\partial \mathbf{z}^T}\mathbf{d}^{(1)}(t|\mathbf{z}_k,t_i) \quad , \quad \mathbf{d}^{(2)}(t_i|\mathbf{z}_k,t_i) = \mathbf{0} \\
&\vdots
\end{aligned}
\right\} \qquad (3-413)
$$

where the partial differentiation with respect to the forward state $\mathbf{z}$ concerns the drift vector $\mathbf{c}(\mathbf{z},t)$. Relationships (3-402), (3-413) represent a coupled system of $n+n+n+\cdots$ non-linear 1st order differential equations for the determination of $\mathbf{d}(t|\mathbf{z}_k,t_i)$, $\mathbf{d}^{(1)}(t|\mathbf{z}_k,t_i)$, $\mathbf{d}^{(2)}(t|\mathbf{z}_k,t_i),\ldots$. The indicated method was given by Köylüoğlu, Nielsen and Çakmak (1995) in a somewhat more involved outline. Rather than formulating the differential equations for $\mathbf{d}^{(1)}(t|\mathbf{z}_k,t_i)$, $\mathbf{d}^{(2)}(t|\mathbf{z}_k,t_i),\ldots$ directly as shown in (3-413), differential equations were specified for the gradients $\frac{\partial}{\partial \mathbf{z}^T}\mathbf{d}(t|\mathbf{z}_k,t_i)$, $\frac{\partial^2}{\partial \mathbf{z}\partial \mathbf{z}^T}\mathbf{d}(t|\mathbf{z}_k,t_i),\ldots$. Taking the symmetry into consideration there will be $n+n^2+\frac{1}{2!}n^3+\cdots$ such different coupled differential equations. Hence, the specification (3-413) represents a significant saving if n is of even moderate magnitude. Even so the original formulation by Köylüoğlu, Nielsen and Çakmak (1995) proved extremely advantageous compared to Monte Carlo simulation results as indicated below in example 3-13.

For a linear system the drift vector is a linear function of the state vector, so $\frac{\partial^2}{\partial \mathbf{z}\partial \mathbf{z}^T}\mathbf{c}(\mathbf{z},t) \equiv 0$. Due to the homogeneous initial values it then follows from (3-413) that $\mathbf{d}^{(2)}(t|\mathbf{z}_k,t_i) \equiv 0$. Generally, it can be shown that $\mathbf{d}^{(N)}(t_0|\mathbf{z}_k,t_0) \equiv 0$, $N \geq 1$, in this case. Hence, the Taylor expansion (3-411) becomes linear in P for linear systems. At small transition time intervals $\mathbf{c}\big(\mathbf{Z}(t),t\big)$ can be approximated by a linear function as stated by (3-385). Since this approach works well even for rather large time steps in case of white noise driven systems, it will also do so in the present case of compound Poisson driven systems. Consequently, it can be concluded that one can chop all terms higher than the 1st power in P in the expansion (3-411) with pretty good accuracy. Notice, that this approximation merely concerns the drift vector, and puts no restrictions on the magnitudes of the impulse strength P, as may appear at first sight.

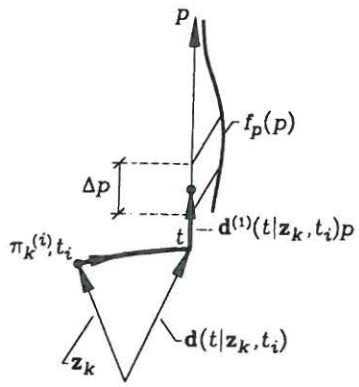

Fig. 3-75: Path integration of compound Poisson process driven system. Method 2: Convection and lumping of probability mass.

As an approximation assuming the linear expansion in P in (3-411) even for non-linear systems, the convection and lumping of probability mass can be explained in the following way, see fig. 3-75. The probability mass $\pi_k^{(i)}$ at the node $\mathbf{z}_k$ at the time t_i is convected to the position $\mathbf{d}(t|\mathbf{z}_k,t_i)$ according to the 0th order term in (3-411), where a probability mass of magnitude $\pi_k^{(i)}P_0(t,t_i)$ is lumped. As specified by the 1st order term in (3-411) the remaining probability mass $\pi_k^{(i)}\big(1-P_0(t,t_i)\big)$ is distributed along the line with the direction $\mathbf{d}^{(1)}(t|\mathbf{z}_k,t_i)$ according to the probability density function $f_P(p)$ of the impulse intensity P. At the position $\mathbf{d}(t|\mathbf{z}_k,t_i)+\mathbf{d}^{(1)}(t|\mathbf{z}_k,t_i)p$ a probability mass of magnitude $\pi_k^{(i)}\big(1-P_0(t,t_i)\big)f_P(p)\Delta p$ is then lumped as sketched in fig. 3-75. Again, all lumped probability masses are redistributed to the 4 neighbouring nodal points, weighted according to their distances.

Example 3-13: Duffing oscillator subjected to compound Poisson process. Methods 1 and 2.

The Duffing oscillator (3-44), (3-45), (3-46) is considered, when driven by a stationary compound Poisson process.

For Method 1 the following system data are used

$$m=1.0\quad,\quad \omega_0=1.0\quad,\quad \zeta=0.01\quad,\quad \epsilon=0.2 \qquad (3-414)$$

The impulse strength of the compound Poisson process is assumed to be zero-mean normally distributed, $P\sim N(0,\sigma_P^2)$ with the variance chosen, so $\frac{\nu\sigma_P^2}{4\zeta\omega_0^3m^2}=1$, corresponding to the stationary standard deviations $\sigma_{X,0}=\sigma_{\dot{X},0}=1$ of a linear oscillator exposed to an equivalent Gaussian white noise. Three values of ν are considered, namely $\nu=0.01\omega_0=\frac{0.02\pi}{T_0}$, $\nu=0.1\omega_0=\frac{0.2\pi}{T_0}$, $\nu=1.0\omega_0=\frac{2\pi}{T_0}$, which may be categorized as the cases of sparse, medium level and dense pulse arrival rates, respectively. Basically, the path integration has been performed by a uniform 20×20 mesh with the

limits $[-4\sigma_{X,0}, 4\sigma_{X,0}] \times [-4\sigma_{\dot{X},0}, 4\sigma_{\dot{X},0}]$. However, in the case of $\nu = 0.01\omega_0 = \frac{0.02\pi}{T_0}$, where very peaked distributions occur at the origin, a non-uniform 25×25 mesh has been applied with a 4 times finer spacing close to origin. In establishing the transition probability matrix, all convection problems have been solved numerically, using a 4th order Runge-Kutta scheme. The transition time interval Δt is passed by 3 uniformly distributed steps for diffusion, i.e. $\Delta\tau = \frac{1}{3}\Delta t$, see fig. 3-74. An ensemble of 100000 Monte Carlo samples of the state vector is generated in order to estimate the stationary joint probability density of $X(t)$ and $\dot{X}(t)$ by the same way as explained in Example 3-8. Stationarity of the response is assumed after $50T_0$, at which time the stationary distributions have been sampled. In all cases, simulation results for the pdfs have been obtained with the same class-width as applied in the path integration scheme.

In figs. 3-76 - 3-79 are shown the stationary marginal probability density functions of the displacement and the velocity for the case of sparse pulse arrivals $\nu = 0.01\omega_0$. To emphasize on the tails the results have been indicated both in linear and semi-logarithmic scale. Transition is passed with the relatively large transition time interval $\Delta t = T_0$, so $\nu\Delta t = 0.02\pi$. The stationary joint probability density functions have been obtained from (3-383) with start in the origin using 100 iterations until stationarity. As seen the probability density functions reveal pronounced peaks at the origin. This is because the vibrations for sparse pulse arrivals almost extinct between the impulses as it can be observed in fig. 2-24. The oscillator is then in a position close to the origin for a large part of time, and hence there is a high probability density for the oscillator to be there. Since the dissipation of impulses is increased at large values of ζ, the peaks will even increase as the damping ratio is increased. Actually, the controlling parameter for the peakedness turns out to be the fraction $\frac{\zeta\omega_0}{\nu}$. In order to catch the peaks, results for the finer 25×25 mesh have also been obtained as explained above. The stationary standard deviations obtained from path integration are $\sigma_X(\infty) = 0.787$ and $\sigma_{\dot{X}}(\infty) = 0.958$, respectively. The corresponding Monte Carlo simulation results are $\sigma_X(\infty) = 0.799$ and $\sigma_{\dot{X}}(\infty) = 0.999$. Especially for the fine mesh high accuracy is achieved, when compared to Monte Carlo simulations.

Figs. 3-80 - 3-83 show the correponding results for the case of medium level pulse arrivals $\nu = 0.1\omega_0$. The transition time interval is still kept at $\Delta t = T_0$, so $\nu\Delta t = 0.2\pi$. The stationary standard deviations obtained from path integration are $\sigma_X(\infty) = 0.868$ and $\sigma_{\dot{X}}(\infty) = 1.022$, respectively, whereas the corresponding Monte Carlo simulation results are $\sigma_X(\infty) = 0.842$ and $\sigma_{\dot{X}}(\infty) = 0.999$. As seen from the results high accuracy compared to Monte Carlo simulation is obtained even in this case with $\nu\Delta t = 0.2\pi$, which may be considered the outermost limit for the theory.

In figs. 3-84 - 3-87 the results for the case of dense pulse arrivals $\nu = 1.0\omega_0$ are shown. Under the restriction that $\nu E[P^2]$ is kept constant at the value $4\zeta\omega_0^3 m^2$ the response then resembles that of a Gaussian white noise driven system. For this reason the analytical solution for the white noise case has also been shown. Stationarity was achieved after 50 iterations of (3-383). Even though the transition time was reduced to $\frac{T_0}{2}$ the method is now performing rather poor. Of course this is due to fact that the restriction on the method, (3-404), is no longer fulfilled with the present value of $\nu\Delta t = \pi$. The exact standard deviations for the white noise case are $\sigma_X(\infty) = 0.851$ and $\sigma_{\dot{X}}(\infty) = 1.000$. The corresponding results for Monte Carlo simulation are $\sigma_X(\infty) = 0.852$ and $\sigma_{\dot{X}}(\infty) = 0.997$. The conclusion is that for dense pulse arrivals an equivalent white noise approximation is doing better than the indicated path integration method.

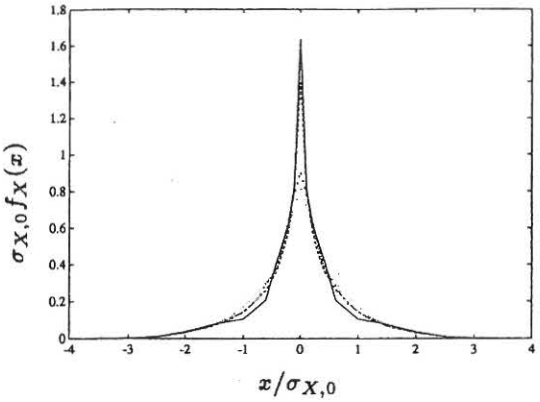

Fig. 3-76: Method 1. Pdf of displacement, $f_X(x)$. Linear scale. $\nu = 0.01\omega_0$, $\Delta t = T_0$. Fine mesh: (- - -) simulation, (—) path integration. Uniform mesh: (-·-·-) simulation, (· · ·) path integration. Köylüoğlu, Nielsen and Iwankiewicz (1995).

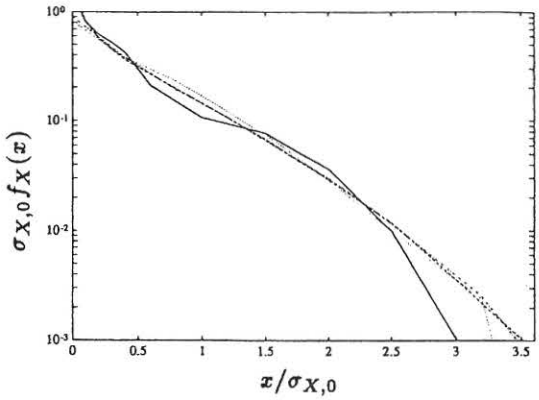

Fig. 3-77: Method 1. Pdf of displacement, $f_X(x)$. Semi-log scale. $\nu = 0.01\omega_0$, $\Delta t = T_0$. Fine mesh: (- - -) simulation, (—) path integration. Uniform mesh: (-·-·-) simulation, (· · ·) path integration. Köylüoğlu, Nielsen and Iwankiewicz (1995).

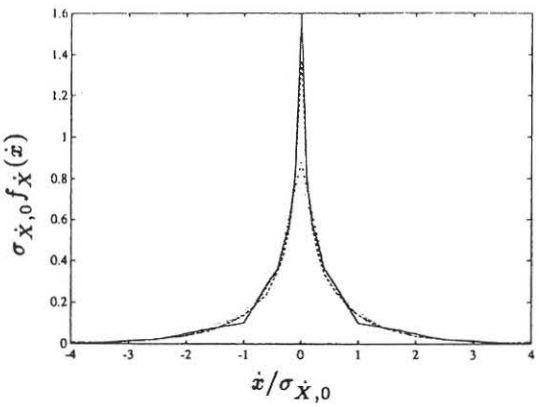

Fig. 3-78: Method 1. Pdf of velocity, $f_{\dot{X}}(\dot{x})$. Linear scale. $\nu = 0.01\omega_0$, $\Delta t = T_0$. Fine mesh: (- - -) simulation, (—) path integration. Uniform mesh: (-·-·-) simulation, (· · ·) path integration. Köylüoğlu, Nielsen and Iwankiewicz (1995).

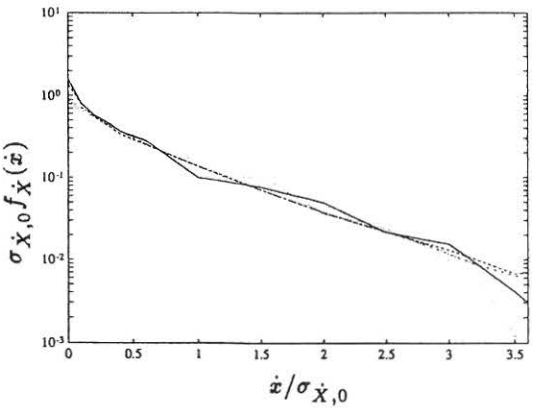

Fig. 3-79: Method 1. Pdf of velocity, $f_{\dot{X}}(\dot{x})$. Semi-log scale. $\nu = 0.01\omega_0$, $\Delta t = T_0$. Fine mesh: (- - -) simulation, (—) path integration. Uniform mesh: (-·-·-) simulation, (· · ·) path integration. Köylüoğlu, Nielsen and Iwankiewicz (1995).

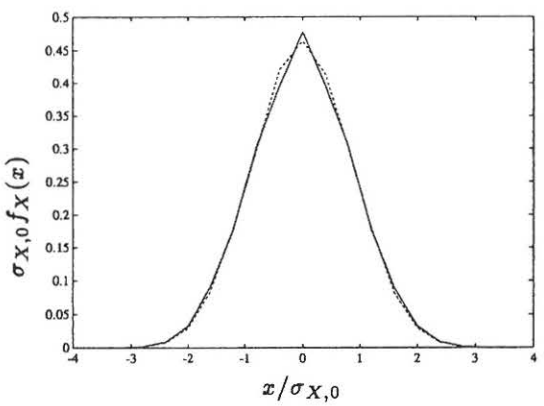

Fig. 3-80: Method 1. Pdf of displacement, $f_X(x)$. Linear scale. $\nu = 0.1\omega_0$, $\Delta t = T_0$. Uniform mesh: (- - -) simulation, (—) path integration. Köylüoğlu, Nielsen and Iwankiewicz (1995).

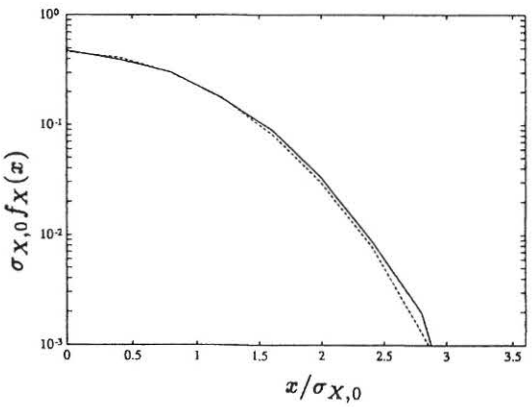

Fig. 3-81: Method 1. Pdf of displacement, $f_X(x)$. Semi-log scale. $\nu = 0.1\omega_0$, $\Delta t = T_0$. Uniform mesh: (- - -) simulation, (—) path integration. Köylüoğlu, Nielsen and Iwankiewicz (1995).

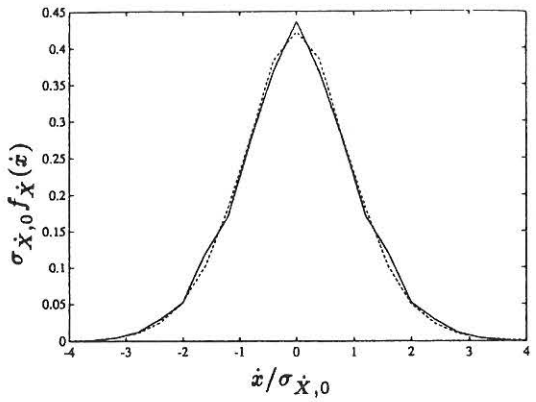

Fig. 3-82: Method 1. Pdf of velocity, $f_{\dot{X}}(\dot{x})$. Linear scale. $\nu = 0.1\omega_0$, $\Delta t = T_0$. Uniform mesh: (- - -) simulation, (—) path integration. Köylüoğlu, Nielsen and Iwankiewicz (1995).

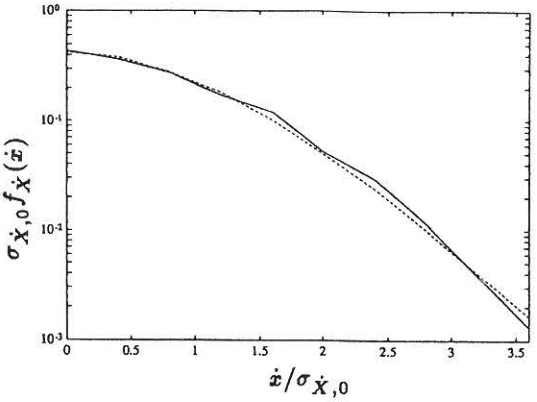

Fig. 3-83: Method 1. Pdf of velocity, $f_{\dot{X}}(\dot{x})$. Semi-log scale. $\nu = 0.1\omega_0$, $\Delta t = T_0$. Uniform mesh: (- - -) simulation, (—) path integration. Köylüoğlu, Nielsen and Iwankiewicz (1995).

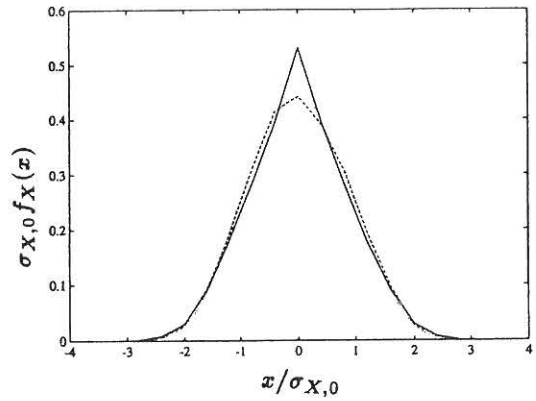

Fig. 3-84: Method 1. Pdf of displacement, $f_X(x)$. Linear scale. $\nu = 1.0\omega_0$, $\Delta t = \frac{T_0}{2}$. Uniform mesh: (- - -) simulation, (—) path integration, $(\cdots)$ exact solution to white noise excitation. Köylüoğlu, Nielsen and Iwankiewicz (1995).

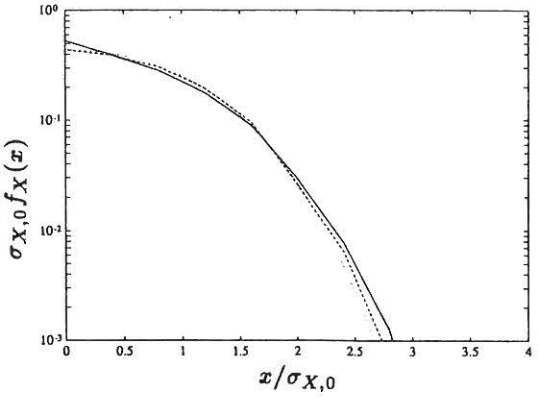

Fig. 3-85: Method 1. Pdf of displacement, $f_X(x)$. Semi-log scale. $\nu = 1.0\omega_0$, $\Delta t = \frac{T_0}{2}$. Uniform mesh: (- - -) simulation, (—) path integration, $(\cdots)$ exact solution to white noise excitation. Köylüoğlu, Nielsen and Iwankiewicz (1995).

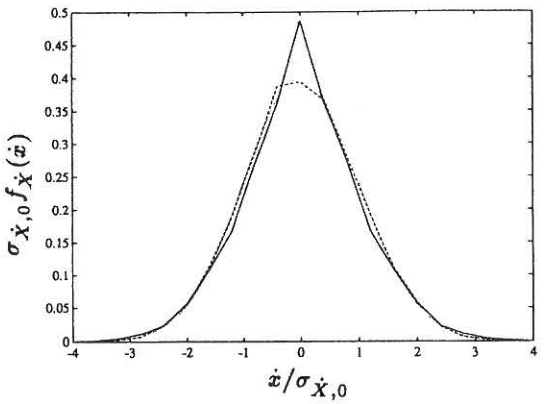

Fig. 3-86: Method 1. Pdf of velocity, $f_{\dot{X}}(\dot{x})$. Linear scale. $\nu = 1.0\omega_0$, $\Delta t = \frac{T_0}{2}$. Uniform mesh: (- - -) simulation, (—) path integration, $(\cdots)$ exact solution to white noise excitation. Köylüoğlu, Nielsen and Iwankiewicz (1995).

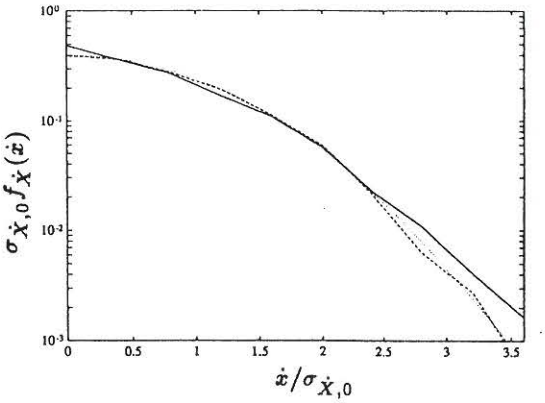

Fig. 3-87: Method 1. Pdf of velocity, $f_{\dot{X}}(\dot{x})$. Semi-log scale. $\nu = 1.0\omega_0$, $\Delta t = \frac{T_0}{2}$. Uniform mesh: (- - -) simulation, (—) path integration, $(\cdots)$ exact solution to white noise excitation. Köylüoğlu, Nielsen and Iwankiewicz (1995).

Figs. 3-88 and 3-89 show the time dependence of the reliability function $R(t|\mathbf{0}) = 1 - F_{T_1}(t|\mathbf{0})$ and the first-passage time probabilty density function $f_{T_1}(t|\mathbf{0})$ for the case of sparse pulse arrivals $\nu = 0.01\omega_0$. The considered first-passage problem has symmetrically constant double barriers, $b = -a = 1.0\sigma_{X,0}$ with deterministic start problem in $\mathbf{Z}(0) = \mathbf{0}$. Results obtained by path integration with a transition time interval $\Delta t = \frac{T_0}{2}$ have been compared to those obtained by Monte Carlo simulations. The simulation results are based on 100000 independent sample functions obtained by numerical integration with the average time step $\frac{T_0}{40}$, by means of a 4th order Runge-Kutta scheme. The first-passage time probability density functions for path integration and Monte Carlo simulation have been obtained by numerical differentiation of the reliability function. As is the case for the white noise case, cf. figs. 3-72 - 3-73, the path integration method underestimates the probability of failure during the first periods of excitation, because of the large transition time interval, made necessary by the coarseness of the applied uniform 20×20 mesh.

Figs. 3-90 and 3-91 show the corresponding results for the case of medium level pulse arrivals, $\nu = 0.1\omega_0$. The obtained results have also been compared to those obtained by approximating the excitation process with an equivalent Gaussian white noise excitation, which was obtained upon solving the boundary value problem (3-138), using a Petrov-Galerkin variational formulation as explained in Section 3.5. As seen the results for $\nu = 0.1\omega_0$ deviate significantly from those for the white noise case, whereas the path integration results are in much better agreement with Monte Carlo simulation.

Figs. 3-92 - 3-93 show the reliability function and first-passage time probability density function for a single constant barrier problem problem with stationary start in the safe domain. The barrier level is $b = 1.0\sigma_{X,0}$. The initial distribution $\boldsymbol{\pi}^{(0)}$ was obtained from the analytical solution for the Gaussian white noise case, which was lumped at the nodes of the mesh, and normalized, so the probability mass within the safe domain amounts to 1. The simulation results were obtained by ergodic sampling based on (2-31) with 10000 out-crossing events. As seen, the staircase character of the first-passage time probability density function during the initial stages of first-passages cannot be caught by the path integration results. Nevertheless, the correct limiting exponential decay, corresponding to a discrete eigen-spectrum of the backward Kolmogorov-Feller operator with absorbing exit boundaries, cf. (2-117), is clearly captured by the path integration method.

Figs. 3-94 and 3-95 show the corresponding solutions for the case of medium level arrival rate of impulses, $\nu = 0.1\omega_0$. Notice that the transition time interval has been reduced to $\Delta t = \frac{T_0}{2}$. Again the correct limiting decay rate is captured. Hence, the method provides an alternative to the results (2-162), (2-166) for the determination of the lowest eigenvalue of the backward or forward Kolmogorov-Feller operator with absorbing exit or entrance boundaries, respectively.

For Method 2 a slightly larger damping ratio of $\zeta = 0.03$ has been used, resulting in the system data specified in (3-395). The impulse strength of the compound Poisson process is still assumed to be zero-mean normally distributed, $P \sim N(0, \sigma_P^2)$, with the variance chosen, so $\frac{\nu\sigma_P^2}{4\zeta\omega_0^3 m^2} = 1$. The mean arrival rates of impulses are chosen as $\nu = \frac{0.1}{\pi}\omega_0$. Then the fraction $\frac{\zeta\omega_0}{\nu}$ is approximately the same as for the system in figs. 3-76 - 3-79, and markedly peaked behaviour should be expected. In establishing the transitional probability matrix, the coupled differential equations (3-402), (3-413) have been solved by a 4th order Runge-Kutta scheme. The path integration is performed by a uniform 20×20 mesh with the limits $[-4\sigma_{X,0}, 4\sigma_{X,0}] \times [-4\sigma_{\dot{X},0}, 4\sigma_{\dot{X},0}]$, and the transition time interval is taken as $\Delta t = T_0$. Solutions for the stationary marginal pdfs of $X(\infty)$ and $\dot{X}(\infty)$ have been obtained both by iteration of (3-383) with start in the origin using 50 iterations until stationarity, and by the eigenvector solution (3-384). Monte Carlo simulation results have been based on an ensemble of 100000 Monte Carlo realizations of $X(t)$ and $\dot{X}(t)$. Stationarity of the response is assumed after $50T_0$, at which time the stationary distributions have been sampled, using the same class-width as applied in the path integration scheme.

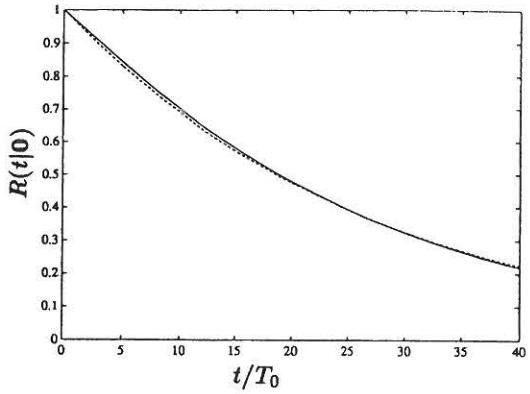

Fig. 3-88: Method 1. Reliability function, $R(t|\mathbf{0})$. Deterministic start, double barrier problem. $b = -a = \sigma_{X,0}$, $\nu = 0.01\omega_0$, $\Delta t = \frac{T_0}{2}$. Uniform mesh: (- - -) simulation, (—) path integration. Köylüoğlu, Nielsen and Iwankiewicz (1995).

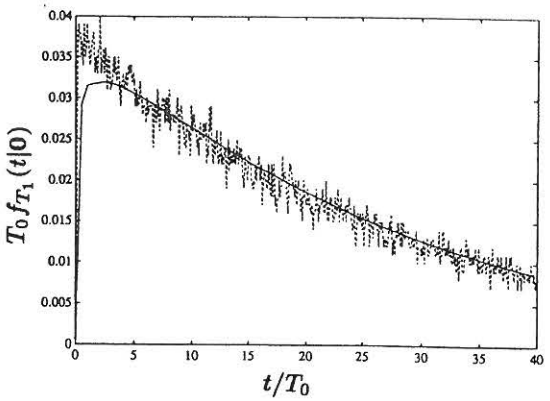

Fig. 3-89: Method 1. First-passage time pdf, $f_{T_1}(t|\mathbf{0})$. Deterministic start, double barrier problem. $b = -a = \sigma_{X,0}$, $\nu = 0.01\omega_0$, $\Delta t = \frac{T_0}{2}$. Uniform mesh: (- - -) simulation, (—) path integration. Köylüoğlu, Nielsen and Iwankiewicz (1995).

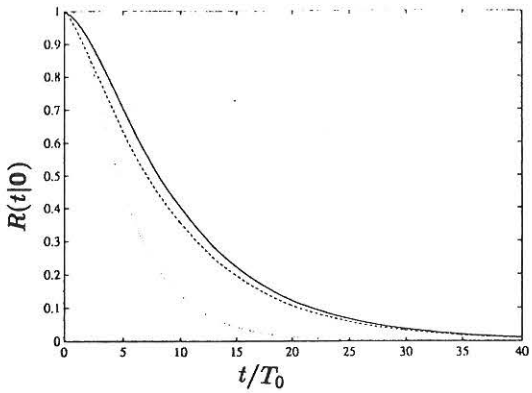

Fig. 3-90: Method 1. Reliability function, $R(t|\mathbf{0})$. Deterministic start, double barrier problem. $b = -a = \sigma_{X,0}$, $\nu = 0.1\omega_0$, $\Delta t = \frac{T_0}{2}$. Uniform mesh: (- - -) simulation, (—) path integration, mesh: (· · ·) white noise excitation. Köylüoğlu, Nielsen and Iwankiewicz (1995).

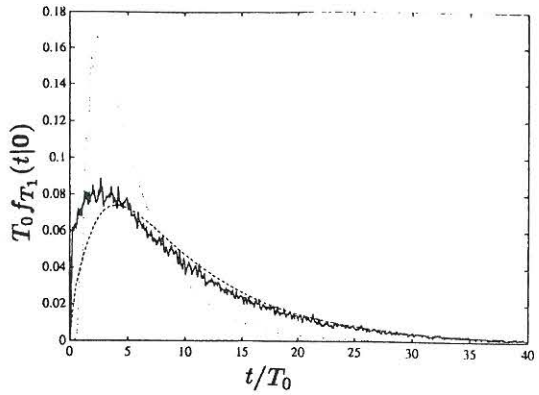

Fig. 3-91: Method 1. First-passage time pdf, $f_{T_1}(t|\mathbf{0})$. Deterministic start, double barrier problem. $b = -a = \sigma_{X,0}$, $\nu = 0.1\omega_0$, $\Delta t = \frac{T_0}{2}$. Uniform mesh: (- - -) simulation, (—) path integration, mesh: (· · ·) white noise excitation. Köylüoğlu, Nielsen and Iwankiewicz (1995).

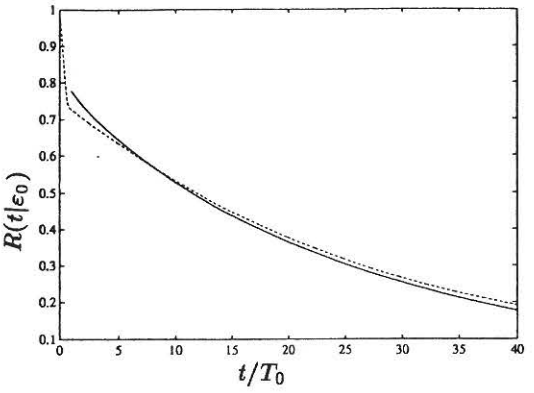

Fig. 3-92: Method 1. Reliability function, $R(t|\mathcal{E}_0)$. Stationary start, single barrier problem. $b = \sigma_{X,0}$, $\nu = 0.01\omega_0$, $\Delta t = T_0$. Uniform mesh: (- - -) simulation, (—) path integration. Köylüoğlu, Nielsen and Iwankiewicz (1995).

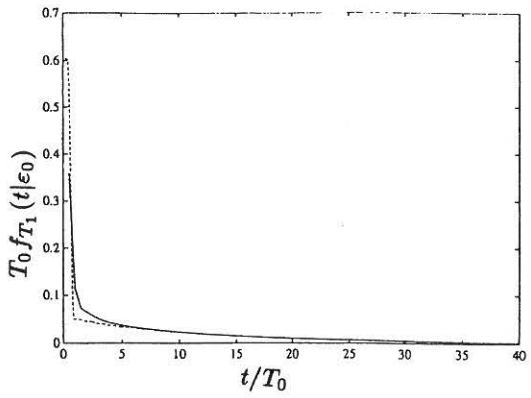

Fig. 3-93: Method 1. First-passage time pdf, $f_{T_1}(t|\mathcal{E}_0)$. Stationary start, single barrier problem. $b = \sigma_{X,0}$, $\nu = 0.01\omega_0$, $\Delta t = T_0$. Uniform mesh: (- - -) simulation, (—) path integration. Köylüoğlu, Nielsen and Iwankiewicz (1995).

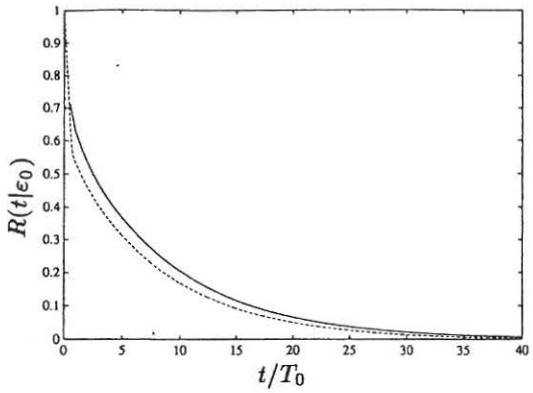

Fig. 3-94: Method 1. Reliability function, $R(t|\mathcal{E}_0)$. Stationary start, single barrier problem. $b = \sigma_{X,0}$, $\nu = 0.1\omega_0$, $\Delta t = \frac{T_0}{2}$. Uniform mesh: (- - -) simulation, (—) path integration. Köylüoğlu, Nielsen and Iwankiewicz (1995).

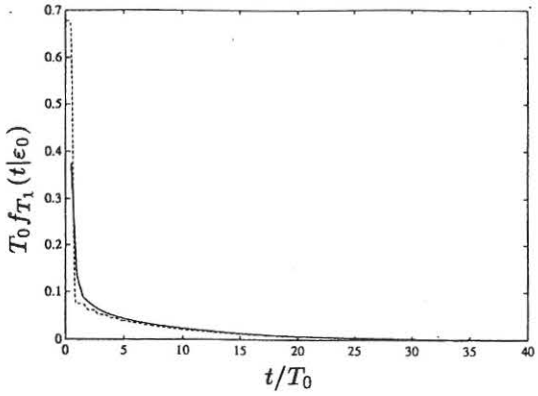

Fig. 3-95: Method 1. First-passage time pdf, $f_{T_1}(t|\mathcal{E}_0)$. Stationary start, single barrier problem. $b = \sigma_{X,0}$, $\nu = 0.1\omega_0$, $\Delta t = \frac{T_0}{2}$. Uniform mesh: (- - -) simulation, (—) path integration. Köylüoğlu, Nielsen and Iwankiewicz (1995).

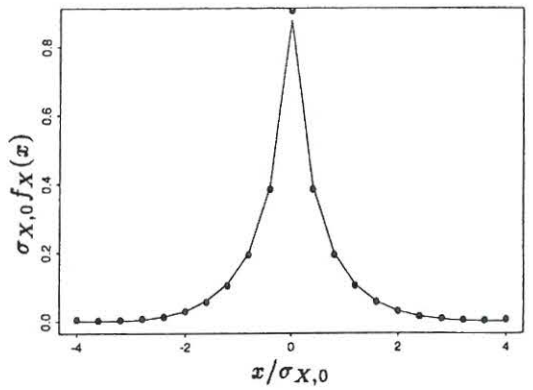

Fig. 3-96: Method 2. Pdf of displacement, $f_X(x)$. Linear scale. $\nu = \frac{0.1}{\pi}\omega_0$, $\Delta t = T_0$. Uniform mesh: (—) simulation, • path integration, iteration, (o) path integration, eigenvector solution. Köylüoğlu, Nielsen and Çakmak (1995).

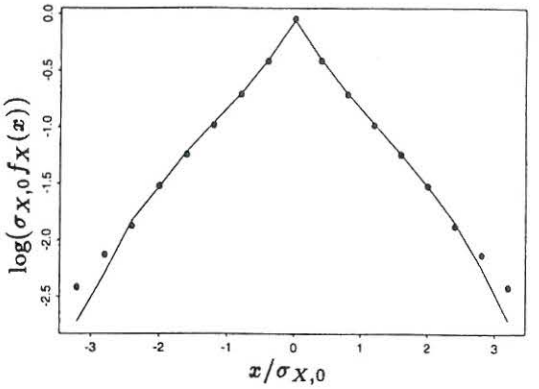

Fig. 3-97: Method 2. Pdf of displacement, $f_X(x)$. Semi-log scale. $\nu = \frac{0.1}{\pi}\omega_0$, $\Delta t = T_0$. Uniform mesh: (—) simulation, • path integration, iteration, (o) path integration, eigenvector solution. Köylüoğlu, Nielsen and Çakmak (1995).

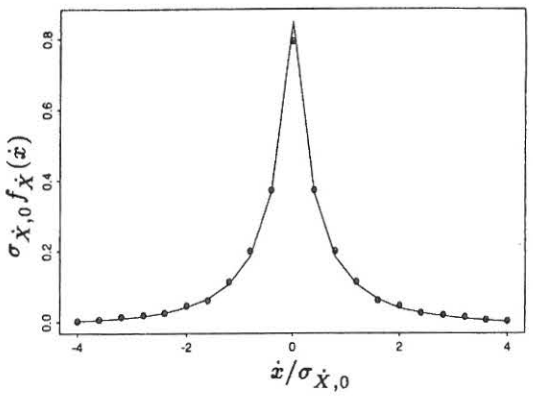

Fig. 3-98: Method 2. Pdf of velocity, $f_{\dot{X}}(\dot{x})$. Linear scale. $\nu = \frac{0.1}{\pi}\omega_0$, $\Delta t = T_0$. Uniform mesh: (—) simulation, • path integration, iteration, (o) path integration, eigenvector solution. Köylüoğlu, Nielsen and Çakmak (1995).

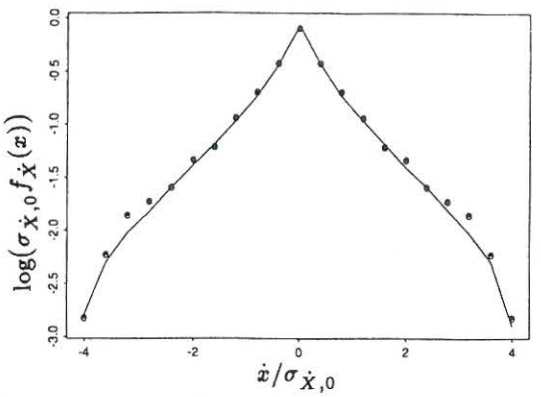

Fig. 3-99: Method 2. Pdf of velocity, $f_{\dot{X}}(\dot{x})$. Semi-log scale. $\nu = \frac{0.1}{\pi}\omega_0$, $\Delta t = T_0$. Uniform mesh: (—) simulation, • path integration, iteration, (o) path integration, eigenvector solution. Köylüoğlu, Nielsen and Çakmak (1995).

In figs. 3-96 - 3-99 the obtained stationary marginal probability density functions of the displacement and the velocity in linear and semi-logarithmic scale are shown. Upon comparison with the corresponding results in figs. 3-76 - 3-79 obtained by Method 1 with a uniform mesh it is concluded that the present distribution and lumping scheme is performing at least equally well. At the same time the scheme is significantly simpler and faster to use. The necessary computing times for the path integration method based on iteration, on eigenvector solution and for the Monte Carlo simulation were 37s, 31s, and 13950s, respectively, which concludes that path integration offers extreme computational advantages over the Monte Carlo simulation method.

The main conclusion to be drawn from this example is that both the convection and diffusion schemes explained in figs. 3-74 and 3-75 provide accurate estimates of the probability density functions, even with the mesh as coarse as 20×20. In reliability applications, the probabilty of failure is underestimated during the initial periods of first-passages with such a mesh, and a finer mesh should be applied. However, even with the coarse mesh the methods are capable of capturing the correct limiting exponential decay of the reliability function and the first-passage time probability density functions.

The path integration schemes of Method 1 and Method 2 are both based on the asymptotic expansion (3-403), which is valid under the restriction (3-404). For the present example of a Duffing oscillator with moderate non-linearity parameter this criterion turns out to be fulfilled for $\nu \leq 0.1\omega_0$. As mentioned in Example 3-8, moment methods work at best at the other extreme of very dense pulse arrivals. Upon using the modified cumulant neglect closure schemes (3-234), (3-235), devised for closure at the order $N = 4$, it was possible to extend the applicability of moment methods for the present example to mean arrival rates down to $\nu \geq 0.05\omega_0$. Hence the whole range of mean arrival rates has been covered by the two methods in combination.

The differential equations for a dynamic system driven by Lévy α-stable motion is given by (3-119) with $\{V(t), t \in [t_0, \infty[\}$ signifying a Lévy α-stable motion. During the interval $[\tau, \tau + d\tau[, \tau \in]t_i, t[$, an increment (impulse) of magnitude $dV(\tau)$ is assumed to occur. With the same approximation as assumed in Method 2 for compound Poisson process driven systems, the state vector at the time t from the impulse $dV(\tau)$ can then be written, cf. (3-411), $\mathbf{Z}(t) \simeq \mathbf{d}(t|\mathbf{z}_k, t_i) + \mathbf{d}^{(1)}(t|\mathbf{z}_k, t_i)dV(\tau)$. Since, $\mathbf{Z}(t)$ is independent of τ and depends linearly on $dV(\tau)$, the state vector from all such differential impulses becomes

$$\mathbf{Z}(t) \simeq \mathbf{d}(t|\mathbf{z}_k, t_i) + \mathbf{d}^{(1)}(t|\mathbf{z}_k, t_i)\Delta V(t_i) \quad , \quad \Delta V(t_i) = \int_{t_i}^{t} dV(\tau) = V(t) - V(t_i) \quad (3\text{-}415)$$

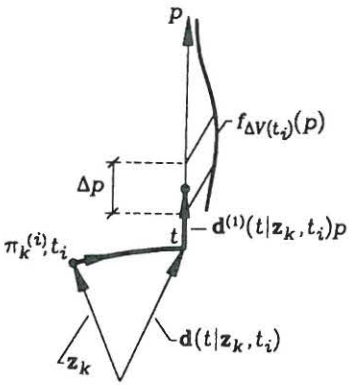

Fig. 3-100: Path integration of compound Lévy α-stable motion driven system. Convection and lumping of probability mass.

$\Delta V(t_i)$ in (3-415) is an α-stable random variable $\Delta V(t_i) \sim S_\alpha\big((a\Delta t)^{1/\alpha}, \beta, 0\big)$, cf. (3-23). According to (3-415) the probability mass $\pi_k^{(0)}$ at the node $\mathbf{z}_k$ at the time t_i is then convected to the position $\mathbf{d}(t|\mathbf{z}_k, t_i)$, where it is diffused along the direction of $\mathbf{d}^{(1)}(t|\mathbf{z}_k, t_i)$, according to the probability density function $f_{\Delta V(t_i)}(p)$. At the position $\mathbf{d}(t|\mathbf{z}_k, t_i) + \mathbf{d}^{(1)}(t|\mathbf{z}_k, t_i)p$ a probability mass of magnitude $\pi_k^{(i)} f_{\Delta V(t_i)}(p)\Delta p$ is then lumped as sketched in fig. 3-100.

As shown by (3-356) - (3-360) a system driven by an Erlang renewal process can be reduced to an equivalent Poisson driven system at the expense of the introduction of a number of auxiliary state variables in addition to the structural state variables $\mathbf{X}(t)$, which control that only every kth Poisson generated impulse is applied to the structure. This suggests that the devised path integration schemes for compound Poisson driven systems can be applied also to compound Erlang driven systems as well. However, a modification of the convection and diffusion scheme is needed to ensure that only every kth Poisson impulse causes a convection and diffusion in the mesh. A modification of the Method 2 path integration scheme has been devised by Iwankiewicz and Nielsen (1996), and will be explained in detail in what follows.

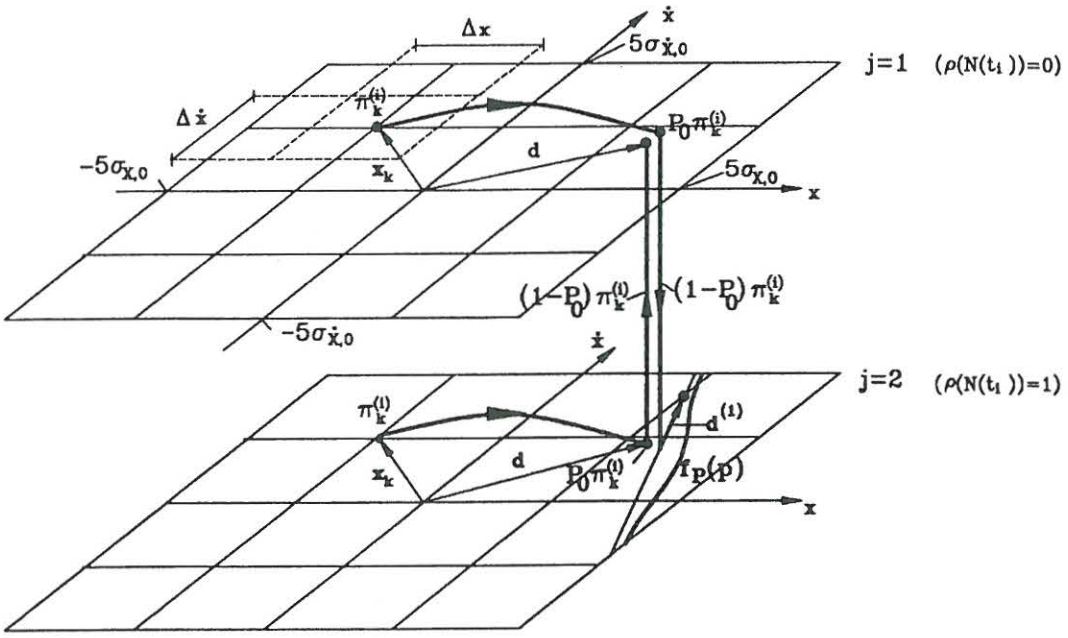

Fig. 3-101. Discretization of the state space for the case $k = 2$. Convection and lumping of the probability mass.

The function $\rho\big(N(t)\big)$ defined by (3-345) repeats itself periodically, attaining the value $\rho\big(N(t)\big) = 0$ during the first $k-1$ Poisson events, followed by a value $\rho\big(N(t)\big) = 1$ in the kth event. To each Poisson event in the cycle a path integration mesh is defined for convection and diffusion calculation in the discretized structural state space variables,

so totally k such meshes should be pointed out, as illustrated in fig. 3-101 for the case $k = 2$ for a 2-dimensional structural sample space.

Assume that the system at the time t_i is in the structural state $\mathbf{X}(t_i) = \mathbf{x}_k$ after the $(j-1)$th Poisson event in the sequence has occurred, $j = 1, \ldots, k-1$. During the interval $]t_i, t]$ the probability mass $\pi_k^{(i)}$ of being at the node $\mathbf{x}_k$ of mesh j at the time t_i is convected to the position $\mathbf{d}(t|\mathbf{x}_k, t_i)$ according to the 0th order term in (3-411). At this position a probability mass of magnitude $\pi_k^{(i)} P_0$ is lumped, where $P_0 = P_0(t, t_i)$ signifies the probability that no Poisson impulse has occurred in $]t_i, t]$. If $j < k-1$ the remaining probability mass $\pi_k^{(i)}(1-P_0)$ is transferred to the succeeding mesh $j+1$, where it is lumped at the same position $\mathbf{d}(t|\mathbf{x}_k, t_i)$. However, if $j = k-1$ the probability mass $\pi_k^{(i)}(1-P_0)$ is distributed along the line $\mathbf{d}^{(1)}(t|\mathbf{x}_k, t_i)$ in the mesh $j = k$, according to the probability density function $f_P(p)$ as in the original formulation of Method 2. In either case the probability mass $\pi_k^{(i)}(1-P_0)$ is attached to the succeeding mesh $j+1$, because the distribution is performed on the condition that one extra Poisson event has occured during $]t_i, t]$. If the system at the time t_i is in the structural state $\mathbf{X}(t_i) = \mathbf{x}_k$ after the $(k-1)$th Poisson event in the sequence has occurred, the probability mass $\pi_k^{(i)} P_0$ is still lumped at the position $\mathbf{d}(t|\mathbf{x}_k, t_i)$ of mesh $j = k$. The remaining probability mass is transferred to mesh $j = 1$, where it is lumped at the position $\mathbf{d}(t|\mathbf{x}_k, t_i)$ to start a new sequence. As previously, all lumped probability masses are finally redistributed to the adjacent grid points in all k meshes.

As specified by (3-357) and (3-359) the total number of auxiliary state variables amounts to $k-1$, so the dimension of the state vector $\mathbf{Z}(t)$ of the integrated dynamic system becomes $n+k-1$. Appearently, using N cells per state variable in the discretized mesh, the number of states of the Markov chain becomes $(N+1)^{n+k-1}$. However, the number of states of the described path integration scheme only amounts to $k(N+1)^n$, i.e. the growth is linear with k rather than exponential.

Example 3-14: Duffing oscillator subjected to compound Erlang process with k=2

The Duffing oscillator (3-44), (3-45), (3-46) is considered with the following system data

$$m = 1.0 \quad , \quad \omega_0 = 1.0 \quad , \quad \zeta = 0.01 \quad , \quad \varepsilon = 0.5 \qquad (3-416)$$

The strength of the impulses is assumed to be zero-mean normally distributed, $P \sim N(0, \sigma_P^2)$ with the variance chosen, so $\frac{\nu}{k} \frac{\sigma_P^2}{4\zeta \frac{3}{\omega} m^2} = 1$, corresponding to the stationary standard deviations $\sigma_{X,0} = \sigma_{\dot{X},0} = 1$ of a linear oscillator exposed to an equivalent Gaussian white noise. Only the case $k = 2$ is considered with the following three values of $\frac{\nu}{k\omega_0}$

$$\frac{\nu}{k\omega_0} = \begin{cases} 0.01 \\ 0.10 \\ 1.00 \end{cases} \quad , \quad \frac{\Delta t}{T_0} = \begin{cases} 1.00 \\ 0.20 \\ 0.05 \end{cases} \quad \Rightarrow \quad \nu\Delta t = \begin{cases} 0.126 \\ 0.251 \\ 0.628 \end{cases} \qquad (3-417)$$

The indicated values of $\frac{\nu}{k\omega_0}$ make comparison possible to the compound Poisson cases considered in example 3-13. Again the indicated arrival rates may be categorized as the cases of sparse, medium level

and dense pulse arrival rates. The corresponding transition time intervals, Δt, have been selected to meet the upper bound requirement (3-404). Obviously, the lower bound $\frac{\Delta t}{T_0} \geq \frac{1}{2\pi}$, as stated subsequent to (3-405), is not met by the specification of Δt for the case of sparse pulses. Hence, rather poor results are to be expected in this case. The path integration has been performed by a uniform 44×44 mesh with the limits $[-5\sigma_{X,0}, 5\sigma_{X,0}] \times [-5\sigma_{\dot{X},0}, 5\sigma_{\dot{X},0}]$. The stationary marginal pdfs of $X(\infty)$ and $\dot{X}(\infty)$ were estimated from (3-383) with start in the origin of the mesh $j = 1$ using 60 iterations until stationarity. Again, comparison has been made with the results obtained by Monte Carlo simulation. The stationary marginal pdfs were obtained by ergodic sampling, using a time-series of the length $4000000T_0$, which was obtained by numerical integration of the equations of motions by means of a 4th order Runge-Kutta scheme with the time-step $\frac{T_0}{40}$. The generation of the underlying compound Erlang process, and the succeeding numerical integration procedure, was performed as explained in example 3-11. The sampling was performed with the same class-width as applied in the path integration scheme at the end of each integration time-step. Sampling was not initiated until the elapse of an initial transient phase of length $200T_0$.

$\frac{\nu}{k\omega_0}$	$\frac{\Delta t}{T_0}$	$\sigma_X(\infty)$		$\sigma_{\dot{X}}(\infty)$	
		sim.	num.	sim.	num.
0.01	1.00	0.69938	0.70703	0.99768	1.00295
0.10	0.20	0.75587	0.79073	1.00138	1.06577
1.00	0.05	0.76174	0.64546	1.00151	0.80115

Table 3.5: Stationary standard deviations $\sigma_X(\infty)$, $\sigma_{\dot{X}}(\infty)$ of displacement and velocity response as a function of $\frac{\nu}{k\omega_0}$.

In table 3.5 the predictions of the stationary standard deviations obtained from path integration in comparison to those of Monte Carlo simulation are shown. As seen, the results are excellent in the case of sparse pulses $\frac{\nu}{k\omega_0} = 0.01$, they are still quite good in the case of medium level pulse arrivals, $\frac{\nu}{k\omega_0} = 0.10$, but they are not satisfactory for $\frac{\nu}{k\omega_0} = 1.00$.

Below, in figs. 3-102 – 3-105 the stationary marginal probability density functions of the displacement and the velocity for the case of sparse pulse arrivals, $\frac{\nu}{k\omega_0} = 0.01$ are shown, with the non-dimensional transition time interval $\frac{\Delta t}{T_0} = 1.0$. To emphasize on the tails, the results have been indicated both in linear and semi-logarithmic scale. As seen, the agreement with Monte Carlo simulation is very good. Similarly to the comparable Poisson driven system in example 3-13 the marginal pdfs reveal pronounced peaks at the origin in case of sparse pulse arrivals.

Figs. 3-106 and 3-107 show the prediction of path integration method in semi-logarithmic scale for the case $\frac{\nu}{k\omega_0} = 0.01$ for various values of the non-dimensional transition time interval $\frac{\Delta t}{T_0}$. The results for $\frac{\Delta t}{T_0} = 5.0$ are not very good, because the upper bound criterion (3-404) has been violated in this case. The case $\frac{\Delta t}{T_0} = 0.2$, which is close to the lower bound for allowable transition time intervals, still provides good results. However, the best results are obtained for $\frac{\Delta t}{T_0} = 1.0$, which is well within the admissible interval for the transition time interval.

Figs. 3-108 - 3-111 show the corresponding results for the stationary marginal probability density functions of the displacement and the velocity for the case of medium level pulse arrivals $\frac{\nu}{k\omega_0} = 0.1$ with the non-dimensional transition time interval $\frac{\Delta t}{T_0} = 0.2$, which is close to the acceptable lower limit for the transition time interval. As expected the results are not so good as those of the previous case of sparse impulses.

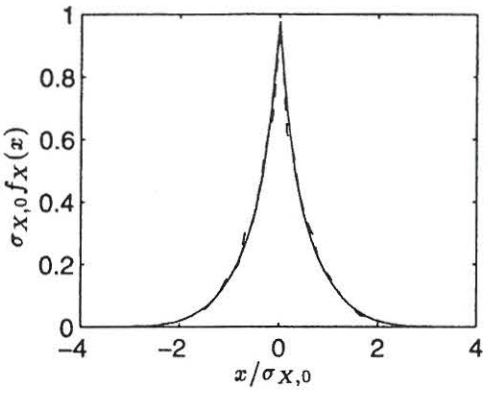

Fig. 3-102: Stationary pdf of displacement, $f_X(x)$. Linear scale. $k = 2$, $\frac{\nu}{k\omega_0} = 0.01$, $\frac{\Delta t}{T_0} = 1.0$. Uniform mesh: (—) simulation, (- - -) path integration. Iwankiewicz and Nielsen (1996).

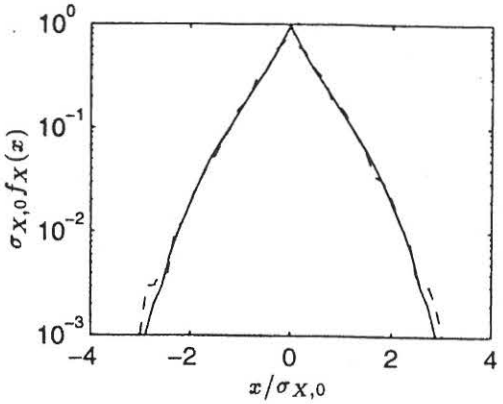

Fig. 3-103: Stationary pdf of displacement, $f_X(x)$. Semi-log scale. $k = 2$, $\frac{\nu}{k} = 0.01\omega_0$, $\frac{\Delta t}{T_0} = 1.0$. Uniform mesh: (—) simulation, (- - -) path integration. Iwankiewicz and Nielsen (1996).

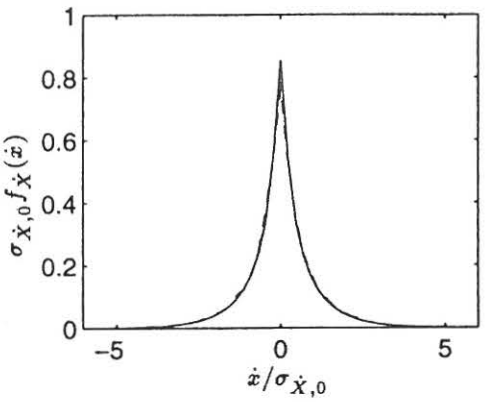

Fig. 3-104: Stationary pdf of velocity, $f_{\dot{X}}(\dot{x})$. Linear scale. $k = 2$, $\frac{\nu}{k\omega_0} = 0.01$, $\frac{\Delta t}{T_0} = 1.0$. Uniform mesh: (—) simulation, (- - -) path integration. Iwankiewicz and Nielsen (1996).

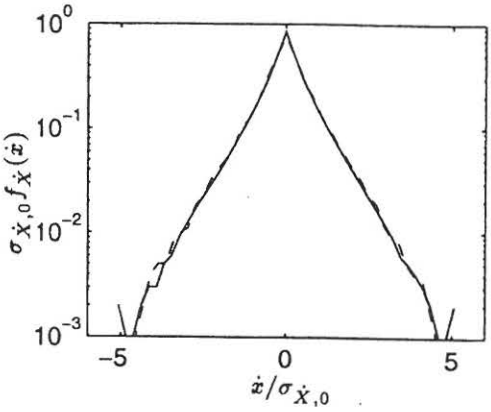

Fig. 3-105: Stationary pdf of velocity, $f_{\dot{X}}(\dot{x})$. Semi-log scale. $k = 2$, $\frac{\nu}{k} = 0.01\omega_0$, $\frac{\Delta t}{T_0} = 1.0$. Uniform mesh: (—) simulation, (- - -) path integration. Iwankiewicz and Nielsen (1996).

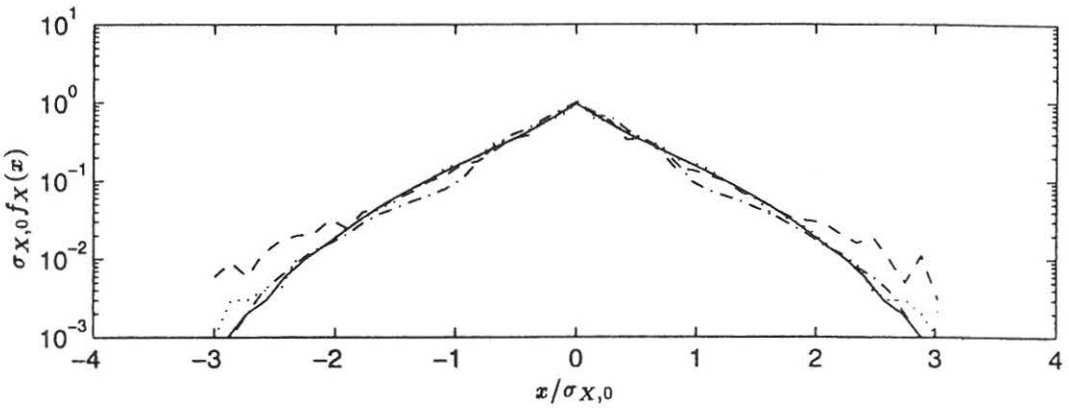

Fig. 3-106: Dependence of path integration results on the length of transition time interval Δt. Stationary pdf of displacement, $f_X(x)$. Semi-log scale. $k = 2$, $\frac{\nu}{k\omega_0} = 0.01$, uniform mesh.
(—): simulation, (- - -): $\frac{\Delta t}{T_0} = 5.0$, ($\cdots$): $\frac{\Delta t}{T_0} = 1.0$, (-·-·-): $\frac{\Delta t}{T_0} = 0.2$. Iwankiewicz and Nielsen (1996).

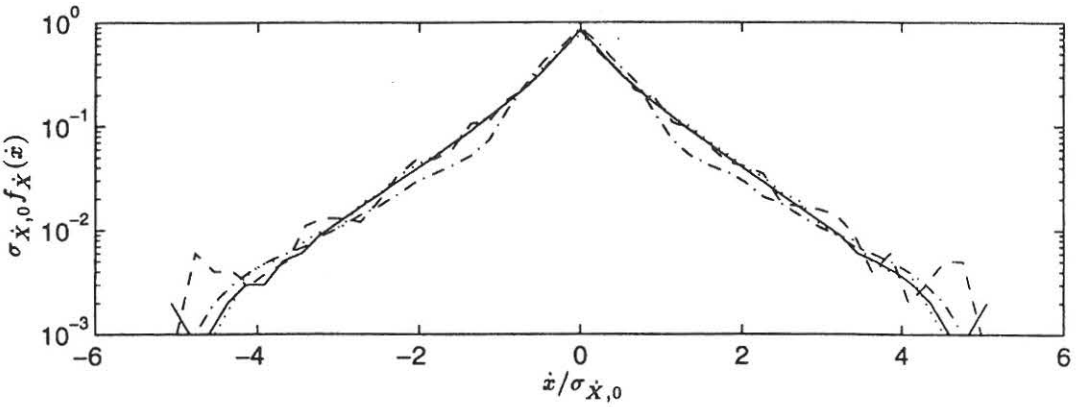

Fig. 3-107: Dependence of path integration results on the length of transition time interval Δt. Stationary pdf of velocity, $f_{\dot{X}}(\dot{x})$. Semi-log scale. $k = 2$, $\frac{\nu}{k\omega_0} = 0.01$, uniform mesh.
(—): simulation, (- - -): $\frac{\Delta t}{T_0} = 5.0$, (· · ·): $\frac{\Delta t}{T_0} = 1.0$, (-·-·-): $\frac{\Delta t}{T_0} = 0.2$.
Iwankiewicz and Nielsen (1996).

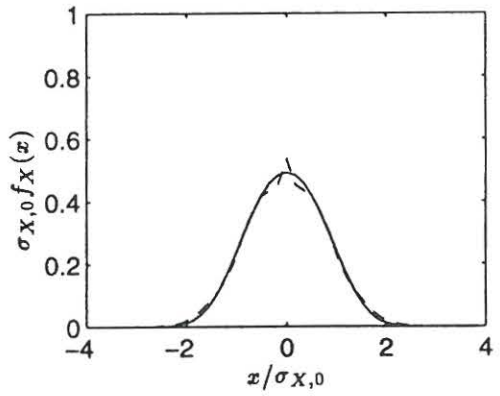

Fig. 3-108: Stationary pdf of displacement, $f_X(x)$. Linear scale. $k = 2$, $\frac{\nu}{k\omega_0} = 0.1$, $\frac{\Delta t}{T_0} = 0.2$. Uniform mesh: (—) simulation, (- - -) path integration. Iwankiewicz and Nielsen (1996).

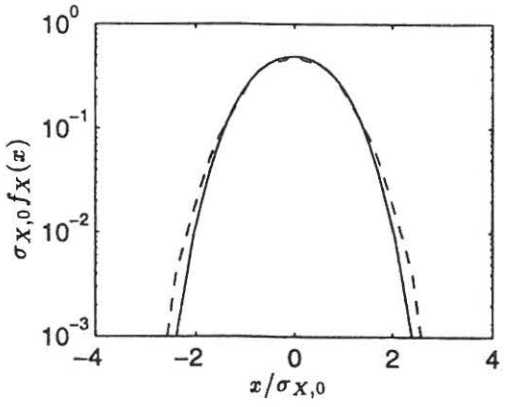

Fig. 3-109: Stationary pdf of displacement, $f_X(x)$. Semi-log scale. $k = 2$, $\frac{\nu}{k\omega_0} = 0.1$, $\frac{\Delta t}{T_0} = 0.2$. Uniform mesh: (—) simulation, (- - -) path integration. Iwankiewicz and Nielsen (1996).

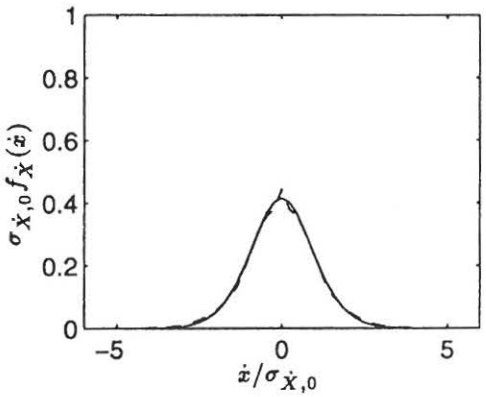

Fig. 3-110: Stationary pdf of velocity, $f_{\dot{X}}(\dot{x})$. Linear scale. $k = 2$, $\frac{\nu}{k\omega_0} = 0.1$, $\frac{\Delta t}{T_0} = 0.2$. Uniform mesh: (—) simulation, (- - -) path integration. Iwankiewicz and Nielsen (1996).

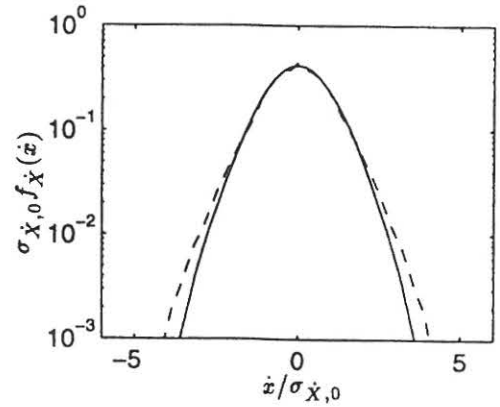

Fig. 3-111: Stationary pdf of velocity, $f_{\dot{X}}(\dot{x})$. Semi-log scale. $k = 2$, $\frac{\nu}{k\omega_0} = 0.1$, $\frac{\Delta t}{T_0} = 0.2$. Uniform mesh: (—) simulation, (- - -) path integration. Iwankiewicz and Nielsen (1996).

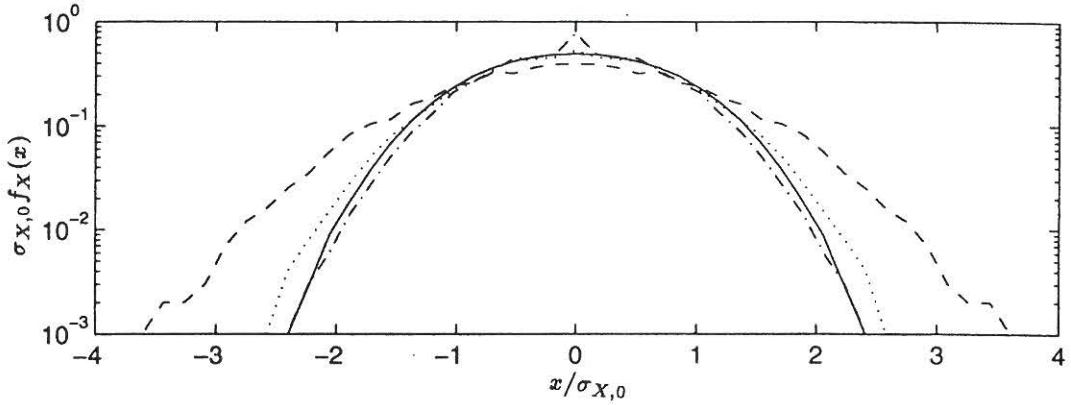

Fig. 3-112: Dependence of path integration results on the length of transition time interval Δt. Stationary pdf of displacement, $f_X(x)$. Semi-log scale. $k = 2$, $\frac{\nu}{k\omega_0} = 0.1$, uniform mesh.
(—): simulation, (- - -): $\frac{\Delta t}{T_0} = 1.0$, (· · ·): $\frac{\Delta t}{T_0} = 0.2$, (-·-·-): $\frac{\Delta t}{T_0} = 0.1$.
Iwankiewicz and Nielsen (1996).

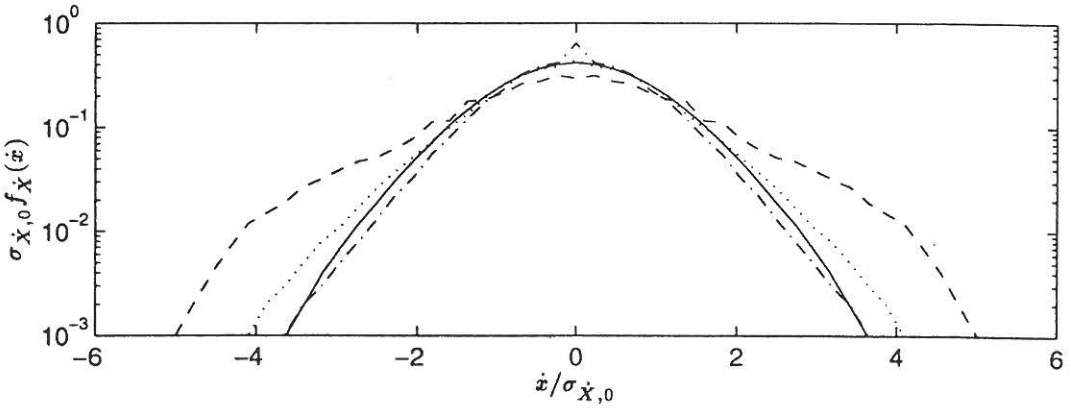

Fig. 3-113: Dependence of path integration results on the length of transition time interval Δt. Stationary pdf of velocity, $f_{\dot{X}}(\dot{x})$. Semi-log scale. $k = 2$, $\frac{\nu}{k\omega_0} = 0.1$, uniform mesh.
(—): simulation, (- - -): $\frac{\Delta t}{T_0} = 1.0$, (· · ·): $\frac{\Delta t}{T_0} = 0.2$, (-·-·-): $\frac{\Delta t}{T_0} = 0.1$.
Iwankiewicz and Nielsen (1996).

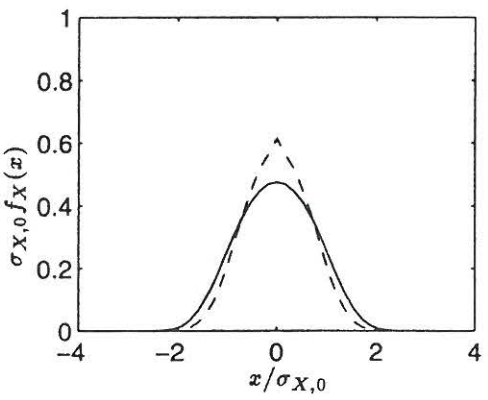

Fig. 3-114: Stationary pdf of displacement, $f_X(x)$. Linear scale. $k = 2$, $\frac{\nu}{k\omega_0} = 1.0$, $\frac{\Delta t}{T_0} = 0.05$. Uniform mesh: (—) simulation, (- - -) path integration. Iwankiewicz and Nielsen (1996).

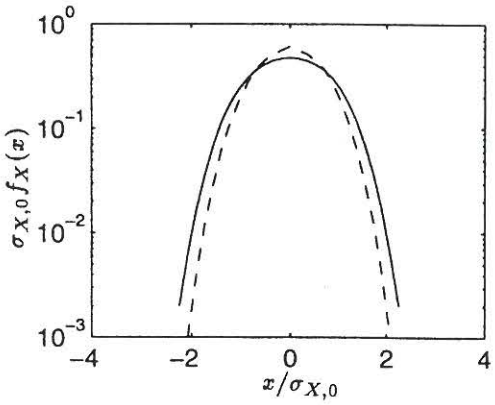

Fig. 3-115: Stationary pdf of displacement, $f_X(x)$. Semi-log scale. $k = 2$, $\frac{\nu}{k\omega_0} = 1.0$, $\frac{\Delta t}{T_0} = 0.05$. Uniform mesh: (—) simulation, (- - -) path integration. Iwankiewicz and Nielsen (1996).

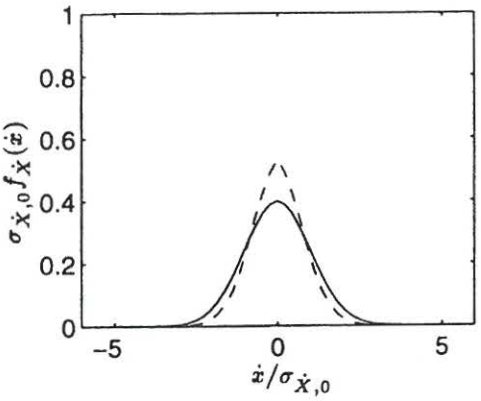

Fig. 3-116: Stationary pdf of velocity, $f_{\dot{X}}(\dot{x})$. Linear scale. $k = 2$, $\frac{\nu}{k\omega_0} = 1.0$, $\frac{\Delta t}{T_0} = 0.05$. Uniform mesh: (—) simulation, (- - -) path integration. Iwankiewicz and Nielsen (1996).

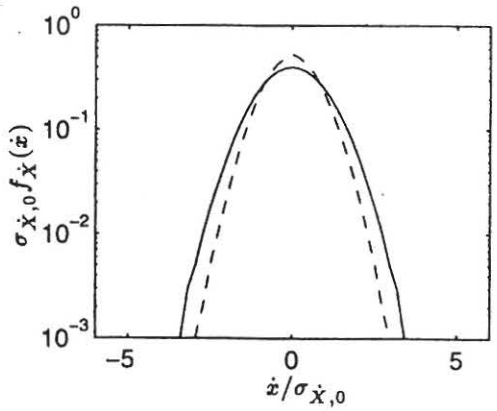

Fig. 3-117: Stationary pdf of velocity, $f_{\dot{X}}(\dot{x})$. Semi-log scale. $k = 2$, $\frac{\nu}{k\omega_0} = 1.0$, $\frac{\Delta t}{T_0} = 0.05$. Uniform mesh: (—) simulation, (- - -) path integration. Iwankiewicz and Nielsen (1996).

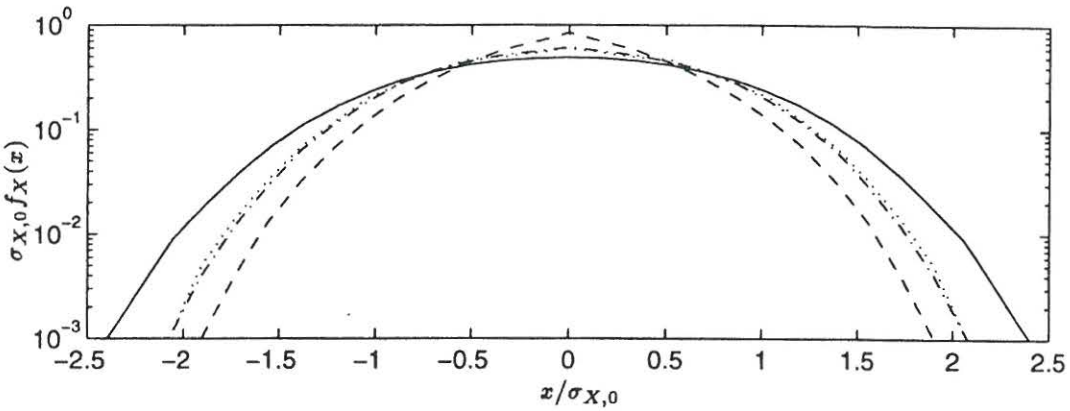

Fig. 3-118: Dependence of path integration results on the length of transition time interval Δt. Stationary pdf of displacement, $f_X(x)$. Semi-log scale. $k = 2$, $\frac{\nu}{k\omega_0} = 1.0$, uniform mesh.
(—): simulation, (- - -): $\frac{\Delta t}{T_0} = 0.02$, ($\cdots$): $\frac{\Delta t}{T_0} = 0.1$, (-·-·-): $\frac{\Delta t}{T_0} = 0.05$.
Iwankiewicz and Nielsen (1996).

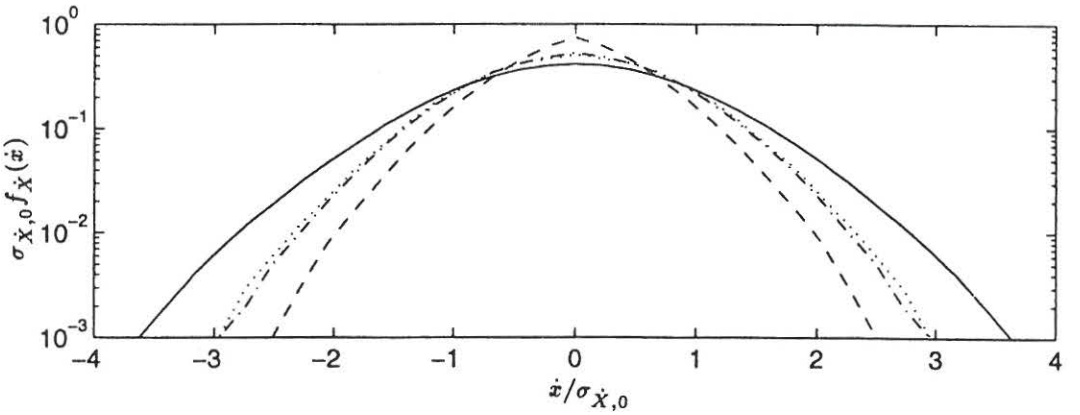

Fig. 3-119: Dependence of path integration results on the length of transition time interval Δt. Stationary pdf of velocity, $f_{\dot{X}}(\dot{x})$. Semi-log scale. $k = 2$, $\frac{\nu}{k\omega_0} = 1.0$, uniform mesh.
(—): simulation, (- - -): $\frac{\Delta t}{T_0} = 0.02$, ($\cdots$): $\frac{\Delta t}{T_0} = 0.1$, (-·-·-): $\frac{\Delta t}{T_0} = 0.05$.
Iwankiewicz and Nielsen (1996).

Figs. 3-112 and 3-113 show the dependence of the path integration results on $\frac{\Delta t}{T_0}$ for the same case. The results for $\frac{\Delta t}{T_0} = 1.0$ are unacceptably poor, because the upper bound criterion (3-404) has been violated in this case. The cases $\frac{\Delta t}{T_0} = 0.2$ and $\frac{\Delta t}{T_0} = 0.1$ both provide more accurate results. However, in the latter case a peak is predicted at the origin, which is not present in the simulation result. This may be attributed to the application of too small transition intervals.

Finally, figs. 3-114 - 3-117 show the results for the stationary marginal probability density functions of the displacement and the velocity for the case of dense pulse arrivals, $\frac{\nu}{k\omega_0} = 1.0$, with the non-dimensional transition time interval $\frac{\Delta t}{T_0} = 0.05$. Due to the application of too small transition time intervals the path integration results are neither qualitatively nor quantitatively in agreement with simulation results. Again a peak is predicted at the origin, which is not present in the simulation results.

The dependence on $\frac{\Delta t}{T_0}$ for the same case is shown in figs. 3-118 and 3-119. Although none of the cases provide acceptable results, the accuracy is much better for the cases $\frac{\Delta t}{T_0}$=0.05 and 0.1, than for the case $\frac{\Delta t}{T_0} = 0.02$.

The example demonstrates the applicability of path integration technique for a Duffing oscillator subjected to impulses driven by an Erlang renewal process of order $k = 2$. The applied path integration scheme was a modification of the Method 2 for compound Poisson driven systems. Again, it has been demonstrated that the path integration method provides accurate results for the case of sparse pulses, whereas unaccaptable results are obtained if the non-dimensional transition interval $\frac{\Delta t}{T_0}$ is either too small or too large.

3.5 Diffusion methods

Attempts to solve the forward or backward integro-differential Chapman-Kolmogorov equations (3-94), (3-96), as well as the related reliability problems (3-128), (3-131) and (3-134), (3-138) by means of conventional finite difference or finite element schemes have proved to be unsuccessful, due to large convection velocities compared to the diffusion velocities present in the phase space at large values of the velocity component $\dot{x}$, which renders such schemes unstable, when the local Peclet number becomes large, Zienkiewicz and Taylor (1991). Such instability problems have also been found in convective heat transport problems at large convection velocities, in fluid dynamic problems at high Reynolds number and other mixed convection-diffusion problems with high velocities. For the forward and backward Fokker-Planck equation Bergman and his co-workers demonstrated in a number of papers on non-hysteretic simple oscillators, Bergman and Heinrich (1982), Bergman and Spencer (1983), as well as hysteretic oscillators, Spencer (1986), that corrections for the convection flows could be achieved by applying a Petrov-Galerkin type of weighting with upwind differentiation to the weak formulation of the ruling differential equations. Similar approaches have been proposed by Langley (1988b), Langtangen (1990), and others.

In this section the reliability problem is considered for the non-linear, non-hysteretic time-invariant SDOF oscillator (3-45), (3-46), subject to a stationary compound Poisson process $\{F(t), t \in [0, \infty[\}$ with the mean arrival rate ν. The weak counterpart of (3-138) with the Kolmogorov-Feller operator given by (3-123) or (3-125) is solved by a Petrov-Galerkin approach. Because of the severe requirements of differentiability and continuity in the $\dot{x}$-direction, the shape and weighting functions for the $\dot{x}$-component have to be globally specified, which rules out the possibility of any finite element formulation of the applied variational approach.

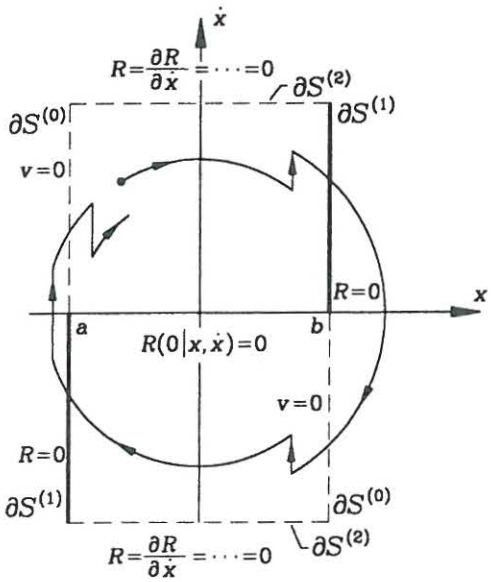

Fig. 3-120: Boundary and initial conditions.

A double barrier problem with constant barriers is considered, i.e. the safe domain S is given as $S = \{(x,\dot{x})|\ a < x < b\ \wedge\ -\infty < \dot{x} < \infty\}$. The boundary and initial value problem for the reliability function $R(\tau \mid \mathbf{z}) = 1 - F_{T_1}(\tau \mid \mathbf{z})$ then becomes, see fig. 3-120 and (3-138)

$$\left.\begin{array}{l} \frac{\partial}{\partial\tau}R(\tau \mid x,\dot{x}) - \dot{x}\frac{\partial}{\partial x}R(\tau \mid x,\dot{x}) + u(x,\dot{x})\frac{\partial}{\partial\dot{x}}R(\tau \mid x,\dot{x}) - \\ \nu\sum\limits_{k=1}^{\infty}\frac{1}{k!}\frac{E[P^k]}{m^k}\frac{\partial^k}{\partial\dot{x}^k}R(\tau \mid x,\dot{x}) = 0\ ,\ \forall\tau\in]0,\infty[\ ,\ \forall(x,\dot{x})\in S \\ R(0 \mid x,\dot{x}) = 1\ ,\ \forall(x,\dot{x})\in S \\ R(\tau \mid x,\dot{x}) = 0\ ,\ \forall\tau\in]0,\infty[\ ,\ \forall(x,\dot{x})\in \partial S^{(1)}\cup\partial S^{(2)} \\ \frac{\partial^n}{\partial\dot{x}^n}R(\tau \mid x,\dot{x}) = 0\ ,\ n = 1,2,\dots\ ,\ \forall\tau\in]0,\infty[\ ,\ \forall(x,\dot{x})\in\partial S^{(2)} \end{array}\right\} \qquad (3-418)$$

The Kramer-Moyal expansion for the backward Kolmogorov-Feller operator (3-125) has been applied in (3-418). Hence, it is assumed that moments $E[P^n]$ of the impulse strength P exist for any order n. In what follows a scheme for obtaining numerical solutions of (3-418) will be devised. First, the weak counterpart of (3-418) will be derived. Assuming the weighting function $v(x,\dot{x})$ to fulfil the boundary conditions $v(x,\dot{x}) = 0$, $(x,\dot{x})\in\partial S^{(0)}$, and using $u(x,\dot{x}) = R(\tau \mid x,\dot{x})$ in (3-110) it follows that

$$\int_S R(\tau \mid x,\dot{x})\mathcal{K}_{\mathbf{z}}\big[v(x,\dot{x})\big]dxd\dot{x} = \int_S v(x,\dot{x})\mathcal{K}^T_{\mathbf{z}}\big[R(\tau \mid x,\dot{x})\big]dxd\dot{x} \quad \Rightarrow$$

$$\int_S v(x,\dot{x})\frac{\partial}{\partial\tau}R(\tau \mid x,\dot{x})dxd\dot{x} - \int_S R(\tau \mid x,\dot{x})\mathcal{K}_{\mathbf{z}}\big[v(x,\dot{x})\big]dxd\dot{x} = 0 \qquad (3-419)$$

(3-419) provides the weak counterpart of the considered problem. $\mathcal{K}_{\mathbf{z}}\big[v(x,\dot{x})\big]$ is the forward Kolmogorov-Feller operator given by (3-124). The variational equation (3-419) is discretized upon expanding $R(\tau \mid x,\dot{x})$ into the following product form

$$R(\tau \mid x,\dot{x}) = \sum_{I=1}^{I_0}\sum_{J=1}^{J_0} R_{IJ}(\tau)N_I^{(1)}(x)N_J^{(2)}(\dot{x}) \qquad (3-420)$$

The variational field $v(x,\dot{x})$ is also restricted to a subspace of functions expanded by the following linearly independent basis

$$V_{IJ}(x,\dot{x}) = V_I^{(1)}(x)V_J^{(2)}(\dot{x}) \quad ,\quad I = 1,\dots,I_0,\ J = 1,\dots,J_0 \qquad (3-421)$$

The shape functions $N_I^{(1)}(x)$ are continuous and the weight functions $V_I^{(1)}(x)$ are both continuous and piecewise differentiable in $]a,b[$. Additionally, $N_I^{(1)}(x)$ vanishes on $\partial S^{(1)}$ and $V_I^{(1)}(x)$ vanishes on $\partial S^{(0)}$. In the $\dot{x}$-direction, the weight functions $V_J^{(2)}(\dot{x})$ are

continuous and infinitely many times differentiable in $]-\infty,\infty[$. Further, $V_J^{(2)}(\dot{x})$ and all its derivatives vanish on $\partial S^{(2)}$. In principle the shape functions $N_J^{(2)}(\dot{x})$ need only be piecewise continuous, and are not requested to fulfil any boundary conditions on $\partial S^{(2)}$.

The fulfilment of (3-419) for any variation $w(x,\dot{x})$ within the considered subspaces leads to the following discrete variational equations

$$\sum_{I_2=1}^{I_0}\sum_{J_2=1}^{J_0} M_{I_1J_1I_2J_2}\dot{R}_{I_2J_2} + \sum_{I_2=1}^{I_0}\sum_{J_2=1}^{J_0} K_{I_1J_1I_2J_2}R_{I_2J_2} = 0$$

$$I_1 = 1,\ldots,I_0 \quad , \quad J_1 = 1,\ldots,J_0 \qquad (3-422)$$

The components of the "mass"-tensor $M_{I_1J_1I_2J_2}$ and the "stiffness"-tensor $K_{I_1J_1I_2J_2}$ are given as

$$M_{I_1J_1I_2J_2} = \int_a^b V_{I_1}^{(1)}(x)N_{I_2}^{(1)}(x)dx \int_{-\infty}^{\infty} V_{J_1}^{(2)}(\dot{x})N_{J_2}^{(2)}(\dot{x})d\dot{x} \qquad (3-423)$$

$$K_{I_1J_1I_2J_2} = \int_a^b \frac{dV_{I_1}^{(1)}(x)}{dx}N_{I_2}^{(1)}(x)dx \int_{-\infty}^{\infty} \dot{x}\, V_{J_1}^{(2)}(\dot{x})N_{J_2}^{(2)}(\dot{x})d\dot{x} -$$

$$\int_a^b\int_{-\infty}^{\infty} V_{I_1}^{(1)}(x)N_{I_2}^{(1)}(x)\frac{\partial}{\partial\dot{x}}\Big(u(x,\dot{x})V_{J_1}^{(2)}(\dot{x})\Big)N_{J_2}^{(2)}(\dot{x})dxd\dot{x} -$$

$$\int_a^b V_{I_1}^{(1)}(x)N_{I_2}^{(1)}(x)dx\ \nu\sum_{k=1}^{\infty}\frac{(-1)^k}{k!}\frac{E[P^k]}{m^k}\int_{-\infty}^{\infty}\frac{d^kV_{J_1}^{(2)}(\dot{x})}{d\dot{x}^k}N_{J_2}^{(2)}(\dot{x})d\dot{x} \qquad (3-424)$$

All integrals on the right-hand sides of (3-423) and (3-424) are the products of one-dimensional quadratures, except the 2nd term on the right-hand side of (3-424). However, this term is also reducible to such a form if $u(x,\dot{x})$ is given as a polynomial of the state variables x and $\dot{x}$, as is the case of usually considered non-linear oscillators (Duffing, van der Pol, etc), i.e.

$$u(x,\dot{x}) = \sum_{i=0}^{n}\sum_{j=0}^{m} a_{ij}x^i\dot{x}^j \qquad (3-425)$$

If $N_I^{(1)}(x) = V_I^{(1)}(x)$ and $N_J^{(2)}(\dot{x}) = V_J^{(2)}(\dot{x})$, the conventional Galerkin approach is obtained. By analogy with the corresponding white noise excited problem, this turns out to render the numerical scheme unstable due to the large convection velocities at $|\dot{x}| \to \infty$. Numerical inaccuracies and instabilities can be overcome by introducing a

Petrov-Galerkin type of weighting to consider upwind differencing. Petrov-Galerkin finite element schemes have been employed in numerous applications in convection dominated problems, Zienkiewicz and Taylor (1991). Therefore, instead of the Galerkin formulation, a Petrov-Galerkin approach will be applied to solve (3-419), (3-422). The gist for the success of the Petrov-Galerkin solution is the proper selection of the upwind parameter controlling the approximation for the correction of the convection flows.

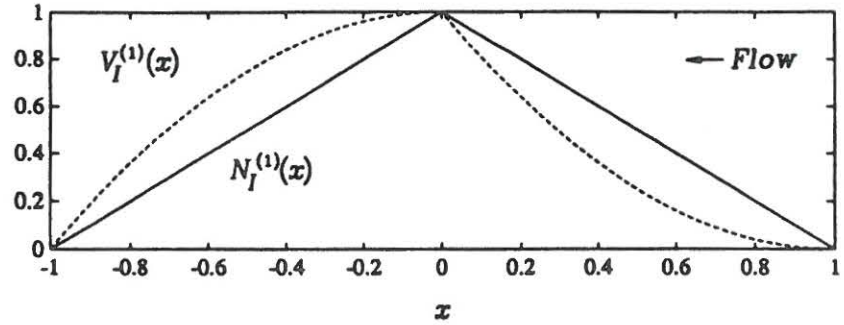

Fig. 3-121: Shape and weight functions in the x-direction. ($\alpha = 1$, $\Delta x = 1$).

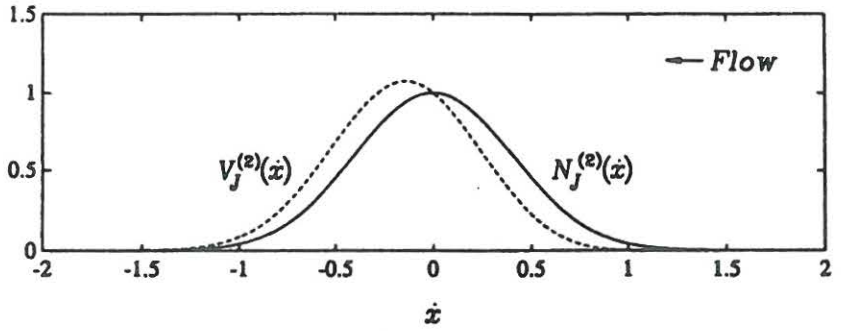

Fig. 3-122: Shape and weight functions in the $\dot{x}$-direction. ($\beta = \sqrt{\frac{2}{\pi}}$, $\gamma = 1$, $\Delta\dot{x} = \frac{1}{\sqrt{2\pi}}$).

In the variational formulation shape and weight functions will be indicated, which fulfils all the requirements of differentiability, continuity and boundary values. These functions clearly constitute a basis for the finite dimensional subspaces for the spaces of the trial functions and the weighting functions. In the x-direction, the following linear shape functions and quadratic weighting functions are utilized, fig. 3-121

$$N_I^{(1)}(x) = \begin{cases} \frac{1}{\Delta x}(x - I\Delta x) + 1 & , \quad x \in [(I-1)\Delta x, I\Delta x] \\ -\frac{1}{\Delta x}(x - I\Delta x) + 1 & , \quad x \in [I\Delta x, (I+1)\Delta x \\ 0 & , \quad \text{elsewhere} \end{cases} \qquad (3-426)$$

$$V_I^{(1)}(x) = \begin{cases} N_I^{(1)}(x) + \alpha F_{I,1}(x) & , \quad x \in [(I-1)\Delta x, I\Delta x] \\ N_I^{(1)}(x) - \alpha F_{I,2}(x) & , \quad x \in [I\Delta x, (I+1)\Delta x] \\ 0 & , \quad \text{elsewhere} \end{cases} \qquad (3-427)$$

$$F_{I,1}(x) = 3\Big(\frac{x}{\Delta x} - I\Big)\Big(I - 1 - \frac{x}{\Delta x}\Big) \quad , \quad F_{I,2}(x) = 3\Big(\frac{x}{\Delta x} - I\Big)\Big(I + 1 - \frac{x}{\Delta x}\Big) \tag{3-428}$$

$$\alpha = \coth\Big(\frac{\Gamma_x}{2}\Big) - \frac{2}{\Gamma_x} = \begin{cases} 1 & , \quad \dot{x} < 0 \\ -1 & , \quad \dot{x} > 0 \end{cases} \tag{3-429}$$

$$\Gamma_x = \begin{cases} +\infty & , \quad \dot{x} < 0 \\ -\infty & , \quad \dot{x} > 0 \end{cases} \tag{3-430}$$

where Γ_x is the local Peclet number and α is the upwind parameter. As shown in fig. 3-122, the shape and weighting functions in the $\dot{x}$-direction are specified globally in order to fulfil the severe requirements of differentiability and continuity in this direction. Shape functions are chosen as normal probability density functions with varying means

$$N_J^{(2)}(\dot{x}) = \frac{1}{\sqrt{2\pi}\gamma\Delta\dot{x}} \exp\Big(-\frac{(\dot{x} - J\Delta\dot{x})^2}{2(\gamma\Delta\dot{x})^2}\Big) \tag{3-431}$$

Weighting functions are chosen as the scaled first derivative of normal probability density functions superimposed on the Gaussian curve

$$V_J^{(2)}(\dot{x}) = N_J^{(2)}(\dot{x}) + \frac{\beta}{\sqrt{8\pi}\gamma^2\Delta\dot{x}}\Big(\frac{\dot{x} - J\Delta\dot{x}}{\gamma\Delta\dot{x}}\Big) \exp\Big(-\frac{(\dot{x} - J\Delta\dot{x})^2}{2(\gamma\Delta\dot{x})^2}\Big) \tag{3-432}$$

$$\beta = \coth\Big(\frac{\Gamma_{\dot{x}}}{2}\Big) - \frac{2}{\Gamma_{\dot{x}}} \tag{3-433}$$

$$\Gamma_{\dot{x}} = \frac{2\Big(u(x,\dot{x}) - \frac{\nu E[P]}{m}\Big)}{\overline{\frac{\nu E[P^2]}{m^2}}}\Delta\dot{x} \tag{3-434}$$

The parameter γ, used in the definition of the standard deviation of the shape and weight functions, can be termed as the interaction parameter, since it somehow represents the interaction degree of two weighting functions. The local Peclet number $\Gamma_{\dot{x}}$ and the upwind parameter β are defined as position dependent in the $(x, \dot{x})$-plane.

The white noise case is obtained if the sum in the backward Kolmogorov equation, (3-418), is truncated at $k = 2$. The optimal choice for the denominator of (3-434) then becomes $\overline{\nu E[P^2]/m^2} = \nu E[P^2]/m^2$. In this case, $\Gamma_{\dot{x}}$ can be interpreted as a measure of the relative strength of convective and diffusive velocities in the $\dot{x}$-direction, and stability is guaranteed if $\Gamma_{\dot{x}} < 2$, Bergman and Heinrich (1982), Bergman and Spencer (1983),

Spencer (1986). In the compound Poisson case, a straightforward generalization would be to introduce the following quantity in (3-434) as the average diffusion constant

$$\frac{\overline{\nu E[P^2]}}{m^2} = \nu \frac{\sum_{k=2}^{\infty} \frac{(-1)^k}{k!} \frac{E[P^k]}{m^k} \frac{\partial^k}{\partial \dot{x}^k} R(\tau \mid x, \dot{x})}{\frac{1}{2} \frac{\partial^2}{\partial \dot{x}^2} R(\tau \mid x, \dot{x})} \qquad (3-435)$$

After inserting (3-420) into (3-435), highly nonlinear differential equations are obtained from (3-422). In order to preserve linearity, the following approximate diffusion coefficient is suggested as an alternative

$$\frac{\overline{\nu E[P^2]}}{m^2} = \nu \frac{\sum_{k=2}^{\infty} \frac{(-1)^k}{k!} \frac{E[P^k]}{m^k} \frac{\partial^k}{\partial \dot{x}^k} N_J^{(2)}(\dot{x})}{\frac{1}{2} \frac{\partial^2}{\partial \dot{x}^2} N_J^{(2)}(\dot{x})} \qquad (3-436)$$

With $N_J^{(2)}(\dot{x})$ given by (3-431), the right-hand side of (3-436) can be evaluated as a closed form expression. Using (3-436), the stability requirement on $\Gamma_{\dot{x}}$ is no longer exactly fulfilled. However, since (3-436) is qualitatively correct, it follows from (3-434) that the fraction $\frac{\nu E[P^2]/m^2}{\nu E[P^2]/m^2}$ is an indication of the number of times the mesh width, $\Delta\dot{x}$, must be reduced, compared to the white noise case, in order to ensure stability.

The semi-discrete equation of (3-422), which can be interpreted as a coupled system of ordinary differential equations, is solved using the following unconditionally stable and second order accurate Crank-Nicolson scheme.

$$\Big(\mathbf{M} + 0.5\Delta\tau\mathbf{K}\Big)\mathbf{R}(\tau + \Delta\tau) = \Big(\mathbf{M} - 0.5\Delta\tau\mathbf{K}\Big)\mathbf{R}(\tau) \qquad (3-437)$$

Initial values $\mathbf{R}(0)$ are obtained from equation (3-420) after constraining the reliability function to unity at $\tau = 0$. Each period is passed by 50 time steps to achieve convergence in the Crank-Nicholson scheme.

The first-passage time probability density function $f_{T_1}(t \mid x, \dot{x})$ on condition of deterministic start in $(x, \dot{x}) \in S$ can be evaluated from (3-420)

$$f_{T_1}(t \mid x, \dot{x}) = -\frac{\partial}{\partial \tau} R(\tau \mid x, \dot{x}) = -\sum_{I=1}^{I_0} \sum_{J=1}^{J_0} \dot{R}_{IJ}(\tau) N_I^{(1)}(x) N_J^{(2)}(\dot{x}) \qquad (3-438)$$

where the derivatives $\dot{R}_{IJ}(t)$ are calculated from (3-422) as given by the matrix solution $\dot{\mathbf{R}}(\tau) = -\mathbf{M}^{-1}\mathbf{K}\mathbf{R}(\tau)$.

The indicated variational scheme and solution approach were suggested by Köylüoğlu, Nielsen and Iwankiewicz (1994), who also derived the somewhat lengthy analytical expression for the components of the mass tensor and the stiffness tensors (3-423) and (3-424) for the case of a Duffing oscillator exposed to a compound Poisson process as considered in the following example 3-15.

Example 3-15: Reliability analysis of Duffing oscillator driven by a compound Poisson process

The Duffing oscillator (3-44), (3-45), (3-46) is considered, when driven by a stationary compound Poisson process. Generally, the following system data are used $m = 1.0$, $\omega_0 = 1.0$. The considered values of the damping ratio ζ and non-linearity parameter ε are indicated in the legend of the figures. The impulse strength of the compound Poisson process is assumed to be zero-mean normally distributed, $P \sim N(0, \sigma_P^2)$. The safe domain S in fig. 3-120 is meshed into 30×30 identical rectangles. Boundaries of the mesh in the $\dot{x}$-direction are chosen as 5 times the stationary standard deviation $\sigma_{\dot{X}}(\infty)$. This bound is reduced to 2 times the standard deviation of the stationary response, when stability requirements could not be met by the indicated mesh size. It should be noted that stability of the Petrov-Galerkin solution is fully correlated to the local Peclet numbers. Hence, unstable results are expected for coarse meshes. This will be illustrated in the coming examples. For the specification of the mesh width, the standard deviation of the stationary response of the nonlinear oscillator is obtained from an initial Monte Carlo simulation in which stationarity is assumed after 20 periods. Results are obtained for the reliability function, $R(t|\mathbf{0})$, and first-passage time probability density function, $f_{T_1}(t|\mathbf{0})$, only for symmetric time-invariant double barrier problems, $-a = b$, with deterministic start in the origo, $[x, \dot{x}] = [0, 0]$.

Figs. 3-123 and 3-124 illustrate the convergence of the numerical scheme to the solution of the Fokker-Planck equation as $\nu \to \infty$ under the restriction of constant $\frac{\nu E[P^2]}{4\zeta\omega_0^3 m^2}$ for the cases of the relatively large damping ratio $\zeta = 0.08$ and the medium level damping ratio $\zeta = 0.01$, respectively. The Gaussian white noise results have been obtained from the variational principle and weighting functions proposed in this study upon truncating the sum in (3-418) after the first two terms. The dashed line indicated the corresponding results obtained upon using the present solution with the excessive large mean arrival rate of $\nu = 100\omega_0$. As seen, the results are in excellent agreement. The examples covered in figs. 3-423 and 3-424 have been taken from Bergman and Spencer (1983), who used somewhat simpler and different weighting functions.

Fig. 3-125 shows the effect of the non-linearity parameter, ε on the reliability function and the first-passage time probability density function. The following values, $\varepsilon = 0.00$, $\varepsilon = 0.25$ and $\varepsilon = 0.50$, are considered, representing the cases of linear, medium non-linear and significantly non-linear restoring forces. In order to make comparison meaningful the barrier level b is adjusted in proportion to the stationary standard deviation of the displacement, $\sigma_X(\infty)$, which is obtained by Monte Carlo simulation. Corresponding to the indicated values of ε the following standard deviations are obtained $\sigma_X(\infty) = 1.004$, $\sigma_X(\infty) = 0.827$, $\sigma_X(\infty) = 0.759$. From the results shown it is concluded that the reliability function and the first-passage time probability density function are significantly dependent on the non-linearity parameter.

Fig. 3-126 shows the dependence on the damping ratio, ζ. The following damping ratios have been considered, $\zeta = 0.05$, $\zeta = 0.10$ and $\zeta = 0.15$. The corresponding stationary standard deviations of the displacement are $\sigma_X(\infty) = 0.759$, $\sigma_X(\infty) = 0.587$, $\sigma_X(\infty) = 0.501$. From the results it is concluded that the reliability function and the first-passage time probability density function are rather insensible to the damping ratio.

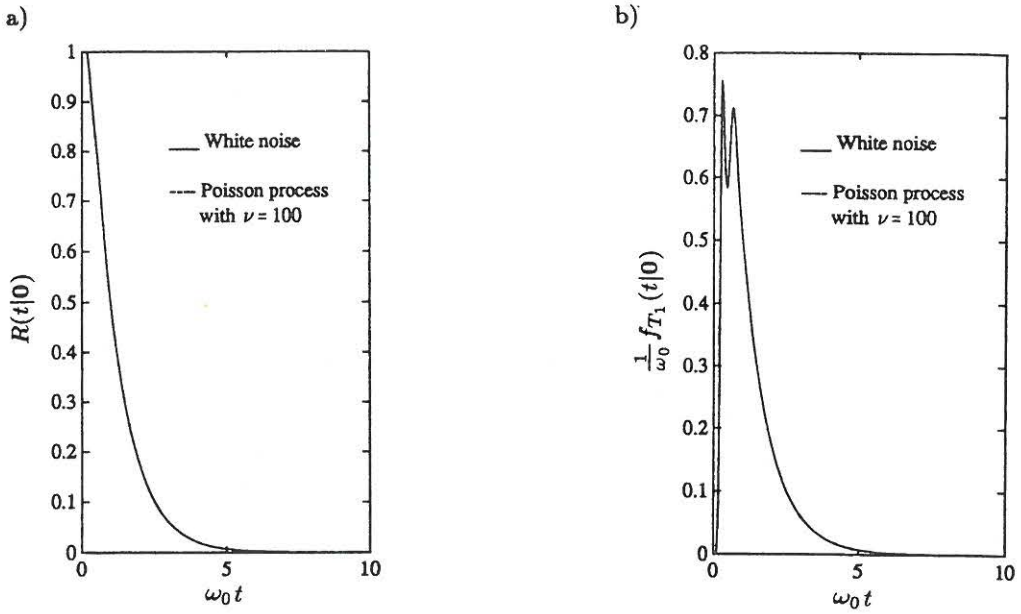

Fig. 3-123: Comparison with Gaussian white noise. a) Reliability function, $R(t|\mathbf{0})$. b) First-passage time pdf, $f_{T_1}(t|\mathbf{0})$. Deterministic start, constant double barrier problem. $b = -a = \sigma_X(\infty)$, $\zeta = 0.08$, $\epsilon = 0.2$, $\nu E[P^2] = 4\zeta\omega_0^3 m^2 = 0.32$. Köylüoğlu, Nielsen and Iwankiewicz (1994).

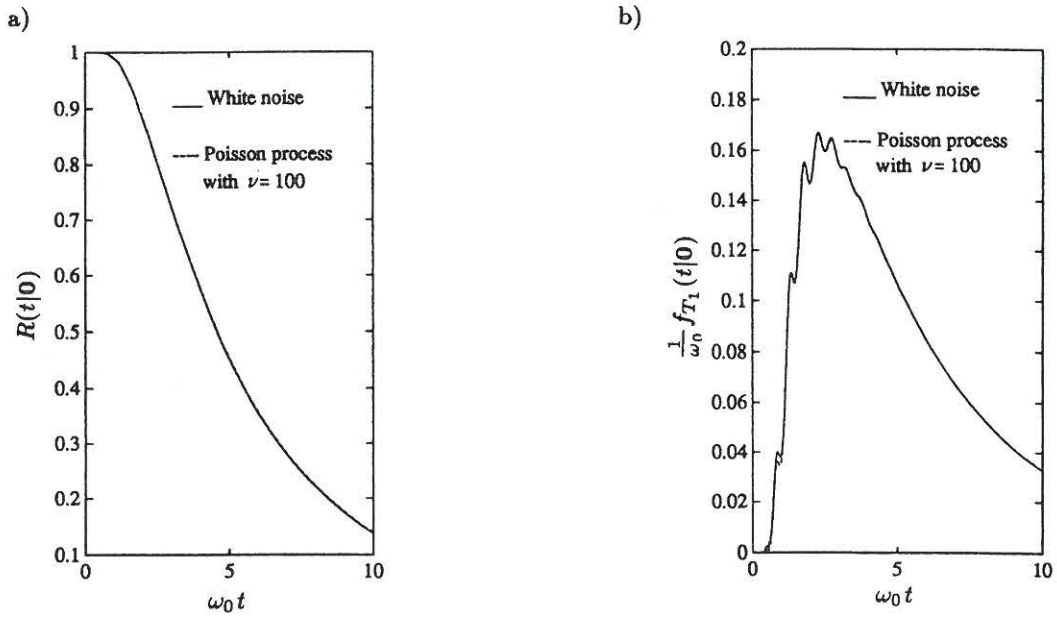

Fig. 3-124: Comparison with Gaussian white noise. a) Reliability function, $R(t|\mathbf{0})$. b) First-passage time pdf, $f_{T_1}(t|\mathbf{0})$. Deterministic start, constant double barrier problem. $b = -a = \sigma_X(\infty)$, $\zeta = 0.01$, $\epsilon = 0.2$, $\nu E[P^2] = 4\zeta\omega_0^3 m^2 = 0.04$. Köylüoğlu, Nielsen and Iwankiewicz (1994).

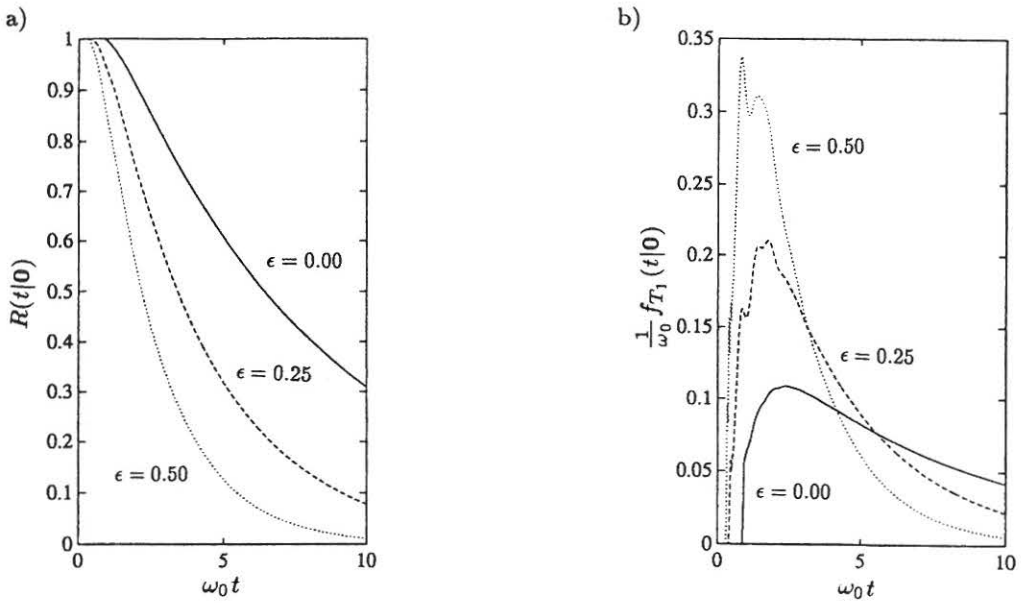

Fig. 3-125: Dependence on non-linearity parameter, ε. a) Reliability function, $R(t|\mathbf{0})$. b) First-passage time pdf, $f_{T_1}(t|\mathbf{0})$. Deterministic start, constant double barrier problem. $b = -a = 2\sigma_X(\infty)$, $\zeta = 0.05$, $\nu E[P^2] = 4\zeta\omega_0^3 m^2 = 0.20$, $\nu = 5\omega_0$. Köylüoğlu, Nielsen and Iwankiewicz (1994).

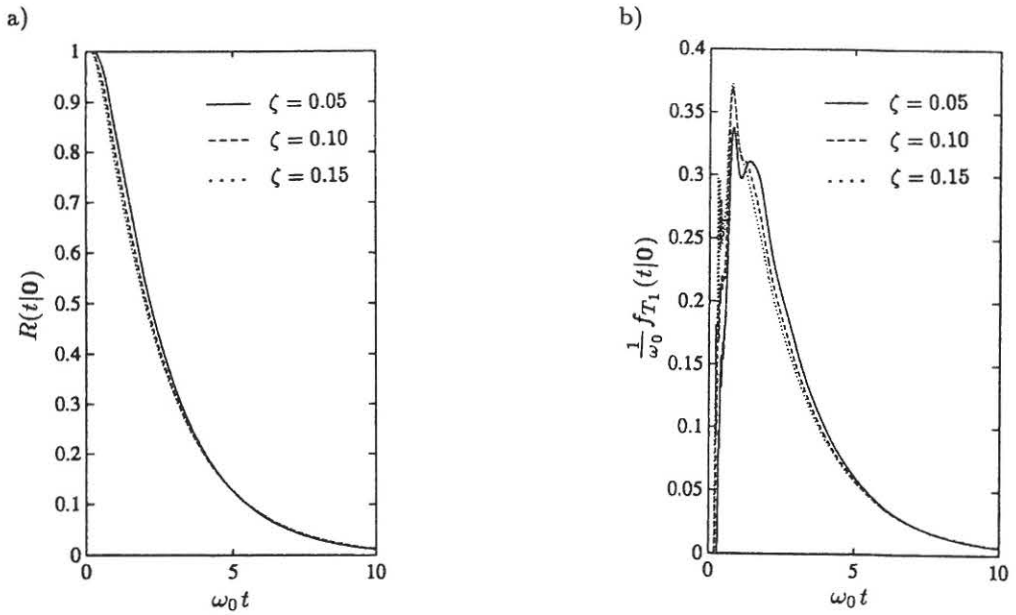

Fig. 3-126: Dependence on damping ratio, ζ. a) Reliability function, $R(t|\mathbf{0})$. b) First-passage time pdf, $f_{T_1}(t|\mathbf{0})$. Deterministic start, constant double barrier problem. $b = -a = 2\sigma_X(\infty)$, $\varepsilon = 0.5$, $\nu E[P^2] = 4\zeta\omega_0^3 m^2 = 0.20$, $\nu = 5\omega_0$. Köylüoğlu, Nielsen and Iwankiewicz (1994).

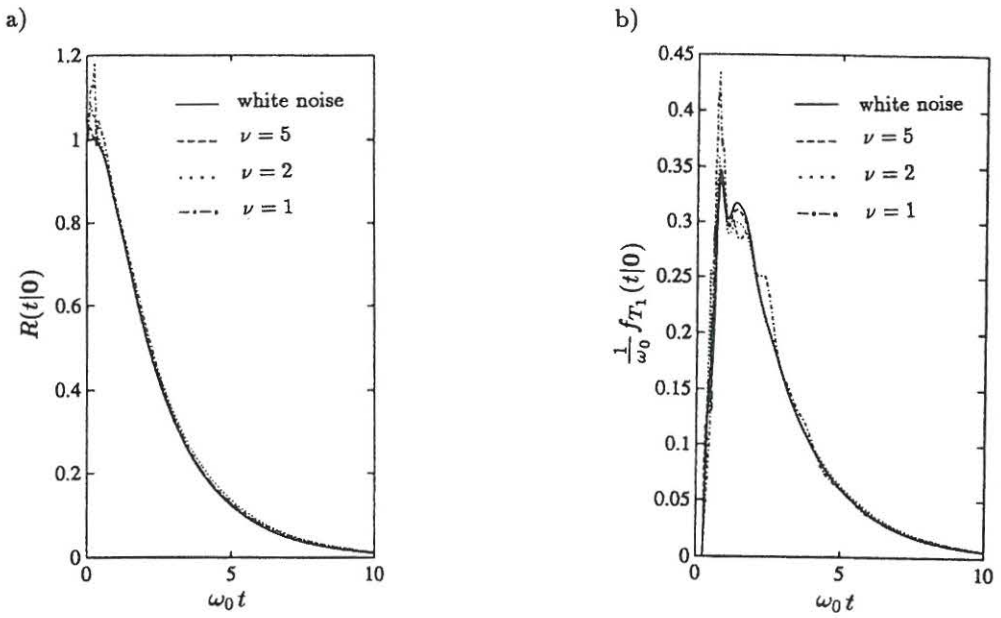

Fig. 3-127: Dependence on mean arrival rate, ν. a) Reliability function, $R(t|0)$. b) First-passage time pdf, $f_{T_1}(t|0)$. Deterministic start, constant double barrier problem. $b = -a = 2\sigma_X(\infty)$, $\zeta = 0.05$, $\epsilon = 0.5$, $\nu E[P^2] = 4\zeta\omega_0^3 m^2 = 0.20$. Köylüoğlu, Nielsen and Iwankiewicz (1994).

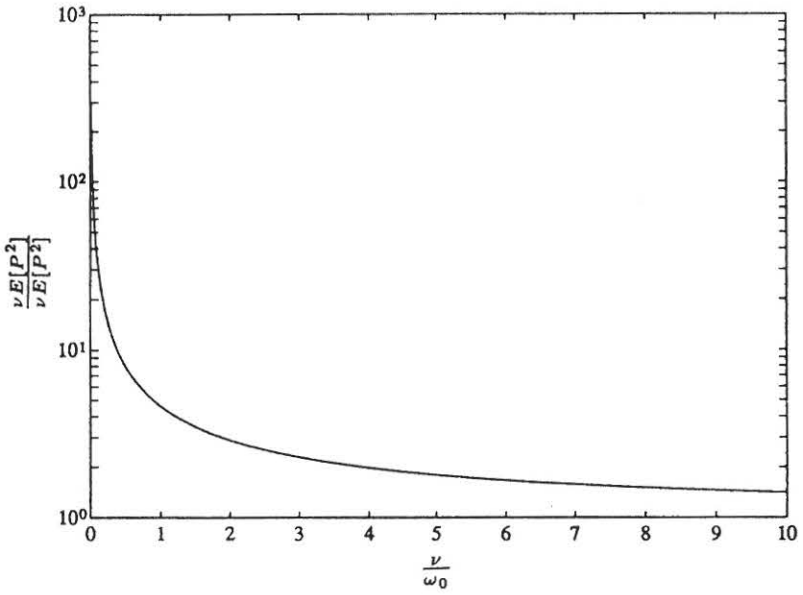

Fig. 3-128: Mesh refinement fraction, $\frac{\nu E[P^2]}{\nu E[P^2]}$ for $\nu \in [0.01, 10.0]$ at $\dot{x} = 0$. Köylüoğlu, Nielsen and Iwankiewicz (1994).

Fig. 3-127 shows the dependence on the mean arrival rate, ν. The following damping ratios have been considered, $\nu = 5.0\omega_0$, $\nu = 2.0\omega_0$ and $\omega_0 = 1.0\omega_0$. The corresponding stationary standard deviations of the displacement are $\sigma_X(\infty) = 0.760$, $\sigma_X(\infty) = 0.758$, $\sigma_X(\infty) = 0.757$. For comparison, the white noise case has also been shown in the figure. As seen, the results are quite insensible to variations in ν. Hence, the case $\nu = 1.0\omega_0$, corresponding to averagely 6.28 impulse arrivals per linear eigenperiod T_0 is effectively equivalent to Gaussian white noise for the reliability problems considered for the Duffing oscillator. Notice, in example 3-9 it was demonstrated that signifantly deviating displacement responses were obtained for a compound Poisson process with $\nu = 1.297\omega_0$ and for the comparable white noise process. However, this was observed for a hysteretic oscillator with small values of the elastic fraction of the restoring force, α. Attempts to reduce ν beyond $\nu = 1.0\omega_0$ with $\nu E[P^2]$ kept constant imply numerical instability with the present 30×30 mesh. Although, these instabilities can be cured by decreasing the mesh size, limitations in the memory allocations of the avaliable computer facilities prevented the application of finer meshes. The fraction $\frac{\nu E[P^2]}{\nu E[P^2]} = \frac{\Delta\dot{x}(\infty)}{\Delta\dot{x}(\nu)}$, which indicates the necessary mesh refinement to ensure stability for finite values of ν relative to the stable white noise mesh, is plotted in fig. 3-128. As shown in the figure, a reduction factor of 32 in the mesh width is necessary to obtain stability for mean arrival rates equal to $\nu = 0.1\omega_0$.

The main conclusion drawn from this example is, that the numerical integration of the backward Kolmogorov-Feller equation for the reliability function of a SDOF non-linear and non-hysteretic oscillator subject to a stationary Poisson driven train of impulses, based on a Petrov-Galerkin variational formulation may be performed for relatively high values of the mean arrival rate, ν. In the example the limit was $\nu \geq 1.0\omega_0$ using a coarse 30×30 mesh. If smaller mean arrival rates are applied numerical instability is observed. It is addressed how these instabilities can be cured using finer meshes. However, the necessary width of the calculation mesh is decreasing dramatically as ν decreases. As is the case for moment methods the Petrov-Galerkin variational method is working at best at relatively large mean arrival rates. A short parameter study for the Duffing oscillator was performed in the example, which demonstrated that the reliability function and the first-passage time probability density function is insensible to the value of the damping ratio, and highly sensible to the non-linearity parameter.

3.6 Summary and conclusions

Initially, in section 3.1 Wiener processes, compound Poisson and α-stable Lévy motions are introduced and briefly described. All these stochastic processes have independent increments. It is discussed how some other actual random excitations can be modelled using a filtration of processes with independent increments through a sharpening filter. Thus the attention has been focused on the processes for which the response of the dynamic system may be regarded as a Markov process. The general state vector formulation for geometric non-linear elastic as well as hysteretic systems is given. Especially, in example 3-1 equivalent hysteretic SDOF and MDOF shear models are formulated for instrumentated reinforced concrete structures exposed to earthquakes. The models are aimed at the prediction of the stochastic response and reliability and the global and localized damage of the structure, based on a sequential updating of a few number of system parameters. The accuracy of the predictions of the models as compared to available model tests is primarily due to a modelling of the elastic fraction of the restoring force as a degrading function of the damage, corresponding to gradual transition from elastic to plastic response, as larger and larger parts of the structure become plastic.

In section 3.2 the forward and backward integro-differential Chapman-Kolmogorov equations for transition probability density function of the Markov vector have been indicated as a reference for later sections for system driven Wiener processes, compound Poisson processes and α-stable Lévy motions. Further, the first-passage time problem has been formulated based on the solution of the forward or backward integro-differential Chapman-Kolmogorov equation with absorbing boundary conditions.

Section 3.3 deals with stochastic response analysis of Markov systems based on moment equation methods. Initially, the generalized Itô differential rule for diffusion and jump excited systems is derived, from which the generic equation for moments is derived. Especially, explicit expressions for joint central moments have been indicated.

In Section 3.3.1 the closure problem for the hierarchy of moment equations is treated, i.e. the specification of an approximate joint pdf for the state variables from which unknown expectations may be calculated. The free parameters of the closure assumption is calibrated, so that the said joint pdf displays the joint moments provided by the retained moment equations. The moment neglect closure, the cumulant neglect closure, the quasi-moment neglect closure and the Hermite moment neglect closure schemes are adressed. It is emphasized that most of these methods are likely to work well for systems, which are almost Gaussian, i.e. of the monomodal and smooth type. In fact they may all be considered as expansions from Gaussian probability densities with the remainder in the expansion beyond the first two terms measuring the deviation from Gaussianity. Systems with joint pdf of the multimode or mixed continuous-discrete type are often met in stochastic structural dynamics. For these cases the rate of convergence of series expansions from Gaussianity may be very slow or convergence may be totally lacking. Instead, modified closure schemes need to be formulated, guided by physical insight into the system dynamics. A modified cumulant neglect closure scheme is presented for the socalled double-well potential oscillator with a bimodal joint pdf. Even at closure at the covariance level rather accurate results are obtained. In contrast the rate of convergence

of the ordinary cumulant neglect closure scheme is extremely slow as demonstrated in example 3-7. Next, a similar modification is suggested for the Hermite moment neglect closure scheme applied to the Bouc-Wen oscillator exposed to high intensity Gaussian white noise, in which case the marginal pdf of the hysteretic component displays a marked double-peaked behaviour. Again substantial improvements are registered as compared to the ordinary Hermite moment neglect closure scheme. Finally, a modified closure scheme is proposed for Poisson driven systems with low mean arrival rate, where a transient discrete probability component is present in the joint pdf, representing the deterministic drift from the initial values on condition that no impulses have yet arrived. Explicit expressions for the modified cumulant neglect closure scheme have been derived for systems with polynomial non-linear drift vectors at closure at the order $N = 4$.

In section 3.3.2 moment equations for Wiener process driven dynamic systems are derived. Especially, formulas for systems with cubic polynomial drift vectors (such as the Duffing and the van der Pol oscillators) are addressed. Besides, the conditions are determined for replacing a system with non-analytical (e.g. hysteretic) drift vector by an equivalent system with polynomial non-linear drift vector. A theorem is proved, stating that exact joint moments up to the order $N + 1$ are provided by the equivalent system, if an equivalent polynomial expansion of the order N is applied, and the expansion coefficients of the equivalent expansion are determined from a least mean square criterion with the unknown expectations evaluated with the exact joint pdf. In example 3-3 the method of equivalent polynomial expansion is applied to the stochastic analysis of a bilinear hysteretic oscillator exposed to stationary Gaussian white noise. The idea is to replace merely the constitutive equation for the hysteretic component by an equivalent polynomial expansion, whereas the linear equations are left unchanged. In contrast, the global mean least square criterion of the mentioned theorem assumes that all components are replaced by equivalent polynomial expansions of the order N. In the numerical example it is demonstrated that such an approach introduces quite ignorable additional errors in the analysis. The benefit of the method is that only a marginal joint pdf of the velocity and the hysteretic component need to be calibrated at the calculation of the coefficients of the equivalent cubic expansion. The said tentative joint pdf is selected as a truncated 2-dimensional Gram-Charlier series with a Minai-Suzuki modification for the discrete probability of attaining the plastic branches. Two equivalent linearization strategies are investigated. Both of these predict a stationary displacement variance for the case of an ideal elastic-plastic oscillator ($\alpha = 0$), in contrast to the Brownian motion type of variance growth displayed by the Monte-Carlo simulation and the cubic polynomial expansion method. This suggests that the variance growth phenomenon is caused by joint moments of the 4th and higher order. The main discrepancies between the cubic polynomial expansion method and the simulation results can be attributed to the application of an ordinary cumulant neglect closure scheme with no modification for discrete probability components in the global moment equations. This problem has been further investigated in example 3-4, which includes a reliability analysis of the bilinear hysteretic oscillator. The reliability analysis is based on the observation of a damage indicator, which is selected as the accumulated energy dissipated by the system during plastic deformations. The failure event of the system occurs, when the non-decreasing damage indicator makes a first-passage of some critical

level, d_{cr}. The damage indicator is included in the state vector as an extra state variable, and a differential equation has been formulated specifying its development with time. The load process of the system is obtained from rational filtration of time-modulated Gaussian white noise through a time-invariant rational filter of the order $(r, s) = (1, 2)$. The state variables of the filter is also included in the state vector of the integrated dynamic system along with the displacement, the velocity, the hysteretic component and the damage indicator. Only the differential equations for the hysteretic component and the damage indicator are replaced by equivalent polynomial expansions. The consistant expansions turn out to be of the 3rd order for the hysteretic component and of the 2nd order for the damage indicator. At the evaluation of the equivalent expansion coefficients a least square criterion is applied, and the joint pdf for the evaluation of the unknown expectations is selected as a truncated 2-dimensional Gram-Charlier series with a Minai-Suzuki modification. Besides, a modified cumulant neglect closure scheme is devised for the global moment equations, which takes the discrete probability components in the joint pdf into account. The closure scheme only requires the same joint pdf of the velocity and hysteretic component as applied in the equivalent polynomial expansions of the hysteretic and damage indicator differential equations. In the example results obtained with the ordinary and the modified cumulant neglect closure scheme have been compared with those obtained by Monte Carlo simulation. The conclusion drawn from this comparison is that significantly better results are obtained with the modified cumulant neglect closure scheme than with the ordinary scheme. Hence, the same tentative joint pdf should be applied at the local and at the global level. Example 3-5 deals with the stochastic analysis of hysteretic multi-storey plane frames. Initially a differential formulation of the constitutive equations for elasto-plastic beam elements has been indicated, connecting the rate of the generalized stresses and strains of the element. This is next specialized to yield hinge models, where the generalized strains and stresses are made up of the end-section rotations and end-section bending moments. The frame is subjected to a horizontal earthquake excitation obtained upon filtering modulated Gaussian white noise through a Kanai-Tajimi filter, which is merely a rational filtration of the order $(r, s) = (1, 2)$ with physically interpretable filter constants. The state vector components for the integrated dynamic system consist of nodal displacements and nodal velocities, the generalized stresses from all plastic elements, and the filter state variables. The resulting differential equations on state vector form represent a MDOF generalization of the corresponding differential equations for the elasto-plastic oscillator in example 3-4 with the generalized stresses forming the multi-variate hysteretic components. Only the constitutive equations for the generalized stresses (the hysteretic components) are replaced by equivalent polynomial expansions in the local generalized stresses and generalized strain rates. Hence, the equivalent polynomial expansion is performed at element level, which facilitates the formulation of a global equivalent polynomial system significantly. The global joint moment equations are next closed by an ordinary cumulant neglect closure scheme. The theory has been applied to a simply supported two-storey single-bay plane frame with the Kanai-Tajimi filter exposed to a stationary Gaussian white noise. Severe plastic deformations are most likely to occur in the lower storey columns. Equivalent cubic expansions are only applied to the constitutive equations for these elements, whereas equivalent linear

expansions are introduced for the remaining elements. The joint expectations of the rate of the end-section rotations and bending moments, entering the least mean square equations for the determination of the coefficients of the equivalent polynomial expansions, are evaluated by means of a Gram-Charlier expansion to the 4th order of the joint pdf with a Minai-Suzuki modification for plastic deformations. From the results obtained it is concluded that equivalent linearization for all elements with Gaussian evaluation of the expansion coefficients provides results for the displacement response of the storeys that neither quantitatively nor quantitatively are in agreement with those obtained by Monte Carlo simulation. Only slightly better results are obtained by an equivalent linearization scheme, where a Gram-Charlier expansion to the 2nd order with a Minai-Suzuki modification for plastic deformations has been applied for the evaluation of the linear expansion coefficients. In both cases a stationary variance is predicted for the storey displacements in contrast to the simulation results, which shows a similar Brownian motion type of variance drift, as addressed in example 3-3. The inevitable conclusion seems to be that equivalent linearization techniques should not be used for elasto-plastic structures exposed to severe stationary excitations. Instead, the analysis should involve at least the 4th order moments. In contrast the application of a cubic polynomial expansion for the lower storey columns provided results, which are in much better agreement with the simulation results. No significant difference is noticed in the results, if the equivalent linearization for the remaining elements is performed with Gaussian closure or with a joint normal pdf or with Gram-Charlier expansion to the 2nd order with a Minai-Suzuki modification. In example 3-6 the theory has been applied to the reliability analysis of saturated sand deposits under horizontal shear earthquake excitations (SH waves), assuming liquefaction to be the principal failure mode of the soil. Liquefaction is assumed to take place, when the accumulated dissipated energy per unit of volume of the soil reaches a critical level. In the example the applicability of this damage indicator is verified by triaxial testing of various sand samples exposed to cyclic testing with variable amplitudes. The triaxial tests also show that the rate of the mobilization factor, which for the present plane strain case can be defined as the shear stress in proportion to the shear strength, can be related to rates of the shear strain by a Bouc-Wen hysteretic model. The shear strength is a decreasing function with time as the pore pressure builds up, and turns out to deteriorate proportionally to the deterioration of the shear modulus. Both have been related to the damage indicator by a simpel linear relation. A statically admissible stress field is prescribed, from which the subsoil continuum is discretized into a SDOF system. The acceleration process at the top of the bedrock is obtained from filtration of modulated Gaussian white noise through a time-invariant rational filter of the order $(r, s) = (1, 2)$. The differential equation for the evolution of the damage indicator becomes cubicly polynomial, whereas the differential equation for the velocity becomes quadratic. The constitutive equation for the mobilization factor is replaced by an equivalent linear expansion, with the expansion coefficients evaluated by a Gram-Charlier expansion truncated at the order $N = 2$, whereas the linear, the quadratic and the cubic equation are left unchanged. The resulting global hierarchy of moment equations is truncated at the order $N = 4$ by means of an ordinary cumulant neglect closure scheme. The obtained results for the variance response of the displacement and the mobilization factor are rather poor in comparison

to simulation results, as can be expected from the application of equivalent linearization to the hysteretic equation. However, excellent results are obtained for the mean value and standard deviation of the damage indicator, whereas the skewness parameter of this variable is less accurately estimated. The reason for the improved results for the lower order statistical moments of the damage indicator in comparison to those for the other state variables is merely the exact cubic polynomial form of the differential equation of this variable. Improved results for the skewness parameter requires application of higher order equivalent polynomial expansion of constitutive differential equation for the hysteretic component and global closure at higher than the order $N = 4$.

Section 3.3.3 deals with the stochastic analysis of compound Poisson process driven systems by means of moment equations. Initially, the differential equations for the joint central moments of dynamic systems exposed to a multi-dimensional or scalar compound Poisson process are indicated. Especially, the moment equations for systems with cubic polynomial drift vectors are derived. In example 3-8 the theory is applied to a Duffing oscillator. The idea of the example is to demonstrate the applicability of the modified cumulant neglect closure scheme, devised for Poisson counting processes with low mean arrival rates. Ordinary cumulant neglect closure schemes at the orders $N = 3$, $N = 4$ and $N = 5$, and modified cumulant neglect closure at the order $N = 4$ are considered. The excitation process has Rayleigh distributed impulse strengths, and is obtained as output process from a filtration of a homogeneous compound Poisson process through a rational filter of the order $(r, s) = (0, 2)$. For the relatively high mean arrival rate of impulses of $\nu = 0.1\omega_0$, the considered ordinary cumulant neglect closure schemes work well and all give acceptable results, although the best result is obtained for closure at the order $N = 5$ as expected. In comparison to ordinary cumulant neglect closure at the order $N = 4$ the modified cumulant neglect closure scheme gives substantially improved results for the mean value functions and for the variance functions in the initial part of the excitation, where the modification of the joint pdf is most important. Application of a pulse train with the lower mean arrival rate of $\nu = 0.05\omega_0$ renders the ordinary cumulant neglect closure schemes numerically unstable, whereas the modified scheme still produces accurate estimates for the mean value functions and variance functions. From the example it is then concluded that more accurate and numerically stable results are obtained by the modified cumulant neglect closure scheme. However, even the modified cumulant neglect closure scheme eventually renders into numerical instability as ν is reduced. In the present example this occurs for $\nu \simeq 0.01\omega_0$, which is approximately one order of magnitude less than the corresponding limit for the comparable ordinary cumulant neglect closure scheme. In example 3-9 a reliability analysis of a Bouc-Wen oscillator exposed to both an unfiltered and a filtered homogeneous compound Poisson process has been performed by means of the equivalent polynomial expansion technique. The reliability analysis is based on a damage indicator, which is selected as the accumulated energy dissipated by the hysteretic component. Then the said damage indicator is quadratically polynomial. Only the constitutive equation for the hysteretic component is replaced by a cubic polynomial expansion, whereas the remaining linear or quadratic non-linear differential equations are kept unchanged. As in previous applications the expansion coefficients of the equivalent polynomial expansion are determined by a least mean square criterion. Evaluation of the unknown expectations entering the mean least

square criterion is performed by a quasi-moment neglect closure scheme, truncated at the order $N = 4$. Besides, equivalent linear expansions of the hysteretic differential equation are considered with the expansion coefficients evaluated by means of quasi moment expansions truncated at the order $N = 2$ and $N = 4$, respectively. The former linearization scheme is equivalent to a white noise excitation with Gaussian closure. The hierarchy of global moment equations is closed at the order $N = 4$ by means of an ordinary cumulant neglect closure scheme for both equivalent linear expansions and for the equivalent cubic polynomial expansion. First, the case of excitation with an unfiltered compound Poisson process is considered. Two alternative distributions for the impulse strength are assumed. The first of these concerns an ordinary Rayleigh distribution, while the other is a zero-mean centered Rayleigh distribution. The relatively high mean arrival rate of impulses of $\nu = 1.297\omega_0$ is applied. For the case of an ordinary Rayleigh distribution of the impulse strength the obtained results for the mean value functions of the displacement, the hysteretic component and the damage indicator are all in good agreement with the simulation results, both for the two equivalent linearization schemes and for the cubic polynomial expansion method, although the Gaussian closure algorithm overestimates the mean value function of the hysteretic component somewhat at larger excitation intervals. The variance response of the displacement and the hysteretic component is significantly underestimated by the equivalent linearization methods, and these methods completely fail to predict the variance response of the damage indicator. In contrast, the variances predicted by the equivalent cubic polynomial expansion method are acceptable for the displacement and hysteretic component and very good for the damage indicator. For the case of a zero-mean centered Rayleigh distribution of impulse strengths it is demonstrated that significant non-zero mean values for the displacement and the hysteretic component are present even at the relatively high mean arrival rate of $\nu = 1.297\omega_0$, which is a consequence of non-zero higher order odd moments of the impulse strength in combinations with small values of the elastic fraction of the total restoring force, α. In contrast, the equivalent linearization scheme with Gaussian closure predicts zero mean responses. Hence the replacement of a compound Poisson process with a comparable Gaussian white noise process should be performed with some caution for such systems even at relatively high mean arrival rates of the impulses. The equivalent linearization scheme based on a 4th order quasi-moment neglect series expansion captures the qualitative behaviour of the mean values, but the quantitative predictions are not good. In contrast, the predictions of the equivalent polynomial expansion are in excellent agreement with the Monte Carlo simulation results. Both equivalent linearization techniques underestimate the variances of the displacement and the hysteretic component. Only the equivalent cubic polynomial expansion gives acceptable variance estimates, and is the only one of the methods that provide meaningful and even accurate results for the damage indicator. Next, the case of excitation with a compound Poisson process filtered through a time-invariant and rational filter of the order $(r, s) = (0, 2)$ is considered. Only the case of an ordinary Rayleigh distribution of the impulse strength is considered, and only the equivalent linearization scheme with expansion coefficients evaluated from the quasi-moment expansion at the order $N = 4$ is investigated. The mean arrival rate is selected as relatively high as $\nu = 1.0\omega_0$. As for the non-zero mean case for unfiltered impulses the considered methods give acceptable

results for the mean values. Again, the equivalent linearization method underestimates the variance responses of the displacement and the hysteretic component, and completely fails to predict the variance response of the hysteretic component, whereas the equivalent cubic polynomial expansion technique provides acceptable variance estimates for all considered state variables. The conclusion to be drawn from the results of this example is that equivalent linearization methods fail to predict the variance response of all state variables. Especially for the damage indicator the results are completely misleading. Hence equivalent linearization methods should not be used in a reliability analysis of hysteretic oscillators exposed to compound Poisson processes if response statistics beyond the mean value function of the damage indicator is requested. Only equivalent polynomial expansion techniques of at least the 3rd order in combination with an ordinary cumulant neglect closure scheme provide accurate estimates of the mean value and variances of the damage indicator, and in fact seems to be the best available semi-analytical scheme for the analysis of such response statistics. The computer time in comparison to Monte Carlo simulation for the methods in the example is 0.88% for the equivalent linearization methods and 6% for the equivalent cubic polynomial expansion technique.

Section 3.3.4 deals with dynamic systems driven by compound Erlang renewal processes. Initially, it is demonstrated that such systems can be reduced to an equivalent system driven by a compound Poisson process at the expense of the introduction of some auxiliary state variables. Next, the stochastic differential equations specifying the development of these extra state variables are formulated. The integrated dynamic system with the state vector made up of the structural state variables in combination with the auxiliary state variables then form a Markov system, and the moment equations for systems driven by a compound Poisson process can be applied in a slightly changed form. Also the modified closure schemes for sparse pulse arrivals need to be changed slightly. In example 3-10 the general conditions for reducing a system driven by a compound regular counting process to an equivalent system driven by a compound Poisson process are settled, and it is shown that the compound Erlang process is obtained as a special case of the general formulation. In example 3-11 the stochastic response of a Duffing oscillator exposed to compound Erlang processes with the parameters $k = 2$, $k = 3$ and $k = 4$ is analysed. The impulse strength is assumed to be ordinary Rayleigh distributed. To make comparison between the indicated cases meaningful the mean arrival rate of Poisson events is selected as $\frac{\nu}{k} = 10\omega_0$. Then the average number of renewal impulses per unit of time is the same for the three cases of k, and any differences in the calculated response moments can be attributed to the different interarrival time distributions. The indicated mean arrival rate of impulses is very large, so the hierarchy of moment equations can be closed at the order $N = 4$ by means of an ordinary cumulant neglect closure scheme. The obtained mean value functions and variance functions for the displacement are all in excellent agreement with the simulation results. The mean value functions are practically the same for the three cases of k. However, the variances have a marked tendency to decrease with increasing value of k. From these observations is concluded that the moment equation method can be used for the stochastic analysis of a class of non-linear systems exposed to a compound Erlang renewal process after reduction to an equivalent compound Poisson process driven system. The mean value

function of the displacement response is believed to be rather insensible to the choice of distribution for the interarrival times, and depends primarily on the mean arrival rate of impulses. In contrast the variance function shows significant dependency on this distribution. The application of compound Poisson processes as a load model for cases where the interarrival times are far from exponentially distributed should then be done with caution.

Section 3.4 deals with the numerical integration of the forward integro-differential Chapman-Kolmogorov equation by means of path integration. Initially the applied discretization scheme is described, which reduces the time and space continuous Markov vector process to an irreducible, positive recurrent and aperiodic Markov chain. In case of stationary processes observed at equidistant time intervals it is next demonstrated, how the stationary distribution may be obtained from a linear eigenvalue problem with the known eigenvalue $\lambda = 1$.

In section 3.4.1 the application of path integration to Wiener process driven systems is dealt with. Since the state vector process does not perform any jumps in this case, the drift vector may the approximated by a piecewise linear vector function and the diffusion matrix by a piecewise constant matrix. For sufficiently small transition time intervals the system then behaves as local Gaussian, and the differential equations for the development of the conditional mean value functions and the conditional covariances, as well as the transitional joint pdf can be specified at once. Four alternative linearization strategies are indicated in ascending order of complexity. Especially, the running mean linearization scheme and the equivalent linearization scheme are promising, since much larger transition time intervals may be used, then allowed for the other two mentioned linearization schemes. The use of the latter schemes is due to the simple solutions obtained for the conditional mean value function and the conditional covariance matrix function. In example 3-12 the linearization schemes have been explicitly stated for a Duffing oscillator subjected to Gaussian white noise. Next, the running mean linearization scheme has been chosen with a uniform coarse 20×20 mesh extending four linear stationary standard deviations in the positive and negative displacement and velocity directions, and with a transition interval of $\Delta t = \frac{T_0}{4}$. Excellent agreement with Monte Carlo simulation results is obtained both at the central part of the marginal distributions and at their tails. The first-passage time problem for a deterministic start problem with a single constant barrier is also solved. The first-passage time probability distribution function obtained by path integration overestimates the probability of failure somehow during the first period as compared to Monte Carlo simulation results, which is an effect of using the indicated coarse mesh in combination with the relatively large transition interval. From the results of the example it is concluded that the stochastic response can be determined by path integration with a very coarse mesh without affecting the accuracy significantly, whereas a somewhat finer mesh must be used in reliability problems.

In section 3.4.2 path integration methods are devised for systems driven by compound Poisson processes, Lévy α-stable motions and compound Erlang processes. First the case of a dynamic system driven by a scalar compound Poisson process is considered. An asymptotic expansion is derived for the transitional joint pdf, valid under the re-

striction $\nu\Delta t \ll 1$, and involving only the transitional joint pdfs on condition of zero and one impulse arrivals during the transition interval. The transitional joint pdf on condition of zero impulses specifies the eigenvibrations of the system from the initial conditions, which is obtained by numerical integration. The various path integration schemes are sorted out in the same way as the transitional joint pdf on condition of one impulse arrival during the transitional time interval is specified. Due to the restriction on $\nu\Delta t$, path integration methods are likely to work best for small values of ν in contrast to moment equation methods. For fixed ν the restriction indicates an upper bound for the choice of Δt. On the other hand it is shown that a lower bound for this quantity also exists, so the optimal results are obtained, when Δt is confined to some interval. Two methods are presented for the convection and diffusion of the probability mass on condition of one impulse arrival during the transition time interval. Method 1 is based on the fact that the arrival time of the impulse is uniformly distributed in the transitional interval for homogeneous Poisson processes. The transition interval is then divided into a finite number of sub-intervals, and the convection and diffusion of the probability mass are performed for each sub-interval in a sequence on condition that the impulse arrives in the said interval. Method 2 is based on a Taylor expansion of the state vector at the end of the transition interval in terms of the strength of the impulse, P. The Taylor expansion coefficients only depend on the start- and terminal time and the position of the system at the start of the transition, but not on the time where the impulse actually occurs. Next, coupled ordinary non-linear differential equations for the determination of these expansion coefficients are formulated and solved numerically. It is shown that the Taylor expansion for linear systems becomes linear in P. Since a local linear replacement of the drift vector is always possible at sufficiently small transition time intervals, it follows that the Taylor expansion of the state vector in P becomes asymptotically linear as the transition time interval goes to zero. This observation is the background for Method 2, which assumes such a linear Taylor expansion to be exactly valid. It should be noticed that the linearization approximation concerns the drift vector as a function of the state vector and puts no restriction on the magnitude of the impulse strength. In example 3-13 the stochastic response and reliability analysis of a Duffing oscillator is performed both by Method 1 and Method 2. The Duffing oscillator is lightly damped with a medium level non-linearity parameter. Basically the path integration analysis is performed with a coarse and uniform 20×20 mesh extending four linear stationary standard deviations in the positive and negative displacement and velocity directions. The strength of the impulses is assumed to be zero-mean normally distributed. For Method 1 three values of ν are considered corresponding to sparse, medium, and dense impulse arrivals. For the case of sparse impulse arrivals very peaked distributions occur at the origin. For this case a non-uniform 25×25 mesh has been applied with a four times finer spacing close to the origin. The transition time interval Δt is passed through by three sub-divisions. The stationary marginal pdf of the displacement and velocity has been obtained by iterating the transition equation of the Markov chain into stationarity. The transition intervals for the three cases of ν are $\Delta t = T_0$, $\Delta t = T_0$ and $\Delta t = \frac{T_0}{2}$, respectively. For the cases of sparse and medium level impulse arrivals excellent results are obtained in comparison with results obtained by Monte Carlo simulation even with the present relatively coarse

meshes, both at the central part of the distributions and at the tails. However, for the case of dense pulse arrivals path integration provides rather poor results because the upper bound restriction on Δt is no longer fulfilled. Next, the first-passage time problem for a deterministic start problem with symmetrically constant double barriers is solved for the cases of sparse and medium level impulse arrivals. As is the case for the corresponding white noise excitation the path integration method underestimates the probability of failure during the first periods of exitation as a consequence of the coarseness of the mesh and the large transition time interval. For the case of medium level impulse arrivals a comparison has been made with the probability of failure obtained by approximating the excitation process by an equivalent Gaussian white noise process. The results obtained by Method 1 are in much better agreement with Monte Carlo simulation results than those of the white noise excitation are. Hence a replacement of the compound Poisson process by an equivalent Gaussian white noise is misleading in reliability analyses with mean arrival rates of the considered magnitude. Next a single barrier problem with stationary start in the safe domain is considered for the cases of sparse and medium level impulse arrival rates. In neither case the staircase character of the first-passage time probability density function is captured by the path integration. However, the correct limiting exponential decay, corresponding to a discrete eigenvalue spectrum of the backward or forward Kolmogorov-Feller operator with absorbing exit or entrance boundaries, respectively, is captured by the path integration method for both deterministic and stationary start problems. Next, Method 2 has been used for the determination of the stationary marginal pdfs of the displacement and velocity in case of relatively sparse mean arrival rate of impulses. The obtained results for the marginal distributions are of the same quality as the corresponding results of Method 1. However, the algorithm of Method 2 is significantly simpler and faster to use. The computer time for performing the path integration analysis with Method 2 in the considered example is 0.22% in proportion to the computer time for the simulation, which concludes that the method offers extreme computational advantages over the Monte Carlo simulation method. Next, Method 2 is modified for path integration of systems driven by Lévy α-stable motions and compound Erlang processes. The modification for systems driven by a Lévy α-stable motion merely consists of replacing the actual process by an equivalent compound Poisson process with α-stable distributed impulse strengths. No example has been indicated for this theory. For systems driven by Erlang renewal processes a more involved modification of the method needs to be devised. Instead of a single mesh for the discretized space of the structural state variables it becomes nescessary to define k such meshes, one for each of the k Poisson events per Erlang event. For each of the first $k-1$ Poisson events the probability mass at a certain node of the mesh related to this event is convected on the same mesh according to the eigenvibrations from the initial values. The fraction of probability mass corresponding to the probability of no impulse arrivals in the transition interval is lumped at the terminal point of the system, whereas the remaining probability is tranferred to the next mesh in line. If this next mesh is the kth and final mesh the transferred probability mass is diffused in this plane. Else it is lumped at the same terminal point on the new mesh as in the previous one. If the system starts on the kth mesh, the probability mass on condition of one impulse arrival is transferred to the first mesh to start a new sequence. It follows that

the number of states of the resulting Markov chain only grows linearly with k rather than exponentially. Hence the introduction of the auxiliary state variables, necessary at the reduction of the Erlang process driven system into an equivalent Poisson driven system, has relatively small influence on the computational effort of the devised path integration scheme. In example 3-14 the method has been applied to a Duffing oscillator with relatively high non-linearity parameter subject to a compound Erlang process with parameter $k = 2$. The strength of the renewal impulses is assumed to be zero-mean normally distributed. Three cases of mean arrival rates of Poisson events are considered, corresponding to sparse, medium level and dense renewal impulse arrivals. The path integration is performed with two uniform 44×44 meshes extending five linear stationary standard deviations in the positive and negative displacement and velocity directions. For the case of sparse impulse arrivals excellent results are obtained for the marginal pdfs of the displacement and the velocity in comparison to results obtained by Monte Carlo simulation. In this case the lower and upper bounds on the allowable interval for the transition time interval can easily be met. The importance of these requirements is demonstrated in a study of the quality of the obtained results as a function of the length of the transition time interval. Results obtained with the very large transition interval of $5.0T_0$ in the case of sparse impulse arrivals are useless because the upper bound criterion has been violated in this case. The corresponding results for the medium level pulse arrival rate are acceptable but not so good as those obtained with sparse pulses. The transition time interval is selected as $\Delta t = 0.2T_0$ to meet the upper-bound criterion. However, this choice is also close to the acceptable lower-bound value, as demonstrated in the performed study of the dependence on the transition interval with the used value of ν, where transition time intervals smaller or larger than the selected value provide less accurate results. The path integration results for the case of dense impulse arrivals are even worse. The path integration has been performed with the transition time interval of $\Delta t = 0.05T_0$ to meet the upper-bound criterion, but the lower-bound criterion is certainly violated. Hence the observations of the example confirm the previous results for systems exposed to compound Poisson processes that path integration methods for pulse driven systems provide accurate results for the case of sparse impulse arrivals with properly selected transition time interval, whereas useless results are obtained if the transition time interval is either too small or too large.

Section 3.5 deals with the numerical solution of the reliability problem for the non-linear, non-hysteretic time-invariant SDOF oscillator subjected to a homogeneous stationary compound Poisson process by means of a Petrov-Galerkin approach. Based on the general formulation in section 3.2.2, the boundary and initial value problem for the determination of the reliability function for a double barrier problem with constant barriers is stated, and the weak counterpart of the boundary and initial problem is derived. In the formulation a Kramer-Moyal expansion of the backward Kolmogorov-Feller operator is assumed, requiring that moments of the impulse strength of arbitrary order exists. In the displacement direction triangular shape functions are applied, and the weight functions are obtained from these by adding a quadratic upwind differencing. In the velocity direction the shape functions are chosen as normal probability density functions with varying means to meet the severe requirements on differentiability. The weight functions are obtained by adding upwind differencings chosen as the scaled first

derivative of the shape functions. Expressions for the scaling factor of the upwind differencing and the local Peclet number are suggested. The discretized system of coupled first order differential equations for the reliability function is solved by means of a Crank-Nicolson scheme. In example 3-15 the method has been applied to a symmetric double barrier first-passage time problem with deterministic start in the origin for a Duffing oscillator driven by a compound Poisson process. The damping ratio and the non-linearity parameter of the oscillator is varied in the example to analyse their influence on the reliability function. The impulse strength is assumed to be zero-mean normally distributed. The safe domain is divided into a uniform 30×30 mesh extending five stationary standard deviations in the positive and negative velocity directions. The stationary standard deviations are obtained from an initial Monte-Carlo simulation, but may be obtained from the method as well. It is demonstrated that the numerical scheme converges to the results obtained by Gaussian white noise as $\nu \to \infty$. The parameter studies show that the reliability function is significantly dependent on the non-linearity parameter, whereas is it rather insensible to the damping ratio. A study of the dependence of the reliability function on the mean arrival rate shows that the method with a 30×30 mesh renders into numerical instability for $\nu < 1.0\omega_0$, and that the obtained results are rather insensible to values of the mean arrival rate above this limit. It is demonstrated that attempts to achieve numerical stability for mean arrival rates below the indicated stability limit demand drastical reduction of the mesh width. Hence, the Petrov-Galerkin variational approach shares the drawback of the moment equation method for compound Poisson process driven systems that these methods are most effective for excitation processes with large mean arrival rate of impulses.

4. REFERENCES

Ahmadi, G. (1980). *Mean Square Response of a Duffing Oscillator to a Modulated White Noise Excitation by the Generalized Method of Equivalent Linearization.* Journal of Sound and Vibration, **71**, pp. 9-15.

Ahmadi, G., and Orabi, I.I. (1987). *Equivalence of Single-Term Wiener-Hermite and Equivalent Linearization Techniques.* Journal of Sound and Vibration, **118**, pp. 307-311.

Allen, M.P. (1982). *Algoritms for Brownian Dynamics.* Molecular Physics, **35**, pp. 599-601.

Andronov, A.A., Pontriagin, L.S., and Vitt, A.A. (1933). *On the Statistical Considerations of Dynamic Systems.* Zhurnal Exper. Teoret. Fiz., Vol. 3, No. 3, pp. 165-180. (In Russian). Reprinted in *Selected Works*, Andronov, A.A., Academy of Sciences, USSR, 1956.

Arnold, L. (1974). *Stochastic Differential Equations: Theory and Applications.* New York: John Wiley and Sons.

Atalik, T.S., and Utku, S. (1976). *Stochastic Linearization of Multi-Degree-of-Freedom Non Linear Systems.* Earthquake Engineering and Structural Dynamics, **4**, pp. 411-420.

Baber, T.T. (1986). *Non-Zero Mean Random Vibration of Hysteretic Frames.* Computers and Structures, **23**, pp. 265-277.

Baber, T.T., and Wen, Y.-K. (1982). *Stochastic Response of Multistorey Yielding Frames.* Earthquake Engineering and Structural Dynamics, **10**, pp. 403-416.

Bharucka-Reid, A.T. (1960). *Elements of the Theory of Markov Processes and Their Applications.* New York: McGraw-Hill, Inc.

Belyaev, Y.K. (1968). *On the Number of Exits Across the Boundary of a Region by a Vector Stochastic Process.* Theory of Probability and its Application, **13**, pp. 320-324.

Bergman, L.A., and Spencer, B.F. Jr. (1983). *Solution of the first passage problem for simple linear and nonlinear oscillators by the finite element method.* T. & A.M. Report No. 461, Department of Theoretical and Applied Mechanics, University of Illinois at Urbana-Champaign.

Bergman, L.A., and Heinrich, J.C. (1982). *On the reliability of the linear oscillator and systems of coupled oscillators.* International Journal for Numerical Methods in Engineering, **18**, pp. 1271-1295.

Bergman, L.A., Wojtkiewicz, S.F., Johnson, E.A., and Spencer, B.F.Jr. (1994). *Some Reflections on the Efficacy of Moment Closure Methods.* Proceedings of the 2nd International Conference on Computational Stochastic Mechanics, Athens, Greece, June 12-15, 1994, pp. 87-95.

Bernard, M.C., and Shipley, J.W. (1972). *The first passage problem for stationary random structural vibration.* Journal of Sound and Vibration, **24**, pp. 121-132.

Bolotin, V.V. (1967). *Statistical aspects in the theory of structural stability.* Proceedings of an International Conference in the Theory of Structural Stability, pp. 67-81. Northwestern University, Illinois. Ed. G. Hermann: Pergamon Press.

Booton, R.C. (1954). *The Analysis of Nonlinear Control Systems with Random Inputs.* IRE Transactions in Circuit Theory, **CT-1**, pp. 9-18.

Bouc, R. (1967). *Forced Vibration of a System with Hysteresis.* Proceedings of the 4th International Conference on Nonlinear Oscillations, Prague, pp. 315.

Casciati, F., and Farivelli, L. (1984). *Reliability Assessment for Non-Linear Random Frames.* Proceedings of the Weibull IUTAM Symposium on Probabilistic Methods in the Mechanics of Solids and Structures. Stockholm, Sweeden, June 19-21, 1984, pp. 469-478.

Caughey, T.K. (1963). *Equivalent Linearization Techniques.* Journal of the Acoustical Society of America, **35**, pp. 1706-1711.

Cecen, H. (1979). *Response of Ten Storey, Reinforced Concrete Model Frames to Simulated Earthquakes.* Ph.D. Thesis, University of Illinois at Urbana-Champaign, Illinois, U.S.A.

Clough, R.W., and Johnston, S.B. (1966). *Effects of Stiffness Degradation on Earthquake Ductility Requirements.* Proceedings of the 2nd Japan Earthquake Engineering Symposium, pp. 227-232.

Clough, R.W., and Penzien, J. (1974). *Dynamics of Structures.* New York: McGraw-Hill.

Cook, R.G. (1964). *Digital Simulation of Random Vibrations.* Ph.D. Thesis, Department of Mechanical Engineering, M.I.T., Cambridge, Massachusetts.

Cox, D.R. (1962). *Renewal Theory.* London: Methuen.

Cox. D.R., and Isham, V. (1980). *Point Processes.* London: Chapman and Hall.

Cramér, H., and Leadbetter, M.R. (1967). *Stationary and Related Stochastic Processes. Sample Function Properties and Their Applications.* New York: John Wiley and Sons, Inc.

Crandall, S.H., Chandiramani, K.L., and Cook, R.G. (1966). *Some First-Passage Problems in Random Vibration.* Journal of Applied Mechanics, **33**, pp. 532-538.

Crandall, S.H. (1980). *Non-Gaussian Closure for Random Vibration of Non-Linear Oscillators.* International Journal of Nonlinear Mechanics, **15**, pp. 303-313.

Crandall, S.H. (1985). *Non-Gaussian Closure Techniques for Stationary Random Vibration.* International Journal of Nonlinear Mechanics, **20**, pp. 1-8.

Dash, P.K., and Iyengar, R.N. (1982). *Analysis of Randomly Time Varying Systems by Gaussian Closure Technique.* Journal of Sound and Vibration, **83**, pp. 241-251.

Davenport, A.G. (1964). *The Distribution of Largest Values of a Random Function with Application to Gust Loading.* Proc. Inst. Civil Eng., London, **22**, pp. 187-196.

DiPasquale, E., and Çakmak, A.Ş. (1990). *Seismic Damage Assessment using Linear Models.* Soil Dynamics and Earthquake Engineering, **9**, No. 4, pp. 194-215.

Einstein, A. (1905). *Über die von der molekular-kinetischen Theorie der Wärme geforderte Bewegung von in ruhenden Flüssigkeiten suspendierten Teilchen.* Ann. Phys., **17**, pp. 549.

Ermak, D.L., and Buckholtz, H. (1980). *Numerical Integration of the Langevin Equation: Monte Carlo Simulation.* Journal of Computational Physics, **35**, pp. 162-182.

Fan, F.-G., and Ahmadi, G. (1990). *On Loss of Accuracy and Non-Uniqueness of Solutions Generated by Equivalent Linearization and Cumulant-Neglect Methods.* Journal of Sound and Vibration, **137**, No. 3, pp. 385-401.

Fichera, G. (1960). *On a Unified Theory of Boundary Value Problems for Elliptic-Parabolic Equations of Second Order.* In *Boundary Problems in Differential Equations*, (R.E. Langer, ed.). University of Wisconsin Press, Madison, 1960, pp. 97-120.

Gardiner, G.W. (1985). *Handbook of Stochastic Methods for Physics, Chemistry and the Natural Sciences, 2nd Ed.* Berlin, Heidelberg, New York: Springer-Verlag.

Iwan, W.D., and Mason, A.B. (1980). *Equivalent Linearization for Systems Subjected to Non-Stationary Random Excitation.* International Journal of Nonlinear Mechanics, **15**, pp. 71-82.

Iyengar, R.N., and Dash, P.K. (1978). *Study of the Random Vibration of Nonlinear Systems by the Gaussian Closure Technique.* Journal of Applied Mechanics, **45**, pp. 393-399.

Janicki, A., and Weron, A. (1994). *Simulation and Chaotic Behaviour of α-stable Stochastic Processes.* New York: Marcel Dekker.

Janssen, R.A., and Lambert, R.F. (1967). *Numerical Calculation of Some Response Statistics for a Linear Oscillator under Impulsive Noise Excitation.* Journal of the Acoustical Society of America, **41**, pp. 827-835.

Johnsen, J.M. (1992). *Response Statistics of Nonlinear Dynamic Systems.* Ph.D. Thesis 1992:42, Norwegian Institute of Technology, Trondheim, Norway.

Kac, M., and Slepian, D. (1959). *Large Excursions of Gaussian Processes.* Annals of Mathematical Statistics, **30**, pp. 1215-1228.

Kaul, M.K., and Penzien, J. (1974). *Stochastic Seismic Analysis of Yielding Offshore Towers.* Journal of the Engineering Mechanics Division, American Society of Civil Engineers, **100**, No. EM5, pp. 1025-1038.

Kazakov, I.E. (1956). *Approximate Probability Analysis of Operational Precision of Essential Nonlinear Feedback Control Systems.* Automation and Remote Control, **17**, pp. 423-450.

Kimura, K., Yagasaki, K., and Sakata, M. (1987). *The Level Crossing Problem of Linear Systems Subjected to Nonwhite Excitation.* Nippon Kikai Gakkai Ronbunsha C Hen, Vol. 53, No. 492, pp. 1653-1662. (in Japanese).

Kleinert, H. (1992). *Path Integrals in Quantuum Mechanics.* Singapore: World Scientific.

Langley, R.S. (1988a). *An Investigation of Multiple Solutions Yielded by the Equivalent Linearization Method.* Journal of Sound and Vibration, **127**, pp. 271-281.

Langley, R.S. (1988b). *A Variational Formulation of the FPK Equations with Application to the First Passage Problem in Random Vibration.* Journal of Sound and Vibration, **123**, No. 2, pp. 213-227.

Langtangen, H.P. (1990). *Estimation of Reliability of Dynamic Systems by Numerical Solution of Fokker-Planck and Backward Kolmogorov Equations.* Proceedings of the 1st Scandinavian Forum for Stochastic Mechanics, Lund, Sweden, August 30-31, 1990, Swedish Council for Building Research, Stockholm, 1991, pp. 41-47.

Lin, Y.K. (1967). *Probabilistic Theory of Structural Dynamics.* New York: McGraw-Hill, Inc.

Lin, Y.K. (1969). *On first-Excursion Failure of Randomly Excited Structures.* Proceedings of the AIAA Struc. Dyn. Aeroelast. Spec. Conf., pp. 102-111. New Orleans, April, 1969.

Lin, Y.K. (1970). *First-Excursion Failure of Randomly Excited Structures.* AIAA Journal, **8**, No. 4, pp. 720-725.

Longuet-Higgins, M.S. (1964). *Modified Gaussian distributions for slightly nonlinear variables.* RADIO SCIENCE Journal of Research NBS/USNC-URSI, **68D**, No. 9, pp. 1049-1062.

Lyon, R.H. (1960). *On the Vibration Statistics of Randomly Excited Hard-Spring Oscillator.* Journal of the Acoustical Society of America, **32**, No. 6, pp. 716-719.

Lyon, R.H. (1961). *On the Vibration Statistics of Randomly Excited Hard-Spring Oscillator II.* Journal of the Acoustical Society of America, **33**, No. 10, pp. 1395-1403.

Madsen, P.H., and Krenk, S. (1984). *An Integral Equation Method for the First-Passage Problem in Random Vibration.* Journal of Applied Mechanics, **51**, pp. 674-679.

Marcienkiewicz, J. (1939). *Sur une propriété de la loi de Gauss.* Mathematische Zeitschrift, **44**, pp. 612-618.

Mark, W.D. (1966). *On False Alarm Probabilities of Filtered Noise.* Proceedings of the IEEE, **54**,

pp. 316-317.

Minai, R., and Suzuki, Y. (1985). *Seismic Reliability Analysis of Building Structures.* Proceedings of the ROC-Japan Joint Seminar on Multiple Hazards Mitigation, Taipei, Taiwan, ROC, March 1985, pp. 193-208.

Mullen, C.L., Micaletti, R.C. Jr., and Çakmak, A.Ş. (1995). *A Simple Method for Estimating the Maximum Softening Damage Index.* Proceedings of the 7th International Conference on Soil Dynamics and Earthquake Engineering, Crete, Greece, May 24-26, 1995, pp. 371-378.

Mørk, K.J. (1989). *Stochastic Response and Reliability Analysis of Hysteretic Structures.* Ph.D. Thesis, Aalborg University, Aalborg, Denmark.

Mørk, K.J. (1992). *Stochastic Analysis of Reinforced Concrete Frames Under Seismic Excitation.* Soil Dynamics and Earthquake Engineering, **11**, No. 3, pp. 145-161.

Mørk, K.J. (1993). *Response Analysis of Reinforced Concrete Structures under Seismic Excitation.* Earthquake Engineering and Structural Dynamics, **23**, No. 1, pp. 33-48.

Naess, A., and Johnsen, J.M. (1991).*Response Statistics of Nonlinear Dynamic Systems by Path Integration.* Proceedings of IUTAM Symposium on Nonlinear Stochastic Mechanics, Eds.: Bellomo and Casciati, Torino, Italy, July 1991, Springer-Verlag 1991.

Noori, M., and Davoodi, H. (1988). *Comparison Between Equivalent Linearization and Gaussian Closure.* In *Probabilistic Methods in Civil Engineering.* (Ed. P. D. Spanos), pp. 293-296.

Osaki, S. (1992). *Applied Stochastic System Modelling.* Berlin, Heidelberg, New York, Tokyo: Springer Verlag.

Renger, A. (1979). *Eine Dichtegleichung für Schwingungssysteme bei gleichzeitigen kontinuierlichen und diskreten stochastishen Erregungen.* Zeitschrift für angewandte Mathematik und Mechanik **59**, No. 1, pp. 1-13.

Ricciardi, L.M., Sacerdote, L., and Sato, S. (1984). *On an Integral Equation for First-Passage-Time Probability Densities.* Journal of Applied Probability, **21**, pp. 302-314.

Rice, J.R. (1964). *Theoretical Prediction of Some Statistical Characteristics of Random Loading Relevant to Fatigue and Fracture.* Ph.D. Thesis, Lehigh University, Betlehem, Pennsylvania.

Rice, J.R., and Beer, F.P. (1966). *First Occurrence-Time of High-Level Crossings in a Continous Random Process.* The Journal of the Acoustical Society of America, **39**, pp. 323-335.

Rice, S.O. (1944) in *Mathematical Analysis of Random Noise.* Reprinted in *Selected Papers on Noise and Stochastic Processes* (N. Wax, ed.). New York: Dover Publications, 1954, pp. 133-294.

Risken, H. (1984). *The Fokker-Planck Equation. Methods of Solution and Applications.* Berlin, Heidelberg, New York, Tokyo: Springer-Verlag.

Roberts, J.B. (1968). *An Approach to the First-Passage Problem in Random Vibration.* Journal of Sound and Vibration, **8**, No. 2, pp. 301-328.

Roberts, J.B. (1972). *System Response to Random Impulses.* Journal of Sound and Vibration, **24**, pp. 23-34.

Roberts, J.B., and Spanos, P.D. (1990). *Random Vibration and Statistical Linearization.* New York: John Wiley and Sons.

Samorodnitsky, G., and Taqqu, M. (1994). *Non-Gaussian Stable Processes: Stochastic Models with Infinite Variance.* London: Chapman and Hall.

Shinozuka, M., and Yang, J.-N. (1969). *On the Bound of First Excursion Probability.* Journal of the Engineering Mechanics Division, American Society of Civil Engineers, **95**, No. EM2, pp. 363-377.

Shipley, J.W., and Bernard, M.C. (1972). *The First Passage Time Problem for Simple Structural Systems.* Journal of Applied Mechanics, **39**, pp. 911-917.

Siegert, A.J.F. (1951). *On the First Passage Time Probability Problem.* Physical Review, **81**, pp. 617-623.

Slepian, D. (1961). *First Passage Time for a Particular Gaussian Process.* Annals of Mathematical Statistics, **32**, pp. 610-612.

Snyder, D.L. (1975). *Random Point Processes.* New York: John Wiley and Sons, Inc.

Sobczyk, K. (1991). *Stochastic Differential Equations with Applications to Physics and Engineering.* Dordrecht, Boston, London: Kluver Academic Publishers.

Soong, T.T., and Grigoriu, M. (1993). *Random Vibration of Mechanical and Structural Systems.* Englewood Cliffs, New Jersey: Prentice Hall.

Spanos, P.-T.D., and Iwan W.D. (1978). *On the Existence and Uniqueness of Solutions Generated by Equivalent Linearization.* International Journal of Non-Linear Mechanics, **13**, pp. 718.

Spanos, P.-T.D. (1981). *Stochastic Linearization in Structural Dynamics.* Applied Mechanics Review, **34**, pp. 1-8.

Spencer, B.F. Jr. (1986). *Reliability of Randomly Excitated Hysteretic Structures.* Lecture Notes in Engineering, **21**, Berlin, Heidelberg, New York: Springer Verlag.

Srinivasan, S.K. (1974). *Stochastic Point Processes and their Applications.* London: Griffin.

Stratonovich, R.L. (1963). *Topics in the Theory of Random Noise. Volume I.* New York: Gordon and Breach.

Sun, J.-Q., and Hsu, C.S. (1987). *Cumulant Neglect Closure Method for Nonlinear Systems under Random Excitation.* Journal of Applied Mechanics, **54**, pp. 649-655.

Sun, J.-Q., and Hsu, C.S. (1988). *First-Passage Time Probability of Non-Linear Stochastic Systems by Generalized Cell Mapping Method.* Journal of Sound and Vibration, **124**, No. 2, pp. 233-248.

Sun, J.-Q. and Hsu, C.S. (1990). *The Generalized Cell Mapping Method in Nonlinear Random Vibration based upon Short-Time Gaussian Approximations.* Journal of Applied Mechanics, ASME, **57**, pp. 1018-1025.

Suzuki, Y., and Minai, R. (1985). *Seismic Reliability Analysis of Hysteretic Structures Based on Stochastic Differential Equations.* Proceedings of the 4th International Conference on Structural Safety and Reliability, ICOSSAR'85, **II**, pp. 177-186.

Tajimi, H. (1973). *A Statistical Method of Determining the Maximum Response of a Building During an Earthquake.* Proceedings of the 2nd World Conference on Earthquake Engineering, Tokyo, **2**, pp. 781-797.

Toro, G.R., and Cornell, C.A. (1986). *Extremes of Gaussian Processes with Bimodal Spectra.* Journal of the Engineering Mechanics Division, American Society of Civil Engineers, **112**, No. 5, pp. 465-484.

Wang, M.C., and Uhlenbeck, G.E. (1945). *On the Theory of Brownian Motion II.* Reviews of Modern Physics, **17**, No. 2 and 3, pp. 323-342.

Wehner, M.F. and Wolfer, W.G. (1987). *Numerical Evaluation of Path-Integral Solutions to Fokker-Planck Equations. III. Time and Functionally Dependent Coefficients.* Physical Review A, **34**, No. 4, pp. 1795-1801.

Wen, Y.K. (1976). *Method for Random Vibration of Hysteretic Systems.* Journal of the Engineering Mechanics Division, American Society of Civil Engineers, **102**, No. EM2, pp. 249-263.

Wen, Y.K. (1980). *Equivalent Linearization for Hysteretic Systems under Random Vibration.* Journal of Applied Mechanics, **47**, pp. 150-154.

Wong, E., and Zakai, M. (1965). *On the Relationship between Ordinary and Stochastic Differential Equations.* International Journal of Engineering Science, **3**, pp. 213-229.

Wu, W.F., and Lin, Y.K. (1984). *Cumulant-Neglect Closure for Non-Linear Oscillators under Random Parametric and External Excitations.* International Journal of Non-linear Mechanics, **19**, pp. 349-362.

Zienkiewicz, O.C., and Taylor, R.L. (1991). *The Finite Element Method, Fourth Edition, Volume 2.* London: McGraw Hill.

The present thesis has been based on the following papers and publications:

Aşkar, A., Köylüoğlu, H.U., Nielsen, S.R.K., and Çakmak, A.Ş. (1996). *Faster Simulation Methods for the Nonstationary Random Vibrations of Nonlinear MDOF Systems.* Probabilistic Engineering Mechanics, **11**, pp. 63-72. Also published in Proceedings of the 2nd International Conference on Computational Stochastic Mechanics, pp. 287-296, Athens, Greece, June 13-15, 1994.

Iwankiewicz, R., and Nielsen, S.R.K. (1992a). *Dynamic Response of Non-Linear Systems to Poisson-Distributed Random Impulses.* Journal of Sound and Vibration, **156**, No. 3, pp. 407-423.

Iwankiewicz, R., and Nielsen, S.R.K. (1992b). *Dynamic Response of Hysteretic Systems to Poisson-Distributed Pulse Trains.* Probabilistic Engineering Mechanics, **7**, pp. 135-148.

Iwankiewicz, R., and Nielsen, S.R.K. (1994). *Dynamic Response of Non-Linear Systems to Renewal-Driven Random Pulse Trains.* International Journal of Non-Linear Mechanics, **29**, No. 4, pp. 555-567.

Iwankiewicz, R., and Nielsen, S.R.K. (1995). *Sensitivity of Reliability Estimates in Partially Damaged RC Structures subject to Earthquakes, using Reduced Hysteretic Models.* Structural Reliability Theory, Paper No. 139. ISSN 0902-7513 R9507, Aalborg University.

Iwankiewicz, R., and Nielsen, S.R.K. (1996). *Dynamic Response of Non-Linear Systems to Renewal Impulses by Path Integration.* Journal of Sound and Vibration, **195**, No. 2, pp. 175-193.

Iwankiewicz, R., Nielsen, S.R.K., and Thoft-Christensen, P. (1990). *Dynamic Response of Non-Linear Systems to Poisson-Distributed Pulse Trains: Markov Approach.* Structural Safety, **8**, pp. 223-238.

Kirkegaard, P.H., Nielsen, S.R.K., Micaletti, R.C., Jr., and Çakmak, A.Ş. (1996). *Identification of a Maximum Softening Damage Indicator of RC-Structures using Time-Frequency Techniques.* Proceedings of the 3rd European Conference on Structural Dynamics, EURODYN'96, Florence, Italy, June 5-8, 1966, pp. 971-979.

Köylüoğlu, H.U., and Nielsen, S.R.K. (1996). *System Dynamics and Modified Cumulant Neglect Closure Schemes.* Proceedings of the 7th Specialty Conference on Probabilistic Mechanics and Structural Reliability, ASCE, Worcester, Massachusetts, USA, August 7-9, 1996, pp. 380-383.

Köylüoğlu, H.U., Nielsen, S.R.K., Abbott, J., and Çakmak, A.Ş. (1996). *Local and Modal Damage Indicators for Reinforced Concrete Shear Frames subject to Earthquakes.* Submitted to Journal of Engineering Mechanics, ASCE.

Köylüoğlu, H.U., Nielsen, S.R.K., and Çakmak, A.Ş. (1995). *Fast Cell-to-Cell Mapping (Path Integration) for Nonlinear White Noise and Poisson Driven Systems.* Structural Safety, **17**, pp.

151-165. Also published in Proceedings of the 2nd International Conference on Computational Stochastic Mechanics, pp. 361-370, Athens, Greece, June 13-15, 1994.

Köylüoğlu, H.U., Nielsen, S.R.K., and Çakmak, A.Ş. (1996a). *A Faster Simulation Method for the Stochastic Response of Hysteretic Structures subject to Earthquakes.* Soil Dynamics and Earthquake Engineering, **15**, No. 6, pp. 359-368.

Köylüoğlu, H.U., Nielsen, S.R.K., and Çakmak, A.Ş. (1996b). *Approximate Forward Difference Equations for the Lower Order Nonstationary Statistics of Nonlinear MDOF Systems subject to Random Excitation.* Proceedings of 3rd International Conference on Stochastic Structural Dynamics, San Juan, Puerto Rico, January 1995. Submitted to Probabilistic Engineering Mechanics.

Köylüoğlu, H.U., Nielsen, S.R.K., Çakmak, A.Ş., and Kirkegaard, P.H. (1996). *Prediction of Global and Localized Damage and Future Reliability for RC-Structures subject to Earthquakes.* Accepted for publication in Journal of Earthquake Engineering and Structural Dynamics.

Köylüoğlu, H.U., Nielsen, S.R.K., and Iwankiewicz, R. (1994). *Reliability of Non-Linear Oscillators subject to Poisson Driven Impulses.* Journal of Sound and Vibration, **176**, No. 1, pp. 19-33.

Köylüoğlu, H.U., Nielsen, S.R.K., and Iwankiewicz, R. (1995). *Response and Reliability of Poisson Driven Systems by Path Integration.* Journal of Engineering Mechanics, ASCE, **121**, No. 1, pp. 117-130.

Micaletti, R.C., Çakmak, A.Ş., Nielsen, S.R.K. and Kirkegaard, P.H. (1996). *Construction of Time-Dependent Spectra Using Wavelet Analysis for Determination of Global Damage.* Proceedings of the ISMA21 1996 International Conference on Noise and Vibration Engineering (ed. P. Sas), Conference, Leuven, Belgium, September 18-20, 1996, **II**, pp. 993-1004.

Mørk, K.J., and Nielsen, S.R.K. (1990). *Reliability of Soil Sublayers under Earthquake Excitation.* Proceedings of the 1st European Conference on Structural Dynamics, EURODYN'90, Bochum, Germany, June 1990, **1**, pp. 225-236.

Mørk, K.J., and Nielsen, S.R.K. (1991a). *System Reduction for Random Dynamically Loaded Elasto-Plastic Structures.* Proceedings of the 1st Scandinavian Forum for Stochastic Mechanics, Lund, Sweden, August 30-31, 1990, pp. 145-157.

Mørk, K.J., and Nielsen, S.R.K. (1991b). *Program for Stochastic Analysis of Plane Reinforced Concrete Frames under Seismic Excitation.* Structural Reliability Theory, Paper No. 91. ISSN 0902-7513 R9129, Aalborg University.

Nielsen, S.R.K. (1980). *Probability of Failure of Structural Systems under Random Vibration, Part I.* Department of Building Technology and Structural Engineering, Aalborg University, Report No. 8001.

Nielsen, S.R.K. (1990a). *Approximations to the Probability of Failure in Random Vibration by Integral Equation Methods.* Journal of Sound and Vibration, **137**, No. 2, pp. 305-317.

Nielsen, S.R.K. (1990b). *Probability of Failure by Integral Equation Methods.* Structural Reliability Theory, Paper No. 81. ISSN 0902-7513 R9037, Aalborg University.

Nielsen, S.R.K. (1993). Vibration Theory, Vol. 3. Linear Stochastic Vibration Theory. Aalborg Tekniske Universitetsforlag.

Nielsen, S.R.K., and Çakmak, A.Ş. (1991). *Evaluation of Maximum Softening as a Damage Indicator for Reinforced Concrete under Seismic Excitation.* Proceedings of the 1st International Conference on Computational Stochastic Methods, Corfu, Greece, Sept. 17-19, 1991, pp. 169-184.

Nielsen, S.R.K., and Iwankiewicz, R. (1996). Vibration Theory, Vol. 4. Advanced Methods in Stochastic Dynamics of Non-Linear Systems. Aalborg Tekniske Universitetsforlag.

Nielsen, S.R.K., Iwankiewicz, R., and Skjærbæk, P.S. (1996). *Moment Equations for Non-Linear Systems under Renewal-Driven Random Impulses with Gamma-Distributed Interarrival Times.* Proceedings of the IUTAM Symposium on Advances in Nonlinear Stochastic Mechanics, Trondheim, Norway, July 3-7, 1995, pp. 331-340.

Nielsen, S.R.K., Iwankiewicz, R., and Thoft-Christensen, P. (1989). *Dynamic Response of Hysteretic Structures to Random Pulse Trains: Markov Approach.* Structural Reliability Theory, Paper No. 60. ISSN 0902-7513 R8914, Aalborg University. Presented at the 5th International Conference on Structural Safety and Reliability, ICOSSAR'89, San Francisco, August 7-11, 1989.

Nielsen, S.R.K., and Köylüoğlu, H.U. (1996). *Path Integration Applied to Structural Systems with Uncertain Properties.* Proceedings of the 7th Specialty Conference on Probabilistic Mechanics and Structural Reliability, ASCE, Worcester, Massachusetts, USA, August 7-9, 1996, pp. 6-9.

Nielsen, S.R.K., and Köylüoğlu, H.U. (1997). *Moment Closure Schemes for Multi-Peaked Systems.* (Submitted to Journal of Sound and Vibration).

Nielsen, S.R.K., Köylüoğlu, H.U., and Çakmak, A.Ş. (1992). *One- and Two-Dimensional Maximum Softening Damage Indicators for Reinforced Concrete Structures under Seismic Excitation.* Soil Dynamics and Earthquake Engineering, **11**, No. 8, pp. 435-443. Also published in Proceedings of the 6th International Conference on Structural Safety and Reliability, ICOSSAR'93, pp. 1809-1816, Innsbruck, Austria, August 9-13, 1993.

Nielsen, S.R.K., Mørk, K.J., and Thoft-Christensen, P. (1989). *Response Analysis of Hysteretic Multi-Storey Frames under Earthquake Excitation.* Earthquake Engineering and Structural Dynamics, **18**, pp. 655-666, 1989. Also printed in Proceedings of Research Workshop on Stochastic Mechanics, Department of Structural Engineering, Technical University of Denmark, Report No. 244, 1989.

Nielsen, S.R.K., Mørk, K.J., and Thoft-Christensen, P. (1990a). *Stochastic Response of Hysteretic Systems.* Structural Safety, **9**, pp. 59-71.

Nielsen, S.R.K., Mørk, K.J., and Thoft-Christensen, P. (1990b). *Reliability of Hysteretic Systems Subjected to White Noise Excitation.* Structural Safety, **8**, pp. 369-379.

Nielsen, S.R.K., Skjærbæk, P.S., Köylüoğlu, H.U., and Çakmak, A.Ş. (1995). *Prediction of Global Damage and Reliability based upon Sequential Identification and Updating of RC Structures subject to Earthquakes.* Proceedings of the 7th International Conference on Soil Dynamics and Earthquake Engineering, Crete, Greece, May 24-26, 1995, pp. 361-369.

Nielsen, S.R.K., and Sørensen, J.D. (1988). *Probability of Failure in Random Vibration.* Journal of Engineering Mechanics, ASCE, **114**, No. 7, pp. 1218-1230.

Nielsen, S.R.K., Thoft-Christensen, P., and Moust Jacobsen, H. (1989). *Reliability of Soil Sublayers under Earthquake Excitation: Markov Approach.* Structural Dynamics and Soil-Structure Interaction, Proceedings of the 4th International Conference on Soil Dynamics and Earthquake Engineering, Mexico City, Mexico, October 23-26, 1989, pp. 19-37.

Sigurdsson, G., and Nielsen, S.R.K. (1991). *Stress-Response of Offshore Structures by Equivalent Polynomial Expansion Techniques.* International Journal of Offshore and Polar Engineering, **1**, No. 1, pp. 71-76.

Thoft-Christensen, P., and Nielsen, S.R.K. (1982). *Bounds on the Probability of Failure in Random Vibration.* Journal of Structural Mechanics, **10**, No. 1, pp. 67-91.

5. NOTATION

$\mathbf{A}(t)$	Vector of 1st order tensor components $A_i(t)$.
A	Cross-sectional area of beam element.
A_i	Cross-sectional area of beam element i.
$A_i(t)$	1st order tensor components in cubic expansion of drift vector.
$A_i(t)$	Time-dependent slope in Clough-Johnston hysteretic model.
$\mathbf{a}(\mathbf{X}(t), t)$	Drift vector of compound Erlang process driven system.
a	Parameter in α-stable random variable.
a_0	Mode participation factor.
a_{ij}	Coefficients in polynomial expansion of $u(x, \dot{x})$.
$a(t)$	Lower barrier level.
a_i	Parameter in hysteretic model for shear force between $(i-1)$th and ith storey in shear building.
a_i	Coefficients in closure expression for $Y_{k+1}(t)$.
$\dot{a}(t)$	$\frac{d}{dt}a(t)$.
$[a, b]$	Closed interval from a to b.
$]a, b[$	Open interval from a to b.
a_{peak}	Peak value of $\ddot{u}_g(t)$.
$\mathbf{B}(t)$	Matrix of 2nd order tensor components $B_{im}(t)$.
B_{im}	2nd order tensor components in cubic expansion of drift vector.
$\mathbf{b}(t)$	Position vector to surface area element da_t.
$\dot{\mathbf{b}}(t)$	$\frac{d}{dt}\mathbf{b}(t)$.
$\mathbf{b}(\mathbf{X}(t), t)$	Diffusion vector of compound Erlang driven system.
b	Decay rate of intensity function of white noise excitation.
b_1, b_2	Coefficients in equivalent cubic expansion of constitutive equation for hysteretic beam with a single yield hinge.
b_i	Expansion coefficients in solution to AR difference equation for $\rho(N(t))$.
$b(t)$	Upper barrier level.
$\dot{b}(t)$	$\frac{d}{dt}b(t)$.
$\mathbf{C}$	Covariance matrix.
$\mathbf{C}$	Linear viscous damping matrix.
$C^{(k)}$	Local Courant number for the kth cell.

C_{imn}	3rd order tensor components in cubic expansion of drift vector.
$C_j(t)$	$\mathrm{Re}\,(U_j)$. Auxiliary state variable at the transformation of Erlang process driven system into equivalent Poisson process driven system.
$\mathcal{C}_t$	Event that a crossing through ∂S_t takes place.
$\mathcal{C}_{]t,t+\Delta t]}$	Event that a crossing through ∂S_t takes place during $]t, t+\Delta t]$.
$\mathcal{C}_t^-$	Event that an in-crossing to S_t takes place.
$\mathcal{C}_{]t,t+\Delta t]}^-$	Event that an in-crossing to S_t takes place during $]t, t+\Delta t]$.
$\mathcal{C}_t^+$	Event that an out-crossing from S_t takes place.
$\mathcal{C}_{]t,t+\Delta t]}^+$	Event that an out-crossing from S_t takes place during $]t, t+\Delta t]$.
$C_i(\mathbf{z},t)$	Derivate moment of the 1st order of Markov vector process $\{\mathbf{Z}(t), t \in [t_0,\infty[\}$. $(C_i(\mathbf{z},t) = \lim_{\Delta t\to 0} \frac{1}{\Delta t} E[Z_i(t+\Delta t) - Z_i(t) \mid \mathbf{Z}(t) = \mathbf{z}])$.
$\mathbf{c}(\mathbf{Z}(t),t)$	Drift vector in Markov system.
$\mathbf{c}^0(\mathbf{Z}(t),t)$	$\mathbf{c}(\mathbf{Z}(t),t) - E[\mathbf{c}(\mathbf{Z}(t),t)]$. Zero-mean centralized drift vector.
$c_{eq,i}(\mathbf{Z}(t),t)$	ith component in equivalent polynomial expansion of drift vector.
$c_i(\mathbf{Z}(t),t)$	ith component of $\mathbf{c}(\mathbf{Z}(t),t)$.
$c_i^0(\mathbf{Z}(t),t)$	ith component of $\mathbf{c}^0(\mathbf{Z}(t),t)$.
$c(t \mid \mathbf{z}_0, t_0)$	Deterministic displacement drift (eigenvibration) from initial state $\mathbf{z}_0$ at the time t_0 of single-degrees-of-freedom system.
$\dot{c}(t \mid \mathbf{z}_0, t_0)$	$\frac{\partial}{\partial t} c(t \mid \mathbf{z}_0, t_0)$. Deterministic velocity drift (eigenvibration) from initial state $\mathbf{z}_0$ at the time t_0 of single-degrees-of-freedom system.
$c^{(k)}$	$\lvert\mathbf{c}(\mathbf{Z}_k,t)\rvert$. Length of drift-vector at the centre of the kth cell at the time t.
c_n	Coefficient in eigenfunction expansion of first-passage time probability density function.
$c_{\{Z\}}(b(t),t \mid \mathcal{E}_{t_0})$	Probability current of Markov scalar process $\{Z(t), t \in [t_0,\infty[\}$ through barrier $b(t)$ at the time t on condition of $\mathcal{E}_{t_0}$.
$c_{\{Z\}}(b(t),t \mid z_0, t_0)$	Probability current of Markov scalar process $\{Z(t), t \in [t_0,\infty[\}$ through barrier $b(t)$ at the time t on condition of deterministic start at $z_0 \in S_0$ at the time t_0.
$\mathbf{D}(t)$	Vector of damage indicators.
D	Diffusion coefficient.
$D(t)$	Damage indicator. Bilinear and Bouc-Wen hysteretic oscillators.

$D_i(t)$	Damage indicator between $(i-1)$th and ith storey in shear building.
$D_i^+(t), D_i^-(t)$	Accumulated plastic deformation at positive and negative yielding between $(i-1)$th and ith storey in shear building.
D_{imnp}	4th order tensor components in cubic expansion of drift vector.
$D_N(z,t)$	Derivate moment of order N of scalar Markov process $\{Z(t), t \in [t_0, \infty[\}$. $(D_N(z,t) = \lim_{\Delta t \to \infty} \frac{1}{\Delta t} E[(Z(t+\Delta t) - Z(t))^N \mid Z(t) = z])$.
$D_{i_1 \cdots i_N}(\mathbf{z}, t)$	Derivate moment of order N of Markov vector process $\{\mathbf{Z}(t), t \in [t_0, \infty[\}$. $(D_{i_1 \cdots i_N}(\mathbf{z},t) = \lim_{\Delta t \to \infty} \frac{1}{\Delta t} E[(Z_{i_1}(t+\Delta t) - Z_{i_1}(t)) \cdots (Z_{i_N}(t+\Delta t) - Z_{i_N}(t)) \mid \mathbf{Z}(t) = \mathbf{z}])$.
$\mathbf{d}(\mathbf{Z}(t), t)$	Diffusion vector in Markov system due to excitation by Wiener processes.
$\mathbf{d}(t \mid \mathbf{z}_0, t_0)$	Deterministic drift (eigenvibrations) during interval $]t_0, t]$ from initial value $\mathbf{Z}(t_0) = \mathbf{z}_0$.
$\mathbf{d}_0$	Vector for scaling of external normalized Wiener vector process $\{\mathbf{W}(t)\}$.
$\mathbf{d}_0(t)$	Diffusion vector in path integration of Wiener process driven systems. Piecewise constant as a function of $\mathbf{Z}(t)$.
$\mathbf{d}^{(1)}(t \mid \mathbf{z}_k, t_i)$	$\frac{\partial \mathbf{d}(t \mid \mathbf{z}_k, t_i)}{\partial \mathbf{z}_k^T}\mathbf{e}$. 1st order expansion vector in Taylor expansion of $\mathbf{Z}(t)$ on condition of one impulse arrival in $]t_i, t]$.
$\mathbf{d}^{(2)}(t \mid \mathbf{z}_k, t_i)$	$\frac{1}{2}\mathbf{e}^T \frac{\partial^2 \mathbf{d}(t \mid z_k, t_i)}{\partial \mathbf{z}_k \partial \mathbf{z}_k^T}\mathbf{e}$. 2nd order expansion vector in Taylor expansion of $\mathbf{Z}(t)$ on condition of one impulse arrival in $]t_i, t]$.
$d(t)$	Diffusion function.
d_0	Amplitude of white noise intensity function.
$d_1, \ldots, d_4$	Coefficients in equivalent cubic expansion of constitutive equation for hysteretic beam with a single yield hinge.
da_t	Area element of surface ∂s_t.
d_{er}	Critical value of $D(t)$.
$d_i(t \mid \mathbf{z}_0, t)$	ith component of $\mathbf{d}(t \mid \mathbf{z}_0, t_0)$.
$d_{i\alpha}(\mathbf{Z}(t), t)$	Component in ith row and αth column of $\mathbf{d}(\mathbf{Z}(t), t)$.
d_n	Coefficient in eigenfunction expansion for $F_{T_1}(t \mid \mathbf{z})$.
E	Modulus of elasticity.
E	Dissipated energy per unit volume of soil.
$E[\cdot]$	Expectation operator.
$E[\,]_0$	Expectations with respect to $f_{\mathbf{V}}(\mathbf{v}, t)$.
$\mathcal{E}$	Event.

$\mathcal{E}_{t_0}$	Event that a subset of initial values belongs to S_{t_0}.
$\mathcal{E}_{]t_0,t]}$	Event $\cap_{\tau\in]t_0,t]} S_\tau$.
$\mathcal{E}^{(n)}_{]t_0,t]}$	Event that at least n out-crossings take place from the safe domain during the interval $]t_0,t]$ of sample curves originating in S_{t_0}.
$\mathbf{e}(\mathbf{Z}(t),t)$	Diffusion vector in Markov system due to excitation by jump process.
$\mathbf{e}_0$	Vector for scaling of external jump vector process $\{\mathbf{V}(t)\}$.
$\mathbf{e}^0(\mathbf{Z}(t),t)$	$\mathbf{e}(\mathbf{Z}(t),t) - E[\mathbf{e}(\mathbf{Z}(t),t)]$. Zero-mean centralized diffusion matrix.
$\mathbf{e}_\alpha(t)$	αth column matrix of $\mathbf{e}(t)$.
$e(t)$	Diffusion function.
e_1, e_2, e_3, e_4	Parameters for specification of amplitude d_0 of white noise intensity function.
$e_{i\alpha}(\mathbf{Z}(t),t)$	Component in ith row and αth column of $\mathbf{e}(\mathbf{Z}(t),t)$.
$e^0_{i\alpha}(\mathbf{Z}(t),t)$	Component in ith row and αth column of $\mathbf{e}^0(Z(t),t)$.
$\{\mathbf{F}(t),\ t\in]t_0,t_1]\}$	Vector load process.
$\{F(t),\ t\in]t_0,t_1]\}$	Scalar load process.
$F_{I,1}(x), F_{I,2}(x)$	Quadratic upwind correction of weighting functions in x-direction in Petrov-Galerkin variational approach.
$F_L(\cdot)$	Probability distribution function of L.
$F^-_{n,j}(t_1,\ldots,t_n,t)$	Integral of $f^{-\cdots-}_{n+j+1}{}^{-\cdots-+}(t_1\ldots,t_n,t_{n+1},\ldots,t_{n+j},t)$ over one triangle of $[t_n,t]^j$ with respect to $t_{n+j},\ldots,t_{n+1}$.
$F^+_{n,j}(t_n,\ldots,t_1 \mid \mathcal{E}_{t_0})$	Integral of $f^{+\cdots+}_{n+j}{}^{++\cdots+}(t_{n+j},\ldots,t_{n+1},t_n,\ldots,t_1 \mid \mathcal{E}_{t_0})$ over one triangle of $[t_0,t_n]^j$ with respect to $t_{n+j},\ldots,t_{n+1}$.
$F_P(p)$	Probability distribution function of P.
$F_{T_1}(t \mid \mathcal{E}_{t_0})$	First-passage time probability distribution function.
$F_{X_{\max}}(x;[0,t])$	Probability distribution function of $X_{\max} = \max_{\tau\in[0,t]} X(\tau)$.
$\mathcal{F}^{(1)}_t$	Event that a first-passage takes place at the time t.
$\mathcal{F}^{(1)}_{]t,t+\Delta t]}$	Event that a first-passage takes place during $]t,t+\Delta t]$.
$\mathcal{F}^{(n)}_t$	Event that an nth-passage takes place at the time t.
$\mathcal{F}^{(n)}_{]t,t+\Delta t]}$	Event that an nth-passage takes place during $]t,t+\Delta t]$.
$f_1(t)$	Unconditioned first order crossing rate through ∂S_t.
$f_1^-(t_1 \mid \mathcal{C}^+_t)$	First order in-crossing rate to S_{t_1} on condition of an out-crossing from S_t, $t_0 < t_1 < t$.
$f_1^-(t_1 \mid \mathcal{L}_{t_2,t})$	Kernel in integral equations for $f_{L^+_t}(t-t_1)$. Rate of in-

crossings to S_{t_1} on condition of an in-crossing to S_{t_2}, on condition of an out-crossing from S_t and on condition that the sample curves are not leaving the safe domain in the interval $]t_2, t[$, $t_0 < t_1 < t_2 < t$.

$f_1^-(t_{n+1} \mid \mathcal{C}_{t_1}^- \cap \cdots \cap \mathcal{C}_{t_n}^- \cap \mathcal{L}_{t_{n+2},t})$ Kernel in integral equations for $f_{L_t^+}(t - t_{n+1} \mid \mathcal{C}_{t_1}^- \cap \cdots \cap \mathcal{C}_{t_n})$. Rate of in-crossings to $S_{t_{n+1}}$ on condition of an in-crossing to $S_{t_1}, \ldots, S_{t_n}, S_{t_{n+2}}$, on condition of an out-crossing from S_t and on condition that the sample curves are not leaving the safe domain in the interval $]t_{n+2}, t[$, $t_0 < t_1 < \cdots < t_n < t_{n+1} < t_{n+2} < t$.

$f_1^+(t)$ Unconditioned first order out-crossing rate from S_t.

$f_1^+(t \mid \mathcal{E}_{t_0})$ First order out-crossing rate from S_t on condition of $\mathcal{E}_{t_0}$.

$f_1^+(t \mid x_1, \dot{x}_1, t_1)$ First order out-crossing rate from S_t on condition of deterministic start in $[X(t_1), \dot{X}(t_1)] = [x_1, \dot{x}_1]$ at the time $t_1 < t$.

$f_1^+(t \mid \mathcal{C}_{t_1}^- \cap \mathcal{F}_{t_2}^{(1)})$ Kernel in integral equation for $f_{L_{t_1}^-}(t - t_1)$. Rate of out-crossings from S_t on condition of $\mathcal{C}_{t_1}^-$ and on condition of a first-passage at the time $t_2 \in]t_1, t[$.

$f_1^+(t \mid \mathcal{E}_{t_0} \cap \mathcal{F}_{t_1}^{(1)})$ Kernel in integral equation for $f_{T_1}(t \mid \mathcal{E}_{t_0})$. Rate of out-crossings from S_t on condition of $\mathcal{E}_{t_0}$ and on condition of a prior first-passage at the time $t_1 \in]t_0, t[$.

$f_1^+(t \mid \mathcal{E}_{t_0} \cap \mathcal{U}_{t_1,t_2})$ Kernel in integral equation for $f_{U_{t_1}^-}(t - t_1 \mid \mathcal{E}_{t_0})$. Rate of out-crossings from S_t on condition of $\mathcal{E}_{t_0}$ and on condition of $\mathcal{U}_{t_1,t_2}$, $t_0 < t_1 < t_2 < t$.

$f_1^+(t_1 \mid \mathcal{E}_{t_0} \cap \mathcal{U}_{t_2,t})$ Kernel in integral equation for $f_{U_t^+}(t - t_1 \mid \mathcal{E}_{t_0})$. Rate of out-crossings from S_{t_1} on condition of $\mathcal{E}_{t_0}$ and on condition of $\mathcal{U}_{t_2,t}$.

$f_1^+(t; \mathcal{E}_{\tau_1}, \cdots, \tau_m \mid \mathcal{E}_{t_0})$ Rate of out-crossings from S_t on condition $\mathcal{E}_{t_0}$ of sample curves in the safe domain at instants of times $\tau_1, \cdots, \tau_m$.

$f_1^+(t; \mathcal{E}_{\tau_1}, \cdots, \tau_m \mid \mathcal{E}_{t_0} \cap \mathcal{F}_{t_1}^{(1)})$ Kernel in integral equation for $f_{T_1}(t \mid \mathcal{E}_{t_0})$. Rate of out-crossings from S_t on condition of $\mathcal{E}_{t_0}$ and on condition of a first-passage at the time $t_1 \in]t_0, t[$ of sample curves in the safe domain at instants of times $\tau_1, \cdots, \tau_m$.

$f_1^+(t_n \mid \mathcal{E}_{t_0} \cap \mathcal{C}_{t_{n-1}}^+ \cap \cdots \cap \mathcal{C}_{t_1}^+ \cap \mathcal{C}_t^+)$ Rate of out-crossing from S_{t_n} on condition of $\mathcal{E}_{t_0}$ and on condition of out-crossings from $S_{t_{n-1}}, \cdots, S_{t_1}, S_t$, $t_0 < t_n < t_{n-1} < \cdots < t_1 < t$.

$f_1^+(t_n \mid \mathcal{E}_{t_0} \cap \mathcal{F}_{t_{n+1}}^{(1)} \cap \mathcal{C}_{t_{n-1}}^+ \cap \cdots \cap \mathcal{C}_{t_1}^+ \cap \mathcal{C}_t^+)$

Kernel in integral equations for $f_{T_1}(t_n \mid \mathcal{E}_{t_0} \cap \mathcal{C}_{t_{n-1}}^+ \cap \cdots \cap \mathcal{C}_{t_1}^+ \cap \mathcal{C}_t^+)$. Rate of out-crossings from S_{t_n} on condition of $\mathcal{E}_{t_0}$, on condition of a first-passage at the time t_{n+1} and on condition of out-crossings from $S_{t_{n-1}}, \ldots, S_{t_1}, S_t$, $t_0 < t_{n+1} < t_n < t_{n-1} < \cdots < t_1 < t$.

$f_2^{--}(t_1, t_2; \mathcal{E}_{]t_2,t[} \mid \mathcal{C}_t^+)$ 2nd order rate of in-crossings to S_{t_1} and S_{t_2} of sample curves which does not leave the safe domain in $]t_2, t[$ on condition of an out-crossing at the time t.

$f(D)$ — $\frac{\sigma_{12,y}(x_2,t)}{\sigma_{12,y}(x_2,0)} = \frac{\mu(x_2,t)}{\mu(x_2,0)}$. Deterioration function for shear strength and shear modulus.

$f_e(\mathbf{Q}_e)$ — Yield function.

$f_I(\cdot)$ — Probability density function of interarrival times $I_2, I_3, \cdots$.

$f_{I_1}(\cdot)$ — Waiting time probability density function of first impulse arrival of renewal counting process.

$f_{L_t^-}(l)$ — Probability density function of L_t^-.

$f_{L_{t_1}^-}(l \mid \mathcal{C}_{t_n}^+ \cap \cdots \cap \mathcal{C}_{t_2}^+ \cap \mathcal{C}_t^+)$ — Probability density function of $L_{t_1}^-$ on condition of joint outcrossings from $S_{t_n}, \ldots, S_{t_2}, S_t$, $t_0 < t_1 < t_1 + l < t_n < \cdots < t_2 < t$.

$f_{L_t^+}(l)$ — Probability density function of L_t^+.

$f_{L_t^+}(l \mid \mathcal{C}_{t_1}^- \cap \cdots \cap \mathcal{C}_{t_n}^-)$ — Probability density function of L_t^+ on condition of prior joint in-crossings to $S_{t_1}, \ldots, S_{t_n}$, $t_0 < t_1 < \cdots < t_n < t - l < t$.

$f_n(t_1, \ldots, t_n)$ — Unconditioned nth order crossing rate through $\partial S_{t_1}, \ldots, \partial S_{t_n}$.

$f_n(t_1, \ldots, t_n \mid \mathcal{E})$ — nth order crossing rate through $\partial S_{t_1}, \ldots, \partial S_{t_n}$ on condition of event $\mathcal{E}$.

$f_n(t_1, \ldots, t_n; \mathcal{E})$ — nth order crossing rate through $\partial S_{t_1}, \ldots, \partial S_{t_n}$ of samples in event $\mathcal{E}$.

$f_n(t_n, \ldots, t_1; \mathcal{E}_{\tau_1,\ldots,\tau_m} \mid \mathcal{E}_{t_0})$ — nth order crossing rate through $\partial S_{t_1}, \cdots, \partial S_{t_n}$ on condition of $\mathcal{E}_{t_0}$ of sample curves in the safe domain at instants of times $\tau_1, \cdots, \tau_m$.

$f_n^{-\cdots-}(t_1, \ldots, t_n \mid \mathcal{C}_t^+)$ — nth order in-crossing rate to $S_{t_1}, \ldots, S_{t_n}$ on condition of an out-crossing from S_t, $t_0 < t_1 < \cdots < t_n < t$.

$f_n^{+\cdots+}(t_2, \ldots, t_{n+1} \mid \mathcal{C}_{t_1}^-)$ — nth order out-crossing rate from $S_{t_2}, \ldots, S_{t_{n+1}}$ on condition of event $\mathcal{C}_{t_1}^-$. $t_0 < t_1 < t_2 < \cdots < t_{n+1}$.

$f_n^{+\cdots++}(t_n, \ldots, t_3, t_2, t \mid \mathcal{C}_{t_1}^- \cap \mathcal{F}_{t_{n+1}}^{(1)})$ — Kernel in integral equation for $f_{L_{t_1}^-}(t - t_1)$. nth order outcrossing rate from $S_{t_n}, \ldots, S_{t_3}, S_{t_2}, S_t$ on condition of $\mathcal{C}_{t_1}^-$ and on condition of a first-passage at time t_{n+1}, $t_0 < t_1 < t_{n+1} < t_n < \cdots < t_3 < t_2 < t$.

$f_n^{+\cdots+}(t_1, \ldots, t_n \mid \mathcal{E}_{t_0})$ — nth order out-crossing rate from $S_{t_1}, \ldots, S_{t_n}$ on condition of event $\mathcal{E}_{t_0}$.

$f_n^{+\cdots++}(t_{n-1}, \ldots, t_1, t \mid \mathcal{E}_{t_0} \cap \mathcal{F}_{t_n}^{(1)})$ — Kernel in integral equation for $f_{T_1}(t \mid \mathcal{E}_{t_0})$. nth order outcrossing rate from $S_{t_{n-1}}, \ldots, S_{t_1}, S_t$ on condition of $\mathcal{E}_{t_0}$ and on condition of a first-passage at the time $t_n, t_0 < t_n < t_{n-1} < \cdots < t_1 < t$.

$f_{n,g}(t_1,\ldots,t_n)$ — nth order product density of generalized renewal counting process.

$f_{n,o}(t_1,\ldots,t_n)$ — nth order product density of ordinary renewal counting process.

$f_{T_1}(t \mid \mathcal{E}_{t_0})$ — First-passage time probability density function on condition

of initial values in $\mathcal{E}_{t_0}$.

$f_{T_1}(t \mid \mathcal{E}_{t_0} \cap \mathcal{C}_{t_1}^+ \cap \cdots \cap \mathcal{C}_{t_n}^+)$ First-passage time probability density function on condition of $\mathcal{E}_{t_0}$ and on condition of later joint out-crossings from $S_{t_1}, \ldots, S_{t_n}$, $t_0 < t < t_1 < \cdots < t_n$.

$f_{T_n}(t \mid \mathcal{E}_{t_0})$ nth-passage time probability density function on condition of initial values in $\mathcal{E}_{t_0}$.

$f_P(p)$ Probability density function of P.

$f_{U_t^-}(u \mid \mathcal{E}_{t_0})$ Probability density function of U_t^- on condition of $\mathcal{E}_{t_0}$.

$f_{U_{t_1}^-}(u \mid \mathcal{E}_{t_0} \cap \mathcal{C}_{t_2}^+ \cap \cdots \cap \mathcal{C}_{t_n}^+ \cap \mathcal{C}_t^+)$ Probability density function of $U_{t_1}^+$ on condition of $\mathcal{E}_{t_0}$ and on condition of joint out-crossings from $S_{t_2}, \ldots, S_{t_n}, S_t$, $t_0 < t_1 < t_1 + l < t_2 < \cdots < t_n < t$.

$f_{U_t^+}(u \mid \mathcal{E}_{t_0})$ Probability density function of U_t^+ on condition of $\mathcal{E}_{t_0}$.

$f_{U_t^+}(u \mid \mathcal{E}_{t_0} \cap \mathcal{C}_{t_1}^+ \cap \cdots \cap \mathcal{C}_{t_n}^+)$ Probability density function of U_t^+ on condition of $\mathcal{E}_{t_0}$ and on condition of prior joint out-crossings from $S_{t_1}, \ldots, S_{t_n}$, $t_0 < t_1 < \cdots < t_n < t - l < t$.

$f_{\{\mathbf{V}\}}(\mathbf{z}, t)$ Joint probability density of $\mathbf{Z}(t)$ on condition of at least one pulse arrival.

$f_{\{\mathbf{V}\}\{\mathbf{Y}\}}(\mathbf{x}, \mathbf{y}, t)$ Joint monomodal probability density function of $\mathbf{V}(t)$ and auxiliary state vector $\mathbf{Y}(t)$.

$f_{V\dot{X}}(v, \dot{x}, t)$ Auxiliary monomodal joint probability density function in two-well Duffing oscillator problem.

$f_{\{\mathbf{X}\}\{\dot{X}_n\}}(\mathbf{x}_1, \dot{x}_1, t_1; \ldots; \mathbf{x}_n, \dot{x}_n, t_n \mid \mathcal{E}_{t_0})$ Joint nth order probability density function of vector process $\{\mathbf{X}(t), t \in [t_0, \infty[\}$ and relative normal velocity vector process $\{\dot{X}_n(\mathbf{b}(t)), t \in [t_0, \infty[\}$ on condition of $\mathcal{E}_{t_0}$. Joint conditioned probability density function of stochastic variables $\mathbf{X}(t_1), \dot{X}_n(\mathbf{b}(t_1)), \ldots, \mathbf{X}(t_n), \dot{X}_n(\mathbf{b}(t_n))$.

$f_{\{\mathbf{X}\}\{\dot{\mathbf{X}}\}}(\mathbf{x}_1, \dot{\mathbf{x}}_1, t_1; \ldots; \mathbf{x}_n, \dot{\mathbf{x}}_n, t_n)$ Joint unconditioned probability density function of stochastic variables $\mathbf{X}(t_1), \dot{\mathbf{X}}(t_1), \ldots, \mathbf{X}(t_n), \dot{\mathbf{X}}(t_n)$.

$f_{\{\mathbf{X}\}\{\dot{\mathbf{X}}\}\{\dot{X}_n\}}(\mathbf{x}_0, \dot{\mathbf{x}}_0, t_0; \mathbf{x}_1, \dot{x}_1, t_1; \ldots; \mathbf{x}_n, \dot{x}_n, t_n)$

Joint unconditioned probability density function of stochastic variables $\mathbf{X}(t_0), \dot{\mathbf{X}}(t_0), \mathbf{X}(t_1), \dot{X}_n(\mathbf{b}(t_1)), \ldots, \mathbf{X}(t_n), \dot{X}_n(\mathbf{b}(t_n))$, $t_0 < t_1 < \cdots < t_n$.

$f_{\{X\}\{\dot{X}\}}(x_1, \dot{x}_1, t_1; \ldots; x_n, \dot{x}_n, t_n)$ Joint unconditioned nth order probability density function of scalar processes $\{X(t), t \in [t_0, \infty[\}, \{\dot{X}(t), t \in [t_0, \infty[\}$. Joint probability density function of stochastic variables $X(t_1), \dot{X}(t_1), \ldots, X(t_n), \dot{X}(t_n)$.

$f_{\{X\}\{\dot{X}\}}(x_1, \dot{x}_1, t_1; \ldots; x_n, \dot{x}_n, t_n \mid \mathcal{E}_{t_0})$ Joint nth order probability density function of scalar processes $\{X(t), t \in [t_0, \infty[\}, \{\dot{X}(t), t \in [t_0, \infty[\}$ on condition of $\mathcal{E}_{t_0}$. Joint conditioned probability density function of stochastic variables $X(t_1), \dot{X}(t_1), \ldots, X(t_n), \dot{X}(t_n)$.

$f_{X\dot{X}V}(x, \dot{x}, v, t)$ Auxiliary monomodal joint probability density function in Bouc-Wen oscillator problem.

$f_{\dot{\mathbf{X}}T_1}(\mathbf{b}(t), \dot{\mathbf{x}} \mid \mathcal{E}_{t_0})$	Joint probability density function of first-passage time T_1 and associated out-crossing velocity vector $\dot{\mathbf{X}}$ per unit of area of ∂s_t at position $\mathbf{b}(t)$ on condition of initial values in $\mathcal{E}_{t_0}$. Markov vector processes.
$f_{\dot{X}L^-_{t_1}}(b, \dot{x}, t - t_1)$	Joint probability density function of the time interval spent in the safe domain after an in-crossing at the time t_1 and the associated out-crossing velocity $\dot{X}$ at the time t at the constant barrier b. 2-dimensional Markov vector processes.
$f_{\dot{X}T_1}(b, \dot{x}, t \mid \mathcal{E}_{t_0})$	Joint probability density function of first-passage time T_1 and associated out-crossing velocity $\dot{X}$ at constant barrier b on condition of initial values in $\mathcal{E}_{t_0}$. 2-dimensional Markov vector processes.
$f_{\dot{X}QT_1}(b, \dot{x}, q, t \mid \mathcal{E}_{t_0})$	Joint probability density function of first-passage time T_1 and associated out-crossing velocity $\dot{X}$ and hysteretic component Q at barrier b on condition of initial values in $\mathcal{E}_{t_0}$.
$f_{\dot{X}U^-_{t_1}}(b, \dot{x}, t - t_1 \mid \mathcal{E}_{t_0})$	Joint probability density function of the time interval between two succeeding out-crossings from the safe domain after an out-crossing at the time t_1 and the associated out-crossing velocity $\dot{X}$ at the time t at the barrier b on condition of $\mathcal{E}_{t_0}$. 2-dimensional Markov vector processes.
$f_{\{\mathbf{Y}\}}(\mathbf{y}, t)$	Joint probability density function of auxiliary state vector $\mathbf{Y}(T)$ at the transformation of Erlang process driven system into equivalent Poisson process driven system.
$f(\mathbf{Z}(t), t)$	Sufficiently smooth function.
$f_{\{\mathbf{Z}\}}(\mathbf{z}_1, t_1; \dots; \mathbf{z}_n, t_n)$	Joint unconditioned nth order probability density function of state vector $\mathbf{Z}(t)$. Joint probability density function of $\mathbf{Z}(t_1), \cdots, \mathbf{Z}(t_n)$.
$f(\alpha, \beta, \text{sign}(p))$	Function for specification of jump probability intensity function of α-stable Lévy motion.
$f_{\Delta V(t)}(v)$	Probability density function of α-stable random variable $\Delta V(t) \sim S_\alpha((a\Delta t)^{1/\alpha}, \beta, 0)$.
$f_{\{\mathbf{Z}\}}(\mathbf{z}, t \mid N(t) > 0)$	Joint probability density of $\mathbf{Z}(t)$ on condition of at least one pulse arrival. Equal to $f_{\{\mathbf{V}\}}(\mathbf{z}, t)$.
$G_{i_1 \dots i_k}(\mathbf{z}; \boldsymbol{\mu}, \boldsymbol{\kappa})$	Hermite polynomial adjoint to $H_{i_1 \dots i_k}(\mathbf{z}; \boldsymbol{\mu}, \boldsymbol{\kappa})$.
$\mathbf{g}$	Global geometrical matrix.
$\mathbf{g}_e$	Local geometrical matrix for plastic element e.
$g(\dot{X}, Q)$	State dependent function specifying the development of damage indicator $D(t)$.
$g(X)$	Nonlinear displacement dependent damping coefficient. $(u(X, \dot{X}) = g(X)\dot{X} + k(X)X)$.
$g_n^{+\cdots+}(t_1, \dots, t_n \mid \mathcal{E}_{t_0})$	Functions in formal inclusion–exclusion expansion of $h_{T_1}(t \mid \mathcal{E}_{t_0})$.

$H(x)$	Heaviside's unit step function.
$H(\omega)$	Frequency response function.
$H_i(x)$	Univariate Hermite polynomial generated by $\varphi(x)$.
$H_{i_1 \ldots i_k}(\mathbf{z}; \boldsymbol{\mu}, \boldsymbol{\kappa})$	Multivariate Hermite polynomial generated by $\varphi_n(\mathbf{z}; \boldsymbol{\mu}, \boldsymbol{\kappa})$.
$H_{mn}(\xi_1, \xi_2 \; ; \rho)$	Bivariate Hermite polynomial generated by $\varphi_2(\xi_1, \xi_2; \rho)$.
$\mathcal{H}^{(1)}_{]t,t+\Delta t]}$	Event that an out-crossing through ∂S_t takes place during $]t, t+\Delta t]$ on condition of $\mathcal{E}_{[t_0,t]} = \cap_{\tau \in [t_0,t]} S_\tau$.
$\mathcal{H}^{(n)}_{]t,t+\Delta t]}$	Event that an out-crossing through ∂S_t takes place during $]t, t+\Delta t]$ on condition of $\mathcal{E}^{(n)}_{]t_0,t]}$.
h	Thickness of soil layer.
$h(t)$	Impulse response function of linear time-invariant system.
$\dot{h}(t)$	$\frac{\mathrm{d}}{\mathrm{d}t} h(t)$. Velocity impulse response function of linear time-invariant system.
$h_{\max}$	Maximum of $h(t)$ for $t \in [0, \infty[$.
$h_{T_1}(t \mid \mathcal{E}_{t_0})$	Hazard rate on condition of $\mathcal{E}_{t_0}$.
$h_{T_n}(t \mid \mathcal{E}_{t_0})$	Hazard rate for the nth out-crossing event on condition of $\mathcal{E}_{t_0}$.
I_0	Bending moment of inertia for yield hinge element.
I_i	Bending moment of inertia for beam element i.
I_i	Interarrival time-interval between impulses.
$J_{\{\mathbf{Z}\}}(\mathbf{x}\|\mathbf{z}, t)$	Jump probability intensity function for the state vector process $\{\mathbf{Z}(t), t \in [t_0, t_1]\}$ for jump into interval $]\mathbf{x}, \mathbf{x} + d\mathbf{x}]$ per unit of time t on condition of start in $\mathbf{Z}(t) = \mathbf{z}$ at the time t.
$J_{\{V_\alpha\}}(p_\alpha, t)$	Jump probability intensity function for the component jump process $\{V_\alpha(t), t \in]t_0, t_1]\}$ for jump into interval $]p_\alpha, p_\alpha + dp_\alpha]$ per unit of time at the time t.
$\mathbf{K}$	"Stiffness"-tensor in Petrov-Galerkin variational approach.
$\mathbf{K}_0$	Global stiffness matrix for linear elastic structural elements.
$K_{I_1 J_1 I_2 J_2}$	Component of "stiffness"-tensor $\mathbf{K}$ in Petrov-Galerkin variational approach.
$\mathcal{K}_{\mathbf{z},t}[\cdot]$	Forward Chapman-Kolmogorov differential-integro operator (Fokker-Planck operator). Time-invariant version: $\mathcal{K}_{\mathbf{z}}[\cdot]$.
$\mathcal{K}^T_{\mathbf{z},t}[\cdot]$	Backward Chapman-Kolmogorov differential-integro operator. Time-invariant version: $\mathcal{K}^T_{\mathbf{z}}[\cdot]$.
k	Parameter in Gamma-distributed interarrival times $I_i \sim G(k-1, \nu)$ of Erlang renewal process.
k_0	Equal to $\left[\frac{k+1}{2}\right]$.

$k(X)$	Nonlinear displacement dependent stiffness coefficient. $(u(X,\dot{X}) = g(X)\dot{X} + k(X)X)$.
L	Length of time interval spent in safe domain. Stochastic start problem of stationary processes with time-invarient safe domain.
L_t^-	Length of time interval spent in safe domain after an in-crossing to S_t.
L_t^+	Length of time interval spent in safe domain before an out-crossing from S_t.
$\mathcal{L}_{t_2,t}$	Joint event $\mathcal{C}_{t_2}^- \bigcap_{\tau\in]t_2,t[} \mathcal{S}_\tau \cap \mathcal{C}_t^+$.
l	Chord length of beam element in the deformed state.
$\mathbf{M}$	Mass matrix.
$\mathbf{M}$	"Mass"-tensor in Petrov-Galerkin variational approach.
$\mathbf{M}_e(t)$	Vector of member end-section moments $M_1(t)$ and $M_2(t)$.
$M_{I_1J_1I_2J_2}$	Component of "mass"-tensor $\mathbf{M}$ in Petrov-Galerkin variatioal approach.
$M(\Delta t, t, \Delta p, p)$	Random measure specifying number of jumps (impulses) of generating source $\{V(t),\ t \in [t_0,\infty[\}$ into the interval $]p, p+\Delta p]$ during the time interval $]t, t+\Delta t]$.
$M_1(t), M_2(t)$	Member end-section moments.
$M_\alpha(\Delta t, t, \Delta P, P)$	Random Poisson measure for αth component of compound Poisson vector process.
$M_P(\theta)$	Characteristic function of impulse strength P.
$M_y, M_{y,i}$	Yield moment of beam. Yield moment of beam i.
$M_{\{X\}\{\dot{X}\}}(\theta_1,\theta_2,t \mid \mathbf{z}_0, t_0)$	Joint characteristic function of $X(t), \dot{X}(t)$ on condition of the state $\mathbf{z}_0^T = [x_0, \dot{x}_0]$ at the time t_0.
$M_{\mathbf{V}}(\boldsymbol{\theta}; t_1, \ldots, t_n)$	Joint characteristic function of random vector $\mathbf{V}^T(t) = [V(t_1), \ldots, V(t_n)]$.
$M_{\{\mathbf{Z}\}}(\boldsymbol{\theta}, t)$	Joint characteristic function of state vector $\mathbf{Z}^T(t) = [Z_1(t), \ldots, Z_n(t)]$.
m	Mass of single-degree-of-freedom oscillator.
m_i	Mass of ith storey in shear building.
$m_N(\mathbf{z})$	Nth order moment of first-passage time T_1 on condition of deterministic start in $\mathbf{Z}(t_o) = \mathbf{z}$. $(E[T_1^N \mid \mathbf{Z}(t_0) = \mathbf{z}_0])$.
$N_I^{(1)}(x)$	Continuous shape function. $N_I^{(1)}(x) = 0$ for $(x,\dot{x}) \in \partial S^{(1)}$.
$N_J^{(2)}(\dot{x})$	Continuous shape function.
$\{N(t), t \in]t_0,\infty[\}$	Non-stationary Poisson counting process.
$\{N^-(t), t \in]t_0,\infty[\}$	Counting process specifying the number of in-crossings to the safe domain.
$\{N^+(t), t \in]t_0,\infty[\}$	Counting process specifying the number of out-crossings from

	the safe domain.
$N(\mu, \sigma^2)$	Class of normal distributed stochastic variables with mean value μ and variance σ^2.
N_e	Axial force along chord line of beam member.
$\{N_r(t),\ t \in]t_0, \infty[\}$	Renewal counting process.
$\mathbf{n}(\mathbf{b}(t))$	Unit normal vector in outward direction to ∂s_t at position $\mathbf{b}(t)$.
n	Parameter in Bouc-Wen hysteretic model.
n	Number of iterations until stationarity is achieved in path integration technique.
n	Dimension of state vector $\mathbf{Z}(t)$.
n_1	Dimension of $\mathbf{X}(t)$.
n_2	Dimension of $\mathbf{Q}(t)$ and $\mathbf{q}(t)$.
n_3	Dimension of $\mathbf{W}(t)$.
n_4	Dimension of $\mathbf{V}(t)$.
$\mathrm{O}(x)$	Order notation symbol. ($\lim_{x \to 0} \mathrm{O}(x) \leq A\,x$, A being a positive constant).
P	Intensity of impulses of compound Poisson process.
$P(z)$	Numerator polynomial of rational frequency response function.
$P_0(t, t_0)$	Probability of no Poisson events in the interval $]t_0, t]$.
P_α	Intensity of impulses of αth component of compound Poisson vector process.
$P(\mathcal{E})$	Probability of the event $\mathcal{E}$.
$\mathcal{P}$	Sample space of impulse strength, P.
$P_f([t_0, t_1])$	Probability of failure in the time interval $[t_0, t_1]$.
$P_f([0, t]; x)$	Probability of failure in the time interval $[0, t]$ for single barrier problem with variable upper barrier x.
P_{jk}	Parameter entering modified cumulant neglect closure scheme for bilinear oscillator.
$P_{\{N\}}(n, t, t_0)$	Probability function of the first order of Poisson counting process $\{N(\tau), \tau \in]t_0, t]\}$.
$\mathbf{p}_1, \cdots, \mathbf{p}_r$	Real matrices in linear output filter differential equations for $\mathbf{F}(t)$.
p	Sample value of P.
$p_1, \cdots, p_r$	Real constants in linear output filter differential equation for $F(t)$.
p_i, α	Coefficients in Hermite polynomial $H_i(x)$.

$\mathbf{Q}(t)$	Vector of generalized stresses from all plastic elements.
$\mathbf{Q}_e(t)$	Vector of local generalized stresses for plastic element e.
$\mathbf{Q}^{(i)}$	Transition probability matrix of Markov chain during ith transition.
$Q(t)$	Hysteretic component of restoring force in single-degree-of-freedom system.
$Q(z)$	Denominator polynomial of rational frequency response function.
$Q^0(t)$	$Q(t) - E[Q(t)]$. Zero-mean centralized hysteretic component.
$Q_i(t)$	Hysteretic component of shear force between $(i-1)$th and ith storey in shear building.
$Q_{jk}^{(i)}$	Component in jth row and kth column of $\mathbf{Q}^{(i)}$. Probability of transition from $\mathbf{z}_k$ to jth cell during interval $]t_i, t_i + \Delta t_i]$.
$\mathbf{q}(t)$	Vector of generalized strains from all plastic elements.
$\mathbf{q}_e(t)$	Vector of local generalized strains for plastic element e.
$\mathbf{q}_1, \cdots, \mathbf{q}_s$	Real matrices in linear input filter differential equations for $\mathbf{F}(t)$.
$q^{(0)}(\mathbf{z}, t)$	Abbreviation for $q_{\{\mathbf{Z}\}}(\mathbf{z}, t \mid \mathbf{x}, t_0)$.
$q^{(1)}(\mathbf{z}, t)$	Abbreviation for $q_{\{\mathbf{Z}\}}(\mathbf{y}, t_1 \mid \mathbf{z}, t)$.
q_0	Modal value for peaks in Bouc-Wen oscillator problem.
$q_1, \cdots, q_s$	Real constants in linear input filter differential equation for $F(t)$.
q_a	Amplitude of harmonic varying shear stress.
q_y	Yield value of hysteretic restoring force component.
$q_{y,i}$	Yield value of hysteretic component of shear force between $(i-1)$th and ith storey in shear building.
$q_{\{\mathbf{Z}\}}(x, \dot{x}, t \mid \mathcal{C}_{t_1}^-)$	Joint probability density function of displacement x and velocity $\dot{x}$ at the time t on condition of an in-crossing at the time $t_1 < t$. 2-dimensional Markov processes.
$q_{\{\mathbf{Z}\}}(x, \dot{x}, t \mid \mathcal{E}_{t_0})$	Joint probability density function of displacement x and velocity $\dot{x}$ at the time t on condition of $\mathcal{E}_{t_0}$. 2-dimensional Markov processes.
$q_{\{\mathbf{Z}\}}(x, \dot{x}, t \mid \mathcal{E}_{t_0} \cap \mathcal{C}_{t_1}^+)$	Joint probability density function of displacement x and velocity $\dot{x}$ at the time t on condition of $\mathcal{E}_{t_0}$ and on condition of an out-crossing at the time t_1, $t_0 < t_1 < t$. 2-dimensional Markov processes.
$q_{\{\mathbf{Z}\}}(\mathbf{z}, t \mid \mathbf{z}_0, t_0)$	Joint transition probability density function of Markov vector process $\{\mathbf{Z}(t), t \in [t_0, \infty[\}$. Transition from state $\mathbf{z}_0$ at the time t_0 to state $\mathbf{z}$ at the time t.
$q_{\{\mathbf{Z}\}}^{(n)}(\mathbf{z}, t \mid \mathbf{z}_0, t_0)$	Joint transition probability function of Markov vector process

	$\{\mathbf{Z}(t), t \in [t_0, \infty[\}$ on condition of exact n pulses in $[t_0, t[$.
$q_{\{Z\}}(z, t \mid z_0, t_0)$	Transition probability density function of Markov scalar process $\{Z(t), t \in [t_0, \infty[\}$. Transition from state z_0 at the time t_0 to state z at the time t.
$\mathbf{R}(\tau)$	Vector of expansion coefficients $R_{IJ}(\tau)$ in Petrov-Galerkin variational approach.
R	Set of real numbers.
$R_{IJ}(\tau)$	Expansion coefficients in Petrov-Galerkin variational approach for the solution of $R(\tau\|\mathbf{z})$.
$R(\tau\|\mathbf{z})$	$1 - F_{T_1}(\tau\|\mathbf{z})$. Reliability function for first-passage time problem with deterministic start in $\mathbf{Z}(0) = \mathbf{z}$.
$R(t_1, t_2)$	Correlation coefficient of point process.
$R[q^{(0)}(\mathbf{z}, t), q^{(1)}(\mathbf{z}, t)]$	Boundary value terms in variational equation (3-103). Cancels for adjoint operators.
$R_{T_1}^{(n)}(t)$	nth lower bound to the first-passage time probability density function.
$r_{l,i}$	Coefficient in expansion for $E[X^l(t)\dot{X}^m(t)Q^n(t)]$ for bilinear oscillator.
$S_i(t)$	$\mathrm{Im}(U_j)$. Auxiliary state variable at the transformation of Erlang process driven system into equivalent Poisson process driven system.
$S(i\theta_1, i\theta_2)$	Part of log-characteristic function of $q_{\{\mathbf{Z}\}}(\mathbf{z}, t \mid \mathbf{z}_0, t_0)$ in case of compound Poisson driven system.
S_0	Auto-spectral density function of Gaussian white noise.
$S_{T_1}^{(n)}(t)$	nth upper bound to the first-passage time probability density function.
S_t	Safe domain at the time t.
S_t^c	Unsafe domain at the time t. Complement to S_t.
$S(t)$	Weighted integral of $R(\tau, t)$.
$\mathcal{S}_t$	Event that $\mathbf{X}(t)$ attains value in S_t.
$s_i(t)$	Equivalent linear stiffness of hysteretic component of shear force between $(i-1)$th and ith storey in shear building.
$s_{n,k}$	Coefficient in expansion for $E[X^l(t)\dot{X}^m(t)Q^n(t)]$ for bilinear oscillator.
T_0	Period of linear undamped eigenvibrations of single-degree-of-freedom system.
T_1	First-passage time.
T_i	Shear force between $(i-1)$th and ith storey in shear building.
T_m	Time for maximum value of intensity function of white noise excitation.

T_n	nth-passage time. Elapsed time until the nth out-crossing from the safe domain.
t	Time.
t_0	Initial time of excitations.
t_1	Terminal time of excitations.
t_i	Arrival time of impulse of compound Poisson process.
$t_k(\beta)$	Auxiliary function in analytical solution for $s_{n,k}$.
$t_{\max}$	Time for maximum value of $h(t)$.
$\mathbf{U}$	Vector specifying the stiff-body motion of all global degrees-of-freedom due to unit horizontal translation of ground surface.
$U(x)$	Potential function of two-well Duffing oscillator problem.
$U_i(t)$	Auxiliary complex state variable at the transformation of Erlang process driven system into equivalent Poisson process driven system.
U_t^-	Elapsed time interval until the next out-crossing after an out-crossing from S_t.
U_t^+	Elapsed time interval between an out-crossing from S_t and the previous out-crossing.
$\mathcal{U}_{t_2,t}$	Joint event $\mathcal{C}_{t_2}^+ \cap \{\text{exactly one in-crossing in }]t_2, t[\} \cap \mathcal{C}_t^+$.
$u(\mathbf{z})$	Sufficiently smooth function of state vector in Petrov-Galerkin variational approach. $u(\mathbf{z}) = 0$ for $\mathbf{z} \in \partial S_t^{(1)}$.
$u(X(t), \dot{X}(t))$	Restoring force per unit mass of single-degree-of-freedom time-invariant non-linear oscillator.
$u(x_2, t)$	Horizontal displacement of soil.
u_e	Elongation along chord line of beam member.
$\ddot{u}_g(t)$	Ground surface acceleration.
$\{\mathbf{V}(t), t \in]t_0, t_1]\}$	Vector jump process with independent increments.
$V_I^{(1)}(x)$	Continuous and piecewise differentiable weight function. $V_I^{(1)}(x) = 0$ for $(x, \dot{x}) \in \partial S^{(0)}$.
$V_J^{(2)}(\dot{x})$	Continuous and infinitely many times differentiable weight function. $V_J^{(2)}(\dot{x}) = 0$ for $(x, \dot{x}) \in \partial S^{(2)}$.
$V_{IJ}(x, \dot{x})$	Weight function. Equal to $V_I^{(1)}(x) V_J^{(2)}(\dot{x})$.
$V(t)$	Auxiliary random variable with monomodal probability density function.
$\{V(t), t \in]t_0, t_1]\}$	Scalar jump process with independent increments.
$V_i(v)$	Orthonormal polynomials of probability density function $f_V(v)$ of $V(t)$.

$\{V_\alpha(t), t \in]t_0, t_1]\}$	αth component process of $\{\mathbf{V}(t), t \in]t_0, t_1]\}$.
$v_{i,\alpha}$	Coefficients in orthonormal polynomials $V_i(v)$.
$v(\mathbf{z})$	Sufficiently smooth function of state vector in Petrov-Galerkin variational approach. $v(\mathbf{z}) = 0$ for $\mathbf{z} \in \partial S_t^{(0)}$.
$\{\mathbf{W}(t), t \in]t_0, t_1]\}$	Vector Wiener process.
$\{W(t), t \in]t_0, t_1]\}$	Scalar Wiener process.
$\{W_\alpha(t), t \in]t_0, t_1\}$	αth component process of $\{\mathbf{W}(t), t \in]t_0, t_1]\}$.
$\{\dot{W}(t), t \in]t_0, t_1]\}$	Stationary white noise process.
$\{\mathbf{X}(t), t \in [t_0, t_1]\}$	Vector displacement process.
$\{\mathbf{X}(t), t \in [t_0, t_1]\}$	Structural state vector process of compound Erlang process driven system.
$\{\dot{\mathbf{X}}(t), t \in [t_0, \infty[\}$	Velocity process of $\{\mathbf{X}(t), t \in [t_0, \infty[\}$.
X_0	Initial value of displacement.
$\dot{X}_0$	Initial value of velocity.
$\{X(t), t \in [t_0, \infty[\}$	Scalar displacement process.
$\{X_i(t), t \in [0, \infty[\}$	ith modal coordinate process.
$\{\dot{X}(t), t \in [t_0, \infty)\}$	Velocity process of $\{X(t), t \in [t_0, \infty[\}$.
$\dot{X}^0(t)$	$\dot{X}(t) - E[\dot{X}(t)]$. Zero-mean centralized velocity component.
$\dot{X}_n(\mathbf{b}(t))$	Component of relative velocity vector $\dot{\mathbf{X}}(t) - \dot{\mathbf{b}}(t)$ at failure surface in direction of $\mathbf{n}(\mathbf{b}(t))$.
$X_{\max}$	Maximum value of $\{X(\tau), \tau \in [0, t]\}$.
$X(\infty)$	Stationary displacement response as $t \to \infty$.
$\dot{X}(\infty)$	Stationary displacement velocity as $t \to \infty$.
$\mathbf{x}_e$	Vector of nodal point degrees-of-freedom $x_1, \ldots, x_6$ of beam element relative to local coordinates.
$\mathbf{x}_k$	$\mathbf{X}(t_i) = \mathbf{x}_k$. Initial value at time t_i of structural state vector process for compound Erlang process driven system.
x_0	Modal value for peaks in two-well Duffing oscillator problem.
$x_1, \ldots, x_6$	Nodal point degrees of beam element relative to local coordinates.
$\mathbf{Y}(t)$	Auxiliary vector of state variables of filter differential equations for $\mathbf{F}(t)$.
$\mathbf{Y}^{(s)}(t)$	$\frac{d^s}{dt^s}\mathbf{Y}(t)$. Auxiliary vector of state variables of differential equations for $\mathbf{F}(t)$.
$Y(t)$	Auxiliary state variable of filter differential equation for $F(t)$.
$Y_j(t)$	Equal to $\rho(N(t)+j-1)$. Auxiliary state variable at the transformation of arbitrary regular counting process $\{N(t), t \in$

	$]t_0, \infty[\}$ into equivalent Poisson process.
$Y^{(s)}(t)$	$\frac{d^s}{dt^s}Y(t)$. Auxiliary state variable in filter differential equation for $F(t)$.
$\mathbf{Z}(t)$	Markov state vector.
$\{\mathbf{Z}(t), t \in [t_0, t_1]\}$	Markov state vector process.
$\mathbf{Z}_0$	Initial value of Markov state vector.
$\{Z(t), t \in [t_0, t_1]\}$	Scalar Markov process.
$\{Z_i(t), t \in [t_0, t_1]\}$	ith component process.
$Z_i^0(t)$	$Z_i(t) - \mu_i(t)$. Mean value centered state variable.
$\mathbf{z}_k$	Centre of kth cell in path integration technique.
z_j	Root of $Q(z) = 0$.
α	Non-hysteretic fraction of total restoring force in single-degree-of-freedom system.
α	Parameter of α-stable random variable.
α	Decay rate coefficient ($\alpha = \lambda_1 / f_1^+$).
α	Upwind parameter for flow in x-direction in Petrov-Galerkin variational approach.
α_i	Elastic fraction of restoring force between $(i-1)$th and ith storey in shear building.
$\alpha_i(\Theta_i, M_i)$	Indicator function. Equal to 1 at yielding in yield hinge i else 0.
α_y	Fraction $\frac{q_y}{q_y - q_0}$.
β	Skewness or asymmetry parameter of α-stable random variable.
β	Parameter in Bouc-Wen hysteretic model.
β	Fraction $\frac{q_y}{\sigma_V}$.
β	Upwind parameter for flow in $\dot{x}$-direction in Petrov-Galerkin approach.
β_i	Mode participation factor.
$\beta_{i_1 \ldots i_k}(t)$	Zero time-lag joint quasi-moments of the order k.
Γ_x	Local Peclet number for flow in x-direction in Petrov-Galerkin variational approach.
$\Gamma_{\dot{x}}$	Local Peclet number for flow in $\dot{x}$-direction in Petrov-Galerkin variational approach.
γ	Parameter in Bouc-Wen hysteretic model.
γ	Interaction parameter specifying the relative width of the upwind correction for the weighting functions in $\dot{x}$-direction in Petrov-Galerkin variational approach.

$\gamma_{i_1 \ldots i_k}(t)$	Joint Hermite moments of the order k.
$\Delta \mathbf{z}_k$	Volume of kth cell in path integration technique.
$\Delta N^-(t)$	Increment $N(t+\Delta t)-N^-(t)$ of $\{N^-(t)\}$ in the interval $]t, t+\Delta t]$.
$\Delta N^+(t)$	Increment $N^+(t+\Delta t)-N^+(t)$ of $\{N^+(t)\}$ in the interval $]t, t+\Delta t]$.
Δt	Length of time-interval.
$\Delta V(t)$	Increment $V(t+\Delta t)-V(t)$ of $\{V(t)\}$ in the interval $]t, t+\Delta t]$.
$\Delta W(t)$	Increment $W(t+\Delta t)-W(t)$ of $\{W(t)\}$ in the interval $]t, t+\Delta t]$.
Δx	Spacing of finite elements in x-direction in Petrov-Galerkin variational approach.
$\Delta \dot{x}$	Spacing of finite elements in $\dot{x}$-direction in Petrov-Galerkin variational approach.
$\Delta \tau$	Time step for diffusion of impulse in Method 1 for path integration of Poisson process driven systems.
δ	Maximum softening damage indicator.
$\delta(x)$	Dirac's delta function.
δ_c	Critical level of maximum softening damage indicator.
$\delta_i(t)$	Local softening between $(i-1)$th and ith storey in shear building.
$\delta\alpha\beta$	Kronecker's delta.
∂S_t	Failure surface at the time t.
$\partial S_t^{(a)}$	Accessible part of failure surface ∂S_t.
$\partial S_t^{(0)}$	Entrance part of failure surface ∂S_t.
$\partial S_t^{(1)}$	Exit part of failure surface ∂S_t.
$\partial S_t^{(2)}$	Non-accessible part of failure surface ∂S_t.
∂s_t	Failure surface at the time t. Trace in displacement space of ∂S_t.
ε	Nonlinearity parameter of Duffing oscillator.
ε_{12}	Shear strain.
ϵ_i	$c_i - c_{eq,i}$. Error vector.
ζ	Damping ratio.
$\zeta_{0,i}$	Nondimensional linear viscous damping coefficient between $(i-1)$th and ith storey in shear building.
ζ_i	Modal damping ratio in the ith mode.
ζ_f	Damping ratio of 2nd order sharpening filter.

ζ_g	Damping ratio of subsoil. Parameter in Kanai-Tajimi filter.
$\boldsymbol{\kappa}$	Covariance vector of Gaussian stochastic vector.
$\boldsymbol{\kappa}(\dot{\mathbf{q}}, \mathbf{Q})$	State dependent stiffness matrix for all plastic elements.
$\boldsymbol{\kappa}_0, \boldsymbol{\kappa}_1, \boldsymbol{\kappa}_2$	Coefficient matrices in state dependent stiffness matrix $\boldsymbol{\kappa}_e(\dot{\boldsymbol{\Theta}}_e, \mathbf{M}_e)$ for yield hinge element e.
$\boldsymbol{\kappa}_e(\dot{\mathbf{q}}_e, \mathbf{Q}_e)$	State dependent stiffness matrix for plastic element e.
$\boldsymbol{\kappa}_{e,0}$	Elastic stiffness matrix for plastic element e.
$\kappa(\dot{X}(t), Q(t))$	State dependent stiffness coefficient of hysteretic component.
$\kappa_{i_1 \ldots i_k}(t)$	Zero time-lag joint cumulants of the order k.
$\kappa_{mn}[X(t), \dot{X}(t) \mid \mathbf{z}_0, t_0]$	Joint cumulant of order $m+n$ of $X(t)$ and $\dot{X}(t)$ at the time t, conditioned on the state $\mathbf{z}_0$ at the time t_0. $\frac{\partial^{n+m}}{\partial(i\theta_1)^m \partial(i\theta_2)^n} \ln M_{\{X\}\{\dot{X}\}}(\theta_1, \theta_2, t \mid \mathbf{z}_0, t_0) \mid_{\theta_1=\theta_2=0}$.
$\kappa_n[V(t_1), \ldots, V(t_n)]$	Joint nth order cumulant of random vector $\mathbf{V}^T(t) = [V(t_1), \ldots, V(t_n)]$.
$\kappa_{XX}(t_1, t_2)$	Auto-covariance function of $\{X(t), t \in [t_0, \infty[\}$.
$\kappa_{X_\alpha X_\beta}(t_1, t_2)$	Cross-covariance function of $\{X_\alpha(t), t \in [t_0, \infty[\}$ and $\{X_\beta(t), t \in [t_0, \infty[\}$.
Λ_t	Set of out-crossing velocity vectors with $\dot{X}_n > 0$.
$\boldsymbol{\lambda}(t)$	Covariance matrix for $t > t_i$ of Gaussian stochastic vector on condition of $\mathbf{Z}(t_i) = \mathbf{z}_k$.
$\dot{\lambda}$	Plastic potential multiplier.
λ_i	Solution to characteristic equation.
$\lambda_{i_1 \ldots i_k}(t)$	$E[(Z_{i_1}(t) - \mu_{i_1}(t)) \cdots (Z_{i_k}(t) - \mu_{i_k}(t))]$. Zero time-lag joint central moments of the order k.
$\lambda^0_{i_1 \ldots i_k}(t)$	$E[(V_{i_1}(t) - \mu^0_{i_1}(t)) \cdots (V_{i_k}(t) - \mu^0_{i_k}(t))]$. Zero time-lag joint central moments of the order k on condition of at least one pulse arrival.
λ_n	nth eigenvalue of the forward and backward integro-differential Chapman-Kolmogorov operator.
$\lambda_n(t)$	Fraction used for closing inclusion-exclusion series. Method by Roberts and Kimura et al.
λ_{mn}	Normalized joint conditioned cumulant of order $m+n$ of $X(t)$ and $\dot{X}(t)$.
$\boldsymbol{\mu}(t)$	Mean value vector of Gaussian stochastic vector. Also used as mean value vector for $t > t_i$ of Gaussian stochastic vector on condition of $\mathbf{Z}(t_i) = \mathbf{z}_k$.
μ	Shift or location parameter of α-stable random variable.
$\mu_D(t)$	Mean value function of damage indicator $D(t)$.
μ_i	Mass ratio. Mass of ith storey in proportion to mass of $(i-1)$th storey in shear building.

μ_i	Mass per unit length for beam i.
$\mu_i(t)$	$E[Z_i(t)]$. Mean value function of ith component.
$\mu_{i_1 \ldots i_k}(t)$	$E[Z_{i_1}(t) \cdots Z_{i_k}(t)]$. Zero time-lag joint moments of the order k.
$\mu^0_{i_1 \ldots i_k}(t)$	$E[V_{i_1}(t) \cdots V_{i_k}(t)]$. Zero time-lag joint moments of the order k on condition of at least one pulse arrival.
$\mu_X(t)$	Mean value function of $\{X(t), t \in [t_0, \infty[\}$.
$\mu[X(t) \mid \mathbf{z}_0, t_0]$	Mean value function of $\{X(t), t \in [t_0, \infty[\}$ on condition of initial values $\mathbf{z}_0$ at the time t_0.
$\mu[\dot{X}(t) \mid \mathbf{z}_0, t_0]$	Mean value function of $\{\dot{X}(t), t \in [t_0, \infty[\}$ on condition of initial value $\mathbf{z}_0$ at the time t_0.
$\mu(x_2, t)$	Position and time-dependent shear modulus.
$\overline{\frac{\nu E[P^2]}{m^2}}$	Average diffusion coefficient in Petrov-Galerkin approach for Poisson process driven systems.
$\nu(t)$	Mean arrival rate of impulses of Poisson counting process $\{N(t), t \in]t_0, \infty[\}$.
$\nu_\alpha(t)$	Mean arrival rate of αth component Poisson counting process $\{N_\alpha(t), t \in]t_0, \infty[\}$.
ξ_i	Sample of stochastic variable normalized to zero mean and unit standard deviation.
$\xi_i(t)$	$\frac{Z_i(t) - \mu_i(t)}{\sigma_{Z_i}(t)}$. Zero-mean centered state variable, normalized to unit standard deviation.
$\boldsymbol{\pi}^{(i)}$	Vector of state probabilities $\pi^{(i)}_j$.
$\boldsymbol{\pi}^{(\infty)}$	Stationary distribution of states.
$\pi^{(i)}_j$	Probability of being in the jth cell at the time $t_i = i\Delta t$.
ρ	Mass density of soil.
$\rho(N(t))$	Zero-memory transformation of Poisson counting process into Erlang renewal process.
$\rho_{XX}(\tau)$	Auto-correlation coefficient function of the displacement process.
$\rho_{X_i X_i}(\tau)$	Auto-correlation coefficient function of the modal coordinate process $\{X_i(t), t \in [0, \infty[\}$.
$\rho[X(t)\dot{X}(t) \mid \mathbf{z}_0, t_0]$	Auto-correlation coefficient of $X(t)$ and $\dot{X}(t)$ on condition of initial values $\mathbf{z}_0$ at the time t_0.
σ	Scale or dispersion parameter of α-stable random variable.
σ	Parameter in Rayleigh distribution.
σ_{12}	Shear stress.
$\sigma_{12,y}(x_2, t)$	Position and time-dependent shear strength.
$\sigma_D(t)$	Standard deviation of damage indicator $D(t)$.

$\sigma_{M_i}(t)$	Time-dependent standard deviation of end-section moment $M_i(t)$.
σ_P	Standard deviation of P.
$\sigma_{X,0}$	Stationary value of standard deviation of $X(t)$ for linear oscillator.
$\sigma_X(\infty)$	Stationary value of standard deviation of $X(t)$ for non-linear oscillator.
σ_{X_i}	Stationary standard deviation of response from the ith mode.
$\sigma_{\dot{X},0}$	Stationary value of standard deviation of $\dot{X}(t)$ for linear oscillator.
$\sigma[X(t) \mid \mathbf{z}_0, t_0]$	Standard deviation of $X(t)$ on condition of initial values $\mathbf{z}_0$ at the time t_0.
$\sigma^0_{\ddot{u}g}$	Stationary standard deviation of ground surface acceleration.
$\sigma_{Z_i}(t)$	Time-dependent standard deviation of ith state vector component.
$\sigma_{\dot{\Theta}_i}(t)$	Time dependent standard deviation of end-section rotational velocity $\dot{\Theta}_2(t)$.
$\Phi(x)$	Distribution function of standardized normal variable.
$\Phi^{(n)}(\mathbf{z})$	Eigenfunction of forward integro-differential Chapman-Kolmogorov equation with absorption on the entrance part of the boundary.
$\Phi(\xi)$	Non-dimensional shape function as a function of $\xi = \frac{x_2}{h}$.
$\varphi(x)$	Probability density function of standardized normal variable.
$\varphi_2(\xi_1, \xi_2; \rho)$	Joint probability density function of bivariate normal stochastic variable with correlation coefficient ρ, standardized to zero mean values and unit standard deviations.
$\varphi_n(\mathbf{z}; \boldsymbol{\mu}, \boldsymbol{\kappa})$	Multivariate Gaussian joint probability density function with mean value vector $\boldsymbol{\mu}$ and covariance matrix $\boldsymbol{\kappa}$.
$\varphi_{2n}(\mathbf{x}, \dot{\mathbf{x}}; \mathbf{C})$	$2n$-dimensional joint probability density function of zero mean normal distributed stochastic vector $[\mathbf{X}, \dot{\mathbf{X}}]^T$ with covariance matrix $\mathbf{C}$.
$\Psi^{(n)}(\mathbf{z})$	Eigenfunction of backward integro-differential Chapman-Kolmogorov equation with absorption on the exit part of the boundary.
$\boldsymbol{\Theta}_e(t)$	Vector of member end rotations $\Theta_1(t)$ and $\Theta_2(t)$
$\Theta_1(t), \Theta_2(t)$	Member end rotations.
ω_0	Circular undamped eigenfrequency of linear single-degree-of-freedom system.
$\omega_{0,i}$	Parameter for specification of linear elastic fraction of shear force between $(i-1)$th and ith storey in shear building.

ω_f	Circular eigenfrequency of 2nd order sharpening filter.
ω_g	Circular eigenfrequency of subsoil. Parameter in Kanai-Tajimi filter.
$\binom{n}{j}$	Binomial coefficient.
$\{\cdot\}_s$	Permutation operator.

6. SUMMARY IN DANISH

I afsnit 2.1 er indledningsvis udledt identiteter mellem førstepassage sandsynlighedstæthedsfunktionen under betingelse af hændelsen $\mathcal{E}_{t_0}$, $f_{T_1}(t \mid \mathcal{E}_{t_0})$, og sandsynlighedstæthed-funktionenerne $f_{L_t^+}(t-t_1)$ og $f_{U_t^+}(t-t_1 \mid \mathcal{E}_{t_0})$ for henholdsvis længden af tidsintervallet tilbragt i det sikre område fra den foregående indkrydsning til tidspunktet t_1 til udkrydsningen til tidspunktet t, og den forløbne tid fra den foregående udkrydsning til tidspunktet t_1 til udkrydsningen til tidspunktet t under betingelse af hændelsen $\mathcal{E}_{t_0}$. $\mathcal{E}_{t_0}$ betegner hændelsen, at en mængde af begyndelsesværdier tilhører det sikre område til tiden t_0. Forbindelsen mellem svigtsandsynligheden $P_f([t_0,t])$ og disse størrelser er ligeledes anført.

I afsnit 2.2 opstilles en Volterra integralligning for $f_{T_1}(t \mid \mathcal{E}_{t_0})$, hvor kernefunktionen introduceres som en ny ukendt funktion. Baseret på denne integralligning er udledt inclusion-exclusionrækker for $f_{T_1}(t \mid \mathcal{E}_{t_0})$, og for tælleren og nævneren af kernefunktionen i integralligningen, udtrykt i de simultane betingede udkrydsningsfrekvenser $f_n^{+\cdots+}(t_1,\ldots,t_n \mid \mathcal{E}_{t_0})$. Herefter formuleres en integralligning for førstepassage sandsynlighedstæthedsfunktionen til tiden t under betingelse af efterfølgende udkrydsninger til tiderne $t_1,\ldots,t_n$, der er betegnet $f_{T_1}(t \mid \mathcal{E}_{t_0} \cap \mathcal{C}_{t_1}^+ \cap \cdots \cap \mathcal{C}_{t_n}^+)$, $t_0 < t < t_1 < \cdots < t_n$. Denne størrelse forekommer i restleddet af inclusion-exclusionrækken for $f_{T_1}(t \mid \mathcal{E}_{t_0})$. Ideen er at bestemme en approksimativ løsning til den pågældende integralligning. Ved indsætning heraf i restleddet for rækkeudviklingen af $f_{T_1}(t \mid \mathcal{E}_{t_0})$ kan hurtig konvergens herved forventes. I forbindelse hermed er tillige udledt en integralligning formuleret for n-passage sandsynlighedstæthedsfunktionen $f_{T_n}(t \mid \mathcal{E}_{t_0})$, og den tilhørende inclusion-exclusionrække er udledt for denne størrelse og for nævneren og tælleren af kernefunktionen. Dernæst vises, at alle de anførte integralligninger og tilhørende inclusion-exclusionrækker alternativt kan formuleres i simultane udkrydsningsfrekvenser for realisationer, der er i det sikre område til diskrete tidspunkter $\tau_1,\ldots,\tau_m$ under betingelse af $\mathcal{E}_{t_0}$. Disse er betegnet $f_n^{+\cdots+}(t_1,\ldots,t_n\ ;\ \mathcal{S}_{\tau_1} \cap \cdots \cap \mathcal{S}_{\tau_m} \mid \mathcal{E}_{t_0})$. Ved passende valg af de intermediære tidspunkter $\tau_1,\ldots,\tau_m$ opnås nøjagtigere approksimationer til de forskellige integralligninger og hurtigere konvergens af inclusion-exclusionrækkerne. Dernæst er formuleret en inclusion-exclusionrække for hazard hastigheden, en størrelse der er direkte anvendelig i pålidelighedsproblemer, og en ikke-lineær integralligning af Volterra typen er formuleret for denne. Et grundlæggende problem for alle de omtalte inclusion-exclusionrækkeudviklinger er, at disse er divergent ved afrunding af vilkårlig endelig orden, når påvirkningstiden vokser mod uendelig. Yderligere kan kun et stærkt begrænset antal led normalt beregnes. I eksempel 2-1 undersøges forskellige måder at afrunde disse rækker. Konklusionerne, der drages heraf, er, at alle tilgængelige lukningsmetoder er baseret på svage forudsætninger og synes motiveret primært af deres mulighed for at udregne rækken på sluttet form. I stedet foreslås anvendt integralligningsmetoder med passende approksimationer til kernefunktionen, der involverer de samme beregningsmæssige omkostninger, men fører til mere rationelt begrundede og nøjagtige resultater. Endelig betragtes dynamiske systemer påvirket af processer med uafhængige tilvækster, såsom Wiener processen eller en sammensat Poisson proces. Tilstandsvektoren sammensat af flytningskomponenter, hastighedskomponenter og eventuelle hysteresekomponenter udgør da en Markov vektor. Integralligninger

af Volterra typen er formuleret for den simultane sandsynlighedstæthedsfunktion for førstepassagetiden og den tilknyttede udkrydsningshastighed. Førstepassage sandsynlighedstæthedsfunktionen opnås dernæst ved marginalisering. Kernen i disse integralligninger dannes af gennemgangssandsynlighedstæthedsfunktionen for Markov vectoren, der antages at være kendt med tilstrækkelig nøjagtighed. Der introduceres herved ingen ny ukendt funktion, og eksakte løsninger kan i princippet opnås. Integralligninger er formuleret for enkelt- og dobbeltbarriere problemer for en ikkelineær oscillator af 1 frihedsgrad uden hysteresevirkning, for et ikkelineært multifrihedsgraderssystem uden hysteresevirkning, og for en oscillator af 1 frihedsgrad med hysteresevirkning. I eksempel 2-2 er undersøgt forskellige kerneapproximationer og øvre- og nedreværdiløsninger i forbindelse med integralligninger for $f_{T_1}(t \mid \mathcal{E}_{t_0})$. Det betragtede system udgøres af en lineær oscillator af 1 frihedsgrad påvirket af gaussisk hvid støj. Konklusionen af undersøgelsen er, at den bedste approximation til kernen opnås, hvis tælleren og nævneren af denne trunkeres efter det første led. Dette skyldes, at såvel tælleren som nævneren i så fald udgør øvreværdier, der til en vis grad afbalancerer hverandre. To sådanne kerneapproksimationer er nærmere undersøgt. Den første af disse er formuleret i simultane betingede udkrydsningsfrekvenser af 2. orden af typen $f_2^{++}(t_1, t_2 \mid \mathcal{E}_{t_0})$, mens den anden er udtrykt i de simultane ubetingede udkrydsningsfrekvenser af 2. orden, $f_2^{++}(t_1, t_2)$. De tilsvarende løsninger for førstepassage sandsynlighedstæthedsfunktionen er betegnet ved $f_{T_1}^{(a)}(t \mid \mathcal{E}_{t_0})$ og $f_{T_1}^{(b)}(t \mid \mathcal{E}_{t_0})$. I eksempel 2-3 er formuleret øvre- og nedreværdier for $f_{T_1}(t \mid \mathcal{E}_{t_0})$ udtrykt ved de simultane udkrydsningsfrekvenser $f_n^{+\cdots+}(t_1, \ldots, t_n; S_{\tau_1} \cap \cdots \cap S_{\tau_m} \mid \mathcal{E}_{t_0})$, og den optimale placering af kontrolpunkterne $\tau_1, \ldots, \tau_m$ undersøges med henblik på at indsnævne afstanden mellem disse grænser. Det behandlede førstepassage problem udgøres af et enkeltbarriere problem med stationær start i det sikre område for den lineære oscillator af 1 frihedsgrad betragtet i eksempel 2-2. Af de opnåede resultater er konkluderet, at øvre- og nedreværdier til $f_{T_1}(t \mid \mathcal{E}_{t_0})$ med optimalt placerede kontrolpunkter er væsentlig skarpere end tilsvarende grænser uden kontrolpunkter. Det er yderligere konkluderet, at optimalt placerede kontrolpunkter er begrænset til relativt snævre intervaller bestemt af systemets dynamik. Disse kan derfor fastlægges relativt enkelt. En approksimation til førstepassage sandsynlighedstæthedsfunktionen er formuleret baseret baseret på den 1. øvreværdi uden kontrolpunkter. Approksimationen tager i betragtning sammenklunpningen af udkrydsninger, der forekommer for smalbåndede responsprocesser ved middel og ved lave tærskelniveauer. I eksempel 2-4 er formuleret approksimationer til kernefunktionen af integralligningen for $f_{T_1}(t \mid \mathcal{E}_{t_0} \cap C_{t_1}^+)$. Specielt er betragtet en kernefunktion, der involverer de simultane ubetingede udkrydsningsfrekvenser af 3. orden, $f_3^{+++}(t_2, t_1, t)$. Den tilhørende løsning for førstepassage sandsynlighedstæthedsfunktionen er betegnet $f_{T_1}^{(f)}(t \mid \mathcal{E}_{t_0})$. Et enkeltbarriere problem med stokastisk start er undersøgt for såvel en lineær oscillator af 1 frihedsgrad som et lineært 2 frihedsgraders system, begge påvirket af gaussisk hvid støj. I begge tilfælde er opnået væsentlig hurtigere konvergens mod resulterne bestemt ved Monte-Carlo simulering, end for de tilsvarende løsninger baseret på ubetingede 2. ordens udkrydsningsfrekvenser. I alle de omtalte eksempler tenderer graferne for de approksimative førstepassage sandsynlighedstæthedsfunktioner til at forløbe parallelt med den simulerede kurve. Følgelig kan den såkaldte limiting decay rate af førstepassage sandsyn-

lighedstæthedsfunktionen, karakteristisk for tidsinvariante Markov systemer under stationær påvirkning og med tidsinvariante sikkert område, estimeres ved metoden. Denne størrelse er intet andet end den laveste egenværdi af Kolmogorovs forud og Kolmogorovs bagud operatorer med absorbtion på henholdsvis indgangs- og udgangsdelen af den tilgængelige del af svigtfladen. I eksempel 2-5 er løsninger opnået for enkeltbarriere problemet med stokastisk start for en lineær tidsinvariant oscillator af 1 frihedsgrad påvirket af gausisk hvid støj eller en sammensat Poisson process ved numerisk integration af integralligningen for den simultane sandsynlighedstæthedsfunktion for førstepassagetiden og den tilhørende hastighed ved udkrydsning af barrieren b, $f_{T_1\dot{X}}(b,\dot{x},t \mid \mathcal{E}_{t_0})$. I tilfælde af påvirkning med gaussisk hvid støj opnås eksakte løsninger i et omfang fastlagt af nøjagtigheden af det benyttede numeriske skema. I tilfælde af påvirkning med en sammensat Poisson process er kun opnået approximative resultater, fordi gennemgangssandsynlighedstæthedsfunktionen er approksimeret ved hjælp af en Gram-Charlier række afrundet efter 6. orden. Endelig er angivet en approksimation til førstepassage sandsynlighedstæthedsfunktionen for dynamiske systemer påvirket af en sammensat Poisson proces med meget lille middelankomstfrekvens af impulserne, baseret på antagelsen om stokastisk uafhængighed af egensvingningerne fra to på hinanden følgende impulser. Approksimationen bliver asymptotisk korrekt, når middelankomstfrekvensen af impulserne går mod 0 eller den strukturelle dæmpning øges.

I afsnit 2.3 er formuleret en Volterra integralligning for $f_{L_t^+}(t-t_1)$. På baggrund heraf er udledt inclusion-exclusion rækker for $f_{L_t^+}(t-t_1)$ og for tælleren og nævneren i kernefunktionen af den pågældende integralligning, alle udtrqykt ved simultane ubetingede krydsningsfrekvenser af typen $f_{n+1}^{-\cdots-+}(t_1,\ldots,t_n,t)$. Ved hjælp af relationen mellem $f_{T_1}(t \mid \mathcal{E}_{t_0})$ og $f_{L_t^+}(t-t_1)$ opnås herved en alternativ inclusion-exclusion series for $f_{T_1}(t \mid \mathcal{E}_{t_0})$ udtrykt i de anførte ubetingede simultane krydsningsfrekvenser. Dernæst formuleres en integralligning for sandsynlighedstæthedsfunktionen for L_t^+ under betingelse af indkrydsning til det sikre område til tidspunkterne $t_1,\ldots,t_n$ placeret forud for indkrydsningen til tidspunktet t_{n+1} i starten af intervallet L_t^+. Denne størrelse, der er betegnet $f_{L_t^+}(t-t_{n+1} \mid C_{t_1}^- \cap \cdots \cap C_{t_n}^-)$, $t_1 < \cdots < t_n < t_{n+1} < t$, forekommer i restleddet for inclusion-exclusion rækken for $f_{L_t^+}(t-t_1)$. Hvis en tilnærmet løsning til integralligningen for denne størrelse kan opnås, kan hurtig konvergens forventes af inclusion-exclusion rækken for $f_{L_t^+}(t-t_1)$ og dermed for $f_{T_1}(t \mid \mathcal{E}_{t_0})$. Identiteterne $f_{T_1}(t_2 \mid \mathcal{E}_{t_1}) = f_1^+(t;\cap_{\tau\in]t_1,t[}S_\tau \mid \mathcal{E}_{t_1})$ og $f_{L_{t_1}^-}(t-t_1) = f_1^+(t;\cap_{\tau\in]t_1,t[}S_\tau \mid C_t^-)$ kan bevises. Det fremgår, at de anførte funktioner kun afviger med hensyn til forskellig konditionering. Baseret på denne observation er en integralligning formuleret for $f_{L_{t_1}^-}(t-t_1)$, identisk med den tidligere omtalte for $f_{T_1}(t \mid \mathcal{E}_{t_1})$, hvor blot konditioneringen på hændelsen $\mathcal{E}_{t_1}$ er erstattet med hændelsen C_t^- i de betingede krydsningsfrekvenser. På basis heraf er udledt inclusion-exclusion rækker for $f_{L_t^-}(t-t_1)$ og for tælleren og nævneren af kernefunktionen til den pågældende integralligning, alle udtrykt i simultane ubetingede krydsningsfrekvenser af typen $f_{n+1}^{-+\cdots+}(t_1,\ldots,t_n,t)$. Baseret på den omtalte relation mellem $f_{L_t^-}(t-t_1)$ og $f_{L_t^+}(t-t_1)$ kan en alternativ inclusion-exclusion række i disse ubetingede krydsningsfrekvenser herved udledes for $f_{T_1}(t \mid \mathcal{E}_{t_0})$. Dernæst betragtes enkeltbarriere problemet med stationær start for en lineær oscillator af 1 frihedsgrad påvirket ag gaussisk hvid støj, for hvilket flytningen og hastigheden dan-

ner en Markov vektor. Ud fra den omtalte formelle lighed mellem integralligningerne for $f_{T_1}(t \mid \mathcal{E}_{t_1})$ og $f_{L_t^-}(t-t_1)$ kan en integralligning umiddelbart formuleres for den simultane sandsynlighedstæthedsfunktion $f_{\dot{X}L_{t_1}^-}(b,\dot{x},t-t_1)$ af udkrydsningshastigheden $\dot{X}$ til tiden t og L_t^- ved sammenligning med den tilsvarende integralligning for $f_{\dot{X}T_1}(b,\dot{x},t \mid \mathcal{E}_{t_1})$. $f_{L_t^-}(t-t_1)$ bestemmes af den numeriske løsning til denne integralligning ved marginalisering. $f_{L_t^+}(t-t_1)$ og endelig $f_{T_1}(t \mid \mathcal{E}_{t_0})$ bestemmes dernæst ved relationerne, der forbinder disse størrelser med $f_{L_t^-}(t-t_1)$. I eksempel 2-6 er undersøgt approksimationer til kernefunktionen i integralligningen for $L_t^+(t-t_1)$. To approksimationer er undersøgt, hvoraf den ene er baseret på simultane krydsningsfrekvenser af 3. orden af typen $f_3^{--+}(t_1,t_2,t)$, mens den anden er baseret på simultane krydsningsfrekvenser af 2. orden af typen $f_2^{--}(t_1,t_2)$. De tilhørende løsninger for førstepassage sandsynlighedstæthedsfunktionen er betegnet henholdsvis $f_{T_1}^{(g)}(t \mid \mathcal{E}_{t_0})$ og $f_{T_1}^{(h)}(t \mid \mathcal{E}_{t_0})$. Et enkeltbarriere problem med stationær start er betragtet for såvel en lineær oscillator af 1 frihedsgrad som for et lineært system af 2 frihedsgrader, begge påvirket af gaussisk hvid støj. For begge systemer findes, at approksimationen $f_{T_1}^{(h)}(t \mid \mathcal{E}_{t_0})$ giver omtrent samme resultater som $f_{T_1}^{(b)}(t \mid \mathcal{E}_{t_0})$, der ligeledes er baseret på ubetingede krydsningsfrekvenser af 2. orden. Dog giver approksimationen $f_{T_1}^{(h)}(t \mid \mathcal{E}_{t_0})$ bedre resultater i løbet af de første perioderaf førstepassager. Under alle omstændigheder er $f_{T_1}^{(g)}(t \mid \mathcal{E}_{t_0})$ bedre end approksimationen $f_{T_1}^{(f)}(t \mid \mathcal{E}_{t_0})$, der ligeledes er baseret på ubetingede krydsningsfrekvenser af 3. orden. Den overordnede konklusion, der drages af eksemplet, er, at approksimationerne $f_{T_1}^{(g)}(t \mid \mathcal{E}_{t_0})$ og $f_{T_1}^{(h)}(t \mid \mathcal{E}_{t_0})$ er de bedste af de betragtede approksimationer baseret på henholdsvis simultane ubetingede krydsningsfrekvenser af 3. og 2. orden. I eksempel 2-7 er angivet passende approksimative kernefunktioner til anvendelse i integralligningen for henholdsvis $f_{L_t^+}(t-t_2 \mid C_{t_1}^-)$ og $f_{L_t^+}(t-t_{n+1} \mid C_{t_1}^- \cap \cdots \cap C_{t_n}^-)$, der forekommer i restleddet af inclusion-exclusion rækken for $f_{L_t^+}(t-t_1)$. Der er ikke anført noget numerisk eksempel, men disse approksimationer kan med henvisning til konklusionen i eksempel 2-6 forventes at give de bedste tilnærmede løsninger baseret på simultane ubetingede krydsningsfrekvenser af orden $n+3$. Endelig er i eksempel 2-8 angivet en approksimativ kernefunktion til anvendelse i integralligningen for $f_{L_{t_1}^-}(t-t_1)$. Den pågældende kerneapproksimation forventes at give resultater af samme kvalitet som $f_{T_1}^{(g)}(t \mid \mathcal{E}_{t_0})$, baseret på integralligningen for $f_{L_{t_1}^-}(t-t_1)$, omend dette ikke er dokumenteret ved et numerisk eksempel.

I afsnit 2.4 er indledningsvist formuleret en Volterra integralligning for $f_{U_t^+}(t-t_1 \mid \mathcal{E}_{t_0})$. På baggrund af heraf er udledt inclusion-exclusion rækker for $f_{U_t^+}(t-t_1 \mid \mathcal{E}_{t_0})$ og for tælleren og nævneren af kernefunktionen til den pågældende integralligning, alle udtrykt i simultane betingede udkrydsningsfrekvenser af typen $f_n^{+\cdots+}(t_1,\ldots,t_n \mid \mathcal{E}_{t_0})$, der også var grundlaget for rækkeudviklingen af $f_{T_1}(t \mid \mathcal{E}_{t_0})$. Med baggrund i sammenhængen mellem $f_{T_1}(t \mid \mathcal{E}_{t_0})$ og $f_{U_t^+}(t-t_1 \mid \mathcal{E}_{t_0})$ kan alternative inclusion-exclusion rækker i disse betingede udkrydsningsfrekvenser herved udledes for $f_{T_1}(t \mid \mathcal{E}_{t_0})$. Dernæst er formuleret en integralligning for sandsynlighedstæthedsfunktionen for U_t^+ under betingelse af hændelsen $\mathcal{E}_{t_0}$ og under betingelse af udkrydsninger fra det sikre område til tidspunkterne $t_1,\ldots,t_n$, placeret forud for udkrydsningen i slutningen af intervallet U_t^+. Denne

størrelse, der er betegnet $f_{U_t^+}(t - t_{n+1} \mid \mathcal{E}_{t_0} \cap \mathcal{C}_{t_1}^+ \cap \cdots \cap \mathcal{C}_{t_n}^+)$, $t_1 < \cdots < t_n < t - l < t$, forekommer i restleddet for inclusion-exclusion rækken for $f_{U_t^+}(t - t_1 \mid \mathcal{E}_{t_0})$. Hvis en approksimativ løsning til denne integralligning kan opnås, kan hurtig konvergens for inclusion-exclusion rækken for $f_{U_t^+}(t - t_1 \mid \mathcal{E}_{t_0})$, og dermed for rækkeudviklingen for $f_{T_1}(t \mid \mathcal{E}_{t_0})$, opnås ved indsætning heraf i restleddet. Dernæst er formuleret en integralligning for sandsynlighedstæthedsfunktionen $f_{U_t^-}(t - t_1 \mid \mathcal{E}_{t_0})$, hvor U_t^- betegner det forløbne tidsinterval indtil næste udkrydsning, efter at en udkrydsning fra det sikre interval har fundet sted til tidspunktet t. Ved hjælp af denne integralligning er udledt en inclusion-exclusion række for $f_{U_t^-}(t - t_1 \mid \mathcal{E}_{t_0})$ og for tælleren og nævneren af kernefunktionen, stadig udtrykt i de simultane betingede udkrydsningsfrekvenser $f_n^{+\cdots+}(t_1, \ldots, t_n \mid \mathcal{E}_{t_0})$. Baseret på en relation mellem $f_{U_t^-}(t-t_1 \mid \mathcal{E}_{t_0})$ og $f_{U_t^+}(t-t_1 \mid \mathcal{E}_{t_0})$ kan en tredje inclusion-exclusion række bestemmes for $f_{T_1}(t \mid \mathcal{E}_{t_0})$, udtrykt i disse betingede udkrydsningsfrekvenser. Heraf følger at de tre alternative rækker i princippet repræsenterer forskellige udviklinger af restleddet af inclusion-exclusion rækken. Herefter betragtes igen enkeltbarriere problemet med stationær start for en lineær oscillator af 1 frihedsgrad påvirket ag gaussisk hvid støj, for hvilket flytningen og hastigheden danner en Markov vektor. En integralligning er formuleret for den simultane sandsynlighedstæthedsfunktionen $f_{\dot{X}U_{t_1}^-}(b, \dot{x}, t - t_1 \mid \mathcal{E}_{t_0})$ af udkrydsningsfrekvensen $\dot{X}$ til tiden t og intervallængden U_t^- under betingelse af $\mathcal{E}_{t_0}$. Ud fra den numeriske bestemte løsning til denne ligning kan $f_{U_t^-}(t - t_1 \mid \mathcal{E}_{t_0})$ dernæst bestemmes ved marginalisering. $f_{U_T^+}(t - t_1 \mid \mathcal{E}_{t_0})$ og sluttelig $f_{T_1}(t \mid \mathcal{E}_{t_0})$ beregnes herefter af relationerne, der knytter disse til $f_{U_t^-}(t - t_1 \mid \mathcal{E}_{t_0})$. Intet numerisk eksempel er anført for teorien i afsnit 2-4.

Afslutningsvis skal det anføres, at det væsentligste problem ved alle de præsenterede metoder er, at anvendelsesområdet er begrænset til problemer for hvilke de nødvendige krydsningsfrekvenser kan beregnes. For øjeblikket betyder dette, at kun lineære og en meget begrænset klasse af ikkelineære systemer kan analyseres. Yderligere, må dimensionen af den betragtede responsvektor være lav. Selv for gaussiske vektorprocessor af moderat dimensionalitet bliver beregningen af simultane krydsningsfrekvenser hurtigt uoverkommelig.

Indledningsvis i afsnit 3.1 betragtes Wiener processer, sammensatte Poisson processer og α-stabile Lévy motions, og der gives en kort omtale af disses væsentligste egenskaber. Disse stokastiske er alle karakteriseret ved at have uafhængige tilvækster. Det diskuteres, hvorledes andre aktuelle stokastiske processer kan modelleres ved filtrering af processer med uafhængige tilvækster gennem et sharpening filter. Herved er betragtningen indskrænket til processer, for hvilke responset af det dynamiske system kan beskrives ved en Markov vektor. Den generelle tilstandsvektor for såvel geometrisk ikkelineære som fysisk ikkelineære (i.e. systemer med hysteresevirkning) er anført. Specielt er i eksempel 3-1 formuleret ækvivalente SDOF og MDOF forskydningsmodeller med hysteresevirkning for instrumenterede jernbetonkonstruktioner udsat for jordskælv. Modellerne tænkes anvendt til prediktion af stokastisk respons og pålidelighed samt globale og lokale skader i konstruktionen, baseret på sekventiel opdatering af nogle få systemparameter. Nøjagtigheden af modelforudsigelserne ved sammenligning med tilgængelige

modelforsøg skyldes primært en modellering af den elastiske del af tilbageføringskraften som en faldende funktion af skaden, svarende til en gradvis overgang fra elastisk til plastisk response, når større og større dele af konstruktionen bliver plastisk.

I afsnit 3.2 er forud og bagud Chapman-Kolmogorov integro-differentialligningen for gennemgangssandsynlighedstæthedsfunktionen af Markov tilstandsvektoren angivet med henblik på senere anvendelse på systemer påvirket af Wiener processer, sammensatte Poisson processer og α-stabile Lévy motions. Yderligere er førstepassage problemet formuleret, baseret på løsningen af den forud eller bagud Chapman-Kolmogorov integro-differentialligning med absorberende randbetingelser.

Afsnit 3.3 omhandler stokastisk responsanalyse af Markov systems baseret på momentligningsmetoder. Indledningsvis er den generaliserede Itô differentiationsregel udledt, gældende både for diffusionssystemer og for systemer med hop. Momentligningerne er herefter udledt ved hjælp af denne ligning. Specielt er eksplicitte udtryk angivet for de simultane centraliserede statistiske momenter.

I afsnit 3.3.1 er lukningsproblemet for hirarkiet af momentligninger behandlet, dvs. specifikationen af en approksimativ simultan sandsynlighedstæthedfunktion for tilstandsvariablerne ved hjælp af hvilken ukendte forventningsværdier kan beregnes. De frie parametre i lukningsantagelsen kalibreres, således at den pågældende simultane sandsynlighedstæthedsfunktion repræsenterer alle simultane momenter bestemt af momentligningerne. Moment neglect closure, cumulant neglect closure, quasi-moment neglect closure and Hermite moment neglect closure omtales. Det fremhæves, at de fleste af disse metoder kan forventes at virke for tilnærmet normalfordelte systemer med simultan sandsynlighedstæthedsfunktion af kontinuert og monomodal type. De kan alle betragtes som rækkeudviklinger fra Gaussiske sandsynlighedstæthedsfunktioner, hvor restleddet i rækkerne måler afvigelsen fra gaussianitet. Systemer med multimodal eller blandet kontinuert-diskret sandsynlighedstæthedsfunktion mødes ofte i stokastisk dynamik. I disse tilfælde vil konvergenshastigheden af rækkeudviklingerne ud fra normalfordelingen være langsom, eller konvergensen kan helt mangle. I stedet bør man formulere såkaldte modificerede lukningsskemaer, baseret på fysisk indsigt i det konkrete problem. Et modificeret cumulant neglect closure skema er angivet for en såkaldt double-well potential oscillator, for hvilken den simultane sandsynlighedstæthedsfunktion er bimodal. Selv ved lukning på covariansniveau opnås relativt nøjagtige resultater. I modsætning hertil er konvergenshastigheden af et sædvanligt cumulant neglect closure skema overordentligt langsom, som demonstreret i eksempel 3-7. Dernæst foreslås en lignende modification anvendt i forbindelse med Hermite moment neglect closure for en Bouc-Wen oscillator påvirket af gaussisk hvid støj af høj intensitet, i hvilket tilfælde den marginale sandsynlighedstæthedsfunktion for hysteresekomponenten har dobbeltspidser. Igen opnås væsentlige forbedringer sammnelignet med det sædvanlig Hermite moment neglect closure skema. Endelig er foreslået anvendt et modificeret lukningsskema for Poisson drevne systems med lav middel ankomstfrekvens, hvor der forekommer en transient diskret sandsynlighedskomponent i den simultane sandsynlighedstæthedsfunktion, repræsenterende den deterministiske drift fra begyndelsesværdierne under betingelse af, at ingen impulser endnu er ankommet. Eksplicitte udtryk for det modificerede cumulant neglect closure skema er udledt for systemer med polynomial

ikkelineær drift vektor ved lukning ved orden $N = 4$.

I afsnit 3.3.2 er udledt momentligninger for dynamiske systemer drevet af Wiener processer. Specielt er anført udtryk for systemer med kubisk polynomial drift vektor (eksempelvis ved Duffing og van der Pol oscillatorer). Endvidere fastlægges betingelserne for at erstatte et system med ikkeanalytisk drift vektor (f.eks. systemer med hysteresevirkning) med et system med polynomial ikkelineær drift vektor. Der bevises sætningen, at eksakte simultane momenter op til orden $N + 1$ opnås ved hjælp af det ækvivalente polynomiale system, forudsat at dette afrundes ved orden N, og forudsat at udviklingskoefficienterne af det ækvivalente system bestemmes ved hjælp at et least mean square kriterium med ubestemte forventningsværdier udregnet med den eksakte simultane sandsynlighedstæthedsfunktion. I eksempel 3-3 benyttes ækvivalent polynomial udvikling til stokastisk analyse af en biliniær hysterese oscillator påvirket af gaussisk hvid støj. Ideen er kun at erstatte den konstitutive ligning for hysterese komponenten med en ækvivalent polynomial udvikling, medens de lineære ligninger er uændret. I modsætning hertil forudsætter det globale least mean square kriterium i den anførte sætning, at alle komponenter erstattes med ækvivalente polynomiale udviklinger af orden N. I det numeriske eksempel er det demonstreret, at en sådan fremgangsmåde introducerer helt ubetydelige ekstra fejl i analysen. Nytten af metoden ligger i, at kun en marginal simultan sandsynlighedstæthedsfunktion for hastigheden og hysteresekomponenten behøver at blive kalibreret ved beregningen af koefficienterne i den ækvivalente kubiske udvikling. Den pågældende simultane sandsynlighedstæthedsfunktion vælges som en trunkeret 2 dimensional Gram-Charlier række med en Minai-Suzuki modifikation for den diskrete sandsynlighed for at befinde sig på de plastiske grene af arbejdskurven. To ækvivalente lineariseringsstrategier undersøges. Begge af disse forudsiger en stationær værdi for variansen af flytningen for en ideal elastisk-plastisk oscillator ($\alpha = 0$), i modsætning til den ikkestationære Brownian motion agtige variansvækst, der fremgår af resultaterne opnået ved Monte-Carlo simulering og ved den kubiske polynomiale udvikling. Dette antyder, at variansvæksten forårsages af simultanmomenter af 4. eller højere orden. Den væsentligste afvigelse mellem resultaterne opnået ved ækvivalent kubisk udvikling og simulering skyldes anvendelsen af et sædvanligt cumulant neglect closure skema uden modifikation for diskrete sandsynlighedskomponenter i de globale momentligninger. Dette problem er yderligere undersøgt i eksempel 3-4, der tillige indeholder en pålidelighedsanalyse af den biliniære hysterese oscillator. Pålidelighedsanalysen er baseret på observationen af en skadesindikator, der er valgt som den akkumulerede energy dissiperet af systemet, når dette undergår plastiske deformationer. Svigthændelsen indtræffer, når den ikkeaftagende skadesindikator foretager en førstepassage af et kritisk niveau, d_{cr}. Skadesindikatoren er indkluderet i tilstandsvektoren som en ekstra tilstandsvariabel, og en differentialligning er formuleret, der fastlægger udviklingen i tiden af denne. Belastningsprocessen på systemet modelleres som tidsmoduleret gaussisk hvid støj filtreret gennem et tidsinvariant rationalt filter af orden $(r, s) = (1, 2)$. Filterets tilstandsvariable er ligeledes indkluderet i tilstandsvektoreren sammen med flytningen, hastigheden, hysteresekomponenten og skadesindikatoren. Kun differentialligningerne for hysteresekomponenten og skadesindikatoren erstattes med ækvivalente polynomiale udviklinger. De konsistente udviklingerne viser sig at være af 3. orden for hystere-

sekomponenten og af 2. orden for skadesindikatoren. Ved udregningen af udviklingskoefficienter i de ækvivalente udviklinger er anvendt et least mean square kriterium, og den simultane sandsynlighedstæthedsfunktion til udregning af ukendte forventningsværdier vælges som en afrundet 2 dimensional Gram-Charlier række med en Minai-Suzuki modifikation. Herudover er udviklet en modificeret cumulant neglect closure skema for de globale moment ligninger, der tager de diskrete komponenter i den simultane sandsynlighedstæthedsfunktion i regning. Lukningsskemaet kræver kun kendskab til samme simultane sandsynlighedstæthedsfunktion af hastigheden og hysteresekomponenten, som er anvendt i den ækvivalente polynomiale udvikling af differentialligningerne for hysteresekomponenten og skadesindikatoren. I eksemplet sammenlignes resultater opnået ved hjælp af det sædvanlige og det modificerede cumulant neglect skema med Monte Carlo simuleringsresultater. På basis heraf er konkluderet, at væsentligt bedre resultater opnås med det modificerede cumulant neglect skema end med det sædvanlige. Følgelig bør anvendes approksimative simultane sandsynlighedstæthedsfunktioner af samme nøjagtighed på det lokale og på det globale niveau. Eksempel 3-5 omhandler stokastisk analyse af plane rammer med hysteresevirkning. Indledningsvis er anført en differentiel formulering af de konstitutive ligninger for elasto-plastiske bjælkeelementer, der forbinder generaliserede spændings- og tøjningshastigheder af elementet. Disse specialiceres dernæst til flydeledsmodeller, hvor de generaliserede tøjninger og spændinger udgøres af rotationer og bøjningsmomenter ved elementets knuder. Rammen påvirkes af et horizontalt jordskælv, der opnås ved filtrering af moduleret gaussisk hvid støj gennem et Kanai-Tajimi filter. Dette er i princippet et rationalt filter af orden $(r, s) = (1, 2)$ med filterkonstanter, der tillader fysisk fortolkning. Tilstandsvektorkomponenterne for det integrerede dynamiske system består af knudeflytninger og knudehastigheder, generaliserede spændinger fra alle plastiske elementer og filtertilstandsvariablerne. De resulterende differentialligninger formuleret på tilstandsvektorform udgør en generalisering til multifrihedsgraderssystemer af de tilsvarende differentialligninger for den elasto-plastiske oscillator i eksempel 3-4, hvor de generaliserede spændinger udgør hysteresekomponenterne. Kun de konstitutive ligninger for de generaliserede spændinger (hysteresekomponenterne) erstattes med ækvivalente polynomiale udviklinger i de lokale generaliserede spændinger og generaliserede tøjningshastigheder. Følgelig udføres den ækvivalente polynomiale udvikling på elementniveau, hvilket letter formuleringen af et globalt ækvivalent polynomialt system væsentligt. De globale simultane momentligninger lukkes dernæst ved hjælp af et sædvanligt cumulant neglect closure skema. Teorien er anvendt på en simpelt understøttet 2 etagers plan ramme med Kanai-Tajimifilteret påvirket af en stationær gaussisk hvid støj. Væsentlige plastiske deformationer er mest sandsynlige at forekomme i de nederste etagesøjler. Ækvivalent kubisk udvikling er derfor kun benyttet for de konstitutive ligninger for disse elementer, hvorimod ækvivalent linearisering indføres for de resterende elementer. De simultane forventningsværdier af rotationshastigheder og bøjningsmomenter i elementets endeknuder, der indgår i least mean square ligningerne til bestemmelse af koefficienterne i de ækvivalente polynomiale udviklinger, er udregnet ved hjælp af en Gram-Charlier udvikling af den simultane sandsynlighedstæthedsfunktion trunkeret ved orden $N = 4$ med en Minai-Suzuki modifikation for plastiske deformationer. På basis af resultaterne er konkluderet, at ækvivalent linearisering for alle elementer med udregning af udviklingskoefficienterne ved hjælp

af en simultan normalfordeling (gaussisk lukning) giver resultater for flytningsresponset, der hverken kvalitativt eller kvantitativt er i overenstemmelse med Monte Carlo simuleringsresultaterne. Resultater, der kun er en ubetydelighed bedre, opnås ved et lineariseringsskema, hvor en Gram-Charlier udvikling til orden $N = 2$ med en Minai-Suzuki modifikation for plastiske deformationer er benyttet ved udregningen af de lineære udviklingskoefficienter. I begge tilfælde forudsiges et stationært varians respons for etageflytningerne i modsætning til simuleringsresultaterne, der udviser en lignende Brownian motion agtigt variansdrift, som beskrevet i eksempel 3-3. Den uundgåelige konklusion synes at være, at ækvivalent linearisering ikke bør anvendes for elastoplastiske konstruktioner påvirket af væsentlige stationære påvirkninger. I stedet bør anvendes en analyse, der mindst indbefatter 4. ordens momenterne. I modsætning til ækvivalent linearisering giver kubisk polonomial udvikling for de lavere etagesøjler resultater, der er i langt bedre overensstemmelse med simuleringsresultaterne. Der registreredes ingen væsentlige forskelle i resultaterne, hvis ækvivalent linearisering for de øvrige elementer udføres ved hjælp af gaussisk lukning eller ved hjælp af en Gram-Charlier udvikling til 2. orden med en Minai-Suzuki modifikation. I eksempel 3-6 er teorien anvendt til en pålidelighedsanalyse af en vandmættet sandaflejring påvirket af et horizontalt forskydningsjordskælv (SH bølger), idet likvidfaktion antages at være den væsentligste brudmåde for jorden. Likvidfaktion antages at finde sted, når den akkumulerede dissiperede energy per enhedsvolumen af jorden når et kritisk niveau. I eksemplet er anvendeligheden af denne skadesindikator verificeret ved hjælp af triaksialforsøg på forskellige sandprøver udsat for cyklisk påvirkning med variable amplituder. Triaksialforsøgene viser tillige, at den tidsafledede af mobiliseringsfaktoren, der for den betragtede plane tøjningstilstand kan defineres som forskydningsspændingen i forhold til forskydningsbrudspændingen, kan relateres til forskydningstøjningshastigheden ved hjælp af en Bouc-Wen hysterese model. Forskydningsbrudspændingen er en aftagende funktion af tiden i takt med poretryksopbygningen, og viser sig at svækkes proportionalt med svækkelsen af forskydningsmodulet. Begge er relateret til skadesindikatoren ved hjælp af en simpel lineær sammenhæng. Et statisk tilladeligt spændingsfelt foreskrives, ved hjælp af hvilket det kontinuerte jordlag diskretiseres til et frihedsgraders system. Accelerationsprocessen ved oversiden af grundfjeldet opnås ved filtrering af moduleret gaussisk hvid støj gennem et tidsinvariant rationalt filter af orden $(r, s) = (1, 2)$. Differentialligningen for udviklingen af skadesindikatoren bliver kubisk polynomial, hvorimod differentialligningen for hastigheden bliver kvadratisk. Den konstitutive ligning for mobiliseringsfaktoren erstattes af en ækvivalent lineær udvikling med udviklingskoefficienter udregnet ved en Gram-Charlier udvikling afrundet ved orden $N = 2$, hvorimod den lineære, den kvadratiske og den kubiske ligning bibeholdes uændret. Det resulterende globale hirarki af momentligninger er trunkeret ved orden $N = 4$ ved hjælp af et sædvanligt cumulant neglect closure skema. De opnåede resultater for variansresponset af flytningen og mobiliseringsfaktoren er dårlige sammenlignet med simuleringsresultaterne som følge af anvendelsen af ækvivalent linearisering på hystereseligningen. Derimod opnås gode resultater for forventningsværdifunktionen og standardafvigelsen af skadesindikatoren, hvorimod skævhedsparameteren for denne størrelse bestemmes mindre nøjagtigt. Grunden til de forbedrede resultater for de lavere statistiske momenter for skadesindikatoren sammenlignet med de tilsvarende momenter for de

øvrige tilstandsvariable skyldes primært den eksakte kubisk polynomiale form af differentialligningen for denne variabel. Forbedrede resultater for skævhedsparameteren vil kræve anvendelse af højere ordens ækvivalent polynomial udvikling af den konsitutive ligning for hysteresekomponenten og global lukning ved højere orden end orden $N = 4$.

Afsnit 3.3.3 omhandler anvendelsen af momentligninger til stokastisk analyse af systemer drevet af sammensatte Poisson processer. Indledningsvis er differentialligningerne udledt for de simultane centraliserede momenter af et dynamisk system påvirket af en multidimensional eller skalar sammensat Poisson proces. Specielt er momentligningerne fremhævet for systemer med kubisk polynomial drift vektor. I eksempel 3-8 er teorien anvendt på en Duffing oscillator. Ideen i eksemplet er at demonstrere anvendeligheden af det modificerede cumulant neglect closure skema, udviklet for Poisson tælleprocesser med lave middelankomstsfrekvenser. Der undersøges sædvanlige cumulant neglect closure skemaer af orden $N = 3$, $N = 4$ og $N = 5$, og et modificeret cumulant neglect closure skema af orden $N = 4$. Påvirkningsprocessen har Rayleigh fordelte impulser, og opnås som outputproces fra en homogen sammensat Poisson proces filtreret gennem et rationalt filter af ordenen $(r, s) = (0, 2)$. For den relativt høje middelankomstfrekvens på $\nu = 0.1\omega_0$, fungerer de betragtede sædvanlige cumulant neglect closure skemaer udmærket og giver alle acceptable resultater, omend det bedste resultat som forventet opnås ved lukning ved ordenen $N = 5$. I sammenligning med sædvanlig cumulant neglect closure af orden $N = 4$ giver det modificerede cumulant neglect closure skema væsentligt forbedrede resultater for middelværdifunktionerne og variansfunktionerne i den tidlige del af påvirkningen, hvor modifikationen af den simultane sandsynlighedstæthedsfunktion er mest betydningsfuld. Påføringen af en pulsbelastning med den lavere middelankomstfrekvens på $\nu = 0.05\omega_0$ medfører numerisk instabilitet for det sædvanlige cumulant neglect closure skema, hvorimod det modificerede skema stadig frembringer nøjagtige estimater for middelværdifunktionerne og variansfunktionerne. Af eksemplet konkluderes derfor, at nøjagtigere og numerisk mere stabile resultater opnås ved hjælp af det modificerede cumulant neglect closure skema. Imidlertid vil selv det modificerede cumulant neglect closure skema efterhånden blive numerisk instabilt, når ν reduceres tilstrækkeligt. I det aktuelle eksempel sker dette for $\nu \simeq 0.01\omega_0$, hvilket tilnærmet er en størrelsesorden mindre end den tilsvarende grænse for det sammenlignelige sædvanlige cumulant neglect closure skema. I eksempel 3-9 er gennemført en pålidelighedsanalyse af en Bouc-Wen oscillator påvirket af såvel en ufiltreret som en filtreret sammensat Poisson proces ved anvendelse af ækvivalent polynomial udvikling. Pålidelighedsanalysen er baseret på en skadesindikator, som vælges som den akkumulerede energy dissiperet af hysteresekomponenten. Herved er den betragtede skadesindikator kvadratisk polynomial. Kun den konstitutive ligning for hysteresekomponenten erstattes af en kubisk polynomial udvikling, hvorimod de øvrige lineære eller kvadratiske ligninger bibeholdes uændrede. Som ved tidligere anvendelser bestemmes udviklingskoefficienterne af den ækvivalente polynomiale udvikling ved hjælp af et least mean square kriterium. Udregningen af de ukendte forventningsværdier, der indgår i mean least square kriteriet, er foretaget ved hjælp af et quasimoment neglect closure skema, trunkeret ved orden $N = 4$. Desuden er undersøgt ækvivalente lineariseringer af differentialligningen for hysteresekomponenten med udviklingskoefficienterne udregnet ved hjælp af quasimoment neglect closure skemaer trunkeret ved henholdsvis or-

denerne $N = 2$ og $N = 4$. Det førstnævnte lineariseringsskema er ækvivalent med hvid støjspåvirkning med gaussisk lukning. Hirarkiet af globale momentligninger er lukket ved hjælp af et sædvanligt cumulant neglect closure skema ved orden $N = 4$, såvel for de to ækvivalente lineære udviklinger som for den ækvivalente kubiske udvikling. Først analyseres tilfældet med påvirkning af en ufiltreret sammensat Poisson proces. To forskellige fordelinger for impulsstyrken betragtes. Den første af disse er en sædvanlig Rayleighfordeling, mens den anden er en middelværdicentreret Rayleighfordeling. En relativ høj middelankomstfrekvens af impulserne på $\nu = 1.297\omega_0$ er benyttet. For tilfældet med en sædvanlig Rayleigh fordeling of impulsstyrken er de opnåede resultater for forventningsværdifunktionerne for flytningen, hysteresekomponenten og skadesindikatoren alle i god overensstemmelse med simuleringsresultaterne, såvel for de to ækvivalente lineariseringsskemaer som for den kubisk polynomiale udvikling, omend den gaussiske lukningsalgoritme overestimerer middelværdifunktionen for hysteresekomponenten en smule ved store påvirkningsintervaller. Variansresponset for flytningen underestimeres væsentligt ved de ækvivalente lineariseringsmetoder, og disse metoder giver helt misvisende estimater af variansresponset af skadesindikatoren. Derimod er varianserne, der forudsiges af den ækvivalente kubisk polynomiale udviklingsmetode, acceptable for flytnings- og hysteresekomponenten, og meget gode for skadesindikatoren. For tilfældet med en middelværdicentreret Rayleighfordeling af impulsstyrken vises det, at middelværdier væsentligt forskellig fra nul kan forekomme for flytningen og for hysteresekomponenten selv ved den relativt høje middelankomstfrekvens på $\nu = 1.297\omega_0$, hvilket er en følge af, at højere ordens momenter af impulsstyrken af ulige orden er forskellig fra nul i kombination med små værdier af den elastiske brøkdel af den totale tilbageføringskraft, α. I modsætning hertil forudsiger det ækvivalente lineariseringsskema med gaussisk lukning middelværdifunktioner identisk lig nul. Følgelig skal erstatningen af en sammensat Poisson proces med en sammenlignelig gaussisk hvid støjsproces foretages med en vis forsigtighed for sådanne systemer, selv ved relativt høje middelankomstfrekvenser af impulserne. Det ækvivalente lineariseringsskema baseret på en 4. ordens quasimoment neglect række opfanger den kvalitative opfo rsel af middelværdifunktionerne, men de kvantitative estimater er ikke gode. Derimod er estimaterne af den ækvivalente polynomiale udvikling i udmærket overensstemmelse med resultater opnået ved Monte Carlo simulering. Begge ækvivalente lineariseringskemaer underestimerer variansen af flytningen og hysteresekomponenten. Kun den ækvivalente polynomiale udvikling giver acceptable variansestimater, og er den eneste af metoderne, der giver meningsfulde og nøjagtige resultater for skadesindikatoren. Dernæst betragtes tilfældet med påvirkning af en sammensat Poisson proces filtreret gennem et tidsinvariant rationalt filter af orden $(r, s) = (0, 2)$. Kun tilfældet med sædvanlig Rayleighfordeling af impulsstyrken er betragtet, og kun lineariseringsskemaet baseret på en 4. ordens quasimoment neglect række er undersøgt. En relativ høj middelankomstfrekvens af impulser på $\nu = 1.0\omega_0$ er benyttet. Som det er tilfældet for den tilsvarende fordeling af impulser i det ufiltrerede tilfælde giver de betragtede metoder acceptable resultater for middelværdifunktionerne. Igen underestimerer den ækvivalente linearisering variansresponset for flytningen og hysteresekomponenten, og giver helt misvisende resultater for variansresponset, hvorimod den ækvivalente kubisk polynomiale udvikling giver acceptable variansestimater for alle betragtede tilstandsvariable. Af resultaterne opnået

i dette eksempel sluttes, at ækvivalent lineariseringsmetoder ikke er egnet til at estimere variansresponset af alle tilstandsvariable. Specielt for skadesindikatoren er resultaterne helt misvisende. Følgelig bør ækvivalente lineariseringsmetoder ikke benyttes i pålideligsanalyser af oscillatorer med hysteresevirkning, hvis statistiske responsstørrelser udover forventningsværdifunktionen er påkrævet. Kun ækvivalent polynomial udvikling af mindst 3. orden i kombination med et sædvanligt cumulant neglect closure skema giver nøjagtige estimater af middelværdifunktion og variansfunktion af skadesindikatoren, og synes at være den bedst tilgængelige semianalytiske metode til analyse af sådanne responsstørrelser, der er til rådighed. Computertiden i eksemplet er 0.88% for de ækvivalente lineariseringsmetoder og 6% for den ækvivalente kubisk polynomiale metode i forhold til regnetiden for Monte Carlo simuleringen.

Afsnit 3.3.4 omhandler dynamiske systemer påvirket af sammensatte Erlang renewalprocesser. Først vises, hvorledes sådanne systemer kan reduceres til ækvivalente systemer drevet af sammensatte Poisson processer med omkostningen, at ekstra hjælpetilstandsvariable må indføres. Dernæst udledes de stokastiske differentialligninger, der specificerer udviklingen af disse hjælpevariable. Det integrerede dynamiske system med tilstandsvektoren sammensat af de strukturelle tilstandsvariable og hjælpetilstandsvariablerne udgør da et Markov system, og momentligningerne for systemer drevet af sammensatte Poisson processer kan anvendes i lettere tillempet form. I eksempel 3-10 er anført de generelle betingelser for at reducere et system drevet af en sammensat regulær tælleproces til et ækvivalent system drevet af en sammensat Poisson proces, og det vises, at den sammensatte Erlang proces opnås som et specialtilfælde af den generelle formulering. I eksempel 3-11 er analyseret det stokastiske respons af en Duffing oscillator påvirket af en sammensat Erlang proces med parametrene $k = 2$, $k = 3$ og $k = 4$. Impulsstyrken antages at være sædvanlig Rayleighfordelt. For at kunne sammenligne meningsfuldt mellem de anførte tilfælde vælges middelankomstfrekvensen af de underliggende Poisson hændelser som $\frac{\nu}{k} = 10\omega_0$. Herved bliver det gennemsnitlige antal renewalhændelser pr. tidsenhed det samme i de tre tilfælde af k, og eventuelle forskelle i de beregnede statistiske momenter er forårsaget af de forskellige interarrival tidsfordelinger. De anførte middelankomstfrekvenser er meget høje, hvorfor hirarkiet af momentligninger kan lukkes ved orden $N = 4$ ved hjælp af et sædvanligt cumulant neglect closure skema. De opnåede middelværdifunktioner og varianser for flytningen er i alle tilfælde i udmærket overensstemmelse med simuleringsresultaterne. Middelværdifunktionerne er praktisk taget identiske for de tre tilfælde af k. Derimod har varianserne en markant tendens til at falde med øget k. Af disse observationer konkluderes, at momentligningsmetoden kan benyttes til stokastisk analyse af en klasse af ikkelineære systemer påvirket af en sammensat Erlang renewal proces efter reduktion til et ækvivalent system drevet af en sammensat Poisson proces. Middelværdifunktionen af flytningsresponset anses for at være temmelig ufølsom overfor valget af fordeling af interarrival tiden, og afhænger primært af middelankomstfrekvensen af impulser. Derimod viser variansfunktionen væsentlig afhængighed af denne fordeling. Anvendelse af sammensatte Poisson processer som lastmodel for tilfælde, hvor interarrival tidsfordelingen er langt fra en eksponential fordeling, skal derfor foretages med forsigtighed.

Afsnit 3.4 omhandler numerisk integration af den forud Chapman-Kolmogorov integro-

differentialligning ved hjælp af path integration. Først beskrives det anvendte diskretiseringsskema, der reducerer den tids- og stedkontinuerte Markov vektorproces til en ikkereducerbar, positive recurrent og ikkeperiodisk Markovkæde. I tilfælde af stationære processer observeret til ækvidistante tidspunkter vises dernæst, hvorledes den stationære fordeling kan opnås ved løsning af et linært egenværdiproblem, for hvilket egenværdien $\lambda = 1$ er kendt.

Afsnit 3.4.1 omhandler anvendelsen af path integration for systemer påvirket af Wiener processer. Eftersom tilstandsvektoren ikke foretager hop i dette tilfælde, kan denne approksimeres ved en stykkevis lineær vektorfunktion, og diffusionsmatricen ved en stykkevis konstant matrix. For tilstrækkeligt små tidsintervaller opfører systemet sig herved som lokalt gaussisk, og differentialligninger for udviklingen af betingede middelværdifunktioner og betingede kovarianser tillige med den simultane overgangssandsynlighedstæthedsfunktion kan umiddelbart formuleres. Fire alternative lineariseringsstrategier er anført efter voksende grad af kompleksitet. Specielt running mean lineariseringsskemaet og det ækvivalente lineariseringsskema er lovende, eftersom meget større gennemgangstidsintervaller kan benyttes end tilladt ved de to øvrige anførte lineariseringsskemaer. Anvendelsen af de sidstnævnte anførte lineariseringskemaer. Anvendelsen af de sidstnævnte skemaer skyldes, at simple løsninger opnås for de betingede middelværdifunktioner og de betingede kovariansfunktioner. I eksempel 3-12 er eksplicitte udtryk angivet for lineariseringsskemaerne for en Duffing oscillator påvirket af gaussisk hvid støj. Dernæst udvælges running mean lineariseringsskemaet til nærmere undersøgelse i forbindelse med et ensformigt relativt groft 20×20 net, der udstrækkes fire lineære stationære standardafvigelser i de positive og negative flytnings- og hastighedsretninger, og med et gennemgangstidsinterval på $\Delta t = \frac{T_0}{4}$. Udmærket overensstemmelse med simuleringsresultater er opnået både ved de centrale dele af de marginale fordelinger og ved disses haler. Førstepassagetidsproblemet er ligeledes l ost for et deterministisk start problem med en enkelt konstant barriere. Fordelingsfunktionen for førstepassagetiden opnået ved path integration overestimerer svigtsandsynligheden en smule under den første periode sammenlignet med Monte Carlo simulering, hvilket er en følge af brugen af det omtalte grove net i forbindelse med det relativt store gennemgangstidsinterval. Af resultaterne af eksemplet konkluderes, at det stokastiske respons kan bestemmes ved hjælp af path integration med anvendelse af et meget grovt net uden at påvirke nøjagtigheden væsentligt, hvorimod et noget finere net må benyttes i pålidelighedsproblemer.

I afsnit 3.4.2 er path integration metoder udviklet for systemer påvirket af sammensatte Poisson processer, Lévy α-stabile bevægelser og sammensatte Erlang processer. Først betragtes tilfældet med et dynamisk system drevet af en skalar sammensat Poisson proces. En asymptotisk udvikling er udledt for den simultane gennemgangssandsynlighedstæthedsfunktion, gyldig under forudsætningen $\nu \Delta t \ll 1$, og kun involverende de simultane gennemgangssandsynlighedstæthedsfunktioner under betingelse af ankomsten af eksakt nul og en impuls i løbet af gennemgangstidsintervallet. Den simultane gennemgangssandsynlighedstæthedsfunktion under betingelse af nul impulser beskriver egensvingningerne af systemet fra begyndelsesbetingelserne, der opnås ved numerisk integration. De forskellige path integrationsskemaer udskiller sig derefter

ved, på hvilken måde den simultane gennemgangssandsynlighedstæthedsfunktion under betingelse af en impulsankomst i løbet af gennemgangstidsintervallet er bestemt. På grund af restriktionen på $\nu\Delta t$ forventes path integration at virke bedst for små værdier af ν, hvilket er modsat forholdene ved momentmetoder. For fast ν fastlægger restriktionen en øvreværdi for valget af Δt. På den anden side vises det, at en nedreværdi for denne størrelse også eksisterer, således at de optimale resultater opnås, når Δt er beliggende i et vist interval. To metoder præsenteres for konvektion og diffusion af sandsynlighedsmassen under betingelse af en impulsankomst i løbet af gennemgangstidsintervallet. Metode 1 er baseret på kendsgerningen, at ankomsttiden af impulsen er ensformigt fordelt i gennemgangstidsintervallet for homogene Poisson processer. Gennemgangstidsintervallet opdeles derfor i et endeligt antal underintervaller, og konvektionen og diffusionen af sandsynlighedsmasse udføres for hvert unterinterval efter tur, under betingelsen at impulsen ankommer netop i det pågældende interval. Metode 2 er baseret på en Taylorudvikling i impulsstyrken P af tilstandsvektoren ved slutningen af gennemgangstidsintervallet. Koefficienterne af Taylorudviklingen afhænger kun af start- og sluttidspunktet samt af systemets position ved starten af gennemgangen, men ikke af tidspunktet, hvor impulsen faktisk indtræffer. Dernæst er udledt koblede ordinære til bestemmelse af disse udviklingskoefficienter, der løses numerisk. Det vises, at Taylorudviklingen for lineære systemer bliver lineær i P. Eftersom en udskiftning af drift vektoren med en lokal ækvivalent lineær drift vektor altid er mulig ved tilstrækkeligt små gennemgangstidsintervaller følger, at Taylorudviklingen bliver asymptotisk lineær, når gennemgangstidsintervallet går mod nul. Denne observation danner baggrunden for metode 2, som antager, at en sådan lineær Taylorudvikling er eksakt gældende. Det skal her bemærkes, at lineariseringsantagelsen vedrører driftvektoren som funktion af tilstandsvektoren, og at der ikke sættes restriktioner på størrelsen af impulsstyrken. I eksempel 3-13 er foretaget en stokastisk responsanalyse og en pålidelighedsanalyse af en Duffing oscillator, både ved hjælp af metode 1 og metode 2. Duffing oscillatoren er let dæmpet med en middelstor ikkelinearitetsparameter. Grundlæggende udføres path integrationen ved hjælp af et ensformigt grovt 20×20 net, der udstrækkes fire lineære stationære standardafvigelser i de positive og negative flytnings- og hastighedsretninger. Styrken af impulserne antages at være normalfordelt med middelværdien nul. For metode 1 betragtes 3 forskellige værdier af ν, svarende til lav, middel og høj middelankomstfrekvens af impulserne. For tilfældet med lav middelankomstfrekvens opnås fordelinger med meget markante spidser ved origo. For dette tilfælde er benyttet et ikkeensformigt 25×25 net med en fire gange finere inddeling tæt ved origo. Gennemgangstidsintervallet Δt er opdelt i 3 underintervaller. Den stationære marginale sandsynlighedstæthedsfunktion af flytningen og hastigheden er opnået ved at iterere gennemgangsligningen for Markovkæden indtil stationaritet er opnået. Gennemgangstidsintervallet for de tre tilfælde af ν er henholdsvis $\Delta t = T_0$, $\Delta t = T_0$ og $\Delta t = \frac{T_0}{2}$. For tilfældene med lav og middel middelankomstfrekvens er opnået udmærkede resultater i forhold til Monte Carlo simuleringsresultater, både ved de centrale dele af fordelingerne og ved disses haler, selv med de anførte relativt grove net. Derimod giver path integration relativt dårlige resultater i tilfældet med høj middelankomstfrekvens, hvilket skyldes at øvreværdibegrænsningen på Δt ikke længere er overholdt. Dernæst er førstepassagetidsproblemet for et deterministisk start problem med symmetriske kon-

stante dobbeltbarrierer løst for tilfældene med lav og middel middelankomstfrekvens. Som det er tilfældet med den tilsvarende hvidstøjspåvirkning bliver fordelingsfunktionen for førstepassagetiden opnået ved path integration underestimeret i de første perioder af påvirkningen på grund af det grove net og de store gennemgangstidsinterval. For tilfældet af middel middelankomstfrekvens af impulser er foretaget en sammenligning med svigtsandsynligheden opnået ved at approksimere påvirkningsprocessen med en ækvivalent gaussisk hvid støj. Resultaterne opnået ved hjælp af metode 1 er i langt bedre overensstemmelse med simuleringsresultaterne, end det er tilfældet for resultaterne opnået ved den ækvivalente hvid støj. Følgelig fører en erstatning af en sammensat med en ækvivalent gaussisk hvid støj til helt vildledende resultater i pålidelighedsanalyser med middelankomstfrekvenser af den betragtede størrelse. Dernæst er betragtet et enkeltbarriere problem med stationær start i det sikre område for tilfældene med lav og middel middelankomstfrekvens af impulserne. I intet af tilfældene er den trappelignende karakter af sandsynlighedstæthedsfunktionen for førstepassagetiden opnået ved path integrationen. Imidlertid viser resultaterne et korrekt eksponentielt limiting decay, svarende til et diskret egenværdispektrum af bagud eller forud Kolmogorov-Feller operatoren med absorbtion på henholdsvis udgangsdelene og indgagsdelene af randen, for både deterministisk start og stationær start problemer. Dernæst er metode 2 anvendt ved bestemmelsen af de stationære marginale sandsynlighedstæthedsfunktioner for flytningen og hastigheden i tilfælde af relativt lav middelankomstfrekvens af impulserne. De opnåede resultater for de marginale fordelinger er af samme kvalitet som de tilsvarende resultater opnået med metode 1. Imidlertid er algoritmen i metode 2 væsentlig simplere og hurtigere at benytte. Computertiden ved anvendelse af metode 2 i sammenligning med simulering er 0.22%, hvoraf konkluderes, at metoden muliggør ekstreme beregningsmæssige fordele sammenlignet med Monte Carlo simulering. Dernæst er metode 2 modificeret med henblik på anvendelse ved path integration af systemer påvirket af Lévy α-stabile bevægelser og sammensatte Erlang processer. Modifikationen for systemet påvirket af en Lévy α-stabil bevægelse består i det væsentligste i at erstatte den aktuelle proces med en ækvivalent sammensat Poisson process med α-stabil fordelte impulsstyrker. Teorien er ikke illustreret med et numerisk eksempel. For systemer påvirket af sammensatte Erlangprocesser er en mere gennemgribende modifikation af metoden nødvendig. Istedet for et enkelt net for det diskretiserede tilstandsrum af de strukturelle tilstandsvariable bliver det nu nødvendigt at definere k sådanne net, et for hver af de k Poisson hændelser, der indtræffer pr. Erlang hændelse. For hver af de første $k-1$ Poisson hændelser konvekteres sandsynlighedsmassen ved en given knude i det til denne hændelse tilknyttede net svarende til egensvingningerne fra begyndelsesværdierne. Brøkdelen af sandsynlighedsmassen svarende til sandsynligheden for at ingen impulser ankommer i gennemgangstidsintervallet klumpes i slutpositionen på nettet, medens den resterende sandsynlighedsmasse overføres til det næste net i rækken. Er dette net det k. og sidste udspredes sandsynlighedsmassen i dette net. Ellers klumpes sandsynlighedsmassen ved samme slutposition i det nye net som i det forrige net. Hvis systemet starter på det k. net overføres sandsynlighedsmassen i stedet til det første net, og en ny sekvens kan begynde. Det følger heraf, at antallet af tilstande af den resulterende Markovkæde vokser proportionalt med k, og ikke eksponentielt som forventet. Følgelig har introduktionen af hjælpetilstandsvariablerne, nødvendig for at

reducere et Erlang proces drevet system til et ækvivalent Poisson drevet system, relativt lille indflydelse på de beregningsmæssige omkostninger af det udviklede path integrationsskema. I eksempel 3-14 er metoden anvendt på en Duffing oscillator med relativt høj ikkelinearitetsparameter påvirket af en sammensat Erlang proces med parameter $k = 2$. Styrken af renewal impulserne antages at være normalfordelt med middelværdi nul. Tre tilfælde af middelankomstfrekvenser af de underliggende Poisson hændelser betragtes, svarende til lav, middel og høj middelankomstfrekvens af renewal impulserne. Path integrationen udføres med to ensformige 44×44 net, der udstrækkes fem lineære stationære standardafvigelser i de positive og negative flytnings- og hastighedsretninger. For tilfældet med lav middelankomstfrekvens af impulserne opnås udmærkede resultater for de marginale sandsynlighedstæthedsfunktioner for flytningen og hastigheden i forhold til Monte Carlo simulering. I dette tilfælde er der ingen problemer med at overholde såvel øvre- som nedreværdibegrænsningen for gennemgangstidsintervallet. Vigtigheden af disse begrænsninger er demonstreret i en undersøgelse af kvaliteten af de opnåede resultater som en funktion af længden af gennemgangstidsintervallet. Resultater opnået med det store gennemgangstidsinterval på $5.0T_0$ i tilfælde af lav middelankomstfrekvens af impulserne er ubrugelige, fordi øvreværdikriteriet er overskredet i dette tilfælde. De tilsvarende resultater opnået for middel middelankomstfrekvenser er acceptable, men ikke så gode som resultaterne opnået med lav middelankomstfrekvens. Gennemgangstidsintervallet er valgt til $\Delta t = 0.2T_0$ for at overholde øvreværdibegrænsningen. Imidlertid er dette valg samtidigt tæt på nedreværdigrænsen, som demonstreret i undersøgelsen over afhængigheden af gennemgangstidsintervallets størrelse. Det vises, at med den benyttede værdi af ν opnås dårligere resultater med intervaller mindre end eller større end det anførte. Resultaterne opnået ved path integration for tilfældet med høj middelankomstfrekvens af impulserne er endnu dårligere. Path integrationen er her udført med et gennemgangstidsinterval på $\Delta t = 0.05T_0$ for at overholde øvreværdibegrænsningen, men nedreværdibegrænsningen er helt sikkert ikke overholdt. Følgelig bekræfter observationerne, der er gjort i eksemplet, tidligere resultater for systemer påvirket af sammensatte Poissonprocesser, at path integration af pulsdrevne systemer giver nøjagtige resultater for tilfælde med lav middelankomstfrekvens af impulserne med passende valg af gennemgangstidsintervallet, medens uanvendelige resultater opnås, hvis gennemgangstidsintervallet er enten for lille eller for stort.

Afsnit 3.5 omhandler den numeriske løsning ved hjælp af Petrov-Galerkin variation af pålidelighedsproblemet for ikkelineære tidsinvariante oscillatorer af 1 frihedsgrad uden hysteresevirkning påvirket af en homogen sammensat Poisson proces. Baseret på den generelle formulering i afsnit 3.2.2, er rand- og begyndelsesproblemet angivet til bestemmelsen af pålidelighedsfunktionen for et dobbeltbarriere problem, og den svage formulering af dette rand- og begyndelsesværdiproblem er udledt. I formuleringen forudsættes en Kramer-Moyal udvikling af den bagudrettede Kolmogorov-Feller operator at være gyldig, hvilket indebærer, at momenter af vilkårlig høj orden antages at eksistere for impulsstyrken. I flytningsretningen anvendes triangulære formfunktioner, og vægtfunktionerne opnås ved at addere et kvadratisk upwind tillæg hertil. For at overholde de strenge krav til differentiabilitet vælges formfunktionerne i hastighedsretningen som normaltfordelte sandsynlighedstæthedsfunktioner med varierende middelværdi.

Vægtfunktionerne opnås ved at addere upwind tillæg, der vælges som normerede første afledede af formfunktionerne. Udtryk er foreslået for skaleringsfaktoren på disse tillæg og for de lokale Peclet tal. Det diskretiserede system af koblede førsteordens differentialligninger er løst ved hjælp af et Crank-Nicolson skema. I eksempel 3-15 er metoden anvendt på et førstepassagetidsproblem med symmetriske dobbeltbarrierer og deterministisk start i origo for en Duffing oscillator påvirket af en sammensat Poisson proces. I eksemplet varieres dæmpningsforholdet og ikkelinearitetsparameteren af oscillatoren for at undersøge deres indflydelse på pålidelighedsfunktionen. Impulsstyrken antages at være normalfordelt med middelværdi nul. Det sikre område opdeles i et ensformigt 30×30 net, der udstrækker sig fem stationære standardafvigelser i den positive og negative hastighedsretning. De stationære standardafvigelser er tilvejebragt ved Monte Carlo simulering, men kunne også være bestemt ved metoden. Det vises, at det numeriske skema konvergerer til resultaterne opnået ved gaussisk hvid støj, når $\nu \to \infty$. Parameterstudierne viser, at pålidelighedsfunktionen afhænger væsentligt af ikkelinearitetsparameteren, medens den er forholdsvis ufølsom overfor dæmpningsforholdet. En undersøgelse af pålidelighedsfunktionens afhængighed af middelankomstfrekvensen viser, at metoden med det anvendte 30×30 net bliver numerisk instabil for $\nu < 1.0\omega_0$, og at de opnåede resultater er forholdsvis ufølsom overfor værdier af middelankomstfrekvensen over denne grænse. Det vises, at forsøg på at opnå numerisk stabilitet for middelankomstfrekvenser under den anførte stabilitetsgrænse kræver en drastisk reduktion af netvidden. Følgelig deler Petrov-Galerkin variation mangelen ved momentligningsmetoder for systemer påvirket af sammensatte Poisson processer, at disse metoder er mest effektive for påvirkninger med høj middelankomstfrekvens.

ISSN 1395-7953 R9730
Dept. of Building Technology and Structural Engineering
University of Aalborg
Sohngaardsholmsvej 57, DK-9000 Aalborg
Phone: +45 9635 8080 Fax: +45 9814 8243

Printed at Aalborg University